Technical Reports
Consolidated Printing

VOLUMES 1, 2, and 3

113090

SLANTING IN NEW BASEMENTS FOR COMBINED NUCLEAR WEAPONS EFFECTS:
A Consolidated Printing of Four Technical Reports

October 1975

FEASIBILITY STUDY OF SLANTING FOR COMBINED NUCLEAR WEAPONS EFFECTS (Revised), Volumes 1 and 2 — *July 1971*

Slanting for Combined Nuclear Weapons Effects: FIRE HAZARD REDUCTION — *August 1972*

Slanting for Combined Nuclear Weapons Effects: EXAMPLES WITH ESTIMATES, AND AIR BLAST ROOM FILLING — *June 1973*

Slanting for Combined Nuclear Weapons Effects: BLAST-RESISTANT DESIGN/ANALYSIS WITH EXAMPLES — *December 1974*

For:

DEFENSE CIVIL PREPAREDNESS AGENCY
WASHINGTON, D.C. 20301

Contracts DAHC 20-67-C-0136 and 20-71-C-0292
DCPA Work Units 1154E and 1154H

STANFORD RESEARCH INSTITUTE
Menlo Park, California 94025 · U.S.A.

UNCLASSIFIED

SECURITY CLASSIFICATION OF THIS PAGE (When Data Entered)

REPORT DOCUMENTATION PAGE		READ INSTRUCTIONS BEFORE COMPLETING FORM
1. REPORT NUMBER (none)	2. GOVT ACCESSION NO.	3. RECIPIENT'S CATALOG NUMBER
4. TITLE (and Subtitle) SLANTING IN NEW BASEMENTS FOR COMBINED NUCLEAR WEAPONS EFFECTS: A Consolidated Printing of Four Technical Reports		5. TYPE OF REPORT & PERIOD COVERED Technical Report (final)
		6. PERFORMING ORG. REPORT NUMBER
7. AUTHOR(s) H. L. Murphy, J. R. Rempel and J. E. Beck		8. CONTRACT OR GRANT NUMBER(s) DAHC 20-67-C-0136 and DAHC 20-71-C-0292
9. PERFORMING ORGANIZATION NAME AND ADDRESS Stanford Research Institute Facilities and Housing Research Group Menlo Park, California 94025		10. PROGRAM ELEMENT, PROJECT, TASK AREA & WORK UNIT NUMBERS DCPA Work Units 1154E and 1154H
11. CONTROLLING OFFICE NAME AND ADDRESS Defense Civil Preparedness Agency Washington, D. C. 20301		12. REPORT DATE October 1975
		15. SECURITY CLASS. (o UNCLASSIFIED
14. MONITORING AGENCY NAME & ADDRESS (if diff. from Controlling Office)		15a. DECLASSIFICATION/DOWNGRADING SCHEDULE

16. DISTRIBUTION STATEMENT (of this report)

Approved for public release; distribution unlimited.

17. DISTRIBUTION STATEMENT (of the abstract entered in Block 20, if different from report)

18. SUPPLEMENTARY NOTES

19. KEY WORDS (Continue on reverse side if necessary and identify by block number)

Protective Shelter, Nuclear Weapons Effects
Protective Shelter Design
Natural Disasters Shelter
Nuclear Attack Shelter
Combined Nuclear Effects Slanting
Shelter, Nuclear Attack
Shelter, Natural Disasters
Dynamic Design
Design, Shelter
Slanting

20. ABSTRACT (Continue on reverse side if necessary and identify by block number)

This consolidated printing of four Stanford Research Institute Technical Reports, which were published in five volumes, contains only the latest version of any chapter, appendix or other portion of the original reports.

The three early feasibility studies were published in full, including both old and new material, at the end of each research contract period. Later reports[2-4] provide only revised portions for insertion into the latest full feasibility study.[1]

The purpose of this printing is to provide reference copies of the latest material, primarily for internal use in the Defense Civil Preparedness Agency, its field offices and by its contractors. Separation of the printing into three vol-

DD FORM 1 JAN 73 1473 UNCLASSIFIED

EDITION OF 1 NOV 65 IS OBSOLETE

SECURITY CLASSIFICATION OF THIS PAGE (When Data Entered)

20 ABSTRACT (Continued)

umes has been made to facilitate use in ringbinders with 1½-in. (i.d.) rings; users may still want to shift Chapter 11 into the second ringbinder in front of the Volume 2 material.

Since no new material is published herein, the usual distribution given to research reports is not being made.

It is emphasized that protective shelter of the kind contemplated in full slanting - i.e., to protect against 15 psi nuclear air blast and related radiation effects (or even much lower than 15 psi) - provides excellent (full) protection against such natural disasters as earthquakes, hurricanes (including cyclones), and tornadoes. Also, such protective shelter provides fire protection at a level equaling, in most aspects exceeding, fire codes, because fire codes assume continuing availability of professional fire departments and water supply, while their nonavailability is assumed in full slanting. *In short, full slanted basement shelters more than satisfy requirements for protection against all natural disasters except floods.*

Every effort has been made to ensure the accuracy of all guidance and programs included herein. However, no warranty, expressed or implied, is made as to the recommended procedures or programs. The reader-user is expected to make the final evaluation as to the usefulness of all material contained herein. Recommendations made herein should not be substituted for the knowledge, experience, and judgment of the professional engineer or architect, but should be treated as guidance for consideration by the professional, regarding the best method of achieving specific design goals.

---

1. Murphy, H. L., Feasibility Study of Slanting for Combined Nuclear Weapons Effects (Revised), Volumes 1 and 2, SRI Technical Report, for OCD (DCPA), July 1971. (AD-734 831 and 2)

2. Murphy, H. L., and J. R. Rempel, Slanting for Combined Nuclear Weapons Effects: FIRE HAZARD REDUCTION, Stanford Research Institute Technical Report, for Defense Civil Preparedness Agency, August 1972. (AD-763 472)

3. Murphy, H. L., and J. E. Beck, Slanting for Combined Nuclear Weapons Effects: EXAMPLES WITH ESTIMATES, AND AIR BLAST ROOM FILLING, Stanford Research Institute Technical Report, for Defense Civil Preparedness Agency, June 1973. (AD-783 061)

4. Murphy, H. L., and J. E. Beck, Slanting for Combined Nuclear Weapons Effects: BLAST-RESISTANT DESIGN/ANALYSIS WITH EXAMPLES, Stanford Research Institute Technical Report, for Defense Civil Preparedness Agency, December 1974. (AD-A016 631)

Technical Reports
Consolidated Printing

VOLUME 1

SLANTING IN NEW BASEMENTS FOR COMBINED NUCLEAR WEAPONS EFFECTS:

A Consolidated Printing of Four Technical Reports *October 1975*

By: H. L. Murphy, J. R. Rempel and J. E. Beck
Facilities and Housing Research

FEASIBILITY STUDY OF SLANTING FOR COMBINED NUCLEAR WEAPONS EFFECTS (Revised), Volumes 1 and 2 *July 1971*

By: H. L. Murphy

Slanting for Combined Nuclear Weapons Effects: FIRE HAZARD REDUCTION *August 1972*

By: H. L. Murphy and J. R. Rempel

Slanting for Combined Nuclear Weapons Effects: EXAMPLES WITH ESTIMATES, AND AIR BLAST ROOM FILLING *June 1973*

By: H. L. Murphy and J. E. Beck

Slanting for Combined Nuclear Weapons Effects: BLAST-RESISTANT DESIGN/ANALYSIS WITH EXAMPLES *December 1974*

By: H. L. Murphy and J. E. Beck

For:

DEFENSE CIVIL PREPAREDNESS AGENCY
WASHINGTON, D.C. 20301

Contracts DAHC 20-67-C-0136 and 20-71-C-0292
DCPA Work Units 1154E and 1154H

STANFORD RESEARCH INSTITUTE
Menlo Park, California 94025 · U.S.A.

ib

PREFACE

This consolidated printing of four Stanford Research Institute Technical Reports, which were published in five volumes, contains only the latest version of any chapter, appendix or other portion of the original reports.

The early feasibility studies were published in full, including both old and new material, at the end of each research contract period.[1-3*] Later reports[4-6] provide only revised portions for insertion into the latest full feasibility study.[3]

The purpose of this printing is to provide reference copies of the latest material, primarily for internal use in the Defense Civil Preparedness Agency, its field offices and by its contractors. Separation of the printing into three volumes has been made to facilitate use in ringbinders with $1\frac{1}{2}$-in. (i.d.) rings; users may still want to shift Chapter 11 into the second ringbinder in front of the Volume 2 material.

Since no new material is published herein, the usual distribution given to research reports is not being made. The original reports[3-6] are available, as indicated on the last page of this prefatory material.

It is emphasized that protective shelter of the kind contemplated in full slanting - i.e., to protect against 15 psi nuclear air blast and related radiation effects (or even much lower than 15 psi) - provides excellent (full) protection against such natural disasters as earthquakes, hurricanes (including cyclones), and tornadoes. Also, such protective

* Superscript numerals refer to publications listed at the end of the prefatory material.

shelter provides fire protection at a level equaling, in most aspects exceeding, fire codes, because fire codes assume continuing availability of professional fire departments and water supply, while their nonavailability is assumed in full slanting. *In short, full slanted basement shelters more than satisfy requirements for protection against all natural disasters except floods.*

Note

Every effort has been made to ensure the accuracy of all guidance and programs included herein. However, no warranty, expressed or implied, is made as to the recommended procedures or programs. The reader-user is expected to make the final evaluation as to the usefulness of all material contained herein. Recommendations made herein should not be substituted for the knowledge, experience, and judgment of the professional engineer or architect, but should be treated as guidance for consideration by the professional, regarding the best method of achieving specific design goals.

PREFACE AND SUMMARY FROM THE FEASIBILITY STUDY ON FULL SLANTING[3]

The feasibility study and results described in this report had two principal goals:

- To determine the general feasibility of slanting for combined nuclear weapons effects, within a specified scope and stipulated conditions prescribed by the U.S. Office of Civil Defense.*

- To organize the work and resulting report in such a manner that, should the general question of feasibility be answered affirmatively by this study, the later preparation of a prototype guide or manual for use by architects and engineers would be facilitated.

Because of the latter goal, this report is organized as a guide and the word "guide" is used frequently; nonetheless, the report is intended only to cover a feasibility study, not to provide a guide for protective design.

Publication of a report at this stage of work thus has two broad purposes:

- To demonstrate the possibility that full slanting is achievable, i.e., modification of usual building designs to provide protection in basements against 15 psi overpressure and associated nuclear weapons effects appears possible within the prescribed (added cost) limitation of $6/sf (January 1968) of shelter space.

- To serve as a clearly defined point of departure in the further work of several researchers, including not only those working directly on the project but also those working on associated U.S. Office of Civil Defense* research projects that are expected to contribute inputs to this work.

It is hoped that readers will feel free to provide constructive technical comments to the author by whatever means is most convenient to the reviewer. A discussion of planned further work is included at the end of the report (Chapter 11).

---

* Now the U.S. Defense Civil Preparedness Agency

Chapter 1 includes introductory material and sections on Scope, Stipulations, Approach, Preliminary Building Selection for Slanting, and Acknowledgments. Chapters 2 through 6 provide nuclear effects data and design methodology needed by the architect or professional engineer for combined nuclear effects slanting design. Chapters 7 and 8 constitute applications of the data and methodology to certain buildings selected for use as examples or case studies, and for which complete design drawings were at hand. Chapters 9 and 10 will attempt to draw together lessons learned from the case studies. The Appendices, Volume 2, contain supporting data too voluminous to include in Volume 1.

The revised feasibility study includes discussion of open shelter - concept, problems, and types - with two types included as case studies (applications of full slanting, with cost estimates and floor plans); also an open shelter case study of the two below-grade levels of a large parking garage was completed, except for needed review work in some high cost areas such as ventilation, showing a tremendous potential for combined effects shelter. Each case study slanting cost estimate was summarized into four major categories: structural, blast doors, ventilation, and other. An estimate is also shown for that work which must reasonably be performed at the time of original building construction, i.e., non-deferrable work.

Included too are typical designs, using a detailed final design procedure, for simply supported one-way reinforced concrete slabs. Designs using all combinations of three concrete strengths, two dynamic steel strengths, and four positive moment steel ratios are shown by graphs; a graph for one steel ratio shows total estimated steel quantities. All design graphs have scales for slab clear span, effective depth, positive and negative moment steel ratios, and stirrup steel ratio.

REFERENCES USED IN THE PREFATORY MATERIAL

1. Murphy, H. L., Feasibility Study of Slanting for Combined Nuclear Weapons Effects, Stanford Research Institute Technical Report for U.S. Office of Civil Defense (now Defense Civil Preparedness Agency or DCPA), June 1969. (AD-692 312)

2. Murphy, H. L., Feasibility Study of Slanting for Combined Nuclear Weapons Effects (Revised), Volumes 1 and 2, SRI Interim Report for OCD (DCPA), October 1970. (AD-724 711 and 2)

3. Murphy, H. L., Feasibility Study of Slanting for Combined Nuclear Weapons Effects (Revised), Volumes 1 and 2, SRI Technical Report for OCD (DCPA), July 1971. (AD-734 831 and 2)

4. Murphy, H. L., and J. R. Rempel, Slanting for Combined Nuclear Weapons Effects: FIRE HAZARD REDUCTION, Stanford Research Institute Technical Report for Defense Civil Preparedness Agency, August 1972. (AD-763 472)

5. Murphy, H. L., and J. E. Beck, Slanting for Combined Nuclear Weapons Effects: EXAMPLES WITH ESTIMATES, AND AIR BLAST ROOM FILLING, Stanford Research Institute Technical Report, for Defense Civil Preparedness Agency, June 1973. (AD-783 061)

6. Murphy, H. L., and J. E. Beck, Slanting for Combined Nuclear Weapons Effects: BLAST-RESISTANT DESIGN/ANALYSIS WITH EXAMPLES, Stanford Research Institute Technical Report, for Defense Civil Preparedness Agency, December 1974. (AD-A016 631)

* References are all understood to be available for purchase from NTIS, Springfield, Virginia, 22151, including reference 6 (an "AD-" number had not yet been assigned).

CONTENTS

Volume 1

Preceding page blank

CONTENTS (Continued)

CONTENTS (Continued)

CONTENTS (Concluded)

Volume 2

Volume 3

TABLES

FIGURES

Preceding page blank

FIGURES (Continued)

FIGURES (Continued)

FIGURES (Concluded)

Chapter 1

INTRODUCTION

This publication is intended as a prototype or forerunner of a design guide on slanting against all nuclear weapons effects, comparable to the U.S. Office of Civil Defense (OCD) guidance on slanting for fallout radiation protection only, which is the subject of several publications and a film available to practicing architects and engineers, both directly and through formal courses offered by OCD.

The term "slanting" implies making design changes involving little or no extra cost, such that protection against one or more nuclear weapons effects is improved, yet no needed function of the structure is lost. While the term was originated in another government department where protection against one or more effects was intended, slanting as adopted and currently used by OCD has been limited to improved protection against fallout radiation only. This limited meaning is termed "fallout slanting" in this guide. Where protection against all nuclear weapons effects is envisioned, this guide uses "combined (nuclear) effects slanting" or, more simply, "full slanting"; modest additional costs are implied to obtain significantly greater protection than in fallout slanting.

The government publications, The Effect of Nuclear Weapons (ENW)[1]* and Reference 2, are necessary companion volumes to this guide, in that material therein is referenced and not reproduced herein. A general knowledge of nuclear weapons effects is a prerequisite for the user of this guide. Referenced material from other specialized sources will be extracted to the extent necessary to make this guide useful in itself. Standard references as well as the technical skills ordinarily used in various professional fields (structural and mechanical engineering, architecture, etc.) are assumed to be at hand.†

---

* Superscript numerals refer to publications listed at the end of the main body of the report. Numerical sequence in use was not maintained in the revised report.

† OCD regularly offers three graduate-level courses for engineers and architects in Fallout Shelter Analysis, Protective Construction, and Environmental Engineering. Classes meet in principal cities and outside normal business hours. Full-time summer short courses (four to six weeks) are also offered.

Scope

The scope of this guide is limited to:

- Building designs for new construction* where shelter in the slanted or modified design can be provided in basements (defined as space wholly below grade, either existing or obtained by construction of a berm).
- Consideration of free-field nuclear weapons effects no greater than 15 psi air blast peak (<u>design</u>) overpressure,† at least initially, and other comparable primary and secondary effects.
- Basic consideration of effects from a 1-megaton (Mt) weapon yield, although thermal and initial nuclear radiation effects related to a 200-kiloton (kt) yield were reviewed.
- Shelter providing a fallout radiation protection factor (PF) of 100 or more.
- Slanting where estimated capital cost‡ increase over the unslanted version is not more than $6/sf (January 1968) of shelter space,§ for all modifications whether within or outside the shelter space, including emergency ventilating equipment.**

Human tolerances related to nuclear effects, estimates of the survival probability of shelterees in terms of number uninjured and injured, and gross probability functions are within the Scope, but only insofar as they may affect the full slanting design work.

---

* A supplement discussing full slanting for existing buildings was not excluded as a by-product of the project work.

† See first two sections of Ch. 6 for comments on design overpressure definition and selection. Other overpressures (5 to 30 psi) were later added to the initial Scope of 15 psi (103 cb††) only.

‡ Design, contract administration, and construction, including overhead and profit, etc.

§ Calculated for purposes herein using dimensions to the inside face of all exterior walls, ignoring space taken by any interior walls, but deducting any floor space occupied so fully by an equipment item(s) that people cannot sit or lie on or under the equipment.

** Cost-effectiveness studies per se were excluded from the work.

†† 1 cb (centibar) = 0.01 bar = 10^3 N/m^2 = 1 kN/m^2 = 1000 Pa = 0.010197 kg/cm^2 = 0.145038 psi; <u>or</u> 1 psi = 6.894757 cb = 0.0703067 kg/cm^2 (Ref. 45).

Stipulations

The following stipulations are a part of the basis for this guide:

- Purpose of overall slanting is to provide austere shelter as a secondary building function - within the Scope and Stipulations stated - by balancing, to the extent possible, protective measures against each hazard so that shelterees' survival prospects are improved.

- To the extent that such probabilities can be calculated, a survival probability† of 85%-95% against all effects (at or related to design free-field overpressure) is a slanting goal.‡

- Burst eardrums may be an acceptable hazard.

- Slanting must comply with usual building code requirements - that is, the codes covering large geographic areas[3-8] - but only in connection with the primary or nonshelter function of the structure. For the emergency or shelter function, sound engineering practice is to guide the slanting, whether or not such practice complies with codes.

- Shelter entranceways design, in relation to the emergency function just mentioned, must meet the requirements indicated by Table 1.1, which serves only to set minimums for reasonable shelter loading criteria.[9]

- Blast wave arrival time on the ground (6-7 sec. at 1 Mt; 3 sec. at 200 kt*) may be considered for operational use by shelter managers, i.e., to have shelterees lie down, close any blast doors, etc. Where longer warning times are available, movement of stored materials, preliminary fire countermeasures, and other steps may be planned.

- Loss of normal electric power will be assumed.

- Emergency ventilation and other environmental measures are to be included in the slanting.

---

* Ref. 1, Fig. 3.70a.

† Applies after arrival in shelter.

‡ The purpose of the stated survivability range is to establish that bare survival shelter is intended. However, in the full slanting design examples (case studies) and typical designs herein, Chapters 6-8, the blast resistant designed structural members are expected to have a probability of 98+% for protecting against injuries from the blast design overpressure. For other effects, the probabilities should be nearly 100% for protecting against each direct nuclear effect related to the design overpressure (from 1-Mt yield), and the probabilities can be judged from comments on page 8-94 for protecting against the interior jet blast hazards in open shelters.

Table 1.1

SHELTER ENTRANCEWAY RECOMMENDED MINIMUM DIMENSIONS VS SHELTER CAPACITY[9]
(Based on entry needs)

Shelter Capacity per Element	Entranceway Element	Height*	Nominal Width
470	Stair	7'0"	3'0"‡
630	or Ramp†	"	3'8"
780		"	4'8"
940		"	5'6"
1260		8'0"	7'4"
420	Door	6'8"	2'6"‡
630		"	3'0"
840		"	3'8"
1050		"	4'8"§
1260		"	5'6"§
1680		"	7'4"§
420	Corridor	7'0"	2'6"
630		"	3'0"
840		"	3'8"
1050		"	4'8"
1260		"	5'6"
1680		8'0"	7'4"

* Minimum vertical clearance above stair nosings or floor.

† Use only if ramp slope $\leq$ 1 in 6; steeper ramps are not recommended. Treat slopes < 1 in 16 as corridors.[42]

‡ Minimum.

§ Single door maximum is 4'0"; with multiple doors, minimum single opening width is 2'4".

NOTES: 1. Capacity for an element with a width in between two of the tabulated widths shall be the capacity related to the narrower width.

2. Stair minimums: riser height, 7-3/4"; tread width, 9-1/2".

3. Landings: maximum height between landings, 12'0"; minimum landing dimension in direction of travel, 3'8".

GENERAL: Table is based on a 15-minute time period between an announcement to take shelter and completed filling of the shelter; the time period includes consideration of walking and queuing times. Adjustment to other periods is nonlinear with capacity[9] and, in any case, fire exit codes should be considered.[42] In no Chapter 8 case study, however, was a change in original design needed to meet Table 1.1 recommendations.

- Emergency lighting is to be handled as an operational matter* and excluded from slanting; an exception would be where emergency generating equipment is planned for ventilation, in which case emergency lighting power might be included.

- Temporarily reduced space allowances (overcrowding) may be planned for during probable attack periods. Gross shelter space allowance is 10 sf/person (including space for all functions within the protected areas); reduced space allowance (overcrowding) is 6 sf/person. Minimal space allowance (severe overcrowding) is 3 sf/person, excluding any other function than space for people. (Emergency ventilation needs and plans must be adjusted, however, for any changed space allowances.)

- An initial nuclear radiation dose of 50 rads or less may be considered acceptable and used for shelter design; this figure includes allowance for accuracy shortcomings in current shielding calculation techniques.† For shelter design, the acceptable initial nuclear radiation dose of 50 rads and the minimum fallout shelter PF of 100 (stated in the Scope) will be treated independently.

Approach

A case study method using design or as-built drawings of specific buildings was followed. From the case studies, both general and limited application principles were learned and are described in later chapters. This organizational order may be reversed, of course, in any final published guidance on full slanting.

Case buildings were selected to represent current or recent design techniques and methods, as well as to provide examples. Because the greatest current (fallout) shelter deficit is in the residential or outlying areas of cities and metropolitan regions, usual buildings planned for such locations were of particular interest. That such buildings are normally surrounded by open expanses was a strong inducement for selection, considering the lessened fire spread hazard in open areas.

Chapters 2 through 6 provide data and methodology needed by the design professional for full slanting design. Chapters 7 and 8 constitute applications of the data and methodology to certain buildings

---

* For example, pedal-driven lighting kits have been developed.

† The acceptable dose is based on 100 rads with a "safety" factor of 2 to cover the calculation technique shortcomings.

selected for use in case studies. [Chapters 9 and 10 will attempt to draw together lessons learned from the case studies.]*

Preliminary Building Selection for Slanting

The following criteria may be used for the preliminary screening of buildings for their full slanting potential:

- Design must include a basement or be amenable to redesign involving relocation of appropriate functions into a basement.

- Basement must be wholly below grade; or the design must be amenable to either berming or redesign lowering of basement level to meet this criterion.

- Building must be designed with noncombustible exterior walls and Class A or B roof and must otherwise meet the requirements for "Ordinary Construction" (Table B-3), as a minimum basis for further consideration (Appendix B).

- Separation distances from adjacent buildings must be adequate nearly to eliminate the risk of firespread to the shelter building (Chapter 3). However, when one - or two, if opposing - shelter building exterior walls have a 3-hour fire rating and separate the building from an adjacent building(s), an exception may be considered.

- Use of part of a basement as a shelter generally should not be planned, because the cost of full slanting is most likely to exceed the limitation stated in the Scope.

Acknowledgments

Through suggestions, guidance, or supporting work, the technical help of many persons was freely given and is gratefully acknowledged: N. E. Landdeck, G. N. Sisson, and N. A. Meador, U.S. Office of Civil Defense; Professors W. J. Hall and M. A. Sozen, University of Illinois; and, at Stanford Research Institute, J. F. Halsey, J. R. Kwapil, G. G. Hoskins, and especially each author of an appendix hereto: C. K. Wiehle, J. R. Rempel, R. G. Carroll, F. C. Allen and J. H. Iverson.

---

* Brackets around text material herein are used to indicate uncompleted or planned (further) work.

Chapter 2

NUCLEAR WEAPONS EFFECTS

The nuclear weapons effect adopted as the independent variable was free-field air blast peak overpressure,* with 15 psi as the design value against which protection was to be provided. [The slanted designs will also be evaluated against higher and lower free-field peak overpressures, but such work is principally for probability purposes useful to gaming studies.] A specific weapon yield of 1 Mt was stipulated to allow calculation of details on air blast pressures and of comparable radiation effects. [The latter will be reviewed during later work for the consequences of assuming a yield of 200 kt.]

Figures 2-1 through 2-8 are based on zero height-of-burst (HOB), as well as on HOBs optimized to obtain maximum ground range for each value of air blast peak overpressure. The figures were prepared using Reference 1 as the basic source for effects data, because of its general excellence, ready availability, and authority recognition, and because it has been used for many years as a primary reference in OCD courses for architects and professional engineers. However, effects data from other sources may also be shown if significantly different from the Reference 1 data and if considered authoritative. Figure 2-1 provides data on overpressure positive phase duration at ground level; the Brode curves[29] are recommended† for use and are independent of HOB. Other needed data on air blast pressures‡ are in Sections 3.47-3.54, Reference 1, and in Chapter 3, Reference 2.

---

* Overpressure, rather than range, was considered to be the best basic parameter; overpressure strongly affects both structures and people, in contrast to nuclear radiation, which affects only people. Thermal radiation may affect either or both, in widely varying degrees and probably with little correlation with range, at least within ranges of concern. Overpressure-range-yield relationships seem to be well established, whereas radiation-range-yield relationships show substantial differences among authoritative sources.

† Based primarily on acceptance and use of Brode data by leading professionals in protective design[31] and secondarily on a desire to move toward offsetting some conservatism that is built into the design approach, in the author's judgment.

‡ Other air blast parameters stipulated for use herein are zero rise-time and all (shelter) locations in Mach region.

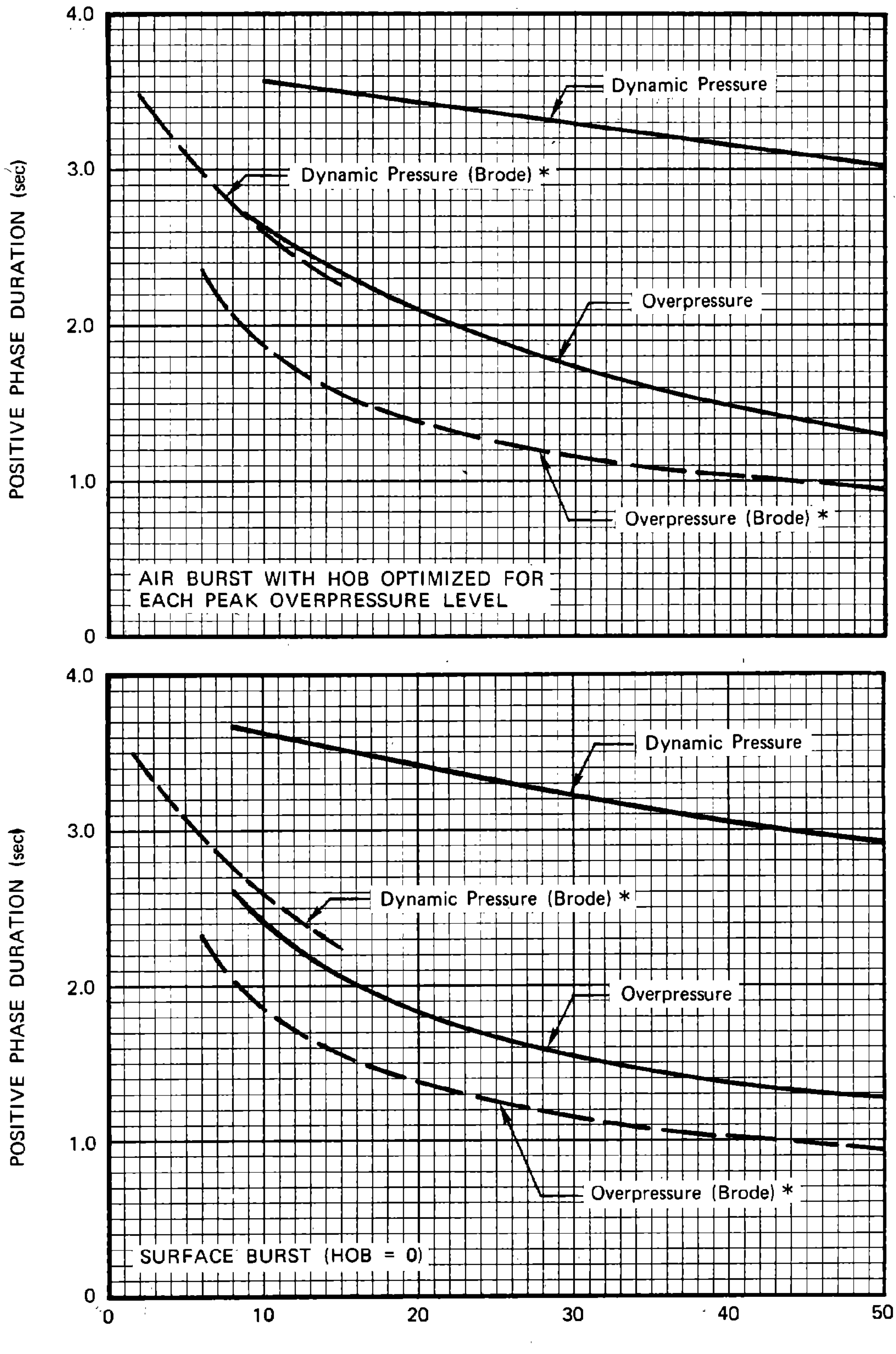

* Recommended for use; see text.

FIG. 2-1 POSITIVE PHASE DURATION VERSUS PEAK OVERPRESSURE (1 Mt)

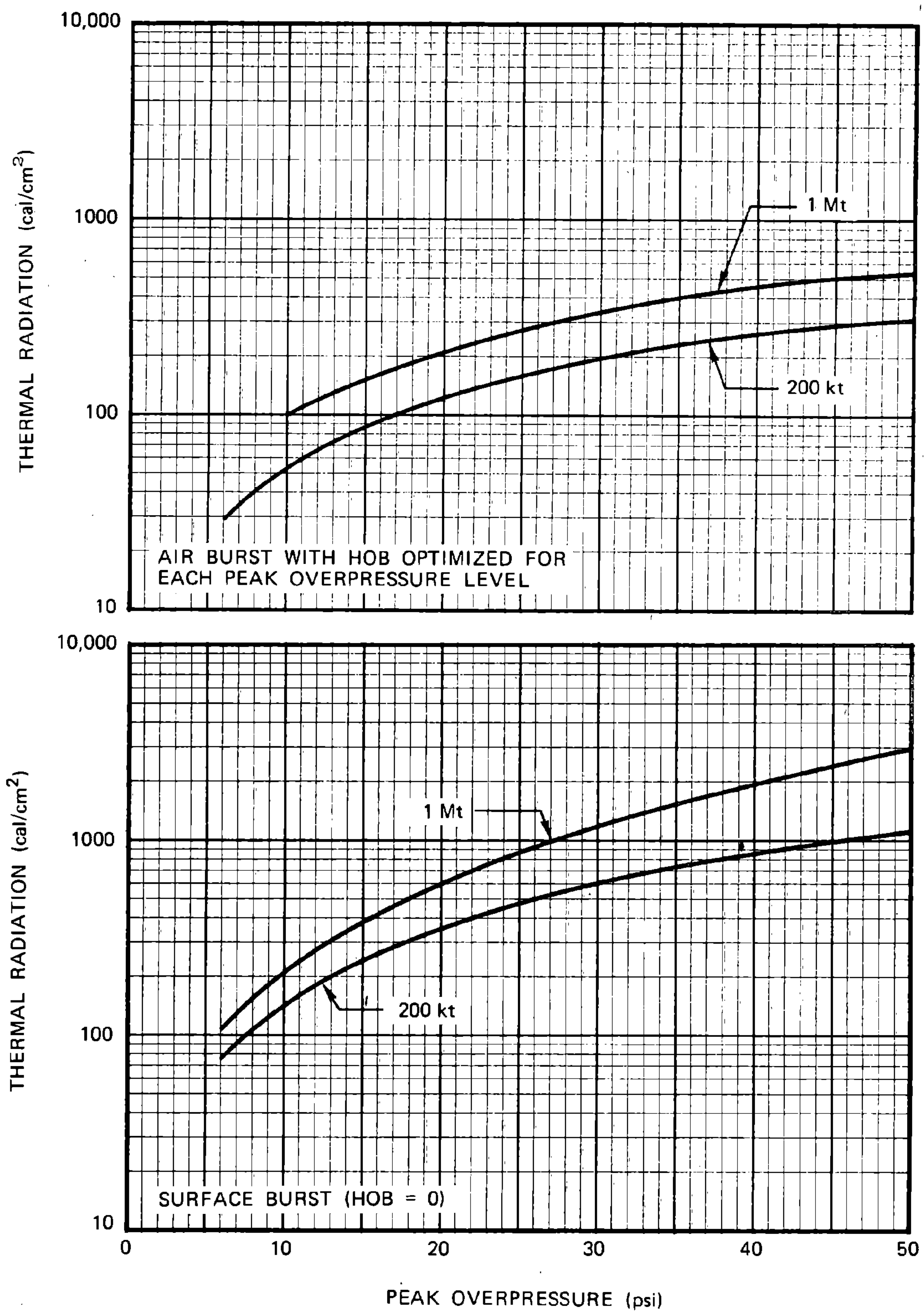

FIG. 2-2 THERMAL RADIATION VERSUS PEAK OVERPRESSURE

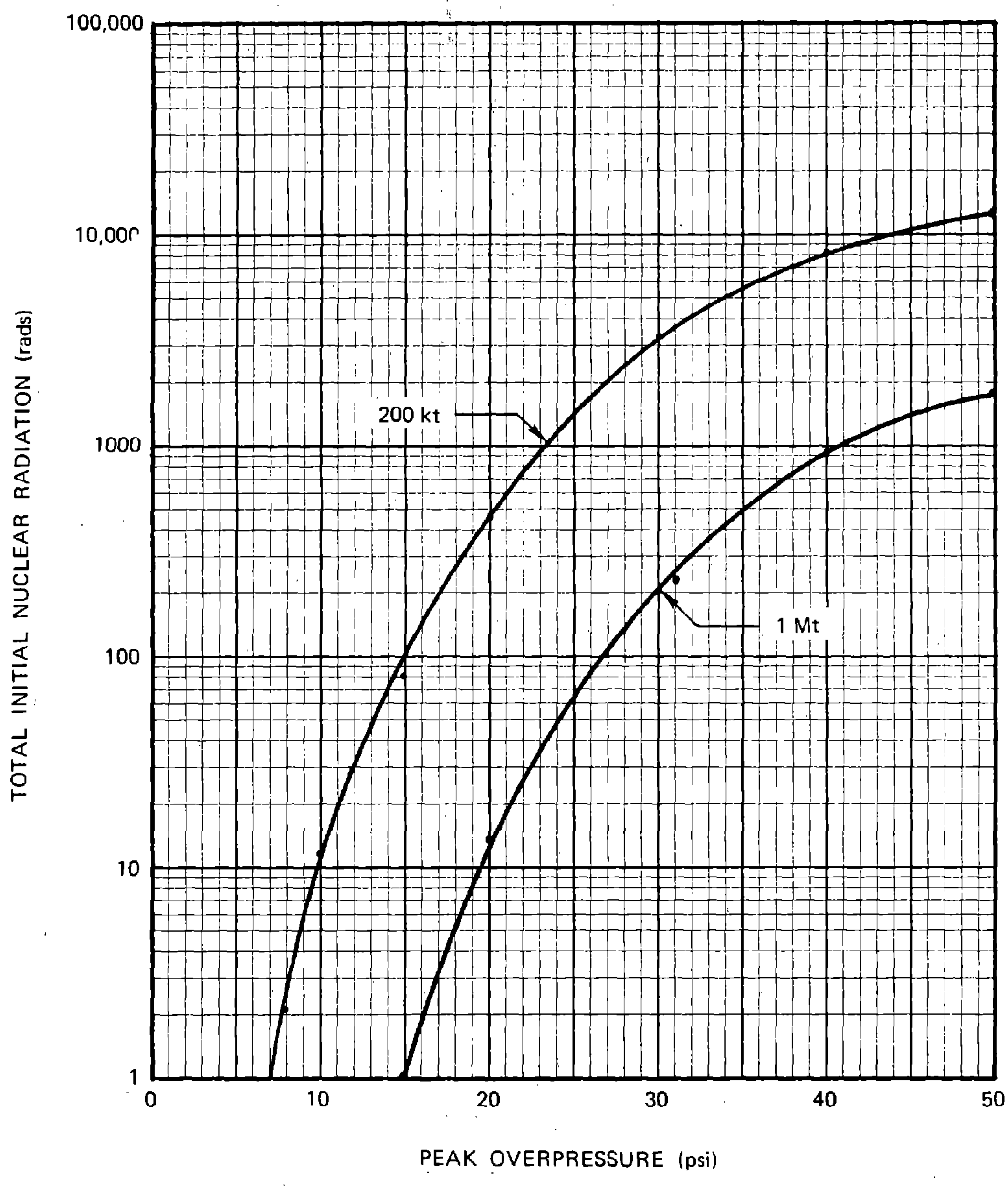

FIG. 2-3 TOTAL INITIAL NUCLEAR RADIATION (GAMMA PLUS NEUTRON) VERSUS PEAK OVERPRESSURE
(Air burst with HOB optimized for each peak overpressure)

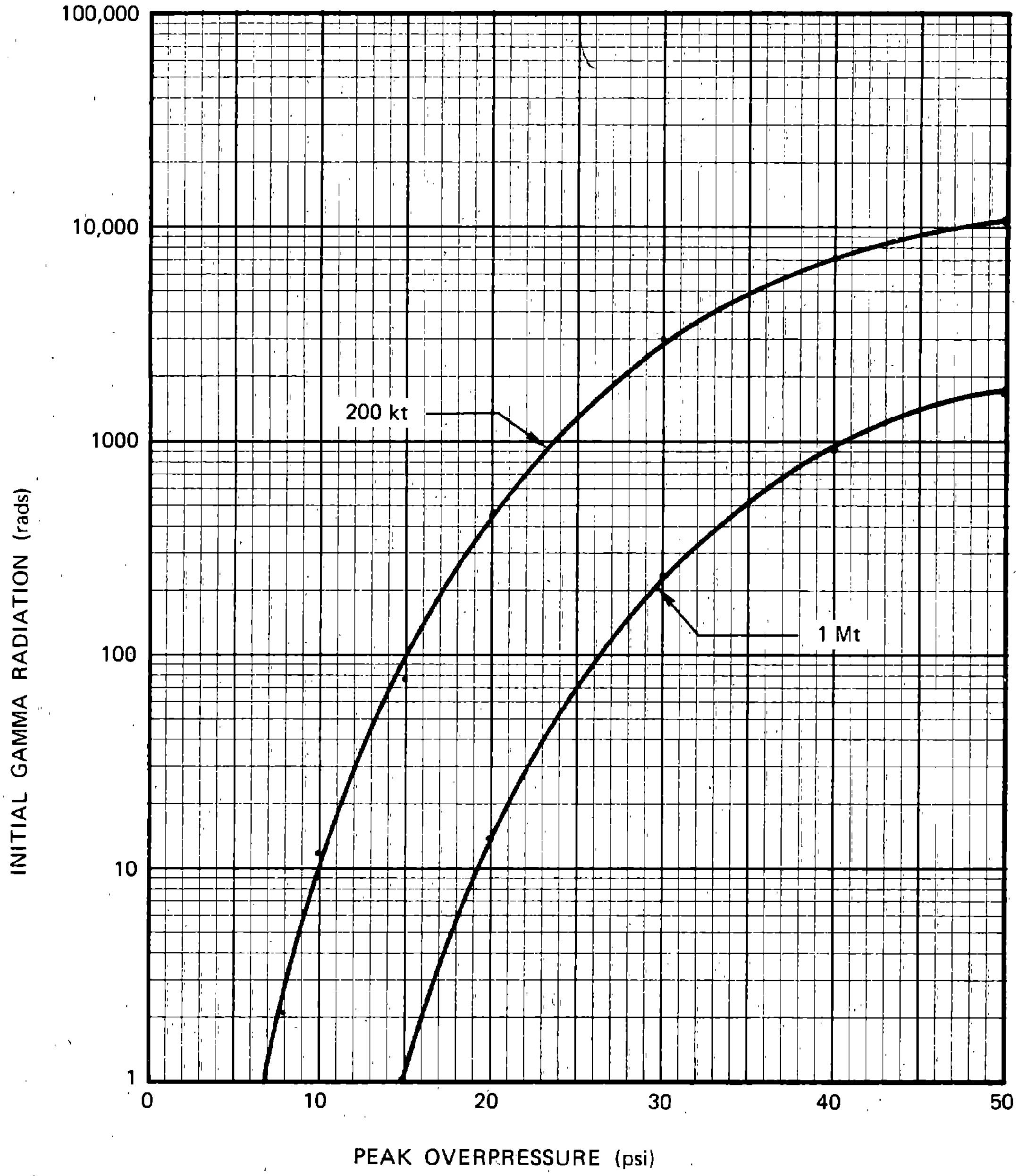

FIG. 2-4 INITIAL GAMMA RADIATION VERSUS PEAK OVERPRESSURE (Air burst with HOB optimized for each peak overpressure)

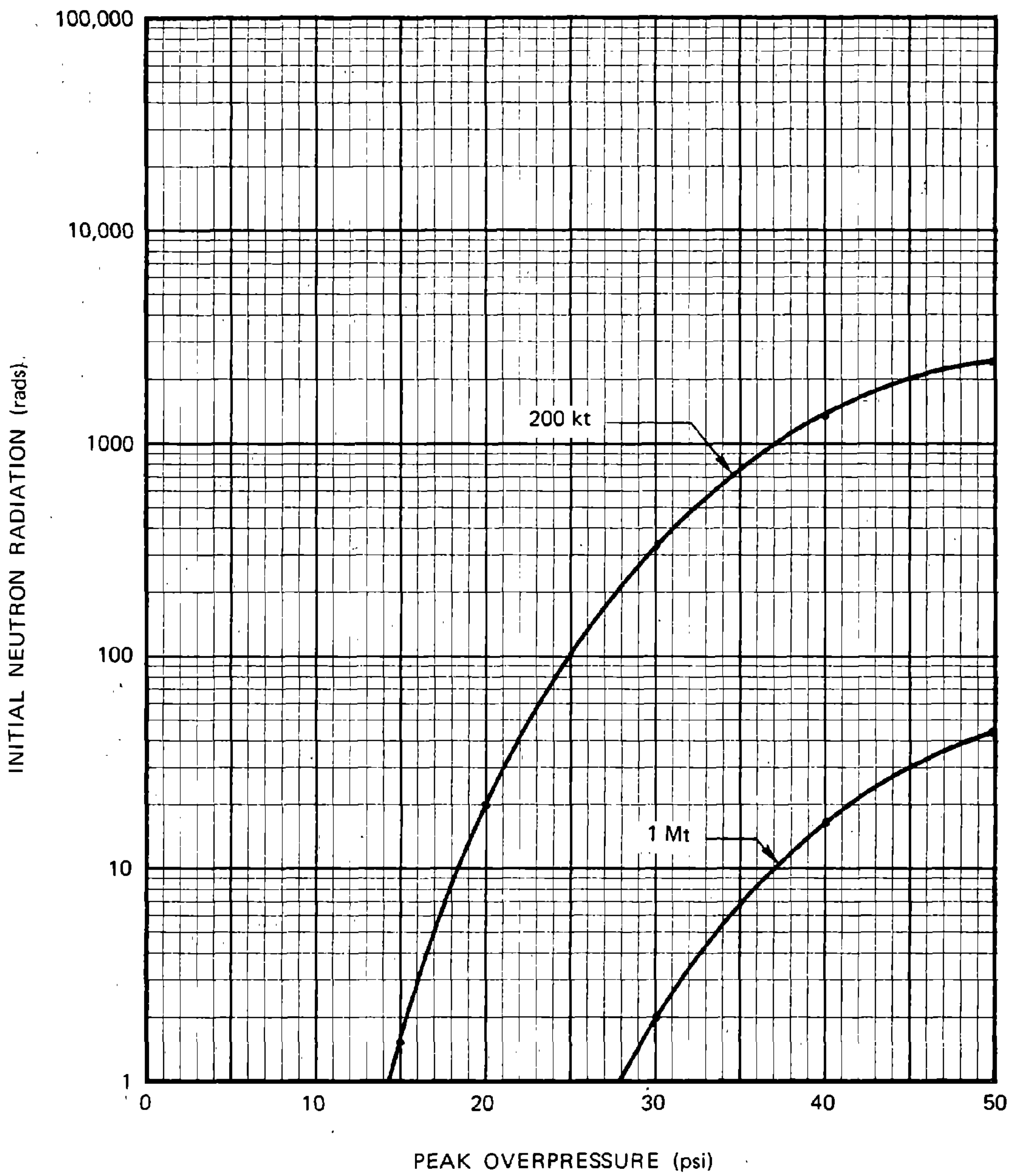

FIG. 2-5 INITIAL NEUTRON RADIATION VERSUS PEAK OVERPRESSURE
(Air burst with HOB optimized for each peak overpressure)

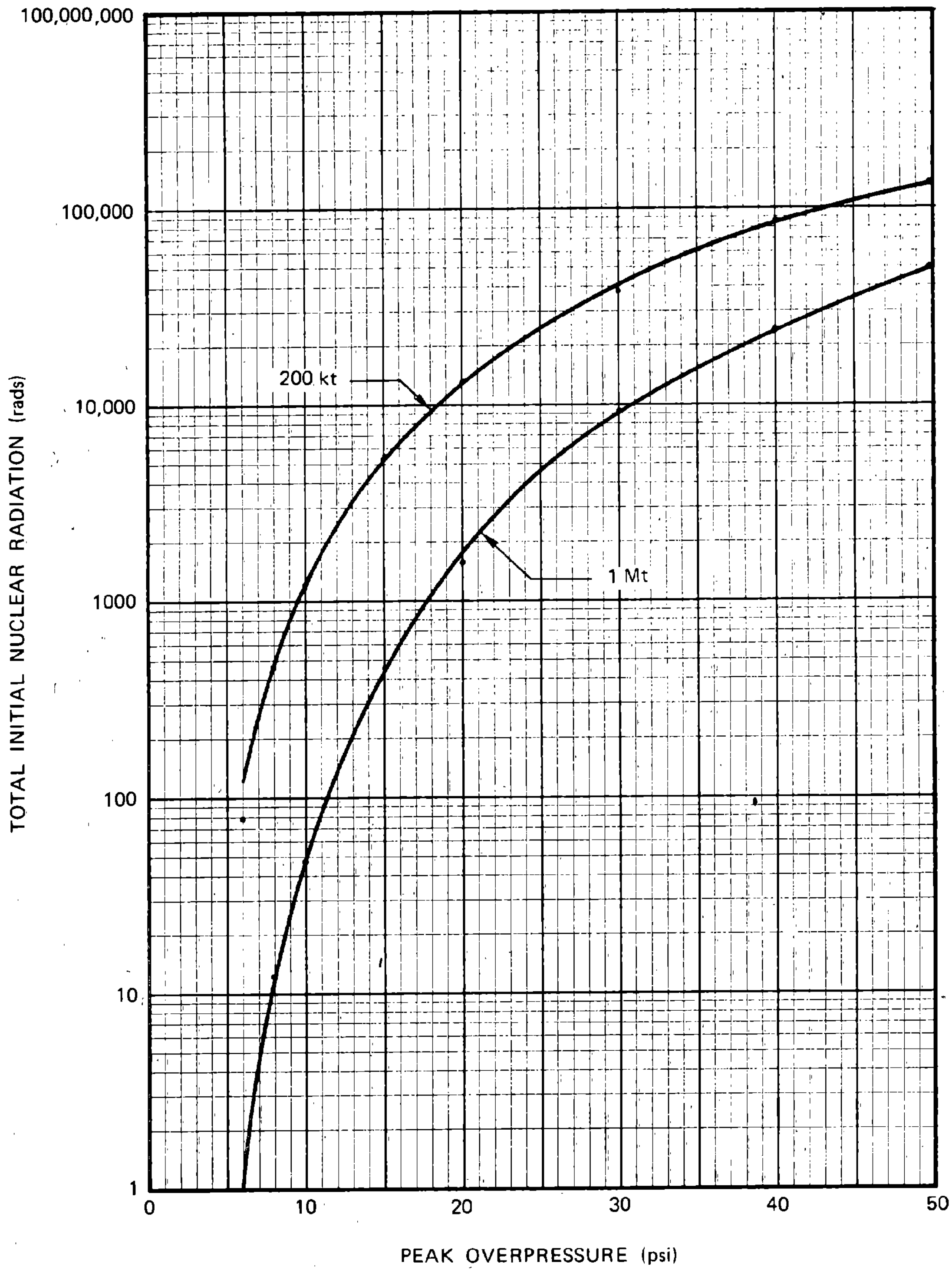

FIG. 2-6 TOTAL INITIAL NUCLEAR RADIATION (GAMMA PLUS NEUTRON) VERSUS PEAK OVERPRESSURE
(Surface burst, HOB = 0)

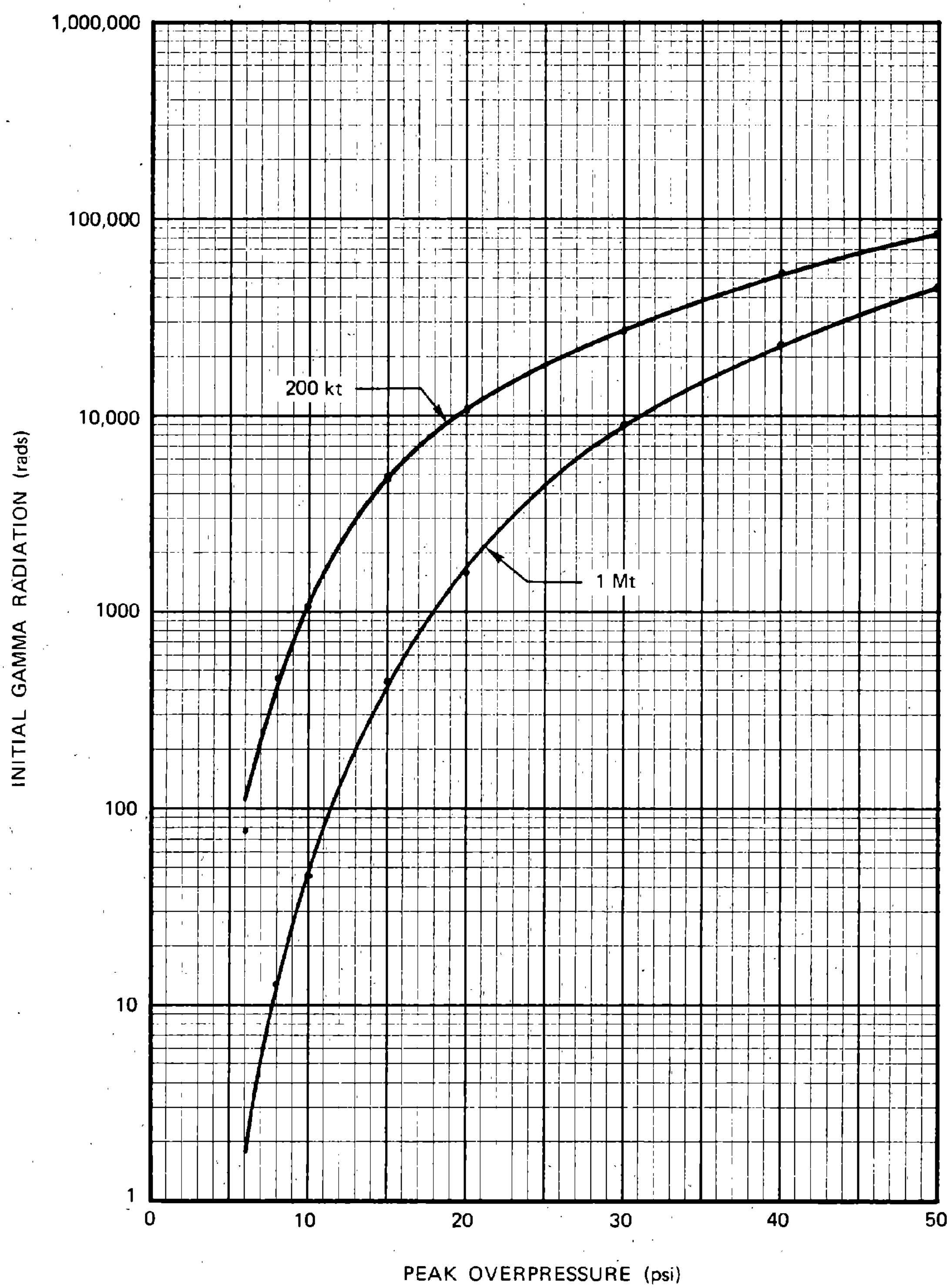

FIG. 2-7 INITIAL GAMMA RADIATION VERSUS PEAK OVERPRESSURE
(Surface burst, HOB = 0)

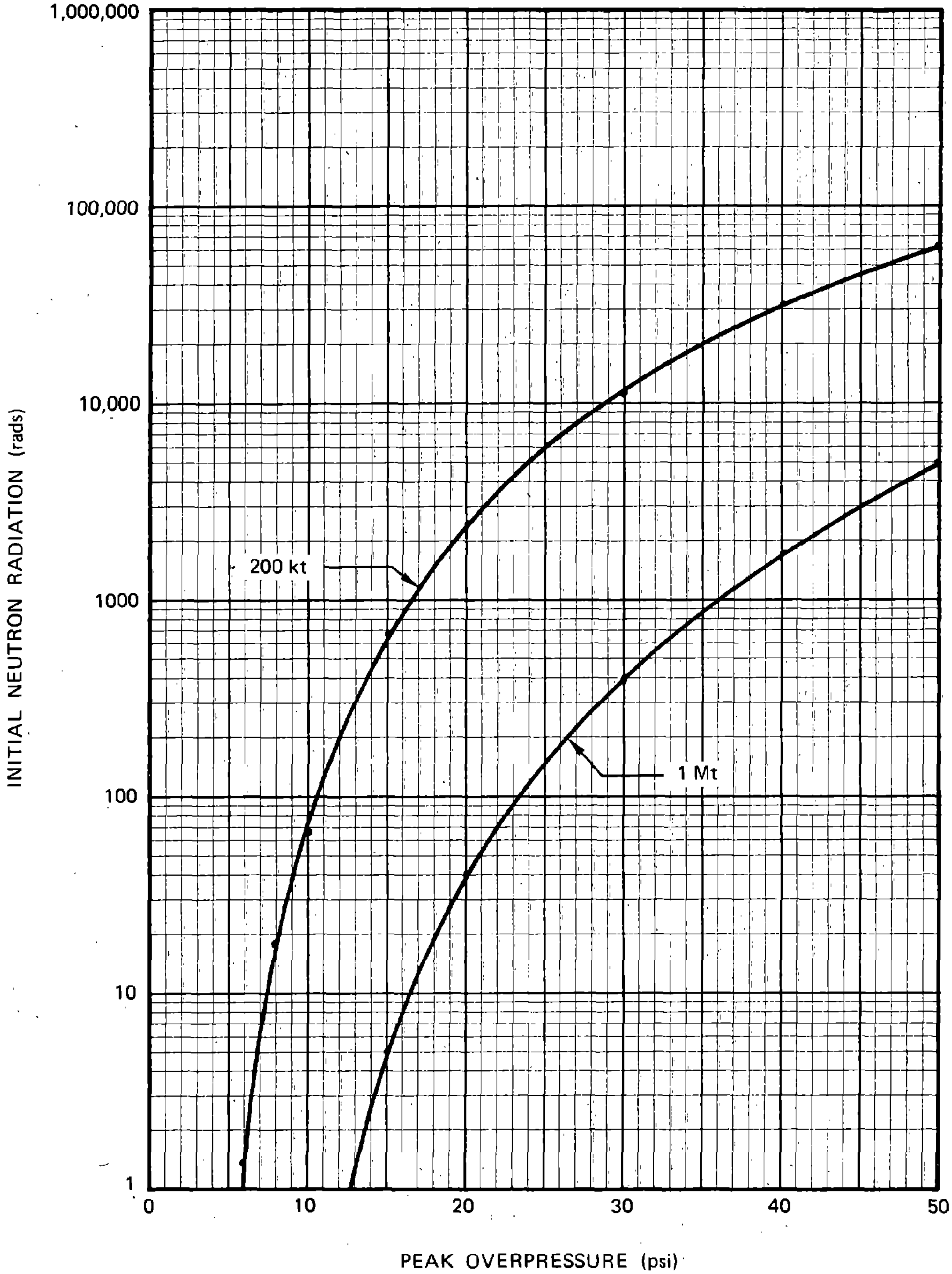

FIG. 2-8 INITIAL NEUTRON RADIATION VERSUS PEAK OVERPRESSURE
(Surface burst, HOB = 0)

Free-field thermal radiation effects (cal/sq cm) versus overpressure (psi) are shown in Figure 2-2 for weapon yields of 1 Mt and 200 kt.

Using similar bases of yield and HOB, Figures 2-3 and 2-6 show combined initial gamma and neutron radiation (rads), and Figures 2-4/2-7 and 2-5/2-8 show separate curves for initial gamma and neutron radiation, respectively.*

Calculation methods and data sources for Figures 2-1 through 2-8 are discussed in Appendix A.

---

* Under guidance provided by the Subcommittee on Radiation Shielding, National Academy of Sciences, and the sponsorship of the U.S. Office of Civil Defense, research on initial nuclear radiation effects is under way in both government and private agencies. At the time of writing this report, key persons in this research effort were reluctant to provide recommended values with which to update Figures 2-3 through 2-8. They advise, however, that values coming out of the work clearly show that the Reference 1 values used for the figures herein may be too low, particularly in the lower nuclear weapon yields (say below 300 kt).

Chapter 3

FIRE HAZARD REDUCTION

The seriousness of the primary and the secondary fire threat from a nuclear attack* is difficult to assess and, therefore, to relate to specific countermeasures, both design and operational. Authoritative sources vary widely both in assessing the threat posed and in prescribing the remedial steps required. It appears that experiences in World War II fire bombing of Hamburg, Germany, and nuclear bombing of Japan can be cited both to support the need for extensive countermeasures and yet to point to human survival where death seemingly should have been certain.

The building design professional taking the lead design role (architect or engineer) will have the same problem in evaluating the fire threat and determining the level of countermeasures that he will have with ventilation, structural, and other such technical areas - any one technical area may easily receive undue emphasis and result in related unwarranted construction costs unless the lead professional exercises a strong leveling influence on all areas.

The fire hazard to full slanted basement shelters is likely to be more severe at overpressures that leave the building upper stories standing, than it would be at overpressures that collapse the building upper stories. Thus the lead professional must suppress too expensive, fire countermeasures, perhaps by considering that evacuation may be necessary when all other fire measures fail, despite the fallout radiation hazard that may exist. However, this should not be seized upon as advocating evacuation as a usual remedy, as it is in normal design against fire hazards. It is <u>not</u> a remedy in the nuclear attack environment at all, but it might be a last ditch survival measure when all else fails.

The purpose of this chapter is, therefore, to provide the lead professional with some background and specific techniques for incorporating reasonable fire countermeasures in the full slanted design. However, he may expect that even reasonable measures will draw criticism of both "too little" and "too much" from various detractors. The material presented here and in Appendix B has been selected to meet only the needs of the design professionals in slanting, not to be a comprehensive or even complete discussion of fire problems in buildings. The material is presented under six headings in an attempt to make it assimilable, but there is considerable interaction among these subareas that must be recognized

---

* Single 1 Mt weapon air or surface burst is assumed (Chapter 1).

by the user. *No building should be eliminated from consideration as a basement shelter location unless the total fire hazard is actually insurmountable; the lead design professional and his staff should treat Chapter 3 and Appendix B as guidance, not definitive as in a building code, and apply considerable professional judgement in using the guidance.*

Introduction

An overview of the fire hazard reduction problem in shelters is presented in Appendix B, Section 1. It includes introductory comments on such things as fire sources; primary and secondary fires; thermal radiation effects from a nuclear detonation and their attenuation by various factors; blast/fire interactions; firespread by wind including firebrands; firestorms; and, radiant firespread and building density. Reading of the overview is urged as a desirable prerequisite to further study of this chapter or Appendix B.

Siting or Building Separation

The primary measure against spread of fire from another building to the building containing the shelter is provision of a clear area around the latter. Appendix B (Section 2 and Annex A) includes several methods for developing the desired separation distance(s) around the shelter building. The shelter building is assumed to have fire-resistant exterior wall construction, a mandatory item in the full slanted building.

A cautionary note: an estimated separation distance should be one highly desirable criterion, but only that, and should certainly not serve to exclude from full slanting an otherwise desirable candidate building. The estimated separation distance may indicate such design modifications as changes in size and location of windows and other openings, or reduction in total area of openings, perhaps to use of a blank wall (note that a 3-hour firewall separating the interior spaces of adjacent buildings reduces the separation distance to zero*). However, even though the separation distance criterion is not met, its estimation will serve to stress the importance of other fire countermeasures.

Other measures to reduce firespread are discussed below.

---

* Appendix B, Table B-3.

Interior Fires and Associated Biological Hazards

These subjects are discussed in Appendix B, Section 3, as background for the designer.

Incipient interior fires on the shelter floor level (inside or outside the shelter) or below must be suppressed (evacuation may be only a last ditch alternative because of the possibility of fallout radiation), and such suppression must be by the shelter occupants using special means, because organized firefighting forces and an adequate water supply will most probably be unavailable. Incipient interior fires on the floor above the shelter should be suppressed if possible, to reduce even the slow heat transmission to the shelter if allowed to burn, and to reduce the risk of smoke and noxious gas travel downward into the basement (even though recent tests, described herein, show that such a risk is negligible).

The most pertinent or primary biological fire hazard factors affecting shelterees are heat, oxygen depletion, carbon dioxide and monoxide build-up, and smoke. Three noxious gases (HCN, SO_2 and NO_2) present in fires have secondary significance in that synergism is strong when any one or more is combined with one of the primary hazard factors. Tests have reasonably demonstrated that these primary and secondary hazard factors apply only to the floor where they are generated and higher floors, except in the unlikely situation of wind pressures driving the gases downward into lower floors. Ventilating air drawn into a basement shelter over or through burning debris is, of course, extremely noxious.

Design Countermeasures

Design countermeasures are discussed in Appendix B, Section 4.

A few key admonitions from that section that are of direct rather than background concern to the designer are:

- Protect against the weapon's thermal pulse by providing aluminized blinds or reflective drapes of noncombustible composition at all exterior wall and roof openings. Painted metal venetian blinds in closed position and having noncombustible tapes will suffice even though the paint will char. As a minimum, such shielding should be provided for the shelter floor(s) and the next floor above.

- Provide 5-gallon (19 liters) stirrup-pump fire extinguishers, with hoses at least 6 ft (1.8 m) long, at one per each 1,250 sf (116 m^2) in shelter (4 minimum) and one per each 5,000 sf (465 m^2) of non-shelter area.

- Use structural components having as a minimum the fire resistance ratings specified in the National Building Code (NBC) under "Ordinary Construction" (Table B-3, Appendix B), except that building separation distances should be calculated by the Law Method, Appendix B.

- Consider providing positive protection against smoke and toxic gases infiltration into the shelter by a ventilation system with an interior positive pressure of uncontaminated air - as low as 0.03 in. (0.76 mm) of water has worked, but 0.25 to 0.5 in. (6.4 to 12.7 mm) may be necessary to turn back wind-driven fumes. Recent tests, however, showed no infiltration in a simple closed-up shelter (Appendix B, Section 3).

- Provide emergency exits compatible with other aspects of the building design, i.e., a high fire load on upper floors (particularly the first) could suggest tunnel exits to get beyond a likely debris and fire perimeter, whereas a low fire load could indicate windowwell and other close-in exits, providing that they are located on three, or preferably four, sides of the building to ensure at least one exit on a debris-free (blastward) side of the building. The more distant exit(s) can probably be fewer in number even if more expensive, and can serve as fresh air intakes likely to be beyond burning debris and the attendant hazard of intaking smoke and fire gases. Emergency exits are discussed in the opening pages of Chapter 8, and in later pages in connection with the various slanting case studies.

- Reduce the combustible fire load on upper floors, especially the one over the basement shelter. For the latter, no more than 15 psf (0.7 cb*) average fire load is urged. Reduced fire loads can be achieved in various ways such as:

  - Assign a use function to the floor over the shelter that carries a low fire load (e.g., open public areas such as reception and waiting rooms);

  - Use noncombustible furniture and furnishings as much as possible;

---

* 1 cb (centibar) = 0.01 bar = 10^3 N/m^2 = 1 kN/m^2 = 1000 Pa = 0.010198 kg/cm^2 = 0.145038 psi; or 1 psi = 6.894757 cb = 0.0703067 kg/cm^2 (Ref. 45).

- Consider available fire retardant treatments of certain combustibles (Appendix B, Section 5);

- Facilitate the emergency strategic removal of combustibles by liberal use of casters on equipment and by doorway and ramp layouts oriented to that purpose.

The case studies or examples of full slanting of building basements, Chapter 8, should be reviewed for the design countermeasures indicated there, e.g., the window-wells and tunnels used for fresh air intakes/ emergency exits, as mentioned above.

Shelter Occupant Countermeasures

These countermeasures are discussed in Appendix B, Section 5. There are many self-help measures that can be done by the shelterees, if proper guidance, training,* and minimal supplies have been provided.†

Most or all of the countermeasures might be considered operational rather than shelter design matters. However, the lead design professional, architect or engineer, must have a good understanding of the fire countermeasures potentially usable by shelterees so that full slanting design may take the countermeasures into account. This is in direct contrast to the usual building design approach, wherein the only fire fighting expected of building occupants is immediate building evacuation and a call to the fire department. The fire department will most likely be unavailable in a nuclear attack situation, and fallout hazards may make evacuation only a last ditch measure.

Some of the shelter occupant countermeasures calling for design consideration are mentioned in the Design Countermeasures section just above; another not mentioned there and worth considering is that of making appropriate provision in the design for shelter occupant selective flooding (controlled from a remote location) of the floor slab over the shelter (Appendix B, Section 5).

---

* Of at least the shelter manager.

† Parking garage fire potential and countermeasures are discussed in connection with Building 4A in Chapter 8.

Miscellaneous

The material in this section, in contrast to that in the preceding sections, is not covered in Appendix B.

The matter of use of plastics in building construction, including their involvement in fires, is a current subject of much controversy among experts from all professions concerned. Strictly for the purposes of design of full slanted shelters, designers should check on two points prior to design and regardless of their views on the controversy: will any contemplated use of plastics adversely affect the insurability of structure or contents; and, will building code enforcement authorities approve of the contemplated use of plastics in their review of the plans and specifications. Insurance carriers have been urged to exercise extreme caution when insuring buildings whose construction used large quantities of plastic products.[46] A plastic panel manufacturer, plus the building owner and architect for the building where the panels were used, were recent defendants in a civil suit over lives lost in a fire; the jury awarded very large damages.[47]

A recent article[48] includes reference to some standard specifications of potential use to the building design professional: Federal Specification CCC-T-191, Method 5903, requires upholstery materials to be self-extinguishing; ASTM D635 does the same for self-supporting plastic materials; ASTM E84 covers pressure treatment of wood with fire retardants; and, U.S. Department of Commerce Standard FF-1-70 concerns carpeting, backing and underlayments.

A recent unpublished letter report[49] covers a study of fire protection problems in underground buildings or other structures. Among the points made in the report was one that many lives had been lost in fires in such structures because of inability to find an exit where natural light is lacking and both normal and emergency lighting are inoperative; smoke frequently compounds the problem. The writer's recommendation was that use be made of the small, battery-operated lanterns frequently seen on high shelves in building hallways (e.g., hospitals, fire and police stations, office buildings); their batteries are kept at full charge by connection to normal electrical sources. These lanterns supplement, not replace, emergency lighting and generators. Their use is recommended for full slanted shelters.

While this report was in press, information was received that a new exit (sign) light (costing about $35) had been approved for use by the International Conference of Building Officials (publishers of the Uniform

Building Code). It is understood that its light comes from a radioactive source, thus obviating the need for electric power or batteries, and that the manufacturer is Canrad Precision Industries, 100 Chesnut Street, Newark, New Jersey, 07105. No further information had been obtained at press time and no descriptive literature had been reviewed.

Chapter 4

THERMAL AND INITIAL NUCLEAR RADIATION RESISTANCE ANALYSIS

Both thermal and initial nuclear radiation effects are discussed in Chapter 2. Figures 2-2 through 2-8 show these effects versus air blast peak overpressure. Chapter 1 includes the Scope and Stiplations applicable to thermal and initial nuclear radiation effects.

Thermal Radiation

No primary thermal radiation hazard* is foreseen for basement shelter occupants protected from 15 psi air blast peak overpressure and related other weapons effects - nor is any foreseen at much higher (twice or so) overpressures and related effects - if simple measures are taken in design to prevent line-of-sight entry of the thermal pulse into the shelter and if fire resistive construction is used.

Secondary fire hazards are treated in Chapter 3.

Initial Nuclear Radiation

No initial nuclear radiation hazard to shelter occupants is foreseen, under the circumstances and for reasons similar to those stated in the preceding paragraph. However, the shelter entranceway, particularly if open or effectively so, must be checked for shielding adequacy. Appendix C was originally prepared for such a purpose[9] and is included herein as published.

---

* Thermal pulse may or may not start primary fires in easily ignited materials, depending on its peak value (cal/cm^2) and shortness of delivery time (sec); e.g., a high value of cal/cm^2 may be delivered in a nonharmful sunbath, but over a lengthy delivery time.

Chapter 5

FALLOUT RADIATION RESISTANCE ANALYSIS

The Scope and Stipulations in Chapter 1 include a shelter requirement to provide a fallout radiation PF of 100 or more, this requirement to be treated independently of the initial nuclear radiation criterion.

Table 5.1 indicates a range of situations, in each case showing the shield mass thickness needed over the basement for PF 100. Thus, a 9.5-inch slab thickness of normal-density reinforced concrete (150 pcf) will be adequate for most situations where the worst case for fallout is assumed (all of the aboveground structure blown clear of the basement by air blast).

Other assumptions may be examined, as needed, by any OCD-certified Fallout Shelter Analyst.[10,11] Such an analyst may also check the shielding adequacy of the shelter entranceway. A technique for the latter analysis is provided by Appendix D, included herein as originally published.[12]

Table 5.1 was prepared using the data and results shown in Table 5.2; no more accuracy is implied in the latter than is inherent in the analysis technique.[10] Calculations for part of Table 5.2 were made using a computer program for roof contributions written by the author for time-sharing use; an equation developed by Suarez[13] was used in the program.

In addition to the shelter shielding, fallout protection requires controlling the ingress of fallout contaminant, whether through the shelter ventilation system or by tracking-in. Means include installation of standard air-conditioning filters, washing-down or simply sweeping-down, and installation of grating traps in entranceway landings.

It should be assumed that the " . . . area within the blast damage circle* may be expected to be heavily contaminated by induced activity, stem fallout, and throwout, regardless of the wind speed."[1]

---

* 7 psi in the quoted portion of ENW[1], so certainly to be considered within the Scope of this guide.

Table 5.1

REQUIRED CONCRETE ROOF SLAB THICKNESS
FOR PF 100 IN BASEMENT SHELTER*

		Roof Slab Thickness (in.)					
	Room area:	250 sf		1000 sf		10,000 sf	
	Story ht.(H):	8 ft	10 ft	8 ft	10 ft	8 ft	10 ft
One Room:	W/L = 1	9"	8.5"	9.5"	9.5"	9.5"	9.5"
	W/L = 0.25	8.5	8	9.5	9	9.5	9.5
Center Room of three rooms of equal size (6" th. common walls)							
	W/L = 1	Same thicknesses as those for one room.					
	W/L = 0.25						

---

* Roof slab at grade, reinforced concrete at 150 pcf, and thicknesses to half-inch to achieve PF 100 minimum.

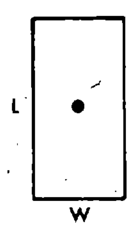

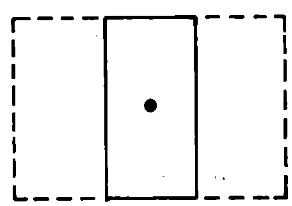

Table 5.2

FALLOUT SHELTER ANALYSIS DATA AND RESULTS
USED IN PREPARING TABLE 5.1

W	L	Z	ØMEGA	REQUIRED PSF SINGLE RØØM	REQUIRED PSF CENTER RØØM
15.8	15.8	5	.5062	110	
15.8	15.8	7	.3785	103	
7.9	31.6	5	.4025	104	
7.9	31.6	7	.2967	95	
31.6	31.6	5	.7263	116	
31.6	31.6	7	.6301	114	
15.8	63.3	5	.6286	114	
15.8	63.3	7	.5217	111	
100.0	100.0	5	.9103	119	
100.0	100.0	7	.8750	119	
50.0	200.0	5	.8704	119	
50.0	200.0	7	.8207	118	
15.8	15.8	5	.5062		
15.8	15.8	5	.5062		
15.8	47.4	5	.6197		110
15.8	15.8	7	.3785		
15.8	15.8	7	.3785		
15.8	47.4	7	.5097		104
7.9	31.6	5	.4025		
7.9	31.6	5	.4025		
23.7	31.6	5	.6828		106
7.9	31.6	7	.2967		
7.9	31.6	7	.2967		
23.7	31.6	7	.5769		97
31.6	31.6	5	.7263		
31.6	31.6	5	.7263		
31.6	94.8	5	.7941		116
31.6	31.6	7	.6301		
31.6	31.6	7	.6301		
31.6	94.8	7	.7195		114
15.8	63.3	5	.6286		
15.8	63.3	5	.6286		
47.4	63.3	5	.8347		115
15.8	63.3	7	.5217		
15.8	63.3	7	.5217		
47.4	63.3	7	.7718		112
100.0	100.0	5	.9103		
100.0	100.0	5	.9103		
100.0	300.0	5	.9331		119
100.0	100.0	7	.8750		
100.0	100.0	7	.8750		
100.0	300.0	7	.9066		119
50.0	200.0	5	.8704		
50.0	200.0	5	.8704		
150.0	200.0	5	.9470		119
50.0	200.0	7	.8207		
50.0	200.0	7	.8207		
150.0	200.0	7	.9259		118

Chapter 6

BLAST-RESISTANT DESIGN/ANALYSIS AND COST ESTIMATING

Introduction

This chapter includes a discussion of full slanting in a planned building for all aspects other than radiation (covered in the preceding two chapters[50]*), i.e., structural, architectural, mechanical (ventilation), and electrical (within the Scope limits). Most of the discussion deals with structural aspects, however, because it is in this technical area that air blast resistance requires the greatest changes in conventionally designed buildings, at least in construction costs.

A difficult problem inevitably arises in protective design wherein architects and engineers of various disciplines must each contribute from their professional field toward the total design of a facility. The problem is that each design professional has a strong tendency to emphasize his own field by designing something a little or a lot better than is required for bare survival, thereby leaving stringent economy to the other design fields. No pat solution to this problem is offered, but an overall bare survival design can at least be hoped for if the lead professional has at least fair technical competence in all applicable fields, or at least in structural and mechanical engineering design, plus building layout and circulation patterns, for it is in such design areas that the significant cost increases for full slanting are found.

It cannot be too strongly emphasized that full slanting has a far greater possibility, both economically and physically, for application to a building designed from the very first conceptual discussion and sketches by a design professional knowledgeable in the techniques of protective structure design and construction. For example, in the earliest conceptual thinking about space allocations versus floor level, the choice of items to be placed in basement space can tremendously affect the full slanting costs. Nonetheless the case studies made for this guide[61] were based on building designs prepared without regard to their slanting potential and, so far as is known, by design professionals unskilled in protective design. (The purpose of the reported work was to reveal conceptual information and methodology; no claim is made that the examples chosen were the best examples.)

---

* Superscript numerals are related to the list of References at the end of the report main text body. Numerical sequence in use was not maintained in revised portions of the report.

Perhaps the single most important point to be made concerning design for blast resistance - a point that most often arises as a touchy one between a designer and a weapons analyst (or operations analyst or target analyst) - is to distinguish between a design overpressure and a weapons analyst overpressure. That there are, in fact, two such very distinct overpressures for each structure is a matter all too often overlooked by competent professionals working in both fields. It would be difficult to state better a clarifying explanation than has been done by the writers* in the following unclassified extract from a classified report (which, therefore, must be excluded from the References list):

Probability Analyses

Weapon Selection vs Protective Design. In general, all of the parameters governing the response of a structure, including the loading and the structural parameters, are subject to variation and uncertainty. In making a design of a structure to resist certain overpressures for a particular yield of weapon, the designer ordinarily makes assumptions on the conservative side in all or nearly all of the cases where he has a choice of parameter values. On the other hand, the weapons analyst who has the assignment of estimating the vulnerability of a structure can work with an overall variation which reflects the variation of the individual parameters. The designer wishes to be able to state, with a high degree of confidence, that his structure will withstand an overpressure (the "design" overpressure) specified to him. He will therefore choose parameter values sufficiently conservative to assign a high confidence value to his statement, say 90 percent or better. The weapon analyst is not bound to the selection of single values for these parameters, for he is not solely interested in being able to state the probability that a single specified overpressure will cause the desired damage, nor that a certain overpressure will cause damage with a high degree of confidence. Instead, he must answer the question, given a specified yield of weapon and height of burst, and considering the possible variations associated with the structural and weapon parameters, what is the probability that the specified damage will occur.

It can be seen, therefore, that the design overpressure is not ordinarily a good guide to the weapons analyst in selecting the overpressure which would be required to cause a structure or structural element to fail. It is because of this discrepancy between the points of view of the designer and the weapons analyst that the principle was adopted in this report that the charts would be given for the median

* Newmark, Hansen & Associates, Urbana, Illinois (AD-346 087; see footnote, p. 11-35).

case, in order that the weapon analyst can, by associating the appropriate variation with the median values, determine the probability of failure.

Probability Charts. The parameters governing the probability analysis . . . cover variations in the following quantities:

(1) Structures and materials

(2) Loading on the ground surface

(3) Loading on underground structures, including attenuation, arching, and horizontal pressures

(4) Attenuation of pressure in ducts or tunnels

(5) Shock effects on equipment

Slanting design should be, of course, solely oriented towards design overpressure, not weapons analyst (or targetting) overpressure, and this guide is so oriented.

Design calculations were carried out only to a reasonable accuracy consistent with possible variations in the inputs - materials behavior and weapons effects (particularly overpressure related to the assumed ideal wave).* The design goal was adequacy for the assumed loading conditions, e.g., 15 psi (103 cb†) air blast peak free-field overpressure, but with no factor of safety included to cover, for example, unwarranted or unexpected load increases, as is done in usual design. Any factor or factors of safety‡ should be incorporated only in the selected design overpressure

---

* Some trial designs were carried out only to a point sufficient to obtain a section suitable for preliminary cost estimating; reinforcing steel was selected only to check for sufficient space, otherwise steel percentage was sufficient for estimating; details around blast doors, anchorages and stirrup locations, etc., were not designed but were allowed for in the steel estimates.[61]

† 1 cb (centibar) = 0.01 bar = 10^3 N/m^2 = 1 kN/m^2 = 1000 Pa = 0.010198 kg/cm^2 = 0.145038 psi; or 1 psi = 6.894757 cb = 0.0703067 kg/cm^2 (Ref. 45).

‡ Ref. 2, page 7-3.

(basically 15 psi herein*), thereby ensuring a comparable factor of safety among structural elements of differing natural periods of vibration, as well as in all the other related weapons effects, because each of the latter is found in terms of the design overpressure by using the charts of Chapter 2.[50] Design for protection against each effect should then be based on barely meeting that effect, i.e., with no further factor of safety for protection against the effect; this approach should retain a reasonable protective balance among the various effects.

Selection of Design Overpressure

The distinction between a selected design overpressure for any full slanting shelter and a weapons analyst overpressure for the same shelter has been discussed in the opening section of this chapter. The selected design overpressure should be applied in such a manner as to give the building owner a high probability of survival, says 95-99%, at that overpressure.

The selection of a design overpressure for a specific case might be analogous to purchase of any kind of insurance coverage - what is the owner's risk or potential loss, and what amount of protection can he afford? Considering the potential life of the kinds of shelter structures considered herein, evaluation of the owner's risk or potential loss calls for defensive targeting, a nonexistent professional skill in the long-range instant case, and for placing dollar values on intangibles such as the value of the owner's life, also an impossible task. Nonetheless, some efforts can be made in the defensive targeting direction, at least to the extent of looking at the proposed building and shelter location with reference to the locations of population-industry centers and military targets, particularly those known to encompass a retaliatory capability; these are basic and only mildly technical matters that can be readily considered.

After selection of a design overpressure, related direct nuclear weapons effects can be found in the charts of Chapter 2,[50] all of which are entered with air blast peak overpressure. Resistance to such related effects has been discussed in Chapters 3-5;[50] blast-resistant structural design is the subject of this chapter and, to a considerable extent, of Chapters 8 and 10.[50,61]

---

* Extended to 5, 10, 20, and 30 psi for some matters.

Notation

The notation used herein follows that generally used in each particular technical field, insofar as possible. In general, the most commonly used reinforced concrete notation[14] and a typical nuclear weapons phenomena notation[15] were adopted as a base. Additions were both originated and made from various sources, particularly one of the companion volumes to this guide.[2] The result was the Notation section at the end of this Chapter.

General Considerations

One of the two publications specified in Chapter 1[(50)] as companion volumes to this guide[1,2] provides a chapter covering general considerations for the full slanting designers (engineers and architects).[2] Some of these considerations are:

- Functions of the facility, including contents, size and space requirements for machinery and equipment, and any special operating conditions, e.g., involving vibration, temperature, humidity (p. 2-2*).

- Utility services such as gas, electric power, water, sewage, and communications (p. 2-2*). Unless fully-buried, all are vulnerable at connection points just outside the structure; connections design that accommodates differential motion between building and surrounding earth may be indicated. One or more auxiliary or independent self-contained services may be required.

- Design structures might, of course, vary from a standard installation in a nonspecific location to an unique installation in a specific location (p. 2-1*). The approach for this guide, however, used a case study method, meaning that unique facilities, usually in specific locations, have been considered for full slanting study.

- Entrances and service openings (p. 2-7*). With the larger openings, for example, single vehicle entrances, the associated problems become quite formidable. Door jambs should be designed to take the reactions of hasty or permanent blast doors. At least two exits (escape routes), on opposite sides of the shelter, should be provided.

---

* In Reference 2.

- Subsoil and weather conditions, water table elevation, and degree of soil saturation (p. 2-8*). All can be very important and difficult to handle, particularly when dealing solely with basement shelters as in this guide.

Loadings - Shelter Exterior Surfaces

Detailed information on air blast loadings is provided by the two companion volumes[1,2] to this guide and by other sources.[9,16,17] Items particularly important among air blast phenomena include:

- Overpressure loadings occurring immediately behind the shock front and the associated dynamic pressures due to "wind" (pp. 3-3 and 3-8*).

- Reflected pressure, generally simplified to normally incident shock but correctable for other angles (p. 3-4*), and clearance time around or over an object.

- Overpressure positive phase duration (p. 3-6*).† This duration is of little significance in most cases, because of the mostly very rigid structural components involved in protective design.

- Simplifications of air blast loading into a pulse having one or more triangles (pp. 3-6 and 3-9*).

- Drag coefficients, used to convert dynamic pressure into a drag pressure loading (p. 3-10*).

- Air blast behavior in tunnels and ducts (pp. 3-23 and 3-24*), particularly when the shock front impinges on a tunnel entrance at various angles (p. 3-25 and Figure 3-22*).

- Soil bearing capacity for air blast loadings and its relation to (primary use) design soil loading (p. 5-45*). In most cases, normal building dead and live loads were so small compared with the air blast loading that only the latter was used as the loading in the dynamic design. Allowable design soil bearing was doubled and added to the design overpressure for a total dynamic allowable soil bearing (p. 9-14*).

---

* In Reference 2; where several consecutive pages are included, only the first is cited.

† But use Brode curves of Figure 2-1[50] for duration values.

- Shelter roof (p. 5-52*) and floor slab loadings (p. 5-54*). Roof transit time for the blast wave was considered in two-way slab design, but zero rise-time was used for one-way slab design because of the unknown horizontal azimuth toward ground zero.

- Fixtures installed in shelter interiors can be potentially more dangerous than the gross weapon effects if not adequately anchored, e.g., light fixtures, ceiling panels, cabinets and racks, utility lines and fixtures, other nonstructural elements, and any stacked materials.

- Loadings on vertical buried surfaces (p. 5-55* and Tables 4-1 and -2*). The usual assumption of the stress wave traveling downward along the wall, with lateral pressure soil coefficients used to obtain related lateral loadings, was used, ignoring attenuation with depth as insignificant for the shallow depths encountered. The average side-wall loading, therefore, had a rise-time (to peak loading) equal to the transit time for the stress wave to reach the base of the wall. Outrunning ground shock may require separate consideration.[1,18] †

- Loadings in stairwells and areaways. Blast loading on the enclosing walls of a stairwell and stair treads and risers - for example, for interior stairs between the ground floor and the shelter (basement) level - is very complex, and infeasible if not impossible of any rational analysis, particularly so for any specific applications. Multiple reflections of the shock and blast waves from stairs (open or closed treads), landings, and walls make this gas dynamics problem impossible of solution.‡

---

* In Reference 2.

† The walls are also subjected to a vertical (in-plane) loading. The load is taken as constant and equal to twice the peak blast overpressure (i.e., a step pulse) applied over the tributary area, <u>or</u> the maximum resistance of (actually the time-varying reaction load from) the supported element, whichever is smaller (p. 8-20*). For some cases, a worse loading condition exists when the vertical load is taken equal to zero rather than an estimated value. Both cases should be checked and the severer condition used for wall design. Outrunning ground shock initial motion may be upward, or afterrunning ground shock (following initial ground shock and airslap) may fall in phase with oscillatory motions and give the worst displacements, all of which further emphasizes the need for good anchorage of all interior equipment, called for in the paragraph just above.

‡ At least for the engineering design work contemplated herein.

For a situation where the stairwell had large windows at the ground floor level, the simplifying assumption was made that the blast wave access was so unencumbered that the loading should approximate that of a front wall (zero rise-time, peak reflected pressure decaying to a stagnation pressure equal to overpressure plus drag pressure), calculated using a clearance distance equal to the story height of the stairwell. This loading was then applied as acting normal to all flat surfaces in the stairwell. A similar assumption was made for outside areaway loadings, using a clearance distance equal to the depth of the areaway floor below ground surface; this assumption was applied to an areaway near a corner of the building. [The assumption was modified for areaways more centrally located along a building wall, by using the clearance distance applicable to the building wall.]

- Loadings on walls between shelter and nonshelter areas.* Where such walls were in a fully-buried basement, a loading was assumed as equal to the free-field overpressure with zero rise-time. The rationale was that, while some part of the reflected pressure might enter from an areaway, use of the overpressure and zero rise-time tended to offset this possibility, and most of the loading was likely to come from blast penetrations through ducts and the first floor slab over the basement nonshelter areas. In-plane loading should be considered for both exterior and interior walls, as described in the preceding section on loadings on vertical buried surfaces.

Loadings - Shelter Interior Surfaces (Room Filling)

The concept of open shelter - that is, where the air blast is allowed to enter the shelter, particularly through personnel entry doors - is within the Scope and Stipulations of this guide.[50]

The prediction of air blast behavior in room filling† is an extremely complex matter and one under continuing research. Prediction techniques for the average room pressure versus time agree fairly well with very small scale model tests and are now being evaluated in a few full size tests. Those for the jet effect through an opening are available but appear to need test verification. Such techniques for the time-varying net (inside-outside) loading for specific points along a wall, or even

* Comments in this paragraph concern closed shelter occupying part of a basement; loadings for walls in an open shelter occupying a full basement are discussed in the related specific case study(ies).[61]

† Table 6.1 data are useful in room filling prediction methods.[61]

Table 6.1

ATMOSPHERIC VARIATIONS AND CALCULATIONS

Properties of the NACA Standard Atmosphere[19]

Symbols: h = altitude above sea level; t = temperature; a = velocity of sound; p = pressure; ρ = density

h (ft)	t (°F)	t (°C)	a (fps)	a (mph)	p (psf)	ρ $\frac{\#\text{-sec}^2}{\text{ft}^4}$	p (psi)
0	59.00	15.00	1117	761.6	2116.2	0.002378	14.70
1,000	55.44	13.02	1113	759.0	2040.9	.002310	14.17
2,000	51.87	11.04	1109	756.3	1967.7	.002242	13.66
3,000	48.31	9.06	1105	753.7	1896.7	.002177	13.17
4,000	44.74	7.08	1102	751.0	1827.7	.002112	12.69
5,000	41.18	5.10	1098	748.4	1760.8	.002049	12.23
6,000	37.62	3.12	1094	745.7	1696.0	.001988	11.78
7,000	34.05	1.14	1090	743.0	1633.0	.001928	11.34
8,000	30.49	-0.84	1086	740.4	1571.9	.001869	10.92
9,000	26.92	-2.82	1082	737.7	1512.8	.001812	10.51
10,000	23.36	-4.80	1078	734.9	1455.4	.001756	10.11

Note: Density values are for dry air; saturated air densities are about 1/2% to 2% less at temperatures of 50°F to 95°F, respectively. (Handbook of Chemistry & Physics, 36th ed., gives 0.0023798 for dry air density at 59°F at 760 mm mercury ambient pressure).

Air Density Calculations (dry air)[19]

$\rho = p/gRT$ where: R = 53.3 ft/°F
p = pressure, absolute psf
T = temperature, absolute (459.4 + °F temperature), °F
g = gravity acceleration (32.1739), fps
ρ = air density, slug/cf (lb-sec^2/ft^4)

For simple corrections (to the tabulated density values shown above) for other temperatures than those tabulated: tabulated and expected ambient temperatures must be converted to absolute temperatures (add 459.4 to °F); their ratio (tabulated/expected) then may be used as a multiplier to the tabulated density, the result being the density corrected to the expected temperature.

the average for a full wall, have been developed (in the form of a massive computer program that will need much more work to reduce it to a working tool), but need verification by at least the few full size tests being conducted. Finally, prediction techniques for the air velocities at many points within a room are under development as a part of those for the time-varying net loading. The prediction techniques for average room pressure versus time and the jet effect through an opening are presented in Appendix E, but were not available during work on the first three case studies.[61]

The first three case study buildings were not, therefore, considered for potential open shelter use, only for closed; one of the buildings was used, however, for a later open-shelter case study.

General Comments on Blast-Resistant Design of a Structural Element

Blast-resistant design, as in much of structural design, is accomplished most often by designing individual/typical structural elements/members, less often by designing bents/frames or full three-dimensional frames. Subsequent sections of this chapter deal with guidance in blast-resistant design of certain structural elements. However, two topics common to all of the elements bear further discussion in this section - single-degree- versus multidegree-of-freedom systems, and a parameter to describe the extent of plastic action, if any, contemplated by the designer:

- Blast-resistant design of most structural elements requires, as in usual structural design, selection of a trial (prismatic) section, then analysis of that section. However, in blast-resistant design, as in any design for dynamic (i.e., nonstatic) loadings, inertia enters into the equations of motion, meaning that there are an infinite number of small masses whose motion must be accounted for, that is, a multidegree-of-freedom system. For most structural elements, there are equations available (e.g., Table 6.3[(50)]) for reducing a system to an equivalent single-degree-of-freedom system; if equations are unavailable, the equivalent system can be calculated.[22(-416),33]

- To describe the extent of structural member plastic action, if any, contemplated by the designer, one yardstick has been adopted widely, even though it has imperfections and must be applied with engineering judgment; it is the ratio of total deflection contemplated to elastic limit deflection calculated for a critical point in the member (or frame, or assemblage). The symbol commonly used for this ductility ratio is μ. No designer should lose sight of the basic assumptions in using μ, however: that one must estimate the elastic limit deflection and total deflection of the member and that these are only estimates, particularly in reinforced concrete.

On the selection of a value for μ for each structural element to be designed, general discussions of this subject are available in some of the references;[2 (Sec. 7-5),16 (p. 111)] attention is invited to a limitation recently suggested[31] in connection with the Ref. 2 citation, that is, that μ have an upper limit of 10 in the equation

$$\mu = 0.1/(p-p')$$

as applied to R/C beams and one-way slabs. Current thinking[31] is that $\mu = 10$ may be high; the designer can readily consider $\mu = 3$ element dimensions (and thus estimated costs) by use of design charts based on $\mu = 3$ (Ch. 9, Ref. 2).

Another general help is available through use of charts, such as those in Figure 6-1,* to gain a judgment for the effect of the μ selection. For example, a R/C member most often has a very short natural period of vibration T and therefore a large value for the ratio of the duration of positive air blast pressure t_d divided by T, all of which means: that the solutions of most interest in the Figure 6-1 charts are located in their right-side areas (i.e., where t_d/T exceeds, say 5 or 10)† and that the equivalent static load q is apt to be about equal to, or to be greater than, the peak blast load p_m.†

A general guide for μ for R/C beams and one-slabs is stated above. For R/C columns or supporting walls, there are too many matters poorly known to, in effect, use more than the elastic limit, which is accomplished herein and elsewhere[2] by using $\mu = 1.3$ and no increase in compressive strength f'_c for dynamic loads. The effect is approximately the same as using $\mu = 1$ and f'_{dc}, which equals about 1.25 or 1.3 times f'_c; this approach has been also used herein.

One caution should be observed when using the larger μ values, such as in the formula above: the maximum deflection should be calculated, particularly for the longer spans, because it may leave insufficient clearance for the sheltered humans or materials.

It is also recommended that beams be designed with a lower μ (say $\mu = 3$ or less) than the larger μ values that might be used for the slabs supported by the beams; the slabs then could be failed yet form lean-tos or tepees with their supporting beams or walls, thus preserving some shelter and contents.

---

* Located in Ch. 11 of Ref. 50

† Recalling that megaton-range weapons are contemplated herein (Ch. 1, Ref. 50).

The solution charts prepared by others (Ref. 2, Ch. 9) were based on $\mu = 1.3$ for such members with high axial loads and on $\mu = 3$ for flexural members; these are μ values often used.

The reader is reminded that this section deals with ". . . Design of a Structural Element," and that all discussion of μ values is in that context; thus, matters of overall structure stability should not be overlooked. Such stability is not, however, of concern in the design of shelters in (below grade) basements, which is one Scope limit of this guide.[50(Ch.1)]

Solution of Single-Degree-of-Freedom Dynamic Systems

Chart solutions are available for the most common single-degree-of-freedom dynamic systems encountered within the Scope of this guide; selected charts[16,20] are provided by Figure 6-1.*†

Solutions are also available using various numerical methods. For this report, the Newmark β Method was used.[21] It provides a capability for handling <u>any</u> loading and resistance functions, without simplification into straight-line graphs, and does not require the mathematical solution of differential equations. To reduce calculation time in preparing the design graphs that follow, a modification of the Newmark β Method was developed and put into the R/C beam and one-way slab design computer program used; details are in Appendix G - Supplement herein.

Slab Design

A seven-step design procedure is provided in Reference 2 (art. 9.2).

Step 1 requires that the percentages of positive reinforcing steel at midspan and of effective negative steel at the supports be assumed; Table 6.2 provides guidance in making this assumption.

Step 7 requires that the preliminary design (from the first six steps) be checked, and a procedure for this checking is stated in the step. However, for those preferring to use load and mass factors in their check of the preliminary design, Table 6.3* provides these factors as well as other useful data.[22]

Table 6.4 includes data from various sources on dynamic strengths of materials; it may be used to provide comparisons with, or to cover

---

* Located in Ch. 11, Ref. 50.

† Three single-triangle, overpressure-time representations have been developed that are useful with chart solutions (Ref. 2, pp. 3-6 and 3-7).

Table 6.2

SELECTION OF STEEL PERCENTAGES IN BEAM AND ONE-WAY SLAB DESIGN

A. Useful equations (ACI ultimate strength design notation, plus p_v for web steel ratio and subscript d for dynamic strengths).

$p' \le p \le 0.02$	(Eq. 1)	(p.8-4*)
$p \ge 0.005$†	(Eq. 2)	(p.9-4*)
$p' \ge 0.0025$	(Eq. 3)	(p.7-10*)
$(p - p') < 0.4\ f'_{dc}/f_{dy}$ (at any section)[31]	(Eq. 4)	(p.8-3*)
p' See rebound resistance, p. B-19*	(or Ref. 16, p. 114); use $r/q_y = p'/p$	
$p_v > 0.0025$ whenever ductility factor μ is > 1.5	(Eq. 5)	(p.8-6*)
$p_v \ge 0.005$ whenever web reinforcement is required by Eq. 6-9a herein	(Eq. 6)	(p.7-10 & 9-5*)

B. Recommended procedure‡

Select p = 0.005 to 0.02 (suggest 0.015 or 0.02),† per Eqs. 1 & 2 above. Note: $p = A_s/bd$, not A_s/(total X-sect. area)

Try $p' = 0.25\ p$ for Mt weapons first trial, but meet Eq. 3 above

Check $p - p'$ against Eq. 4 above

Use p and p' in a trial design for flexural requirements

Check for required rebound resistance, adjusting p' as required

Repeat above steps as necessary to converge on suitable values of p and p'

Design web reinforcement, checking against Eqs. 5 and 6 above

* Reference 2.

† For SS (simply supported); in practice, the values for continuous members become p_e=0.0089 to 0.02 for PC (propped cantilever) and p_c=0.01 to 0.02 for FF (fixed-fixed supports).

‡ As a way to get started in design of beams and one-way slabs. The section on Typical Designs in this Chapter includes some details.

Table 6.3

(Table 6.3 is included in Ch. 11 of Ref. 50)

Table 6.4

DYNAMIC YIELD STRENGTH OF MATERIALS

	Ref.22 1957	Ref.15 1961	Ref. 2 1962	Ref.16 1964
Steel Design				
Structural carbon or weldable steel (A-7 or A-373)[a]				
Tension or compression, ksi	41.6[b]	42[b]	45-50[c]	42
Shear, ksi	21[d,e]	21[d,e]	27-30	25
Modulus of elasticity, ksi	30,000[d]	30,000[d]	(d)	
Rivets* (A141)[16,22] tens, ksi	40			40
compr, ksi	30			30
Reinforced Concrete[f]				
Steel, tens/compr, ksi*				
Structural grade*	43.7[b]	46[b]	40-50	44
Intermediate grade*	52[b]	55[b]	50-60	52
Hard grade or rail steel*		(g)	(d)	52
Steel, modulus of elasticity, ksi	30,000	30,000		
Concrete				
Compression (axial or flexural)[h]	1.3[b]	1.3[b]	1.2-1.4	1.25[b]
Shear[h]	(d,e)	0.2	(d,e)	0.2
Bond, deformed bars[h]	0.15[d,e]			0.15
Tension	(d)			$7.5\sqrt{1.25f'_c}$
Modulus of elasticity, ksi	(d,j)	(d,k)		

a. Reference 15 stresses also apply to A-36; References 2 and 16 mention only A-7.*

b. Recommended for general use; text provides variation for unusual structure response times.

c. Larger for structures with natural period of vibration <100 msec.

d. Use/using static stress.

e. Dynamic stress higher than static, but latter used due to insufficient data to establish former.

f. Flexural members designed so that resistance capacity is governed by steel.

g. For failure loads, stress is less than for intermediate grade. Permissible design stress ≤0.65 times minimum specified yield point for deformed hard grade billet steel bars, rail or hard grade steel.

h. In terms of f'_c (ultimate compressive strength). References 15 and 22 relate f'_c to 28-day strength and reference 2 relates f'_c to time of (dynamic) loading. Note that these are actual or test values, not minimum or specification values.

j. 2,000,000 + 470 f'_c - or approximately 1,000 f'_c where f'_c is 3,000 to 5,000 psi.

k. 2,000,000 + 460 f'_c (psi).

* See Typical Designs section for information on newer reinforcing steels. For bolts: use of A325 is recommended, with no ultimate strength increase for dynamic loadings; use of A490 is not recommended for protective structures.[31]

NOTE: 1 ksi = 1,000 psi (see metric conversion footnote, p. 6-3).

gaps if any in, Reference 2 values. Later data on reinforcing steel are included in the Typical Designs section in this chapter.

Appendix F provides a preliminary design example for a one-way slab, using the foregoing.

The above preliminary design procedure and a modified preliminary design procedure, both as applied to simply supported one-way slabs, are presented in some detail in Appendix G, Section I.[50]

Final design procedures for one-way slabs, simply supported and continuous on simple supports, are presented in the Typical Designs section of this chapter. A few design examples comparing results from the preliminary design procedures with those from the final design procedure and a computer program that uses the final design procedure are also in Appendix G, Section I.[50] A revised computer program is provided later herein (Appendix G - Supplement).

Choice of Slab Types

The preceding section, Slab Design, is concerned solely with solid one-way slabs. This is one of four types of slab commonly used in structural design; all four types are shown in the figure below. One-way slabs may be solid or joist (also termed "ribbed" - or "tin-pan" if so

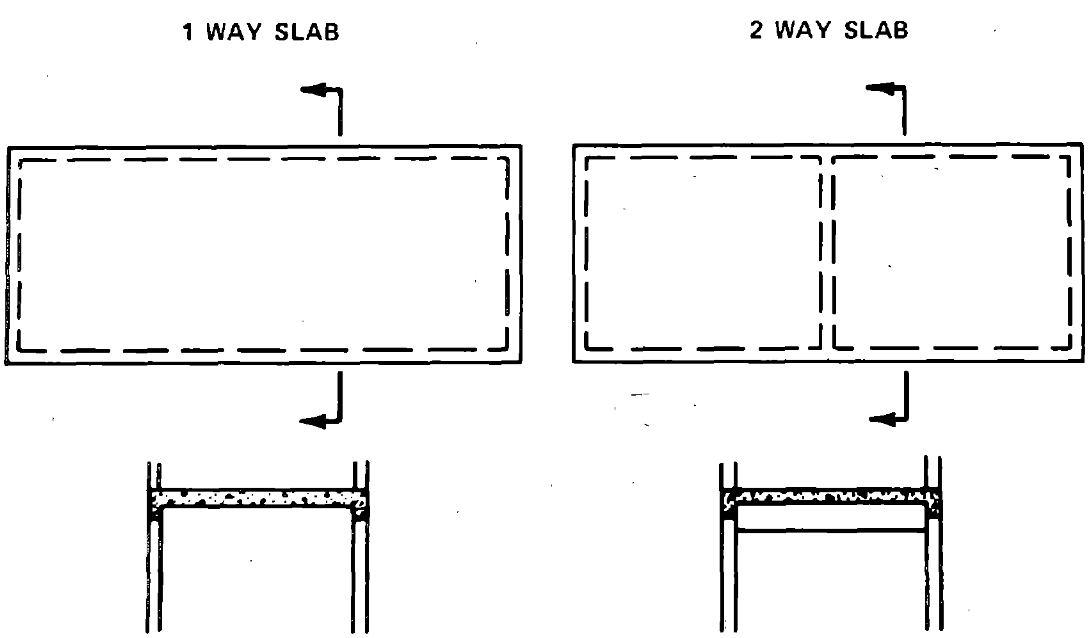

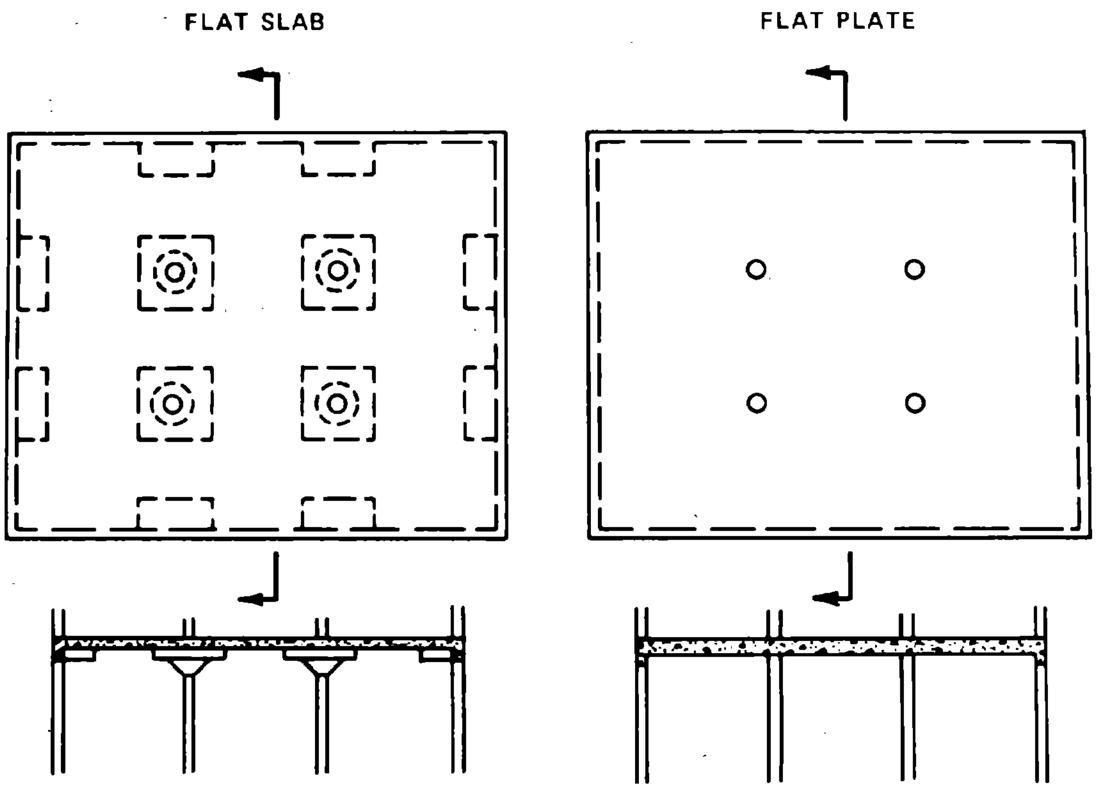

constructed). Two-way slabs may also be solid or joist; for length-width ratios of about 1 to 2, they should be more economical than one-way slabs; for ratios of about 2 to 3, both one- and two-way slab trial designs may be needed to check for best economy; for ratios of about 3 or more, one-way slabs should be more economical than two-way. Most normal design one-way, two-way, and flat slabs will fail in a tensile membrane or yield-line mode, rather than in shear. In contrast, the flat plate type of slab fails in shear around the supporting columns, as demonstrated in collapse analysis studies[74] as well as in some actual and test cases; their use is therefore not recommended for blast-resistant structures.

Wall Design

Reference 2 has no design procedure for walls.

A design procedure capable of including an interaction between in-plane and out-of-plane loadings is presented in the Typical Designs section (later in this Chapter).

Beam Design

The same technique used for one-way slab design was used for beam design.

Where slabs are poured integrally with the beam (or girder) under design, a T-beam approach is often used, wherein a significant slab cross-section area on each side of the beam/girder is taken as a compression area in analyzing the beam/girder resistance. This approach appears to be reasonable for usual design, that is, where only elastic range action is contemplated (whether design approach is by working stress or ultimate strength method); this might be thought of as design for $\mu = 0.5\pm$. When blast-resistant design methods are used, however, one-time ultimate deflections are contemplated that are much larger, say $\mu = 3$ to 10 (note that 3 is recommended earlier herein for beams). In fact, good blast-resistant design looks, before member (or whole structure) collapse, toward use of every bit of member ultimate strength. Such design is therefore based on large deflections of the supported slab, and thus assumes that, as the slab comes close to collapse, there will be tension cracks at the slab edge where it joins the beam. This means that the designer should, in the design of the supporting beam/girder, count on only the slab material situated directly above the beam/girder width as a working part of the beam/girder; in short, consider only the beam/girder rectangular cross-section in design.

Column Design

The procedure of Reference 2 (art. 9.9) was used without modification in preliminary designs for Chapter 8.[50,61] The final design procedure of the Typical Designs section below, however, includes modifications to reflect recent changes in the ACI Code.[4,60] The older code[4] uses equivalent column lengths to handle various support conditions, as well as ℓ/r reduction factors, which approach has become an alternate design method in the newer code.[60] In the latter, a column is designed as a beam-column, that is, an initial deflected shape is assumed, moments and deflections are calculated, and the calculated versus assumed deflected shapes are compared. If agreement is not considered satisfactory, a new deflected shape is assumed and the design cycle is repeated.

Footing Design

The procedure of Reference 2 (art. 9.8) was used without modification in the preliminary designs for Chapter 8[50,61] and in the two footing design examples of Appendix F (herein and in Ref. 50). One typographical error was noted in using Reference 2: "L" should be lower case in Eq. 8-76 (p. 8-48).

The final design procedure presented in the Typical Designs section below includes a slight modification from the Reference 2 procedure, primarily to update compatibility with the current ACI Code.[60]

Door Design

Small steel blast doors, used to cover various openings smaller than doors for people, were not "designed" but were estimated assuming 1/4" plate as a nominal thickness, plus angle framing.

Metal-clad wood doors were designed as blast doors for people; Reference 23 was used, however, because Reference 2 does not cover wood/timber design.

Blast door schemes and designs used in cost studies are discussed in Chapter 8 of Reference 61 (near the end of the Chapter).

Stairwell Design

Design followed the techniques described for appropriate structural elements. Loading was arbitrarily chosen, however, as described earlier in this Chapter; see also loading assumptions shown in Table 8.4A (Item 1a), Reference 61.

Design for Rebound

A member subjected to dynamic loading must be designed to resist the negative displacement, or rebound, that can occur after it reaches maximum positive (initial) displacement.[2]

Design for Expedient Strengthening

Even a slanted shelter can be designed for further strengthening during a warning period; e.g., additional shoring or other supports can be provided to increase the blast resistance of slabs, beams/girders, or columns. This approach is not particularly commended, but the structure's normal use may require clear spans that cannot be reduced except in emergency use of the space(s).

Cost Estimates

The importance of sound cost estimates for the case studies herein[61] is twofold:

- As a check of the success of each case study, measured against the stated Scope of the guide, a specified level of protection for not more than $6/sf* of shelter space. This criterion was found to be achievable at the conclusion of the third case study.

- As a means of convincing architect/engineer users of the guide that personnel shelter capable of considerably reducing the lethal area around a nuclear detonation is possible through full slanting. This criterion is best served by the description that follows of the cost estimating method used.

As described more fully later in this guide,† each case study building was selected based on its potential for full slanting, original and slanted basement floor plans were prepared, and the latter plan was keyed to illustrate a list of planned modifications. The modifications were carried through design only to an extent reasonably sufficient for cost estimating, perhaps analogous to cost estimating from schematics or preliminary design drawings. Cost estimates were made only for those building components to be modified, in which case separate estimates were prepared for the original and slanted versions, the sought for dollar value being the estimated cost difference, whether an increase or decrease, for each modification. The estimated cost difference is shown for each modification item in the case studies that follow; estimated cost differences of less than about $100 were omitted.† (Study time limitations precluded work to optimize slanting estimated costs.)

Since a construction cost estimate strongly reflects the experience and judgment of the estimator, a well-qualified construction cost consultant made the estimates included in this report.† He used a method generally employed by construction contractors and referred to as the "Quantity and Cost, or Materials and Labor, Method" in an OCD report.[24] The estimates reflect construction costs in the San Francisco Bay Region,‡ during June 1968 for the first three case studies. They include all material and labor costs, labor burden, and contractor's profit. Excluded are such costs as those for planning, design, financing, operating

---

* As of January 1968

† In Ch. 8, Ref. 61

‡ But costs are corrected to EN-R's 20-cities average in Table 8-0A, Summary of Slanting Cost Estimates (page 8-69).[61]

and maintenance, etc. The cost estimating approach generally followed that described in another OCD report, which may be consulted for any further details required.[25]

An interesting item came to the author during the preparation of this guide in connection with advertising for construction contract bids for buildings and for alternates with (fallout) slanting incorporated. Invariably the alternates came in at higher bids. An experiment was tried in which a slanted building was used for the basic bid, with the unslanted version to be covered by an alternate - the alternate again came in as the higher bid.*

Ventilation and Air Conditioning

As stated in Chapter 1,(50) possession of appropriate professional capabilities has been assumed for each of the design professionals involved in full slanting of a building. For the mechanical engineer or the architect who is to handle the ventilation, including air conditioning if any, adequate preparation should probably include completion of the OCD/DCPA-sponsored course in Environmental Engineering (footnote, p. 1-1), or the equivalent in private study.[26] The general guide in the field includes some discussion of shelter ventilation.[27]

Shelter space allowances (Chapter 1), and thus the metabolic heat from shelterees, are such that system capacities and configurations are largely determined by requirements for cooling rather than heating. Heating problems can often be minimized by partial recirculation of relatively warm air from the shelter.

When outside temperatures are less than 50 F (10 C†), which is the prescribed minimum temperature for shelters, the local environment near openings through which air enters an occupied space may be too cold, unless the fresh air is either heated or mixed with relatively warm air from the space. As outside temperatures fall, the temperature of mixed air supplied to occupied spaces can be maintained at 50 F by varying the relative quantities of fresh and recirculated air. The mixing process is shown by the example on Figure 6-2A:

---

* Attributed to a private discussion with James E. Roembke, then Deputy Assistant Director of Civil Defense (Technical Services), OCD (now DCPA).

† C = (F - 32) 5/9.

Enter Figure 6-2A at (1) with capacity of ventilating system (17 scfm/person*)† and at (2) with minimum outside air temperature (20 F; -7 C). At intersection read: left to (3) to find required fresh air flow (6 scfm/person†); and up to curve (4) defining T_3, then left to (5) to read resulting exhaust air temperature (66 F). The Change in Humidity Ratio scale and its accompanying formula may be used by interpolating at the first intersection to read about 3.6; i.e., about 0.0036 pounds of moisture per pound of dry air is added to the fresh air while going through the shelter.

Further discussion of the ventilation design process and the basis for it as developed in this study are presented in Appendix H.1.

Ten-year periods of weather observations (hourly dry and wet bulb temperatures, 1949-59) from many representative stations have been used to determine ambient-air ventilation rates required in any climatic locality to maintain an hourly or daily-average, adjusted,‡ effective temperature of 82 F or less during 90% of the time in an average year.§ Per capita ventilation requirements have been determined on both hourly and daily-average bases for each U.S. county. Figure 6-2B summarizes the required ventilation rates in the form of a U.S. map showing isorate contours in scfm (cfm for standard air; density = 0.075 pcf).[28] (For the case studies herein,[61] linear interpolation was used between contours, despite guidance to use the higher contour ventilation rate for the entire zone between each pair of contours. The rationale for such guidance[26, 28] is not understood; the source document is ambiguous, showing both "zone" and specific rates for each county;[28] and use of an annual temperature average for setting either heating or cooling loads is contrary to established professional practice.§)

The Office of Civil Defense has done extensive research on a bicycle-driven ventilator and its applications, culminating in developed kits (PVKs).[26] Their use should be carefully considered.

Where the original building design includes air conditioning, the potential for cooled air use in the shelter, at considerably reduced ventilation rates from those using outside (ambient) air, should be examined.

---

* For Building 4A, Ch. 8, Ref. 61

† 1 cf = 0.02831685 m^3 (Ref. 45).
scfm = cubic feet per minute of "standard air," i.e., air having a specific volume of 13.33 cf per pound of dry air (Appendix H.1 herein).

‡ That is, adjusted slightly for heat losses to the structure.

§ Survival probabilities in the Stipulations section[50] and established professional practice[43] dictate use of ventilation rates for cooling based, not on annual averages, but on four-months averages (June-September).

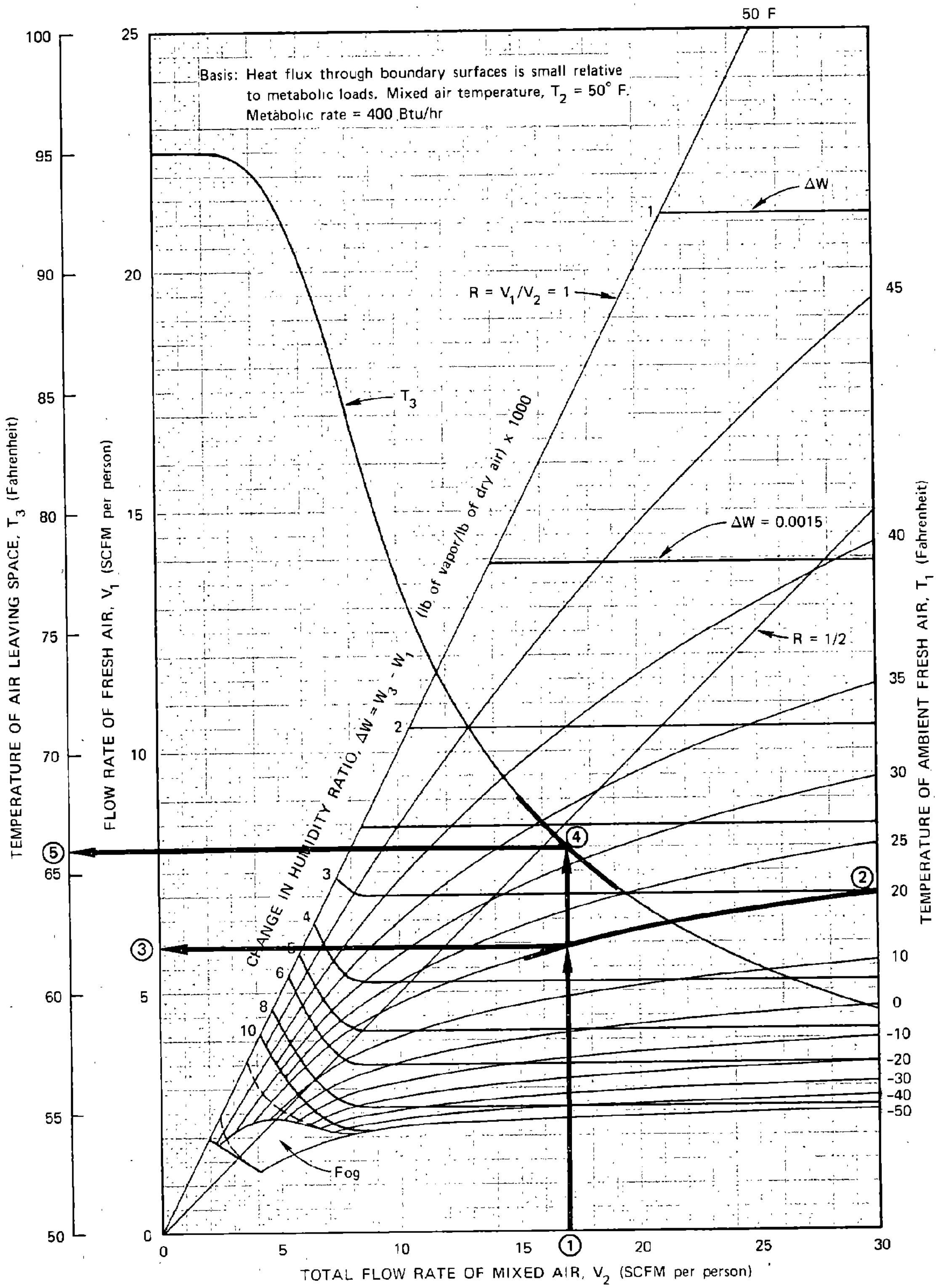

FIG. 6-2A VENTILATION OF AN OCCUPIED SPACE WITH AIR SUPPLY AT 50 F[7]

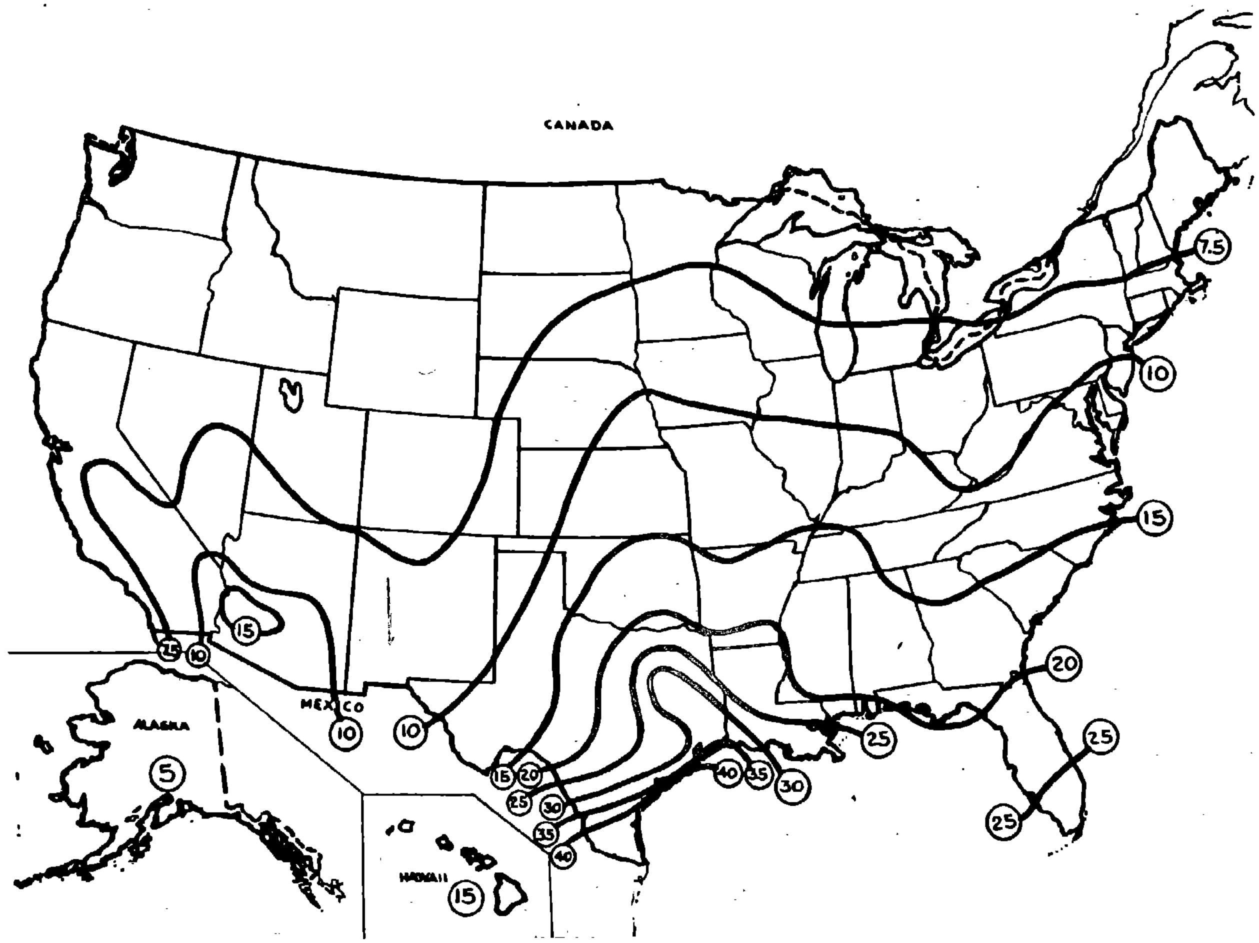

FIG. 6-2B AMENDED MAP OF FORCED VENTILATION REQUIREMENTS (SCFM/OCCUPANT) FOR 82 F ADJUSTED EFFECTIVE TEMPERATURE AND 90% ADEQUACY BASED UPON DAILY AVERAGE DATA (VENTILATION RATES FOR STANDARD AIR, DENSITY = 0.075 pcf)[28]

For discussion purposes, air-conditioning systems can be considered under the following types:

1. High-velocity, double-duct AC system.

   Cold and warm air separately ducted, mixed at using area.

   Air velocity into using space fairly constant.

2. Four-pipe, local fan-coil units.

   Fed by HW and CW pipes, with water mixed at unit per thermostat control.

   Fan usually constant speed, but may have Hi-Lo-Med-Off switch at use point.

3. Central fan-coil unit(s) and ducted air.

   Provides uniform air temperature for large use zones.

   No local temperature control.

4. Ducted air and local reheat coils.

   Central fan-coil unit provides cooling air.

   Reheat coils in local areas warm air to suit.

   Central fan-coil units may be multiple and provide for zoning as in 3.

If air-conditioning equipment is to be installed in the basement, either under the original design or under the fully slanted design, the type indicated as 2 above is unique in its advantages for full slanting use, the reason being that the floor slab over the shelter will be pierced by pipes rather than ducts, for the air conditioning. (If floor slabs are pierced by water pipes rather than ducts, and pipe sleeves are sealed, air blast leakage would be eliminated. Shutoff valves in the pipes would be necessary, however, if the system is to remain operative after the pipes extending outside the shelter are ruptured.) The basement-located equipment used with type 2 requires far less space than the other types. Also, the equipment can be designed to serve only the basement shelter in an emergency, but an emergency power supply would usually be required. A blast-resistant facility for transferring heat to a sink such as water, air, or earth would be necessary. A water well and pump, a reservoir, or a radiator could be used for this purpose. Alternatively, a replacement radiator or cooling tower could be stowed in a protected area and placed in service after the nuclear detonation. (An emergency power

source is a major consideration and a major cost item, if an auxiliary power supply is to be provided.)

Human Tolerances

See note in third item of the Bibliography, and the footnote on page 8-94 of Reference 61. (Project study effort was not available for further work on this topic.)

Typical Designs

The purpose of this section is to provide the manual user - architect or engineer - with several building elements predesigned so that full slanting may be applied, or at least fully considered, with a less than usual design effort.

Typical designs of reinforced concrete elements must recognize steel specifications in current use but not clearly included in Table 6.4 and its sources. These steels are those covered by ASTM Specification Numbers A615 (Billet Steel), A616 (Rail Steel), and A617 (Axle Steel).[30] Use of the latter two steels or A615 Grade 75 is not recommended for protective structures because of possible poor ductility characteristics; if used, they should be handled as indicated in Table 6.4 under "Hard grade or rail steel." A615 Grade 40 has the same specified minimum tensile yield strength (40 ksi) as contemplated by the Table 6.4 "Intermediate grade" entry; A615 Grade 60 has somewhat less ductility, so a ratio of dynamic design tensile yield strength to specified minimum (static) tensile yield strength of 1.2 is recommended.[31]

Values recommended for protective design, and used for the typical designs herein, are therefore as follows.

	Tensile Yield Strength	
	Minimum Static	Dynamic Design
Billet steel, ASTM A615 Grade 40	40 ksi	52 ksi
Billet steel, ASTM A615 Grade 60	60	72

Hook extensions and laps (latter not recommended in blast shelters) in rebars in protective design are recommended to have a 50% increase over the ACI Code[4, 60] requirements in terms of bar diameters. Similarly, any planned welding of rebars must be carefully specified[40]* and be of the highest quality, ensured by excellent construction supervision and inspection methods. Later sections in this chapter, Rebar Design and Details, continue the discussion of rebar use.

---

* Use of latest Code edition and close inspection of all welding are strongly recommended for all shelter construction. Preferably, all rebars in blast shelters would be continuous between excellent anchorages; if welding is unavoidable, all rebars thus connected should be sized so as to develop the full strength of each one.

It is especially important in the construction of protective shelter, where large plastic deflections are contemplated in design, that the highest order of construction inspection be applied, to ensure full and absolute adherence to the design drawings/specifications; extremely careful location of all rebars is vital (improper installation, or non-installation, of even one stirrup, for example, has caused failure of a structure in scale model tests).[31]

A. One-Way Slabs - Simply Supported

This section includes simply supported,* one-way slab, typical designs (Figure 6-3A) and rough estimates of related steel and concrete quantities required (Figure 6-3B). The final design procedure and the rebar estimating approach are described in the two subsections that follow. A preliminary design procedure for such slabs, as well as a modified preliminary design procedure and a discussion of the work leading from one to the other, is described in Appendix G, Section I.[50]

Figure 6-3A is solely for designs where $p = 0.02$; it is entered with the desired clear span and values may then be read for: depth d for any combinations of $f_{dy} = 52$ and 72 ksi, and $f'_c = 3$, 4, and 5 ksi; stirrup steel ratio p_v for the same combinations; and rebound steel ratio p' for the same two f_{dy} values (p' is nearly independent of f'_c). Tics on the d versus L curves show peak slab deflection (in.) for $f'_c = 3$ and 5 ksi. All other design parameters and the design procedure followed are discussed in the following section.†

Figure 6-3B provides approximate slab thickness and total weight of reinforcing steel required per foot of slab width, following the same parameters and methods used in preparing Figure 6-3A.‡

Because the prevailing protective structural design methods [2,15,16,22] all use ductility as their yardstick and maximum deflections several times larger than yield deflection are contemplated in such design, some conservatism in dealing with shear and diagonal tension is indicated. In other words, if design is based on highly ductile structural behavior, the designer must take steps reasonably to ensure against shear-type failures, which are likely to be sudden and catastrophic (entire overhead slab coming straight down, versus a ductile failure where one can hope for some survivors under lean-tos or teepees formed by leaning portions of the failed slab). With this background, vertical stirrups are recommended under the following minimums, even when none may be "required" by the design procedure: (1) first stirrup located at d/4 or less from face of support, (2) maximum stirrup spacing throughout at 0.5 d,§ and (3) stirrups to tie all the top and bottom longitudinal steel together (as discussed in later sections, Rebar Design and Details).

---

* The section is inapplicable if (moment) continuity with walls applies.

† To illustrate use of Figure 6-3A: assume $f_{dy}=52$, $f'_c=3$ and L=300 in.; enter on abscissa scale at L=300 in. and proceed vertically; read maximum deflection about 15.5 in. on curve and d=13.8 in. on right scale; read $p_v=0.0110$ on left scale; read $p'=0.0052$ also on left.

‡ To illustrate use of Figure 6-3B: assume $f_{dy}=52$, $f'_c=3$ and L=300 in.; enter on abscissa scale at L=300 in. and proceed vertically; read total weight of steel about 570 pounds and approximate concrete thickness about 15.6 in.

§ And no smaller than #3 bars, per section A.5.8, Ref. 60.

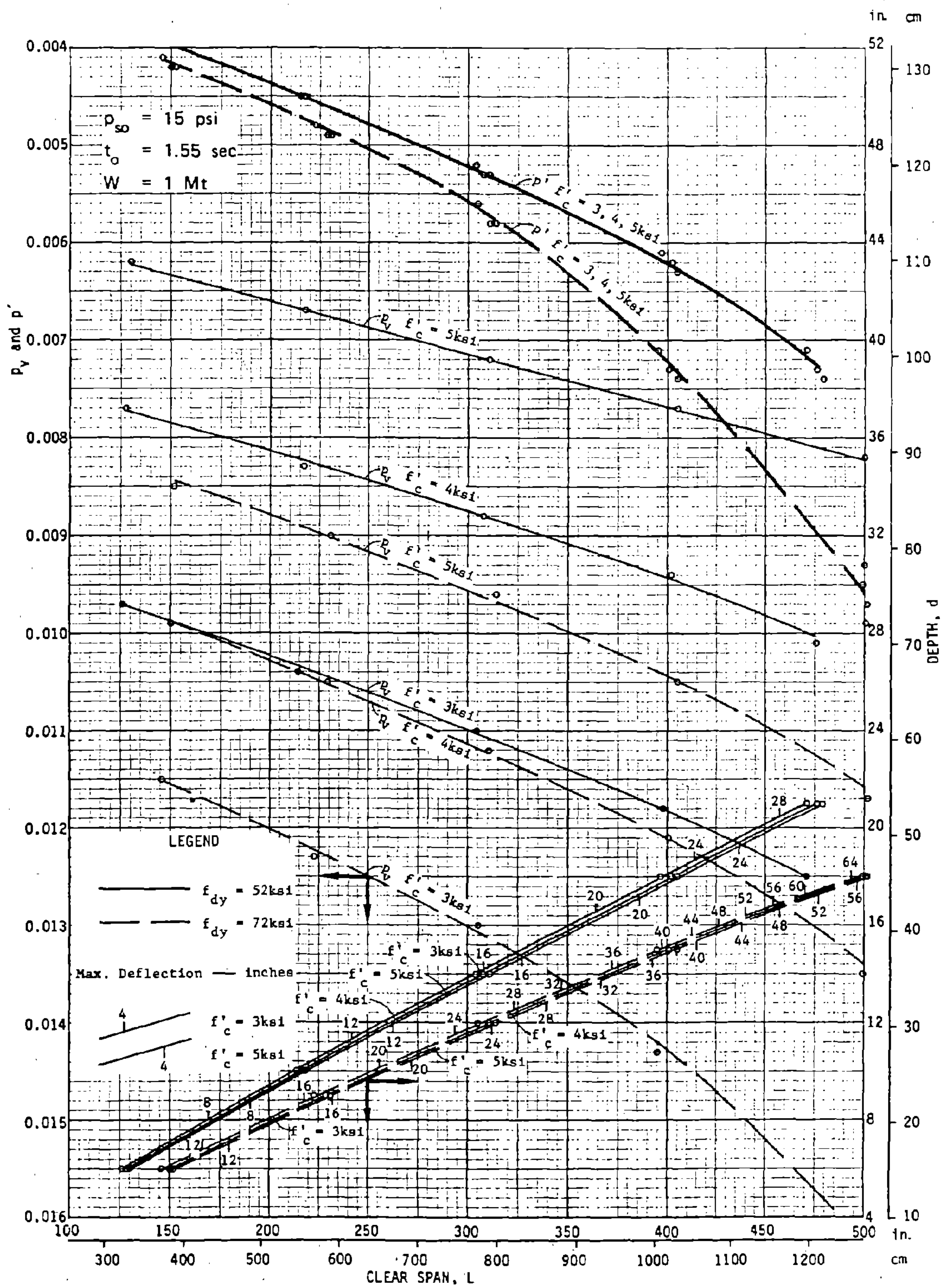

FIG. 6-3A ONE-WAY SLABS, SIMPLY SUPPORTED
Typical Designs – p = 0.020 (15 psi)

Preceding page blank

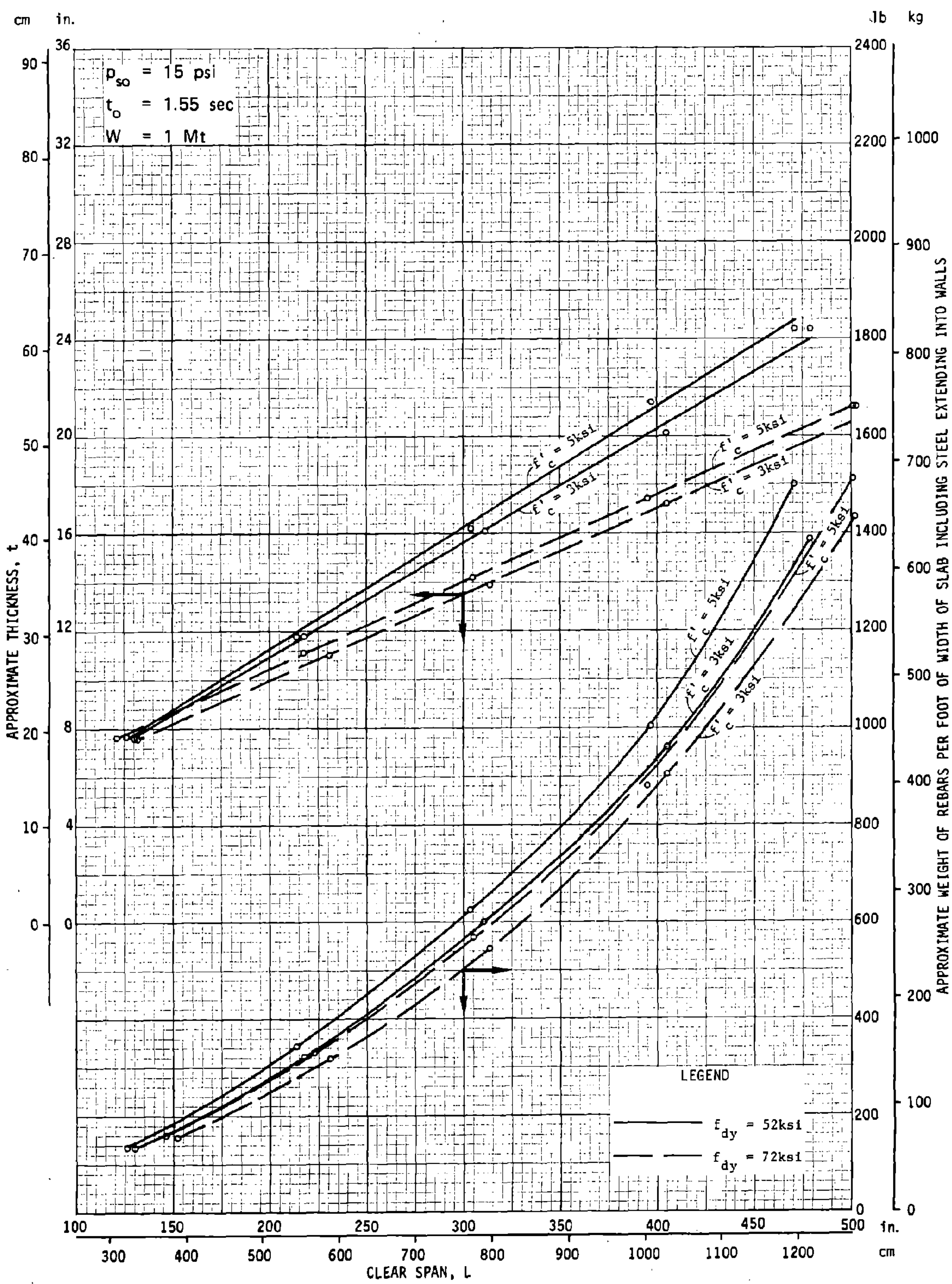

FIG. 6-3B ONE-WAY SLABS, SIMPLY SUPPORTED
Approximate Weight and Thickness – p = 0.020 (15 psi)

Final Design Procedure: This procedure was used in developing the typical designs presented below and is undoubtedly more elaborate than would be justified in normal design use, where only a few one-way slabs might be designed for a building. Shorter procedures are described in Appendix G, Section I, however, as are measures of their accuracy relative to the final procedure used in preparing typical designs.[50] The final design procedure requires several trials through a series of calculations, which include the dynamics aspect, to obtain a "flexural q" (a static unit load, equivalent in terms of assumed flexural response to the actual time-varying/dynamic load). Next, diagonal tension requirements are satisfied by providing web reinforcement as needed so that a diagonal tension q equals or exceeds the flexural q. Then pure shear requirements are similarly handled in terms of the same flexural q. The final design steps followed were:

1. Basic parameter values used were: $f'_c = 3$, 4, and 5 ksi; $f'_{dc} = 1.25\ f'_c$; $f_{dy} = 52$ and 72 ksi; $p_{so} = 15$ psi; $t_o = 1.55$ sec (exponential decay). Further, the desired μ (ratio of maximum center deflection to yield deflection) was to equal $0.1/(p-p')$.* The recommended maximum† flexural steel ($p = 0.02$) was chosen for initial use so that the designed slab might provide protection considerably in excess of the design peak blast load (15 psi), by going through a deep deflection (perhaps membrane) action before collapse. Tentative steel details were also aimed at maximizing ultimate protection, as discussed below.

2. A peak value q (psi) in an elasto-plastic resistance function was assumed, using the first graph in Figure 6-1‡ as a guide in choosing a reasonable trial value. Required flexural resistance led to the first trial set of slab dimensions (Equation 8-1§):

$$M_u = pbd^2 f_{dy}\ [1 - (k'_2/k_1)(pf_{dy}/.85\ f'_{dc})] = aqL^2 c \qquad (6\text{-}1)$$

where a = width of contributory load area (= b for one-way slabs), k_2/k_1 was replaced by 0.554 (Equation 43 of Reference 32), and c = 1/8.

* But $\mu \leq 10$, for R/C beams and one-way slabs.[31]

† See Table 6.2 on selection of p and p′ values.

‡ Ch. 11, Ref. 50.

§ Ref. 2.

3. Cracked section moment of inertia I, elastic phase* stiffness K; and elastic natural period of vibration T were then calculated (Figures 8-1 and 8-3†):

$$I = b(k'd)^3/3 + npbd^3(1 - k')^2 \qquad (6\text{-}2)$$

where $n = 30{,}000/f'_c$ and k′ was as shown in Figure 6-4;‡

$$K = c'E_c I/L^3 \qquad (6\text{-}3)$$

where $c' = 384/5$ and $E_c = 1{,}000\ f'_c$;

$$T = L^2/(c''\, d\sqrt{p}) \quad \text{(sec)} \qquad (6\text{-}4)$$

where $c'' = 425{,}000$.

4. Required rebound steel ratio p′ was initially determined using Figure B-10† ($p'/p = r/q_y$); if the formula $\mu = 0.1/(p-p') \leq 10$ is used (as it was herein), two or three trials are necessary to settle on a μ value. Figure B-10† was constructed for use with an appropriate equivalent triangular load pulse having zero rise-time and duration t_{00}, which may be obtained from Figure 3-7† or an equation thereon, as follows:

$$t_{00} = .87\ \text{sec}[10\ \text{psi}/\hat{p}_{so}]^{1/2}[W/1\ \text{Mt}]^{1/3} \qquad (6\text{-}5)$$

which gives $t_{00} = 0.71$ for the assumed $p_{so} = 15$ psi and W = 1 Mt. Use of Figure B-10† required calculation of the natural period of vibration T, using Eq. 6-4.§ Minimum p′ = 0.0025 (Table 6.2).

---

* Elastic portion of the elastic-plastic deformation diagram (k_1 of p. 11-4, Ref. 50).

† Reference 2.

‡ k′ is identical with k of balanced working stress design (kd = depth to neutral axis), where $k = \sqrt{2np+(np)^2} - np$

§ Reference 2 is unclear on the intended method of calculating T, i.e., whether to use Eq. 6-4 [Figure 8-3 (Ref.2)] or the fundamental equation $T = 2\pi\sqrt{M/K}$ with an appropriate load-mass factor. The latter T was somewhat larger in a typical case, leading to more rebound steel than if the former T were used. Consulting advice[31] and a reference[35] led to the decision to use the smaller T (Eq.6-4), because Figure B-10 (Ref.2) ignores damping, and the statement ". . . when the total duration of the applied force pulse is greater than two or three times the time of maximum positive displacement, damping significantly reduces the required rebound resistance; . . ."[35] was definitely applicable to the typical designs desired. Further, because Eq. B-26 (Ref.2) could

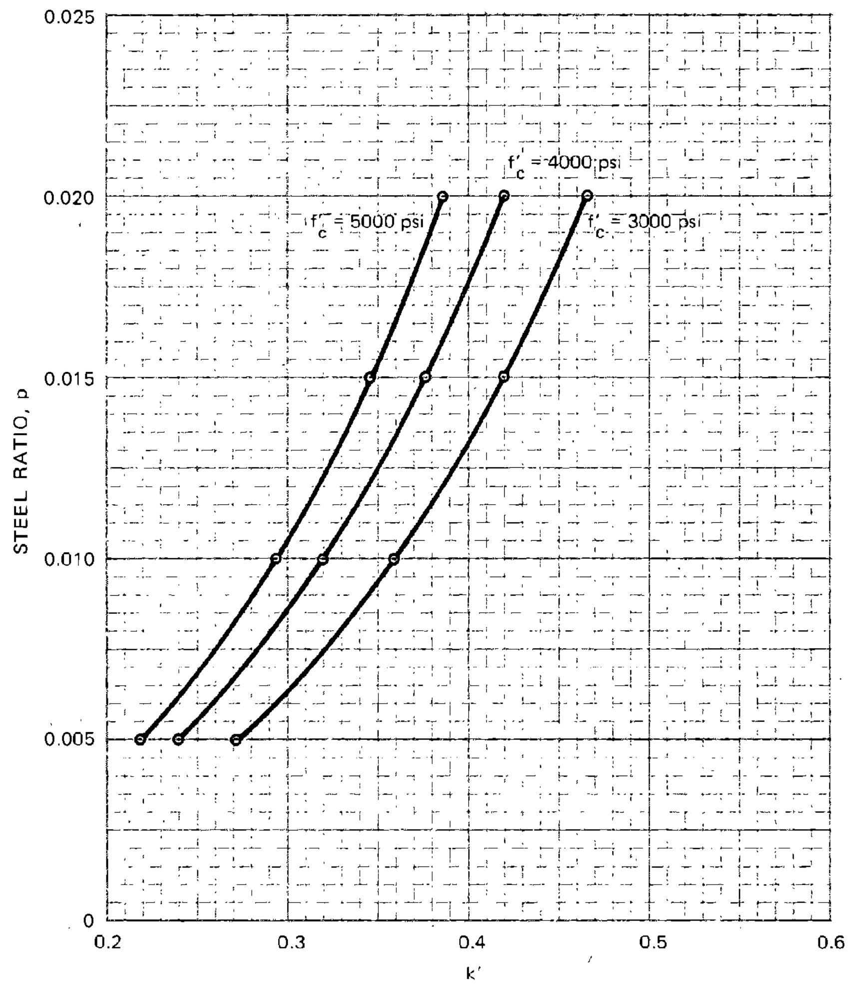

SOURCE: Reference 2

FIG. 6-4 VALUE OF k' VERSUS p

5. Required flexural resistance led to a slight modification of the trial member dimensions, through combining Equations 1 and 4 of Reference 32, the ultimate strength design reference:

---

§ (Continued)
not be made to reproduce Figure B-10 (Ref.2) results, the figure was read for many sets of values, and curve-fitting equations were developed for the design (computer) calculations. The curve-fitting led to a series of equations replacing the region of Figure B-10 (Ref.2), that gives values of r/q_y between -0.1 and -0.5 and that covers values needed for the slab designs of this report section. The series of equations (for computer use) is:

$$y = 3.6916 \ln \mu \qquad x = 3.6916 \ln(t_d/T)$$

$$y' = -0.806 - 0.520x + 0.855y \qquad x' = -4.67 + 0.855x + 0.520y$$

For $y' \leq 0$: $z = x' - 0.15175\, y'^2 - 0.1008$

For $y' > 0$: $z = x' - 0.2811\, y'^2 - 0.2380$

Then: $r/q_y = -0.4008 + 0.04672z - 0.001678z^2 - 0.0003724z^3 + 0.00003552z^4$

To extend coverage in an approximate fashion to the area of Fig. B-10, Ref. 2, that yields values of r/q_y between -0.5 and -1, the following equations are valid for all values of $y > 2.419x$ except for those values of y that are both $< (2.419x + 2.419)$ and < 5:

If $y \geq 2.419x + 7.2905$, then $r/q_y = -1$; otherwise

$$r/q_y = -0.9429 - 0.1839z' + 0.1600(z')^2 - 0.02022(z')^3$$

where $z' = 3.514 + x - y/2.419$

The portions of Fig. B-10, Ref. 2, not covered by either set of equations above are small. For such cases, the user must refer to the figure directly to find rebound steel ratios (as the user should for all non-computer design use).

For preparing the design graphs herein, however, values of r/q_y were all read directly from Fig. B-10, Ref. 2. This technique was necessary because of the discontinuity introduced by going to the figure whenever the above equations found an r/q_y that was out of the equations' specified range. Such discontinuity was slight, however, and is only significant when drawing continuous design graphs as presented in this Chapter. Estimated material quantities (concrete thickness and total rebar weight) from design calculations using the above equations will be within 1% or 2% of those based on reading Fig. B-10 directly.

$$M_u = (p-p')bd^2 f_{dy} [1 - 0.554(p-p')f_{dy}/.85\ f'_{dc}] + p'bd\,f_{dy}\ (d-d')$$
$$= aqL^2 c \qquad (6\text{-}6)$$

where $c = 1/8$, and $d' = 1''$ was assumed (in the trial designs and all one-way slab typical designs)* as reasonable considering the very minor effect of the last term.

6. Using the revised dimensions obtained from Eq. 6-6, steps 3-5 were repeated once before proceeding to step 7, to smooth the design graph plots. For usual design, this step 6 may be omitted.

7. Dynamic equivalent for the static weight of the member was provided by calculating a pseudo-increase in p_{so}; first, the total thickness of the member was estimated:†

$$t = d + d'' = d + 1.3125 \qquad (6\text{-}7)$$

The increase in p_{so} was then calculated:

$$\Delta p_{so} = [1 - 1/(2\mu)]\ 150bt/1728 \qquad (6\text{-}8)$$

where $\mu = 6$ was used,‡ and the term in the brackets is the reciprocal of the dynamic magnification factor for a step loading pulse (zero rise-time to a constant load) applied to a single-degree-of-freedom system, with both considered reasonable in view of the resulting small change in p_{so}.

---

* Only for the SS design graphs for 15 psi was $d' = 1$ in. used. Hand detailing some of the 15 psi designs showed that the minimum $d' = 1.3125$; hence, this value was used for all other design graphs and in the computer program provided later herein (Appendix G - Supplement).

† Initially, $t = 1.27d - 0.006d^2$; the source of this equation is discussed in the Preliminary Design Procedure section of Appendix G, Section I.[50] Later study showed that $t = d + 1.3125$ gives sufficiently accurate results for step 7. If a more accurate estimate of t is desired,

$$t = d + 1.44\,e^{(0.00467\ +\ 0.18A_s)}$$

was derived from detailing approximately 120 slabs.

‡ For early work; later, the formula of step 1 was used for all final slab design procedure work and in the computer program for one-way slabs and beams.

8. Load-mass factors* of 0.78 (elastic) and 0.66 (plastic), Table 6.3, were used to convert to an equivalent single-degree-of-freedom system, which was then solved for maximum deflection (and μ), by using the Newmark β Method[21] or its modification mentioned earlier,† with exponential decay of load and $\beta = 1/6$.‡ (Note: Careful attention must be given to compatibility of units used, particularly in p_{so}, q, mass m, and K.)

9. If the calculated μ was not acceptably close to the desired μ established in the first step of this design procedure, a new q was assumed for use in the second step and the entire procedure was repeated (steps 2 through 8).

10. Diagonal tension requirements were satisfied (Figure 8-2B§) by first checking whether

$$q \le 3.5\sqrt{f'_c}\,(d/L)(b/a)/C \qquad (6\text{-}9a)$$

where C = 1; if Eq. 6-9a was satisfied, required $p_v = 0$ or > 0.0025, for $\mu \le 1.5$ or > 1.5, respectively. (Minimum p_v recommended herein is #3 stirrups spaced as shown in Fig. 6-5.) If Eq. 6-9a was not satisfied, minimum $p_v = 0.005$; also, either of the minimum p_v values (0.0026 or 0.005) was increased as necessary until the flexural q was at least equalled in:

$$q = [1/(2+p'/p)][1000 + 2\,p_v\,f_{dy}]\sqrt{pf'_c}\,(d/L)^2(b/a)C' \qquad (6\text{-}9b)$$

where $C' = 1$ and $p_v = A_v/(s\,b\,\sin\alpha)$, with α being the stirrup inclination angle** from horizontal (from Reference 8-2, p. 77, of Reference 2). Required minimums are also shown in Table 6.2.

11. Pure shear requirements were found to be amply satisfied, without considering inclined steel (not recommended, and not used herein), by checking the allowable peak loading p_m obtained from

---

* Load-mass factors are discussed in more detail in Appendix G, Section I.(50)

† Details are in Appendix G - Supplement herein.

‡ Time increment was 1 msec, later extended to 4 msec in plastic portion only; Eq. 3.51.1 rather than Fig. 3.52 (both in Ref. 1) is recommended and was used for "exponential decay."

§ Reference 2.

** A correction, to source reference, limits the equation application to $\alpha = 90^o$, which was used herein.

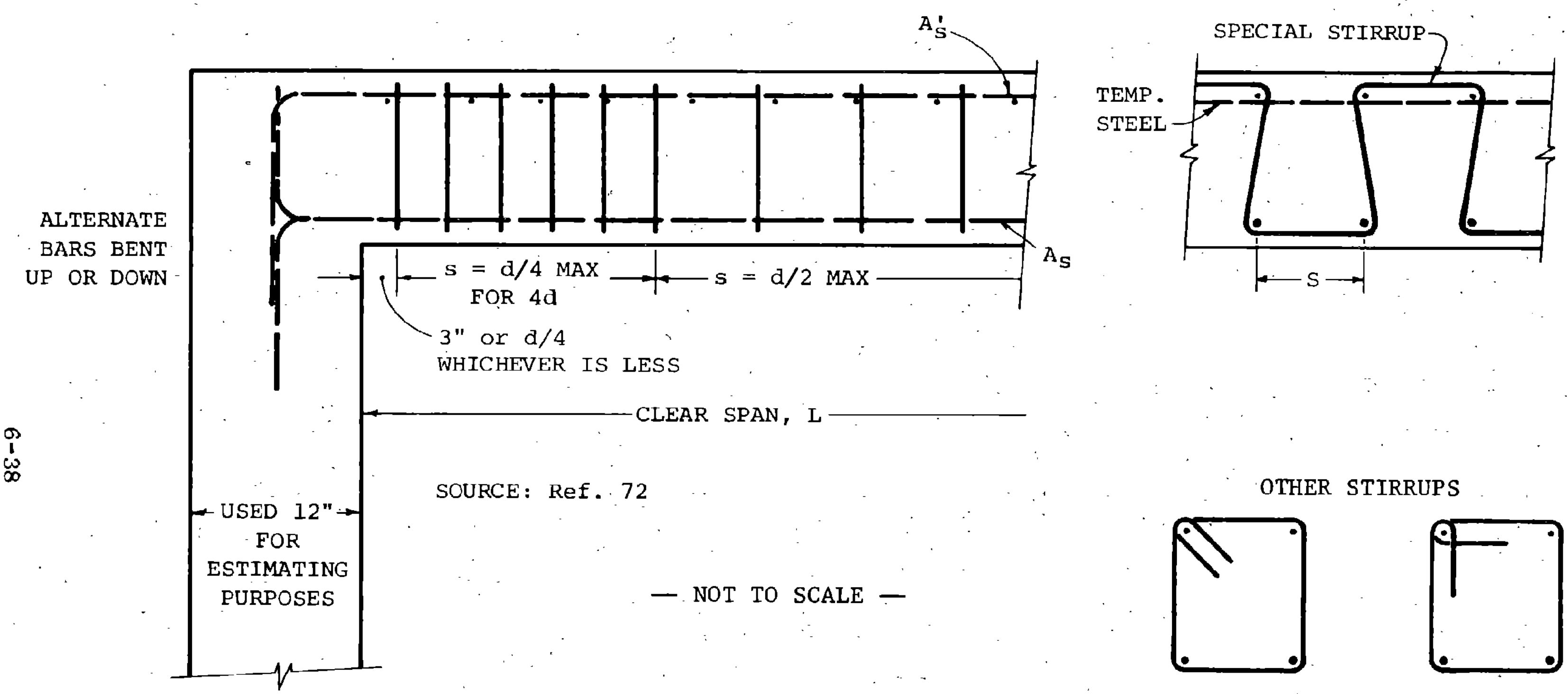

FIG. 6-5 REINFORCING STEEL DETAILING SCHEME
One-Way Slabs, Simply Supported

$$p_m = 0.27\,[\,f'_c d/L](1 - d/L)^{-1}(b/a)/C'' \qquad (6\text{-}10)$$

(applicable only where $d/L \leq 0.2$) against the applied peak loading p_m ($=p_{so} + \Delta p_{so}$); $C'' = 1$. (Section 8.2.4* may be useful if the pure shear check reveals a design situation considered potentially critical.)

The allowable p_m is based on $\mu = 1.3$, which is appropriate for pure shear. Equation 6-10 results from combining Equation 8-10* and $p_m = q[1 - 1/(2\mu)] = 0.6154\,q$ (the term in brackets has been mentioned earlier in connection with Equation 6-8). Equation 8-10* is based on pure shear failure occurring when the average shearing force over the section exceeds 0.2 f'_c, a value that is now considered somewhat high;[31] however, all typical designs calculated for Figure 6-3 showed values far below the 0.2 f'_c. Recommended limit of 0.1 f'_c is considered desirable, with 0.15 f'_c strongly urged as an absolute limit.†

12. Bond strength under blast loads is important for rebar detailing. Most of the usual sources of guidance on blast resistant design cited in this study have no discussion of bond. Two of them, however, provide guidance including allowable dynamic bond stress u_d values: One‡ suggests a general value of 0.15 f'_c for rapid strain rate loadings, whether top or bottom bars; the other§ states that "Tests have indicated that failure in bond . . . will not occur so long as the bond stress does not exceed twice that specified in the ACI Building Code (ACI 318-56). . . . In addition to fulfilling the above limitations on bond stress, bars should be hooked, preferably around other bars, or welded to other bars to insure against possible pulling out of the bars. This last requirement is also desirable in order to provide continuity of the entire reinforcing cage." Both sources are, of

---

* Ref. 2

† While a shear coefficient of 0.1 was desired, for some cases in the design graphs herein, it went as high as 0.148. Shear values > 0.1 in general occurred only with low concrete strength (3,000 psi), high steel ratio (0.02), and overpressures greater than 15 psi for the SS case, or greater than 10 psi for the PC and FF cases.

‡ Ref. 34, p. 46.

§ Ref. 58, p. 27.

course, based on the 1956 Code* and its Working Stress Method, details of which are:

$u = 0.07f_c'$ for top bars (bars near top of member and having 12" or more of concrete under them)*

$u = 0.10f_c'$ for other bars*

$u_d = 0.15f_c'$ is recommended for use under dynamic loadings (per discussion above)

V = total shear at critical section (check at support face and at point of inflection)†

$$V = p_m L/2 \text{ at support face (e.g., psi/in. of slab width)} \tag{6-11}$$

$j = 0.9$ is suggested for general use. (All values contemplated herein will be at or slightly larger than 0.9 and detailed computations are not worthwhile, since no rebar savings will result - at most only a different selection of bar size(s).

Σo = sum of rebar perimeters

$$\Sigma o = V/(u_d jd) \tag{6-12}$$

Equation 6-12 may be solved for use with the areas of both tensile and compressive (rebound) bars, for selecting bar sizes and spacings.

The current ACI Code[60] and its Commentary[63] deal with bond stress under the terms "development length concept" and "development of reinforcement" in Chapter 12 of both references. An excellent state-of-the-art paper has been published by ACI on bond stress and failure.[64]

Regardless of the technique used in dealing with bond stress/ failure, the designer must not lose sight of the objective of a protective structure, as discussed in the following section.

Resulting one-way slab typical designs are shown by Figure 6-3. The rebar scheme and assumptions used are discussed in the next section. The computer program used is provided later herein (Appendix G - Supplement).

---

* ACI 318-56 as quoted in Ref. 59, pp. 7-111 and 7-134.

† Ref. 34, p. 46.

Rebar Design and Details. The general scheme contemplated for steel detailing is shown in Figure 6-5. Because protective construction or shelter may very well be exposed to air blast loadings different or larger than contemplated, the design objective should be members or assemblages that will break up or fail in a predictable and desired mode - for example, a slab loaded to collapse that still preserves some lives by breaking into smaller lean-to or teepee shelters.* On this basis, all top and bottom steel is carried to the slab edges and some is bent into the supporting walls as shown in Figure 6-5; the purpose of bending alternate bottom bars† into the top of the wall is to set up a slab maximum deflection situation wherein the slab center might deflect several times the slab thickness while the walls still support the slab edges (the walls not necessarily wrecked by rigid frame behavior). Also, to maximize protection capability by restraining the top steel for composite action at extreme deflections, vertical stirrups were included for the full span, with maximum spacing of 0.75 d,‡ even including slabs 3 and 4§ where no web steel was "required" by design formulas. A value of p_v greater than 0.0025 is required whenever a ductility factor μ greater than 1.5 is used for diagonal tension (Table 6.2).

The early four slab designs§ were further used to develop the first rough cost estimating relationships for the total steel in one-way, simply supported slabs. Later, rebar detailing was prepared for many slabs, using the slab data in the original Table G.1,§ and rough cost estimating relationships for the total weight of rebars in one-way simply supported slabs were developed. Two correction functions to apply to each required design value (e.g., A_s) appeared necessary - a "fit" correction function relating the required design steel to what it is possible to provide with specific bar diameters and spacings customarily at some multiple of 1/2 in.; e.g., a slab design A_s = 3.6 sq. in., might reasonably be served by number 10 bars at 4 in., giving an actual A_s = 3.81 sq. in., indicating a "fit" correction function is needed. For A_s and A_s' values, a length correction function is also needed, relating clear span length L to the actual steel lengths that include the slab steel extended into the slab ends and the supporting walls. The "fit" correction function for A_s' (top) steel is different than that for A_s (bottom) steel because the former is limited in bar spacing selection to some multiple (usually one or two) of the latter's spacing (to facilitate stirrup and all steel placement). Using the slab data in the orignal Table G.1,§ the "correction" functions averaged out as shown in Table 6.5.

* This yield-line type of failure is understood to be more likely when p is approximately 0.01 (or less) than is a membrane type of failure (like a suspension bridge) that may occur when p is somewhat more than 0.01.

† Alternatively, separate dowel bars could be used, with all slab bottom bars bent up.

‡ Maximum of 0.5 d is now recommended (section A.5.8, Ref. 60).

§ Appendix G, Section I.[50]

Table 6.5

REBAR ESTIMATING FUNCTIONS FOR ONE-WAY SLABS SIMPLY SUPPORTED

Rebar Use	"Fit" Corrected Value*	Rebar Length
A_s	$0.05293 + A_s$	$43.47 + 1.0587\ L$†
A_s'	$0.08532 + 0.998\ A_s'$	$27.83 + 1.0897\ L$†
Temperature and shrinkage ($A = 0.002$ bt) (ACI 318-71)	$0.03122 + 1.037\ A$	Equals slab width
Web steel (volume) (vertical stirrups)	$4.241 + 0.957\ L_v A_v$‡	

* Values of A_s and A_s' (in.^{2}) are per foot width of slab.

† Assumes 12-in. thick supports (L is in.).

‡ Web steel area A_v (in.^{2}) and length L_v (in.) (both per foot of slab width) were derived analytically and empirically from trial detailing (15 psi simply supported slabs), curve-fitting techniques were used, and the results are shown below. The purpose in deriving such unwieldy formulas was to use them in the computer program to obtain rough estimates of the steel quantities when running the large number of design cases needed for design (including quantity) graphs for all other SS, PC, and FF slab cases herein. (Accuracy is not implied by the decimal places shown.)

For $p_v \le \bar{p}$:

$$A_v = SL\bar{p}_v \,/\, p_v$$

For $p_v > \bar{p}_v$:

$$A_v = 0.5\ Sp_v(L + d)\ [1 + (\bar{p}_v / p_v)^2]\ [(L - d) / (L + d)]$$

where $\bar{p}_v = \dfrac{0.11}{0.75\ d^2(0.3 + 0.7\ e^{-0.08\ d})}$

and $L_v = [(1.3 + 0.7\ e^{-0.08\ d})\ d + 1.286\ d' - 0.214\ d'' - 0.25]\ b/S$

Note: S = spacing between main horizontal rebars.
In $\bar{p}_v$ equation, 0.75 should be changed to 0.5 for any future use, to coincide with the change of maximum stirrup spacing from 0.75 d (Ref. 50) to the 0.5 d recommended herein (art. A.5.8, Ref. 60).

As for cost considerations in the choice of thinner versus thicker slabs - that is, reduce steel and increase concrete or vice versa - the thicker slabs appeared to be significantly cheaper. However, lower costs were estimated for slabs with $p = 0.01$ than with $p = 0.005$. In general, the estimated cost difference between using $p = 0.02$ and 0.01 was found to be approximately 9 to 10 percent at all overpressures; therefore, differences were of the order of 24¢ to 36¢ and 80¢ to $1/sf of clear span one-way slabs for short (100 in.) and long (500 in.) spans, respectively. Estimated cost data used were from SS slabs, $f_c' = 3$ psi and $f_{dy} =$ 52 ksi, designed for 5, 10, and 20 psi blast overpressure; material and labor costs were for 1970 (ENR, 6/70, San Francisco area). No consideration was included, however, for thinner slabs requiring less story height, meaning less basement excavation and walls height.

To make cost comparisons possible and to provide for alternative designs, simply supported one-way slab typical designs were prepared, similar to those shown by Figure 6-3A, for p ratios of 0.015, 0.01, and 0.005 and are shown by Figure 6-6. To make design at other overpressures possible, Figure 6-7 was prepared, which gives the designs for simply supported one-way slabs, similar to those in Figure 6-3, for steel ratios of 0.02 and 0.01, and for design blast overpressures of 5, 10, 20, and 30 psi. The computer program used is provided later herein (Appendix G - Supplement).

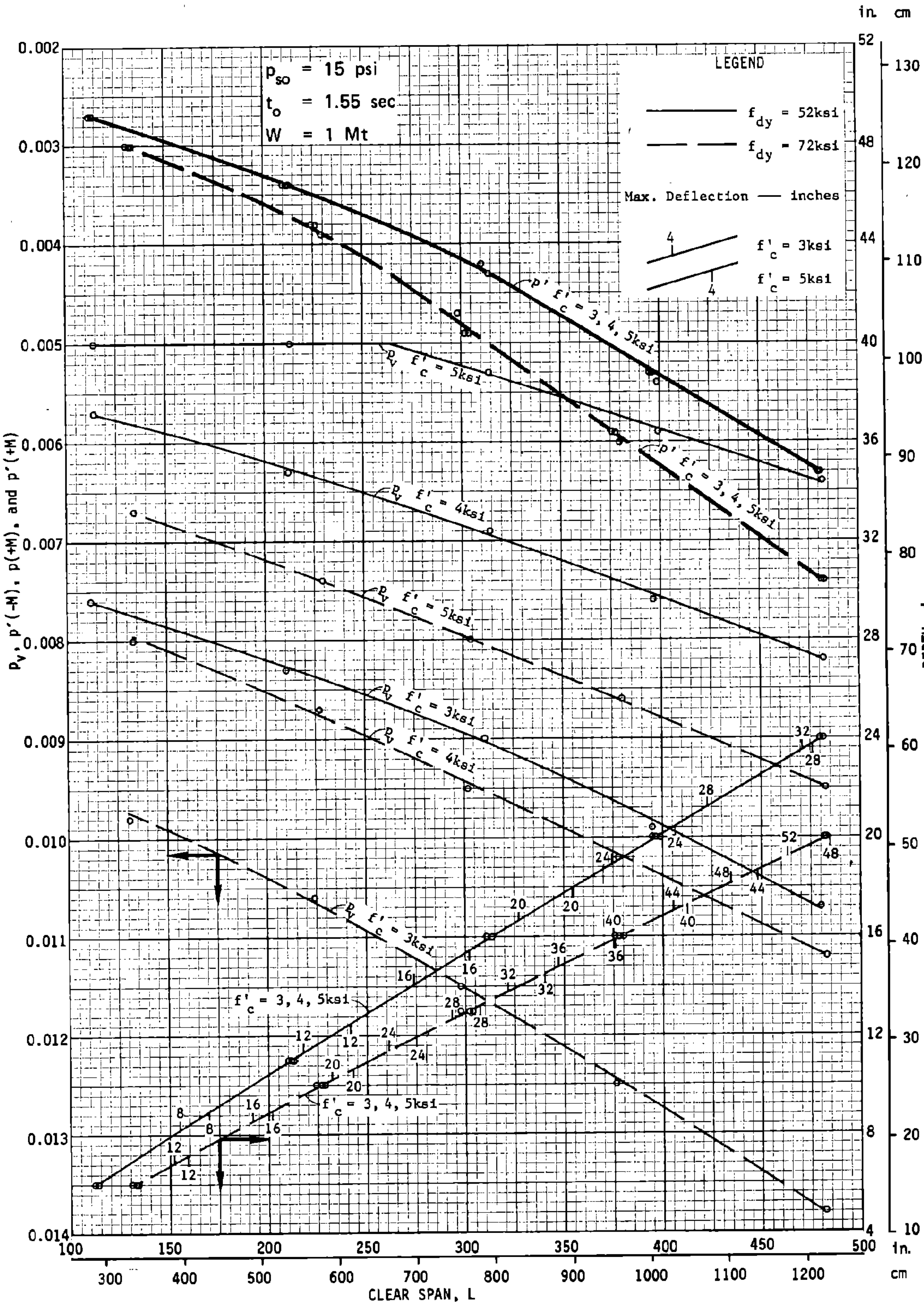

FIG. 6-6A ONE-WAY SLABS, SIMPLY SUPPORTED
Typical Designs — p = 0.015 (15 psi)

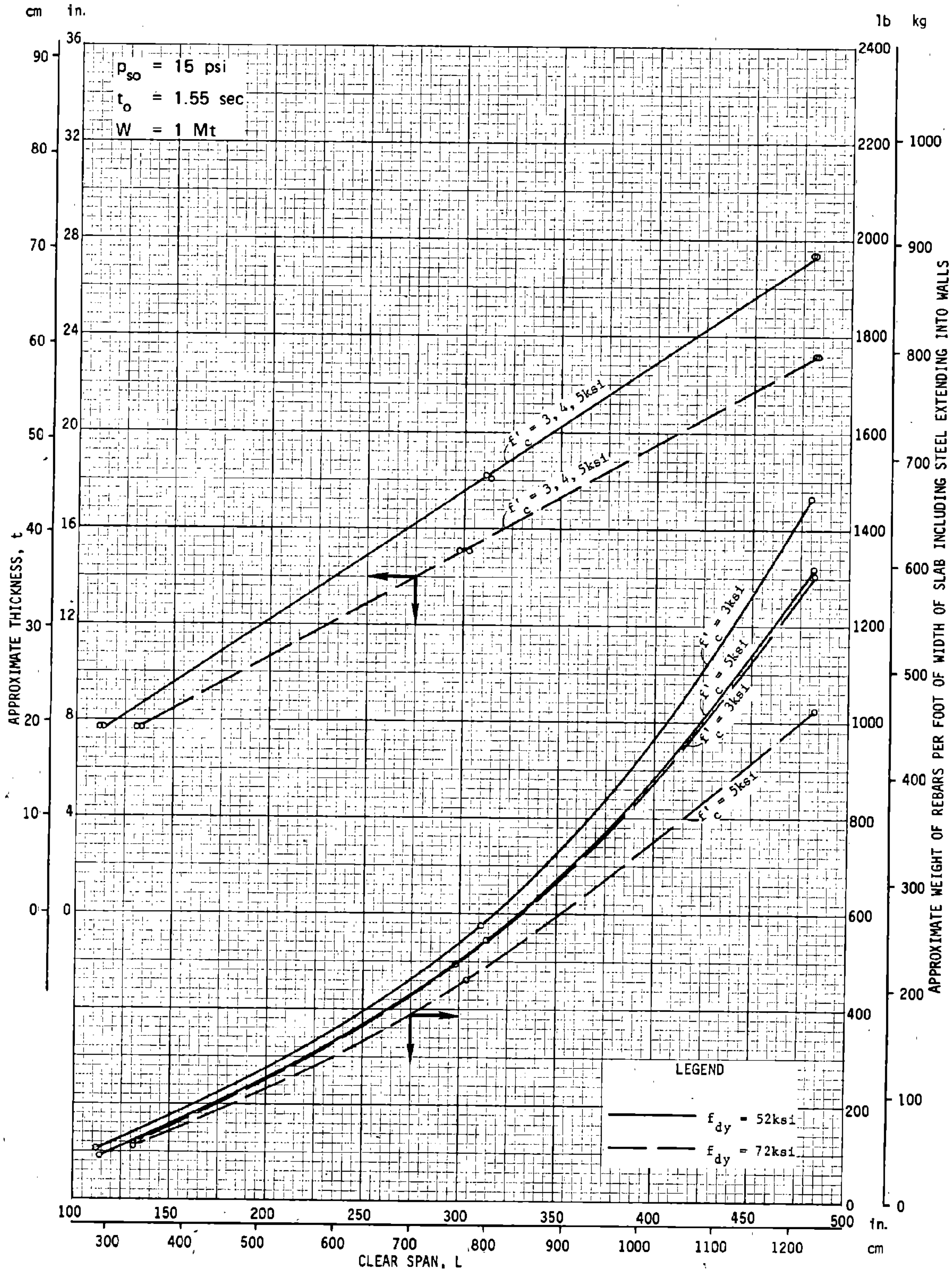

FIG. 6-6B ONE-WAY SLABS, SIMPLY SUPPORTED
Approximate Weight and Thickness – p = 0.015 (15 psi)

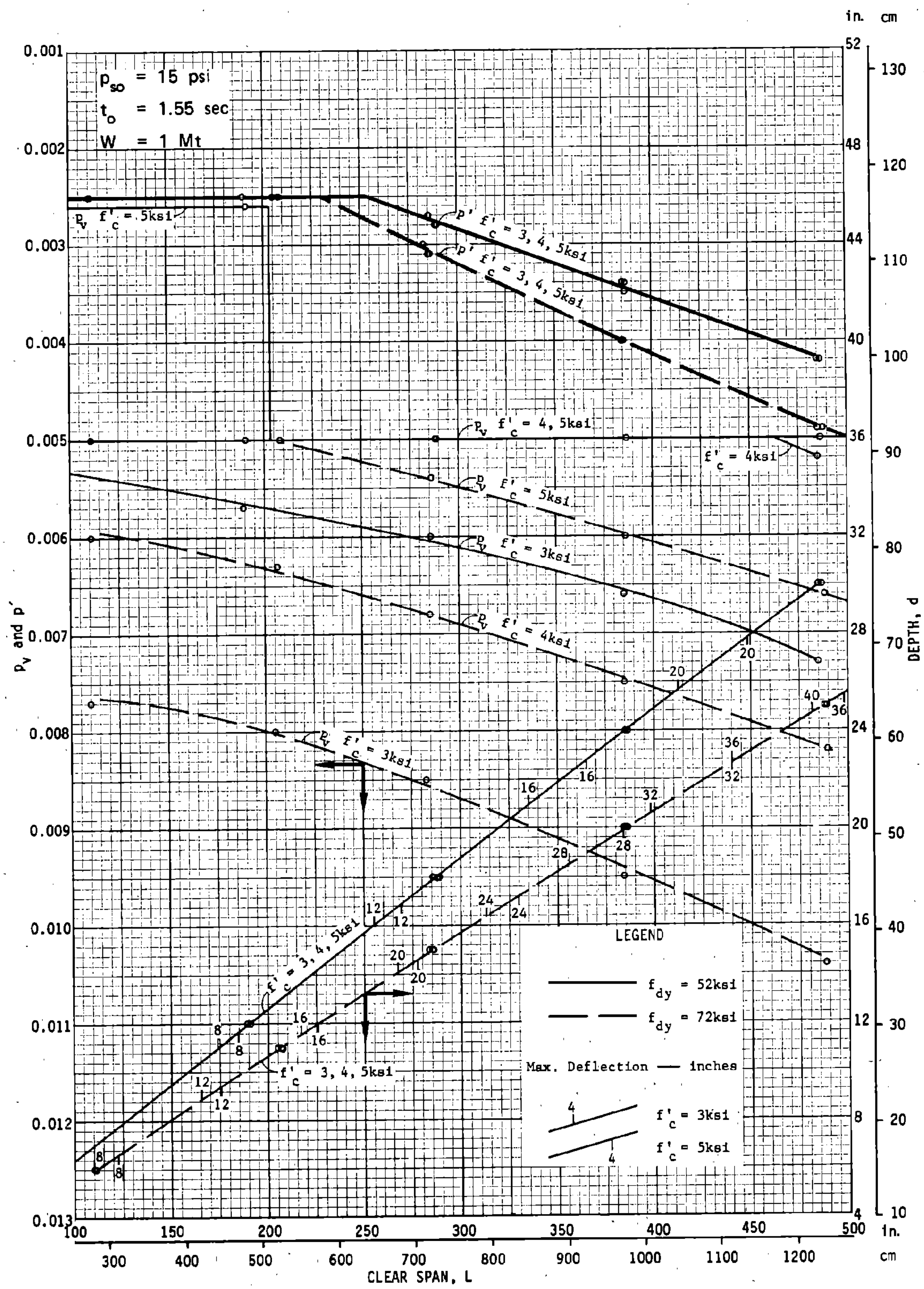

FIG. 6-6C ONE-WAY SLABS, SIMPLY SUPPORTED
Typical Designs – p = 0.010 (15 psi)

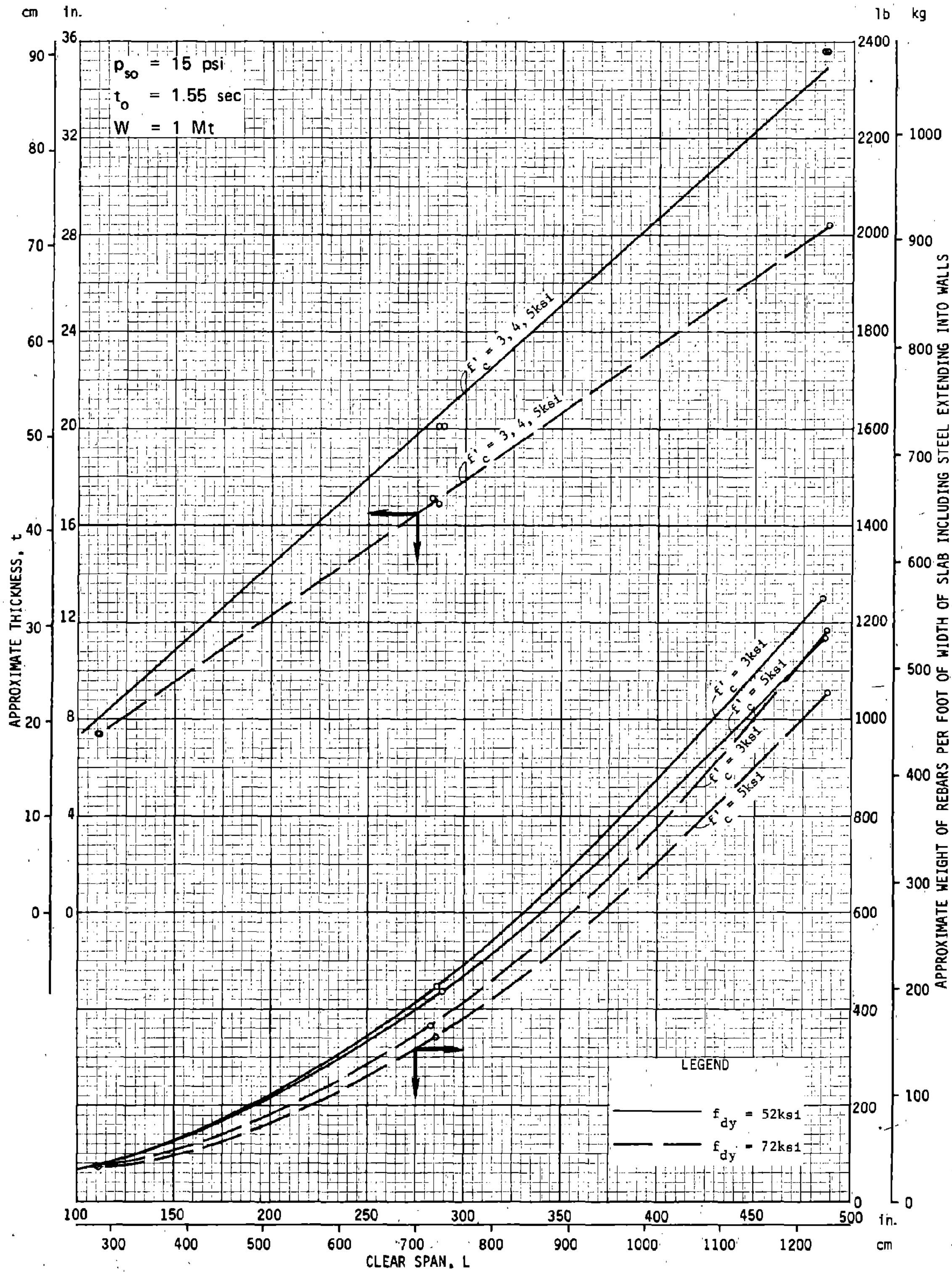

FIG. 6-6D ONE-WAY SLABS, SIMPLY SUPPORTED
Approximate Weight and Thickness – p = 0.010 (15 psi)

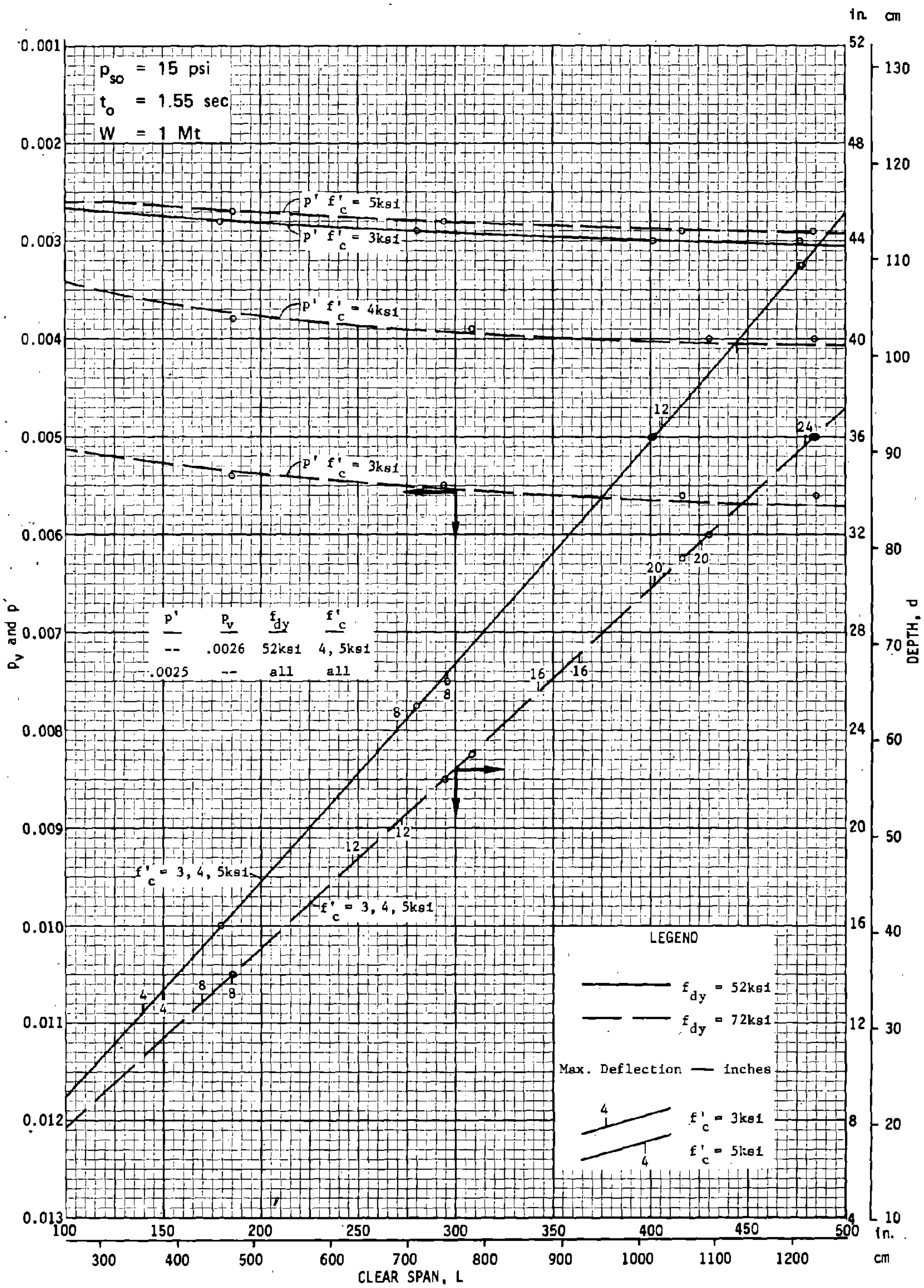

FIG. 6-6E ONE-WAY SLABS, SIMPLY SUPPORTED
Typical Designs – p = 0.005 (15 psi)

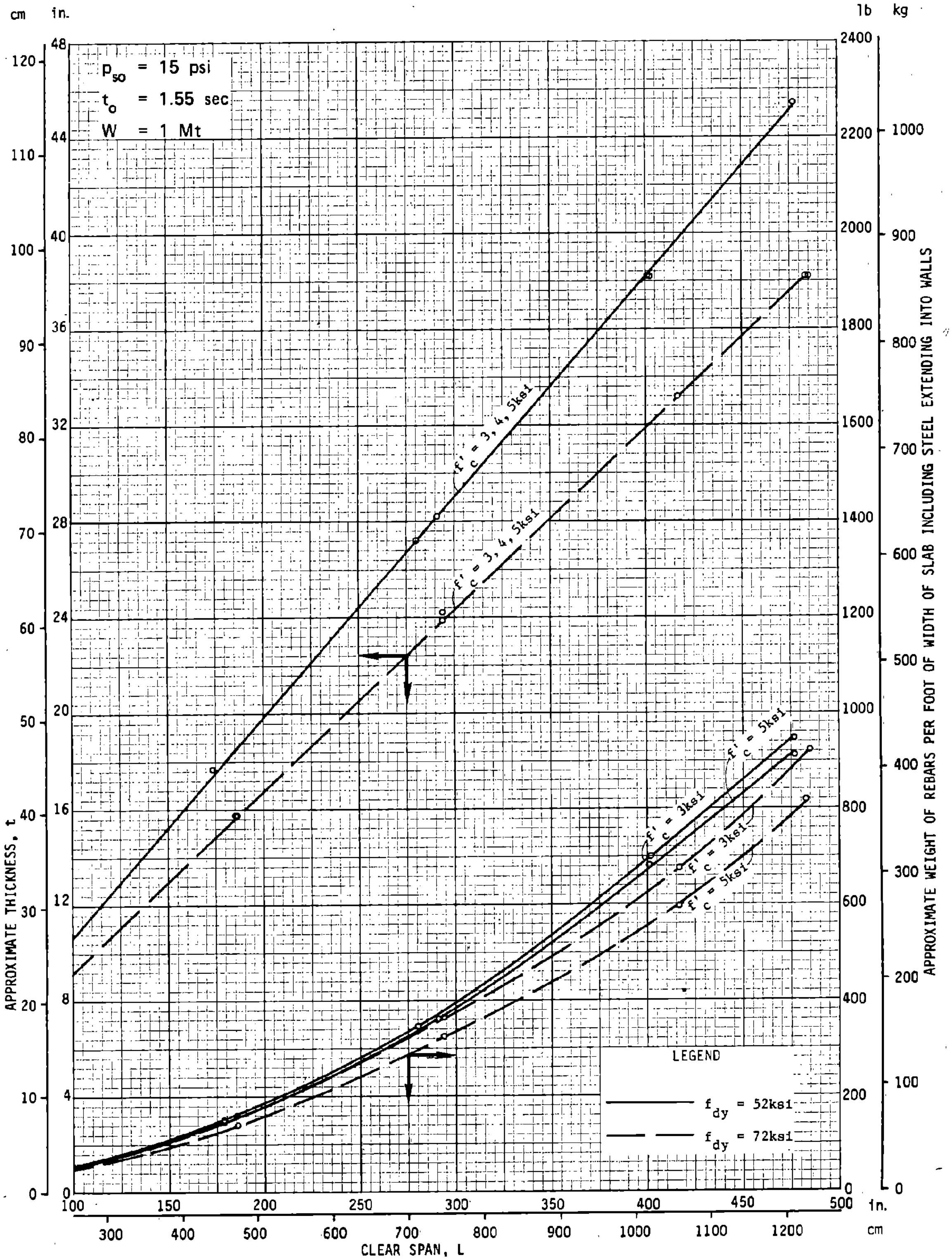

FIG. 6-6F ONE-WAY SLABS, SIMPLY SUPPORTED
Approximate Weight and Thickness – p = 0.005 (15 psi)

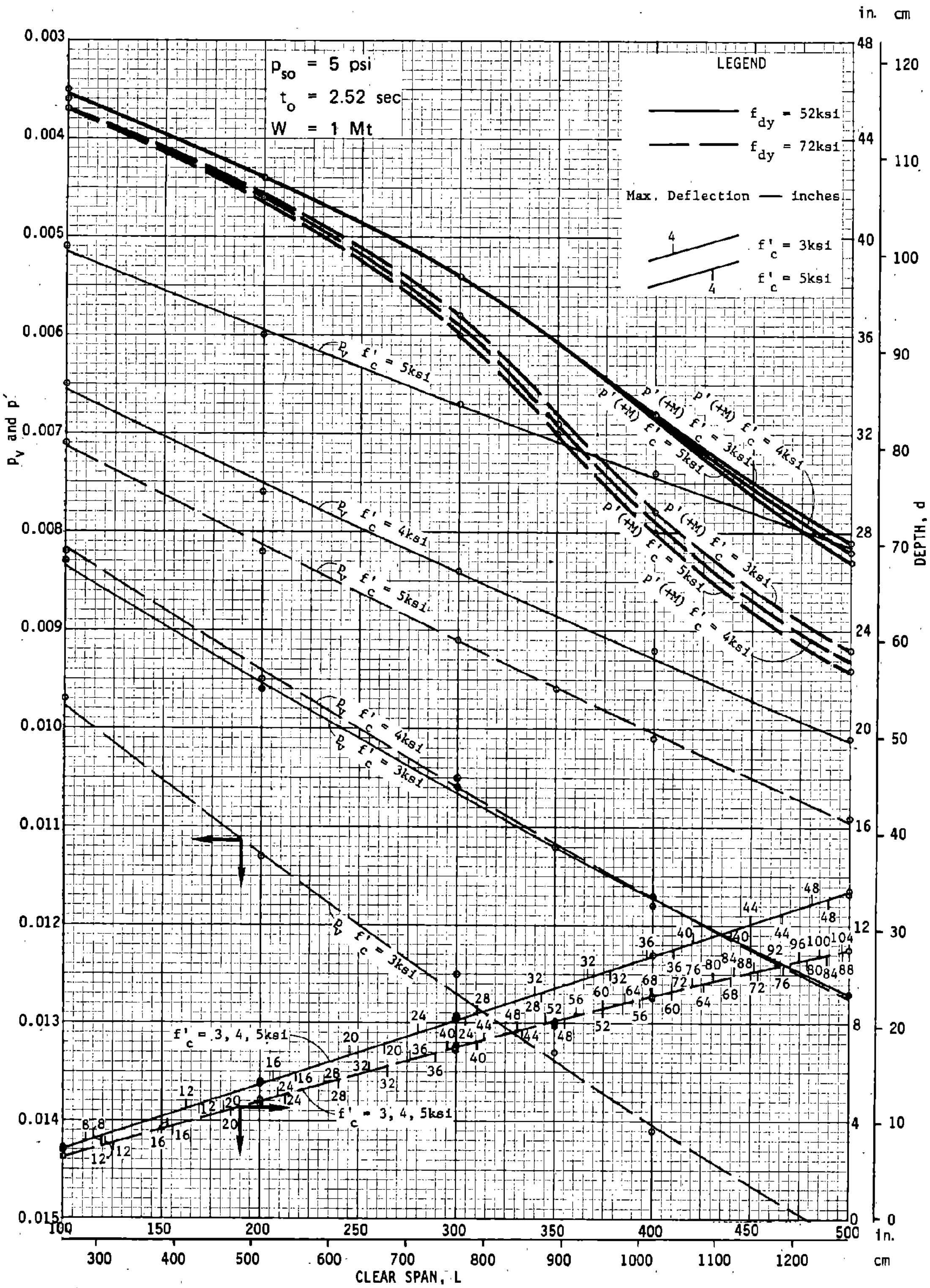

FIG. 6-7A ONE-WAY SLABS, SIMPLY SUPPORTED
Typical Designs — p = 0.020 (5 psi)

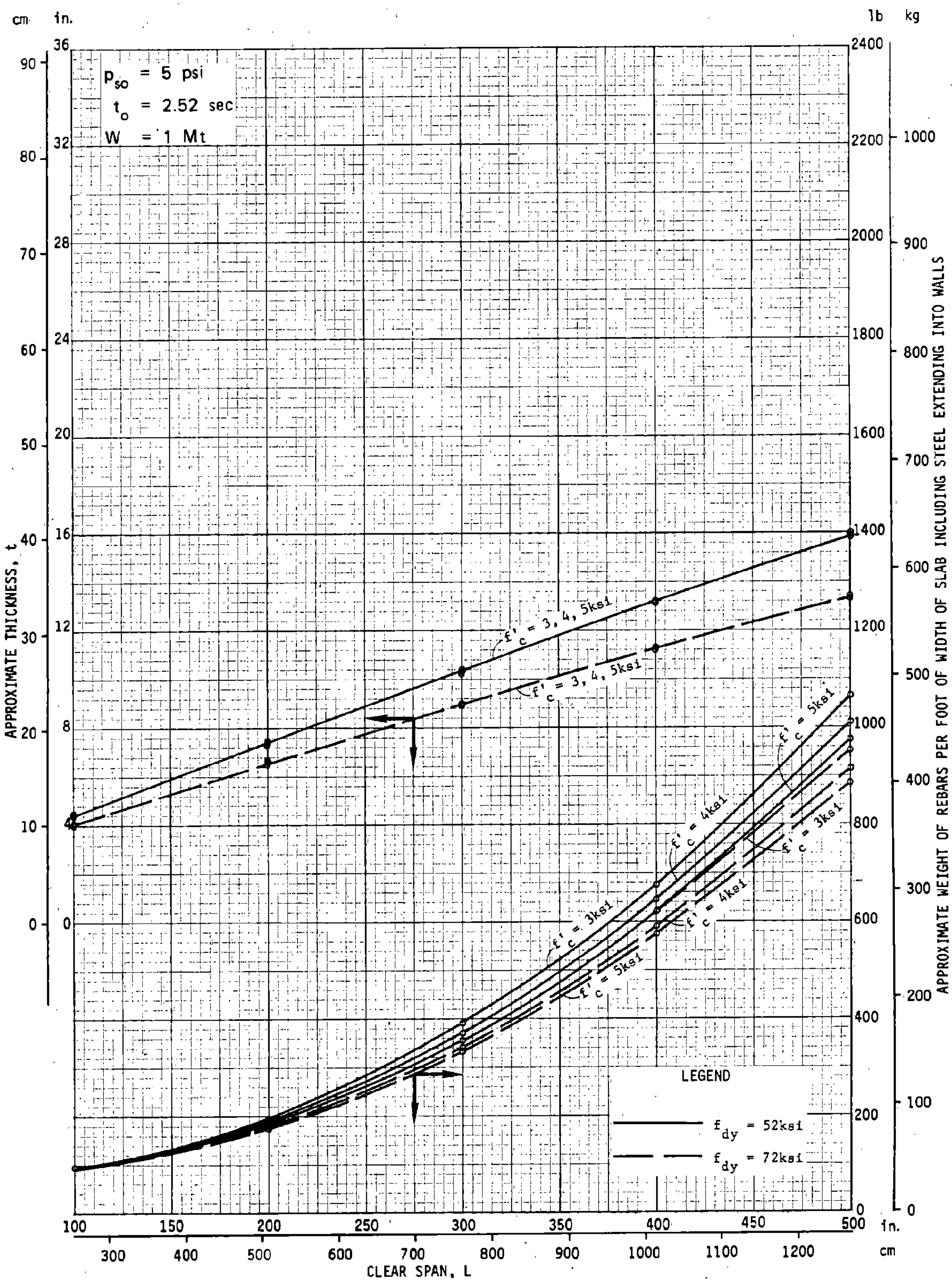

FIG. 6-7B ONE-WAY SLABS, SIMPLY SUPPORTED
Approximate Weight and Thickness – p = 0.020 (5 psi)

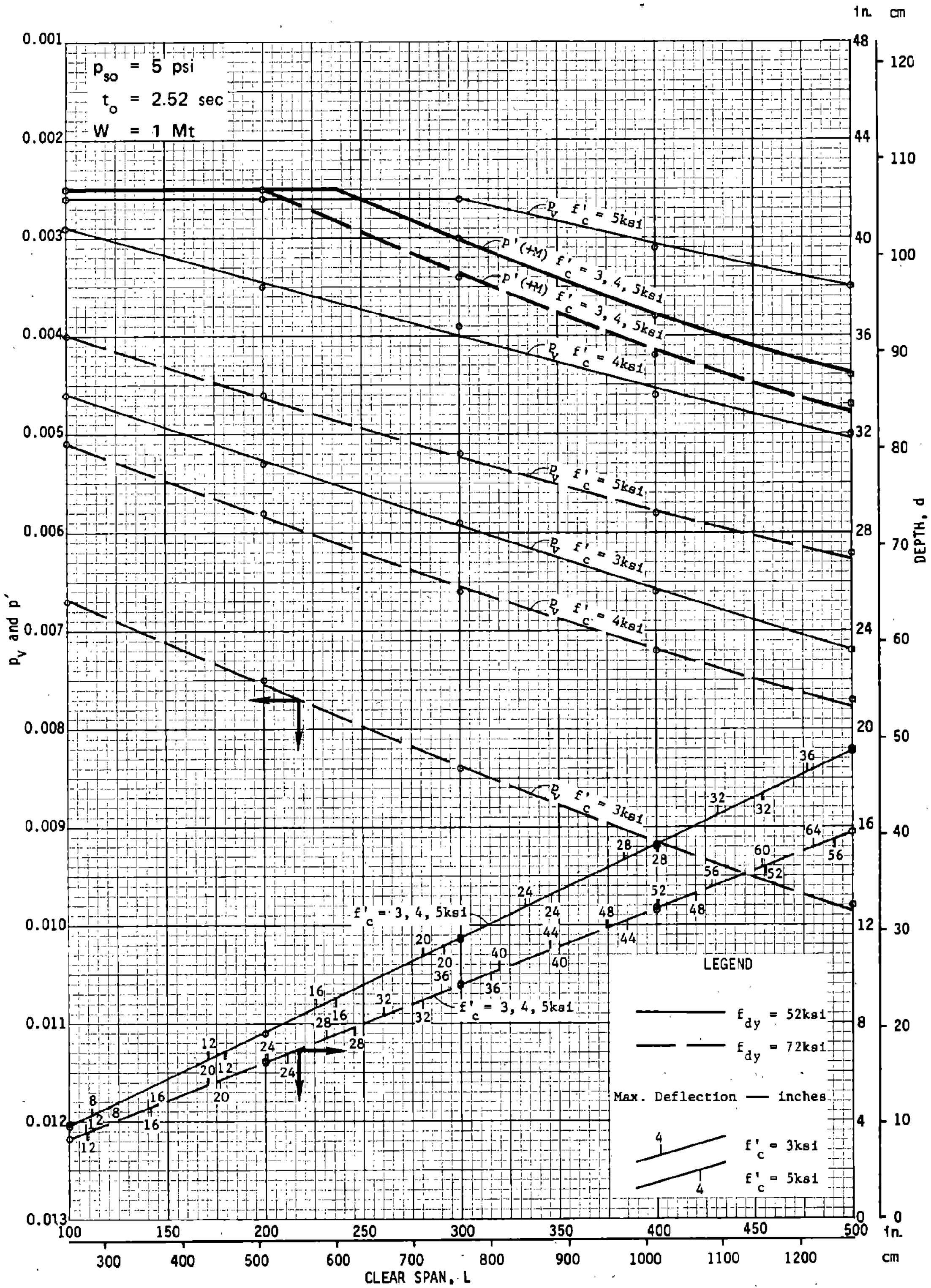

FIG. 6-7C ONE-WAY SLABS, SIMPLY SUPPORTED
Typical Designs — p = 0.010 (5 psi)

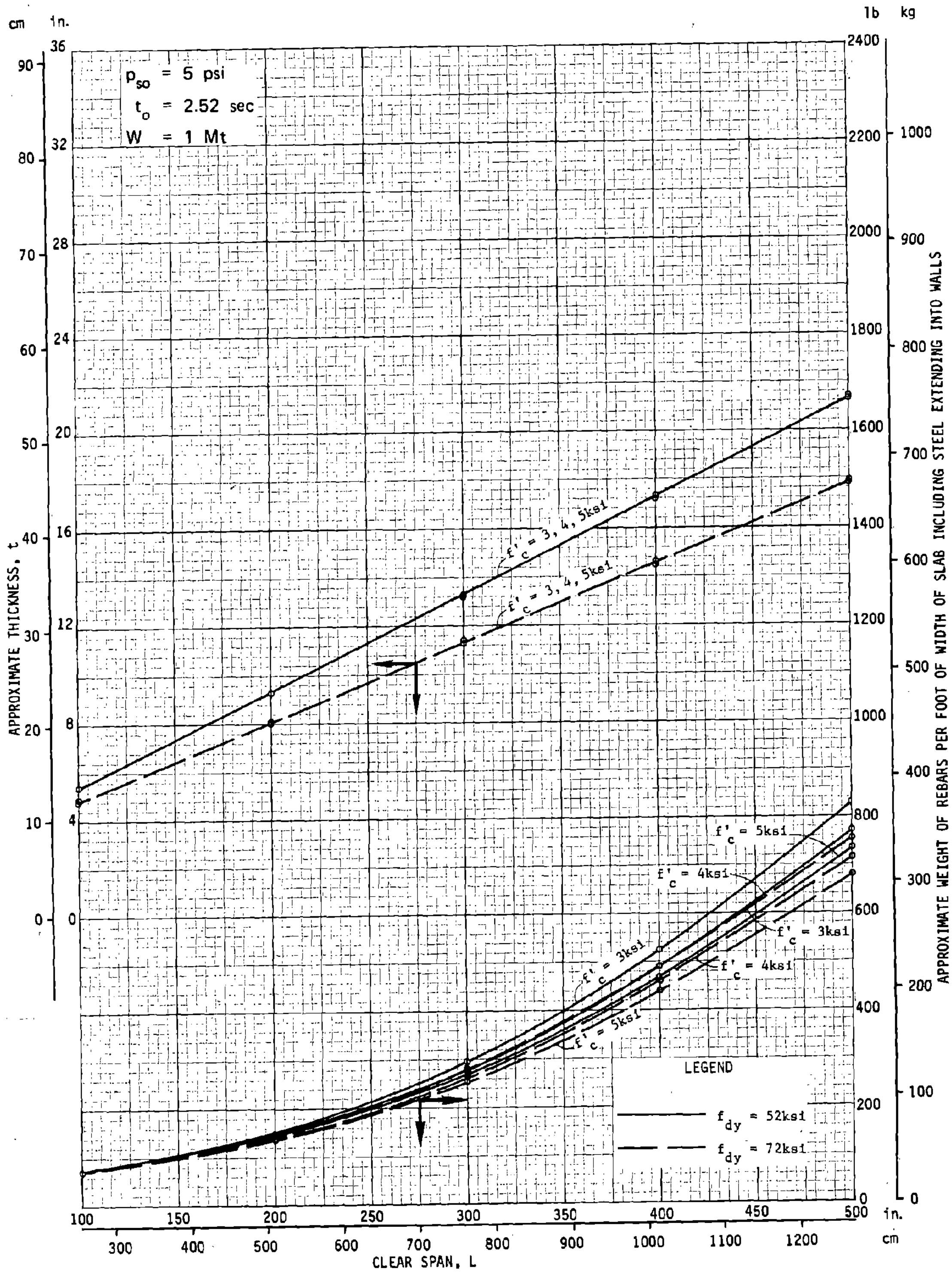

FIG. 6-7D ONE-WAY SLABS, SIMPLY SUPPORTED
Approximate Weight and Thickness – p = 0.010 (5 psi)

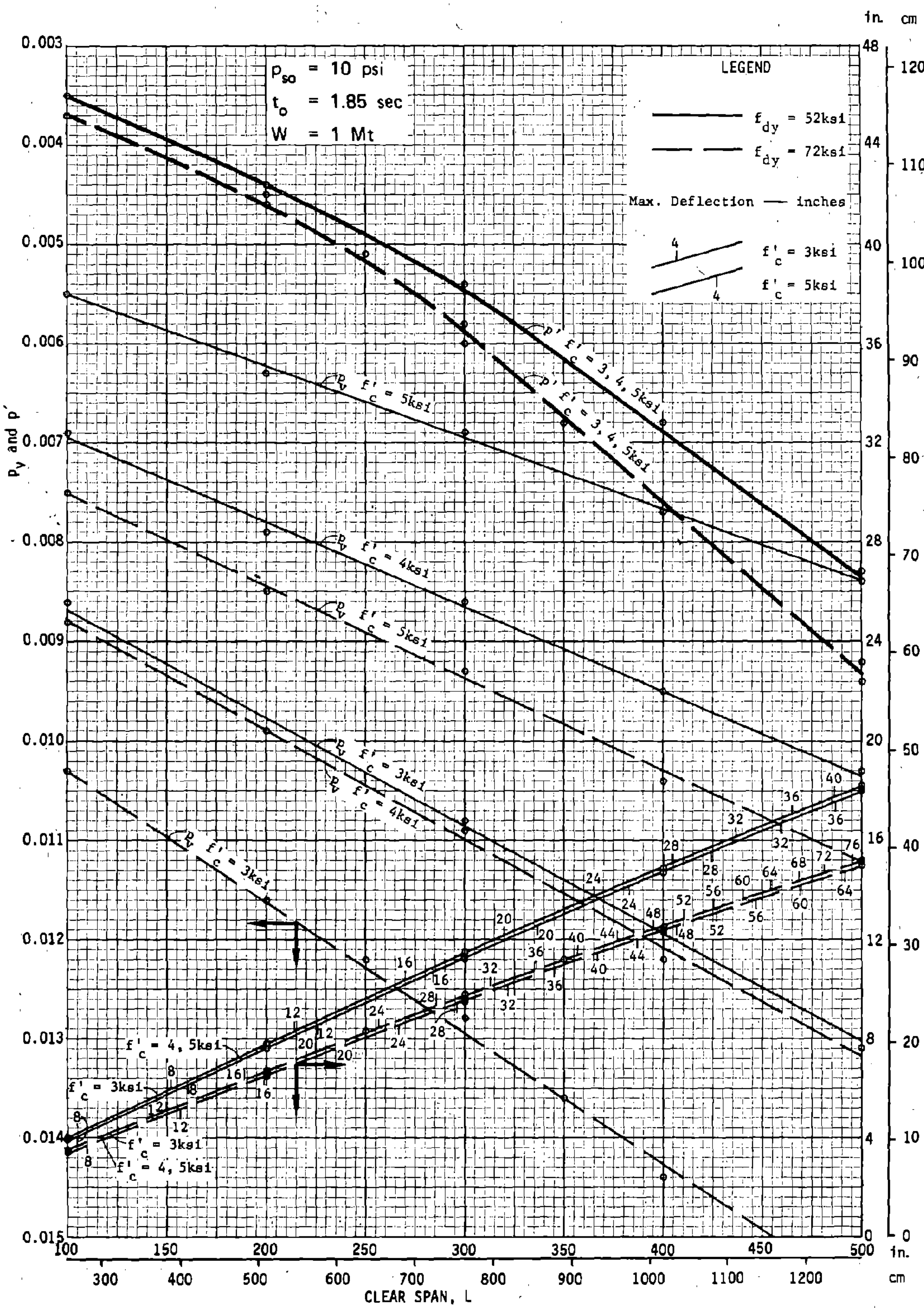

FIG. 6-7E ONE-WAY SLABS, SIMPLY SUPPORTED
Typical Designs — p = 0.020 (10 psi)

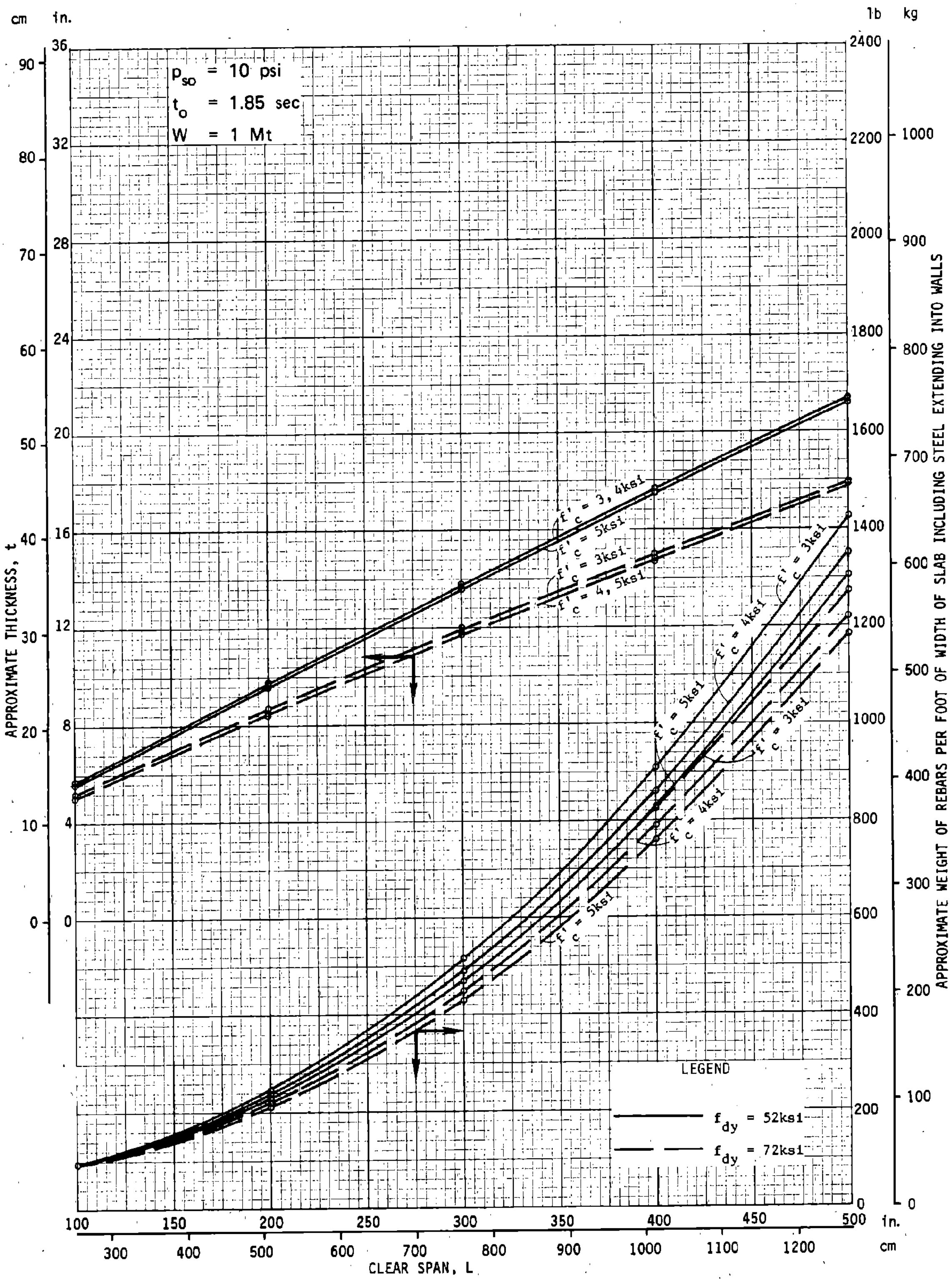

FIG. 6-7F ONE-WAY SLABS, SIMPLY SUPPORTED
Approximate Weight and Thickness – p = 0.020 (10 psi)

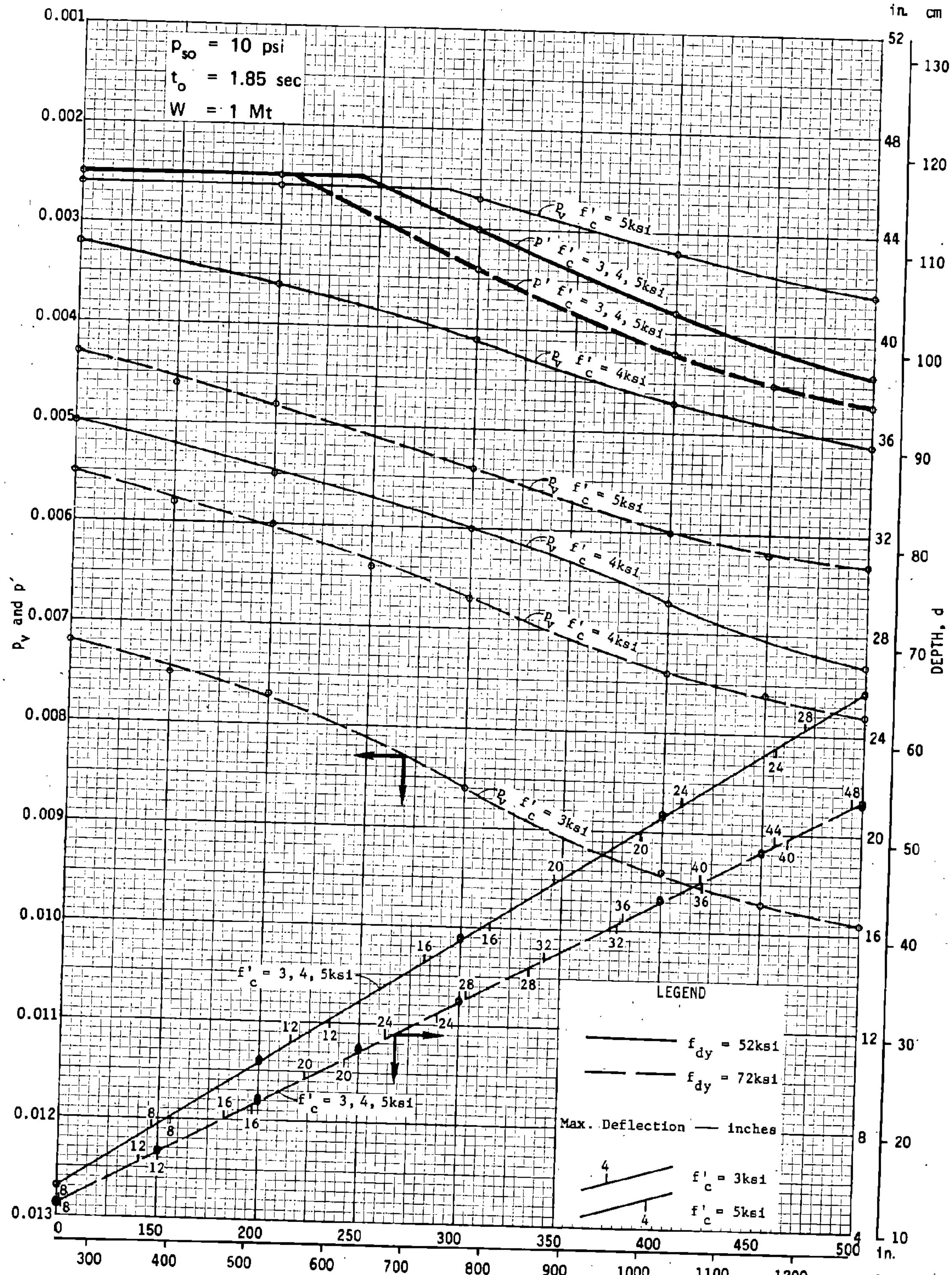

FIG. 6-7G ONE-WAY SLABS, SIMPLY SUPPORTED
Typical Designs – p = 0.010 (10 psi)

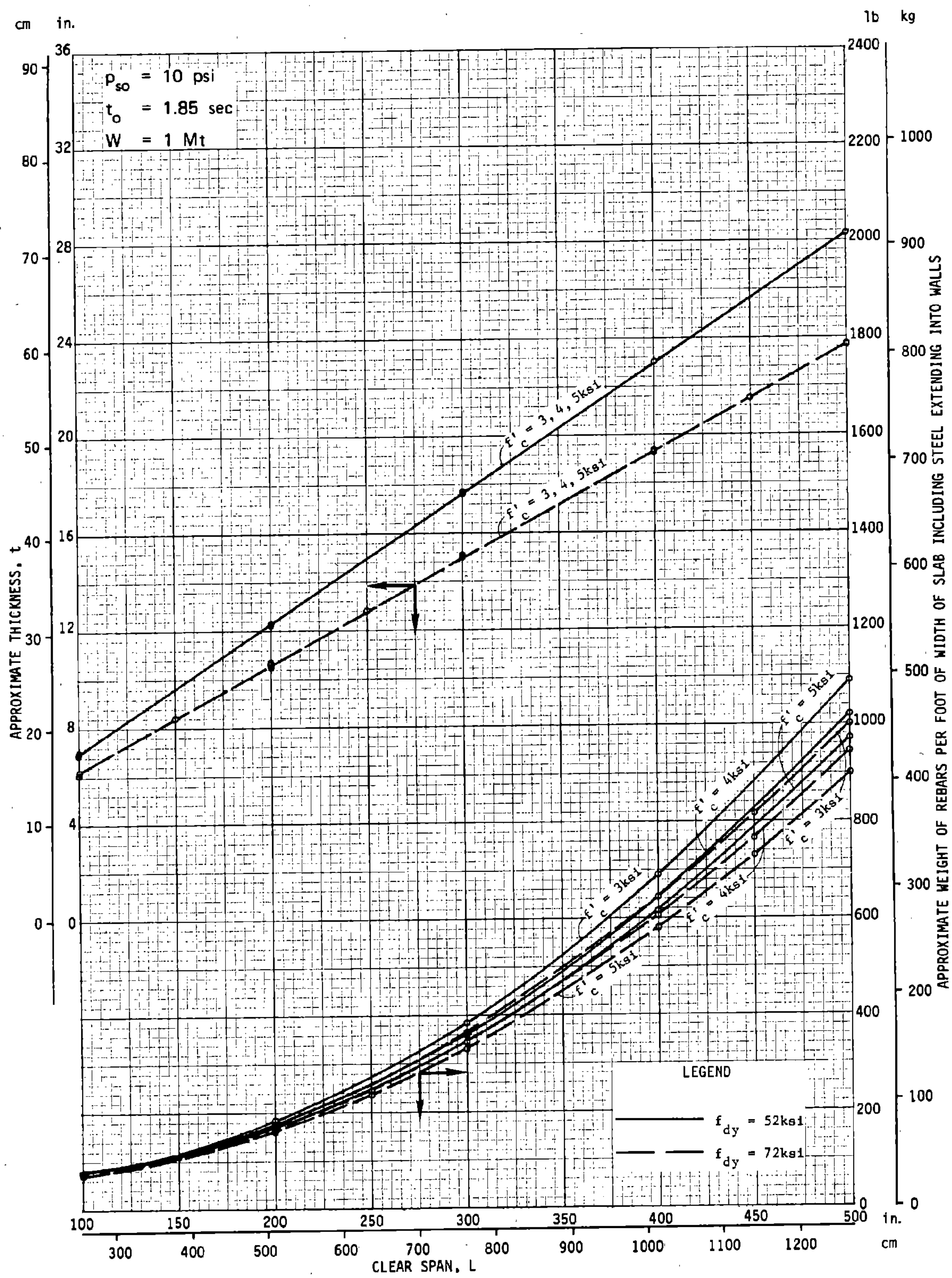

FIG. 6-7H ONE-WAY SLABS, SIMPLY SUPPORTED
Approximate Weight and Thickness – p = 0.010 (10 psi)

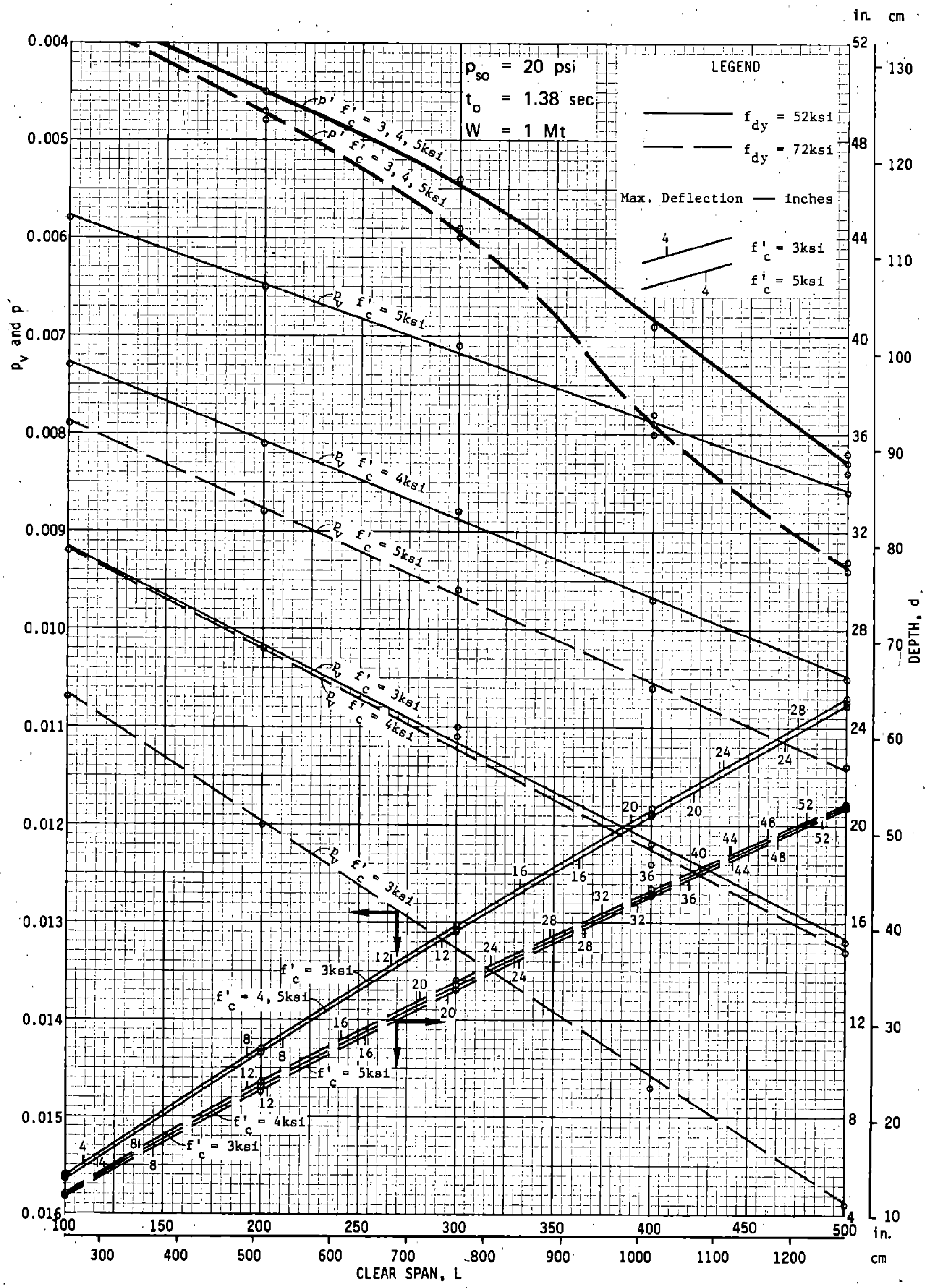

FIG. 6-71 ONE-WAY SLABS, SIMPLY SUPPORTED
Typical Designs — p = 0.020 (20 psi)

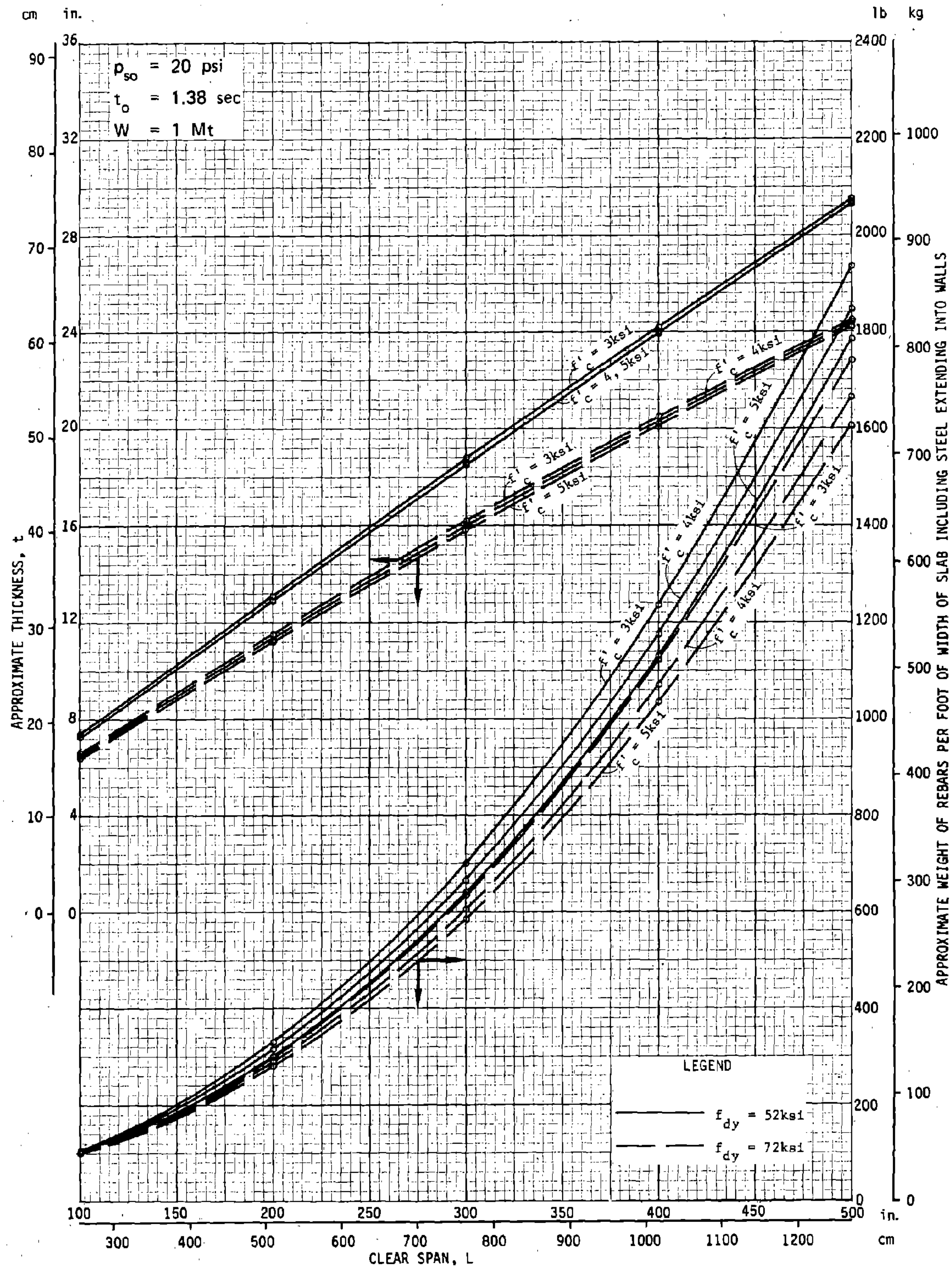

FIG. 6-7J ONE-WAY SLABS, SIMPLY SUPPORTED
Approximate Weight and Thickness – p = 0.020 (20 psi)

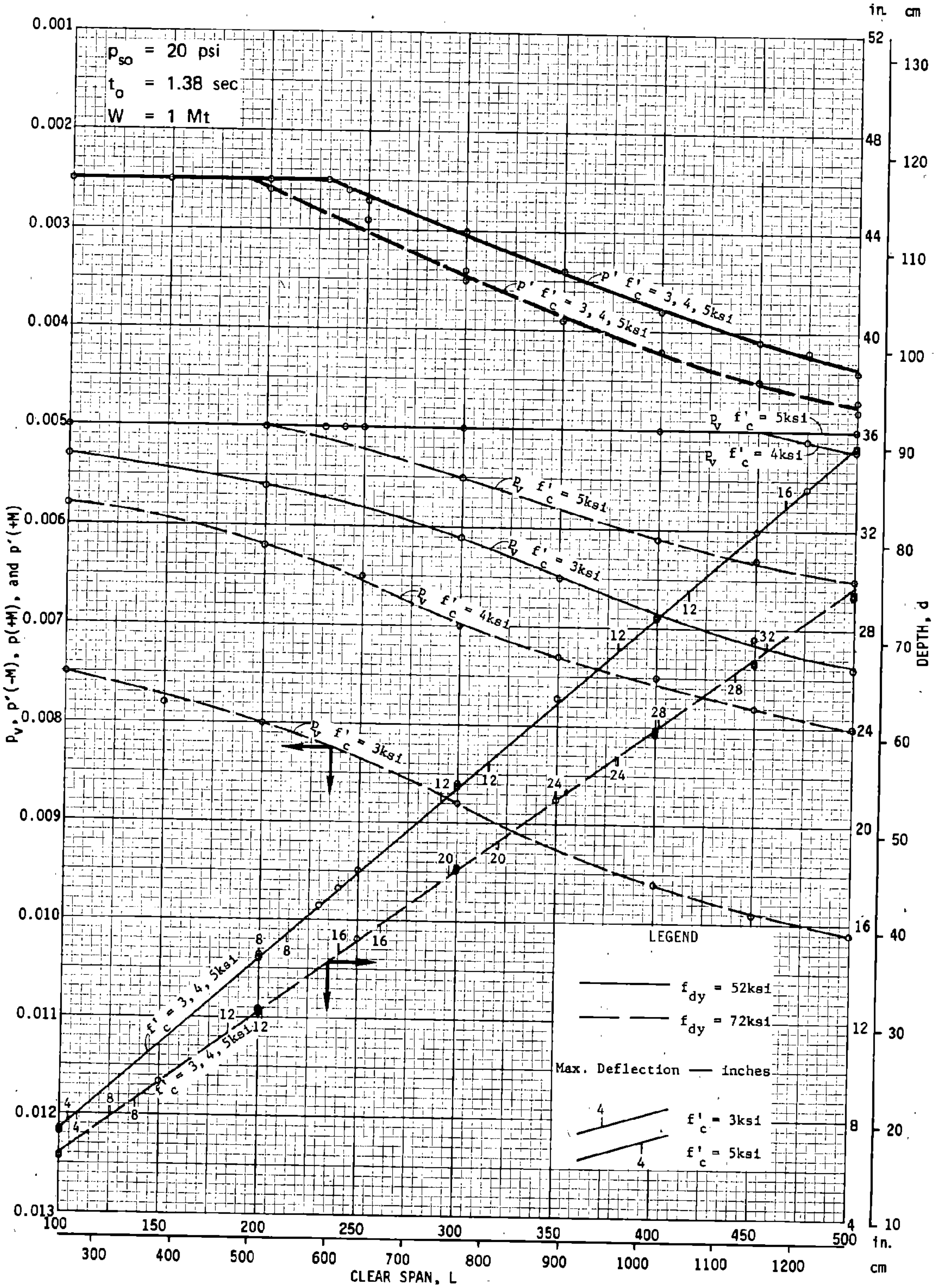

FIG. 6-7K ONE-WAY SLABS, SIMPLY SUPPORTED
Typical Designs – p = 0.010 (20 psi)

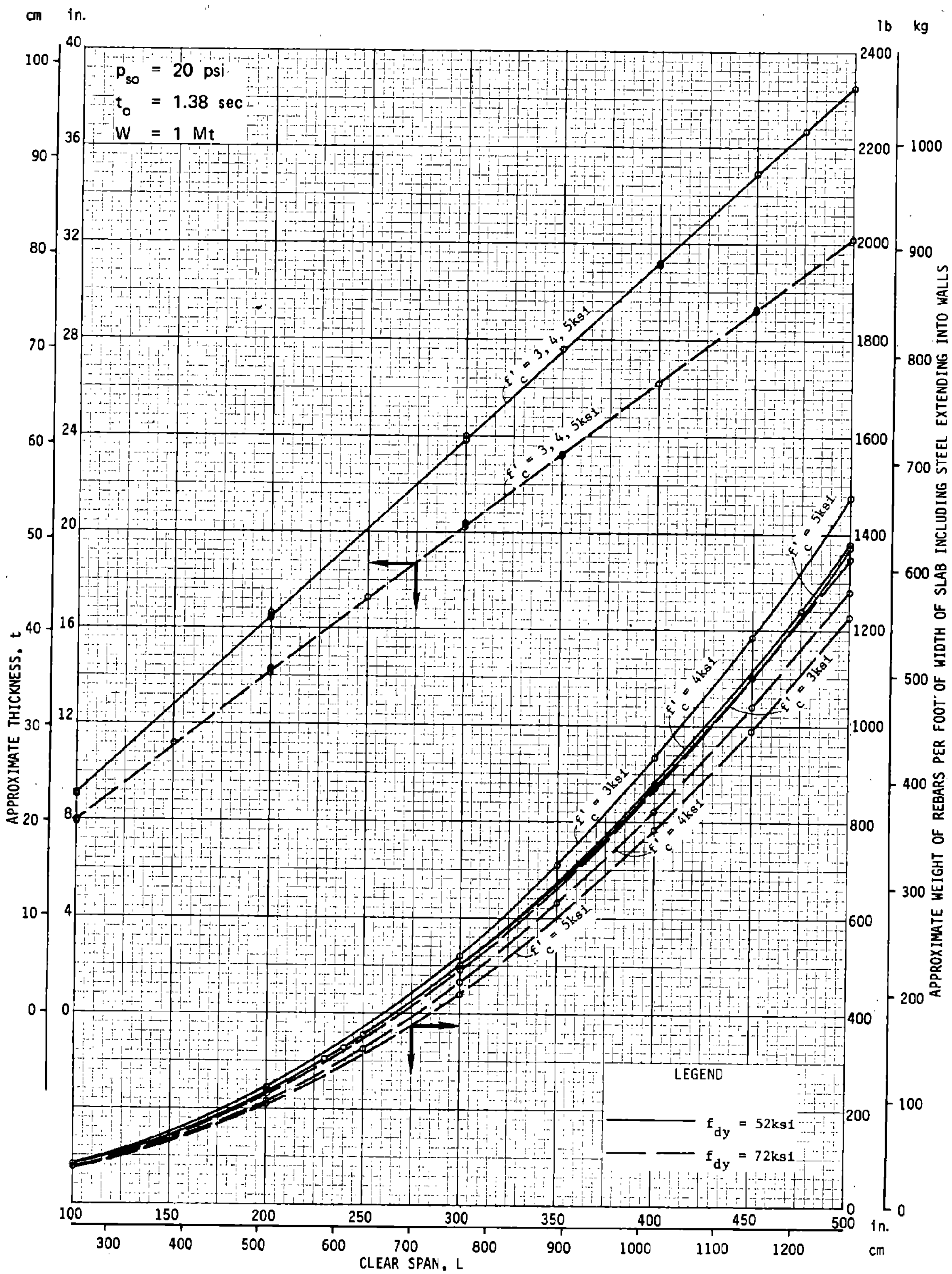

FIG. 6-7L ONE-WAY SLABS, SIMPLY SUPPORTED
Approximate Weight and Thickness — p = 0.010 (20 psi)

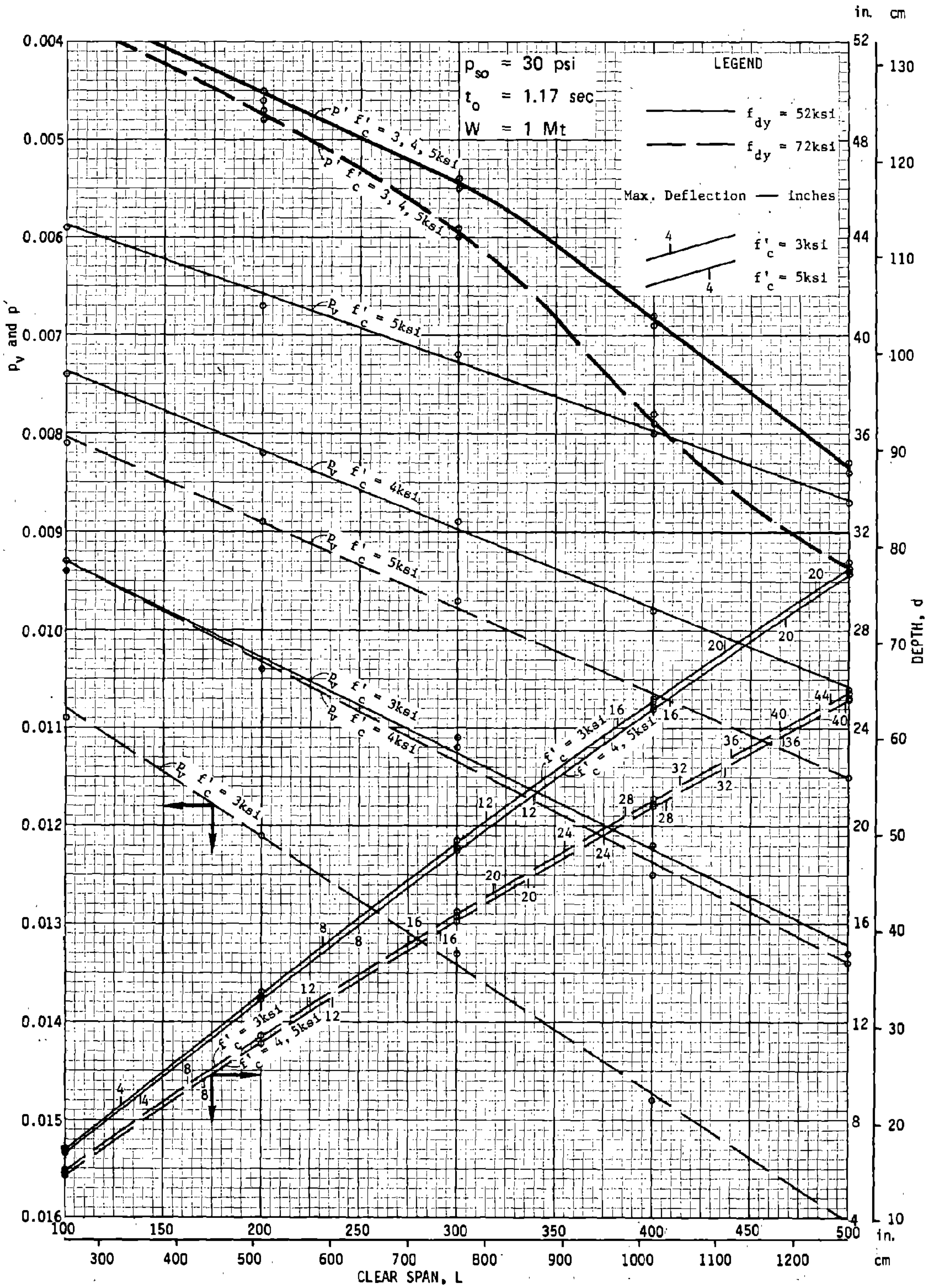

FIG. 6-7M ONE-WAY SLABS, SIMPLY SUPPORTED
Typical Designs — p = 0.020 (30 psi)

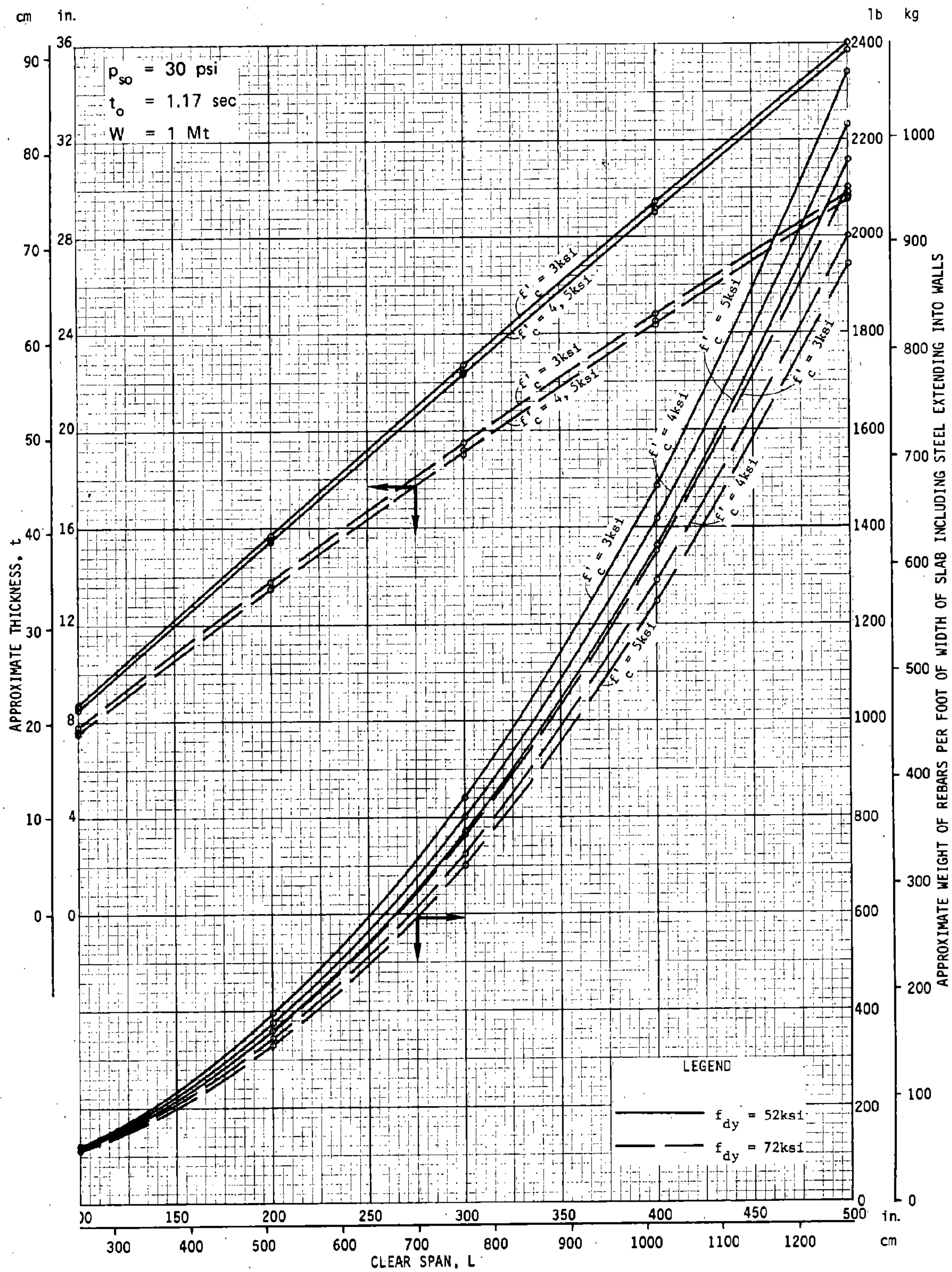

FIG. 6-7N ONE-WAY SLABS, SIMPLY SUPPORTED
Approximate Weight and Thickness – p = 0.020 (30 psi)

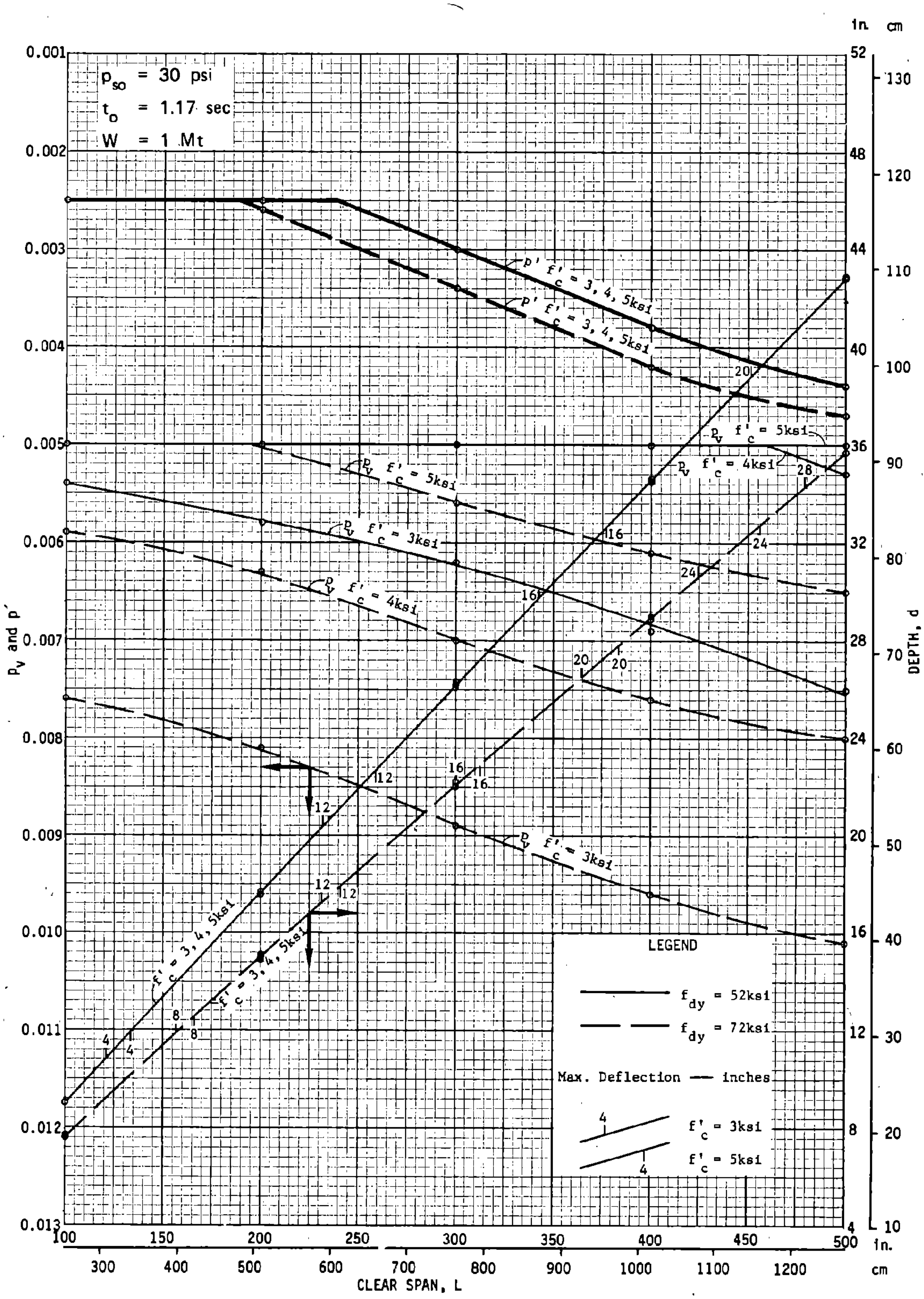

FIG. 6-70 ONE-WAY SLABS, SIMPLY SUPPORTED
Typical Designs — p = 0.010 (30 psi)

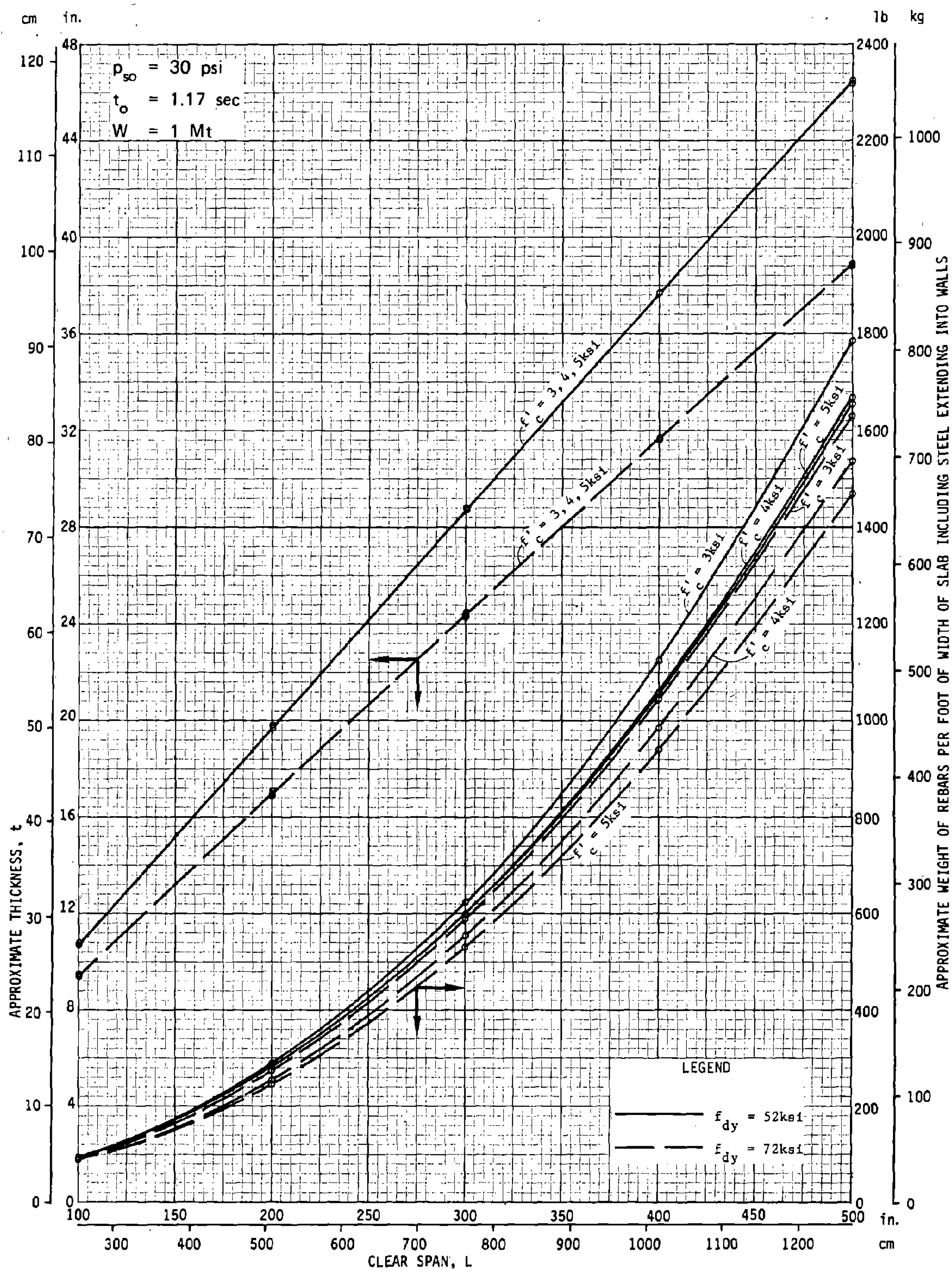

FIG. 6-7P ONE-WAY SLABS, SIMPLY SUPPORTED
Approximate Weight and Thickness – p = 0.010 (30 psi)

B. One-Way Slabs - Continuous

For one-way slabs continuous over two equal spans on simple supports, each span may be designed as a propped cantilever (PC). For one-way slabs continuous over three or more equal spans on simple supports, a departure from normal design procedure is justified; because of the large deflections and mostly plastic behavior contemplated in protective design, one is justified in using design procedures for PC and fixed ends (FF) single-span slabs on simple supports. Thus, for three or more equal spans over simple supports, the PC designs may be used for the end spans and the FF designs for the intermediate spans, for preliminary design if not for final. The slight rotation on the interior simple supports incident to the elastic phase becomes inconsequential as soon as plastic hinges form at the supports.*

The high shear values that may develop along slab edges must be given careful attention (check from edge inward about 1.5 d).[31]

For one-way slab designs that include moment continuity with outer walls, several interaction and other problems arise that are outside the scope of this section.

Final Design Procedure. As before, this procedure was to be used in preparing typical designs† and is probably more elaborate than would be justified in normal or infrequent design use. The final design steps selected parallel those in the simply supported case and were:

1a. Prepare moment and shear diagrams for uniform load conditions and the support conditions prevailing. For a continuous slab with constant span and simple supports, such diagrams are available in handbooks.[3,19] The typical designs herein cover only two continuous slab situations, the propped cantilever (PC) and the single span with fixed ends (FF), which are therefore highlighted in the design steps that follow and which parallel those in the final design procedure for the simply supported (SS) slabs.

1b. Assume values for basic parameters, as before (in the final design procedure for simply supported one-way slabs). Use p and p′ (not p_e and p_e') in $\mu = 0.1/(p-p') \le 10$, if used as before.

---

* Alternatively, using a spans ratio of 1:1.225, for interior (FF) span(s) to end (PC) spans, eliminates the elastic rotation over the the simple interior supports, a rotation expected when interior and end spans are equal. This specific ratio is for a prismatic member on simple supports in a 3-span bent.

† Some (15 psi) chart solutions are described in, and follow, the next section.

2a. Assume a peak value of flexural q, using Figure 6-1[50] for guidance, as before. Calculate a trial set of slab dimensions, based on the maximum end moment, using Equation 6-1 with $c = 1/8$ for PC, 1/12 for FF, and p_e substituted for p (denoting end tensile steel, reserving p for maximum positive moment tensile steel). $p_e = 0.02$ was selected for initial use, per the Table 6.2 criterion for p. Equation 4, Table 6.2, applies to any cross-section of the member, meaning that both $(p-p')$ and (p_e-p_e') must satisfy Equation 4.

2b. Vary p (but ≥ 0.005*) in Equation 6-1, as appropriate to meet maximum positive moment requirements, using $c = 9/128$ for PC, 1/24 for FF. Equation 6-1 may be solved for p, leading to the following form:

$$p = 0.5\left[c_1 - \sqrt{c_1^2 - 4c_1/c_2}\right] \qquad (6\text{-}13)$$

where

$$c_1 = 1.91787\ f_c'/f_{dy}$$

$$c_2 = (b/a)\ f_{dy}(d/L)^2/(cq)$$

3. Calculate I, K, and T by using Equations 6-2, 6-3,† and 6-4, with appropriate changes in constants: in Equation 6-2, k' changes with p (use Figure 6-4); in Equation 6-3, $c' = 160$ for PC, 307 for FF; and in Equation 6-4, $c'' = 638{,}000$ for PC, 850,000 for FF.[2] (Use p not p_e in Equations 6-2 and 6-4.[31])

4. Calculate the rebound steel p' as before (in the simply supported case), then use

$$p_e' = p'p_e/p \qquad (6\text{-}14)$$

where p_e' is the compression steel ratio at the moment-resisting end (PC) or ends (FF). Minimum $p' = 0.0025$,* as should p_e'.

---

* Table 6.2 (footnote† particularly).

† K for continuous beams and one-way slabs is an equivalent elastic phase stiffness (k_1 on p. 11-4, Ref. 50) to simplify the bilinear "elastic" phase of the resistance function that results from formation of a positive moment hinge and a negative moment hinge (PC) or two (FF), with the "elastic" phase ending when all hinges have been formed. The flexural q value is used to complete the resistance function (see k_2 on p. 11-4, Ref. 50). Stated another way, what should be a trilinear resistance function is replaced by an equivalent bilinear elasto-plastic resistance function (as on p. 11-4, Ref. 50).

5. Modify d (or L) slightly, to satisfy Equation 6-6 with $c = 1/8$ for PC, 1/12 for FF. Use p_e and p_c' to replace p and p', respectively. (To check flexural adequacy for maximum positive moment, use Equation 6-6, as written with p and p' and with $c = 9/128$ for PC, 1/24 for FF.)

6. Using the revised dimensions obtained from Equation 6-6, steps 3, 4, and 5 were repeated once before proceeding to step 7, to smooth the design graph plots. For usual design, this step 6 may be omitted.

7. Estimate Δp_{so} using Equations 6-7 and 6-8, as before.

8. Use the Newmark β Method or its modification, with appropriate load-mass factors (unchanged for PC and FF, from the SS case), and solve for μ, as before.

9. If the calculated μ is not acceptable, assume a new q and repeat the foregoing procedure, also as before (steps 2 through 8).

10. Design for diagonal tension requirements, using Equations 6-9a and 6-9b as follows:*

    In Equation 6-9a, C = 1 for symmetrically supported spans (FF) and, for other spans (PC),

$$C = 1 + 0.25\,(\text{max. } p_e - \text{min. } p_e)/p \qquad (6\text{-}15)$$

    where min. p_e is taken as zero for a simply supported end.

    In Equation 6-9b, for both PC and FF:

$$C' = 1 + 1.5\,(\text{average } p_e)/p \qquad (6\text{-}16)$$

    where p_e is taken as zero for the simply supported end of a PC.

11. Design for pure shear as before, using Equation 6-10 with $C'' = 1$ for symmetrically supported spans (FF) and, for other spans† (PC), $C'' = C$ (from Equation 6-15).*

---

* Should different values of d be used for maximum positive and negative moment sections, it is recommended that the smaller d of the two, usually the positive moment d, be used for this design step.

† From Equation 8-14 of Reference 2.

12. Check for bond, as before. The constant of Equation 6-11, 1/2, is unchanged for FF, but becomes 5/8 for PC fixed end and 3/8 for PC free end.

Rebar Design and Details. The general scheme used for FF and PC cases is identical to that for the SS case (Figure 6-5 and related text).

For estimating rebar quantities, the formulas for the SS case (Table 6.5) must be modified in one regard only, that is, rebar length required for PC and FF cases is less than for the SS case because intermediate supports (PC and FF) take less rebar length than end anchorages. Hence, Table 6.5 as shown can be used for estimating all rebar quantities except rebar length for the PC and FF cases. For the PC case, rebar lengths for A_s and A_s' are approximated by (33.74 + 1.02935 L) and (25.67 + 1.04485 L), respectively.* For the FF case, rebar lengths for both A_s and A_s' are approximated by (24 + L).*

To both make estimated cost comparisons possible and provide for alternative designs, PC and FF one-way slab typical designs were prepared (similar to those shown in Figure 6-3A for SS slabs), for p_{so} = 15 psi and p_e ratios of 0.02, 0.015, and 0.01, Figure 6-8. Figure 6-8 also gives gross estimating quantities - thickness of concrete and weight of steel per foot width of slab. The computer program used is provided later herein (Appendix G - Supplement).

---

* Assumes 12 in. thick walls for both interior and end supports.

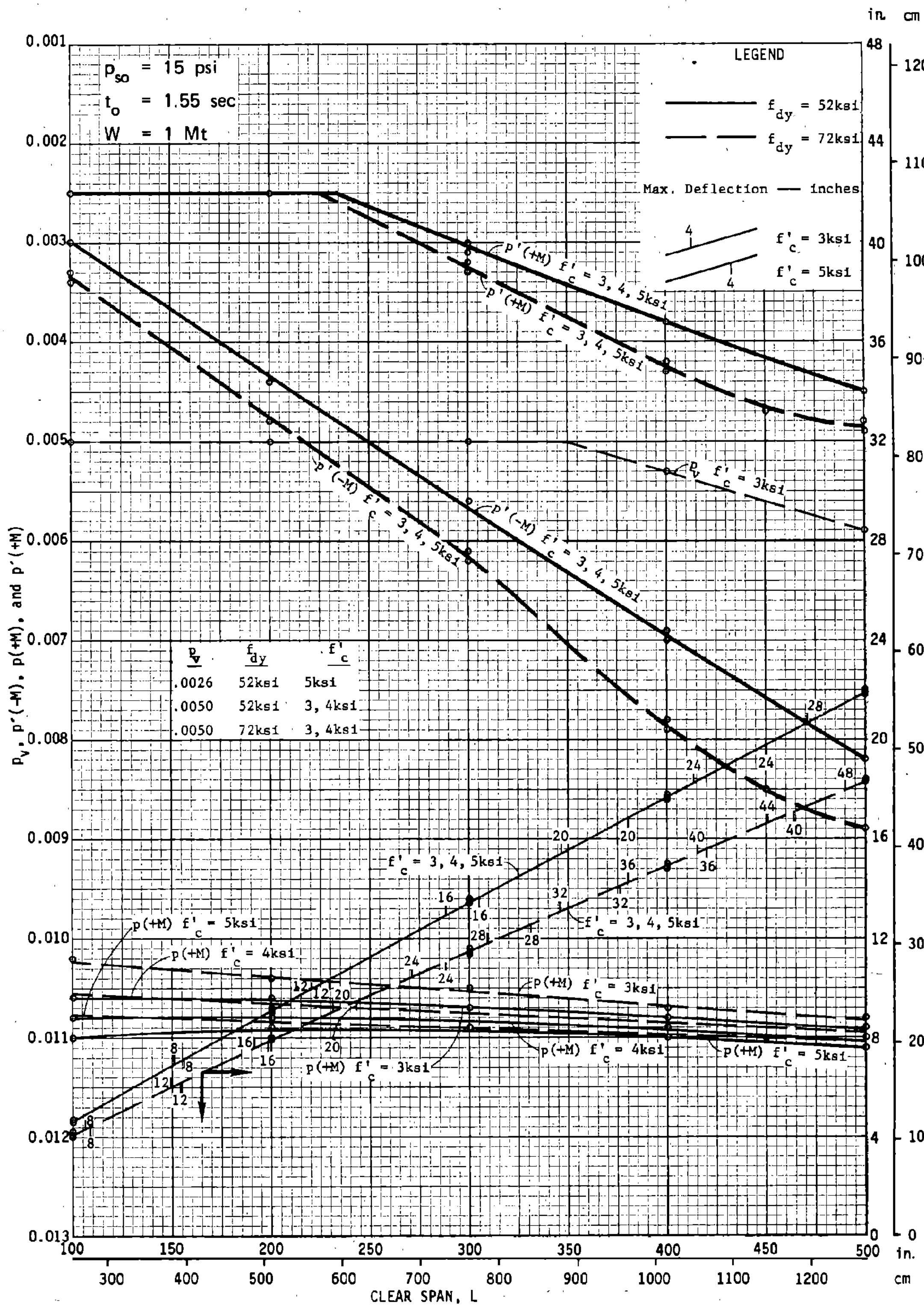

FIG. 6-8A ONE-WAY SLABS, PROPPED CANTILEVER
Typical Designs – p_e = 0.020 (15 psi)

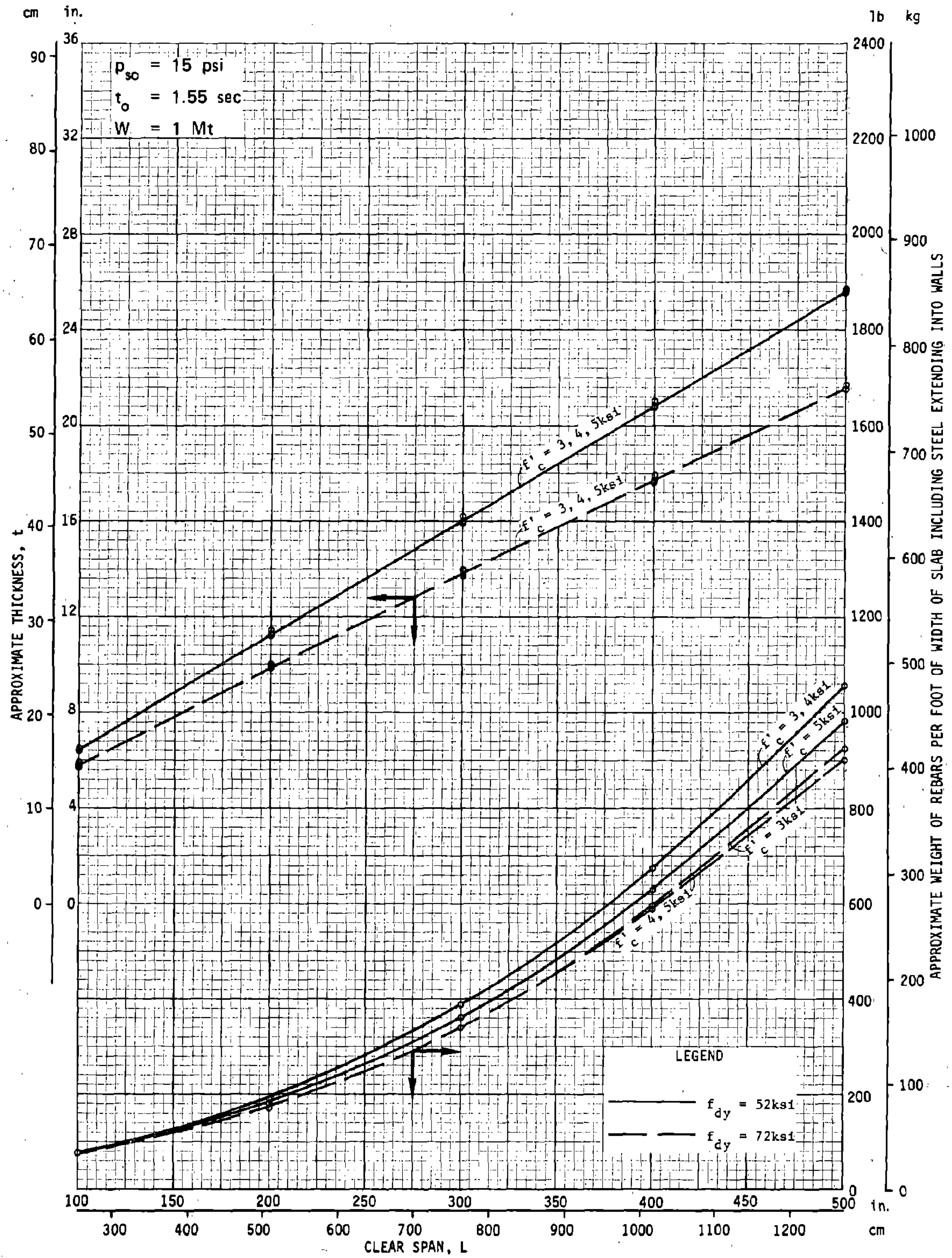

FIG. 6-8B ONE-WAY SLABS, PROPPED CANTILEVER
Approximate Weight and Thickness – p_e = 0.020 (15 psi)

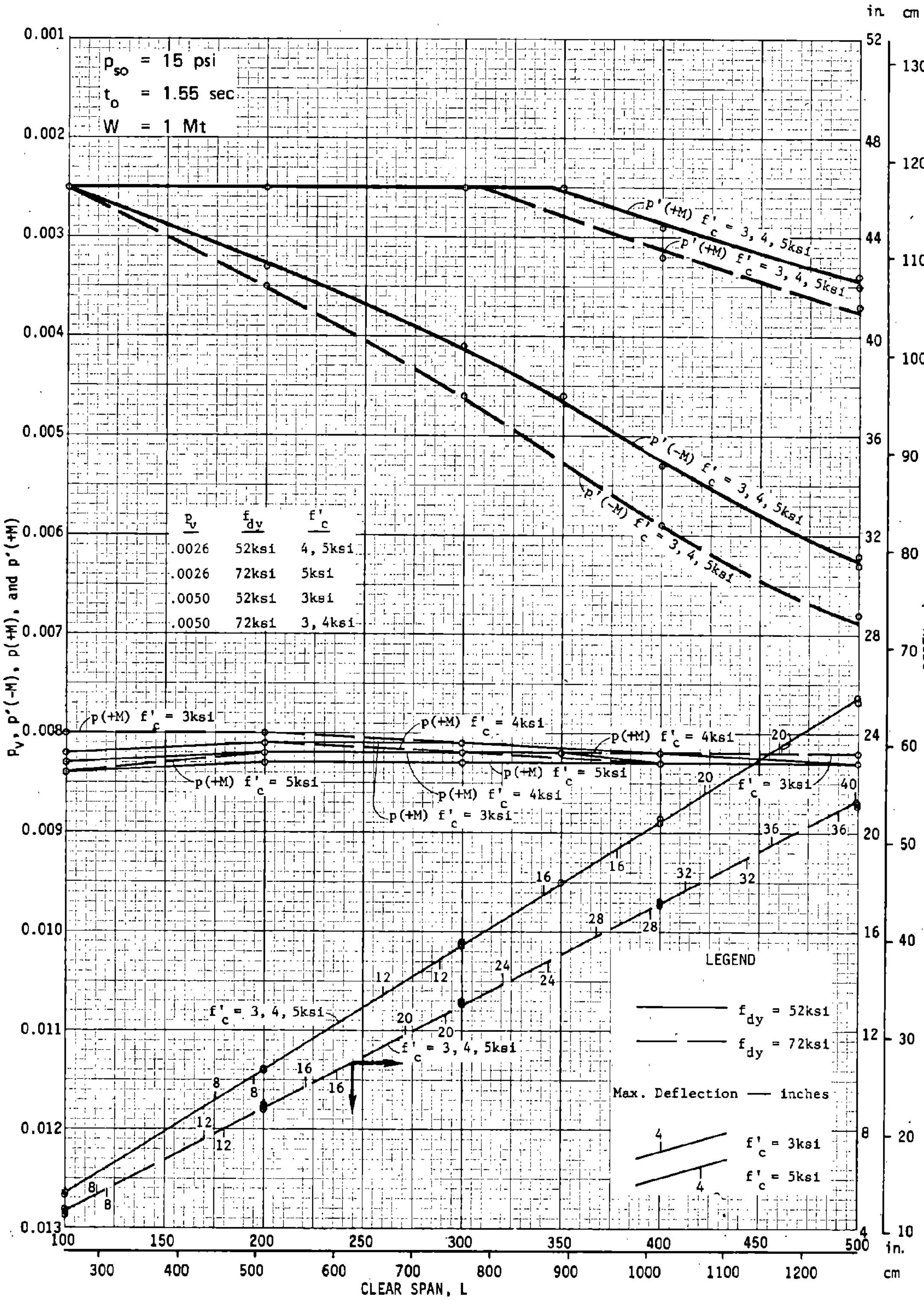

FIG. 6-8C ONE-WAY SLABS, PROPPED CANTILEVER
Typical Designs — p_e = 0.015 (15 psi)

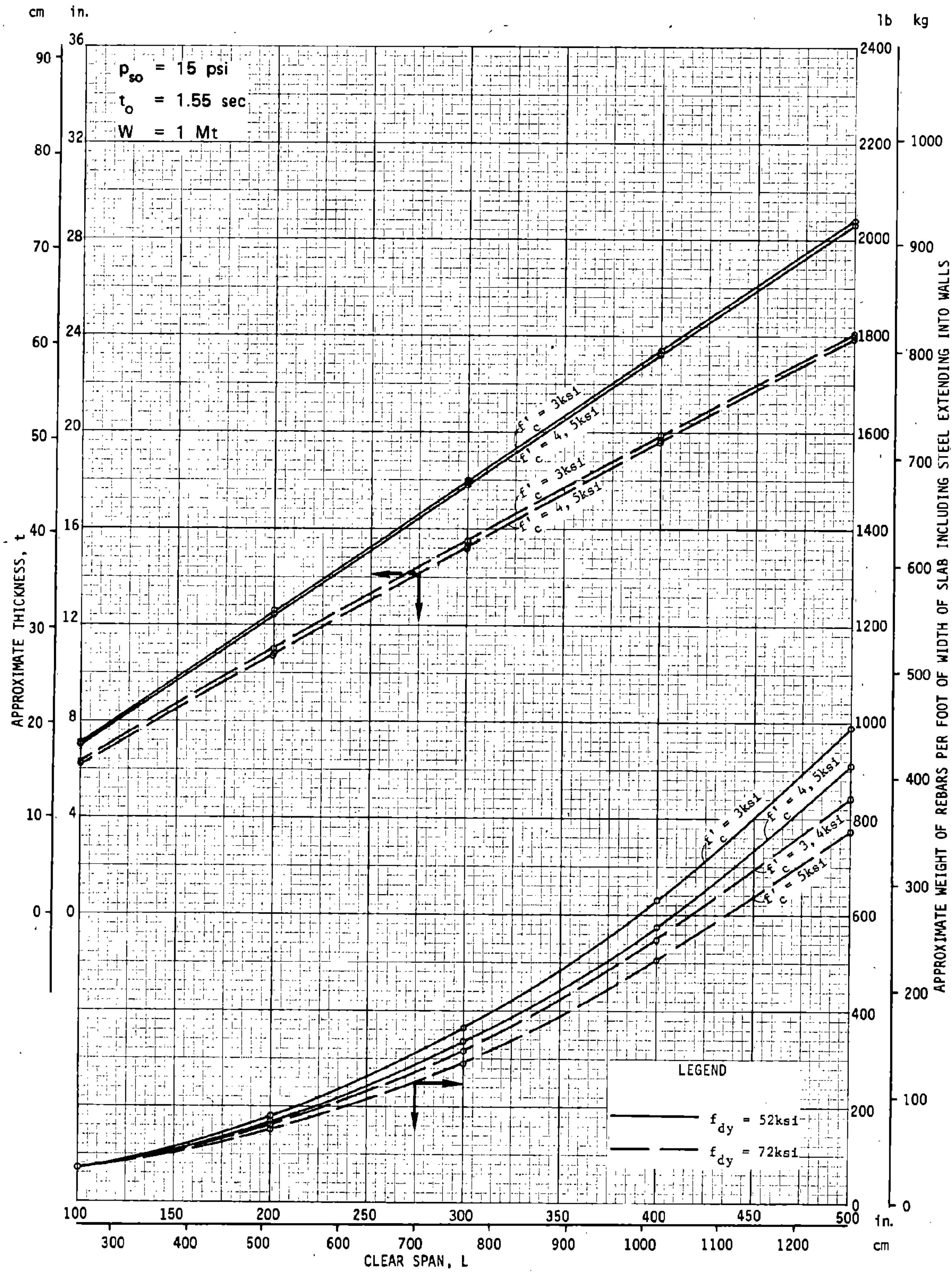

FIG. 6-8D ONE-WAY SLABS, PROPPED CANTILEVER
Approximate Weight and Thickness – p_e = 0.015 (15 psi)

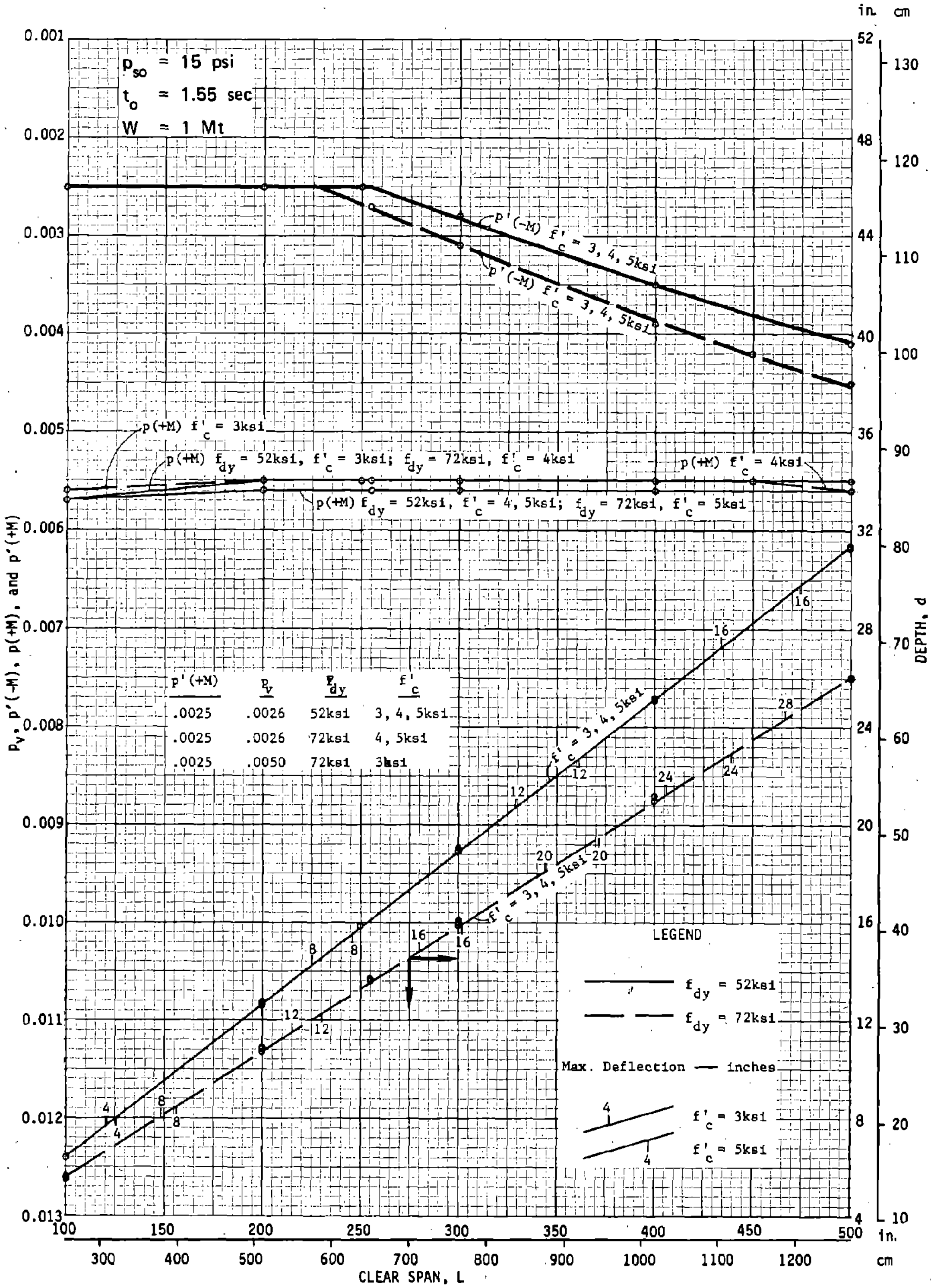

· FIG. 6-8E ONE-WAY SLABS, PROPPED CANTILEVER
Typical Designs – p_e = 0.010 (15 psi)

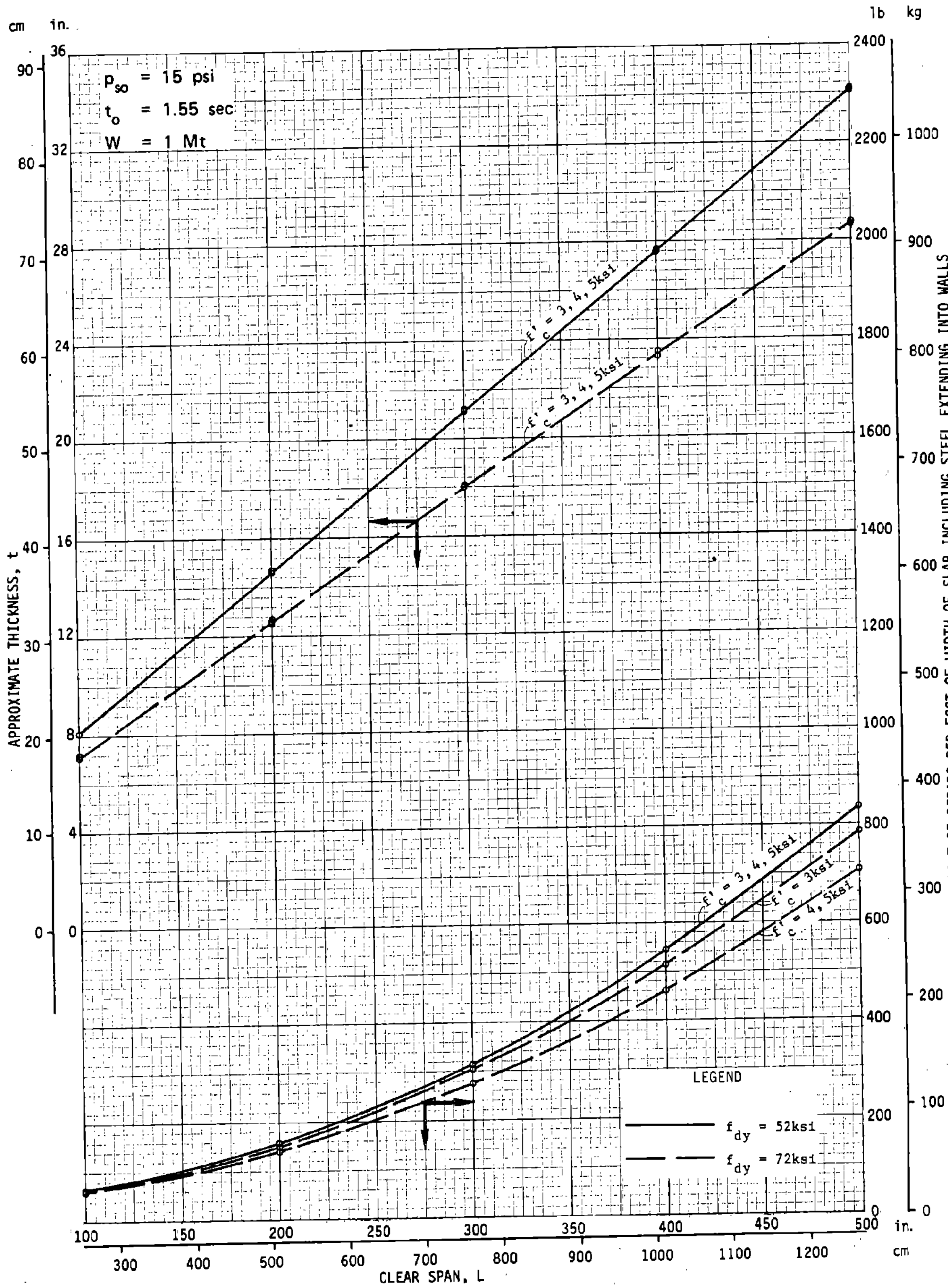

FIG. 6-8F ONE-WAY SLABS, PROPPED CANTILEVER
Approximate Weight and Thickness – p_e = 0.010 (15 psi)

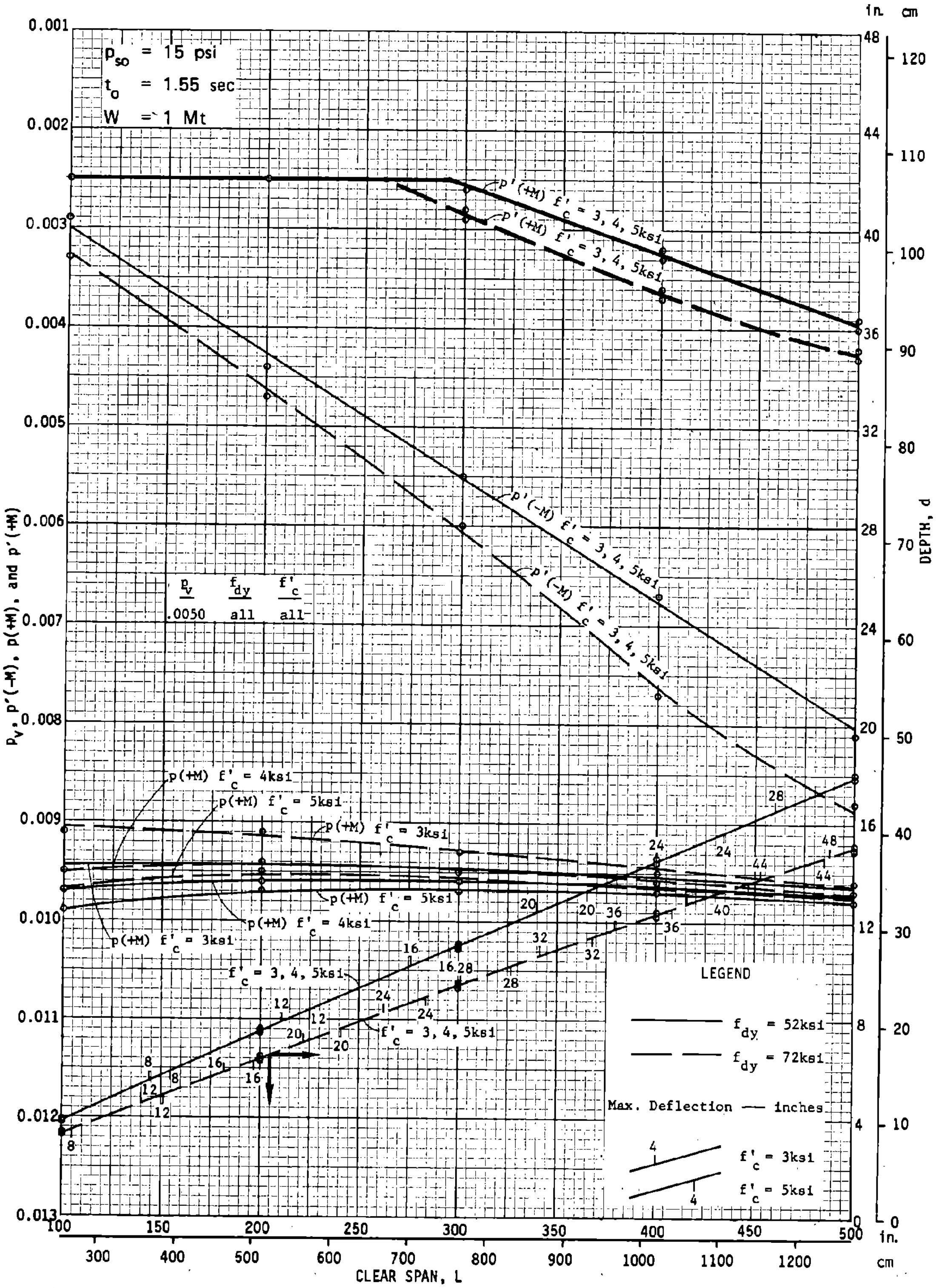

FIG. 6-8G ONE-WAY SLABS, FIXED ENDS
Typical Designs — p_e = 0.020 (15 psi)

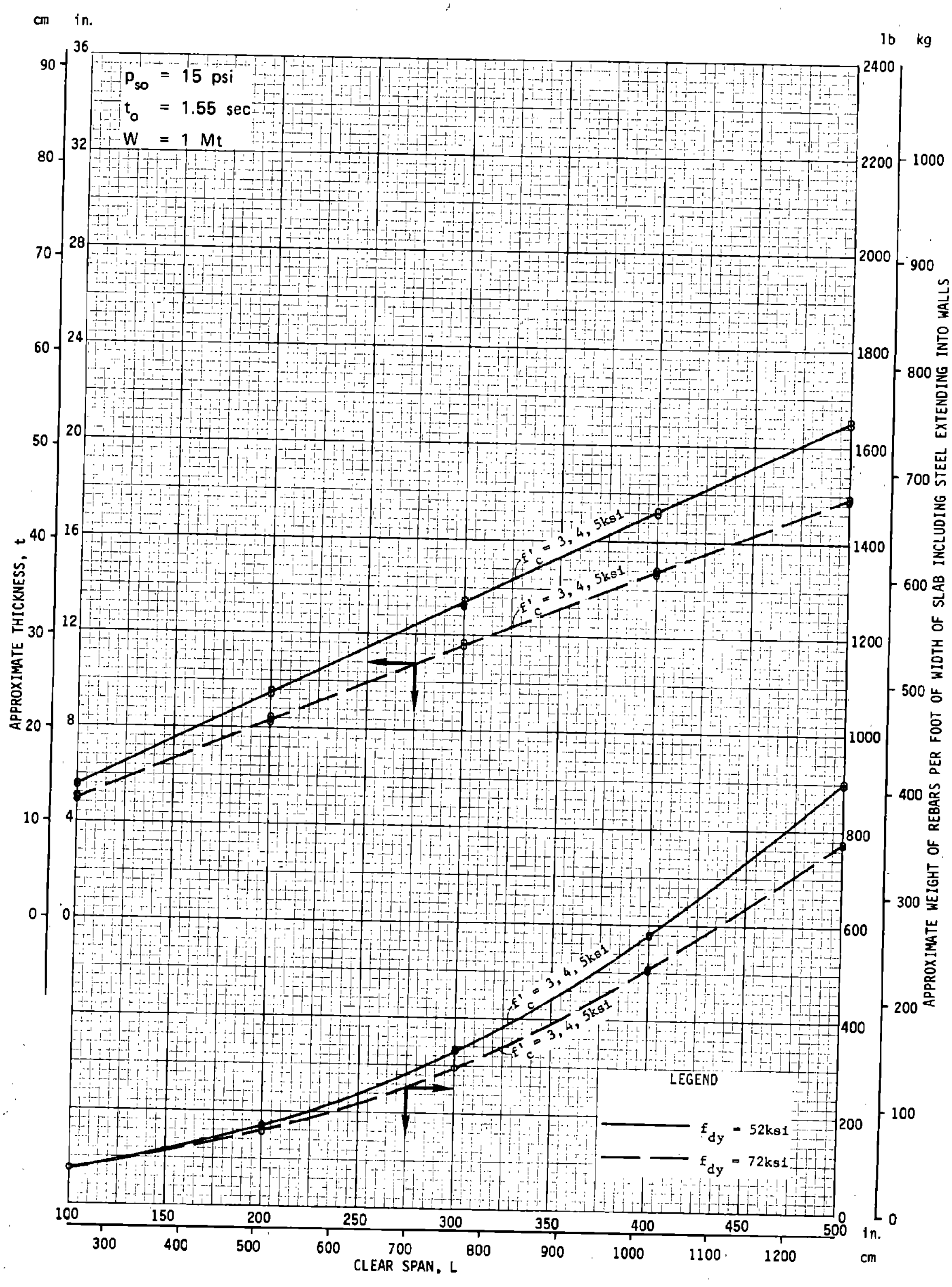

FIG. 6-8H ONE-WAY SLABS, FIXED ENDS
Approximate Weight and Thickness — p_e = 0.020 (15 psi)

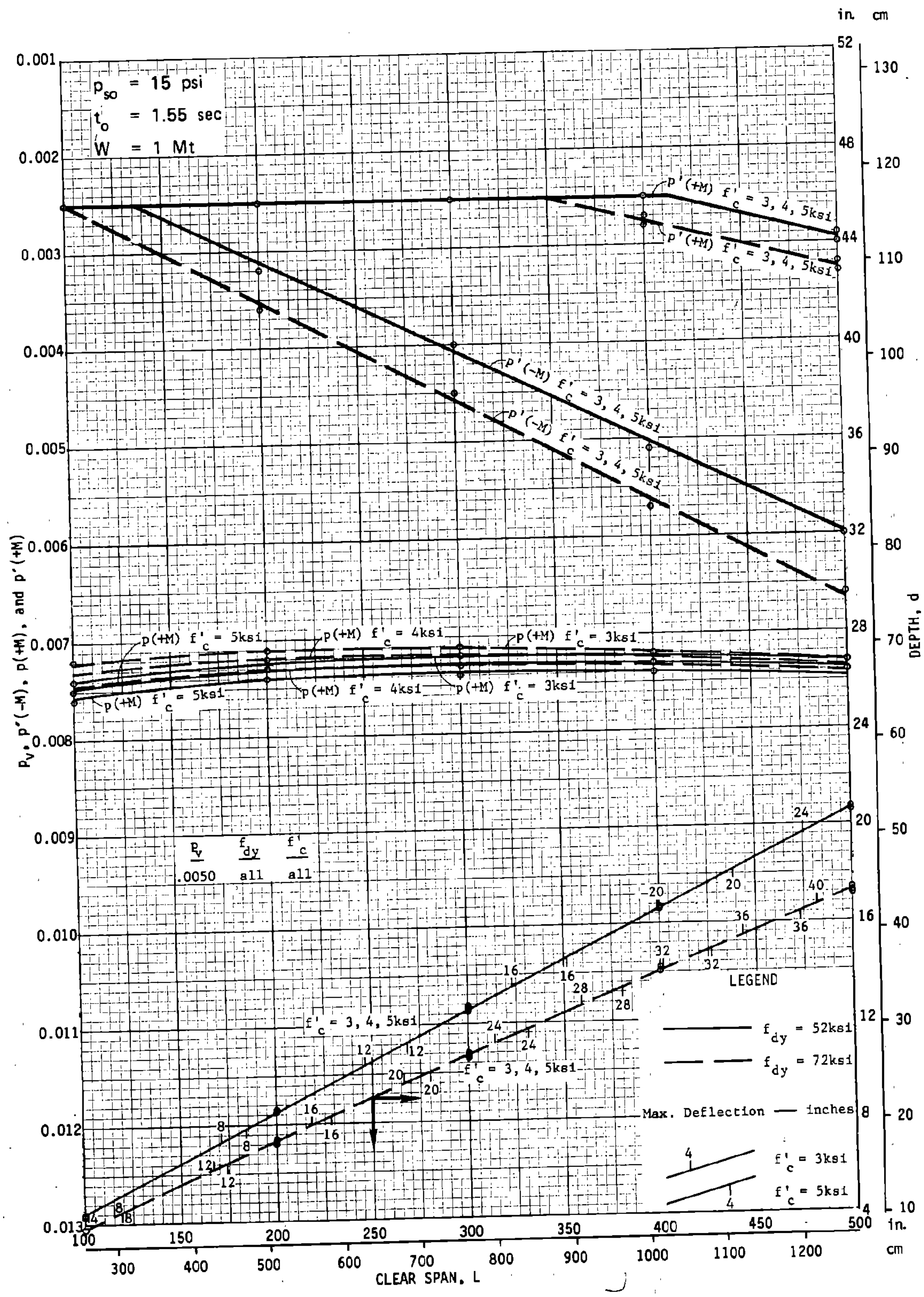

FIG. 6-81 ONE-WAY SLABS; FIXED ENDS
Typical Designs – p_e = 0.015 (15 psi)

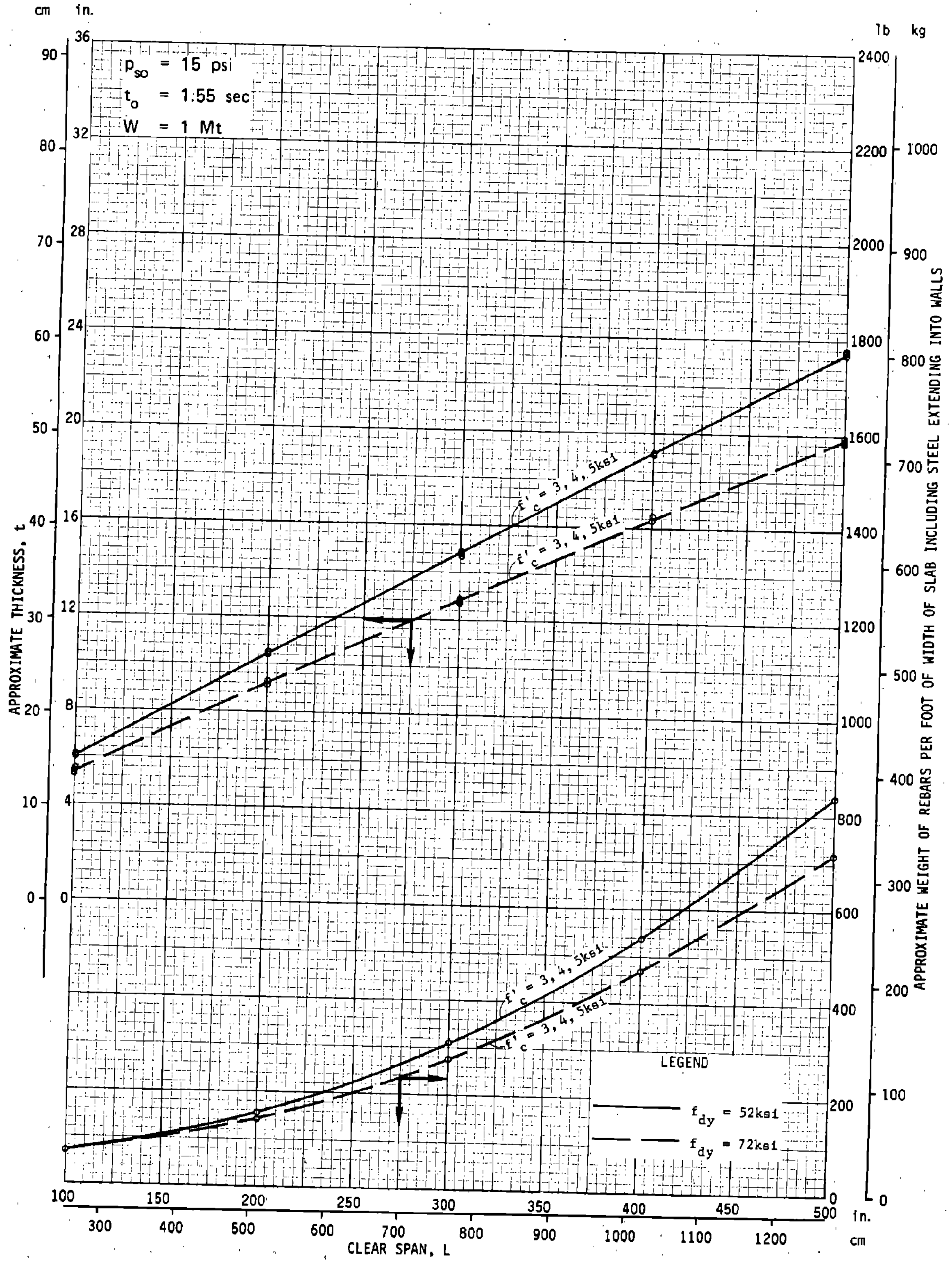

FIG. 6-8J ONE-WAY SLABS, FIXED ENDS
Approximate Weight and Thickness – p_e = 0.015 (15 psi)

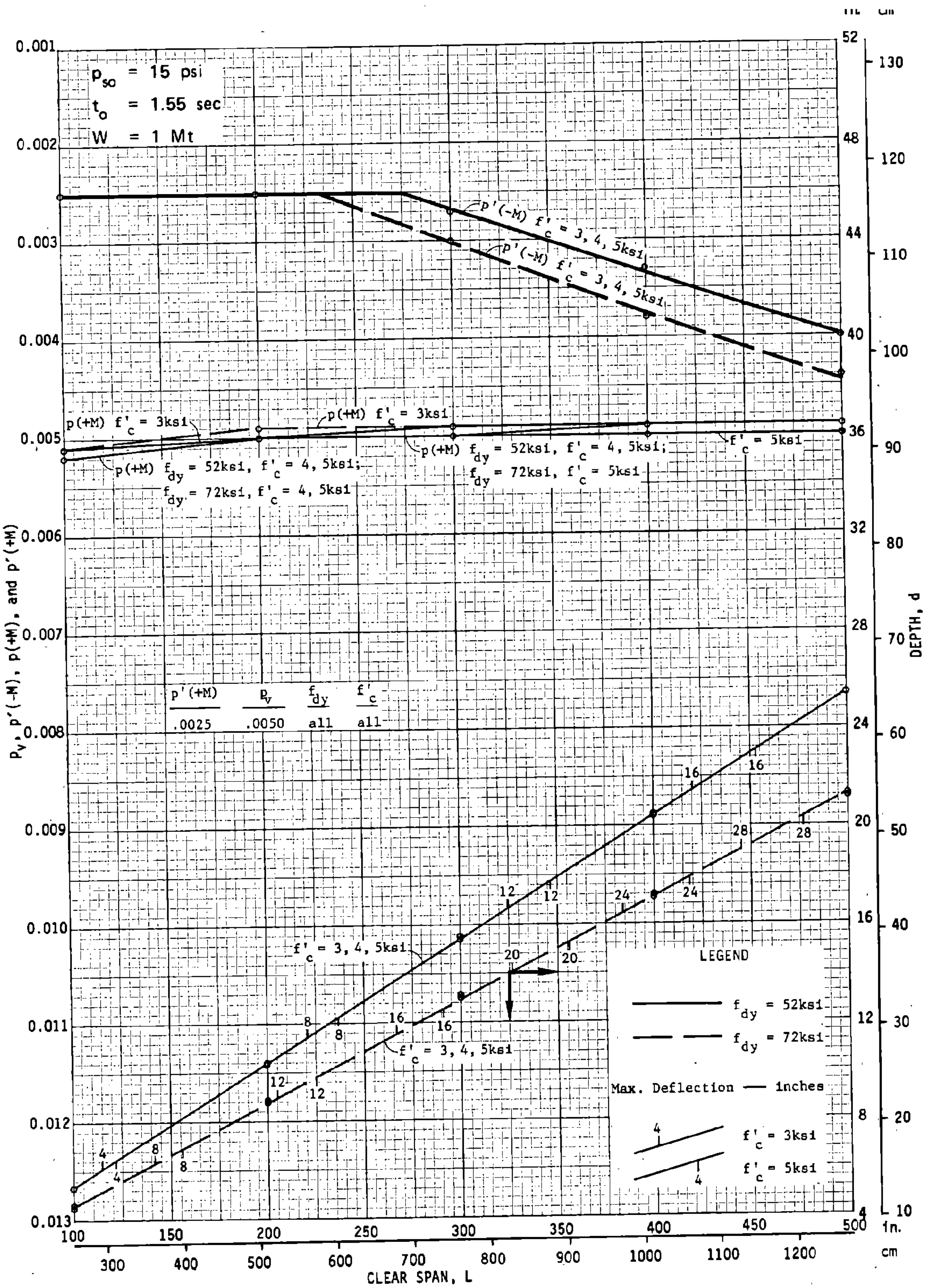

FIG. 6-8K ONE-WAY SLABS, FIXED ENDS
Typical Designs — p_e = 0.010 (15 psi)

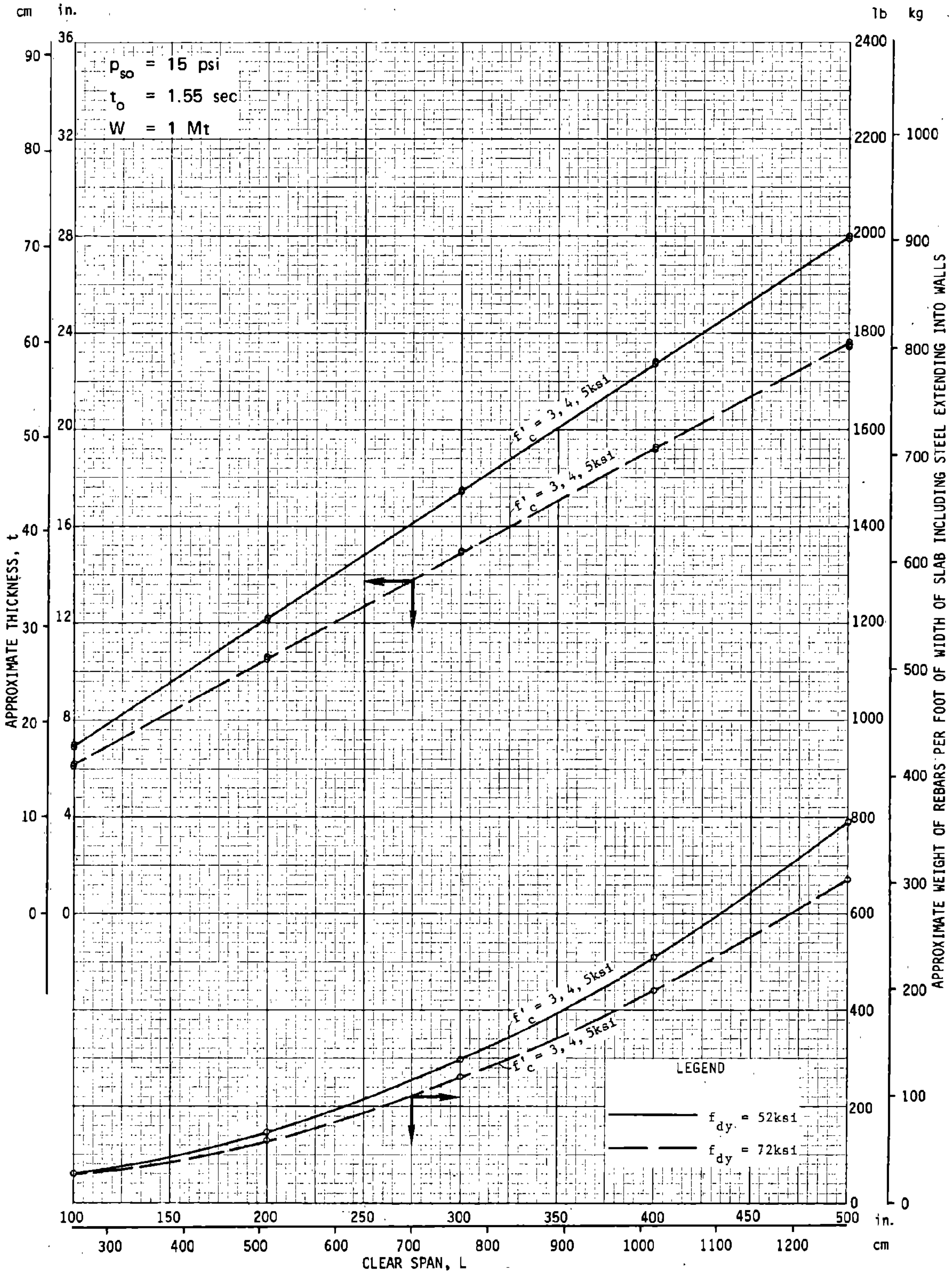

FIG. 6-8L ONE-WAY SLABS, FIXED ENDS
Approximate Weight and Thickness – p_e = 0.010 (15 psi)

C. One-Way Slabs - Design for Rebar Ratios Not in Design Graphs*

To extend the usefulness of the one-way slab design graphs to rebar ratios other than the specific value shown on each graph, study work was performed as follows: Work was restricted to considering interpolation between graphs prepared for the same blast peak overpressure (15 psi), for the PC and FF cases, and therefore, for p_e ratios of 0.01, 0.015, and 0.02. Plots were prepared for each dependent parameter (i.e., all parameters except clear span) shown on the graphs, plus fixed-end-moment (FEM), with a set of plots for each of three clear spans: 100, 300, and 500 in. Plots were made only for f_{dy} = 52 ksi and f_c' = 3 ksi. Spot checking indicated that any conclusions drawn from the plots would also apply to the SS case design graphs for 15 psi.

It was found that the dependent parameters vary so near to linearly between the plotted rebar ratios that a straight line interpolation should be used for slab designs with intermediate ratios, and that use of a higher order (parabolic) interpolation is unwarranted. Examples follow that show both linear and second order (parabolic) interpolations. Errors occur only when interpolating between a graph and parameter whose value was set because of a prescribed minimum, and a graph where the same parameter is above that minimum. The interpolated value will, however, be on the conservative side with one exception: p_v with its two minimums, 0.0026 and 0.005 (see Equations 5 and 6, Table 6.2).

Example of straight line interpolation: Dependent parameter selected for the two examples was FEM because it showed the most curvature on the (arithmetic) plots. Assume a propped cantilever slab with f_{dy} = 72 ksi, f_c' = 3 ksi, L = 400 in., to be designed for p_e = 0.0125. For independent parameter p_e values of 0.01, 0.015, and 0.02 (identify as x_1, x_2, and x_3 herein), step 5 of the final design procedure for PC gave FEM values of 300, 292, and 286 in.-kips (identify as y_1, y_2, and y_3 herein). Let x = 0.0125 and y be the FEM sought. Then

$$y = 300 - (300 - 292) \frac{(0.0125 - 0.01)}{(0.015 - 0.01)} = 296.0 \text{ in.-kips}$$

Example of parabolic interpolation: Using the same inputs as in the first example, the following formulas may be used, provided that the interval is constant between the known values of the independent parameter (i.e., $x_1 - x_2 = x_2 - x_3$):

$$y = A + B\ (x - x_1) + C\ (x - x_1)(x - x_2)$$

---

* Figures 6-3, 6-6, 6-7, and 6-8.

which is the equation for the parabola through three known points, and where;

$$A = y_1$$

$$B = (y_2 - A)/h$$

$$C = (y_3 - A - 2Bh)/(2h^2)$$

with $$h = x_2 - x_1 = x_3 - x_2$$

Use of the above formulas gives y = 295.75, a result which is believed to show that the straight line interpolation should be used.

D. One-Way Walls - Simply Supported

This section includes - for simply supported one-way walls, both exterior (basement) and interior - typical designs and rough estimates of reinforcing steel and concrete quantities. A recommended final design procedure is described below. The procedure for estimating rebars is closely similar to that for one-way slabs;* thus, only deviations from that procedure, plus comments for text continuity, are noted herein. Further, the basic reasoning on use of stirrups in one-way slabs is also applicable to one-way walls, and rebar detailing (Fig. 6-5) should minimize potential moment transfer from basement shelter cover slab into walls or columns designed as simply supported.

Final Design Procedure. This procedure was developed for potential use in making design graphs and is therefore probably more elaborate than would be justified for normal design use. A preliminary design method is introduced later herein (Appendix G - Supplement), as are worked design examples for both final and preliminary design procedures.

1. Basic parameter values considered for use were: $f_c' = 3, 4, 5$ ksi; $f_{dc}' = 1.25\ f_c'$; $f_{dy} = 52, 72$ ksi; $p_{so} = 5, 10, 15, 20, 30$ psi, with $t_o = 2.52, 1.85, 1.55, 1.38, 1.17$ sec, respectively (exponential decay). As recommended earlier herein: for wall and column design, either $\mu = 1.3$ and f_c' with no dynamic loading increase factor, or $\mu = 1$ and f_{dc}' may be used; the latter combination was used herein.

The in-plane loading P_u was assumed constant and taken as twice the design blast peak overpressure,† times the tributary area served.[2] (There is a blast wave transit time, and thus a finite rise-time, in the dynamic loading, which can be handled instead of using zero rise-time, but is generally considered as too design-time consuming and complex to be worthwhile.)

The lateral load p_m (psi) on exterior walls‡ was taken as 0.5 p_{so} (i.e., lateral soil coefficient $K_o = 0.5$§), plus the average static soil

---

* Section A of this chapter.

† Which is equivalent to using a step pulse loading with $\mu = 1$; multiplier is thus $1/(1 - 1/(2\mu))$, or 2.

‡ See earlier section on loadings herein, including lateral loads on exterior (basement) walls; it is suggested there that the transit time of airslap down the wall may be used (thus a finite, or not zero, rise-time), but the simpler approach of a step pulse was adopted in the final design procedure above because of possible outrunning ground motion and other situations, as well as because of the simplicity. For further reading and details on this matter, the following sources are available: References 2 (Ch. 4,5), 16 (Ch. 2,5) and 18.

§ K_o varies with the soil, of course. For airslap, it may vary between about 0.15 and 0.75, but will be 1.0 for any saturated soil.[2(p.4-8), 16(p.10),18] For outrunning blast waves, it should probably be 1.0 applied to the free-field (in soil) loading (not necessarily p_{so}).

pressure acting on the wall multiplied by $(1 - 1/(2\mu))$. For purposes of preparing design graphs, the average soil pressure could be assumed to be 15L/1728 psi.* The lateral load on interior walls is, of course, zero within closed (to blast entry) shelters. The lateral load on interior walls exposed to blast requires some estimation of the interior air blast behavior - inflow rate, reflections, time-rates, etc. - for which reference is made to discussion in Chapter 8 and Appendix E of References 50 and 61. Interior walls in open shelter may be so located as to be potentially exposed to blast from either side (in which case $p = p'$); if only exposed on one side, rebound steel should be included per Section A, step 4.

Rules concerning selection of p and p′ in Table 6.2 also apply to one-way walls; however, for exterior walls where rebound is limited by earthfill, p′ may be taken as 0.25p or 0.0025, whichever is larger.

2. This step was to get a first trial value of d; the approach uses only the lateral loading p_m and ignores for now the axial loading P_u. An alternate approach is to assume d (from code, local practice, or judgment) and move directly to step 3.

2a. A value equal to $2p_m$ was assumed for q (psi), as the peak elastic value in an elasto-plastic resistance function for the wall section under design. Using q led to the first trial value for d as follows:

It was first necessary to compute k_3; (k_3d)† is the distance from extreme fiber to neutral axis in USD[4,60]:

$$k_3 = [pf_{dy} - p'(f_{dy} - 0.85f'_{dc})] / (0.85f'_{dc}\beta_1) \qquad (6\text{-}17)$$

where: $\beta_1 = 0.85$, for $f'_c \leq 4000$; or

$$\beta_1 = 0.85 - 0.00005(f'_c - 4000), \text{ for } f'_c > 4000$$

Next, the strain in the compression steel e'_s was calculated:[65,67]

$$e'_s = 0.00375\ (k_3 - d'/d) / k_3 \qquad (6\text{-}18)$$

where (d'/d) is assumed or estimated (0.1 suggested for first trial); for a trial d′ assume 3/4 in. concrete cover, 3/8 in. stirrup, and half-thickness of 3/8 in. rebar, total 1.3125 in.

---

* L is clear wall height, inches.

† Termed "c" in latest ACI Code.[60]

The e_s' value was then to be compared to the yield strain:

$$e_y = f_{dy} / E_s \qquad (6\text{-}19)$$

where E_s (elastic modulus of rebars) was taken as 3×10^7 psi.

2b. If $e_s' \geq e_y$, then the first trial d was calculated:[65]

$$M_u = [(p - p') bf_{dy}(1 - \beta_1 k_3/2) + p'b (f_{dy} - 0.85 f_{dc}')(1 - d'/d)]d^2$$
$$= bq\, L^2 c \qquad (6\text{-}20)$$

where c = 1/8, and b is the width of wall section under design (usually 1 in., sometimes 1 ft).

2c. If $e_s' < e_y$, then k_3 had to be recomputed from the following quadratic equation solution:[65]

$$k_3 = \frac{-B + [B^2 - 4AC]^{0.5}}{2A} \qquad (6\text{-}21)$$

where: $A = 0.85 \beta_1 f_{dc}'$

$B = p' (0.00375\, E_s - 0.85\, f_{dc}') - pf_{dy}$

$C = -0.00375\, E_s p' (d'/d)$

and a first trial d was computed using[65]

$$M_u = \{0.85 \beta_1 bk_3 f_{dc}' (1 - \beta_1 k_3/2)$$
$$+ p'b [0.00375\, E_s (k_3 - d'/d)/k_3 - 0.85 f_{dc}'](1 - d'/d)\}d^2$$
$$= bq\, L^2 c \qquad (6\text{-}22)$$

where c = 1/8, and b was as defined in step 2b.

3a. The in-plane and flexural loadings interaction was then considered.* Using the applicable one of the six blocks of equations in Table 6.6, or a suitable interaction diagram,† a new M_u was calculated, including the in-plane loading P_u. Values of z_o and x_o were calculated from equations under the General Notes, Table 6.6; thickness of wall t may be estimated from t = d + 1,3125, using some trial assumptions of step 2a.

---

* The complexity of current procedures, both ACI and AISC, for handling the interaction of combined axial and flexural loads on beam-column structural members is the subject of much complaint among structural designers - as is the form of the interaction equations, which is such that no mental image of envisioned structural behavior comes from a study of the equations, as it could from older approaches. Nonetheless, use is made of the interaction equations herein because they are the current practice in design.

† That is, one based on the basic flexural design source,[32] not later sources that include a "safety" factor φ.[4,60]

Table 6.6 INTERACTION EQUATIONS FOR RECTANGULAR SECTIONS WITH REINFORCING STEEL IN BOTH TENSION AND COMPRESSION FACES

Case	Conditions	Equations
1. 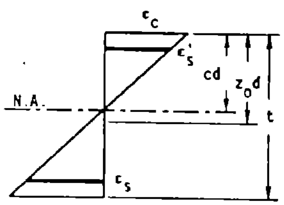	a. $c \le c_b$ b. $\epsilon'_s \ge \epsilon_y$ c. $\epsilon_s \ge \epsilon_y$	$c = [P_u + pdf_{dy} - p'd(f_{dy} - 0.85f'_{dc})]/(0.85f'_{dc}\beta_1 d)$ $M_u = 0.85f'_{dc}\beta_1 cd^2(z_o - \beta_1 c/2) + p'd^2(z_o - d'/d)(f_{dy} - 0.85f'_{dc}) + pd^2 f_{dy}(1 - z_o)$
2. 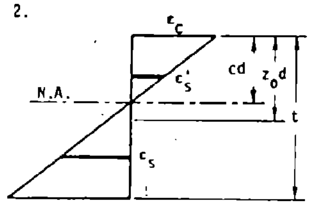	a. $c \le c_b$ b. $\epsilon'_s \le \epsilon_y$ c. $\epsilon_s \ge \epsilon_y$	$C_1 = 0.85f'_{dc}\beta_1$ $C_3 = -0.00375E_s p'd'/d$ $C_2 = p'(0.00375E_s - 0.85f'_{dc}) - P_u/d - pf_{dy}$ $c = [-C_2 + (C_2^2 - 4C_1C_3)^{0.5}]/(2C_1)$ $M_u = 0.85f'_{dc}\beta_1 cd^2(z_o - \beta_1 c/2) + p'd^2(z_o - d'/d)[0.00375E_s(cd - d')/(cd) - 0.85f'_{dc}] +$ $pd^2 f_{dy}(1 - z_o)$
3. 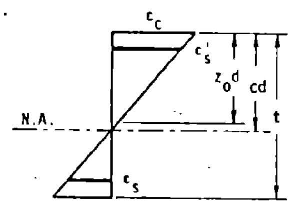	a. $c_b \le c \le t/(d\beta_1)$ b. $\epsilon'_s \ge \epsilon_y$ c. $\lvert\epsilon_s\rvert \le \epsilon_y$	$C_1 = 0.85f'_{dc}\beta_1$ $C_3 = -0.00375E_s p$ $C_2 = p'(f_{dy} - 0.85f'_{dc}) - P_u/d + 0.00375E_s p$ $c = [-C_2 + (C_2^2 - 4C_1C_3)^{0.5}]/(2C_1)$ $M_u = 0.85f'_{dc}\beta_1 cd^2(z_o - \beta_1 c/2) + p'd^2(z_o - d'/d)(f_{dy} - 0.85f'_{dc}) +$ $0.00375E_s pd^2(1 - z_o)(1 - c)/c$
4. 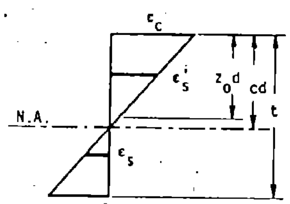	a. $c_b \le c \le t/(d\beta_1)$ b. $\epsilon'_s \le \epsilon_y$ c. $\lvert\epsilon_s\rvert \le \epsilon_y$	$C_1 = 0.85f'_{dc}\beta_1$ $C_3 = -0.00375E_s(p + p'd'/p)$ $C_2 = p'(0.00375E_s - 0.85f'_{dc}) - P_u/d + 0.00375E_s p$ $c = [-C_2 + (C_2^2 - 4C_1C_3)^{0.5}]/(2C_1)$ $M_u = 0.85f'_{dc}\beta_1 cd^2(z_o - \beta_1 c/2) + p'd^2(z_o - d'/d)[0.00375E_s(cd - d')/(cd) - 0.85f'_{dc}] +$ $0.00375E_s pd^2(1 - z_o)(1 - c)/c$

Table 6.6 (Concluded)

5. 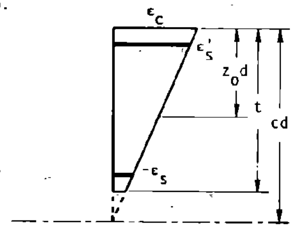 a. $c \geq t/(d\beta_1)$ b. $\epsilon_s' \geq \epsilon_y$ c. $-\epsilon_s \leq \epsilon_y$	$c = 0.00375E_s p/[0.85f_{dc}' t/d + p'(f_{dy} - 0.85f_{dc}') - P_u/d + 0.00375E_s p]$ $M_u = 0.85f_{dc}' td[z_o - t/(2d)] + p'd^2(z_o - d'/d)(f_{dy} - 0.85f_{dc}') +$ $0.00375E_s pd^2(1 - z_o)(1 - c)/c$
6. 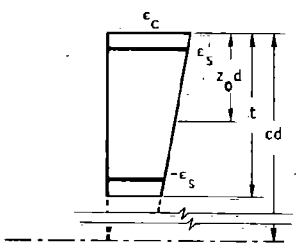 a. $c \geq t/(d\beta_1)$ b. $\epsilon_s' \geq \epsilon_y$ c. $-\epsilon_s \geq \epsilon_y$	$P_u = 0.85f_{dc}' t + d(p+p')(f_{dy} - 0.85f_{dc}')$ $M_u = 0$

HOW TO USE TABLE:

1. Complete Steps 1 and 2 of Final Design Procedure; this Table 6.6 is used in Step 3a (if no graphical or tabular procedures are available).
2. Use Equation Set #1: (a) Calculate c (right side box); (b) Calculate ϵ_y ϵ_s' ϵ_s and c_b (General Notes); (c) Use calculated values in condition equations (to immediate right of figure), to determine whether Equation Set #1 is applicable to your particular problem:
   - If it is, calculate x_o and z_o (General Notes), then M_u (right side box);
   - If it is not applicable, repeat this entire procedure, next using Equation Set #2 and continuing until applicable equation for Mu is found.
3. Experience may help the user to move directly to the applicable Equation Set, rather than starting each time with #1.

GENERAL NOTES:

$\epsilon_y = f_{dy}/E_s$; $\epsilon_s' = \epsilon_c(c - d'/d)/c$; $\epsilon_s = \epsilon_c(1 - c)/c$; $c_b = 0.00375/(0.00375 + f_{dy}/E_s)$

$x_o = (f_{dy} - 0.85f_{dc}')[pd(d - t/2) - p'd(t/2 - d')]/[0.85f_{dc}' t + (f_{dy} - 0.85f_{dc}')(p + p')d]$

$z_o = t/(2d) + x_o/d$ (z_o may be assigned a value of 1 when $P_u = 0$)

Definition: $c = k = k' = k_3$ (for this table)

Source: Adapted from Ref. 65, 68, & 69

3b. Then a new trial value for d was calculated:

$$d_{new} = [M_{u(old)} / M_{u(new)}]^{0.5} \, d_{old} \qquad (6\text{-}23)$$

This step was then repeated until the previously calculated M_u and the new M_u (and of course, the old and new d values) from this step 3 were acceptably close (say, within 2% to 5%); usually no more than 2 or 3 trials are necessary.

4. Cracked section moment of inertia I, and elastic and plastic phase stiffnesses, K and K_p, were then calculated:[67]

$$I = bd^3/12 \, \{12 \, np \, [(1 - k')^2 + r_o(k' - d'/d)^2] + 4(k')^3\} \qquad (6\text{-}24)$$

where: $n = 30{,}000/f'_c$; $r_o = (n-1)\,p'/(np)$; and k' is identical with k of balanced working stress design:

$$k' = [(np(1 + r_o))^2 + 2np(1 + r_o d'/d)]^{0.5} - np(1 + r_o) \qquad (6\text{-}25)$$

$$K = E_c I c'/L^3 \qquad (6\text{-}26)$$

where: $c' = (384/5)/\delta$; $\delta = 12\,[2/\cos(u) - u^2 - 2] / [5\,u^4]$;
$u = 0.5\pi\,(P/P_{cr})^{0.5}$; $P_{cr} = \pi^2 E_c I/L^2$; and $E_c = 1{,}000\, f'_c$ (Ref. 2,60,66,67).*

$K_p = 0$, if $P = 0$; if $P \neq 0$, then $\mu = 1$ and plastic range of resistance function is not used (thus $K_p = 0$ can be used generally, as in a computer program). With $\mu = 1$, the maximum displacement, or deflection at mid-height of the wall, is

$$x_e = qL/K \qquad (6\text{-}27.1)$$

where q is redefined, using the value of δ calculated just above, as

$$q = 8\,M_u/(\delta L^2) \qquad (6\text{-}27.2)$$

5. As in Section A (step 8), load-mass factors of 0.78 (elastic) and 0.66 (plastic), Table 6.3, were used to convert to an equivalent single-degree-of-freedom system, which was then solved for μ and maximum deflection, using the Newmark β Method or a modified version of it (with exponential decay and $\beta = 1/6$). Should chart solutions for the equation

* $\delta \approx 1/(1 - P/P_{cr})$, if $P \leq 0.6\, P_{cr}$ (Ref. 66).

of motion be needed, loading simplification to triangular pulse may be made[2(p.3-6)] and the elastic period of vibration T may be useful:*

$$T = L^2 \delta^{0.5} / [c'' d (p)^{0.5}] \qquad (6\text{-}28.1)$$

where $c'' = 425{,}000$ (Ref. 2,66).† Also needed is the unit mass (i.e., per square inch):

$$m \approx (150/1728)\ t / g \qquad (6\text{-}28.2)$$

where $g = 386.4$ and $t \approx d + 1.3125$ (step 2a trial assumptions). Care should be taken that the equation of motion is dimensionally consistent.)

6. If the calculated μ was not acceptably close (say, within 1% to 5%) to the desired $\mu = 1.0$, a new d was assumed from $d_{new} = [\mu_{calculated} / 1.0]^{1/3} d_{old}$ and step 3a, plus steps 4 through 6, was repeated (i.e., skipping step 3b).

7. The remaining checks - for diagonal tension, pure shear, and bond - were identical to Section A (steps 10, 11, and 12 of simply supported one-way slab design procedure).[2] Note: In step 10, use $a = b$; in step 11, $p_m = p_{so}$ because $\Delta p_{so} = 0$.

Comments on Design for Other Support Conditions. The final design procedure just described is for a simply supported wall, and is based on only two load sources: (1) a uniformly distributed lateral load; and (2) a vertical axial load.‡ The procedure uses the external moment and axial load, applied to the mid-height wall (or column) cross-section; this external moment includes that calculated from the axial load multiplied by the mid-height deflection when the member is under combined axial and lateral loads, i.e., the beam-column stress interaction.

The interaction equations of step 3a are used to examine a trial design cross-section of a wall section or column, for which the axial load just described is known. The equations are used to calculate the ultimate (internal) moment capacity of the trial cross-section, as if it

---

* T is related to behavior under lateral loading; under in-plane loading, the period is so short that a blast load can be handled as a step pulse because the loading lasts much longer than the period.

† $\delta \approx 1/(1 - P/P_{cr})$, if $P \leq 0.6\ P_{cr}$ (Ref. 66).

‡ More precisely, a vertical load applied on top and bottom ends and located along the plastic centroid line (USD) or transformed section centroid line (WSD).
(Note: centroid lines are not neutral axis lines.)

were a short pedestal. This moment capacity is then compared with the applied (external) moment; if not acceptably close, a new trial design cross-section is prepared, then examined as just described.

The interaction equations could be, however, used for examining <u>any</u> trial design wall or column cross-section, providing the axial load and external moment applied to that particular cross-section have been calculated. Therefore, these two values must be known for as many cross-sections as must be examined, and any combination of loadings must be reduced to these two values for each such cross-section, whatever the loadings - vertical axial, vertical eccentric, oblique, and lateral, as well as any kind of applied moment - all wherever applied along the member height.

For the calculations just indicated, an iterative numerical method is valuable if not vital. One such method is suggested for consideration;[73] for the purposes herein, only elastic buckling need be treated. Modification of the final design procedure, for use under other than simply supported assumptions, may also require load-mass (or transformation) factors other than those of step 5; this subject is discussed briefly, and references are cited, in an early section, "General Comments on Blast-Resistant Design . . . ," of this chapter.

<u>Rebar Design and Details</u>. The general scheme for rebars in wall design would be nearly identical to that used for one-way slabs (Section A, text and Figure 6-5). The only difference would be in the computation of rebar lengths in estimating A_s and A_s' quantities. The length would be approximately (12 + L) in both cases, which assumes 12 in. thick overhead slab and/or beam resting on the wall (L = clear height of wall); see Table 6.5 and accompanying text.

E. Columns - Simply Supported

This section covers design of simply supported columns, as well as rough estimates of related steel and concrete quantities. A final design procedure is described below. Comments on loading assumptions in Section D also apply herein. Only circular, spiral reinforcement columns are considered below; they are recommended for shelter use as preferable over square, tied columns.[2,16]

The basis for this recommendation is in the far greater energy absorption capacity of the spiral columns prior to complete collapse. Up to yield point, both types act almost identically, but after reaching this point, a tied column immediately fails with a shearing diagonal failure of the concrete and a buckling failure of the column steel between ties. While the tied and spiral columns act almost identically up to yield point, it is only after this point that the spiral steel becomes significantly effective because of gradual destruction of the shell concrete covering the spiral, which then provides radial compressive forces on the core concrete, thereby adding significantly to the load carrying capacity of the core.[65(p.28-)]

Selecting Column Steel Ratio. Many factors should be considered in selecting the (vertical) steel ratio used in a column (range of 0.01 to 0.06 is recommended*). In general, concrete is less expensive than steel in load-carrying capacity; therefore, as the steel ratio decreases, the total cost of column materials, excluding spiral steel, decreases. However, some of the savings will be offset by the increased spiral steel required as the column diameter increases, which in turn decreases usable space. Another factor in choosing the steel ratio would be the cost effectiveness of having fewer column form sizes by using various steel ratios; present practice is to try to keep column sizes constant throughout a building or at least its major areas. Since there are about as many reasons for selecting a large steel ratio as a small one, it is suggested that a first trial value of, say, 0.03 or 0.04 be used.

Final Design Procedure. This procedure was developed for potential use in making design graphs and is therefore probably more elaborate than would be justified for normal design use. A preliminary design method is introduced later herein (Appendix G - Supplement), as are worked design examples for both final and preliminary design procedures.

1. Basic parameter values used were: f'_c = 3, 4, 5 ksi; f'_{dc} = 1.25 f'_c; f_{dy} = 52, 72 ksi. Select a trial steel ratio p of 0.01 to 0.06

---

* Ref. 60, section A.6.1.

(see preceding section). Desired $\mu = 1$. For design, the axial load P_u to be resisted was taken as the product of the tributary area times twice the assumed blast overpressure p_{so}; by using this value as an independent variable, many combinations of p_{so} and tributary area may be covered by a given value of the load in a design graph or table. The load assumption amounts to use of a step pulse (i.e., resistance must equal peak blast load times $\frac{1}{1-1/(2\mu)}$, or 2 when $\mu = 1.0$); such an assumption is well justified when the structural member is extremely stiff (meaning that it has a very short natural period of vibration), as are columns. Any blast lateral load should be minor relative to P_u.

2. The minimum eccentricity e under the current Code[60] was taken as one inch or 0.05 D (column diameter), whichever was larger. The approximate moment on the column was then calculated:

$$M_u = P_u \delta e \tag{6-29}$$

where δ was assumed as 1.1 for this step, but is defined in step 4 for use after a trial column diameter D has been determined.

3. Using M_u and P_u, a trial D was found through use of suitable interaction diagrams,* equations or tables,† as described below.

Obtaining a trial column D appeared to be a simple matter using M_u and P_u in tables and diagrams.[69,70] It proved troublesome, however, in that the tables are for usual f_y and f'_c values, rather than f_{dy} and f'_{dc}, and include a factor Φ that would not be used for blast design, necessitating multiplication of tabular values by $1/\Phi$ for use. Also, implicit in the procedure herein is that maximum concrete strain[2] is 1.25 times 0.003, whereas the tables[69] are based on 0.003. Finally, in developing a computer program for column design, use of equations was much more convenient than use of tables with a program stop for entry of a value read from a table(s).

Using equations required the following iterative approach:

3a. A trial value for D is provided by

$$D = [4P_u/(0.85\ \pi f'_{dc})]^{0.5} \tag{6-30}$$

---

* See similar footnote to step 4, Section D.

† Equations and tables used herein are in Ref. 69.

3b. Using Table 6.7, values of c were successively tried* until a calculated P_u matched the desired P_u (step 1). Other parameters needing values were D_s and β_1, obtainable as follows: β_1 is as defined in Section D (step 2a); and D_s may be estimated as 0.75 D, at least in early design trials. Figure 6-9 defines several parameters in column design.

3c. An M_u was calculated from Table 6.7. If this value was not satisfactorily close to the trial M_u (from step 2), a new trial D was chosen:

$$D_{(\text{new trial})} = [\text{trial } M_u \ / \ \text{calculated } M_u]^{0.25} \ D_{(\text{old trial value})} \tag{6-31}$$

and steps 3b and 3c were repeated. The latest D value was used for the design steps that follow.

4. Calculations could then be made toward a better check for lateral stability:[60,66]

$$EI = E_c I_g/5 + E_s I_s \tag{6-32}$$

where: $E_c = 1000 \ f_c'$

$E_s = 30{,}000{,}000$ psi

$I_g = \pi D^4/64 = 0.049087 \ D^4$

$I_s = \pi D_s^3 A_{st}/(8\pi D_s) = 0.098175 \ D_s^2 D^2 p$

and $P_{cr} = \pi^2 EI/L^2$

$$\delta = 1/(1 - P_u/P_{cr}) \tag{6-33}$$

Then, using the minimum eccentricity e = 0.05 D or one inch, whichever is larger, a revised trial value of M_u is calculated:

$$M_u = P_u \delta e \tag{6-29}$$

5. This step is the same as step 3 except for the following modification of step "a.":

5a. New trial D was estimated using

$$D = [(\delta e)_{\text{current}} \ / \ (\delta e)_{\text{previous}}]^{0.25} \ D_{\text{previous}} \tag{6-34}$$

where $(\delta e)_{\text{current}}$ is from step 4; $(\delta e)_{\text{previous}}$ is the next earlier one (from step 2 or 4); and D_{previous} is the latest D preceding this step 5a. Steps 5b and 5c are the same as steps 3b and 3c, including the possible iterations.

* First trial c might be D/2.

Table 6.7

CIRCULAR COLUMN INTERACTION EQUATIONS

$$P_u = 0.85\, f_c' D^2\, (\theta_2 - \sin\theta_2\cos\theta_2 - p\theta_5)/4 + f_y p D^2\, (\theta_3 + \theta_4 - \pi)/4 +$$
$$112.5\, pD^2\, [D_s\, (\sin\theta_4 - \sin\theta_3)/2 - (D/2 - c)(\theta_4 - \theta_3)]/(4c)$$

$$M_u = P_u e = 0.85\, f_c' \left[(D\sin\theta_2)^3/12 - (D_s p D^2 \sin\theta_5)/8 \right] + f_y D_s p D^2\, (\sin\theta_3 +$$
$$\sin\theta_4)/8 + 112.5\, D_s p D^2\, [D_s\, (\theta_4 - \theta_3 + \sin\theta_4\cos\theta_4 - \sin\theta_3\cos\theta_3)/4$$
$$(D/2 - c)(\sin\theta_4 - \sin\theta_3)]/(8c)$$

where:

$\theta_1 = \cos^{-1}(1 - 2\, c/D)$; for $2c < D$

$\theta_1 = \pi$; for $2c \geq D$

$\theta_2 = \cos^{-1}(1 - 2k_1c/D)$; for $2k_1c < D$

$\theta_2 = \pi$; for $2k_1c \geq D$

$\theta_3 = \cos^{-1}\{D/D_s - 2_c\, [1 - f_{dy}/(0.00375E_s)]\, /D_s\}$

; for $(D + D_s)/2 > [1 - f_{dy}/(0.00375E_s)] > (D - D_s)/2$

$\theta_3 = 0$; for $[1 - f_{dy}/(0.00375E_s)] \leq (D - D_s)/2$

$\theta_3 = \pi$; for $[1 - f_{dy}/(0.00375E_s)] \geq (D + D_s)/2$

$\theta_4 = \cos^{-1}\{D/D_s - 2_c\, [1 + f_{dy}/(0.00375E_s)]/D_s\}$

; for $(D + D_s)/2 > [1 + f_{dy}/(0.00375E_s)] > (D - D_s)/2$

$\theta_4 = 0$; for $[1 + f_{dy}/(0.00375E_s)] \leq (D - D_s)/2$

$\theta_4 = \pi$; for $[1 + f_{dy}/(0.00375E_s)] \geq (D + D_s)/2$

$\theta_5 = \cos^{-1}(D/D_s - 2k_1c/D_s)$; for $(D + D_s)/2 > k_1c > (D - D_s)/2$

$\theta_5 = 0$; for $k_1c \leq (D - D_s)/2$

$\theta_5 = \pi$; for $k_1c \geq (D + D_s)2$

Source: Adapted from Ref. 69.

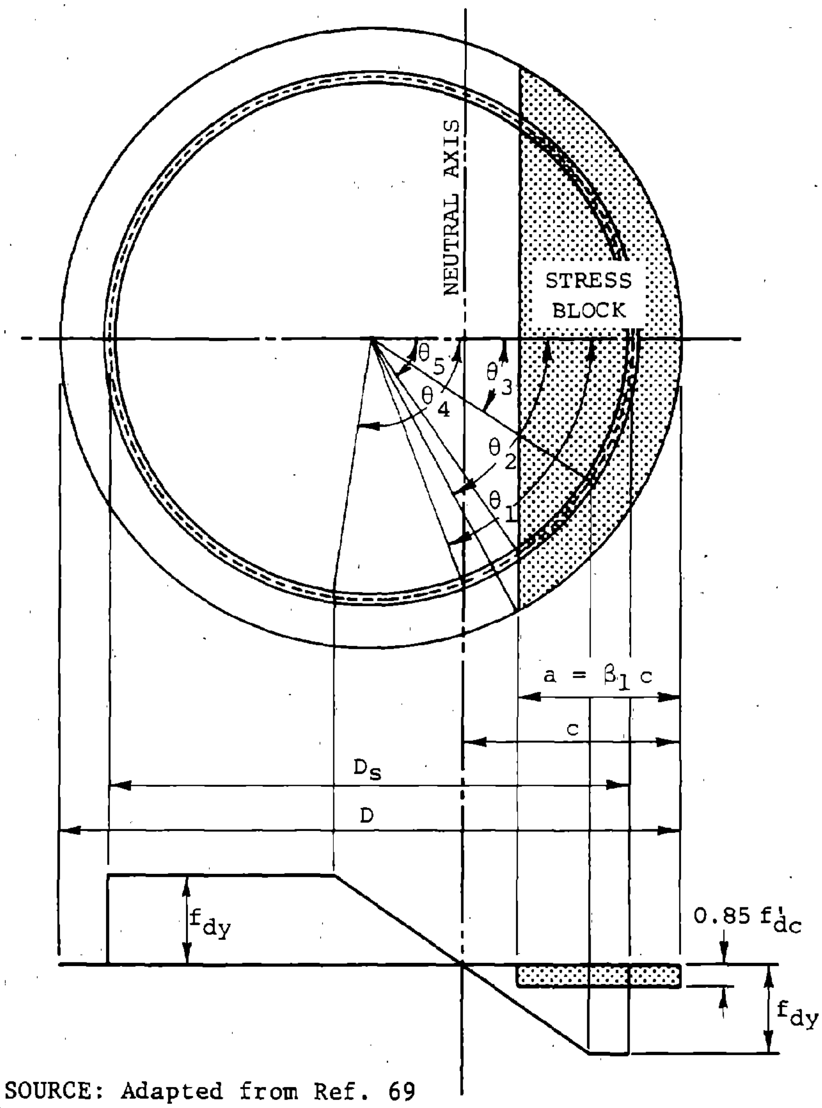

SOURCE: Adapted from Ref. 69

FIG. 6-9 STRESS DISTRIBUTION IN CIRCULAR COLUMNS

6. This step is the same as step 4.

7. If the new M_u value from step 6 was not satisfactorily close to the previous calue of M_u (from step 4 or 6), then steps 5 and 6 were repeated until the current and previous values of M_u from step 6 were satisfactorily close.

8. To complete the design, the required spiral steel ratio was calculated:

$$p_s = 0.45\ (A_g/A_c - 1)\ (f_c'/f_y) \text{ or } = 0.12\ f_c'/f_y \qquad (6\text{-}35)$$

whichever is larger, where: p_s (ρ_s in cited references) is the spiral steel ratio;* A_g is gross area of column; A_c is area of core (measured out-to-out of spiral steel).

The rebar scheme and related assumptions are discussed in the next section.

<u>Rebar Design and Details</u>. The general scheme contemplated for steel detailing is shown in Figure 6-10. In column detailing, required ductility must be maintained to compensate for spalling and is derived from spiral steel serving as web reinforcement (as do stirrups in slabs and beams). Because of this, a design procedure is recommended that complies with the requirements of Ref. 60, Appendix A (Special Provisions for Seismic Design), Section 6 (Special Ductile Frame Columns Subjected to Axial Loads and Bending), some aspects of which are: Spiral reinforcing steel should extend from the floor level in each story up to the lowest horizontal reinforcement of the next floor level:† two extra turns of spiral bar or wire at each end of the spiral unit are required for anchorage; spiral spacers must be provided as shown in Table 6.8; and, minimum suggested bar size for spiral steel is number 3.

Table 6.9 gives percentages and weights of standard steel reinforcing spirals. When computing the length of the column's longitudinal rebars, for estimating required steel quantities, the length used should be from floor level of the story considered up to the floor level of the story above, because only welded, not lapped, bars are contemplated.

---

* For p_s definition: see ρ_s on page 30, Ref. 60. For help on design of spirals: see page 5-17, Ref. 69 or page 34, Ref. 65; and page C-9 is a useful table in Ref. 71 (included later herein as Table 6.8). Source of p_s equations is Ref. 60 (sections 10.9.2 and A.6.4.2).

† See also NOTE, Fig. 6-10.

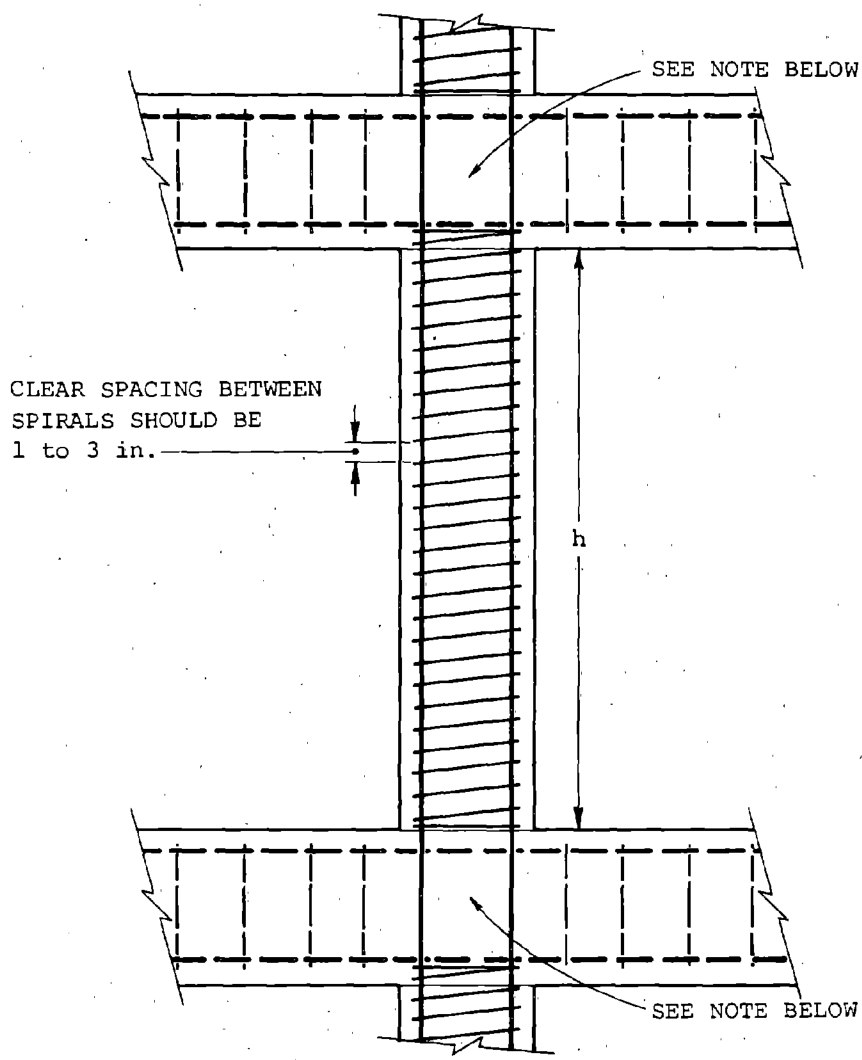

MINIMUM COVER IS 1-1/2 in. ON SPIRAL COLUMNS

SPIRAL EXTENDS FROM FLOOR OR TOP OF FOOTING TO LEVEL OF THE LOWEST BAR IN SLAB, DROP PANEL OR BEAM ABOVE

STEEL RATIO $p = 1$ to 6 percent

SPIRAL STEEL RATIO $p_s = 0.45\ (A_g/A_c - 1)\ f'_c/f_y$
$\geq 0.12\ f'_c/f_y$

SOURCE: Statements are from Ref. 60

NOTE: Ref. 72, p. 164, shows stirrups around this column steel, but they are considered unnecessary in basement shelters, where horizontal movement of the structure is restricted by box action and surrounding earth fill (i.e., lateral floor loads are not carried by the columns).

FIG. 6-10 REINFORCING STEEL DETAILING SCHEME FOR SPIRAL COLUMNS

Table 6.8

SPIRAL COLUMN DETAILING AIDS[71]

SPIRAL SPACERS. Spacers to be used for maintaining the proper pitch of spiral should conform to the following minimum requirements:...

Section Modulus for Spiral Spacers	
Spiral Wire or Rod Dia. (in.)	Min. Spacer Sect. Mod. (in.^{3})
3/8	0.008
1/2	0.030
5/8 (up to 15 ft. high)	0.030
5/8 (over 15 ft. high)	0.050

Number of Spacers per Spiral	
Spiral Core Dia.	Min. No. of Spacers
3/8" or 1/2" wire or rod: 20 in. or less	2
21 to 30 in.	3
More than 30 in.	4
5/8" wire or rod: 24 in. or less	3
More than 24 in.	4

OVERALL DIAMETER OF BARS

Bar diameters are *nominal*, the actual diameter outside of deformations being somewhat greater. The outside diameter may be important when punching holes in structural steel member to accommodate bars or when allowing for the out-to-out width of a group of beam bars crossing and in contact with column verticals. It is close enough to add 1/16 in. for #3, #4, and #5 bars, 1/8 in. for #6, #7, #8, and #9, and 3/16 in. for #10 and #11.

Bar Size	Approx. dia. outside Deformations (inches)
#3	7/16
#4	9/16
#5	11/16
#6	7/8
#7	1

Bar Size	Approx. dia. outside Deformations (inches)
#8	1 1/8
#9	1 1/4
#10	1 7/16
#11	1 5/8
#14	1 7/8
#18	2 1/2

Note that diameters tabulated are approximate size outside of deformations, so clearance should be added.

Table 6.9

PERCENTAGES AND WEIGHTS STANDARD STEEL REINFORCING SPIRALS [71]

WEIGHTS ARE IN POUNDS PER FOOT OF HEIGHT EXCLUSIVE OF SPACERS

Core Dia. in.	% and Wt	PITCH IN INCHES ⅜ϕ 1¾	⅜ϕ 2	⅜ϕ 2¼	⅜ϕ 2½	⅜ϕ 2¾	⅜ϕ 3	⅜ϕ 3¼	⅜ϕ F	½ϕ 2	½ϕ 2¼	½ϕ 2½	½ϕ 2¾	½ϕ 3	½ϕ 3¼	½ϕ 3½	½ϕ F	⅝ϕ 2	⅝ϕ 2¼	⅝ϕ 2½	⅝ϕ 2¾	⅝ϕ 3	⅝ϕ 3¼	⅝ϕ 3½	⅝ϕ F	Core Dia. in.
12	%	2.09	1.83						3.55																	12
	Wt	8.02	7.03																							
13	%	1.93	1.69						3.84																	13
	Wt	8.71	7.63																							
14	%	1.79	1.57	1.40					4.14	2.86	2.54						7.35									14
	Wt	9.35	8.21	7.32						14.92	13.26															
15	%	1.67	1.47	1.30	1.17				4.44	2.67	2.37	2.13					7.87									15
	Wt	10.00	8.82	7.80	7.02					16.00	14.20	12.78														
16	%	1.57	1.37	1.22	1.10				4.73	2.50	2.22	2.00					8.40									16
	Wt	10.71	9.35	8.33	7.51					17.05	15.14	13.64														
17	%	1.48	1.29	1.15	1.03	0.94			5.03	2.35	2.09	1.88	1.71				8.93			2.92	2.65				13.93	17
	Wt	11.40	9.93	8.85	7.93	7.24				18.10	16.10	14.48	13.18							22.48	20.40					
18	%	1.40	1.22	1.09	0.98	0.89	0.81		5.32	2.22	1.97	1.78	1.62	1.48			9.45			2.76	2.51	2.30			14.74	18
	Wt	12.09	10.52	9.42	8.47	7.68	7.00			19.18	17.02	15.38	14.00	12.79						23.83	21.68	19.88				
19	%	1.32	1.16	1.03	0.93	0.84	0.77		5.61	2.10	1.87	1.68	1.53	1.40			9.97		2.90	2.61	2.37	2.17			15.58	19
	Wt	12.70	11.16	9.91	8.95	8.09	7.41			20.21	18.00	16.16	14.72	13.47					27.90	25.10	22.80	20.89				
20	%		1.10	0.98	0.88	0.80	0.73	0.68	5.91		1.78	1.60	1.45	1.33	1.23		10.50		2.76	2.48	2.25	2.07	1.91		16.39	20
	Wt		11.73	10.47	9.40	8.85	7.80	7.26			19.00	17.09	15.48	14.20	13.12				29.45	26.48	24.00	22.10	10.40			
21	%		1.05	0.93	0.84	0.76	0.70	0.65	6.21			1.52	1.39	1.27	1.17	1.09	11.02	2.95	2.62	2.36	2.15	1.97	1.82	1.69	17.21	21
	Wt		12.33	10.93	9.88	8.94	8.22	7.64				17.85	16.34	14.92	13.75	12.81		34.66	30.80	27.75	25.28	23.17	21.40	19.85		
22	%		1.00	0.89	0.80	0.73	0.67	0.62	6.50			1.45	1.32	1.21	1.12	1.04	11.54	2.82	2.51	2.26	2.05	1.88	1.73	1.61	18.03	22
	Wt		12.90	11.48	10.32	9.42	8.65	8.00		18.71	17.02	15.61	14.45	13.42				36.40	32.40	29.19	26.46	24.25	22.30	20.79		
23	%		0.96	0.85	0.77	0.70	0.64	0.59	6.80			1.39	1 26	1.16	1.07	1.00	12.08	2.69	2.40	2.16	1.96	1.80	1.66	1.54	18.84	23
	Wt		13.53	11.98	10.86	9.88	9.02	8.32				19.60	17.76	16.35	15.09	14.10		37.98	33.86	30.45	27.62	25.39	23.40	21.70		
24	%		0.92	0.81	0.73	0.67	0.61	0.56	7.10			1.33	1.21	1.11	1.02	0.95	12.60	2.58	2.30	2.07	1.88	1.72	1.59	1.48	19.68	24
	Wt		14.13	12.43	11.20	10 29	9.37	8.60				20.42	18.59	17.04	15.67	14.59		39.60	35.31	31.80	28.87	26.41	24.41	22.72		
25	%		0.88	0.78	0.71	0.64	0.59	0.54	7.39			1.28	1.16	1.07	0.98	0.91	13.12	2.48	2.21	1.98	1.80	1.65	1.53	1.42	20.48	25
	Wt		14.65	13.00	11.82	10.67	9.83	9.00				21.30	19.32	17.82	16.31	15.15		41 30	36 80	33.00	30.00	27.48	25.48	23.62		
26	%		0.85	0.75	0.68	0.62	0.56	0.52	7.68			1.23	1.12	1.03	0.95	0.88	13.64	2.38	2.12	1.91	1.74	1.59	1.47	1.36	21.30	26
	Wt		15.30	13.50	12.23	11.17	10.08	9.36				22.14	20.18	18.55	17.10	15.84		42.80	38.20	34.40	31.34	28.62	26.46	24.48		
27	%		0.82	0.72	0.65	0.59	0.54	0.50	7.97			1.18	1.08	0.99	0.91	0.85	14 17	2.29	2.04	1.84	1.67	1.53	1.41	1.31	22.12	27
	Wt		15.93	14.00	12.63	11.47	10.50	9.72				22.90	21.00	19.24	17.69	16.52		44.50	39.62	35.79	32.42	29.72	27.40	25.42		
28	%		0.79	0.70	0.63	0.57	0.52		8.27			1.14	1.04	0.95	0.88	0.82	14.70	2.21	1.97	1.77	1.61	1.47	1.37	1.27	22.95	28
	Wt		16.52	14.63	13.18	11.92	10.88					23.82	21.77	19.86	18.40	17.14		46.20	41.20	37.00	33.68	30.78	28.63	26.58		
29	%		0.76	0.67	0.61	0.55	0.51		8.57			1.10	1.00	0.92	0.85	0.79	15.22	2.14	1.90	1.71	1.55	1.43	1.32	1.22	23.79	29
	Wt		17.05	15.03	13.68	12.33	11.43					24.65	22.41	20.63	19.08	17.72		48.00	42.60	38.36	34.79	32.09	29.80	27.39		
30	%		0.73	0.65	0.59	0.53			8.86			1.07	0.97	0.89	0.82	0.76	15 73	2 07	1.84	1.65	1.50	1.38	1.27	1.18	24.60	30
	Wt		17.52	15.60	14.16	12.72						25.70	23.27	21.38	19.69	18.23		49.70	44.20	39.60	36.00	33.10	30.49	28.32		
31	%		0.71	0.63	0.57	0.52			9.16			1.03	0.94	0.86	0 79	0.74	16.28	2.00	1.78	1.60	1.46	1.33	1.23	1.14	25.40	31
	Wt		18.20	16.15	14.62	13.33						26.39	24.10	22.04	20.25	18.98		51.24	45.60	41.00	37.41	34.09	31.54	29.21		
32	%			0.61	0.55	0.50			9.46			1.00	0.91	0.83	0.77	0.71	16.80	1.94	1.72	1.55	1.41	1.29	1.19	1.11	26.22	32
	Wt			16.67	15.03	13.67						27.33	24.89	22.69	21.05	19.40		53.05	47.00	42.35	38.52	35.24	32.50	30.30		
33	%			0.59	0.53				9.76			0.97	0.88	0.81	0.75	0.69	17.32	1.88	1.67	1.50	1.37	1.25	1.16	1.08	27.08	33
	Wt			17.11	15.38							28.15	25.51	23.49	21.75	20.00		54.55	48.49	43.50	39.78	36.25	33.65	31.34		

The above three sizes have been approved through U. S. Department of Commerce Simplified Practice Recommendation R 53-63. For more complete coverage, see *CRSI Design Handbook*.
F = Weight of finishing turns. Total Wt. = Height [spiral wt. per ft. + (spacer wt. per ft. x number of spacers)] + F.
Scale weights may vary from the above values according to the weight tolerances permitted by ASTM specifications applicable to materials used.
Recommended minimum number and section moduli for spacers are shown on page 1-2. 1 in. channel (0.008 in.^{3}) weighs 0.68 lb. per lin. ft.; a 1 x 1 x ⅛ angle (0.03 in.^{3}) weighs 0.80 lb. per lin. ft.; a 1¼ x 1¼ x ⅛ angle (0.050 in.^{3}) weighs 1.01 lb. per lin. ft.

NOTE: F values shown are for 1.5 turns; for 2 turns as recommended herein, multiply tabular values by 4/3.

Source: Ref. 71

F. Footings

After reviewing many USAEWES test reports (see Bibliography), it was concluded that currently the best practical design guidance is outlined in Ref. 2; the method described herein is primarily that suggested by Ref. 2, modified only to update compatibility with the current ACI Code.[60]

The dynamic soil bearing pressure adopted for design use was as follows:

- For rock, in-place crushing strength.
- For granular soil, a bearing pressure that, if applied statically, would produce a settlement of one inch under design blast loading.
- For cohesive soil, a bearing pressure of 3/4 of the failure load.

If detailed soil information is unavailable, the bearing pressure may be taken as the sum of twice the conventional static value (as from a local building code), plus the peak blast pressure existing in soil at the foundation level (footing bottom).

Given the maximum applied load: the plan size of the footings, and then the thickness and steel ratio, are determined. Two detailed footing design procedures are described below, one for strip or wall footings and one for square (column) footings.

Final Design Procedure - Wall Footings. This procedure is less complicated than those described earlier for walls, columns, slabs (and beams); therefore, this procedure was developed for both final and preliminary design, including potential use for making design graphs. It is a static design-analysis approach, except for use of the dynamic strength of steel and soil bearing pressure. The final design steps were:

1. Basic parameter values considered for use were: f'_c = 3,4,5 psi; f_{dy} = 52,72 ksi; p_{so} = 5 to 30 psi; q = dynamic soil bearing pressure = 1 to 14 ksf. For design purposes, the loading P_u was taken as twice the peak blast overpressure times the tributary area of the shelter cover slab; the loading was expressed in lbs/in. (along wall footing).

2. Footing dimension ℓ (width of footing on each side of the supported wall) was calculated:[2]

$$\ell = 0.5 \, (P_u/q - a) \tag{6-36}$$

where a = wall thickness (in.)

3. The equation[2] used for flexural resistance was:

$$q_f = 1.8 \, p f_{dy} (d/\ell)^2 \tag{6-37}$$

and for ultimate shear resistance[2] was:

$$q_v = 250 \, (p f'_c)^{0.5} (d/\ell)^2 \tag{6-38}$$

For balanced design-failure: $q_f = q_v$ and $\overline{p}$ was used to distinguish it from the general rebar ratio p, thus

$$\overline{p} = 19{,}290 \; f'_c \; / \; f_{dy}{}^2 \tag{6-39}$$

Values of $\overline{p}$ were then calculated for various combinations of f'_c and f_{dy}:

f_{dy}	f'_c = 3 ksi	4 ksi	5 ksi
52 ksi	0.0214	0.0285	0.0357
72 ksi	0.0112	0.0149	0.0186

4. Selection of a design value for p is strongly recommended to be such that failure would be expected in flexure rather than shear, meaning $p \le \overline{p}$, in which case the footing d was obtained from:[2]

$$d = \ell \, [0.5556 \, q/(p f_{dy})]^{0.5} \tag{6-40}$$

If the recommendation is not followed, shear is the expected failure mode, meaning $p > \overline{p}$, in which case

$$d = \ell \, [0.004 \, q/p f'_c)^{0.5}]^{0.5} \tag{6-41}$$

Final Design Procedure - Square (Column) Footings. The opening comments under wall footing design apply equally for column footings, except that the dynamic strength of concrete f'_{dc} [= 1.25 f'_c] was also used. The final design steps developed were:

1. Same as step 1 for wall footings, except that total load P_u is in pounds, not in lbs/in. (along wall footing).

2. Length L of square footing was calculated:[2]

$$L = (P_u/q)^{0.5} \tag{6-42}$$

3. Equation[2] used for flexural resistance was:*

$$q_f = 7.2\ pf_{dy}\ [d / (L - a)]^2 \qquad (6\text{-}43)$$

and for ultimate shear resistance[2] was:

$$q_v = 3.5adf'_{dc}\ [0.035 + 130\ \text{psi}/f'_{dc} + 0.07\ q_f/q_v] / [L^2 - (a+2d)^2] \qquad (6\text{-}44)$$

Again, for balanced design-failure: $q_f = q_v$ and d_o was used to distinguish it from the general d, thus

$$d_o/L = [-B + (B^2 - 4\ AC)^{0.5}] / (2A) \qquad (6\text{-}45)$$

where: $A = 4\ q/f'_{dc}$

$B = (a/L)\ [4\ (q/f'_{dc}) + 3.5\ (0.105 + 130\ \text{psi}/f'_{dc})]$

$C = (q/f'_{dc})\ (a^2 - L^2) / L^2$

Then: $$\overline{p} = 0.1389\ (q/f_{dy})\ [(L - a) / d_o]^2 \qquad (6\text{-}46)$$

4. As before, with wall footings, selection of a design value for p is strongly recommended to be such that failure would be expected in flexure rather than shear, meaning $p \leq \overline{p}$, in which case the footing d was obtained from:[2]

$$d = L\ [0.1389\ (q/f_{dy})\ (1 - a/L)^2 / p]^{0.5} \qquad (6\text{-}47)$$

If the recommendation is not followed, shear is the expected failure mode, meaning $p > \overline{p}$, in which case the following cubic equation must be solved for d/L (trial-and-error solution is suggested, using a computer or programmable desk calculator):[2]

$$(d/L)^3\ [1.764\ pf_{dy}f'_{dc}(a/L)] + (d/L)^2\ [4\ q_v^2\ (1 - a/L)^2]$$

$$+ (d/L)\ [q_v\ (1 - a/L)^2\ (a/L)\ (4\ q_v + 0.1225\ f'_{dc} + 455)]$$

$$- q_v^2\ (1 - a/L)^2\ [1 - (a/L)^2] = 0 \qquad (6\text{-}48)$$

Rebar Design and Details. In both one-way reinforced wall footings and two-way reinforced square (column) footings, the reinforcement should be distributed uniformly across the full width of the footing. The wall or column reinforcing steel should be carried down well into the footing.

---

* For round columns, which are recommended for use herein, a = 0.886 D, where D is the column (outside) diameter.

The maximum rebar size to be used in a footing is related to a required "development length,"* which is a function of f_y and f_c', plus A_b or d_b (area of one bar, sq.in., and nominal diameter of bar, wire, or prestressing strand, in., respectively), a procedure replacing the design checking for bond stress; for most cases, the development length required for rebars in tension is

$$\ell_d = 0.04\ \text{in.}^{-1}\ A_b f_y \ /\ f_c'^{0.5} \quad \text{but} \geq 0.0004\ (\text{in.}^2/\text{lb})\ d_b f_y \geq 12\ \text{in.} \tag{6-49}$$

with correction factors required for certain cases.* For blast-resistant design, it is recommended that the required development length, such as that just described, be increased by 50%. The following table of required development lengths includes the 50% recommended increase over Eq. 6-49:

	f_y = 40,000 psi									f_y = 60,000 psi								
	Bar Designation Number									Bar Designation Number								
f_c'	3	4	5	6	7	8	9	10	11	3	4	5	6	7	8	9	10	11
3000	18	18	18	19	26	35	44	56	68	18	18	23	29	39	52	66	83	103
4000	18	18	18	18	23	30	38	48	59	18	18	23	27	34	45	57	72	89
5000	18	18	18	18	20	27	34	43	53	18	18	23	27	31	40	51	65	79

Because the rebars require 3 in. of concrete cover at each end, the available development length ℓ_{da} measured from the wall face in wall footings would be

$$\ell_{da} = \ell - 3\ \text{in.} \tag{6-50}$$

and in square (column) footings

$$\ell_{da} = (L - a - 6\ \text{in.})\ /\ 2 \tag{6-51}$$

In use, therefore, the bar size selected must be such that $\ell_d \leq \ell_{da}$.

For rebars in compression, such as dowels to serve as footing-column connections, the required development length should be*

$$\ell_d = 0.02\ d_b f_y \ /\ f_c'^{0.5} \quad \text{but} \geq 0.0003\ d_b f_y \geq 8\ \text{in.} \tag{6-52}$$

again with correction factors required in certain cases† and a blast-resistant design recommendation of a 50% increase in required development length over the above formula. The following table of required development lengths includes the 50% increase over Eq. 6-52:

---

* Section 12.5, Ref. 60

† Section 12.6, Ref. 60

	f_y = 40,000 psi									f_y = 60,000 psi								
	Bar Designation Number									Bar Designation Number								
f'	3	4	5	6	7	8	9	10	11	3	4	5	6	7	8	9	10	11
3000	12	12	14	16	19	22	25	28	31	12	16	21	25	29	33	37	42	46
4000	12	12	12	14	17	19	21	24	27	12	14	18	21	25	28	32	36	40
5000	12	12	12	14	16	18	20	23	25	12	14	17	20	24	27	30	34	38

Space for the required development length in compression for dowels could be gained either by increasing the pedestal height or bending the rebar 90° near the footing bottom steel (remember that a 3-in. bottom concrete cover is required).

For either bottom steel or dowels, of course, using a smaller bar size reduces the required development length (but not less than 12 in. plus 50% or 8 in. plus 50%, for tension or compression, respectively).

For wall footings, longitudinal reinforcement (i.e., parallel to the wall, also distributed uniformly across the footing) should be provided such that the ratio of reinforcement area to gross concrete area is 0.002.

G. Wood Beams - Simply Supported

The wood contemplated for use under the design procedures described herein is structural or stress-graded lumber, which has been carefully graded in accordance with the standard grading rules for the appropriate trade association (e.g., References 52 and 53). A complete list of such associations is available.[54] It is urged that all lumber contemplated for shelter use - specifically, lumber in structural components or members whose stress-resisting capability is important to the survival of shelterees (in contrast to such things as a door cross-brace that simply holds together the structurally significant members) - be reinspected and regraded by particularly qualified personnel using the appropriate association's grading rules.

Other items for the designer's general consideration are:

- The lack of homogeneity in wood members dictates that every effort be made to design wood structural members so that they interact in such a manner as to transfer load from a weaker or below-standard member to the better members. Examples are: really good blocking between floor joists; and use of tongue-and-groove planking as members used flat in a blast door.

- Only very tight knots (preferably no knots) should be accepted in a situation such as that of an unclad wood shelter blast door where an air blast loading could make a missile or bullet out of a knot that is even slightly loose.

- Metal cladding may be indicated for some situations where wood is used, such as exposure to fires (or where required by local building code), but not necessarily when exposure is only to a nuclear thermal pulse (which may well char the door without setting it on fire, a difficult thing to do to a flat wood wall).

Because this guide is intended for use by engineers and architects with special training in DCPA-conducted courses or their equivalent (as has been stated earlier[50] in a Preface and Chapter 1), technical competence in the usual design of wood structural members is assumed,[54-57] and only those design considerations peculiar to nuclear blast effects loading will be treated in some detail in this section.

Design Procedure. Because wood beams are available in specific dimensions, the general design approach is to select a trial member depth (measured in the direction of the applied load) and width, then find the air blast peak overpressure it can resist; this overpressure is compared

to the specified overpressure to be resisted. The resistance of the selected member is based on elasto-plastic behavior and associated stress resistances in flexure (bending), horizontal shear, and bearing on a support, which resistances are checked in that order. Specifically, the flexure and horizontal shear resistances are found, and then a new trial member is selected, repeating these steps until the lesser of the two resistances is found to be sufficient to meet the expected blast load. The required bearing area is then found directly.

The design steps are as follows:

1. A design air blast peak overpressure is specified, also whether its loading geometry will provide: a side-on overpressure (as in a wood door mounted flush with the earth's surface); a fully reflected overpressure (as in the front wall of a rectangular building); or a peak value of the average loading caused by a combination of side-on and drag pressure (as in the side-wall or roof of a rectangular building[1(§4.80-)]). Related variables, in the same order of loading geometries, look like this:

$$p_m = p_{so} \text{ or } p_r \text{ or } \left[(p_{so} + C_d q)\ L/2U\right] \qquad (6\text{-}53)$$

where q is the dynamic (wind) blast pressure (unlike the q for structural resistance used in the remainder of this section).[1(p. 182-)]

2. A trial size of wood beam (actual depth d, measured in direction of load, and thickness or width b) and kind of structural or stress-graded lumber are selected, then the grading association's design stresses are determined from their publications. Need for the latter may be limited to F_b (extreme fiber stress in bending), F_v (horizontal shear stress), and $F_{c\perp}$ (compression stress perpendicular to grain, or bearing stress as used herein). For the short duration loadings furnished by nuclear air blast, dynamic values of the above three design stresses are recommended[23] as follows:

$$F_{db} = 4F_b \ ; \ F_{dv} = 4F_v \ ; \text{ and } F_{dc\perp} = F_{c\perp}$$

Some grading rules allow increases in design stress values for such things as: repetitive member design values (not recommended for use herein); and members used flatwise (probably appropriate for use herein).[52(p.130-1)]

3. A design ductility ratio μ is selected (see discussion in the earlier section herein, General Comments on Blast-Resistant Design . . .). A value of 3 is recommended,[23] certainly as an upper limit, and with 1.3 or 2 even better.[31]

4. A short design procedure[23] omits use of any loading decay (i.e., uses instead an instantaneously applied long duration load, or step pulse), load-mass factors, modulus of elasticity, elasto-plastic resistance function per se, etc., all in favor of the following approach: A step pulse is assumed, which is reasonable particularly when large yield weapons and short wood beams (therefore having very short periods of natural vibration) are considered.* The other things ignored have been found to have little effect on the structural member selected for most applications; and needed parameters then have the following relationship: $p_m/q = 1 - 1/(2\mu)$ where q is the ultimate resistance to blast loading of the wood beam. Using the recommended value of $\mu = 3$, the equation becomes: $p_m = (5/6)\ q$

5. Clear span L and support conditions are known or assumed. Formulas are included herein for three beam support conditions: simply supported (SS); propped cantilever (PC); and both ends fixed (FF).

6. Flexural or bending resistance q_b (in terms of load/unit area) is calculated for the trial member:

$$M = wL^2c = q_b bL^2c = F_{db}S = F_{db}bd^2/6$$

$$q_b = F_{db}(d/L)^2/(6c) = 2F_b(d/L)^2/(3c) \qquad (6\text{-}54)$$

where c = 1/8 (SS) and (PC), 1/12 (FF).

7. Horizontal shear resistance q_v (in terms of load/unit area) is also calculated for the trial member, with horizontal shear equal to vertical shear and taken at a distance d in from each end of the member: member:[23(p.161),54(p.4-12)]

$$V = w(L-2d)c' = q_v b(L-2d)c' = 2AF_{dv}/3 = 2bdF_{dv}/3$$

$$q_v = 2F_{dv}d/(3c'(L-2d)) = 8F_v d/(3c'(L-2d)) \qquad (6\text{-}55)$$

where c' = 1/2 (SS) and (FF), 5/8 (PC), the latter value being approximate but close enough for the purposes herein.

8. Wood beam resistance q is then equal to the lesser value between q_b and q_v and is converted to peak air blast pressure by using a formula given earlier:

$$p_m = (1 - 1/(2\mu))\ q \qquad (6\text{-}56)$$

or, when the recommended value of $\mu = 3$ is used, $p_m = (5/6)\ q$.

---

* Alternatives to this use of a step pulse are chart solutions and the Newmark β Method, described herein (page 6-12, third paragraph).

9. If p_m is less than the design air blast peak overpressure specified in the first step herein, a larger beam, or a different wood or grade having larger design stresses, must be tried. If p_m is larger than the design overpressure, than it may be desirable to try a smaller beam, or a different wood or grade, in an effort toward closer design. In either case, a new trial member requires that the designer return to the second step and repeat the procedure to this point.

10. Required bearing length L' at <u>each end</u> of the wood beam is calculated as follows:

$$V = qbLc' = F_{c\perp}bL'$$

$$L' = qLc'/F_{c\perp} \qquad (6\text{-}57)$$

where the values of c' are the same as in step 7 above.[55(p.206-7)] It is recommended that L' be at least 1.5 to 2 inches.

<u>Application to a Shelter Door Design</u>. An application of wood beam design occurs when low-cost blast doors must be designed for shelters, in new designs or existing structures. For an application in existing structures, particularly, a pre-design or chart approach was needed as follows:

- An estimate, calculated or judgmental, is made of the blast resistance of the wall adjacent to an aperture (door or window opening) for which a wood blast door is needed. The only <u>designed</u> structural element will be a wood beam, or series of wood beams side-by-side and preferably tongue-and-groove, simply supported on the two <u>sides</u> of the door frame (that has been either strengthened or found adequate to take the load from the door onto the wall).

- Structural grades of various kinds of wood, in standard thicknesses (2, 3, 4, 6 inches, nominal; 1.5, 2.5, 3.5, 5.5 inches, actual) are checked for availability.[52]

The pre-design or chart approach developed for simplified handling of this problem was as follows:

- Obtain a copy of the industry association grading rules for each kind of wood contemplated for possible use; from this, make a tabulation (for each kind of wood and each thickness) of design stresses (psi) stated for use under normal loading for:

- Bending design stress (in extreme fiber), F_b
- Horizontal shear design stress, F_v
- Compression perpendicular to grain design stress, $F_{c\perp}$

- Conversion of design stresses to dynamic values (step 2 above) is unnecessary hereunder; the charts used include this conversion and are therefore entered directly with the design stresses for normal loading.

- For each wood and thickness, determine the blast resistance in terms of free-field overpressure:
  - For the specific thickness, use the pre-design chart, Figure 6-11, which consists of four charts, covering member thicknesses of 1.5, 2.5, 3.5 and 5.5 in. The charts are based on use of Equations 6-53 through 6-56, and assume $\mu = 3$, step pulse and simple supports; the charts are entered with design, not dynamic, stresses (per the preceding paragraph).
  - Enter the chart with the known clear span: first, use the left set of curves, moving up to the known allowable design stress F_b for the selected wood, interpolating as necessary and noting the related applied overpressure (psi) read on the ordinate scale; second, repeat the procedure with the right set of curves (for stress in horizontal shear F_v), again noting the related overpressure. <u>Use only the lower of the two applied overpressures read</u>!

- For each wood and thickness still of interest, determine the required bearing length <u>at each end</u> of the wood beam:
  - Use the last wood pre-design chart, Figure 6-12. The chart is based on use of Equation 6-57, and assumes $\mu = 3$, step pulse and simple supports. Thus $L' = (6/5)\ p_m L\ (1/2) / F_{c\perp}$ (from Eq. 6-57); or $p_m = (5/3)\ L'F_{c\perp} / L$ for which Figure 6-12 is a plot for several specific values of $F_{c\perp}$ and L as the independent variable, all with L' = 1 in.
  - Enter with the clear span, move up to the allowed design stress, and read the applied overpressure on the ordinate scale; this applied overpressure is for <u>one inch</u> of bearing length on <u>each end</u> of the wood beam.

FIG. 6-11A   WOOD BEAM DESIGN, BENDING AND SHEAR

STRUCTURAL OR STRESS-GRADED LUMBER
Actual thickness 1.5 inches

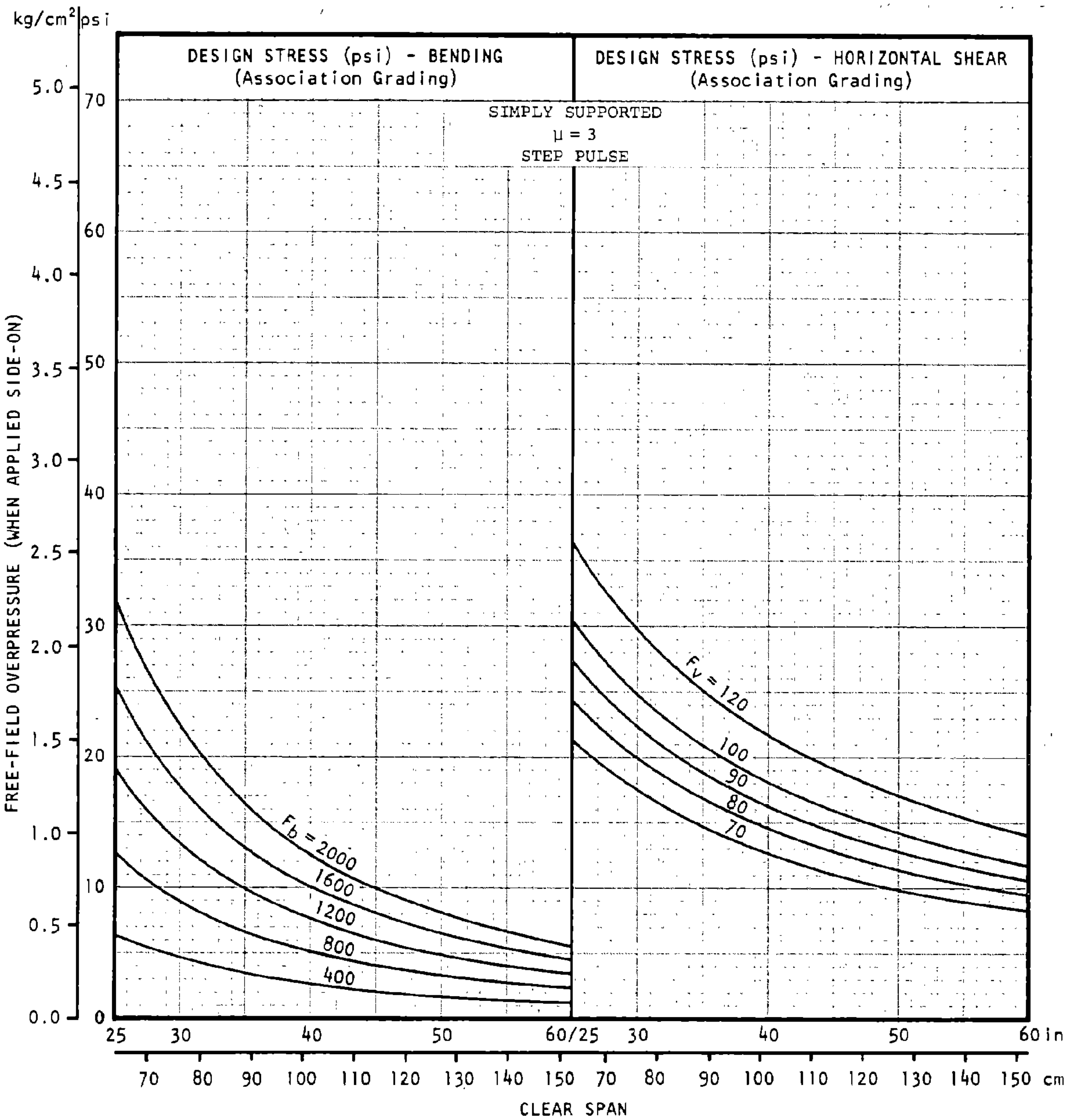

FIG. 6-11B WOOD BEAM DESIGN, BENDING AND SHEAR

STRUCTURAL OR STRESS-GRADED LUMBER
Actual thickness 2.5 inches

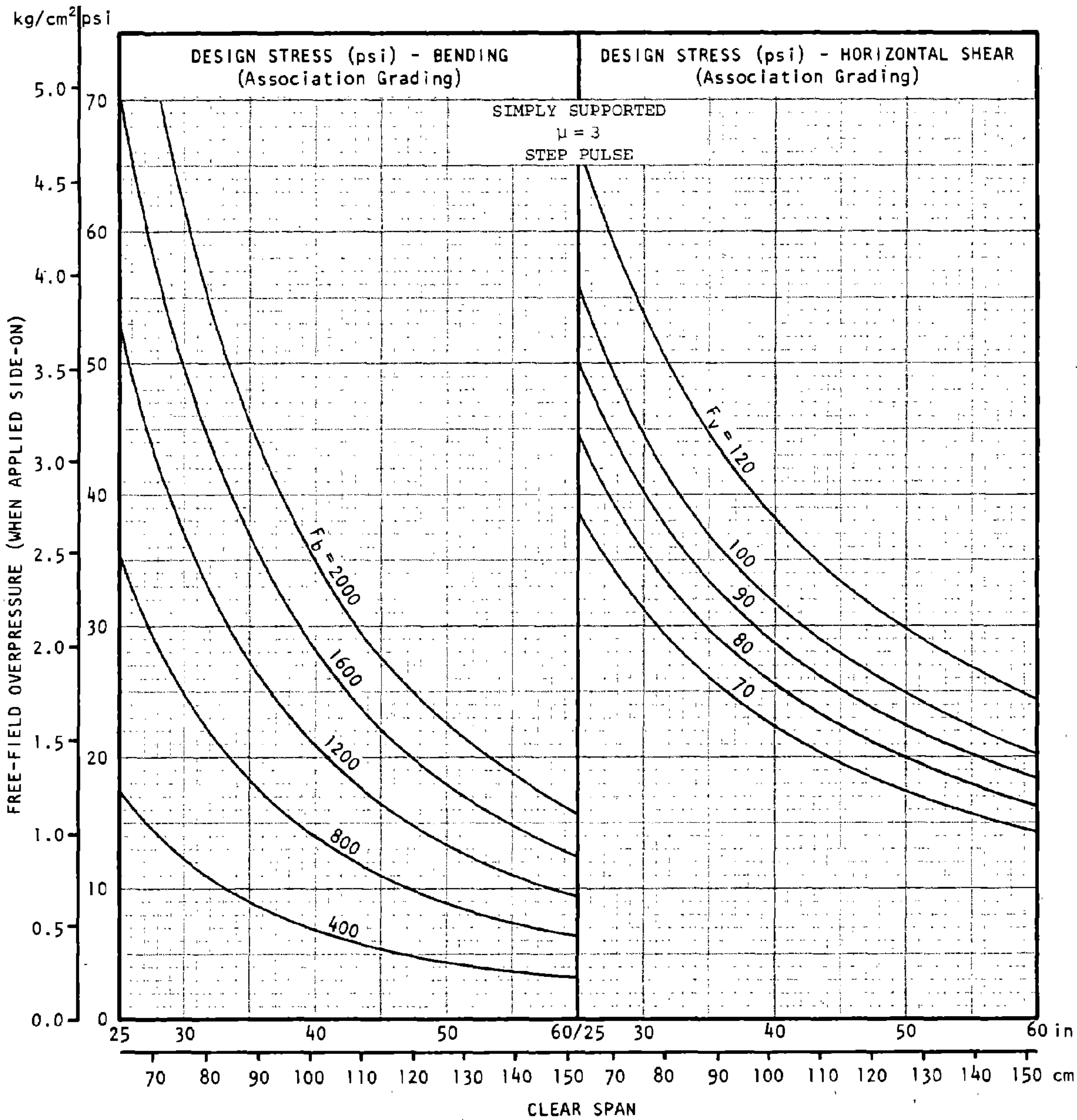

FIG. 6-11C WOOD BEAM DESIGN, BENDING AND SHEAR

STRUCTURAL OR STRESS-GRADED LUMBER
Actual thickness 3.5 inches

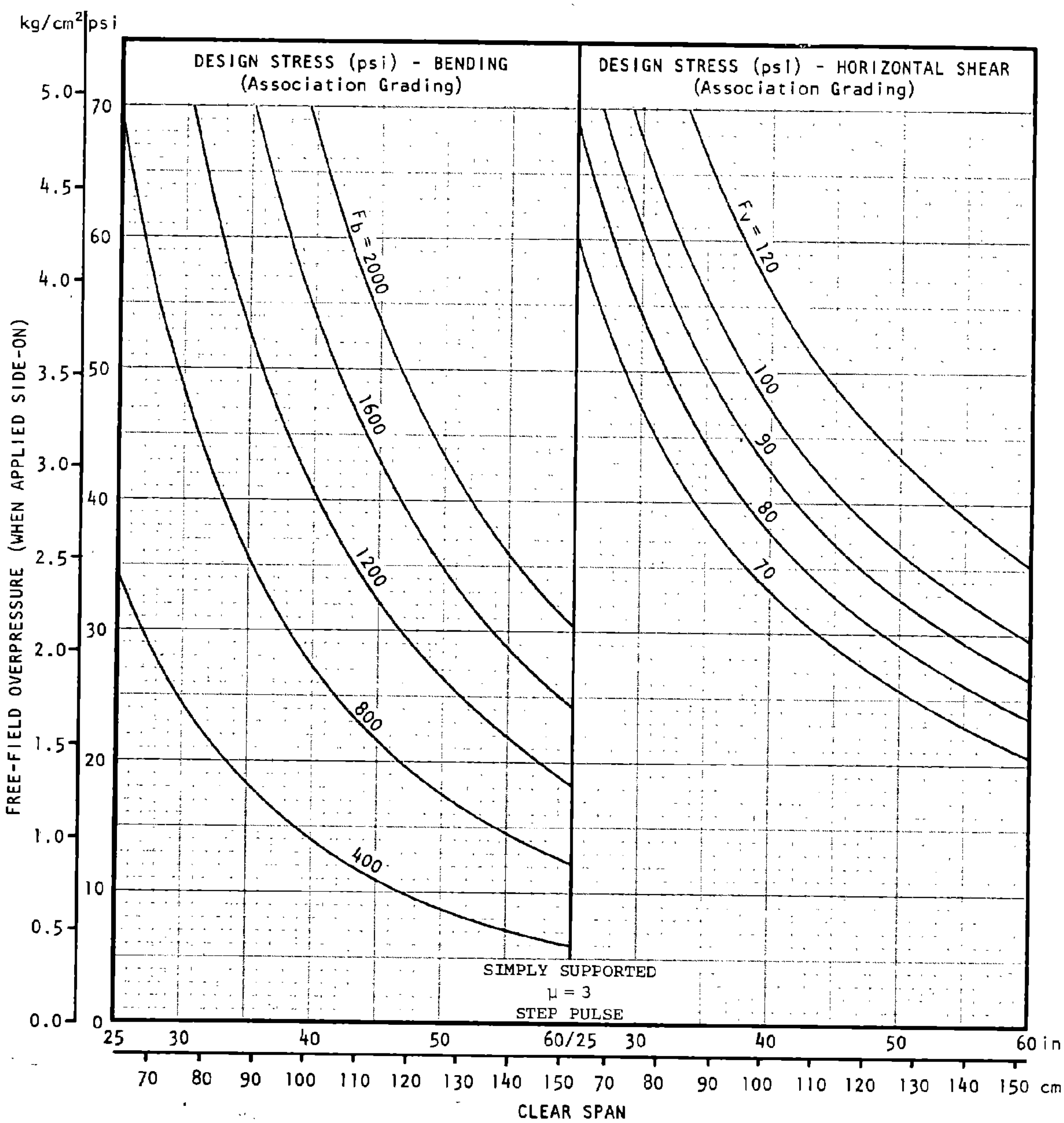

FIG. 6-11D WOOD BEAM DESIGN, BENDING AND SHEAR

STRUCTURAL OR STRESS-GRADED LUMBER
Actual thickness 5.5 inches

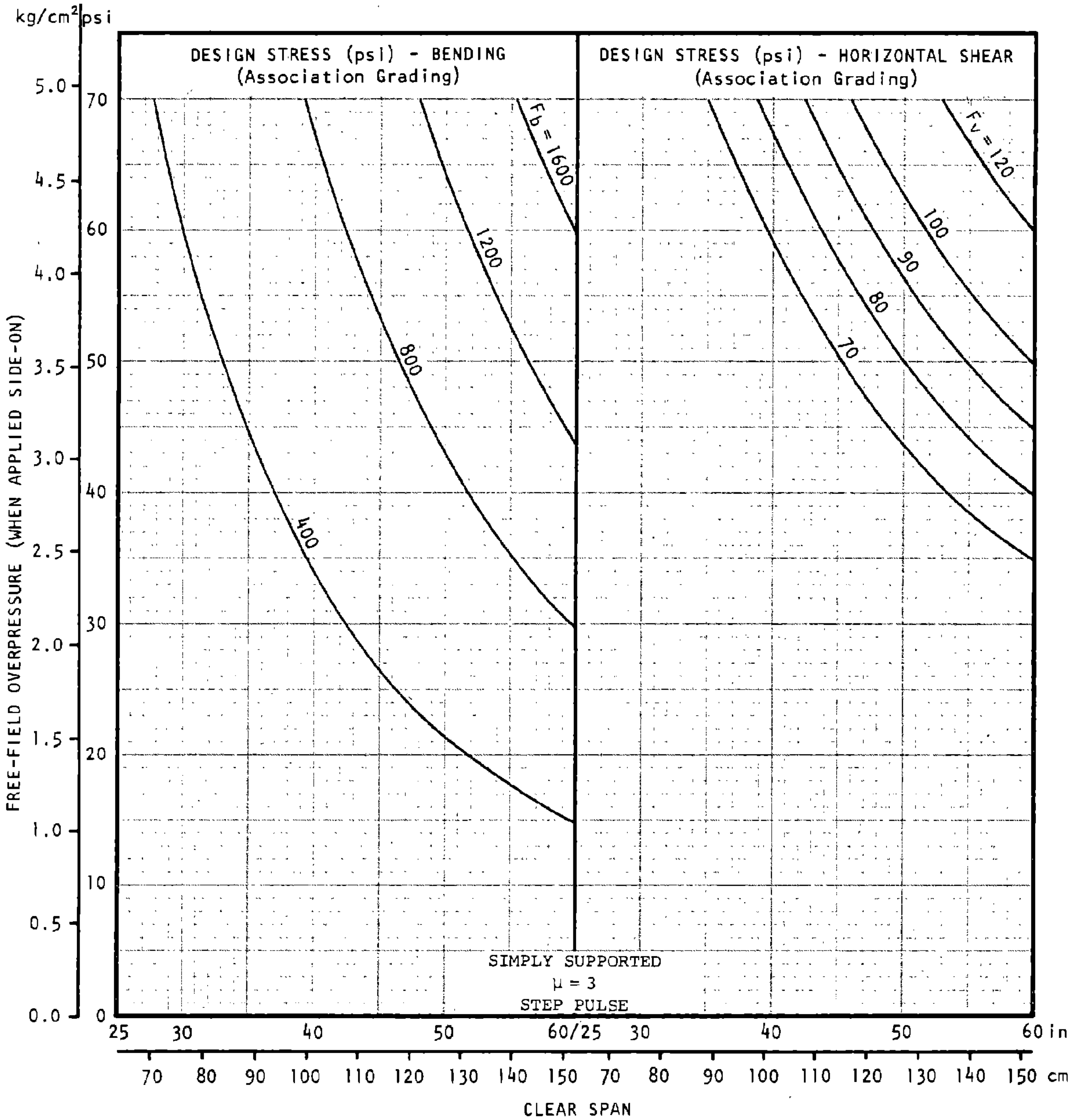

FIG. 6-12 WOOD BEAM DESIGN, END BEARING

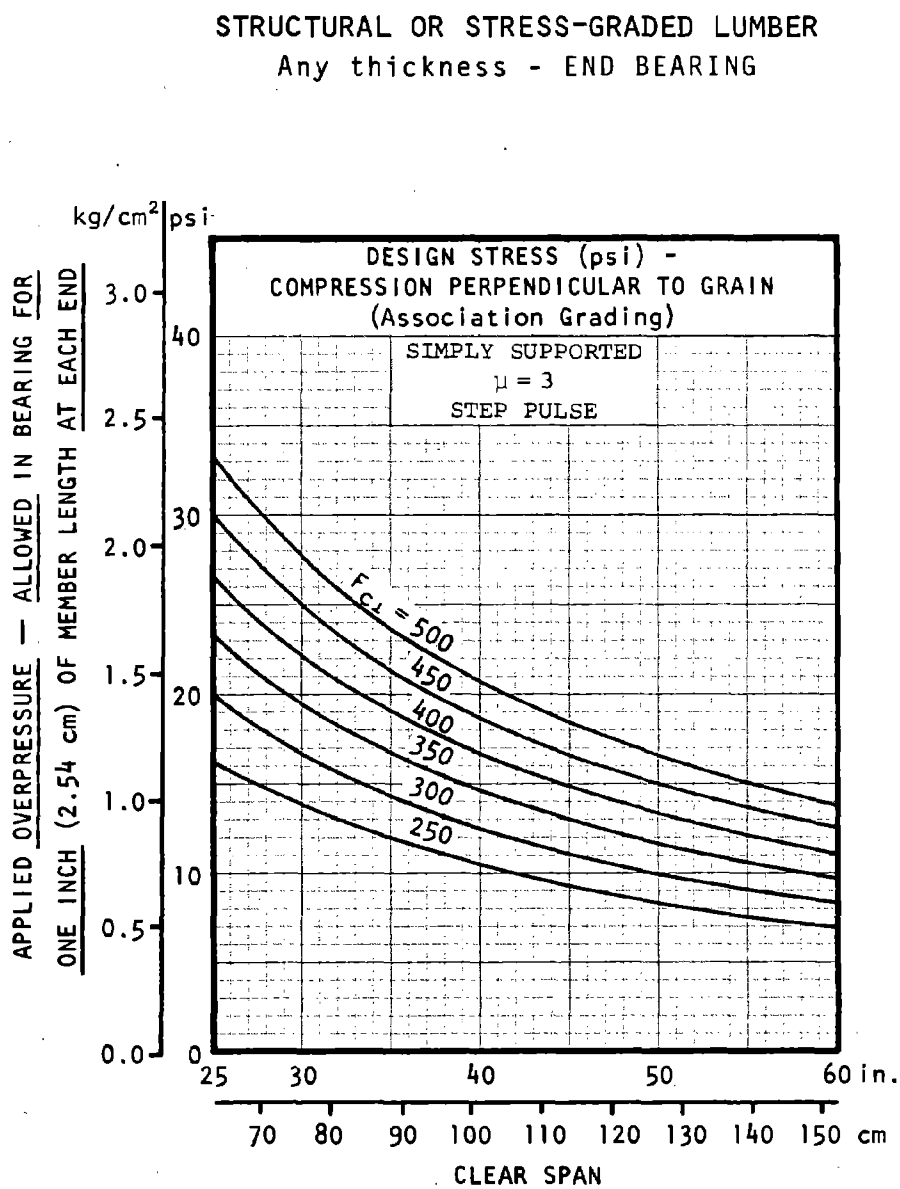

- Divide this applied overpressure for bearing into the overpressure noted at the end of the preceding step (using Figure 6-11); the resulting quotient is the number of inches bearing length required at each end of the wood beam. It is recommended that a minimum length of, say, 1-1/2 or 2 inches be used.

- Applied overpressure, psi, determined above for the particular clear span and kind of wood (with its design stresses from the grading association), was the overpressure when applied side-on, such as if the wood beam were part of a cover or door, mounted flush with the ground and the blast wave passed over it flowing horizontally. If the member is to be used so that the blast wave strikes it head-on, as if the member were part of the front wall of a building struck by the blast wave, then the blast wave is fully reflected, making it equivalent in loading force to a much stronger wave applied only side-on. To relate these two situations by putting both in terms of free-field overpressure resistance (that is, out in the open, unaffected by structures), use the scales below:

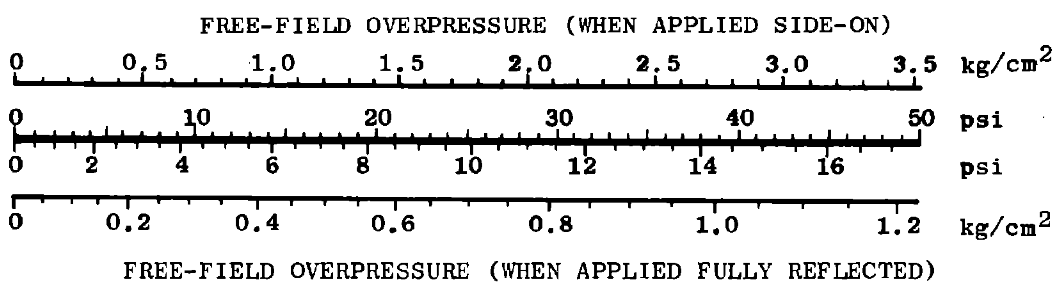

For example, a free-field overpressure of 45 psi hitting the member side-on gives the same peak loading to the member as a free-field overpressure of 16 psi hitting the member head-on, or fully reflected.

A numerical example of this procedure is as follows:

- Clear span 40 inches; bending design stress 1,250 psi; horizontal shear design stress 95 psi; compression perpendicular to grain design stress 385 psi. (These are the values for Douglas Fir, #2 Grade, under Structural Joists and Planks, Table 6.)[52] Assumed blast orientation is head-on, or fully reflected.

- First thickness of above wood to be checked for blast resistance is 3 in. nominal, 2.5 in. actual. Entering the chart, Figure 6-11B, for that thickness, clear span 40 in.: design stress in bending of 1,250 psi gives about 21 psi overpressure; design stress in horizontal shear of 95 psi gives about 30 psi overpressure.

- Required bearing length at each end of the wood beam is obtained by using the last chart, Figure 6-12: entering with a clear span of 40 in., and interpolating for a design stress of 385, gives an applied overpressure (per inch of bearing at each end) of about 16 psi. Dividing the 16 psi. Dividing the 16 psi into the 21 psi noted just above gives a member length at each end, for bearing, of $\frac{21}{16}$ or 1-5/16 in. for which the used length would be rounded (upward ALWAYS) to, say, 1.5 in. at each end (which is a minimum recommended above).

- Free-field overpressure applied head-on, i.e., fully reflected, is found by entering the scale above with the 21 psi side-on (free-field overpressure resistance) and finding this numerical example's answer of about 8.5 psi (free-field overpressure resistance for the wood member loaded by a fully reflected blast wave).

NOTATION

The notation of Tables 6.1 and 6.3 and Figure 6-1 is defined therein and excluded below.

A	area of temperature and shrinkage steel
A, B, C	intermediate equation values used in computing other variables
A_c	area of core of spirally reinforced column measured to the outside diameter of the spiral
A_g	gross area of section
A_s	area of steel in a tension zone
A_s'	area of steel in a compression zone
A_{st}	total area of steel in column
A_v	area of steel in web reinforcement (vertical stirrups) within distance s
a	width of loaded area
a	thickness of wall resting on footing
b	width of beam
$c, c', c'', c_1, c_2, C, C', C''$	dimensionless coefficients
c	ratio of distance between extreme compression fiber of a beam or slab and the neutral axis to depth d (USD)
D	diameter of column
D_s	diameter to the centroid of the vertical bars in a column
d	distance from extreme compression fiber to centroid of tension reinforcement
d'	distance from extreme compression fiber to centroid of compression reinforcement
d''	distance from centroid of tension reinforcement to face of tension reinforcement concrete cover
d_o	distance from extreme compression fiber to the centroid of the tension reinforcement, which produces failure simultaneously in flexure and shear under the same design load

E	modulus of elasticity of section
E_c	concrete modulus of elasticity
E_s	steel modulus of elasticity
e	eccentricity of design load parallel to axis, measured from the plastic centroid
e	base of Napierian or natural logarithms
e_s'	$= \varepsilon_s'$
e_y	$= \varepsilon_y$
F_b	extreme fiber stress in bending
F_{db}	dynamic extreme fiber stress in bending
$F_{c\perp}$	compression stress perpendicular to grain, or bearing stress
$F_{dc\perp}$	dynamic compression stress perpendicular to grain, or bearing stress
F_v	horizontal shear stress (in wood)
F_{dv}	dynamic horizontal shear stress (in wood)
f_c'	static compressive strength of concrete (28-day or later)
f_{dc}'	dynamic compressive strength of concrete
f_{dy}	dynamic (average) yield strength of reinforcing steel
f_y	yield strength of reinforcing steel, specification minimum
f_d	average of dynamic stress factors for steel and concrete
h	same as D, diameter of column
h_e	effective thickness of a column for slenderness
I	cracked section moment of inertia
I_g	moment of inertia of gross concrete area
I_s	moment of inertia of steel area
j	ratio of distance between centroid of compression and centroid of tension, to the depth d (WSD)
K	stiffness factor (elastic phase)
K	weighted dynamic load factor
K_e	dynamic load factor (elastic phase)
K_L	dynamic load factor

K_M	dynamic mass factor
K_o	lateral soil pressure coefficient
K_p	stiffness factor (plastic phase)
K_p	dynamic load factor (plastic phase)
K_R	dynamic resistance factor
k	stiffness factor
k, k'	ratio of distance from the extreme compression fiber to the neutral axis, to depth d (WSD)
k_1, k_2	ratios used in R/C ultimate strength design (see Ref. 32, p. 809-8)
k_3	ratio of the distance from the extreme compression fiber to the neutral axis, to depth d (USD) (same as c)
L	clear height of wall
L	length of structure, or long dimension of rectangular footing, etc.
L	outside (or plan view) dimension of square footing
L	span length of member (clear span, unless otherwise indicated)
L'	bearing length at each end of a wood beam
L_v	length of stirrup steel
ℓ	distance that wall footing protrudes from face of wall
ℓ_d	required development length, in.
ℓ_{da}	available development length, in.
ℓ_n	Napierian or natural logarithms
ℓ/r	ratio of length to radius of gyration
ℓ_u	unsupported length of compression member
M	bending moment
m	mass, unit
n	ratio of steel to concrete moduli of elasticity
P	in-plane applied loading
P_{cr}	critical buckling load of section

P_u	ultimate in-plane capacity of the trial wall section
p	reinforcing steel ratio, tension steel, positive moment
p'	reinforcing steel ratio, compression steel, positive moment
$\bar{p}$	steel ratio that produces a balanced design in footing
p_e	reinforcing steel ratio, tension steel, negative moment
p_e'	reinforcing steel ratio, compression steel, negative moment (end tensile steel)
p_m	peak (unit) value of applied (air blast) loading
p_r	peak reflected (air blast) overpressure
p_s	ratio of volume of spiral reinforcement to total volume of core (out-to-out of spirals) of a reinforced or composite column
p_{so}	peak side-on (air blast) overpressure
p_v	reinforcing steel ratio, web reinforcement ($=A_v/sb$, for vertical stirrups)
$\bar{p}_v$	minimum recommended reinforcing steel ratio, web reinforcement
q	static unit load, equivalent to dynamic load in assumed structural response
q	yield resistance of member, general
q	bearing capacity of footings, psi
q_b	bending resistance
q_f	ultimate flexural resistance of member
q_v	ultimate shear resistance of member
r_o	$= (n-1)p'/(np)$, used in computing cracked (transformed) section properties
r/q_y	ratio of required rebound resistance to direct load resistance
S	spacing between main horizontal bars
s	spacing of web reinforcement (vertical stirrups)
T	natural period of vibration
t	thickness
t_d	effective duration

Preceding page blank

t_m	time to reach maximum deflection
t_o	duration of positive overpressure phase
t_{00}	duration of initially peaked triangular replacement loading pulse (with decay defined by tangent to overpressure-time curve at p_{so})
u	bond stress
u_d	allowable dynamic bond strength
V	total shear at critical section
V	vertical shear in a member
W	weapon yield
x, x' y, y' z, z'	intermediate equation values (dummy variables)
x_e	deflection of member at effective yield point
x_m	max. deflection of member
α	stirrup inclination angle
β	coefficient in Newmark β Method (Ref. 21)
β_1	factor used in computing the effectivd compression area in USD
γ	$= D_s/D$
δ	amplification factor associated with P - Δ effect (i.e. in-plane load)
ϵ_s	strain in tension reinforcing steel
ϵ_s'	strain in compression reinforcing steel
ϵ_c	concrete yield strain
ϵ_y	steel yield strain
μ	ductility factor, ratio of maximum to yield deflections
ρ_s	same as p_s

Chapter 7

DESCRIPTION OF CASE BUILDINGS

General descriptions are given below for each of the buildings selected for the full slanting case studies. The case studies described in later chapters use the same building number as shown below, plus a letter to indicate the case study; for example, Building 1 was used in case studies as Building 1A and Building 1B. Basement floor plans are included in the next chapter.

It was necessary to adopt a working hypothesis for Building 1: that its planned location was such as to provide adequate clearance distance from any other building(s). The real situation was such as to exclude the building from consideration for full slanting.

Building 1

U.S. Post Office and Court House, Newnam, Georgia.
Design and construction by General Services Administration, Public Buildings Service, Washington, D.C. Design (under GSA contract) by Stevens & Wilkinson, Architects & Engineers, Atlanta, Ga.

Site approx 130'x200'; streets on 3 sides. Building 3 stories 104'x130', plus basement 104'x63'. Reinforced concrete frame and pan-joist; exterior walls: concrete masonry units with face brick, except concrete walls at 1st fl. Partitions: concrete masonry units, or metal stud and plaster. Fire resistive Type II Construction. Ducted air conditioning from central fan-coil units in basement and in penthouse.

Building 2

Brentwood Rehabilitation Center, Asheville, North Carolina.
Design by John D. Latimer & Associates, Architects-Engineers, Durham, N.C.

Site approx 950'x600', sloping from elev. 170' to 100' at street end. Building provides beds for 71 patients, dining room, kitchen

offices and treatment rooms, all on one floor of approx 23,000 sf (in 3 wings and connecting structure); laundry and boiler room in partial basement under center wing (45'x82'). Exterior walls brick. Interior partitions: brick, or stud and plaster. Roof framing: steel beams with bar joists. Insulating wood fiber roof deck. Fire resistive Type III Construction. Floors: concrete slab on grade, except concrete slab on bar joists over basement. Heating by baseboard radiation; no cooling; operable windows.

Building 3

Columbus-Muscogee County Court House, Columbus, Georgia. Design by E. Oren Smith and Biggers-Scarbrough-Neal-Crisp and Clark, Associated Architects and Engineers, Columbus, Georgia.

Site approx 300' X 600', essentially level, with cleared areas around all buildings in complex. Complex has central plaza (at one level, 12' above grade) over 3-level parking garage, plus 3 office buildings. Building 3 is tower building, approx 72' X 216'; abuts parking garage on latter's south edge; building basement level between two lower garage levels. Two other 3-story office buildings (approx 72' X 175' each) on east and west sides of plaza directly over two lower garage levels; latter approx 275' X 280'.

Tower building reinforced concrete frame with bronze and glass curtain walls. Structural system of exterior columns plus bearing walls at interior core. Concrete beams support pan joist floors. Type I fire-resistive construction throughout; interior partitions incombustible; 2 firehose cabinets per floor, connected to 500 gpm fire pump serving entire building. Automatic sprinkler system in garage. Tower and garage buildings separated by double wall, each approx. 12" thick R/C. Basement has emergency generator, 500 kva, and special equipment access tunnel extending outward approx. 30' from basement wall, with vertical shaft terminating about 2' below grade (i.e., tunnel use requires excavation and backfill for each use). Typical basement clear height 11' to beams, except 15' in mechanical equipment room because of lowered floor level. Air conditioning system is central equipment single duct (Type 3 of those described in Chapter 6). Central equipment (boiler and refrigeration) housed on top floor together with air-handling equipment for all floors above ground floor. Air-handling equipment for ground floor and basement in basement, served by 4-pipe connection to central equipment. Vertical supply ducts in two mechanical shafts; one (east) is return air plenum, other (west) is toilet exhaust plenum.

Building 4

Columbus-Muscogee County Court House, Columbus, Georgia. Design by E. Oren Smith and Biggers-Scarbrough-Neal-Crisp and Clark, Associated Architects and Engineers, Columbus, Georgia.

Site approx 300' X 600', essentially level, with cleared areas around all buildings in complex. Complex has central plaza (at one level, 12' above grade) over 3-level parking garage, plus 3 office buildings. Tower building, approx 72' X 216', abuts parking garage on latter's south edge; building basement level between two lower garage levels. Two other 3-story office buildings (approx 72' X 175' each) on east and west sides of plaza directly over two lower garage levels; latter approx. 275' X 280'.

Building 4 is parking garage, ground level 38,800 sf, first sub-level 67,600 sf, second sub-level 63,300 sf. R/C construction with exterior bearing walls (except common walls with east-west office buildings); concrete beams support pan joist floors. Plaza paved with concrete and planter areas, all over waterproof membrane on structural slab. Ground floor level 1' above street grade, first sub-level 10' below street, second sub-level 10'6" further below; clear height to pan joist 8'6" all floors. Forced air ventilation only; 48" propeller fans (3) on east side supply air, matching fans on west exhaust air, at both sub-levels; no forced air at ground level. Automatic sprinkler system, all levels.

Ground level access by 18' wide drive, west side to east, adjoining tower; adjacent scissors ramp system for up/down traffic to both sub-levels. Additional access near north end by 11' wide ramps, street to first sub-level, enter east side, exit west; adjacent up/down ramps to second sub-level. Pedestrian access at all 3 levels from all 3 office buildings; two additional stairs connect sub-levels with ground level near south drive.

Chapter 8

SLANTING THE BUILDING

The following sections briefly present the approach and rationale applied to the full slanting in each case study. Preslanting and post-slanting basement floor plans are used, as are tables listing the specific slanting changes (keyed to the appropriate floor plan) and the estimated additional cost of each tabulated item.* These costs clearly show the considerable impact of structural blast-resistant design, and selection of an ultimate deflection criterion μ for flexural structural members strongly affects such design. Selection of this criterion is discussed in the section of Chapter 6 entitled "General Comments on Blast-Resistant Design of a Structural Element," which includes mention of design charts in Ref. 2 tailored to μ=3; the design charts were frequently used in the slanting case studies (examples) described in this Chapter, but the modest conservatism introduced thereby is considered to be balanced by other items that might have been overlooked, or that are mentioned but not estimated. A reasonable upper bound on cost was sought; therefore, use of alternative structural designs, design optimization techniques, or both, is likely to show lower slanting costs than those presented herein. Designs herein were only complete enough, and often only of sample members, for comparative cost estimating.

Case studies shown as Buildings 1A, 1B, and 2A considered only closed shelter, because the room filling prediction method available at the time of the studies did not merit sufficient confidence in its reliability, for predicting even the average room pressure rise-time, to warrant its use for back-loading on a wall or slab in hopes of reducing the member load, design, and related cost. Appendix E presents a later version on room filling than was available for these first three case studies. The concept of open shelter (at least one entry open to shelterees until one full minute or more after arrival of the blast wave; see

* That is, the cost of the slanted (modified design) item minus the cost of the similar item in the original design. Dollar values were tabulated as estimated and do not imply accuracy beyond the usual degree inherent in such estimating.

General note concerning all floor plans herein: any framing indicated is generally for the floor system above the shelter space(s) shown in the floor plan; each slanting scheme (except Bldg. 1A) is described by a table keyed to the floor plan, and the table may describe any modification, whether framing above the space(s) or footings below or any other item(s).

Open Shelter section of this chapter) has many advantages including the important one of making unnecessary a decision as to when and in whose face the shelter door is to be closed. Open shelter is included in full slanting of later case study buildings. Later studies of all the buildings also consider overpressures other than 15 psi. At 15 psi, potential debris loads from the specific case buildings were considered as not controlling on shelter structural design; while this consideration might be inapplicable at 5 or 10 psi, it was nevertheless similarly applied, in the interests of obtaining relative costs for the general case (low-rise buildings).

Figure 8-0A schematically shows a shelter fresh air intake/emergency exit that was used several times, particularly in the first three case studies. Figure 8-0B indicates a version offering more protection against a vehicle being rolled onto and blocking the emergency exit. Figure 8-0C shows a window-well version. Figure 8-0D suggests a ventilation duct/emergency exit scheme; the blast doors are for an "open" shelter discussed later herein. Figure 8-0E illustrates three blast door schemes; all of which were used in full slanting of case study buildings described later in this chapter; further details and cost estimates are provided in a later section of this chapter.

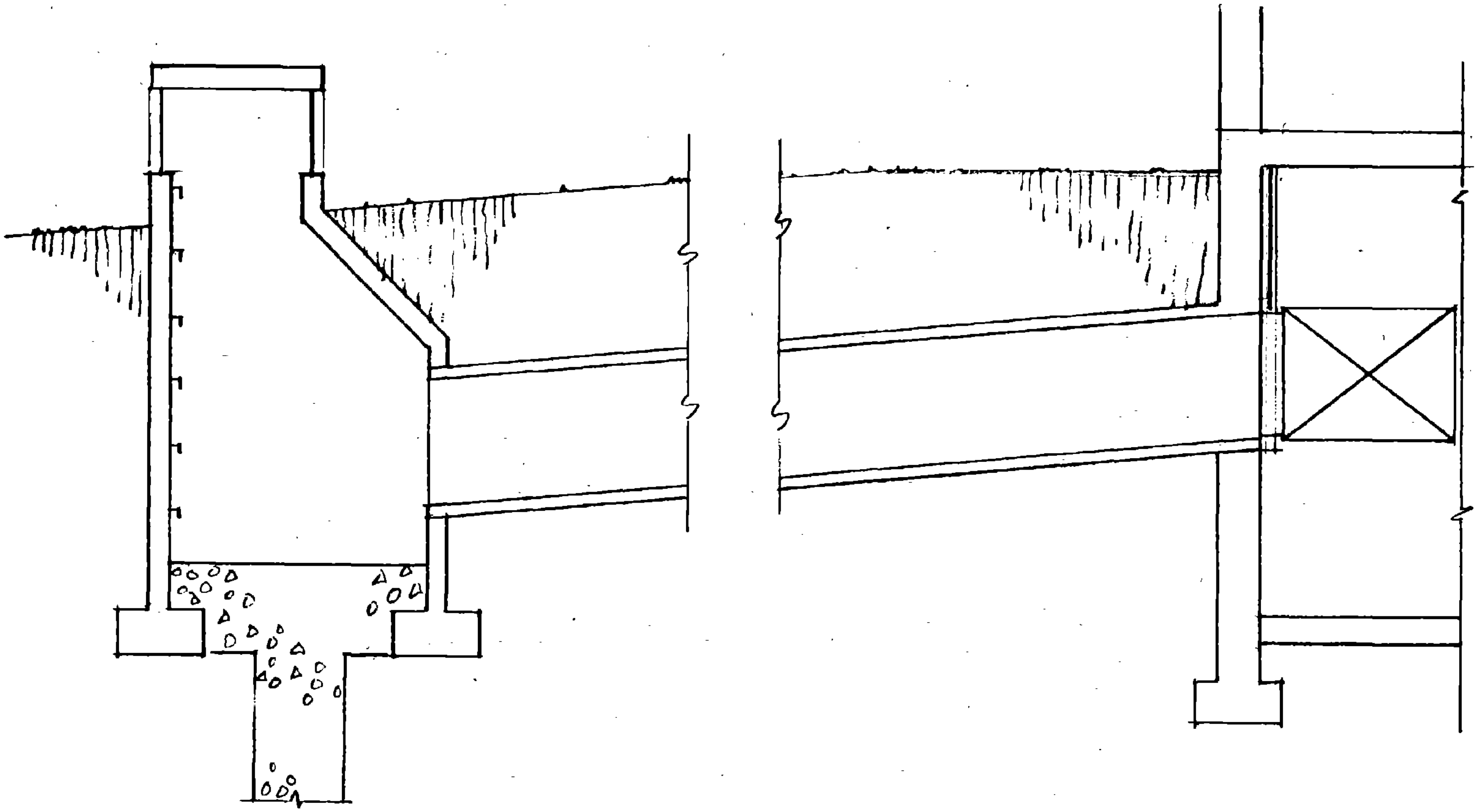

FIG. 8-0A FRESH AIR INTAKE/EMERGENCY EXIT SCHEME

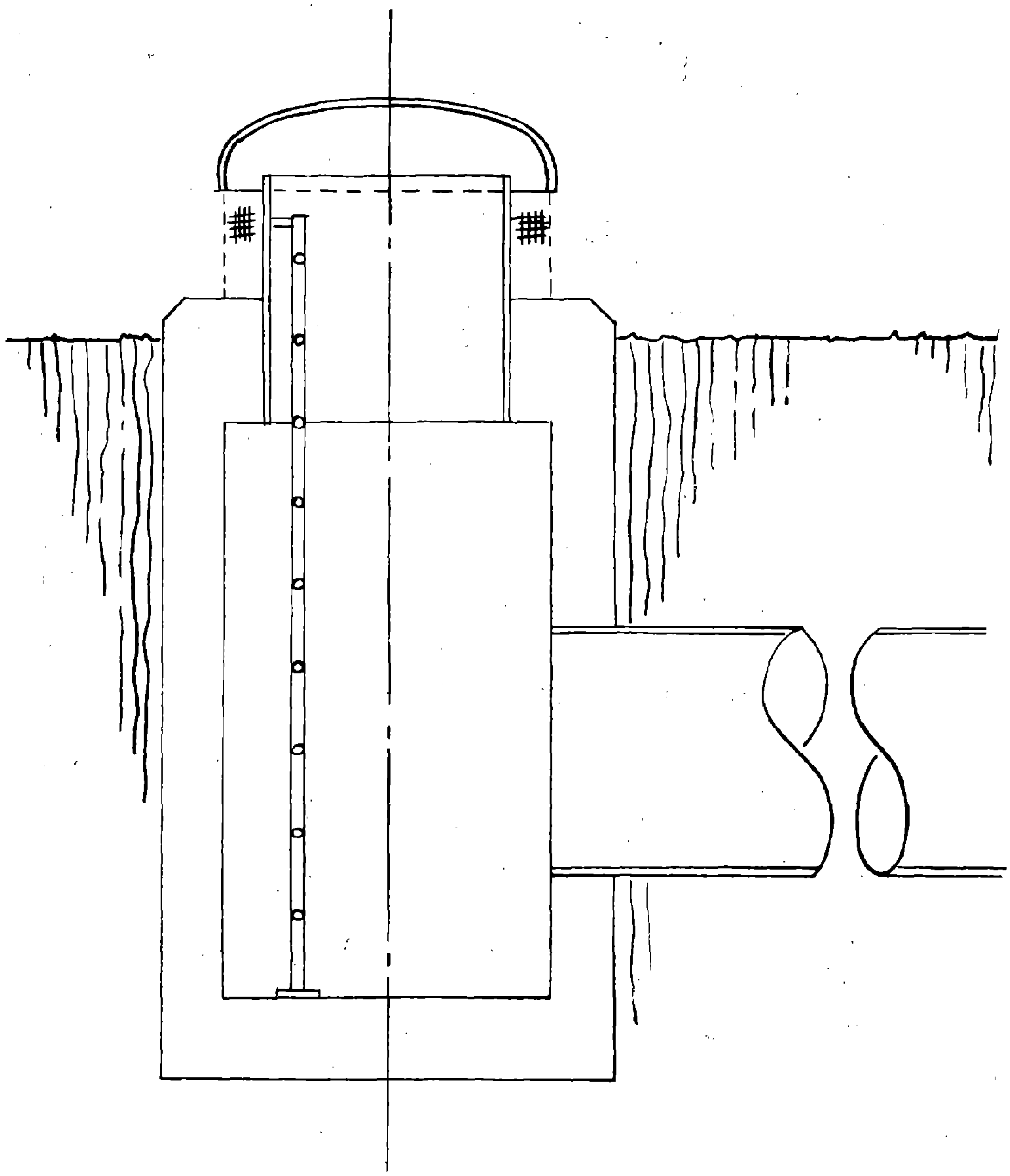

FIG. 8-0B FRESH AIR INTAKE/EMERGENCY EXIT ALTERNATE SCHEME

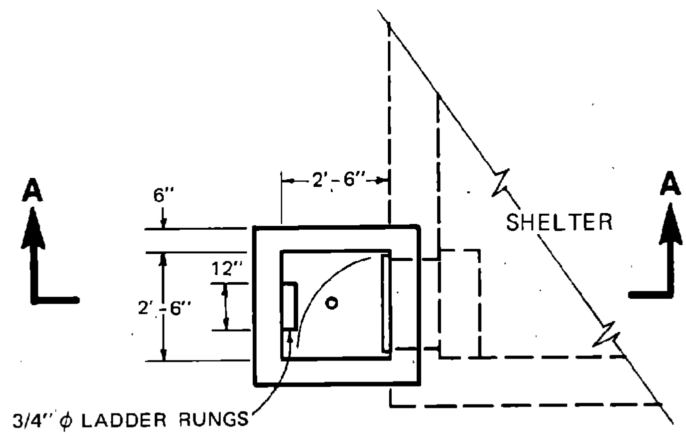

PLAN

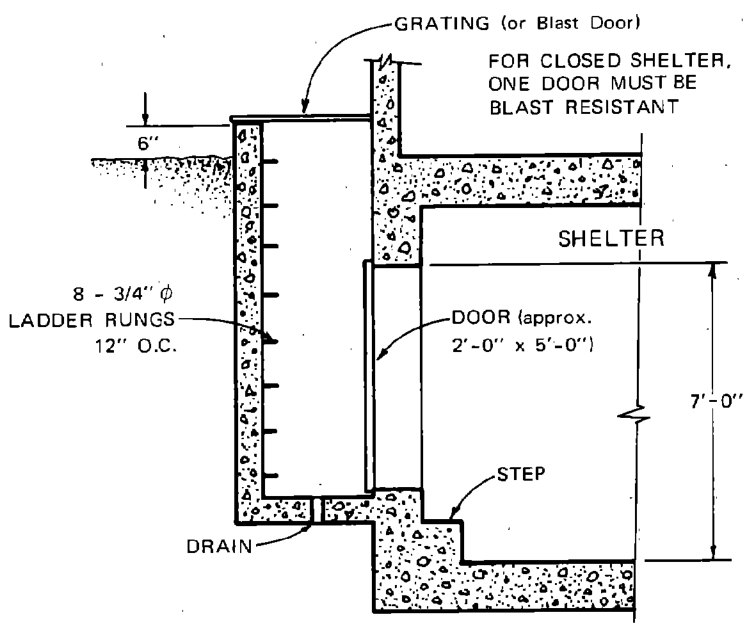

SECTION A–A

SOURCE: Reference 25, plus modifications

FIG. 8-0C BASEMENT SHELTER WINDOW-WELL ESCAPE EXIT

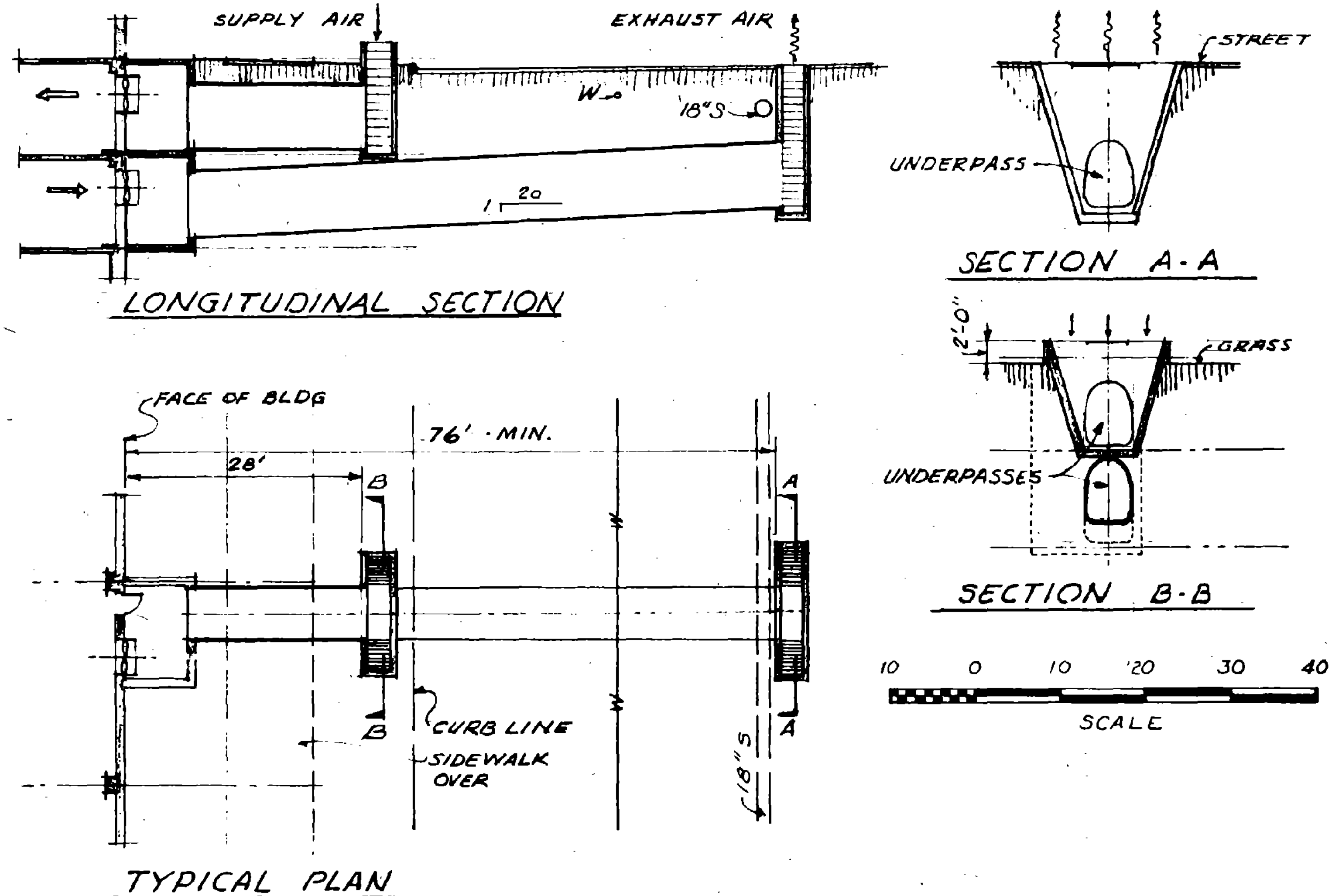

FIG. 8-0D VENTILATION/EMERGENCY EXIT SCHEME – OPEN SHELTER VERSION

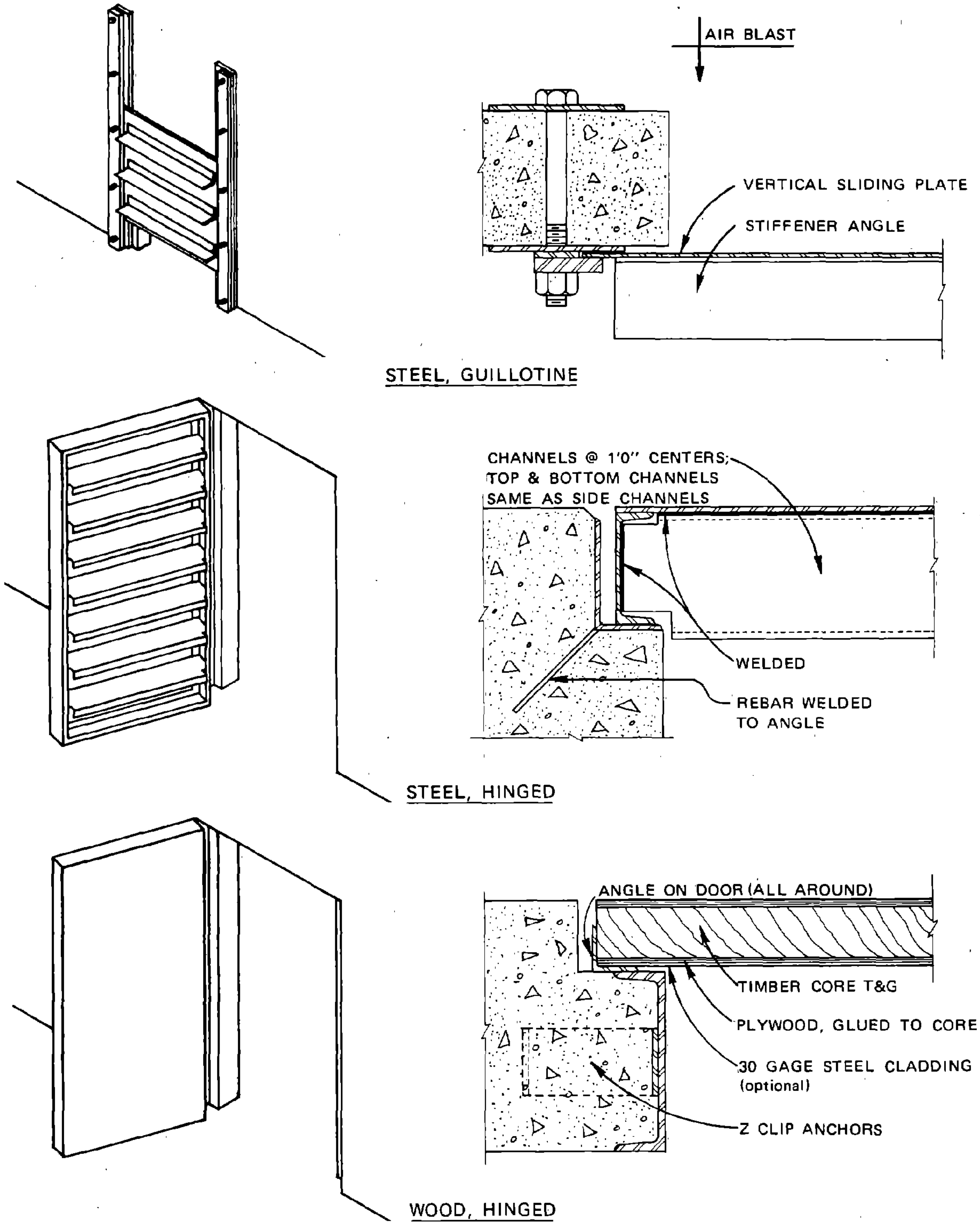

a. ISOMETRIC VIEWS

b. HORIZONTAL SECTIONS IN VERTICAL DOORS

FIG. 8-0E BLAST DOOR SCHEMES USED FOR ESTIMATING

Building 1A

The building is described in general terms in Chapter 7. The designed basement floor plan is shown in Figure 8-1. The slanted version is shown in Figure 8-1A (black lines show slanting changes), the shelter area being L-shaped minus an interior stairwell. A list of slanting changes is not included herein for Building 1A because the estimated additional cost of slanting was many times the Scope limit. The estimates served to confirm what was fairly foreseeable: that too much interior blast-resistant wall was required by this L-shaped shelter and excluded stairwell. The example was useful, however, in learning rough boundaries of possible slanting measures versus the Scope cost limitation; the latter would certainly preclude consideration of this case for any slanting incentive program.

FIG. 8-1

BUILDING 1 BASEMENT FLOOR PLAN

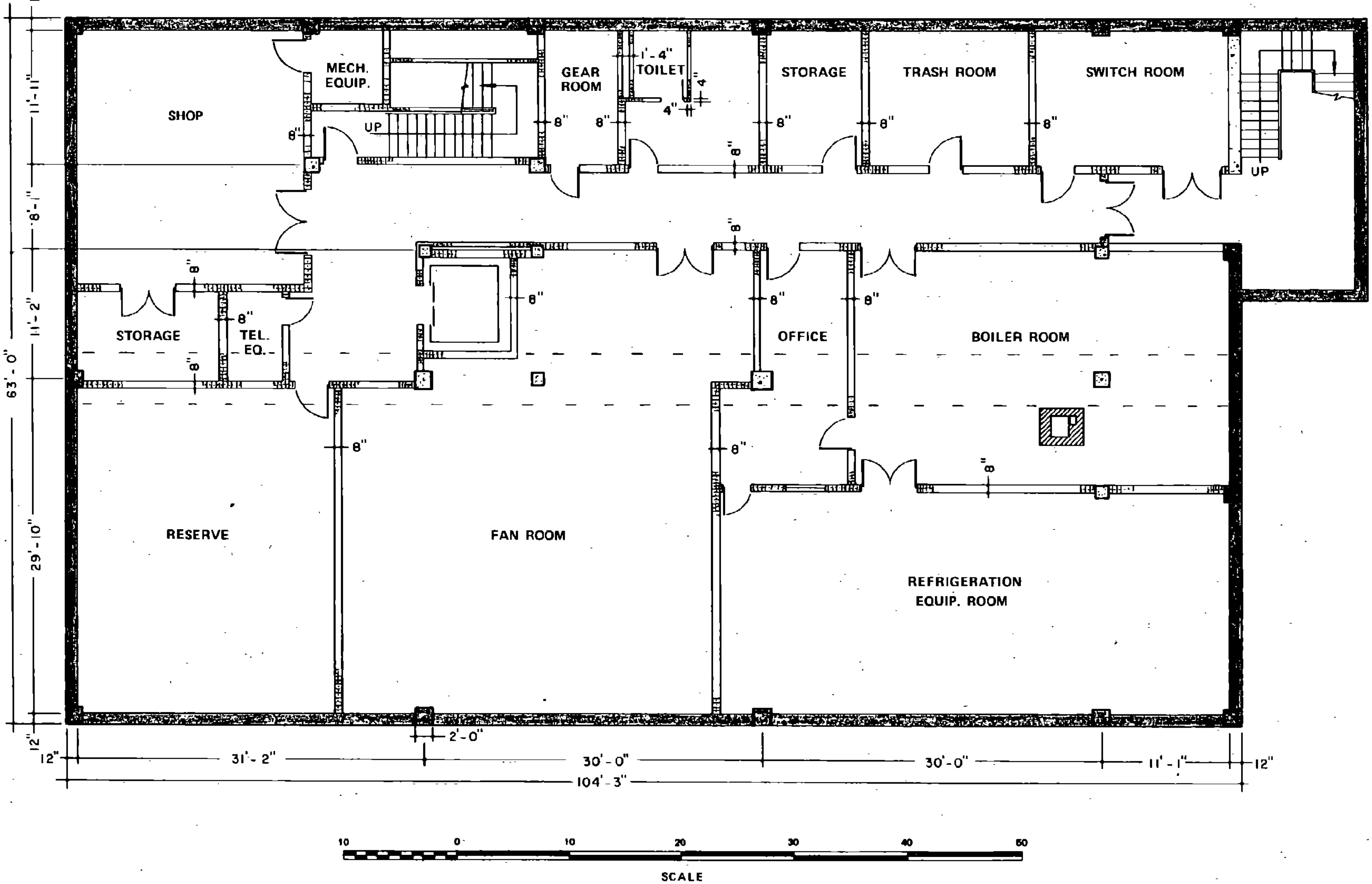

8-6

8-10 BLANK

FIG. 8-1A

BUILDING 1A BASEMENT FLOOR PLAN

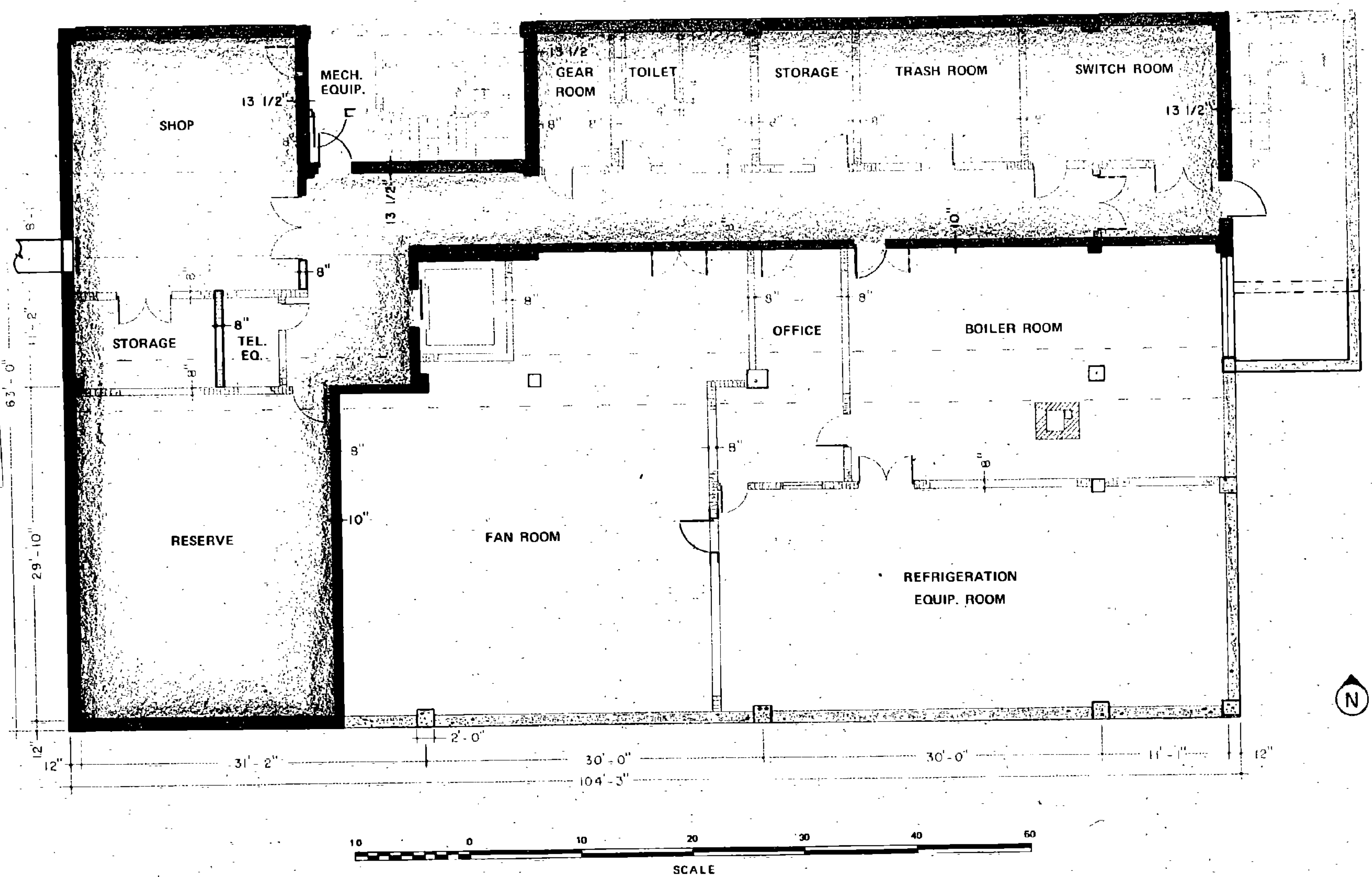

Preceding page blank

8-12 BLANK

Building 1B

The building is described in general terms in Chapter 7.* The designed basement floor plan is shown in Figure 8-1, the slanted version in Figure 8-1B (black lines show slanting structural and layout changes, gray lines show the original design), the shelter being the large rectangular area across the west end. Table 8.1B provides a list of slanting changes, keyed to Figure 8-1B, as well as the estimated additional cost of each change item. Interior shelter walls are not blast-resistant.

The ducted air conditioning from central fan-coil units in the basement and penthouse, plus a boiler room, necessitate about half of the planned partial basement under this building. A slanting change to a four-pipe system (Chapter 6) was not applied because the total basement space requirement might then have been logically reduced. Instead, the many penetrations of the first floor slab for air ducts, pipes, and stairwell were left in a nonshelter area. Items 2 and 9-13, Table 8.1B, describe the slanted shelter ventilation system. The shelter fresh air intake/emergency exit is described in Item 10 and schematically shown by Figure 8-0A.

The second case study results helped in learning the effect of slanting changes versus the Scope cost limitation, in that the estimated additional cost of slanting was improved to about twice the Scope limit. The study illustrates the cost penalty of the fixed cost of Item 10 being borne by a rather small shelter, thereby inordinately increasing unit slanting costs. Further review of the concept and details of this fixed cost item was indicated.

* This second slanting use of the Newnan Post Office has a different shelter layout than the first, Building 1A, in order to reduce the amount of interior blast resistant wall required.

8-14 BLANK

Preceding page blank

FIG. 8-1B

BUILDING 1B BASEMENT FLOOR PLAN

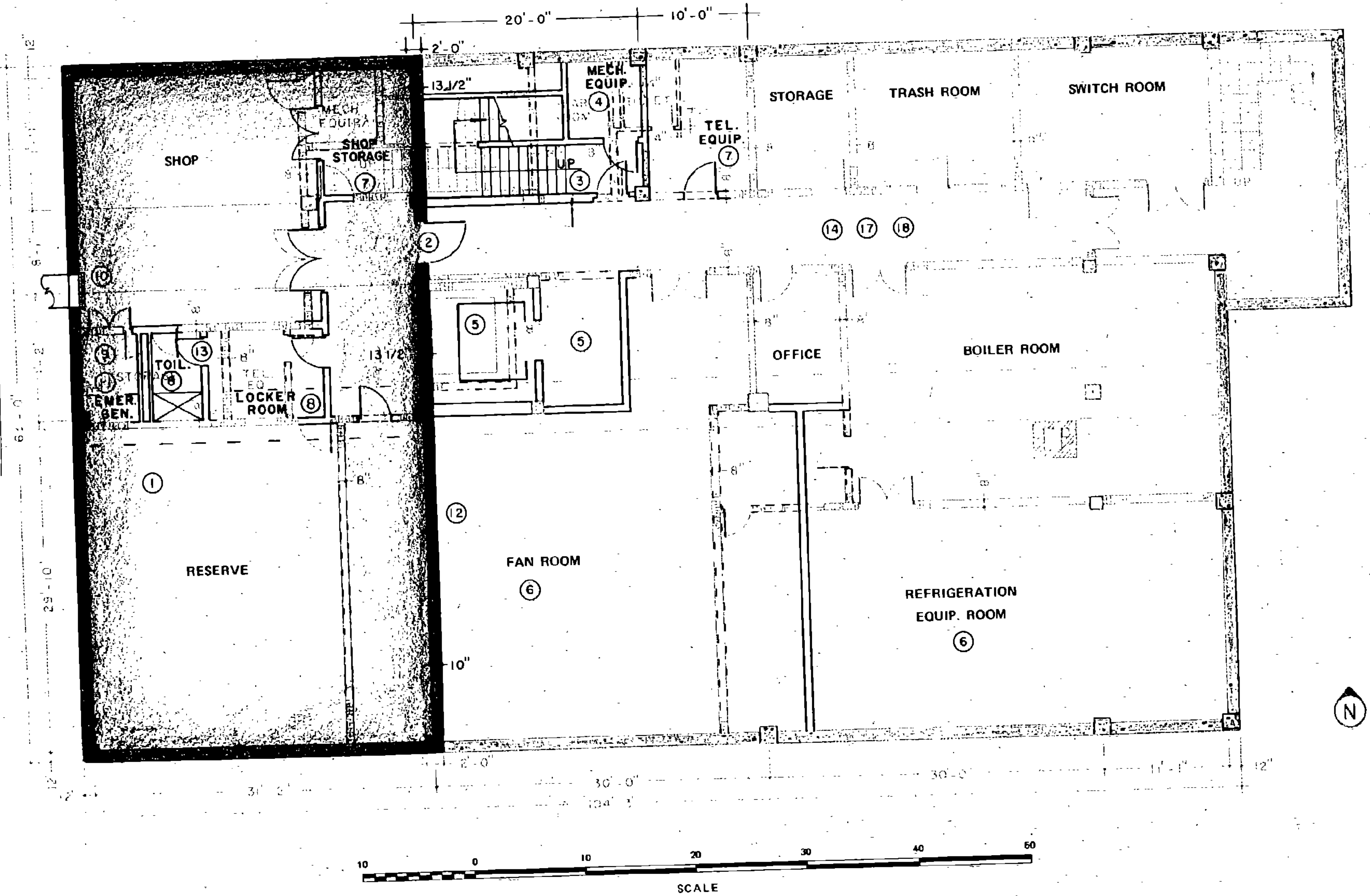

8-16 BLANK

Table 8.1B

BUILDING 1B SLANTING
(Post Office, Newnan, Georgia)

1.	Provide blast walls as shown ($4,385); with blast slab above (15-1/2" thick) and centerline girder increased to 46" overall depth in shelter area ($9,498). All interior partitions in shelter to be nonbearing and detailed to remain so, even with large deflection of slab and/or girder above, say 6" or more.	$13,883
2.	Provide blast door to corridor ($760); with 1'x 4' exhaust air vent ($40) and its own vertical sliding blast door ($160) (both above corridor door). Exhaust air vents into a corridor duct.	960
3.	Relocate stair 10 ft east, as shown; revise stair layout to 3 flights to land at door shown.	*
4.	Relocate Mechanical Equipment Room as shown.	*
5.	Provide elevator with a rear door for basement use only ($1,800); and relocate basement lobby as shown, using space under ducts from Fan Room (*).	1,800
6.	Relocate Fan Room 7'9" to east, maintaining same clear width, as shown. Refrigeration Room can be reduced in size by offsetting two coolers as needed to provide space for disassembly.	*
7.	Relocate Shop Storage and Telephone Equipment Room, as shown.	*
8.	Provide Toilet Room (shower optional) and Mechanic and Labor Locker Room, as shown.	*
9.	Add Generator Room (*) for emergency power unit (5 kva) ($1,400) for shelter lighting and emergency ventilating (fans only; 3500 cfm) (*); provide engine exhaust vent ($100) at grade just outside building wall.	1,500

* Design modification considered achievable at little (<<$100) or no additional cost.

Table 8.1B (concluded)

10.	Provide fresh air intake tunnel, 36" diam. by 55' long ($1,538); plus manhole ($2,204); for use at all times for shelter area, plus emergency use as an exit. Provide vertical sliding blast door in inside face of shelter wall ($394) (dismantle fresh air duct to use tunnel as exit).	$ 4,136
11.	Provide separate air handling system for shelter area use (both normal and emergency), with fan-coil unit located overhead in Generator, Reserve or Shop Storage Room (*). In normal use, unit is to be supplied with HW and CW from existing system. In emergency use, only the fan operates, using emergency power (conduit, wire, and switches: $100).	100
12.	All nonshelter ductwork is to be outside the shelter space.	*
13.	Vent toilet with own fan, and duct out through above-door vent and new duct (#2).	135
14.	Allow no flammable wall and/or ceiling treatment in basement, inside or outside shelter.	*
15.	Metal venetian blinds with fire resistant tapes are to be used on all windows, at least on entire floor above basement.	*
16.	Roof should be Class A or B fire rating (probably normal design).	*
17.	Plumbing vent pipes should be metal (or pass 100 psi internal pressure test) and be tightly grouted (expansion type) for full depth through slab over shelter.	*
18.	All duct risers from nonshelter areas of the basement should have standard fire dampers at first floor slab level.	*
(June 1968)	1,911 sf	$22,514 $11.78/sf

* Design modification considered achievable at little (<<$100) or no additional cost.

Building 2A

The building is described in general terms in Chapter 7. The designed basement floor plan is shown in Figure 8-2, and the slanted version in Figure 8-2A (black lines show slanting structural and architectural changes, gray lines show the original design), the shelter occupying the full basement excluding the interior stairwell and the exit hallway leading to exterior stairs. Table 8.2A provides a list of slanting changes, keyed to Figure 8-2A, as well as the estimated additional cost of each change item. Interior shelter walls are not blast-resistant. Figures 8-2.1 and 8-2A.1 provide perspective views of the building basements, as originally designed and after slanting, respectively (i.e., comparable to the floor plans of Figures 8-2 and 8-2A).

The original, natural cross-ventilation scheme contemplated for the large, open basement portion was slanted to forced fresh air ventilation of the entire basement, as described under Items 2 and 8-12, Table 8.2A. Item 17 covers an unestimated alternate, an air conditioning scheme for the shelter area. The fresh air intake/emergency exit is described in Item 9 and schematically shown by Figure 8-0A.

Table 8.2A (15 psi shelter) was used first for estimates based on June 1968 costs, then later for estimates based on June 1970 costs. Both sets of estimates were shown in the latest version of the complete combined effects slanting study/guide.[50] Only the June 1970 estimates were retained for this Chapter 8 revision, but estimates for new studies of 20 and 30 psi shelters were added.

For this third case study, estimated additional slanting costs were within the Scope limit of $6/sf (about 4% below, when both are corrected to the same time period). The study indicated the need for further review of slanting measures, aimed at reduction in ventilation and blast door costs.

8-20 BLANK

FIG. 8-2

BUILDING 2 BASEMENT FLOOR PLAN

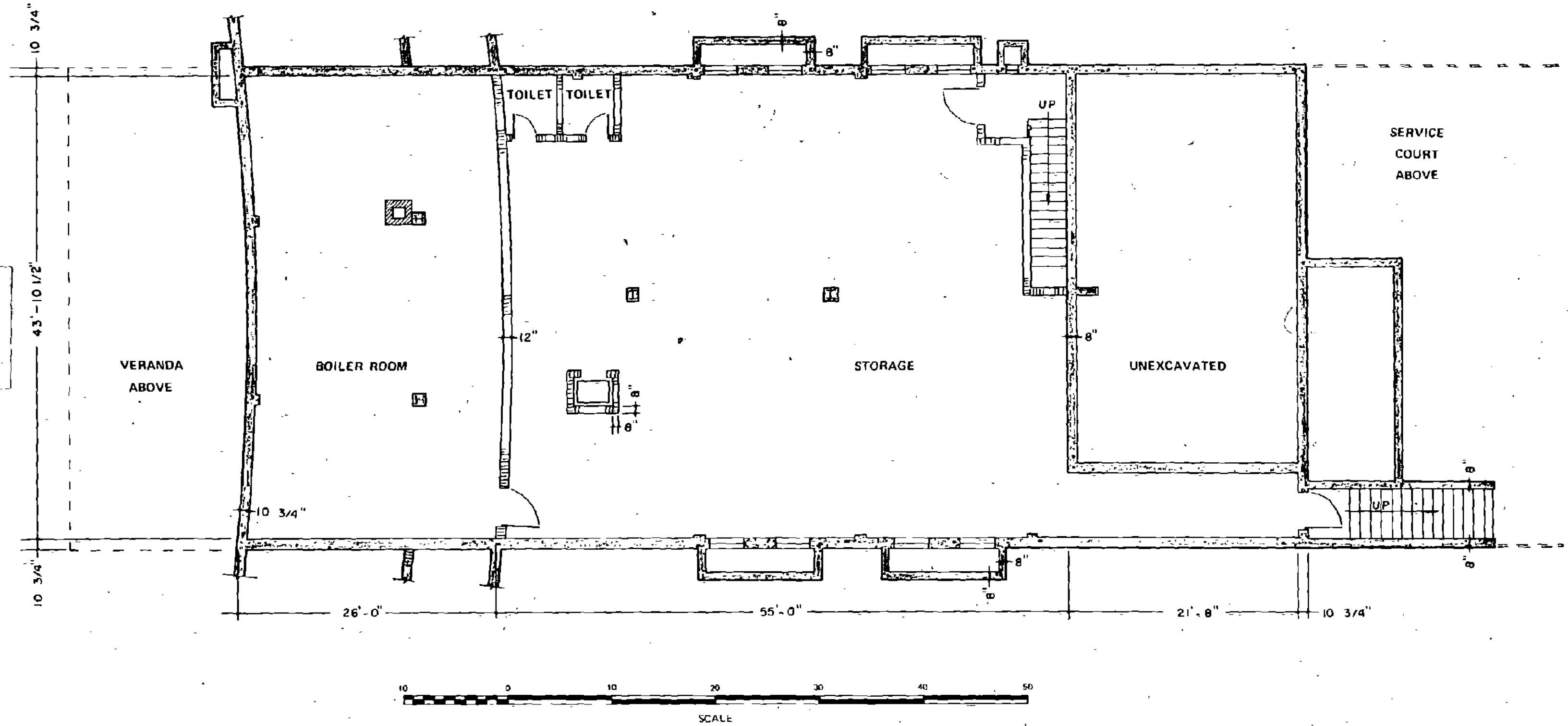

8-22 BLANK

FIG. 8-2A

BUILDING 2A BASEMENT FLOOR PLAN

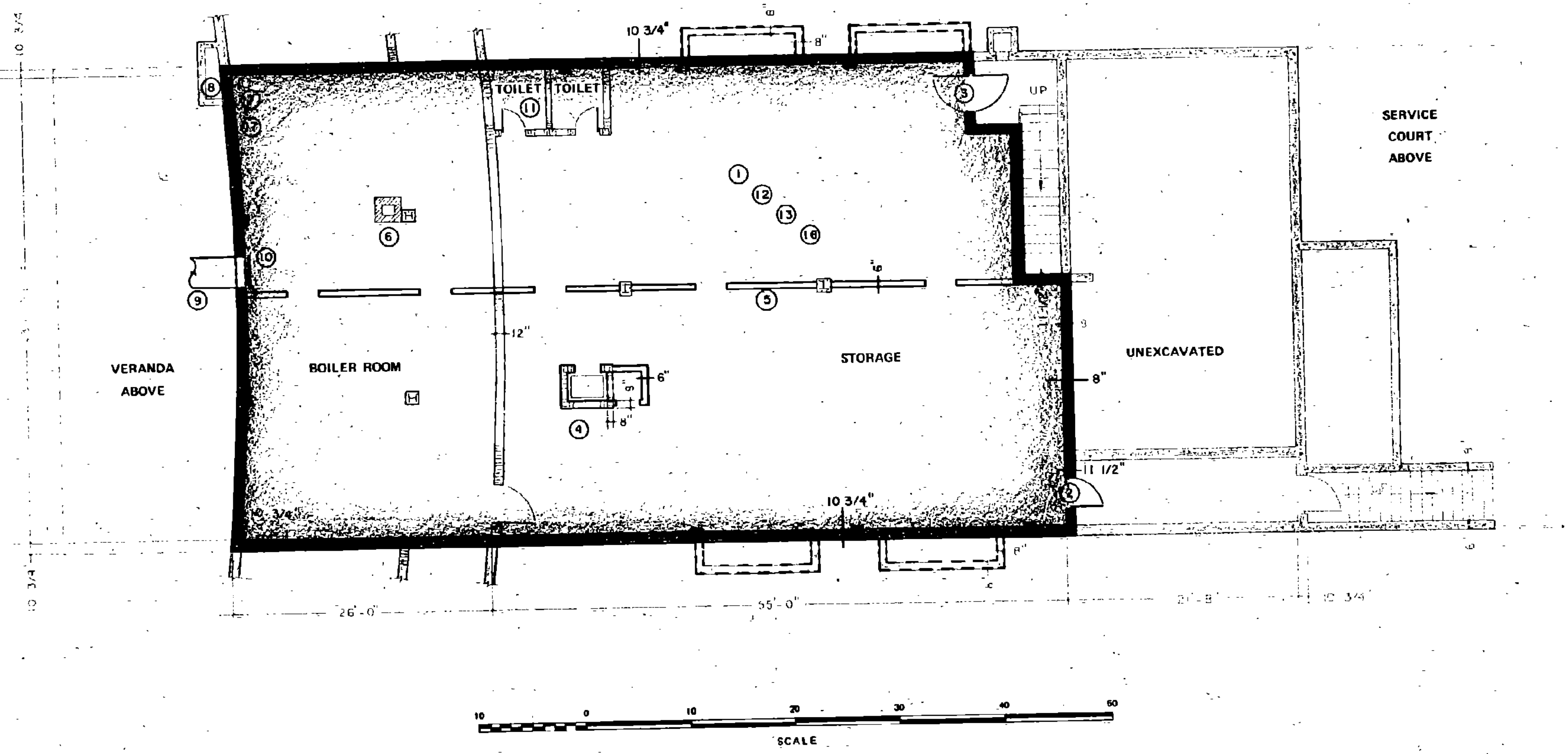

Preceding page blank

8-24 BLANK

Table 8.2A

BUILDING 2A SLANTING
(Brentwood Rehabilitation Center, Asheville, N.C.)

		15 psi shelter	20 psi shelter		30 psi shelter	
1.	Provide blast walls (10-3/4" and 11" thick) as shown (-$99), with blast slab above (14-1/2" thick) ($8,385).	$8,286	(10-3/4" and 12") ($415)(17")($10,587)	$11,002	(12-1/2" and 13-1/2") ($2,166)(20")($13,460)	$15,626
2.	Provide blast door ($747), to also serve as exhaust vent for part of room air by holding door part way open using adjustable door closure ($74).	821	($750) ($74)	824	($755) ($74)	829
3.	Provide blast door between interior stairway and shelter.	747		750		755
4.	Provide blast enclosure (6" thick) around dumbwaiter and laundry chute ($1,174), with vertical sliding blast doors ($99).	1,273	(6") ($1,215) ($105)	1,320	(6") ($1,251) ($111)	1,362
5.	Provide bearing wall (6" thick) along longitudinal column line, with openings as desired.	4,894	(6")	5,074	(6")	6,547
6.	Harden chimney (in shelter) for blast (*), and provide manual blast door ($182) at breeching	182	($210)	210	($257)	257
7.	Provide 7.5 KVA emergency generator ($1,700 + panel + labor), in separate room, for lighting and ventilating.	2,270	($1,700 + +)	2,270	($1,700 + +)	2,270
8.	Convert one remaining areaway (see Plan) into exhaust for room air (passed out through generator room) and generator exhaust; estimate 24" diameter exhaust duct ($99), plus blast door ($182).	281	($99)($210)	309	($99)($257)	356
9.	Provide fresh air intake tunnel, 36" diameter by 55' long ($1,759), leading to manhole ($2,392) in clear area in front of building, to serve as emergency exit as well; vertical sliding blast door ($447) in inside face of shelter wall (dismantle duct for use as exit).	4,598	($1,759)($2,392) ($464)	4,615	($1,759)($2,392) ($519)	4,670
10.	Provide air handling system for entire shelter area, to serve normally as well as in an emergency; 4800 cfm fan ($686), ducts ($1,027) in fan room leading to wall of shelter area; air flows toward stair well, through openings in new center wall and back through boiler room door to vent system. Provide for varying mix of recirculated and fresh air.	1,713	($686)($1,027)	1,713	($686)($1,027)	1,713

8-26 BLANK

Table 8.2A (concluded)

		15 psi shelter	20 psi shelter	30 psi shelter
11.	Vent toilets with own fan and ducts out through areaway (#8)	$ 307	$ 307	$ 307
12.	Delete all present exhaust risers to roof ventilators	*	*	*
13.	Allow no flammable wall and/or ceiling treatment in basement.	*	*	*
14.	Metal venetian blinds with fire resistant tapes are to be used on all windows of building wing above the basement.	*	*	*
15.	Roof of entire building should be Class A or B fire rating (probably not normal design).	*	*	*
16.	Plumbing vent pipes should be metal (or pass 100 psi internal pressure test) and be tightly grouted (expansion type) for full depth through slab over shelter. All heating pipes should be similarly grouted.	*	*	*
17.	If water well is economically available (at least for industrial water), an alternate ventilation system scheme could be considered, using only 1000 cfm fresh air mixed into same 4800 cfm in 10 above, but using well water coils to cool the entire air supply (this scheme not estimated). With this scheme, well water could be used for generator engine radiator cooling, and a blast closure valve could be used over the fresh air intake (it would be reduced enough in vent size).			
18.	Provide for all gas, water, fuel oil, etc., supply lines serving the entire facility to first enter through the Boiler Room, and have cut off valves at entry points.	†	†	†
(June 1970 costs)	3,378 sf	$25,372 $7.51/sf	$28,394 $8.41/sf	$34,692 $10.27/sf

* Design modification considered achievable at little (<<$100) or no additional cost.

† Costs not estimated, but probably minor.

8-28 BLANK

FIG. 8-2.1

BUILDING 2 BASEMENT PERSPECTIVE

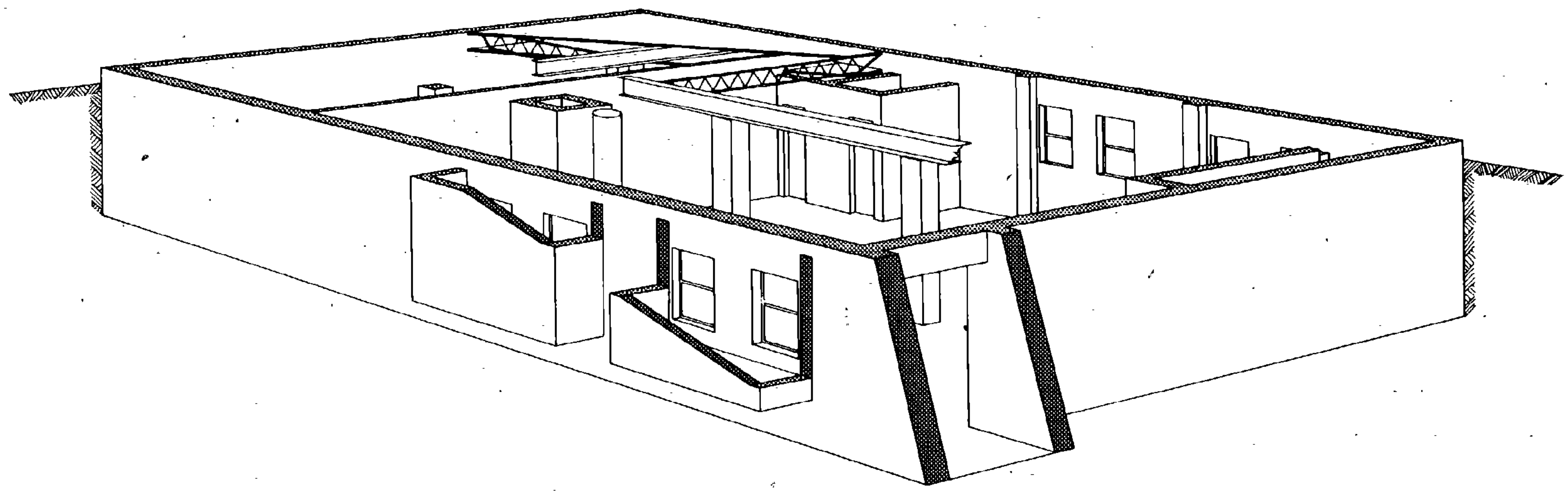

8-30 BLANK

FIG. 8-2A.1

BUILDING 2A BASEMENT PERSPECTIVE

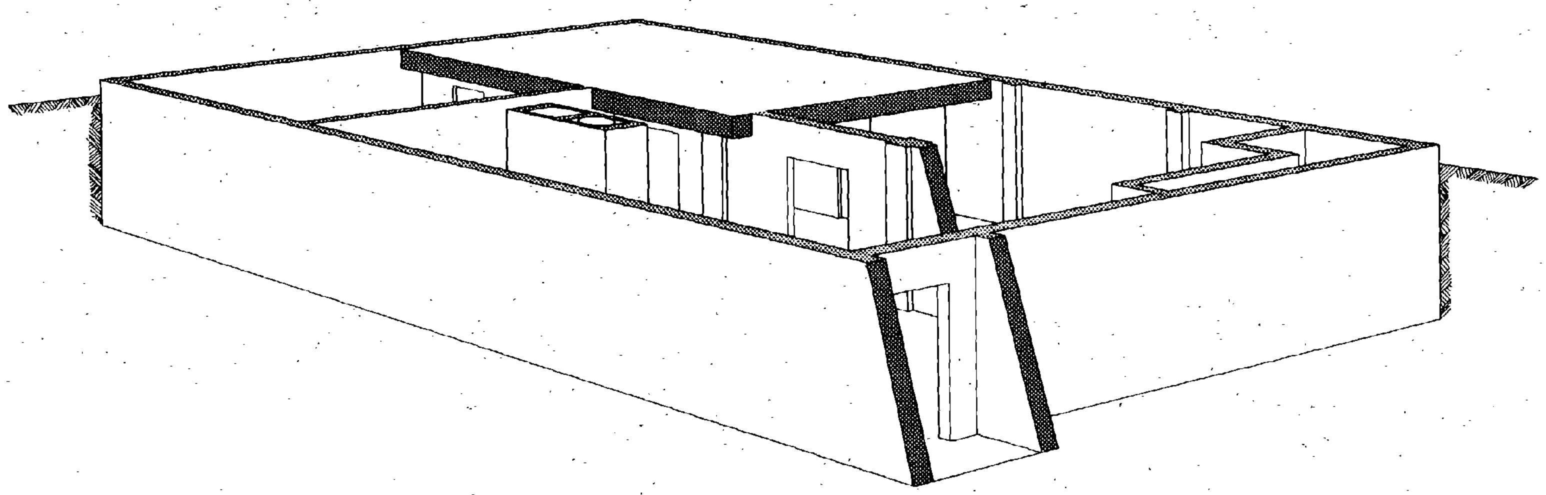

Preceding page blank

8-32 BLANK

Questions Raised by Early Case Studies

Questions arising from these early case studies include:

- Are there slanting ventilation schemes that are more cost-effective (e.g., PVK and Kearny pump) than those used?

- Is the fresh air intake/emergency exit tunnel really required (for blast debris and fire hazards reduction) in an austere, survival shelter situation? Can its cost be markedly reduced by design studies? Are multiple window-wells better? Does the concept of knock-outs in first floor slab have any ventilation potential?

- Can the cost of blast doors be reduced by design studies or eliminated by an open-shelter approach?

- Are the loading assumptions and/or design techniques used on the buried exterior shelter walls too conservative?

Open Shelter

Closed shelters,* as in Buildings 1A, 1B, and 2A, pose the inevitable question: When will the shelter door be closed? This question is avoided in the open shelter concept, defined for purposes herein as shelter where at least one entrance door remains open to shelterees until one full minute or more after the nuclear detonation. Open shelter also merits consideration for its possible lower unit slanting cost, even though the shelterees may face a greater variety of hazards in open than in closed shelter.

Open shelter might be discussed under the following four types:

I. What amounts to a closed shelter but is closed only to the blast wave and other direct nuclear effects, not to people - for example, by having each entrance be a system where people can enter more or less continuously into either of two parallel hallways (really entry locks), with one alternately open to new arrivals while the other is closed to new arrivals but is open to empty an earlier arriving group into the shelter. The alternating is accomplished by sliding doors interlocked so that there is never a passageway for air blast to enter the shelter. Other examples exist.[36]

II. What approaches a closed shelter but is closed only after an early part of the blast wave has entered the shelter - for example, by having an entrance door or doors that are slammed closed by the blast wave, thereby shortening the duration (but not reducing the peak pressure) of the entering air blast to an extent that shelterees (probably prone) will not be accelerated enough to cause injuries/deaths by being thrown into walls or other objects. (Granted that the door may be slammed onto someone rather than going fully closed; in either case the air inflow is reduced quickly and considerably.)

III. An open shelter, but with only one or perhaps two entrance doors open, all other openings being closed not later than during the time interval between nuclear detonation and blast wave arrival at the shelter.

IV. An open shelter with multiple openings (windows and doors) remaining open at least during passage of the blast wave, probably longer for ventilation and access purposes. Openings such

---

* Defined, for use herein, as shelter closed before air blast arrival to all further ingress.

as those for chimneys and ventilation ducts could also remain open, provided that protection is included against chimney and duct parts becoming missiles in the shelter.

No quick conclusions should be drawn about these four types of open shelter. Type I might have all the slanting costs of a closed shelter (such as Building 2A) plus the cost of an elaborate entrance system, leading to a (premature) conclusion that the other types would all cost less than Type I. In Type I, interior walls need not be blast resistant. In the other three types, they must be blast resistant to some degree, a cost item in favor of Type I. Because of such interrelationships among slanting costs, personnel protection, weapons effects, etc., these matters as they relate to the open shelter types are examined in more detail below.

For convenience, the four open shelter types are summarized with shortened descriptions, as follows:

I. Shelter closed to blast but allowing continuous shelteree ingress

II. Shelter with few openings and internal blast duration shortened

III. Shelter with one or two entrances open

IV. Shelter with many openings

The remainder of this section on open shelter is devoted to discussion of certain weapons effects in terms of open shelter and to such general considerations in open shelter as blast resistant construction needed; certain necessary shelter stocks and their storage; and some aspects of shelter management and early recovery tasks applicable to open shelter. A recapitulation closes the section.

A. Weapons Effects and Open Shelter

The shelter designer must exercise care in considering not just the design peak overpressure (15 psi) or higher values and related other effects, but also the full range of all effects below the design level. For example, the fire potential in stories over the basement shelter is likely to be much greater at some overpressure range lying just below an overpressure capable of making debris of the upper stories than at blast levels above this overpressure.

Air Blast - Exterior. At some p_{so} around or above 7 psi, from a surface or air burst, there is a high probability of extensive damage, possibly even collapse, to the entire building above the basement. Also, at p_{so} of about 7 psi or more, from a surface burst, fallout contaminant is likely, even upwind or crosswind from the burst point.[1(Sec.9.87)] At p_{so} of about 1 to 3 psi, exterior and interior aboveground walls may become debris along with the building contents, perhaps blocking egress through downwind window-wells/doors, but providing additional fallout shielding on the shelter (basement) roof. The floors, and perhaps the roof, may not be collapsed, and would contribute to the fallout protection for the shelter. At p_{so} down to about 1/2 psi, there will still be much damage (minor at the lower p_{so} values) to equipment, interiors, and many building elements. All window glass will be shattered.

Air Blast - Interior. This effect is inapplicable to Type I. For the other types, it poses critical problems of estimating interior flow velocities* on shelterees and blast loadings on structure surfaces and shelter equipment, problems that can be only partially solved by Appendix E methods and the present state of knowledge in the field; however, directly applicable research, analytical and experimental, is under way.

Present knowledge suggests that Types III and IV shelter will contain at least some areas of low survival probability and that these types may not meet the 85% to 95% survival probability called for in the Stipulations section herein, unless special efforts are made to vacate dangerous areas before arrival of the air blast. This conclusion is based on calculations such as those discussed in Appendix E, showing that drag forces may be high enough and last long enough to cause prone shelterees to be thrown into walls or other fixed objects with lethal speeds.

For example, when peak free field overpressure is 15 psi, dynamic pressure (jet) in every opening may reach as high as 3.2 psi, enough to accelerate a prone human body to approximate lethal skull impact speed (15 fps)[38 39] in approximately 46 msec. Maximum dynamic pressure in an opening follows a brief diffraction episode of relatively low dynamic pressure and is in turn succeeded by a slow decline of dynamic pressure as the room fills. In a large room the highest values of dynamic pressure are thought to be located within a straight jet issuing from the opening, although a swirling motion entraining most of the air in the room may also occur.

Since, even with all openings open (Type IV shelter), filling time for the basement of Building 2 is approximately 130 msec, it is clear that

---

* Really need dynamic pressures; or, more strictly, drag pressures.

shelterees in the neighborhood of an opening will be threatened. If, in an attempt to spare a large part of the shelter area from these high winds, all but one opening is blast sealed (Type III shelter), the duration of the dangerous inflow is lengthened to approximately 600 msec during which time even relatively weak drag forces remote from the main jet may have the opportunity to accelerate the human body to lethal speed. A steady jet, issuing through an aperture the size of an ordinary door from a reservoir at 15 psi overpressure, will expand, after about 55 ft of travel in an infinite atmosphere, reducing the dynamic pressure to approximately 1.0 psi* (still equivalent to a hurricane wind of about 200 mph).

These approximate and preliminary calculations do not demonstrate that open shelter is infeasible, but they do demonstrate that open shelter of the kind (Type IV) represented by Building 2B presents a survival hazard to some shelterees at the 15 psi range. The magnitude of the hazard and an evaluation of the usefulness of the shelter are matters requiring further knowledge and study. The interior air blast hazard receives a lengthy discussion in the later section herein dealing with Building 4A.

Improved prediction techniques for interior air blast behavior offer a potential for structural savings as well. For example, back pressure on the concrete slab over the basement shelter might have a negligible effect on the slab design when rather small ultimate deflections are considered; however, at the large deflections for longer span slabs, say about 20 ft, the time to maximum deflection becomes of the order of 0.2 sec, which may be sufficient to allow a back pressure build-up of consequence.

Initial Nuclear Radiation. This effect presents no hazard† in an air burst (Figure 2-3), but a surface burst delivers a free-field, gamma-plus-neutron dose of about 450 rads (Figure 2-6, for 1 Mt and 15 psi). The surface burst radiation is likely to be much reduced by shielding from other buildings, but should be considered carefully in relation to protection around all shelter openings. Window-wells and entrances should have only a scattering, not line-of-sight (streaming) hazard because of the low sight angle of even maximum probable height surface bursts.‡ Even then, shelteree mortalities should be improbable and sickness unlikely.

---

* Calculated using Equation 36, Appendix E.

† Using the Scope yield of 1 Mt; if say 200 kt is assumed, the hazard from initial nuclear radiation (INR) may be considerable (Chapter 2), perhaps overshadowing air blast as a structural design criterion.

‡ For air bursts, maximum vertical sight angles (above the horizon) versus air blast peak overpressure might be: 30 psi, 43°; 20 psi, 36°; 15 psi, 33°; and 10 psi, 31°. These values came from considering HOBs to maximize the range for each overpressure (i.e., considering the "knees" of the curves in Figures 3.67a and 3.67b, Reference 1).

Fallout Radiation. This effect was first discussed in connection with exterior air blast and is further discussed below under protective action by shelterees. It should present no serious problems in considering open versus closed shelter.

Thermal Radiation and Secondary Fires. Fires and air blast present the greatest hazards to shelterees within the Scope of this guide.*

The thermal radiation reaching the shelter building exterior should, in a high probability of cases, have been reduced if not eliminated through shielding by other structures and hills. The risk of thermal radiation setting interior fires in the floor above the shelter must be countered by preattack countermeasures (e.g., fire-retardant treatment) and shelteree firefighting capabilities (Chapter 3); the latter are further discussed below. Even at the range of about 2.5 to 3 psi overpressure, the thermal radiation (Figure 2-2) may be sufficient to start fires in the floor above the basement shelter. As the overpressure and thermal radiation levels increase, however, rubble replaces or covers what were exposed building interiors, and there is serious doubt as to whether blast-caused rubble can ignite and burn so as to be a serious threat to shelter occupants. Certainly the threat, if any, is not well understood.

The secondary fire hazard must be countered by the means discussed just above and in Chapter 3, and as discussed further below. This hazard may well be worst at and beyond ranges where overpressures will make debris out of walls and interior equipment and furnishings.

B. General Considerations in Open Shelter†

At least some of the general considerations applicable to open shelter require review in relation to protective shelter design. The more important ones might include those discussed in the paragraphs below.

Blast Resistant Construction Needs. Some of the blast resistant construction needed in and around an open shelter includes:

- All structural elements located in the open shelter space must be blast resistant, including interior walls/partitions (which should therefore be reduced in number to the extent possible).

---

* Footnote † on the preceding page applies here as well.

† Entire section has little application to Type I "open" shelter (closed to air blast, by definition), the exception being some guidance that is useful to both open and closed shelter situations.

- All fixed equipment in the open shelter space must also be blast resistant, both in mounting and as to the equipment itself flying apart.*

- Entranceways, window-wells, and any other openings require attention to blast resistance, generally and for strength around each opening into the shelter.

  Doors should be fire-resistive, capable of being anchored in a protected (open) position for the blast passage, then of being quickly closed as necessary for fire protection. If flying debris, from materials or building elements near but outside the open shelter space, presents a hazard, grating doors may be required in nonentry doors of Type IV shelters.

  Windows should be detailed so that their glazing and other components present no missile hazard to shelterees - for example, glazed sashes could be removable and, at time of shelter occupancy, be moved out of the shelter or to a blast-protected closed space. (Or the sashes might be designed to be anchored safely in an open position, perhaps including use of a new high-strength glazing.)

  Window-wells serving the open shelter should have walls blast strengthened, at least in the walls common to the shelter. The strengthening should extend to all walls in each window-well that may be needed as an emergency exit. Each window-well should have a top grating† for protection against flying debris, but removable for emergency exit use if such use is planned. Window-well bottoms should be sufficiently below their window sills to give protection against direct fallout radiation from contaminant falling onto the bottoms.

- Some closed shelter space appears to be required even in the open shelter concept - if not for people then at least for certain stocks.‡ Examples include the OCD water drums and PVKs (package ventilating kits) in current use.

---

* However, for the blast loading on such equipment, the better interior air blast prediction techniques, mentioned earlier as a subject of ongoing research, are badly needed.

† Sloping, if exterior wall will support upper edge.

‡ Again, better prediction techniques for interior air blast behavior could change this need.

Shelter Stocks. Certain shelter supplies and equipment aspects seem to indicate the following:

- Stocks must not become missiles in the personnel shelter - they must either be removed from the shelter at time of occupancy or must be provided with blast resistant anchorage.* Supplies that cannot be so anchored and cannot withstand air blast damage - such as the water drums and PVKs - must be removed to protected closed space.

- Stocks must be in a space or spaces accessible to the shelterees, both after the direct nuclear effects and without receiving an unacceptable fallout dose.

- Stocks, at least the vital ones, must be protected from destruction by thermal radiation or secondary fires, as well as blast.

- Stocks should include such structural recovery items as building jacks, crowbars, wedges, and sledges.

Shelter Management. For success of an open shelter, shelterees must be informed (and willing) to:

- Move all unanchored items out of the shelter before the blast arrives.

- Move all stocks needing protected shelter to such space.

- Close all blast doors in any closed shelter spaces, either before the detonation or during the few seconds (available with large weapon yields) between detonation and arrival of the air blast wave.

- Take prone positions† at assigned locations, probably with close spacing to provide mutual protection.

- Perform radiation monitoring (for fallout contaminant) on tools, supplies, workers' clothing, etc., to control/reduce the amount of fallout contaminant carried or tracked into the shelter; this

---

* Again, better prediction techniques for interior air blast behavior could change this need.

† Again, better interior air blast prediction techniques could indicate other body positions, as well as specific locations in the shelter.

hazard is considered slight. Also monitor for poor fallout protection places within the shelter, resulting from unexpected contaminant deposition or wind redeposition.

- Work at recovery tasks, including those discussed below.

Early Recovery Tasks and Open Shelter. Many early recovery tasks are vital to the success of an open shelter concept - shelterees must be able to:

- Control fires in spaces adjacent to the shelter, at the same or any lower level and on the level above, or at least keep them small.*

- Control fires elsewhere as necessary to keep the heat on shelterees low enough for survival. This task is magnified in importance if there is a fallout hazard, otherwise the shelter could be evacuated if the heat becomes truly unbearable; even with fallout, evacuation from heat threat may be necessary.

- Clear emergency exits of any building or other debris blocking them.

- Clear any threatening fallout contaminant (that is, perform localized decontamination - e.g., sweeping, washdown, shaking, or brushing) in or near doorways, or deposited on debris in window-wells so as to be dangerously near window-sill height.

- Pile up "clean" debris or shelter stocks wherever needed to create fallout radiation barriers, e.g., near doorways and in window-wells.

Recapitulation. Table 8.0 provides a recapitulation of the general considerations in open shelter.

---

* Shelter building requirements have been stated earlier herein for general fire-resistive construction and fire-resistive or fire retardant treated equipment in, near, and above the shelter.

Table 8.0

OPEN SHELTER GENERAL CONSIDERATIONS

(Recapitulation)

BLAST RESISTANT CONSTRUCTION NEEDS

ALL STRUCTURAL ELEMENTS IN OPEN SHELTER

ALL EQUIPMENT, INTEGRALLY AND MOUNTING

AROUND ALL OPENINGS

DOORS ANCHORED OPEN AND FIRE-RESISTIVE
(PLUS GRATING DOORS?)

GLAZED SASHES: REMOVED, OR ANCHORED SAFELY OPEN

WINDOW-WELL WALLS COMMON TO SHELTER (PERHAPS ALL WALLS)

CLOSED SHELTER SPACE FOR CERTAIN STOCKS

SHELTER STOCKS

SHOULD BE ANCHORED OR REMOVED

ACCESSIBLE SAFELY, AFTER DETONATION

PROTECTED FROM BLAST AND FIRES

INCLUDE STRUCTURAL RECOVERY TIMES

SHELTER MANAGEMENT

MOVE OUT ALL UNANCHORED ITEMS

MOVE SOME STOCKS TO CLOSED SHELTER

CLOSE BLAST DOORS IN CLOSED SHELTER

TAKE PRONE POSITIONS ASSIGNED

MONITOR FALLOUT ENTERING SHELTER

WORK AT RECOVERY TASKS

EARLY RECOVERY TASKS

CONTROL FIRES IN, NEAR AND ABOVE SHELTER

CLEAR EMERGENCY EXITS OF DEBRIS

CLEAR THREATENING FALLOUT CONTAMINANT

ERECT FALLOUT BARRIERS OF DEBRIS/STOCKS

Building 2B

The first application of the open shelter concepts just described was to Building 2, already studied as a closed shelter; the benefits of reuse of Building 2 were economy and a potential for cost comparisons (after two years, a fresh estimate of Building 2A (closed shelter) additional costs for slanting was necessary because of rapidly changing construction costs).

Building 2A costs (from both June 1968 and June 1970 estimates) could be attributed to structural (56%), blast doors (10%), ventilation (25%), and fresh air intake/emergency exit tunnel (18%), the last item being of benefit to ventilation, fire protection, and blast protection, thus rather difficult to assign in terms of the preceding three categories.

Open shelter seemed to offer some potential slanting cost reductions in blast doors, in ventilation (at some increased fire risk), and perhaps in structural changes. However, such reductions may be substantially offset by the cost of closed shelter space required for certain equipment and stocks. Some fire test results[37] were reviewed that seemed to indicate that the noxious gases hazard from fires above the shelter might not be as great as accepted in the past. (See Appendix B.) However, safe ventilation of open shelter in a fire environment requires continuous monitoring of the air taken in and also the capability of changing the source of ventilation air to some extent (or at least the capability of stopping ventilation temporarily if all the sources become contaminated).[51] With such a proviso a well-type escape exit, Figure 8-0C, was considered for use (if used on several basement walls) as an open shelter alternative to the (expensive) fresh air intake/emergency exit tunnel, Figures 8-0A and 8-0B, used in Buildings 1B and 2A. Depending on the fireload on the floors above a basement there may be some danger to basement shelterees from heat. Basement roof slab thickness of one foot appears to be ample to prevent this. For a fuller discussion of all aspects of the fire hazard, see Chapter 3 and Appendix B.

Type IV of the open shelter conceptual types appeared most promising in terms of lower slanting costs, if not in terms of protection provided. Type IV was therefore used for the first case study among the open shelter types.

At the time of writing, serious questions remain concerning the feasibility of Type IV shelter, as discussed in the Open Shelter section of this Chapter. The purpose of this case study, therefore, was to make

some approximate cost comparisons between closed and open shelter, whether or not the latter was of questionable feasibility from a survival standpoint at the time of the study.

Building 2 is described in general terms in Chapter 7. The designed basement floor plan is shown in Figure 8-2 and the slanted version in Figure 8-2B (black lines show slanting structural and architectural changes, gray lines show the original design). The shelter occupies the full basement, excluding the interior stairwell and the exit hallway leading to the exterior stairs. Table 8.2B provides a list of slanting changes, keyed to Figure 8-2B, as well as the estimated additional cost of each change item. Interior shelter walls are blast resistant.

In contrast to Building 2A, Building 2B uses the original, natural cross-ventilation scheme contemplated for the large, open, basement portion used in the slanted version as open shelter. Supplementary ventilation needs could be met by OCD packaged equipment. Some closed shelter space was considered necessary because of the type of equipment in the boiler room and the need for blast resistant storage for certain supply items. However, because the ratio of closed to open shelter areas (49%) is probably atypical, a later summary (Table 8.0A) shows separate estimates for the open, closed, and total shelter areas of Building 2B, in order that the unit costs may be approximately applied to other ratios than 49%.

For this fourth case study, estimated additional slanting costs were close to the Scope limit of $6/sf (about 7% below, when both are corrected to the same time period).

Later work, using this building as the example, made a brief comparison of the centerline support system used in slanting (beams, columns and column footings) with an alternative system (wall and wall footings). The work is described and results provided in a later section of this chapter. The alternative system indicated a potential savings in estimated slanting costs for Building 2B of $3,078 (or about 13% of the total slanting estimate shown in Tables 8.2B and 8.0A).

FIG. 8-2B

BUILDING 2B BASEMENT FLOOR PLAN

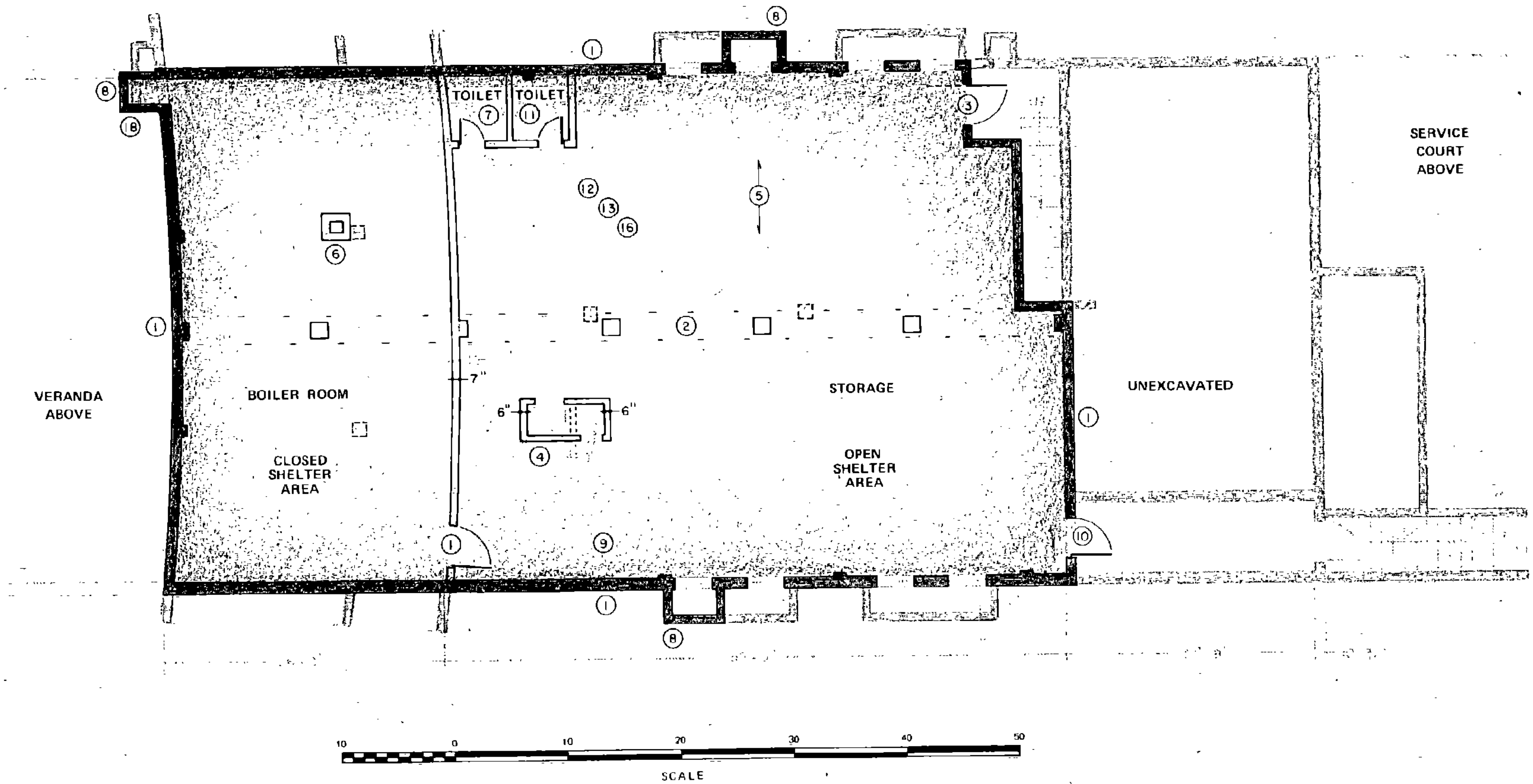

8-46 BLANK

Table 8.2B

BUILDING 2B SLANTING (Type IV Open Shelter)
(Brentwood Rehabilitation Center, Asheville, N.C.)

		15 psi shelter	5 psi shelter		10 psi shelter		20 psi shelter	
1.	Provide blast walls: outer wall (10-3/4" thick)* all around ($3,204), plus main transverse wall 7" thick separating closed and open shelter areas ($1,933), plus blast door ($584). Shelterees allowed in both shelters, but only in prone position in open shelter during blast.	$5,721	(10-3/4") ($859) (7") ($1,412) ($574)	$2,845	(10-3/4") ($2,331) (7") ($1,668) ($579)	$4,579	(10-3/4") ($4,263) (9.5") (2,342) ($590)	$7,195
2.	Provide R/C beam (45" x 24" deep) ($2,539), with R/C columns (tied, 18" square) plus ftgs & end pilasters ($5,145), deleting existing columns	7,684	(45" x 15") ($1,200) (10") ($1,335)	2,535	(45" x 20") ($1,934) (13.5") ($3,122)	5,056	(45"x28.5") ($3,137) (20") ($8,457)	11,594
3.	Provide hardware to anchor stairway door in open position	†		†		†		†
4.	Provide blast enclosure (6" thick) around dumbwaiter and laundry chute ($1,174), with 2 blast doors ($99).	1,273	(6") ($960) (90)	1,050	(6") ($996) ($95)	1,091	(6") ($1,215) ($105)	1,320
5.	Provide blast slab (13-1/2" thick) over both open and closed shelter areas.	7,558	(8.5")	3,165	(11.5")	5,397	(15.5")	9,421
6.	Harden chimney (only in shelter) for blast (†), and provide manual blast door at breeching ($182).	182	($105)	105	($149)	149	($210)	210
7.	Harden toilet spaces: Anchor toilet equipment for blast ($138); detail each door and jamb to open door flat onto a wall and be locked in open position for blast (†); strengthen walls (7" thick) ($889). Prone shelterees allowed during blast.	1,027	($138) (7") ($709)	847	($138) (7") ($810)	948	($138) (7") ($994)	1,132
8.	Convert two areaways, or portions, to Shelter Escape Exits (Figure 8-OC) ($376); convert areaway off Boiler Room to Shelter Escape Exit and into exhaust for all building room air in normal use ($343), with blast door ($373); strengthen all such areaway walls (7" thick) (†).	1,092	($318) ($309) ($369) (7")	996	($346) ($326) ($371) (7")	1,043	($396) ($350) ($375) (7")	1,121

* East wall 11" thick around stairway and main doorway, 8" thick adjacent to remaining (unexcavated) area and at stairwell.

† Design modification considered achievable at little (<<$100) or no additional cost.

Preceding page blank

8-48 BLANK

Table 8.2B (concluded)

	15 psi shelter	5 psi shelter	10 psi shelter	20 psi shelter
9. Provide for blast on all fixed equipment (e.g., laundry tubs), that cannot be moved out during warning periods, by either: a. Blast resistant mounting, with equipment "defanged" (modified as necessary so that no parts can become missiles during blast, or caged in grating heavy enough to contain missiles during blast, preferably the former); OR, b. Provide lockable casters and easily unhooked utility connections (as on home washers), so that equipment can be moved during warning period, either to closed shelter or outside both shelters.	*	*	*	*
10. Take remedial measures about main entrance doorway, based on air blast behavior analysis - at least provide a sliding fire door, mounted and anchored-open-for-blast on inside surface of shelter wall.	*	*	*	*
11. Provide ventilation in toilets: a. Fan in each toilet, ducted out through Boiler Room exhaust areaway (item 8); OR b. Something modified for compatibility with item 9 or no missile hazard; OR c. Some other solution (some ventilation is needed in normal use of building).	†	†	†	†
12-16. As in Table 8-2A.	†	†	†	†
17. As in Table 8-2A.				
18. Provide for all gas, water, fuel oil, etc., supply lines serving the entire facility to first enter through the Boiler Room, and have cut off valves at entry points.	*	*	*	*
(June 1970 costs) 3,378 sf	$24,537 $7.26/sf	$11,543 $3.42/sf	$18,263 $5.41/sf	$31,993 $9.47/sf

† Costs not estimated, but probably minor.
Design modification considered achievable at little (<<$100) or no additional cost.

Preceding page blank

8-50 BLANK

Building 2C

Continuing the application of the open shelter concepts, Building 2C represents a Type I open shelter, thus being like the Building 2A closed shelter (Figure 8-2A) except for having one entrance lock at a time that remains open to entering shelterees. Thus the text remarks under Building 2A apply to Building 2C as well, as does Figure 8-2. Figure 8-2C shows (in black lines) the slanting structural and architectural changes (gray lines show the original design), as applied to the Figure 8-2 basement floor plan. Table 8.2C provides a list of the slanting changes, keyed to Figure 8-2C, as well as the estimated additional cost of each change item. Interior shelter walls are not blast resistant.

For this fifth case study, estimated additional slanting costs were well above the Scope limit of \$6/sf (about 25% high, when both are corrected to the same time period); however, the certainty of the protection level provided was high for an "open" shelter concept.

Table 8.2C

BUILDING 2C SLANTING (Type I Open Shelter)
(Brentwood Rehabilitation Center, Asheville, N.C.)

1 and 3 to 18. Same as in Table 8.2A.		\$24,551
19. Provide special airlock entrance structure (slab 6" thick) (\$6,559) with 3 blast doors (\$2,286) and necessary electrical-mechanical changes (\$365)		9,210
		\$33,761
(June 1970 costs)	3,465 sf	\$9.74/sf

Preceding page blank

8-52 BLANK

FIG. 8-2C

BUILDING 2C BASEMENT FLOOR PLAN

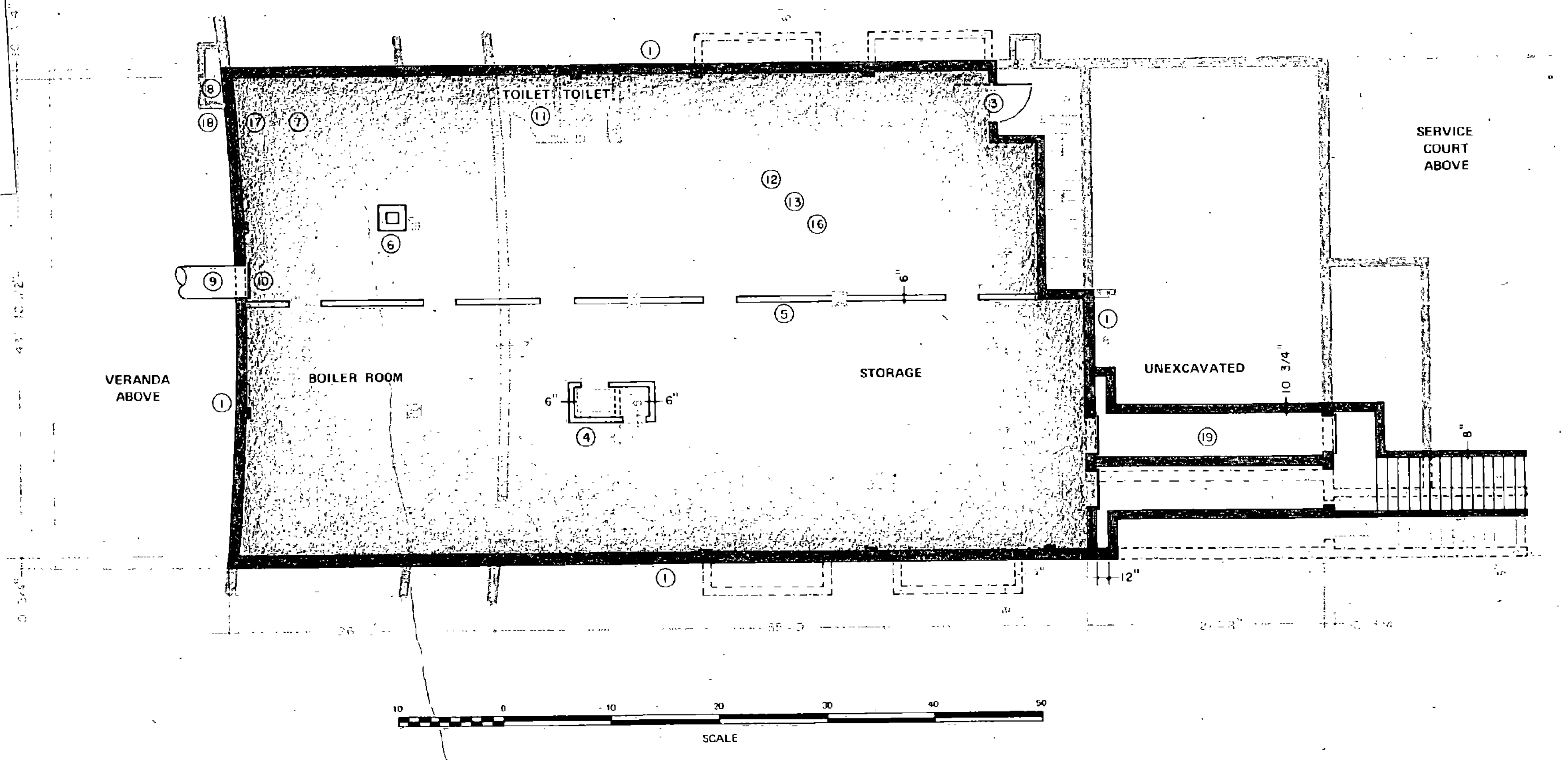

Preceding page blank

8-63

8-54 BLANK

Building 3A

Pursuing slanting case studies into somewhat larger closed shelters seemed appropriate after the lessons of Buildings 1A, 1B, and 2A, to gain some measure of possible lower slanting unit costs with increasing shelter size.

The building is described in general terms in Chapter 7. The designed basement floor plan is shown in Figure 8-3, and the slanted version in Figure 8-3A (black lines show slanting structural and architectural changes, gray lines show the original design). The shelter occupies the full basement excluding the two interior stairwells to upper floors, the elevator shafts, and the police elevator well (no door). Table 8.3A provides a list of slanting changes, keyed to Figure 8-3A, as well as the estimated additional cost of each change item. Interior shelter walls are not blast resistant, except those enclosing the interior stairwells/elevator shafts.

While Items 4, 5, 6, 8, 9, and 10 of Table 8.3A deal with ventilation changes, some further comments on the environmental aspects alone appear to be appropriate. The mechanical plans for the building show a 20,000 cfm exhaust fan that provides cooling air to the transformer vault or removes radiation losses from the emergency diesel-electric set during an emergency. A modified environmental control plan was devised that provides for air conditioning of normally occupied spaces in the basement and also uses this 20,000 cfm of air for ventilating the basement when all habitable spaces are to be densely populated during an attack. For normal use, the central system provides air conditioning for two zones, the Emergency Operating Center (EOC) zone and the Elevator Lobby/Storage Room zone, each of which is supplied with about 5,000 cfm of treated air. With 50% recirculation, the required capacity of the water chiller is about 34 tons. For shelter use, the speed of the zone fans would be doubled and, consequently, the total ventilation rate would be increased to 20,000 cfm, which is about 15 cfm per shelteree (based on 10 sf per person). As early as possible in the postattack period, shelterees in the EOC zone would presumably be relocated to permit EOC personnel to function more effectively. The fan for the EOC zone would then return to normal low speed, and air conditioning would be restored. High speed operation of the fans may be accompanied by objectionable noise. To accommodate requirements for densely populated spaces in the basement shelter, only two changes appeared to be needed in the environmental control system: first, two-speed motors and controllers for the zone supply fans and second, zone supply fans with Class 2 (rather than Class 1) construction that provides reliable operation at high speed.

For this sixth case study, estimated additional slanting costs were under the Scope limit of \$6/sf (about 21% below with mezzanine, about 16% below without mezzanine, when all are corrected to the same time period).

8-56-BLANK

FIG. 8-3

BUILDING 3 BASEMENT FLOOR PLAN AND SECTION

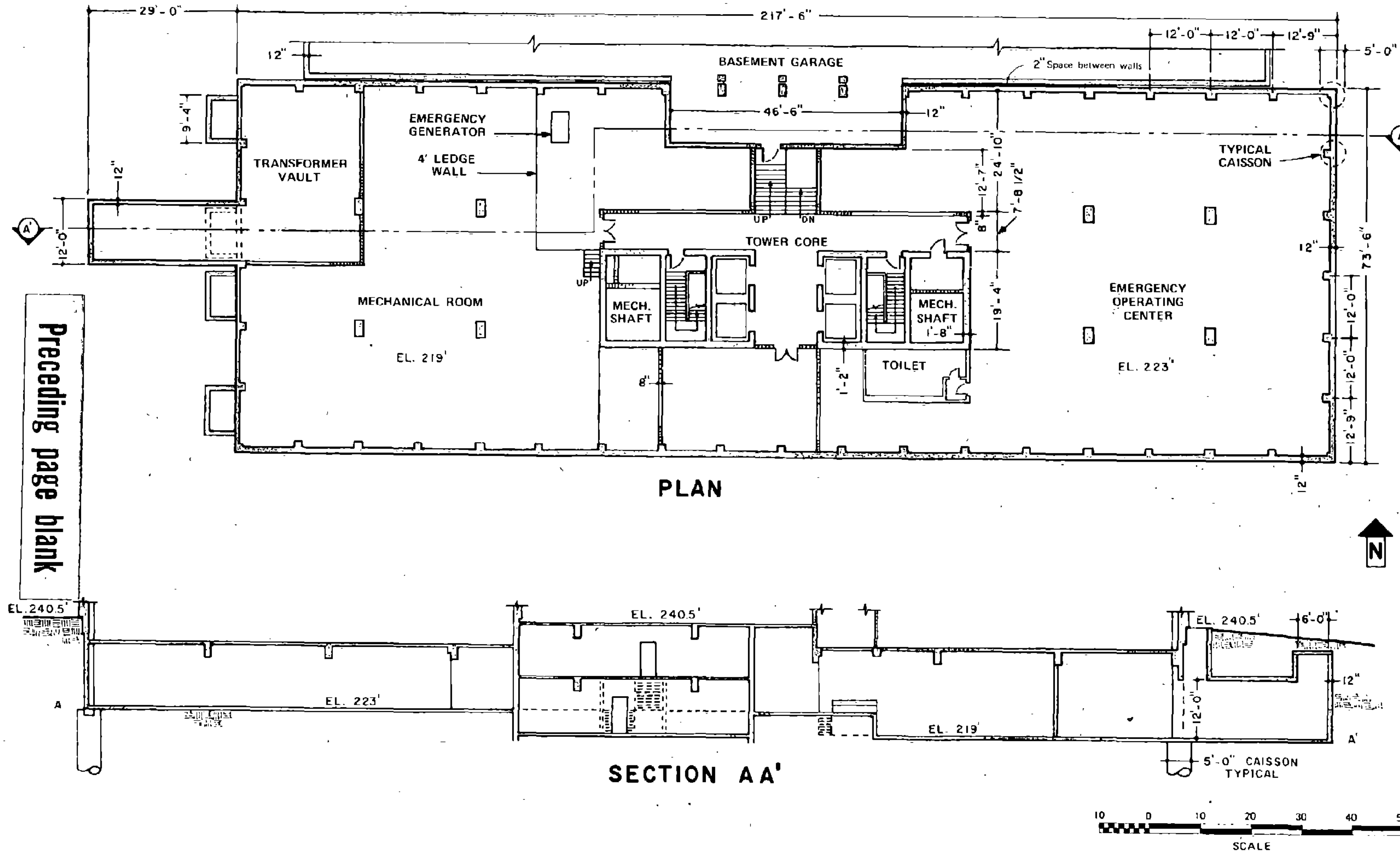

Preceding page blank

8-58 BLANK

FIG. 8-3A

BUILDING 3A BASEMENT FLOOR PLAN AND SECTION

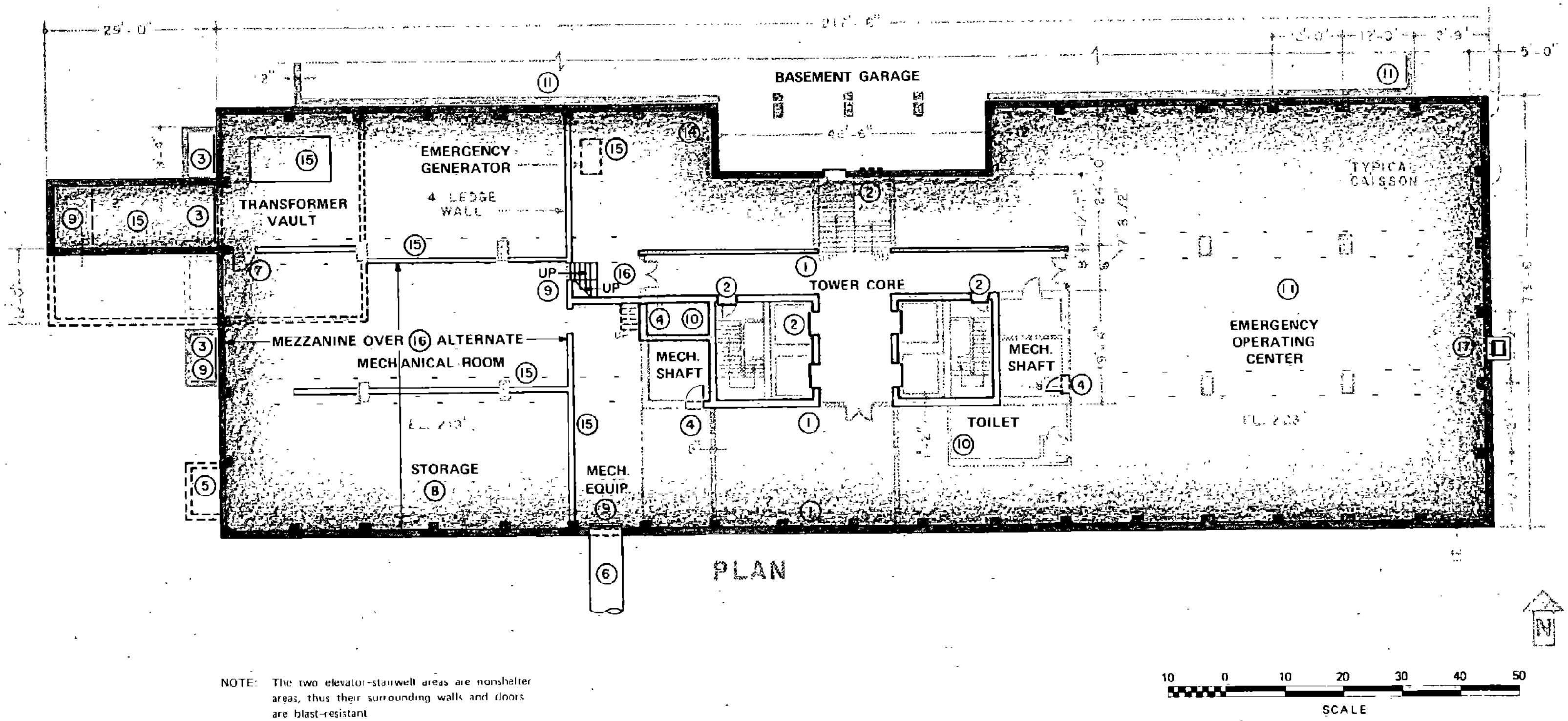

NOTE: The two elevator-stairwell areas are nonshelter areas, thus their surrounding walls and doors are blast-resistant

Preceding page blank

8-59

8-60 BLANK

Table 8.3A

BUILDING 3A SLANTING
(Columbus-Muskogee County Court House, Columbus, Ga.)

		15 psi shelter	20 psi shelter		30 psi shelter	
1.	Strengthen exterior walls (12" thick) for blast ($7,623). Provide interior blast walls enclosing two stairwells (N&S, 13" thick; E&W, 14" thick) and three elevator shafts ($4,200); interior support walls (8" thick with pilaster outer ends) and strengthened columns and footings ($3,709); and blast slab (9" to 14-1/2" thick)* ($32,318) and supporting beams (54" x 37" deep)($4,895).	$52,745	(12")($10,508) (15")(15") ($4,687)(8") ($3,832) (10.5" to 16.5")($38,501) (54" x 42")($7,430)	$64,958	(12")($16,139 (18")(18") ($5,883)(8") ($4,016) (12.5" to 20")($49,185) (54" x 51")($12,264)	$87,487
2.	Provide 8 blast doors at existing doorways: 2 at interior stairways ($1,119); 2 at garage entrance doors ($1,093); and 4 at elevator doors ($10,738).	12,950	($1,209)($1,195) ($10,955)	13,359	($1,427)($1,399) ($13,410)	16,236
3.	Provide 3 horizontal blast doors (or hatches) at areaways.	2,485		2,537		3,100
4.	Modify mechanical shafts: Provide new door to each shaft ($361); close shafts with blast slab (9" thick) above ($1,260); provide R/C blast wall (14" thick) in lieu of existing masonry unit wall between west mechanical shaft and police elevator well (no door)($1,215). Shafts become available as shelter.	2,836	($361)(10-1/2") ($1,344)(15") ($1,322)	3,027	($361)(12-1/2") ($1,495)(18") ($1,471)	3,327
5.	Modify existing air intake #1 to serve ground floor only.	-2,732		-2,732		-2,732
6.	Provide fresh air intake/emergency exit tunnel, approx. 5.5' x 7' corrugated metal cattle-pass by <u>55' long</u> ($8,862), leading to manhole ($3,712) in clear area south of tower building, with vertical sliding blast door ($727) on inside face of shelter wall.	13,301	($8,862) ($3,712) ($780)	13,354	($8,862) ($3,712) ($880)	13,454
7.	Provide new door into transformer vault to add to shelter space (assuming normal power shut off). Door must meet fire standards.	369		369		369

8-62 BLANK

Table 8.3A (continued)

		15 psi shelter	20 psi shelter		30 psi shelter	
8.	Modify ventilation system <u>at and above ground floor level</u>: Relocate AU-1, AU-2, and RA-1 systems to ground floor storage area (Room G-35)($-1,343); relocate storage to basement shelter; relocate return air louvers on all floors from east mechanical shaft to west (*); provide outside air supply openings at ground floor level to outside air plenum (*); duct toilet room exhausts (all floors except basement) via west mechanical shaft to 12th floor exhaust fan to permit open shaft to be used as normal return air duct for all floors ($1,208).	$ -135	($-1,343) ($1,208)	$ -135	($-1,343) ($1,208)	$ -135
9.	Relocate AU-3 unit into new mechanical equipment room; increase AU-3 size to provide required shelter ventilation; provide outside air from fresh air intake tunnel (Item 6); increase exhaust air system (in mechanical equipment room) to provide required shelter exhaust through areaways at transformer vault.	1,284		1,284		1,284
10.	Relocate basement toilet room exhaust duct (15" x 10") from west mechanical shaft to new emergency exit, Item 17 ($560); provide local exhaust fan ($263).	823	($560) ($263)	823	($560) ($263)	823
11.	Provide for all gas, water, fuel oil, etc., supply lines serving entire tower building and nearby garage areas to first enter facility through tower building basement (shelter), and have cut off valves (inside) at entry points.	375		375		375
12.	Grout all pipe penetrations through slab above shelter and through common walls to garage.	1,168		1,168		1,168
13.	If water well is economically available, its development should be considered for two purposes - the obvious one of an emergency water supply in lieu of stored water containers and a second one of a course of cooling water for emergency cooling use in the shelter.					

* Design modification considered achievable at little (<<$100) or no additional cost.

8-64 BLANK

Table 8.3A (concluded)

			15 psi shelter		20 psi shelter		30 psi shelter
14.	Modify present electrical distribution of emergency power supply to provide separate cut-off of nonshelter circuits. Shelter emergency power to serve shelter lighting, heating, ventilation, water pump, and sewage ejector.		*		*		*
15.	Relocate transformers and emergency generator; construct new concrete block partitions for transformer vault and for new mechanical equipment room (Item 9), all to provide for proper shelter ventilation and exhaust circulation; relocate transformer tunnel (*).		$2,214		$2,214		$2,214
16.	Provide new concrete slab (6" thick) and support beams for mezzanine in new basement storage area to provide additional shelter area (2,753 sf) with metal access stairs.		11,646		11,646		11,646
17.	Provide new window-well emergency exit (east end) ($801), including blast door ($373).		1,174	($375)	1,176	($378)	1,179
	June 1970 costs)	16,351 sf	$100,503 $6.15/sf		$113,423 $6.94/sf		$139,795 $8.55/sf
	Omitting mezzanine (Item 16): (June 1970 costs)	13,598 sf	$ 88,857 $6.53/sf		$101,777 $7.48/sf		$128,149 $9.42/sf

Preceding page blank

* Design modification considered achievable at little (<<$100) or no additional cost.

8-66 BLANK

Summary Comments - First Six Case Studies

The first six slanting examples include four closed and two open shelters; the latter are one Type I (closed to blast but open to ingress) and one Type IV (many openings). All of the entranceways have ample capacity (Table 1.1). None of the entranceway configurations was specifically checked for shielding adequacy in terms of initial nuclear and thermal radiation, or fallout, although all appear to be satisfactory if occupant countermeasures can be assumed to have been undertaken. All design changes (slanting) varied between schematic and preliminary, the goal being bare sufficiency to enable the estimator to make a reasonable cost estimate. All estimates were prepared by a professional estimator. For each slanting example, a full set of contract construction plans (i.e., of the original design) was available and used by both designers and the estimator. The usual rounding off of dollar values was not done in the estimates because of their extensive further use in calculations of percentages and other ratios, which were then used in various comparisons; the lack of rounding off does not imply any greater accuracy than usual for building cost estimates (see Cost Estimates section, Chapter 6).

The cost estimates for each of the six slanting examples were summarized into four major items - structural, blast doors, ventilation, and other - to facilitate comparisons and further study. A review was made for construction work that must be done at time of building construction versus work that could be completed later; the former was termed "nondeferrable" for discussion purposes. Percentages were calculated for ratios of each major item's cost to the total slanting cost and also of the nondeferrable to total cost for each major item and total slanting cost. Perhaps of most interest were the total additional costs per square foot of shelter space, for each example and all reduced to the same time period.

Table 8.0A shows the foregoing data.* Building 2B costs (columns 2 to 4) show open portion, closed portion, and total costs. Building 3A costs (columns 6 and 7) show two building options, with and without mezzanine. It should be obvious that many arbitrary decisions had to be made in preparing the table; however, the table was prepared and all estimates/descriptions of work items for all slanted buildings were reviewed by an architect colleague, both because of his diverse background encompassing architecture, structures, mechanical, and estimating experience and to gain another's viewpoint.

---

* Plus data from the case study that follows (Building 4A).

Preceding page blank

The data of Table 8.0A* indicate a potential for lowered slanting costs in open versus closed shelter, considering total, not nondeferrable, costs (note columns 2 and 1, $5.07 versus $5.78, a ratio of 88% for open over closed shelter). The data also indicate that about 60% of slanting costs in closed shelters is nondeferrable (Building 2C, open to shelterees but closed to blast, is more comparable to the closed shelters than to the other open shelter, Building 2B). Building 2B slanting costs (column 4) are about 95% nondeferrable as one might expect for an open shelter.

Considering the data for closed shelters, plus Building 2C (i.e., omitting Buildings 2B and 4A), nondeferrable work under the structural item amounts to 96% to 99% of the nondeferrable totals, but total work under structural amounts fo 57% to 67% of the building totals, blast doors 10% to 19%, and combined structural-blast doors 66% to 85%.

The sparse data indicate that:

- An open shelter (other than Type I such as Building 2C) should probably be considered only for complete work at the time of building construction, because deferrable work may amount to such a small portion of the total work (e.g., 5% in column 5); inflation may reinforce this thinking.

- The results of subsequent work showed that open shelter slanting costs are more sensitive to changes in design overpressure than closed shelter slanting costs. As shelters become smaller in floor area, say below 3000 sf, slanting costs begin to rise markedly.

---

* Holders of earlier versions of this table may note differences among the earlier versions and the version herein. Many new "designs" were required for this report, to cover the range of overpressures and related slanting estimates reported later in this Chapter. Frequently the design approach of the 15 psi shelter studies used for the current Table 8.0A had to be changed from that used earlier, in order to better suit use throughout an overpressure range, i.e., so that the calculation of estimate ratios, say for each overpressure versus a base overpressure, might have better validity. Such 15 psi re-designs, plus simply finding discrepancies in the earlier estimates, generally account for the differences among versions of the table.

Table 8.0A

SUMMARY OF SLANTING COST ESTIMATES (15 psi)

		(1)		(2)		(3)		(4)		(5)		(6)		(7)		(8)	
Building:		2A (closed)		2B (open portion)		2B (closed portion)		2B (total)		2C ("open")		3A (closed) with mezzanine		3A (closed) no mezzanine		4A (open)	
Cost Items		All	Non-deferrable	All	Non-deferrable	All	Non-deferrable	All	Non-deferrable	All	Non-deferrable	All	Non-deferrable	All	Non-deferrable	All	Non-deferrable
Shelter area (sf)		3,378		2,262		1,116		3,378		3,465		16,351		13,598		130,522	
Estimate date		6-70		6-70		6-70		6-70		6-70		6-70		6-70		6-70	
A. Structural	$	14,354	14,354	13,399	13,399	8,154	8,154	21,553	21,553	20,913	20,913	67,667	57,220	56,021	55,220	498,824	498,824
	$/sf	4.25	4.25	5.92	5.92	7.31	7.31	6.38	6.38	6.03	6.03	4.14	3.50	4.12	4.06	3.82	3.82
	%*	57	99	90	91	85	96	88	93	62	>99	67	96	63	96	63	64
	%†		100		100		100		100		100		85		99		100
B. Blast doors	$	2,478	--	99	--	1,139	--	1,238	--	3,943	--	17,265	--	17,265	--	22,738	9,730
	$/sf	.73	--	.04	--	1.02	--	.37	--	1.14	--	1.06	--	1.27	--	.17	.07
	%*	10	--	1	--	12	--	5	--	12	--	17	--	19	--	3	1
	%†		0		0		0		0		0		0		0		43
C. Ventilation	$	6,270	99	376	376	343	343	719	719	6,270	99	11,814	-760	11,814	-760	233,585	233,585
(Incl. emergency	$/sf	1.86	.03	.17	.17	.31	.31	.21	.21	1.81	.03	.72	-.05	.87	-.06	1.79	1.79
exit tunnel,	%*	25	1	3	3	3	4	3	3	19	--	12	-1	13	-1	30	30
if any)	%†		2		100		100		100		<1		-6		-6		100
D. Other	$	2,270	--	1,027	1,027	--	--	1,027	1,027	2,635	--	3,757	3,043	3,757	3,043	35,697	35,697
	$/sf	.67	--	.45	.45	--	--	.30	.30	.76	--	.23	.19	.28	.22	.27	.27
	%*	9	--	7	7	--	--	4	4	8	--	4	5	4	5	5	5
	%†		0		100		0		100		0		81		81		100
Total	$	25,372	14,453	14,901	14,802	9,636	8,497	24,537	23,299	33,761	21,012	100,503	59,503	88,857	57,503	790,844	777,836
	$/sf	7.51	4.28	6.59	6.54	8.63	7.61	7.26	6.90	9.74	6.06	6.15	3.64	6.53	4.23	6.06	5.96
	%†		57		99		90		95		62		59		65		98
‡ Jan. 68:	$/sf	5.78	3.29	5.07	5.03	6.64	5.86	5.59	5.30	7.49	4.66	4.73	2.80	5.03	3.25	4.66	4.58
‡ Jun. 73:	$/sf	9.69	5.51	8.50	8.44	11.14	9.82	9.37	8.90	12.57	7.82	7.93	4.69	8.43	5.45	7.81	7.69

* Percent ratio of item cost to total cost.
† Percent ratio of nondeferrable cost to item (All) cost.
‡ Using Engineering News-Record Building and Construction Cost Indexes (averaged) to convert totals from San Francisco area to EN-R's 20-cities average and from estimate date to date(s) shown.

8-70 BLANK

Building 4A

Building 4 was selected for a case study of a very large, open shelter (Type IV - many openings), thus providing cost and study data to supplement earlier data on a small, open shelter (Building 2B) and to include a shelter some eight times larger than the largest earlier one (Building 3A), open or closed.

The building is described in general terms in Chapter 7. The two below-grade levels of this parking garage are shown, as designed, in Figures 8-4.1 and 8-4.2; the slanted version is shown in Figures 8-4A.1 and 8-4A.2 in which black lines show slanting changes (dashed lines or Xs for deletions) and gray lines show the original design. Slanting was planned to be independent of any slanting of the adjacent tower building (Building 3A), so that costs and problem areas might be more realistic for a general case.

The shelter occupies both sub-levels of the parking garage; however, during passage of the direct effects, it was planned to move personnel and movable equipment out of the more hazardous air blast areas discussed further below. It was considered necessary to cut off by blast doors the air blast that would enter the shelter spaces through stairwells, elevator shafts, and the proposed ventilation ducts/emergency exits; to do otherwise apparently leaves too few "safe" floor areas for the contemplated number of shelterees. Because four large (auto ramp) openings remain, however, the shelter is still an open shelter (Type IV - many openings).

Table 8.4A provides a list of slanting changes keyed to Figures 8-4A.1 and 8-4A.2, as well as the estimated additional cost of each change item. Also indicated in Table 8.4A is the blast loading assumed to act on each of many of the structural components. Such loadings considered results from room filling/jet effect calculations (Appendix E), but were finally based on the judgment of engineers with experience in blast-resistant design and full-scale nuclear tests. Cost data were added to Table 8.0A (column 9) to facilitate various cost comparisons.

For this seventh case study, estimated additional slanting costs were under the Scope limit of \$6/sf (about 22% below the Scope limit when all costs are corrected to the same time period, January 1968).

For the cost estimates for full slanting of Building 4A for overpressures other than the initially used 15 psi, the large number of different structural members in this big shelter precluded as too costly the redesign of each member. Instead, a few members considered typical of their type (e.g., floor cover slabs, beams, walls, columns) were redesigned, then the ratio of their cost to that of the 15 psi design costs was applied to all members of that type.

Preceding page blank

8-72 - BLANK

hazard is considered slight. Also monitor for poor fallout protection places within the shelter, resulting from unexpected contaminant deposition or wind redeposition.

o Work at recovery tasks, including those discussed below.

Early Recovery Tasks and Open Shelter. Many early recovery tasks are vital to the success of an open shelter concept - shelterees must be able to:

o Control fires in spaces adjacent to the shelter, at the same or any lower level and on the level above, or at least keep them small.*

o Control fires elsewhere as necessary to keep the heat on shelterees low enough for survival. This task is magnified in importance if there is a fallout hazard, otherwise the shelter could be evacuated if the heat becomes truly unbearable; even with fallout, evacuation from heat threat may be necessary.

o Clear emergency exits of any building or other debris blocking them.

o Clear any threatening fallout contaminant (that is, perform localized decontamination - e.g., sweeping, washdown, shaking, or brushing) in or near doorways, or deposited on debris in window-wells so as to be dangerously near window-sill height.

o Pile up "clean" debris or shelter stocks wherever needed to create fallout radiation barriers, e.g., near doorways and in window-wells.

Recapitulation. Table 8.2 provides a recapitulation of the general considerations in open shelter.

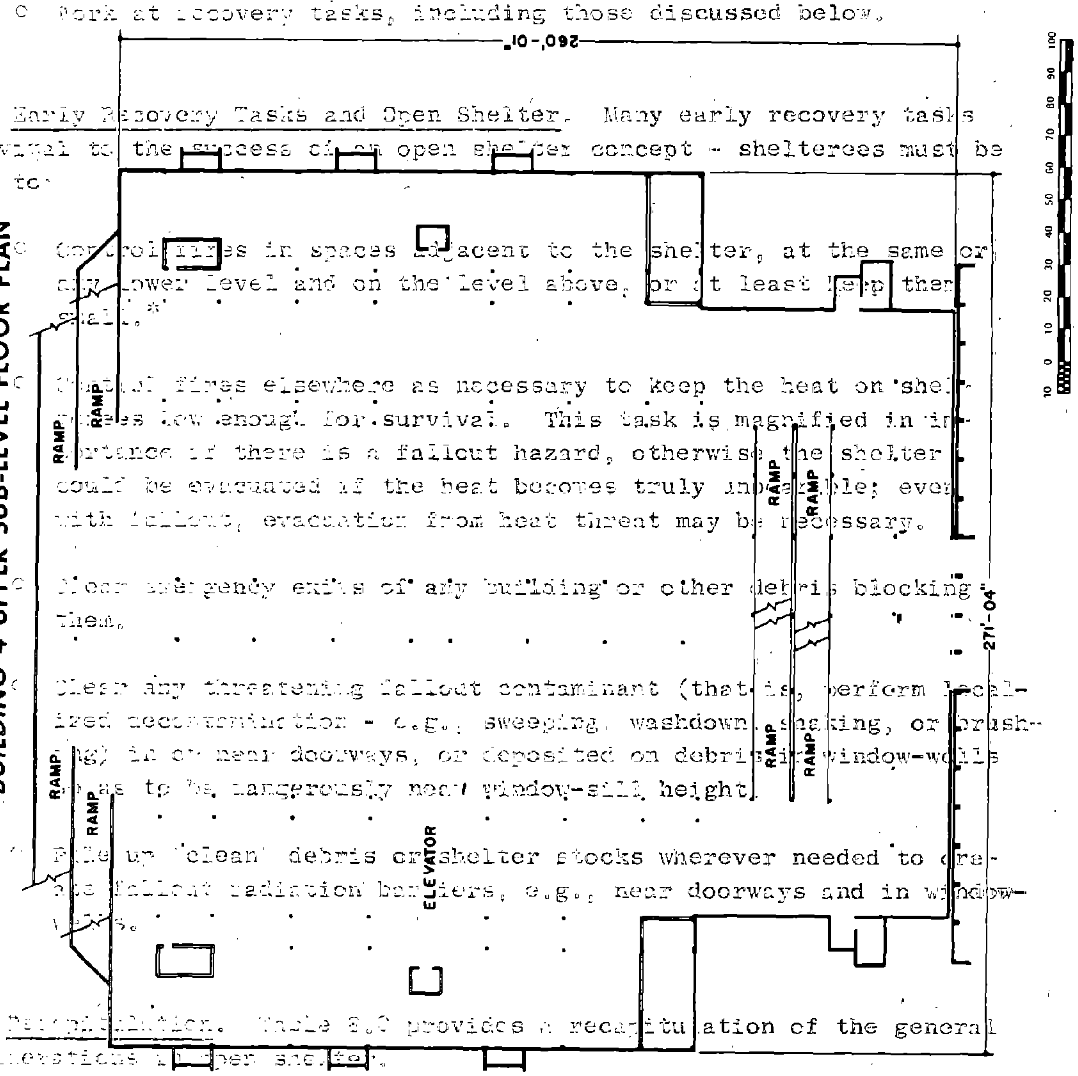

FIG. 8-4.1 BUILDING 4 UPPER SUB-LEVEL FLOOR PLAN

* Shelter building requirements have been stated earlier herein for general fire-resistive construction and fire-resistive or fire retardant treated equipment in, near, and above the shelter.

8-74 BLANK

FIG. 8-4.2

BUILDING 4 LOWER SUB-LEVEL FLOOR PLAN

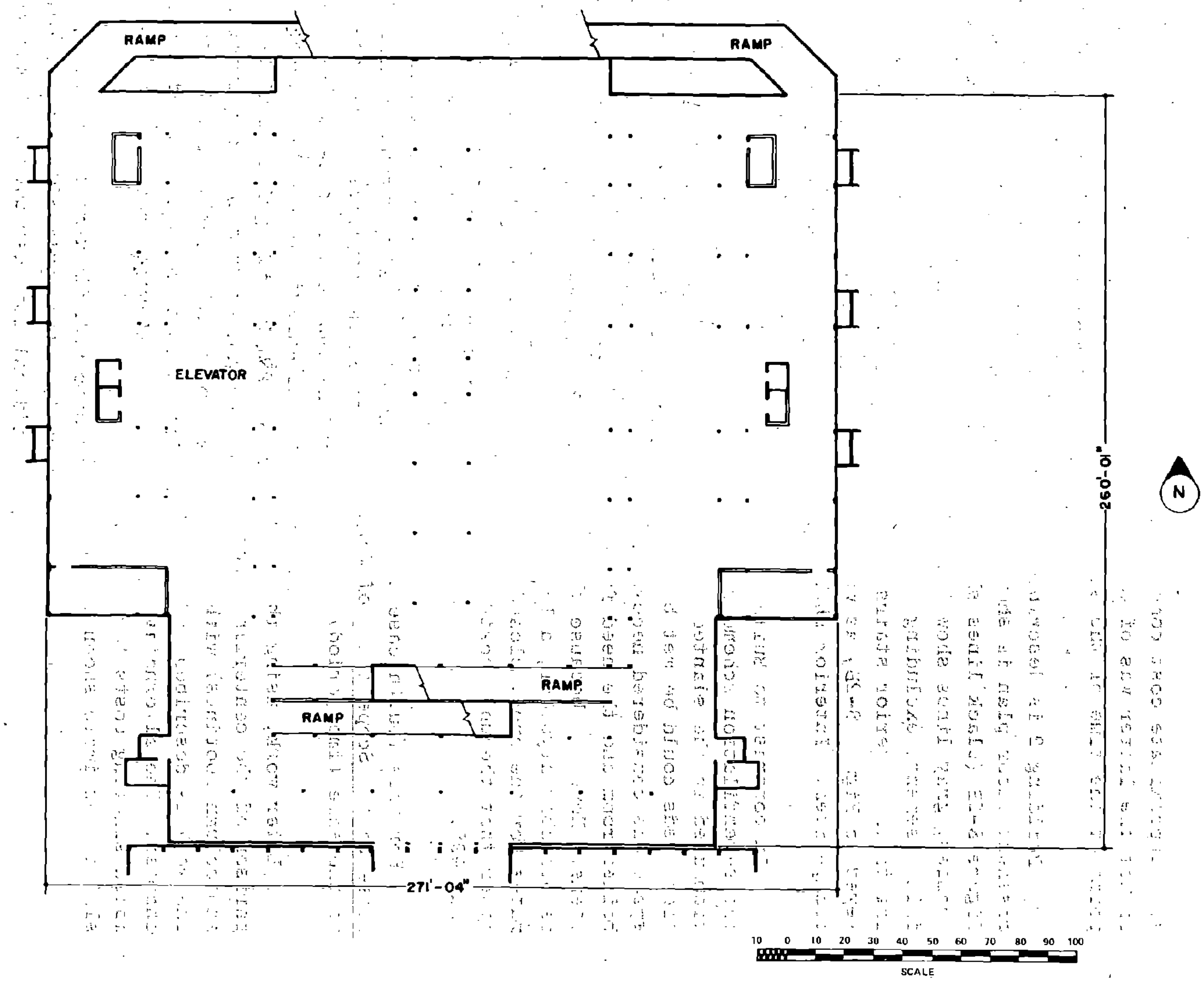

some approximate cost comparisons between closed and open shelter, whether or not the latter was of questionable feasibility from a survival standpoint at the time of the study.

Building 2 is described in general terms in Chapter 7. The designed basement floor plan is shown in Figure 8-2 and the slanted version in Figure 8-2B (black lines show slanting structural and architectural changes, gray lines show the original design). The shelter occupies the full basement, excluding the interior stairwell and the exit hallway leading to the exterior stairs. Table 8.2B provides a list of slanting changes, keyed to Figure 8-2B, as well as the estimated additional cost of each change item. Interior shelter walls are blast resistant.

In contrast to Building 2A, Building 2B uses the original, natural cross-ventilation scheme contemplated for the large, open, basement portion used in the slanted version as open shelter. Supplementary ventilation needs could be met by OCD packaged equipment. Some closed shelter space was considered necessary because of the type of equipment in the boiler room and the need for blast resistant storage for certain supply items. However, because the ratio of closed to open shelter areas (49%) is probably atypical, a later summary (Table 8.0A) shows separate estimates for the open, closed, and total shelter areas of Building 2B, in order that the unit costs may be approximately applied to other ratios than 49%.

For this fourth case study, estimated additional slanting costs were close to the Scope limit of $6/sf (about 7% below, when both are corrected to the same time period).

Later work, using this building as the example, made a brief comparison of the centerline support system used in slanting (beams, columns and column footings) with an alternative system (wall and wall footings). The work is described and results provided in a later section of this chapter. The alternative system indicated a potential savings in estimated slanting costs for Building 2B of $3,078 (or about 13% of the total slanting estimate shown in Tables 8.2B and 8.0A).

8-76 BLANK

FIG. 8-4A.1

BUILDING 4A UPPER SUB-LEVEL FLOOR PLAN

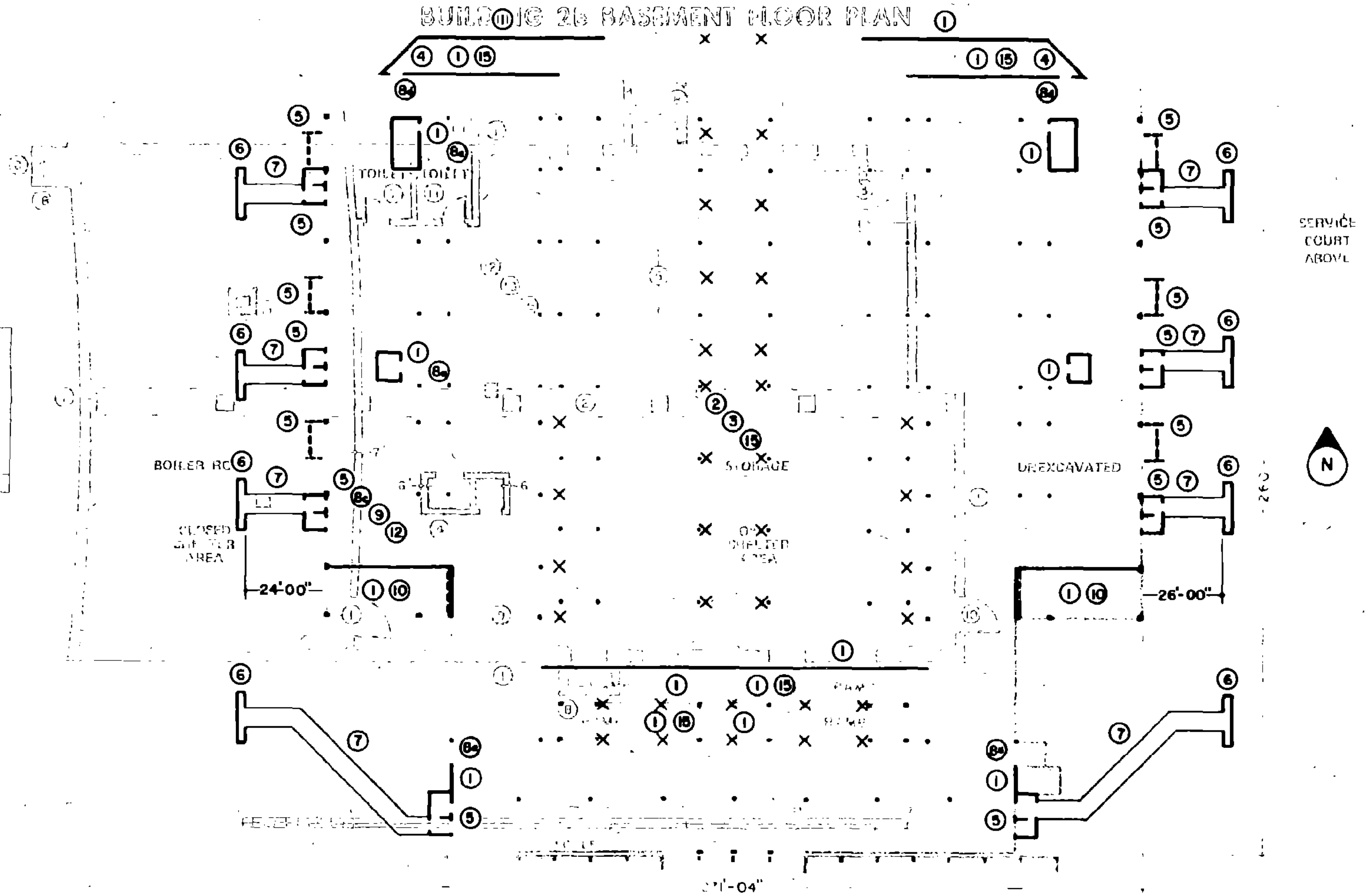

X INDICATES REMOVAL OF COLUMN

--- INDICATES REMOVAL OF WALL

10 0 10 20 30 40 50 60 70 80 90 100
SCALE

8-78 BLANK

FIG. 8-4A.2

BUILDING 4A LOWER SUB-LEVEL FLOOR PLAN

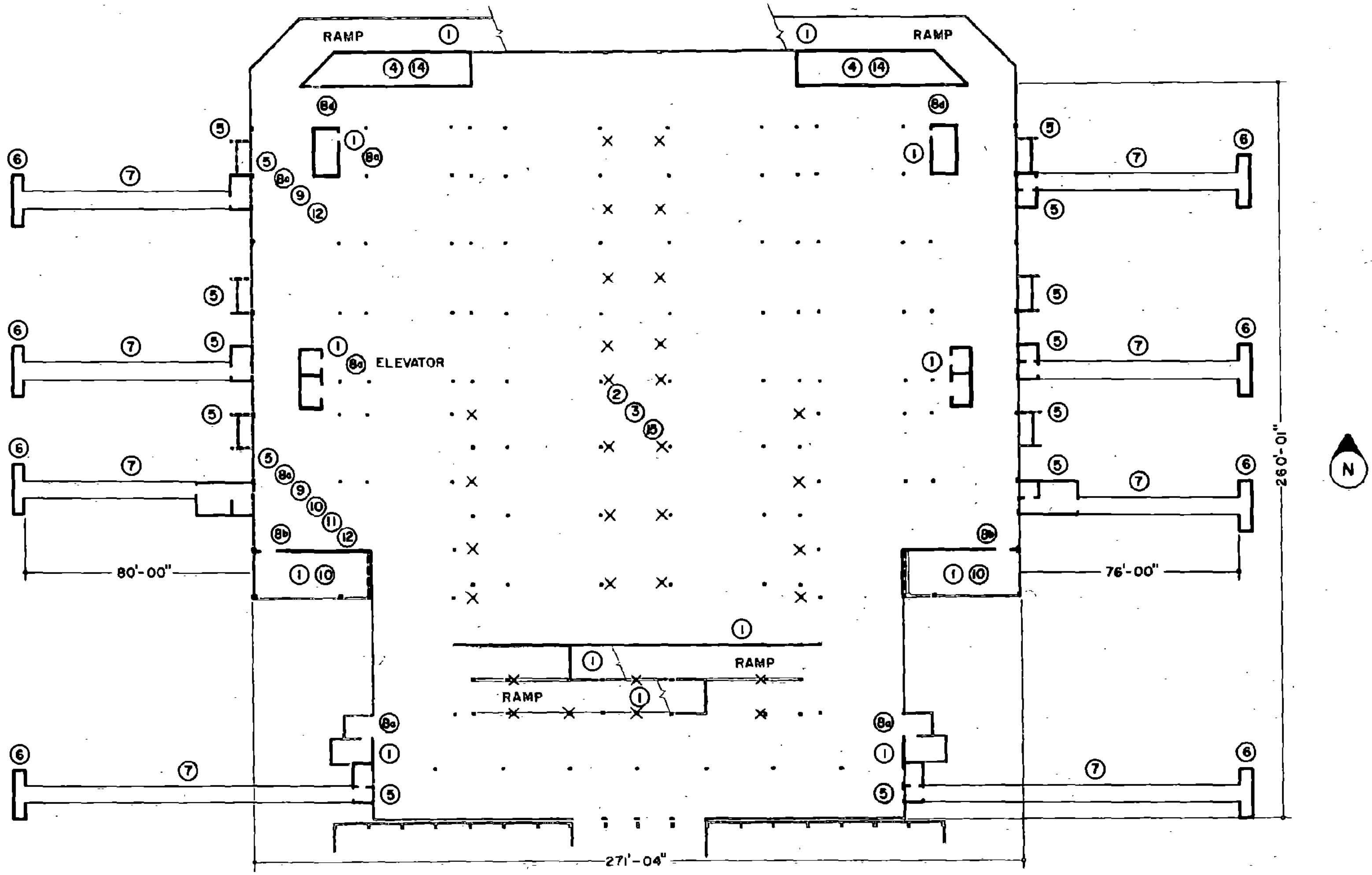

X INDICATES REMOVAL OF COLUMN
--- INDICATES REMOVAL OF WALL

10 0 10 20 30 40 50 60 70 80 90 100
SCALE

8-80 BLANK

Table 8.4A

BUILDING 4A SLANTING

(Columbus-Muskogee County Court House, Columbus, Ga.)

Item	15 psi shelter	5 psi shelter (components)	5 psi shelter	10 psi shelter (components)	10 psi shelter	20 psi shelter (components)	20 psi shelter
1. Strengthen for blast resistance:	$41,805		$ 31,715		$ 37,239		$ 45,914
a. No exterior shelter walls[a] (lateral soil coefficient used for airslap = 1/2); all (4) stairwells[a]; both (2) elevator shafts,[a] each with a machinery room on lower sub-level only; interior walls between garage and 2 mechanical equipment rooms[a] (blast loading either side); ($23,417);		($18,913)		($20,474)		($26,066)	
b. Auto ramps serving upper[a] and lower[b] sub-levels ($6,267) and northernmost wall[a] (also closed openings) of south pair of ramps ($12,121) including their footings.[c] Stairwell, shaft, and mechanical room R/C walls replace concrete block construction.		($5,467) ($9,335)		($5,805) ($10,860)		($6,593) ($13,255)	
2. Relocate interior columns under plaza for reduced spans. Strengthen for blast resistance, all interior columns[d] and their footings,[c] both sub-levels.	197,657		28,340		117,030		294,400
3. Strengthen for blast resistance: Floor slab and beams over upper sub-level (mostly 2-way slabs, 10" to 16-1/2" thick), using worst blast direction[a] ($203,970); floor slab and beams over lower sub-level[b,e] (mostly 2-way slabs, 6" to 12" thick) ($52,596). Both floor slab-and-beam systems replace pan-joist-and-beam systems.	256,566	(7" to 12") ($68,174) (6" to 10")($38,204)	106,378	(9" to 15") ($159,679) (6" to 11")($46,084)	205,763	(11" to 18") ($243,832) (6" to 12")($58,470)	302,302
4. Replace unexcavated space (shown only on lower sub-level plan but extends partly into upper sub-level) with 2 storage rooms approx. 1-1/2 stories high having blast resistant[a] walls and footings; each room to have approx. 7,000 cf.	2,796		2,796		2,796		2,796
5. Replace 6 ventilation wells ($-27,429) with 8 blast resistant[a] ventilating vaults (2-story); two with adjacent generator rooms ($19,105), six without ($31,225); all located exterior to east and west exterior wall lines.	22,901	($-27,429) ($18,168)($29,600)	20,339	($-27,429) ($18,681)($30,490)	21,742	($-27,429) ($19,487)($31,887)	23,945
6. Provide: 8 ventilation exhaust/emergency exit structures in midstreet ($36,744); and 8 ventilation intake/emergency exit structures in sidewalk ($23,192).	59,936	($36,744) ($23,192)	59,936	($36,744) ($23,192)	59,936	($36,744) ($12,192)	59,936

Preceding page blank

8-82 BLANK

Table 8.4A (continued)

	15 psi shelter	5 psi shelter		10 psi shelter		20 psi shelter	
7. Provide: 8 corrugated steel cattle-pass tunnels (approx. 5'6" x 7'), each approx. 68' long, connecting Items 5 and 6 (exhaust at midstreet) ($113,871); and, 8 ditto, each approx. 20' long, connecting Items 5 and 6 (intake at sidewalk) ($25,165).	$139,036		$139,036		$139.036		$ 139,036
		($113,871)		($113,871)		($113,871)	
		($25,165)		($25,165)		($25,165)	
8. Provide 68 blast doors[a] as follows:	22,738		22,106		22,422		23,054
a. One (3' x 7') at each stairwell and elevator shaft (Item 1), at each sub-level ($2,148);		($2,028)		($2,088)		($2,208)	
b. One (3' x 7') for each mechanical room (Item 1), lower sub-level only ($358);		($348)		($353)		($363)	
c. One (3'4" x 7') for each ventilating vault (Item 5) at each sub-level, between garage and vault ($5,888);		($5,728)		($5,808)		($5,968)	
one (5'4" square) for each vault, at each sub-level, between garage and ventilating fan ($6,448);		($6,288)		($6,368)		($6,528)	
one (4' x 6'8") for each vault, at each sub-level, between vault and cattle-pass ventilating duct ($6,560);		($6,400)		($6,480)		($6,640)	
d. One (3' x 7') for each new storage room (Item 4) at lower sub-level and one (3' x 4') at upper sub-level ($1,336).		($1,314)		($1,325)		($1,347)	
9. Provide mechanical equipment for each of 8 ventilation vaults (Item 5): one fan (27,000 cfm), 5-hp motor, and appurtenances for each vault, at each sub-level ($9,725);	11,712	($9,725)	11,712	($9,275)	11,712	($9,725)	11,712
one recirculating air damper for each 2-story vault ($1,987).		($1,987)		($1,987)		($1,987)	
10. Relocate sump pumps from 2 mechanical equipment rooms (outside shelter) to emergency generator rooms (Item 5).	*		*		*		*
11. Provide emergency generators (2 @ 50 kw) and power distribution for ventilating, sump pumps, and partial shelter lighting (Item 5).	23,069		23,069		23,069		23,069
12. Provide shelter lights at each ventilating fan opening (Items 5 and 9), located behind blast door (Item 8c).	3,731		3,731		3,731		3,731
13. Provide normal-use garage lighting fixtures with features to facilitate preattack removal, e.g., hung by strap or chain that can be quickly cut with bolt cutters.	8,160		8,160		8,160		8,160

8-84 BLANK

Table 8.4A (concluded)

	15 psi shelter	5 psi shelter	10 psi shelter	20 psi shelter
14. Provide minimal lighting in new storage rooms (Items 4 and 8d).	$ 737	$ 737	$ 737	$ 737
15. Provide draft curtains at ramps connecting ground level and upper sub-level, for postblast use.	†	†	†	†
16. Reroute all utilities serving complex to reduce or eliminate hazards to shelterees from ruptures.	*	*	*	*
17. If water well is economically available, its development should be considered for two purposes - the obvious one of an emergency water supply in lieu of stored water containers and a second one of a source of cooling water for emergency cooling use in the shelter.				
(June 1970 costs) 130,522 sf‡	$790,844 $6.06/sf	$458,055 $3.51/sf	$653,373 $5.01/sf	$938,792 $7.19/sf

* Design modification considered achievable at little (<<$100) or no additional cost.

† Costs not estimated, but probably minor.

‡ See third footnote on page 1-2; area of ramps connecting sub-levels was counted, but area of ramps connecting upper sub-level and ground level was counted only for those portions lying directly below the ground level floor slab.

a. Blast loading: Design peak free-field overpressure (5, 10, 15 and 20 psi), zero rise-time, 1 Mt yield, no increase for reflection.

b. Blast loading: 1, 1.5, 1 and 1 psi peak, respectively, for design peak overpressure of 5, 10, 15 and 20 psi; zero rise-time, 1 Mt yield, no increase for reflection. 2 psi was used for both 15 and 20 psi design values because choking was assumed to occur above about 14 psi free-field.

c. Allowable bearing pressure for dynamic loading equals twice the conventional allowable static value plus the peak free-field soil pressure at foundation level.[a]

d. Upper sub-level column loading equal to twice the design peak overpressure[a] times loaded area. Lower sub-level column loading equal to twice the design (e.g., 15+2) peak overpressure[a,b] times loaded area.

e. Blast loading, for slabs over lower sub-level in vicinity of ramps: Design peak[b], zero rise-time, 70 msec duration (used for 2 psi peak[b]; proportional durations used for other peaks), no increase for reflection.

f. Blast loading: 15 psi-peak, 100 msec rise-time, 1 Mt yield, no increase for reflection.

8-86 BLANK

The shelter should be cleared of cars to the maximum extent possible following an alert notice. Any remaining cars should have windows open, be located in the "safer" floor areas with respect to the air blast behavior discussed further below, and may be occupied by shelterees. Reported results of recent tests of deliberately set fires in cars parked in an enclosed parking garage[44] showed a modest but entirely survivable fire hazard; the more significant test findings were as follows:

- Intensity and size of car interior fires are closely linked with the additional fire load of objects scattered inside the car.
- Generally the fire remains confined to the car for a very long time and will spread to adjacent cars only under certain conditions.
- Gas tank does not explode, even if the fire rages around the tank (tested at half to two-thirds full); the gasoline burns at the filler cap through the pressure release valve,* the burned-out tank seal and the melted seams.
- Rear tires of burning vehicle explode.
- Room temperature remained bearable† in all tests (but note that only one test fire was burning at any one time).
- With the automatic sprinkler system inoperative, smoke production did not impair visibility until some minutes after the fire had reached its full proportions, even when smoke production was deliberately heightened by burning smoke producing materials (celluloid waste, tires, motor oil).
- With the automatic sprinkler system operative, its opening caused complete smoke obscuration within a few seconds; breathing without auxiliary breathing apparatus was then impossible, as well could be evacuation and firefighting.

---

* Gas tank caps in modern U.S. and European cars are each equipped with a spring-loaded closure that opens, under extraordinary internal pressure, to exhaust vapor to the atmosphere. Under ordinary conditions, the spring holds the cap closed to the seal. It is understood that cars manufactured before 1965 do not have a pressure release valve built into the gas tank cap.

† Probably not if space were full of shelterees, however. The point is that gas tank hazard is not as severe as intuition might indicate, explosion hazard is nil, and time is available for fire countermeasures or evacuation.

- Automatic sprinkler system required a relatively high temperature at ceiling level to respond, could not extinguish a car interior fire, spread pools of burning gasoline and thus the fire, and caused the immediate smoke hazard just described.

Ventilation assumed major proportions because of the large size of this case study shelter. The ventilation planning and preliminary design work is described in Appendix H and is intended to serve as an illustrative example of such mechanical engineering work applied to full slanting of a building. Use of dual emergency generator rooms (Items 5 and 11, Table 8.4A) was adopted for increased reliability (either of the two 50-kw engine-generator sets could operate all of the ventilation fans at their lower or two-thirds speed, 1200 rpm) and because a fan serving a generator room would be inadequate (when operating at the lower speed) to provide sufficient cooling air for a single generator installation (100 kw). Figures 8-4A.3, 8-4A.4, and 8-4A.5 show the contemplated ventilation vaults, the latter figure including a generator room.

FIG. 8-4A.3
TYPICAL VENTILATION VAULT — WEST WALL

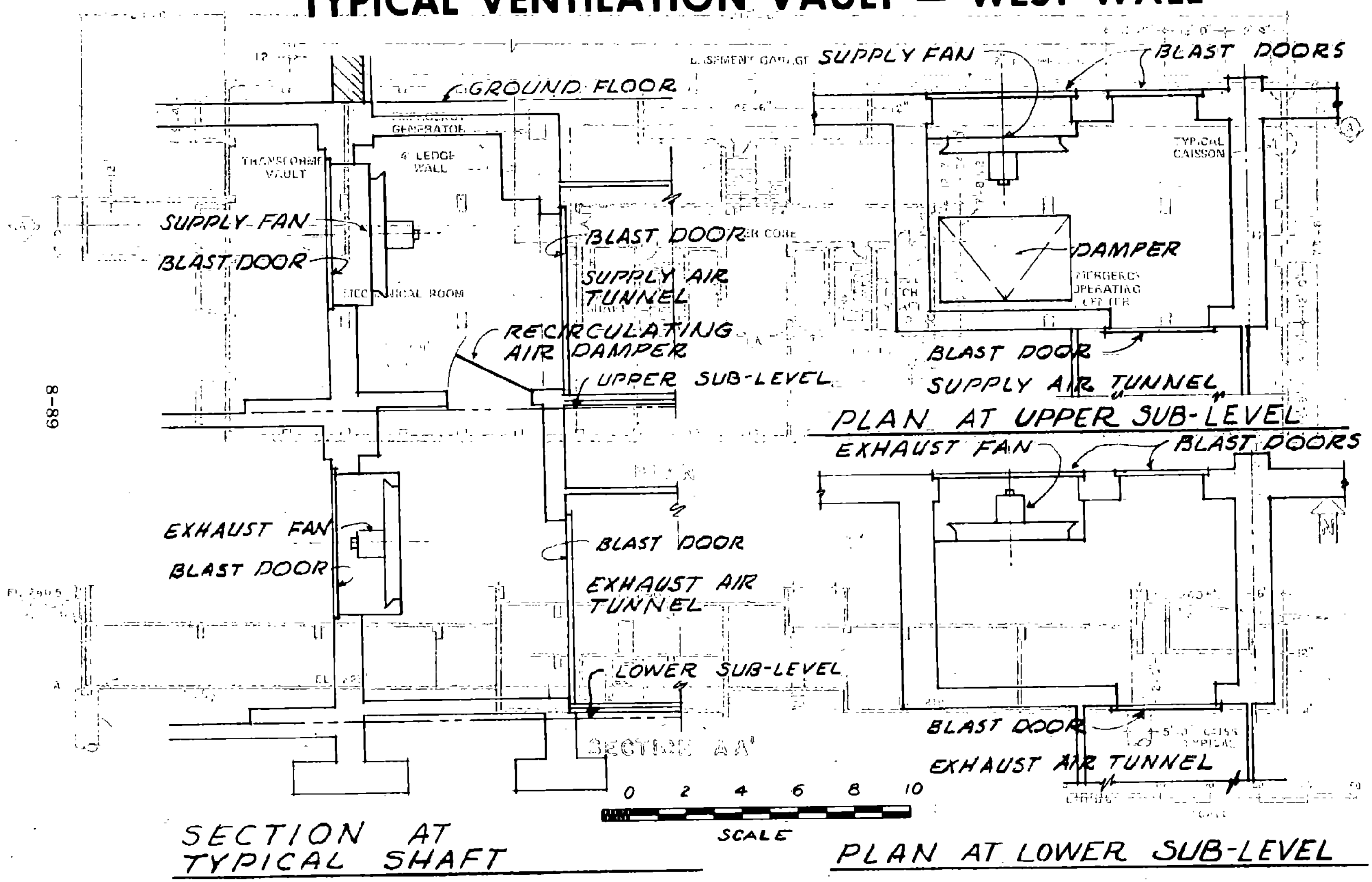

FIG. 8-4A.4
TYPICAL VENTILATION VAULT — EAST WALL

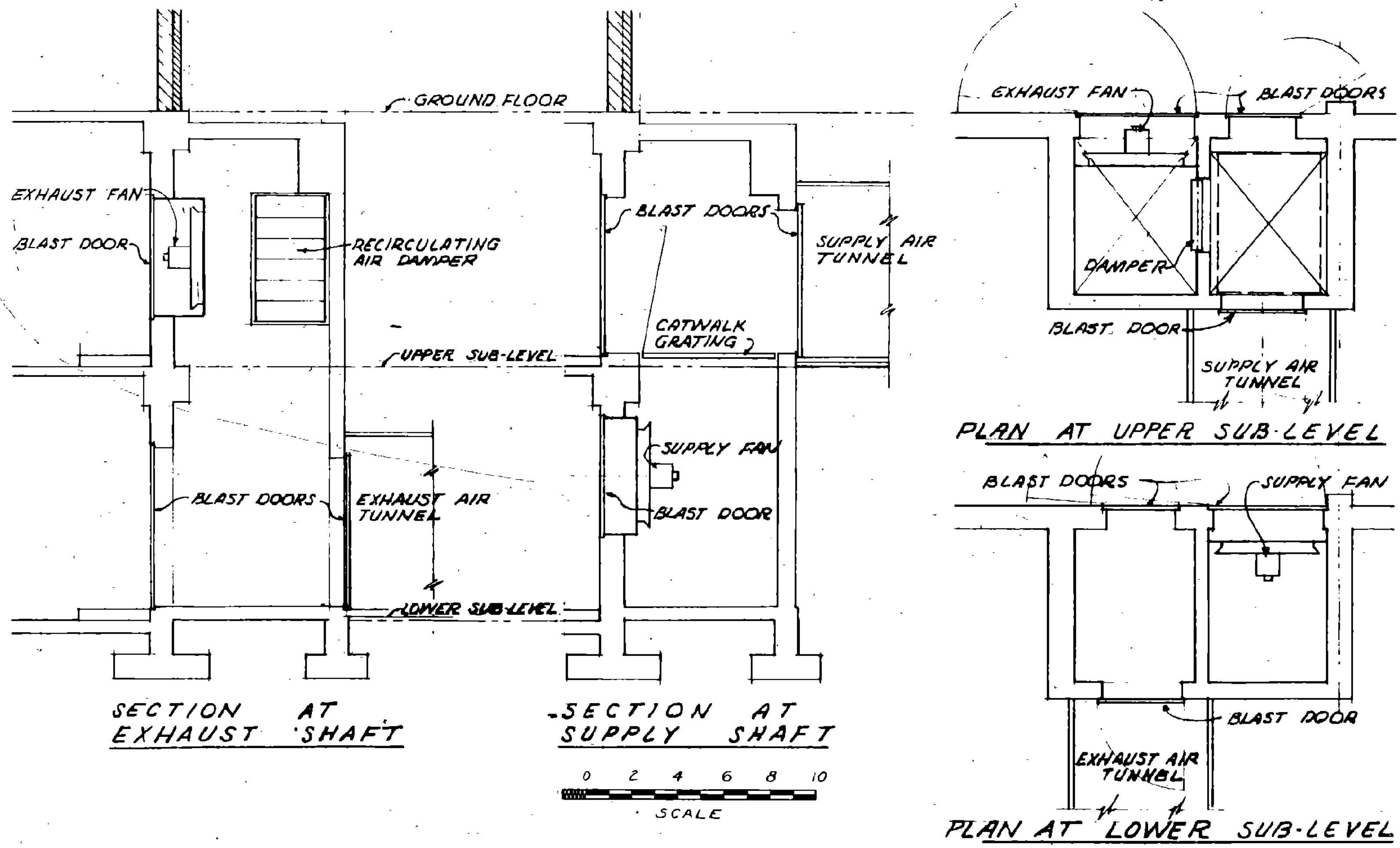

FIG. 8-4A.5

TYPICAL VENTILATION VAULT WITH GENERATOR ROOM

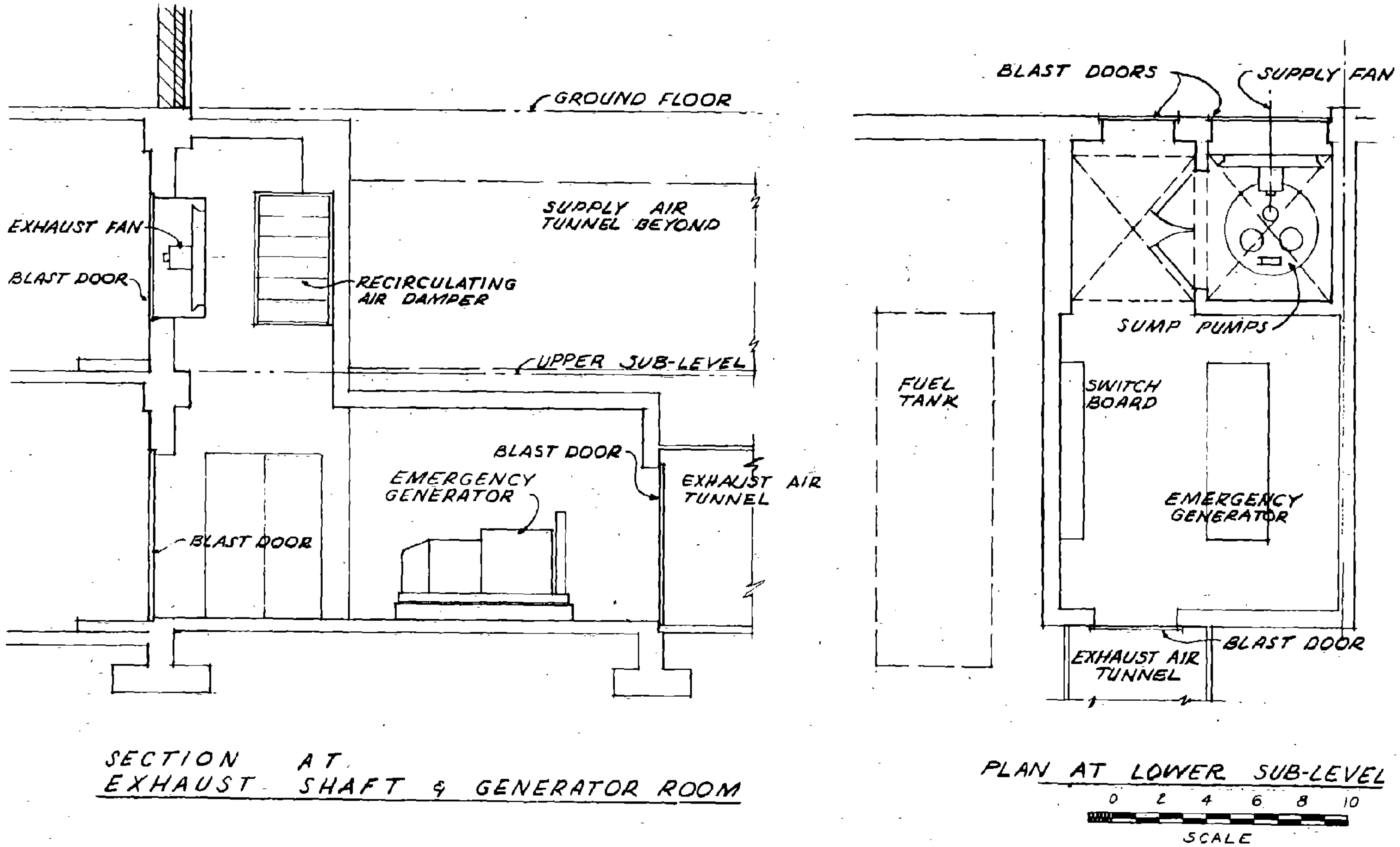

For a review of interior air blast behavior in room filling and jet effects, the general method and theory in Appendix E were used. The work and results are briefly described in the following paragraphs.*

The building was subjected to a hypothetical nuclear blast, and the suitability of its two underground floors as open shelter was evaluated. Peak free-field overpressure was 15 psi, and positive phase duration about 2 sec.† Openings between shelter spaces and the free-field blast environment were assumed to remain free of debris or other obstruction to inflow. As part of the slanting, ramp sidewalls were assumed to have been closed off, at least on the side facing the large parking areas, and the openings from the ventilator wells into the two sub-levels to have been closed. Interior elevator shafts and stairwells were assumed to have been provided with blast doors. The only entries for air blast then would be through the auto ramps.

Detailed results are shown on outline floor plans, Figure 8-4A.6A.‡ In summary, it appears that approximately two-thirds of the upper sub-level area lies outside the more conservatively drawn danger zones and all of the lower sub-level is "safe" except for small areas (not shown in the figure) at the mouths of ramps between sub-levels.

---

* Prepared by a colleague, J. R. Rempel.

† See details below.

‡ Yields of 1 and 10 Mt (1.55 and 3.45 sec. blast duration) are shown, for reasons discussed in footnote of next text page. No estimated hazard areas found on lower sub-level.

FIG. 8-4A.6A

BUILDING 4A AIR BLAST JETS — 15 PSI

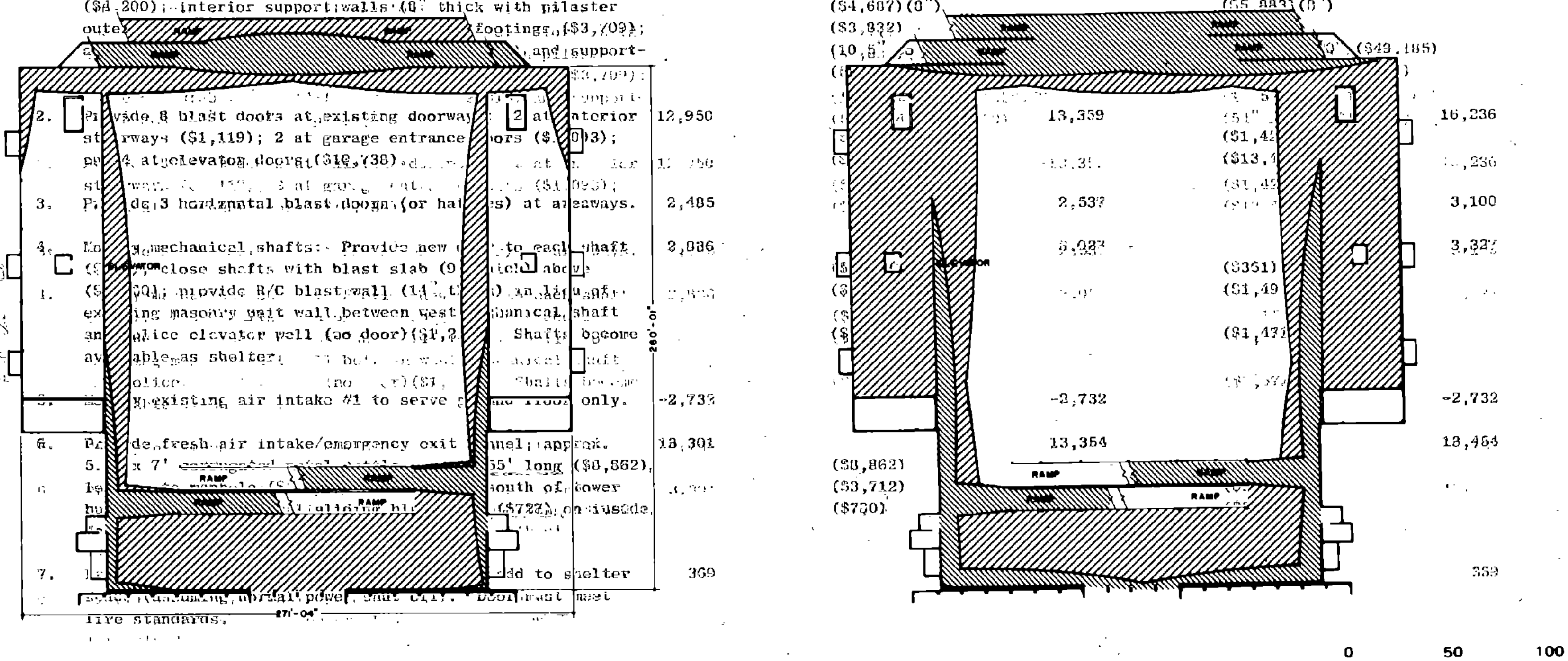

UPPER SUB-LEVEL
(1 Mt)

UPPER SUB-LEVEL
(10 Mt)

LEGEND

20 fps criterion

80 fps criterion

For each opening expected to contribute significant air blast, two areas are outlined. A prone human body located athwart the blast jet within the smaller of the two areas, if not checked or restrained, may be accelerated by the blast wind to 80 fps; within the larger the final speed may be 20 fps. These values correspond approximately to speeds producing death in humans on collision with a massive rigid object: 80 fps for whole body impact, 20 fps for head impact.†

---

† Because of wide individual variability, biological hazard criteria cover a range of values. Available evidence[38, 39] indicates that serious injury or death by head impact against a massive, hard object may occur at a speed between 10 and 20 fps. A few individuals will be seriously hurt or killed when stopped at only 10 fps and some not until a 20 fps speed is reached, but virtually all will experience serious injury or death at some speed within the range. A corresponding hazard range for whole body impact in a direction transverse to the spine (but with head and neck relatively protected) appears to lie near 80 fps but, at the present, data are insufficient to provide a meaningful range. Evidence for these values is presented and discussed in Reference 41. Such values for humans are not precisely known and they may well be subject to some adjustment in the light of further study.

Hazard ranges for impacts against yielding objects and in directions other than transverse to the spine have also been discussed along with some physical evidence in Ref. 41. For example, tolerance to longitudinal impact (in a direction along the spine) appears to lie between 20 and 80 fps; in these cases mortality is probably connected with relatively large displacements of viscera. However, without more detailed analysis of impact parameters, the two limits used in Figure 8-4A.6A are believed to be adequate to suggest the hazard to a prone sliding/rolling body, which will most likely be decelerated by transverse body impact. The results in the figure should be interpreted as showing that the chances of survival in the smaller danger zone (determined by the 80 fps criterion) are slight. However, in the larger danger zone, while some shelterees will be killed by blows to the head, many if not most others will probably survive with nothing worse than broken bones or dislocated joints as they are slammed into walls, pillars, furniture, or each other at speeds between 20 and 80 fps. Outside both zones, even broken bones should be exceptional.

The estimated hazard areas shown in Figure 8-4A.6A are conservative because the following were excluded from the calculations: less dangerous bodily orientations than athwart the blast; sliding friction; any benefit from packing of shelterees; and the possibilities of finding shelter directly under high openings in walls or of a body moving outside the danger area before reaching critical speed. To partly compensate for such conservatism, the upper value of the head impact hazard range, 20 fps, was used in determining the larger hazard areas of Figure 8-4A.6A.

Building 8-4A was also used as an example of a very large open shelter in studies with free-field air blast peak overpressures other than 15 psi, i.e., 5, 10, and 20 psi; the results are described in the next section. This use dictated a need for more estimates of hazard areas, which were made using the same approach as described above for the 15 psi slanting application. Further, the need for blast doors between the two garage levels and each level's 6 elevator and stair wells led to estimates of hazard areas with these 12 blast doors omitted.

Figures 8-4A.6B and C show estimated hazard areas for 20 and 5 psi peak overpressures, respectively, using 10 Mt weapon yield.* While these Figures show no blast doors on the 12 stair and elevator wells, the Figures can be used for study of hazard areas with the 12 blast doors used; the estimated hazard areas from the ramp entrances are about 10% larger when the 12 blast doors are used. Whether the 12 blast doors can or should be omitted, based on the estimated hazard areas shown in the Figures, is a matter of judgment that must in turn consider at least two key matters: the degree of accuracy that can be assigned to the room filling/jet effect calculational method presented by Appendix E; and a conclusion about the discipline of the shelterees in terms of taking carefully spotted locations on each garage level when so instructed.

---

* Positive phase durations of 3.06 and 5.27 psi, respectively, were used; they are for weapon yield of about 10 Mt, as calculated from Brode curves of Figure 2-1. While 1 Mt was used for structural components, they are nearly insensitive to change from 1 to 10 Mt; however, estimated hazard areas, at a single overpressure, vary about as positive phase durations (which in turn vary as cube root of yield). Thus, for 1 Mt positive phase durations, about 1.37 (20 psi) and 2.5 (5 psi) sec., estimated hazard areas would be a little less than half those shown in Figures 8-4A.6B and C (jet lengths would be about two-thirds).

FIG. 8-4A.6B

BUILDING 4A AIR BLAST JETS — 20 PSI

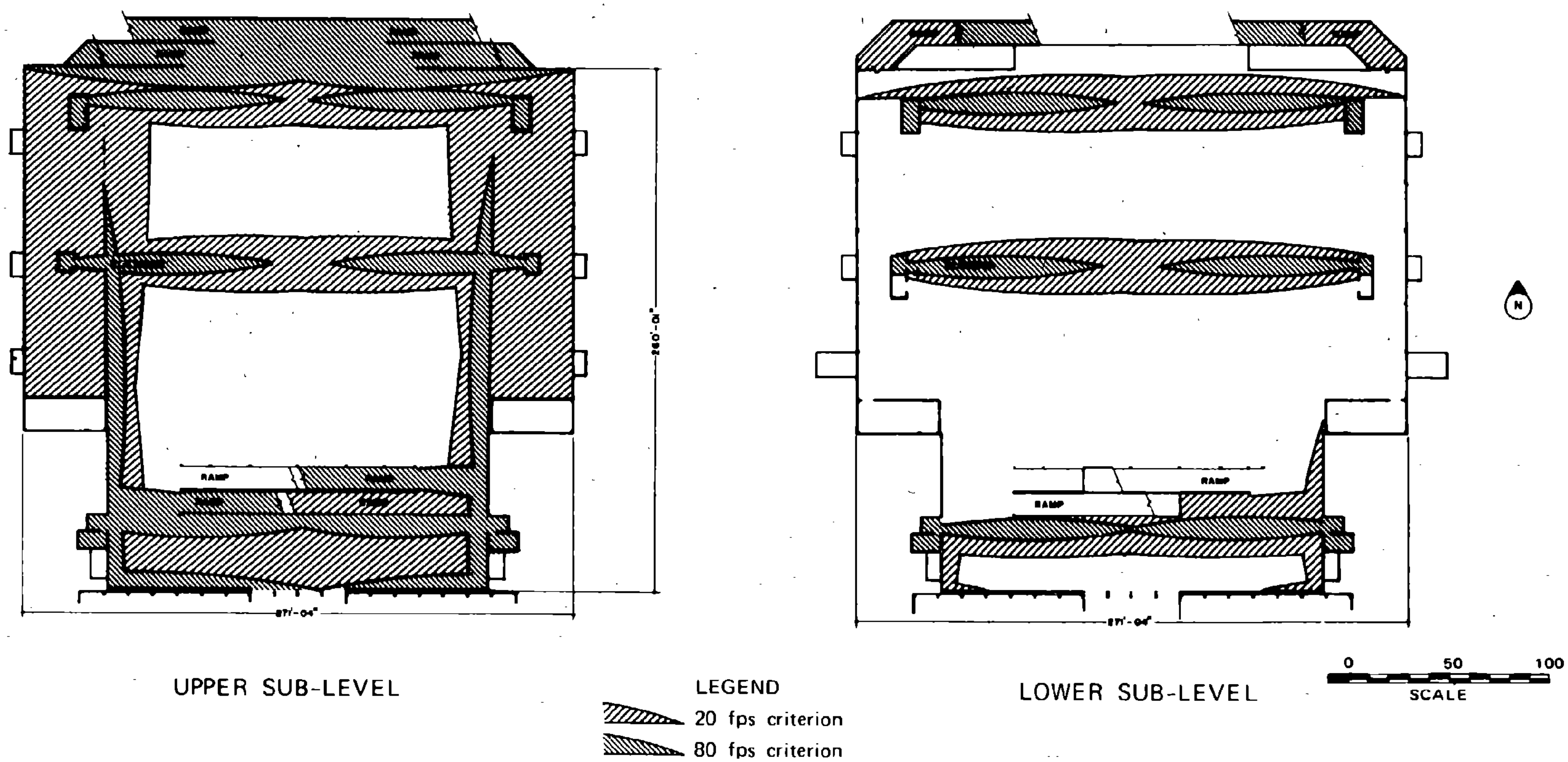

FIG. 8-4A.6C

BUILDING 4A AIR BLAST JETS — 5 PSI

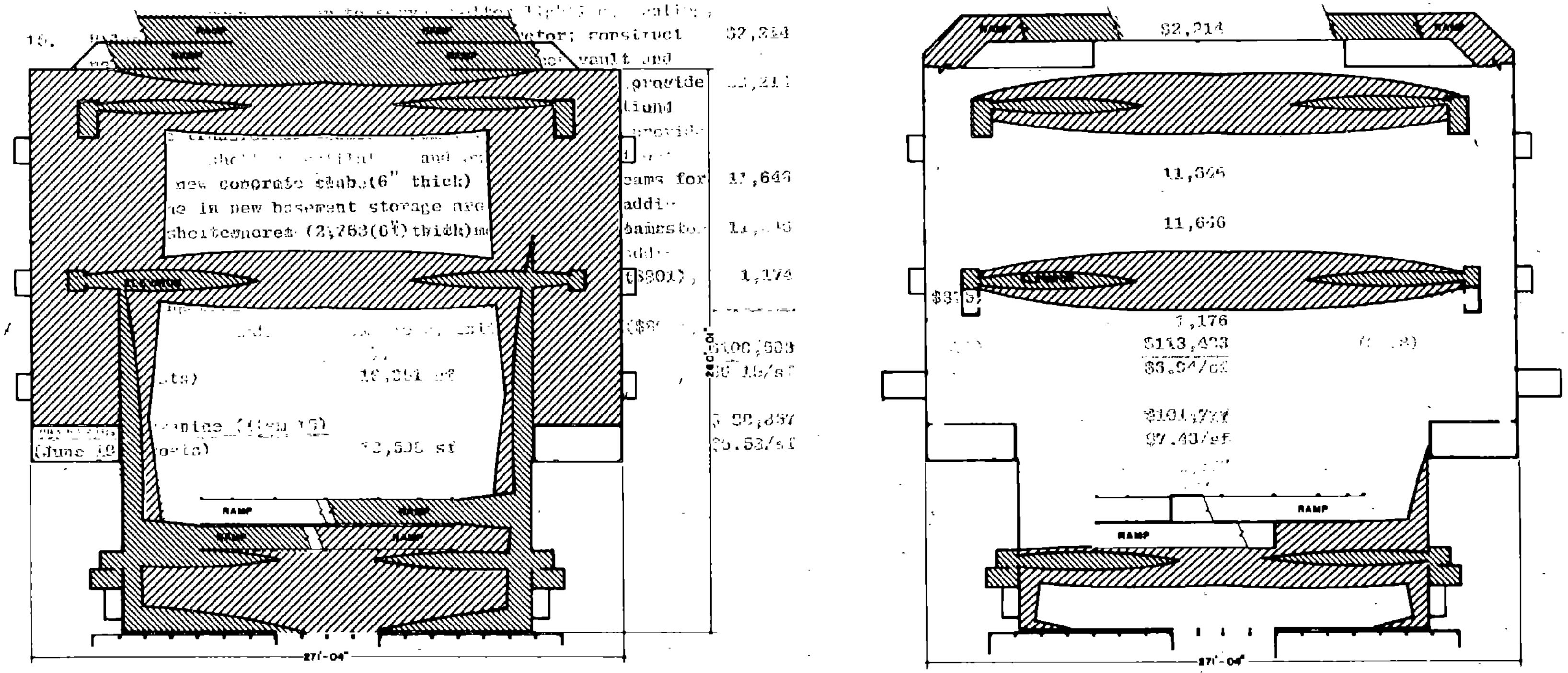

UPPER SUB-LEVEL

LOWER SUB-LEVEL

LEGEND

20 fps criterion

80 fps criterion

0 50 100

SCALE

Slanting Estimated Costs at Peak Overpressures Other Than 15 psi

The study work was extended to cover other peak overpressures than the 15 psi adopted as basic for the original feasibility study (Chapter 1 and other references herein). Two each open and closed shelter example buildings were used: Buildings 2A and 3A for closed, and Buildings 2B and 4A for open. Peak overpressures selected for study, in addition to the original 15 psi, were 5, 10 and 20 psi for the open shelters, and 20 and 30 psi for the closed.

Estimated cost results have been added to each building's estimates table as originally developed for 15 psi; i.e., Tables 8.2A, 8.2B, 8.3A and 8.4A. In addition, cost summary tables, similar to the 15 psi summary table (Table 8.0A), are included herein: Tables 8.0B, 8.0C, 8.0D and 8.0E for peak overpressures of 5, 10, 20 and 30 psi, respectively.

Table 8.0F contains, for each building, at each overpressure, ratios of estimated cost compared to that at 15 psi.

Tentative conclusions might include the following:

- Open shelter estimated slanting costs appear to be more sensitive (or at least equally sensitive) to peak overpressure design changes than those for closed shelters.

- Estimated slanting costs for the larger (open and closed) shelters (Buildings 3A and 4A) were under the Scope limit of $6/sf (4% to 11% below, when all costs are corrected to the same time period) for a design peak overpressure of 20 psi.

Table 8.0B

SUMMARY OF SLANTING COST ESTIMATES (5 psi)

Building:		2B (open portion)		2B closed portion)		2B (total)		4A (open)	
Cost Items		All	Non-deferrable	All	Non-deferrable	All	Non-deferrable	All	Non-deferrable
Shelter area (sf)		2,262		1,116		3,378		130,522	
Estimate		6-70		6-70		6-70		6-70	
A. Structural	$	4,952	4,952	3,979	3,979	8,931	8,931	169,229	169,229
	$/sf	2.19	2.19	3.57	3.57	2.64	2.64	1.30	1.30
	%*	80	81	75	93	77	86	37	38
	%†		*100*		*100*		*100*		*100*
B. Blast doors	$	90	--	1,048	--	1,138	--	22,106	9,418
	$/sf	.04	--	.94	--	.34	--	.17	.07
	%*	1	--	20	--	10	--	5	2
	%†		*0*		*0*		*0*		*43*
C. Ventilation (Incl. emergency exit tunnel, if any)	$	318	318	309	309	627	627	231,023	231,023
	$/sf	.14	.14	.28	.28	.19	.19	1.77	1.77
	%*	5	5	6	7	5	6	50	52
	%†		*100*		*100*		*100*		*100*
D. Other	$	847	847	--	--	847	847	35,697	35,697
	$/sf	.37	.37	--	--	.25	.25	.27	.27
	%*	14	14	--	--	7	8	8	8
	%†		*100*		*0*		*100*		*100*
Total	$	6,207	6,117	5,336	4,288	11,543	10,405	458,055	445,367
	$/sf	2.74	2.70	4.78	3.84	3.42	3.08	3.51	3.41
	%†		*99*		*80*		*90*		*97*
‡ Jan. 68:	$/sf	2.11	2.08	3.68	2.96	2.63	2.37	2.70	2.62
‡ Jun. 73:	$/sf	3.54	3.49	6.17	4.96	4.41	3.97	4.53	4.40
Cost ratio (5 psi/15 psi)	%	42	41	55	50	47	45	58	57

* Percent ratio of item cost to total cost.

† Percent ratio of nondeferrable cost to item (All) cost.

‡ Using Engineering News-Record Building and Construction Cost Indexes (averaged) to convert totals from San Francisco area to EN-R's 20-cities average and from estimate date to date(s) shown.

The data of Table 8.0A* indicate a potential for lower slanting costs in open versus closed shelter, considering total nondeferrable costs (note columns 2 and 1, $5.08 versus $5.78 or a ratio of 83% for open over closed shelter). The data also indicate that about 60% of slanting costs in closed shelters is nondeferrable. Building 2C, open to shelterees but closed to blast, is more comparable to the closed shelters than to the other open shelter, Building 2B. Building 2B slanting costs (column 4) are about 95% nondeferrable as one might expect for an open shelter.

Considering the data for closed shelters plus Building 2C (i.e., omitting Buildings 2B and 4A), nondeferrable work under the structural item amounts to 96% to 99% of the nondeferrable totals, but total work under structural amounts to 57% to 67% of the building totals, blast doors 10% to 19%, and combined structural-blast doors 66% to 85%.

The sparse data indicate that:

- An open shelter (other than Type E such as Building 2C) should probably be considered only for complete work at the time of building construction, because deferrable work may amount to such a small portion of the total work (e.g., 5% in column 5); inflation may reinforce this thinking.

- The results of subsequent work showed that open shelter slanting costs are more sensitive to changes in design overpressure than closed shelter slanting costs. As shelters become smaller in floor area, say below 3000 sf, slanting costs begin to rise markedly.

---

* Holders of earlier versions of this table may note differences among the earlier versions and the version herein. Many new "designs" were required for this report, to cover the range of overpressures and related slanting estimates reported later in this Chapter. Frequently the design approach of the 15 psi shelter studies used for the current Table 8.0A had to be changed from that used earlier, in order to better suit use throughout an overpressure range, i.e., so that the calculation of estimate ratios, say for each overpressure versus a base overpressure, might have better validity. Such 15 psi re-designs, plus simply finding discrepancies in the earlier estimates, generally account for the differences among versions of the table.

Preceding page blank

Table 8.0C SUMMARY OF SLANTING-COST ESTIMATES (10 psi)

Building:		(5) 2C ("open") All	Non-deferable	(6) 3A (closed) with mezzanine All	Non-deferable	(7) 3A (closed) no mezzanine All	Non-deferable	(8) 4A (open) All	Non-deferable
Shelter area (sf)		3,465		13,351		13,598		130,522	
Estimate date		6-70		6-70		6-70		6-70	
A. Structural	$	[illegible]	20,913	68,667	57,220	56,621	55,220	498,824	493,824
	$/sf	[illegible]	6.03	4.14	3.50	4.12	4.06	3.82	3.82
	%*		>99	67	96	63	96	63	64
	%+		100		85		99		100
B. Blast doors	$	[illegible]	---	[illegible]	---	17,265	---	22,738	9,730
	$/sf	[illegible]	---	[illegible]	---	1.27	---	.17	.07
	%*		---	[illegible]	---	19	---	3	1
	%+		0		0				43
C. Ventilation (incl. emergency exit tunnel, if any)	$	[illegible]	99	18,814	-760	13,814	-760	233,565	233,565
	$/sf	[illegible]	.03	.72	-.06	.87	-.06	1.79	1.79
	%*	[illegible]	---	12	-1	13	-1	30	30
	%+		<1		-0		-0		100
D. Other	$	[illegible]	---	3,757	3,043	3,757	3,043	35,697	35,697
	$/sf	[illegible]	---	.28	.19	.28	.22	.27	.27
	%*		---	4	5	4	5	5	5
	%+		0		81		81		100
Total	$	[illegible]	21,012	100,503	59,503	88,857	57,503	790,8[illegible]	777,836
	$/sf	[illegible]	6.06	6.15	3.64	6.53	4.23	6.06	5.96
	%+		62		59		65		98
Cost ratio (10 psi/15 psi)									
‡ Jan. 68:	$/sf	[illegible]	4.66	4.73	2.80	5.03	3.25	4.66	4.58
‡ Jun. 73:	$/sf	[illegible]	7.82	7.93	4.69	8.43	5.45	7.81	7.69

* Percent ratio of item cost to total cost.
\+ Percent ratio of nondeferable cost to item (All) cost.
‡ Using Engineering News-Record Building and Construction Cost Indexes (averaged) to convert totals from San Francisco area to ENR's 20-cities average and from estimate date to date(s) shown.

8-102 BLANK

Table 8.0D

SUMMARY OF SLANTING COST ESTIMATES (20 psi)

Building:		2A (closed)		2B (open portion)		2B (closed portion)		2B (total)		3A (closed) with mezzanine		3A (closed) no mezzanine		4A (open)	
Cost Items		All	Non-deferrable	All	Non-deferrable	All	Non-deferrable	All	Non-deferrable	All	Non-deferrable	All	Non-deferrable	All	Non-deferrable
Shelter area (sf)		3,378		2,252		1,116		3,378		16,351		13,598		130,522	
Estimate date		6-70		6-70		6-70		6-70		6-70		6-70		6-70	
A. Structural	$	17,291	17,291	18,355	18,355	10,480	10,480	28,835	28,835	80,071	69,624	68,425	67,624	645,412	645,412
	$/sf	5.12	5.12	8.15	8.15	9.39	9.39	8.54	8.54	4.90	4.26	5.03	4.97	4.94	4.94
	%*	61	99	92	92	87	97	90	94	71	97	67	97	69	70
	%†		100		100		100		100		87		99		100
B. Blast doors	$	2,563	--	105	--	1,175	--	1,280	--	17,781	--	17,781	--	23,054	9,886
	$/sf	.76	--	.05	--	1.05	--	.38	--	1.09	--	1.31	--	.18	.08
	%*	9	--	1	--	10	--	4	--	16	--	17	--	2	1
	%†		0		0		0		0		0		0		43
C. Ventilation (Incl. emergency exit tunnel, if any)	$	6,270	99	396	396	350	350	746	746	11,814	-760	11,814	-760	234,629	234,629
	$/sf	1.86	.03	.18	.18	.31	.31	.22	.22	.72	-.05	.87	-.06	1.80	1.80
	%*	22	1	2	2	3	3	2	2	10	-1	12	-1	25	25
	%†		2		100		100		100		-6		-6		100
D. Other	$	2,270	--	1,132	1,132	--	--	1,132	1,132	3,757	3,043	3,757	3,043	35,697	35,697
	$/sf	.67	--	.50	.50	--	--	.34	.34	.23	.19	.28	.22	.27	.27
	%*	8	--	6	6	--	--	4	4	3	4	4	4	4	4
	%†		0		100		0		100		81		81		100
Total	$	28,394	17,390	19,988	19,883	12,005	10,830	31,993	30,713	113,423	71,907	101,777	69,907	938,792	925,624
	$/sf	8.41	5.15	8.88	8.83	10.76	9.70	9.47	9.09	6.94	4.40	7.48	5.14	7.19	7.09
	%†		61		99		91		96		63		69		99
‡ Jan. 68:	$/sf	6.46	3.96	6.83	6.79	8.27	7.46	7.28	6.99	5.34	3.38	5.76	3.95	5.53	5.45
‡ Jun. 73:	$/sf	10.84	6.64	11.45	11.39	13.87	12.52	12.21	11.73	8.95	5.67	9.65	6.63	9.28	9.15
Cost ratio (20 psi/15 psi)	%	1.12	1.20	1.34	1.34	1.25	1.27	1.30	1.32	1.13	1.21	1.15	1.22	1.19	1.19

* Percent ratio of item cost to total cost.

† Percent ratio of nondeferrable cost to item (All) cost.

‡ Using Engineering News-Record Building and Construction Cost Indexes (averaged) to convert totals from San Francisco area to EN-R's 20-cities average and from estimate date to date(s) shown.

8-104 BLANK

Table 8.0E

SUMMARY OF SLANTING COST ESTIMATES (30 psi)

Building:		2A (closed)		3A (closed) with mezzanine		3A (closed) no mezzanine	
Cost Items		All	Non-deferrable	All	Non-deferrable	All	Non-deferrable
Shelter area (sf)		3,378		16,351		13,598	
Estimate date		6-70		6-70		6-70	
A. Structural	$	23,424	23,424	102,900	92,453	91,254	90,453
	$/sf	6.93	6.93	6.29	5.65	6.71	6.65
	%*	68	100	74	98	71	98
	%†		*100*		*90*		*99*
B. Blast doors	$	2,728	--	21,324	--	21,324	--
	$/sf	.81	--	1.30	--	1.57	--
	%*	8	--	15	--	17	--
	%†		*0*		*0*		*0*
C. Ventilation (Incl. emergency exit tunnel, if any)	$	6,270	99	11,814	-760	11,814	-760
	$/sf	1.86	.03	.72	-.05	.87	-.06
	%*	18	--	8	-1	9	-1
	%†		*2*		*-6*		*-6*
D. Other	$	2,270	--	3,757	3,043	3,757	3,043
	$/sf	.67	--	.23	.19	.28	.22
	%*	7	--	3	3	3	3
	%†		*0*		*81*		*81*
Total	$	34,692	23,523	139,795	94,736	128,149	92,736
	$/sf	10.27	6.96	8.55	5.79	9.42	6.82
	%†		*68*		*68*		*72*
‡ Jan. 68:	$/sf	7.90	5.36	6.58	4.46	7.25	5.25
‡ Jun. 73:	$/sf	13.25	8.98	11.03	7.47	12.15	8.80
Cost ratio (30 psi/15 psi)	%	1.37	1.63	1.39	1.59	1.44	1.61

* Percent ratio of item cost to total cost.

† Percent ratio of nondeferrable cost to item (All) cost.

‡ Using Engineering News-Record Building and Construction Cost Indexes (averaged) to convert totals from San Francisco area to EN-R's 20-cities average and from estimate date to date(s) shown.

8-106 BLANK

Table 8.0F

SLANTING COST RATIOS - OTHER OVERPRESSURES VS. 15 PSI SHELTERS

BUILDING:	2A Closed		3A w/mezz. Closed		2B Open			4A Open		
AREA, sf:	3,378		16,351		*(total shelter)* *3,378* (open portion only) 2,262			130,522		
OVERPRESSURE:	20	30	20	30	5	10	20	5	10	20
STRUCTURAL	1.20	1.63	1.18	1.52	*0.41* 0.42	*0.72* 0.71	*1.34* 1.37	0.34	0.73	1.29
BLAST DOORS	1.03	1.10	1.03	1.24	*0.92* 0.91	*0.96* 0.96	*1.03* 1.06	0.97	0.99	1.01
VENTILATION	1.00	1.00	1.00	1.00	*0.87* 0.85	*0.93* 0.92	*1.04* 1.05	0.99	1.00	1.00
OTHER	1.00	1.00	1.00	1.00	*0.82* 0.82	*0.92* 0.92	*1.10* 1.10	1.00	1.00	1.00
TOTAL	1.12	1.37	1.13	1.39	*0.47* 0.42	*0.74* 0.73	*1.30* 1.34	0.58	0.83	1.19

NOTE:

PF100 fallout protection generally means an 8.5" to 9.5" cover slab over basement (Table 5.1). In some cases - such as short spans and some of the lower overpressure medium spans - these PF100 thicknesses were controlling.

Support Systems - Beams, Columns and Footings vs. Wall and Wall Footing

Building 2B, a basement shelter offering an open area (2,262 sf) and a closed area (1,116 sf) as described earlier in this Chapter, was subsequently used to briefly compare the slanting costs of two interior support systems: beam, columns and column footings versus wall and wall footing. In this building, the support systems were used on the longitudinal centerline of the shelter, in both open and closed portions. Figure 8-2B shows use of the beam-column system, which in Table 8.2B is Item 2 and the shelter cover slab is Item 5. The interior wall "design" included blast resistance against the very short differential blast loading on its two faces, based on a blast wave incident to a building side parallel to the interior wall and therefore reaching the wall more quickly from openings in the building blastward side than from the leeward side. The following tabulation shows pertinent slanting estimated costs for the two support systems, as applied to Building 2B (15 psi shelter):

	BEAM-COLUMN			WALL		
	Shelter Area			Shelter Area		
	Open	Closed	Total	Open	Closed	Total
Cover slab	$5,195	2,363	7,558 (13.5"th.)	5,475	2,490	7,965 (14.5"th.)
Beam	1,672	867	2,539	-994	-393	-1,387
Columns	488	18	506	-225	-225	-450
Interior wall	-	-	-	3,081	1,285	4,366
Footings	3,157	1,482	4,639	1,185	485	1,670
TOTAL	$10,512	4,730	15,242	8,522	3,642	12,164

(The cover slab cost less in the beam-column than in the wall system, because of a shorter span to the very wide beam than to the wall.) The wall and wall footing system offered a savings of 20 percent compared to the beam, columns and column footings system in this one slanting application.

Blast Door Schemes Used for Estimating

Figure 8-OE shows three blast door schemes used in the case studies of this chapter. Selected details and cost estimates for the three door schemes are shown in Table 8.OG.

Design μ was most often used as 1.3 to 3, but 10 was used for the hinged steel blast doors to close up vents that had no emergency exit function. Designs were not detailed but only complete enough for comparative cost estimating purposes. With blast doors representing as much as about 20% of total slanting cost in a shelter, certainly an early candidate for finished standard designs would be a family of blast doors, should a slanting program be undertaken.

Preventive (not breakdown) maintenance methods would be an absolute requirement for any emergency shelter and components, and the adequacy of such maintenance should be subjected to independent scheduled inspections; this would be particularly applicable to blast doors.

The blast door schemes used were, of course, predicated on manual rather than automatic closing. Manual closing was considered appropriate to the basic nuclear attack and low cost assumptions stated in the Stipulations section of Chapter 1 (first and sixth stipulations). Blast-actuated or other automatic-closing blast doors are generally small, not amenable to the building basement's normal or non-shelter use, and very expensive (say one to two orders of magnitude greater than the doors contemplated herein).

Table 8.0G

BLAST DOORS SCHEMES USED FOR ESTIMATING

Building	Door	Jamb Steel	p_{so}	p_m	q	* Est. $/door	* Est. $/sf
STEEL, GUILLOTINE:							
2A	2'7"x2'7"x1/4" with C3X4.1 stiffeners	PL3/8X2 and PL3/8X3	15	19.5	20.5	44	6.6
2A	3'x3'x1/4" with same	" "	"	"	"	55	6.1
2A	2'7"x2'7"x1/4" with C4X5.4 stiffeners	" "	30	41.5	43.7	50	7.5
2A	3'x3'x1/4" with same	" "	"	"	"	61	6.8
STEEL, HINGED:							
3A	4'3"x8'x1/4" w/C4X5.4 and C5X6.7 stiffeners	L4X3X1/4	15	41.5	44	863	25.4
3A	4'3"x10'x1/4" w/same	"	"	"	"	1,067	25.1
3A	4'3"x8'x1/4" w/C4X5.4 and C6X8.2 stiffeners	"	20	59.5	62.6	879	25.9
3A	4'3"x10'x1/4" w/same	"	"	"	"	1,087	25.6
3A	4'3"x8'x5/16" w/C5X9.0 and C8X11.5 stiffeners	"	30	100.6	105.9	1,052	30.9
3A	4'3"x10'x5/16" w/same	"	"	"	"	1,304	30.7
WOOD (METAL-CLAD), HINGED:							
2A/2B	3'4"x7'3"x3-1/4"	C12X20.7	15	41.5	67.4	747	30.9
2A	" " 4-1/2"	"	30	71	115.4	755	31.2
2B	3'6"x6'11"x3"	C6X8.2	15	30	48.7	584	24.1
†2C	3'10"x6'11"x3-3/4"	C12X20.7	"	41.5	67.4	762	28.7
3A	3'6"x6'11"x2-1/4"	"	"	15	24.4	727	30.0
3A	" " 3-1/2"	"	"	41.5	67.4	735	30.4
3A	" " 3"	2 L6X4X1/2	30	30	48.7	880	36.4
3A	" " 4-1/2"	"	"	100.6	120.4	894	36.9

* June 1970 costs, San Francisco area; use multiple of about 1.29 to June 1973, ENR 20-cities.

† Sliding doors

Notation on structural shapes follows (approximately) AISC Manual of Steel Construction 7th ed., p. 1-10; e.g., C4X5.4 is 4" channel @5.4 plf, PL 3/8X2 is plate 3/8" thick by 2" wide.

Baffle Walls and Blast Drag Pressures (Jet Effect)

Appendix E provides calculational methods for predicting average air blast pressure rise versus time in a shelter space (room filling), as well as drag (wind) pressures for various locations within the shelter (jet effect). The final section of Appendix E describes the use of an interactive (conversational) computer program and includes a listing of the FORTRAN program.

Because of the jet effect hazard to humans, moved directly or by being hit by flying objects, an investigation was made to determine the potential of baffle walls for reducing the jet effect, as well as the usual purpose of turning its direction.

Briefly stated, baffle walls were found to offer only the possibility of flow diversion in shelter from megaton weapons, rather than reduction of the intrinsic hazard within the jet itself. Friction in any reasonable number of turns was found to be too small to be of any consequence. The study ignored the initial shock wave, which is very weak, thus considering (in many short increments of time) only the quasi-steady drag pressures; a discussion of this matter is included in Appendix E. Use of baffles to concentrate hazardous jets within a part of the shelter space should be considered.

After a series of measurements of dynamic pressure in model rooms exposed in a shock tube to overpressures in the range of 5 to 20 psi, Coulter* concluded that a baffle inside the entrance significantly reduced the dynamic pressure in the jet entering the room, although the baffle had no significant effect on the filling time of the room regardless of where in the room the filling time was observed. The mechanism of this reduction in dynamic pressure may be a slight delay in the formation of the jet into the room. It has not been shown that a significant reduction in dynamic pressure would appear in a full size room struck by air blast from a megaton weapon.† In any case, baffles may be valuable in diverting flow from occupied areas.

* Ref. 21 of Appendix E.

† See a discussion of baffles in Section IIC2 of Appendix E.

Room Filling Maximum Interior Pressure

Interest in shelter interior pressure buildup through room filling from a nuclear air blast wave - as it might occur in large spaces, such as caverns or mines, with few or many openings at various angles of incidence to the blast wave - led to the running of several solutions using the computer program shown in the last section of Appendix E.

Two values of free-field blast overpressure were assumed 10 and 20 psi,* and the ratio of total shelter volume (V, cf) to the sum of the area of all apertures/openings (A, sf) was used. Calculations were made for the limits represented by all openings being either hit side-on by the air blast, or hit by a fully reflected wave as if in the front wall of a block-house structure.

When the value of a graph showing all solutions became apparent, sufficient calculations were made to cover the range of V/A from 10 ft to 10^6 ft, and for both side-on and fully reflected angles of blast wave incidence. The results are shown by Figure 8-0F for maximum interior overpressure and by Figure 8-0G for time (seconds) to reach such maximum pressure.

The curves of Figure 8-0F are drawn to two scales of maximum interior pressure, with arrows to indicate which scale applies to each group of curves. In the V/A range of values from 10^3 to 10^4 there are curve groups for both scales. For example, when V/A equals 10^3 a maximum interior pressure value of 7.4 psi may be read on the left side scale for a free-field overpressure of 10 psi (side-on); using the similar curve from the upper group of curves, and reading on the right side scale, the value is 7.45 psi.

* Duration of positive pressure values were based on 5 Mt yield.

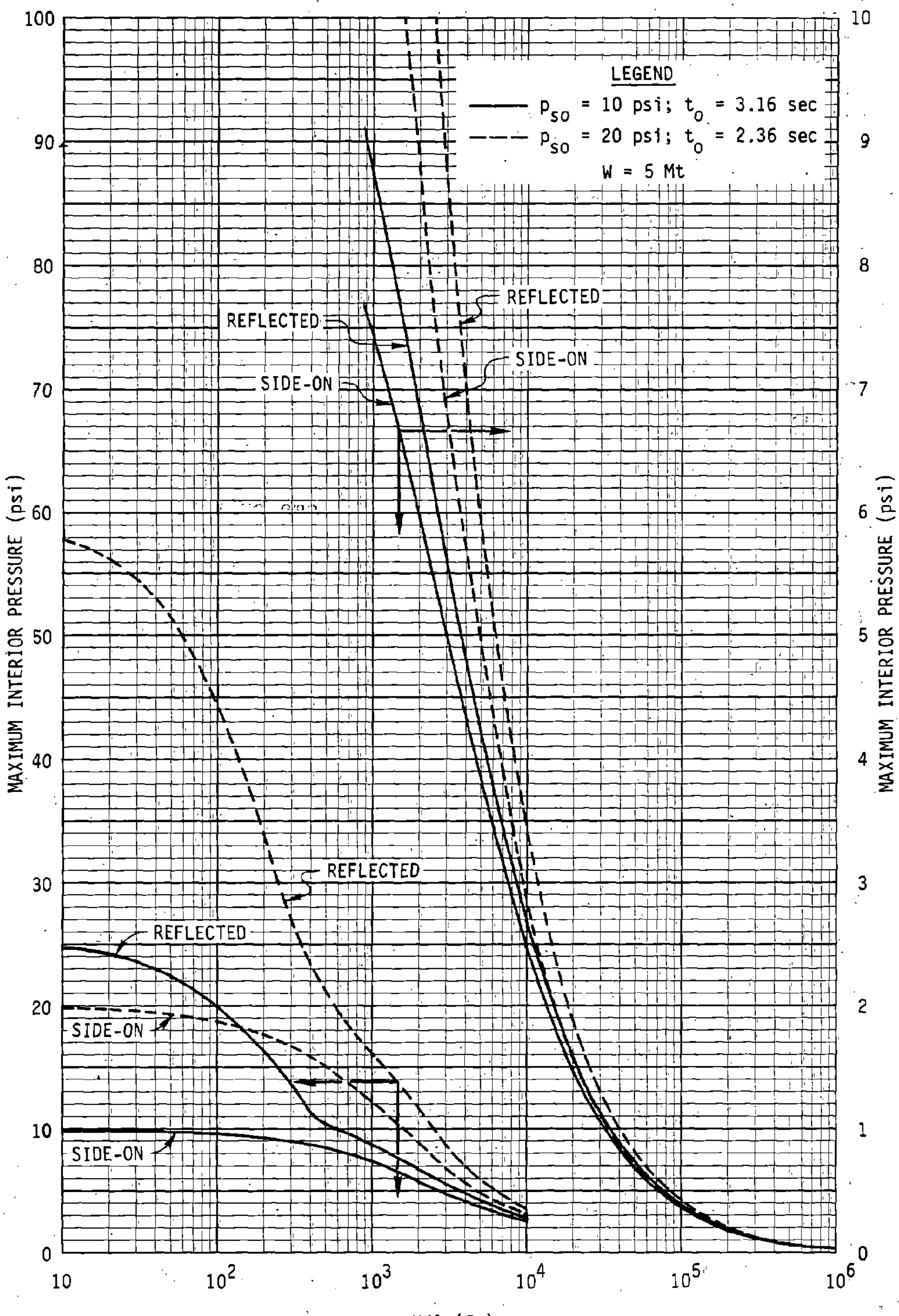

FIG. 8-0F MAXIMUM INTERIOR PRESSURE VERSUS V/A (ROOM VOLUME/TOTAL APERTURE AREA)

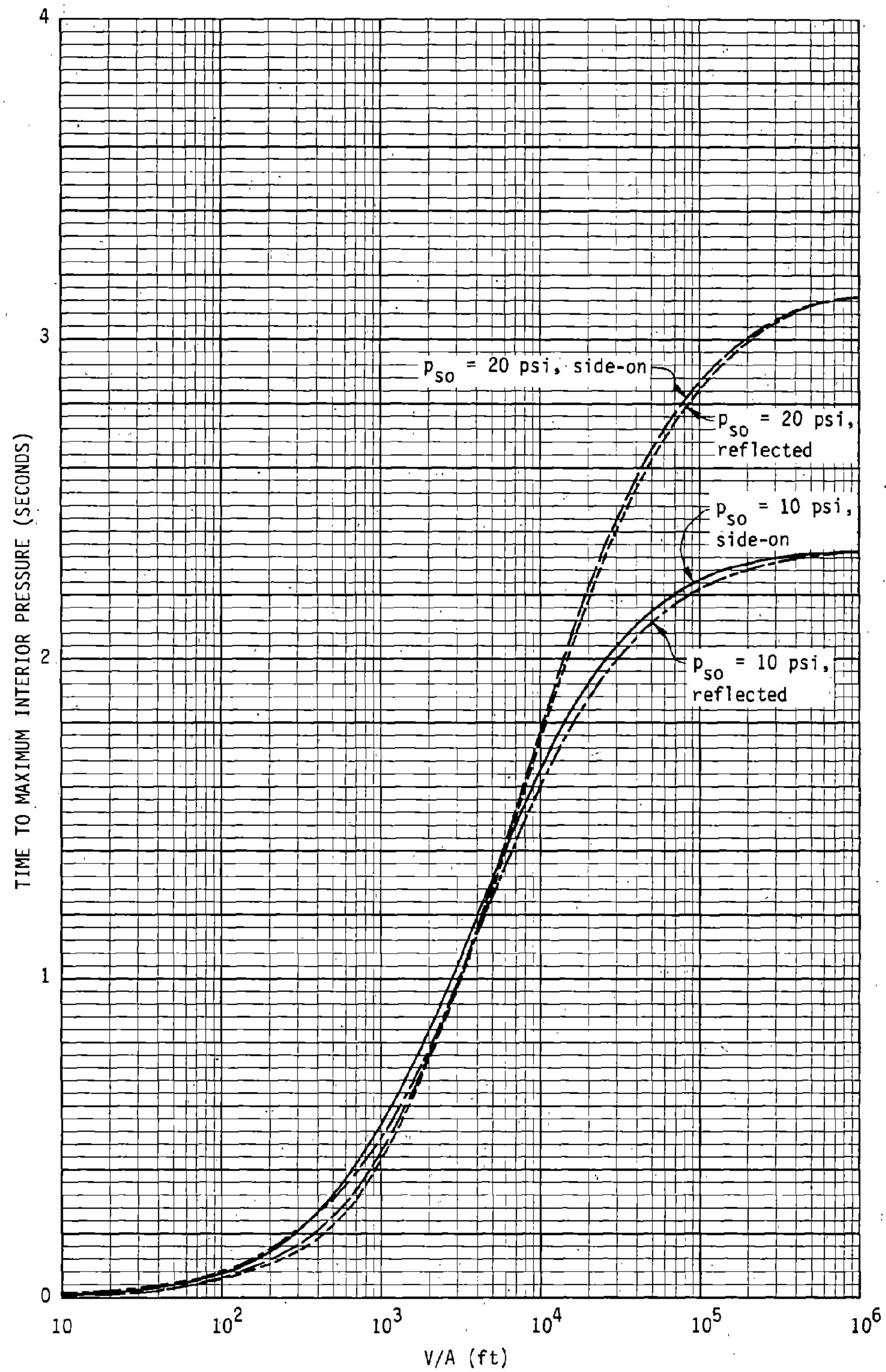

FIG. 8-0G TIME TO MAXIMUM INTERIOR PRESSURE VERSUS V/A (ROOM VOLUME/ TOTAL APERTURE AREA)

Chapter 9

EMP CONSIDERATIONS

EMP or electromagnetic pulse is a nuclear detonation hazard capable of causing significant equipment damage if the height of burst is outside the earth's atmosphere, in other words a high-altitude burst. Such a burst also causes radio blackout over a tremendous area and added thermal radiation hazards. The standard reference on nuclear weapons effects gives a brief description of EMP in its chapter on radio and radar effects, and no hint as to its damaging effects; this in its 1962 edition.[1] (Earlier editions, 1950 and 1957, include no mention of EMP.)

In terms of the electromagnetic radiation spectrum: EMP (electric power through radar), covers a frequency range from 0 to 10^{11} Hz or cps; thermal radiation (through ultra violet) from 10^{11} to 10^{16}+; and initial nuclear radiation (gamma and X-rays) from 10^{16}+ to 10^{21}.

So-called "lightning arrestors" and devices such as spark gaps that are suitable for lightning protection may permit large EMP-induced overvoltages to pass, because the EMP peak is reached much more rapidly, even though lasting a shorter time, than a lightning peak.

Protective measures against EMP must be specifically devised and are necessary to protect equipment and personnel in a manner similar to that for a lightning hazard but more severe.

Effort limitations under the research project supporting the work reported herein precluded more discussion than is presented here all too briefly. Some excellent references are available, however, the first being one intended for use by the emergency planner and operator, whereas the others are more technical and intended for the engineer and communications specialist.[75-78]

A recent technical article briefly describes the design of a major structure to resist nuclear weapons effects, including NEMP; the senior author has an outstanding reputation and many years of work in this design field.[79]

Chapter 10

SUMMARY OF SLANTING TECHNIQUES

One purpose of the case studies, or examples, of the application of full slanting to actual buildings in their early design stage, other than to determine cost and other feasibility factors, is to draw conclusions or learn lessons that may be applied to selection of such buildings for application of combined effects slanting. The results of the first seven case studies[61] seem to point up the following conclusions, generalities, or lessons:

- Blast and secondary fire present much greater hazards than those from initial nuclear and thermal radiation and from fallout.* Thus good building separation and design fire countermeasures (Chapter 3) are very important protective measures, both to inhibit the starting of fires in the shelter building and to facilitate fire evacuation should it become necessary.

- Slanting costs become quite high if full slanting is applied to only part of a basement, in contrast to application to a whole basement. This is demonstrated by: (1) Buildings 1A and 1B and the costs for the latter, amounting to about twice the $6/sf goal (Table 8.1B); and (2) costs encountered in "open shelter" slanting of the separating wall between the large shelter space and a closed blast-resistant storage/equipment room, as in Buildings 2B and 4A (costs in Tables 8.0A, 8.2B, and 8.4A).

---

* Should kiloton-range weapons be stipulated for planning, instead of or in addition to megaton-range, the initial radiation hazard could become extremely important (Chapter 2).

- Full slanting adaptability is considerably enhanced, and slanting costs reduced, if the architects' and engineers' early or conceptual thinking includes slanting potential, because of their training and inclinations. (An obvious example is that of an air-conditioning system, wherein the "four-pipe, local fan-coil units" system is unique in its advantages for full slanting use; this matter is discussed in the Chapter 6 section on "Ventilation and Air Conditioning.")

- Blast slabs, columns or interior supporting walls, and footings (to a lesser extent) represent the major full slanting cost items, especially if normal use of the basement requires long spans (as in a parking garage). In Table 8.0A, costs for the "Structural" category versus three other categories show the former to amount to 57% to 67% of total slanting costs.* The significant magnitude of slab/columns/footings costs is shown by each building's slanting items/costs table (Tables 8.1B, 8.2A/B/C, 8.3A, and 8.4A).

- Multiple-level basements offer lower slanting costs than single-level, because only one blast-resistant floor slab is required (even in open shelters if Building 4A is typical; the slab between the two shelter floors apparently merited a differential blast loading, either way, of no more than 2 psi (Table 8.4A, paragraph 3)).

- Ventilation/emergency exit tunnels and areaways (Figure 8-0A/B/C/D) are significant cost items for both open and closed shelters, especially in the larger ones. However, excluding the tunnels/areaways, the remaining parts of the ventilation systems with emergency generators are not major cost items in larger shelters.

- Open shelters tend to cost about the same as closed,† and fewer basements have normal uses that are adaptable to open shelter - it may be expensive or infeasible to make installed equipment blast-resistant. Potential flying objects in certain building types inhibit open shelter use, e.g., as in retail stores.

- Shelters with large areas cost less per unit area than smaller ones, as might be expected, assuming that clear spans are similar.‡

---

* For open or closed shelters, except Building 2B at 88% with about 1/3 closed and 2/3 open shelter.

† Table 8.0A

‡ In Table 8.0A, compare Buildings 2B with 3A and 4A.

● Nondeferrable full slanting costs (for items that must be included at the time the building is built) are lower for closed than for open shelter.*

● Selection of tensile steel ratio p for the shelter's blast-resistant slab (Figures 6-3, 6-6 and 6-7) has story height (e.g., excavation and wall costs) and slab dead load implications, as well as slab direct cost implications. For the latter alone, the thicker slabs (more concrete, less rebars) cost less, based on June 1970 cost factors (about 9¢/sf/in. thickness for varying the concrete thickness over a rather small range, and about 17¢/lb. for varying the total steel similarly).†

Two comments on the preliminary design work for the case studies[61] may be significant to users of the studies:

a. Generally, the original design's basement story height was retained in the full slanting, meaning that most supporting beams were wide or "over-square." More consideration could well be given to this matter in any actual applications of full slanting; e.g., deeper beams would cost less, but would mean an increase in story height - wider or "over-square" beams cost more, but decrease the span and cost of their supported slabs (which may need to be thicker, though, for radiation protection!).

b. In-plane forces in the cover slab were ignored, even though such consideration would add resistance capacity until a deflection of about half the slab thickness is reached. Considerations in ignoring the in-plane forces were that: (1) soil-rock layer conditions could easily be such that the peak blast (lateral) loads on the slab and the in-plane loads (from airslap or outrunning or other blast-induced ground motion) could arrive at different times; and (2) the approach to steel detailing at the juncture of the cover slab and basement outside walls was to ensure only that the two members were kept in working contact, that is, no moment continuity and some joint cracking, probably just into the wall from the juncture.

---

* In Table 8.0A, compare columns 1 versus 4 and 5, and columns 6 and 7 versus 8.

† For example: the design charts, Figures 6-3, 6-6 and 6-7, are in pairs, the first chart of each pair having the design values and the second the concrete and steel quantities for cost estimating purposes. If the latter charts are used in connection with, say, slabs designed for the same conditions but with one using 2% tension steel and the other 1%, the latter will have more concrete (thickness) and less steel (total weight); the cost <u>difference</u> between the 2% and 1% slabs may be roughly estimated using the 9¢ and 17¢ values mentioned above (corrected from June 1970, of course).

Where a preliminary engineering study of incorporating full slanting in a basement in a new structure is needed, such as for a budget line item, the following outlined steps may be useful:

1. Select a design overpressure level, perhaps also deciding whether to assume the yield is megaton-range or, say, up to 200-300 kilotons (see section so entitled, Chapter 6, which chapter may well be worth a quick review from its beginning up to the section on Typical Designs).

2. Review other weapons effects related to the selected design overpressure (Chapter 2[(50)]).

3. Select a trial support plan for a basement cover slab (solid one-way), with either permanent supports or including crisis-implemented supports.

4. Select a trial basement cover slab, using the charts in the Typical Designs section (Chapter 6) for a solid one-way slab(s) meeting the span and support conditions - recall that going from 2% tensile rebars toward about 1% seems to be less expensive and provides less steel but more concrete, which may be needed for fallout and initial nuclear radiation effects. Check also for concrete thickness fallout protection benefits in Table 5.1[(50)].

5. Use the slab design charts to also obtain approximate rebar and concrete quantities, then make a preliminary cost estimate for the cover slab.

6. If building is multistory, columns/supporting walls/footings may need little added strengthening due to slanting; e.g., planned exterior basement walls reviewed in case studies (Chapter 8[(61)]) invariably needed only some additional steel for 15 psi protection. If building is not multistory, tables[67] are useful for preliminary trials, by multiplying their tabulated load capacity (columns) by 1.7, for use against the loading from the design overpressure.

7. Footings may be similarly handled, again using tables[67] and multiplying tabulated load capacity by 1.5, for use against column/wall overpressure loads (for overpressures of about 15 psi or more, dead loads may be either ignored or very roughly added to blast loads, which are discussed early in Chapter 6). For estimating dynamic soil bearing pressure, see opening paragraph of Section F, Chapter 6.

8. Prepare current preliminary construction cost estimates for the trial structural system above, then refer to data and tables of Chapter 8,(61) especially Tables 8.0A through F, to extend the rough estimate of "Structural" category costs to an estimate of total slanting cost on a unit basis ($/sf), by using the ratios/percentages shown in the tables. Select buildings in the tables that are comparable in total shelter area to the planned shelter. Further estimate refinements may be made by going into other cost categories, e.g., ventilation/emergency exit costs.

[Chapter 11]

FURTHER WORK

As explained in the Preface, this interim report has as one of its purposes the establishment of a framework within which further work may be accomplished. There are some indications of planned work items by statements spread throughout the report and enclosed in brackets (footnote, page 1-5), also by Bibliography annotations. Other work items for consideration include:

- Study additional case buildings and apply full slanting, both open and closed shelter concepts. Implicit in this item is the need for keeping Appendix E current with the state of the art and adding selected available data on human tolerances.

- Make some rough cost analyses of categories of slanting items in case study buildings for variation of costs: with shelter size (a bare start has been made in Chapter 8); between closed and open shelters; of selected structural elements with design peak air blast overpressure (e.g., 10, 15 and 20 psi) and of potential cost-effectiveness.

- Complete all case studies in terms of analysis for resistance to each of the nuclear weapons direct effects, both in original design and full slanted design.* For blast, apply the results of OCD Work Unit 1126C (Existing Structures Evaluation) to obtain resistance values of wall elements for comparison with design resistance values.

- Use the general approach stated in Chapter 10 to reduce full slanting costs, with emergency ventilation design subjected to particular attention.

- Study possible expedient measures to be taken by shelterees to improve radiation shielding around entranceways, in lieu of added structural shielding, particularly for low probability weapon burst orientations.

---

* Such analysis could lead to revision of slab design thinking from using solid slabs (for radiation protection) to using other slabs (waffle, T-beam, tin-pan, etc.).

- Predesign additional repeatedly used shelter structural components, such as flat steel blast doors, and walls and slabs for various spans and support conditions, and prepare appropriate tables and graphs, both to reduce guide case study work and to make full slanting easier for application by the guide user, the practicing architect or engineer.

- Make a limited parametric study aimed at cost reduction and ascertaining cost significance, using the predesigned structural elements described in the preceding item, for example, the cost of a reinforced concrete flat slab versus various spans, support conditions, steel ratios, ultimate concrete strengths, etc.

- Check the full slanting design approach (Chapter 6) for shelter columns, in terms of adequacy when combined (moment and direct stress) loadings from columns carried through from the shelter into upper floors are considered, checking on through failure of the upper story portions of the column.

- Review the full slanting design approach (Chapter 6) for slabs over basements and for basement walls, checking for undue conservatism,* particularly considering OCD research under way at the U.S. Army Engineer Waterways Experiment Station, Vicksburg, Mississippi, and elsewhere.

- Check the full slanting door design approach (Chapter 6) for adequacy in terms of a hazard reportedly noted by Norwegian researchers, that of corners of blastward-opening doors raising and admitting the blast wave into a closed shelter.

- Review the full slanting design approach (Chapter 6) to shear problems in reinforced concrete against the latest proposed ACI code[4] revisions and work by a project consultant, Dr. M. A. Sozen.

---

* Whether the design approach is unduly conservative is perhaps a matter of viewpoint. A building owner buying 15 psi blast overpressure protection expects a high probability, say 99%, of survival at that design overpressure, whereas area survival studies requiring overall or general statistics would need overpressure values related to additional blast survival probabilities, say 50% and 5%. Nonetheless, there are strong indications that the design approach (Chapter 6) may be modified, in view of recent research results, to be less conservative and still provide a high survival probability. Note the second item of this chapter and the discussion on pages 6-2 and -3.

Figure 6-1

CHART SOLUTIONS OF SINGLE-DEGREE-OF-FREEDOM DYNAMIC SYSTEMS[20]

Charts reproduced, without change, from Reference indicated.

Figure 6-1 (continued)

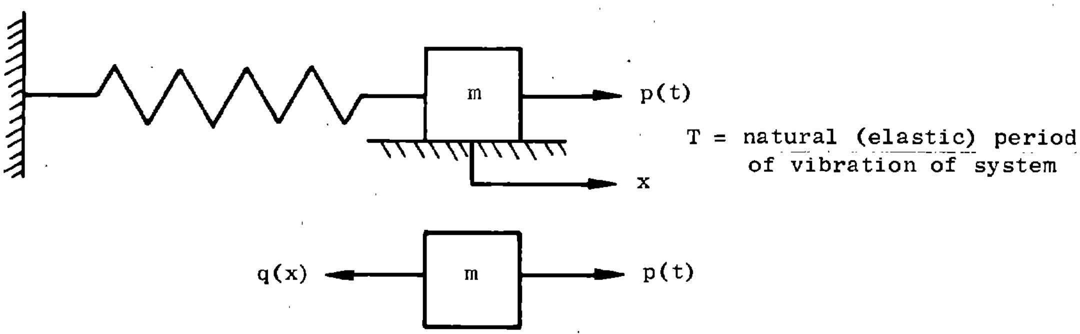

Single Degree of Freedom System

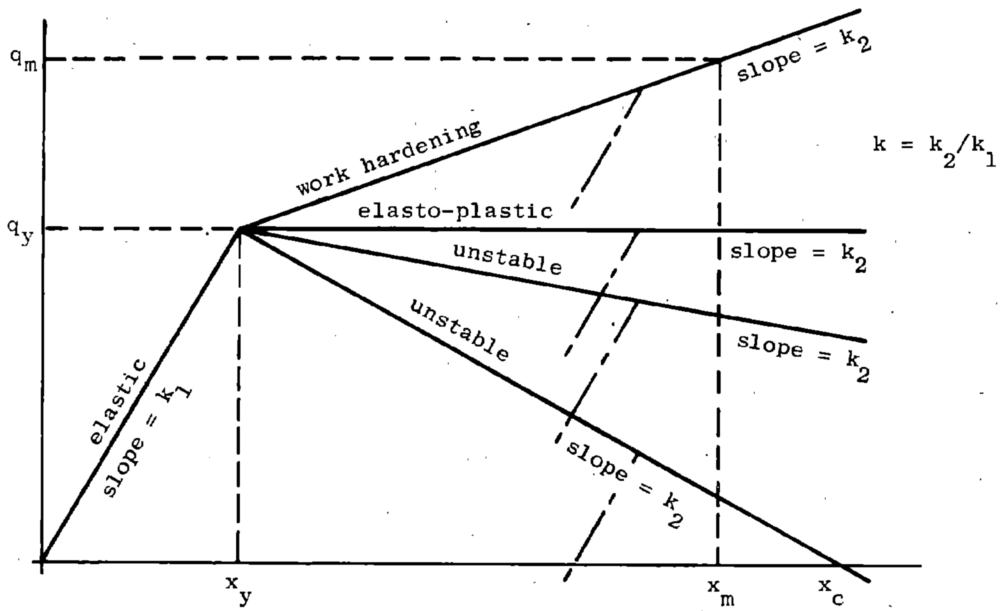

Bilinear Force-Displacement Function

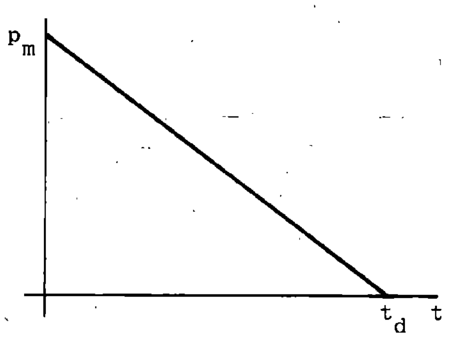

Initial Peak Triangular Pulse

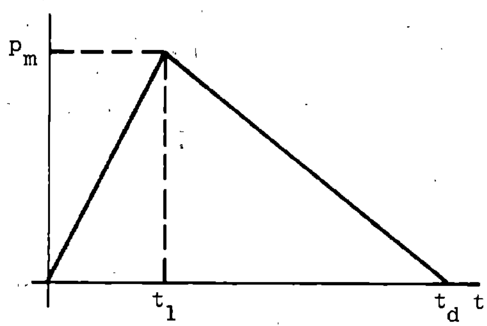

General Triangular Pulse

Figure 6.1 (continued)

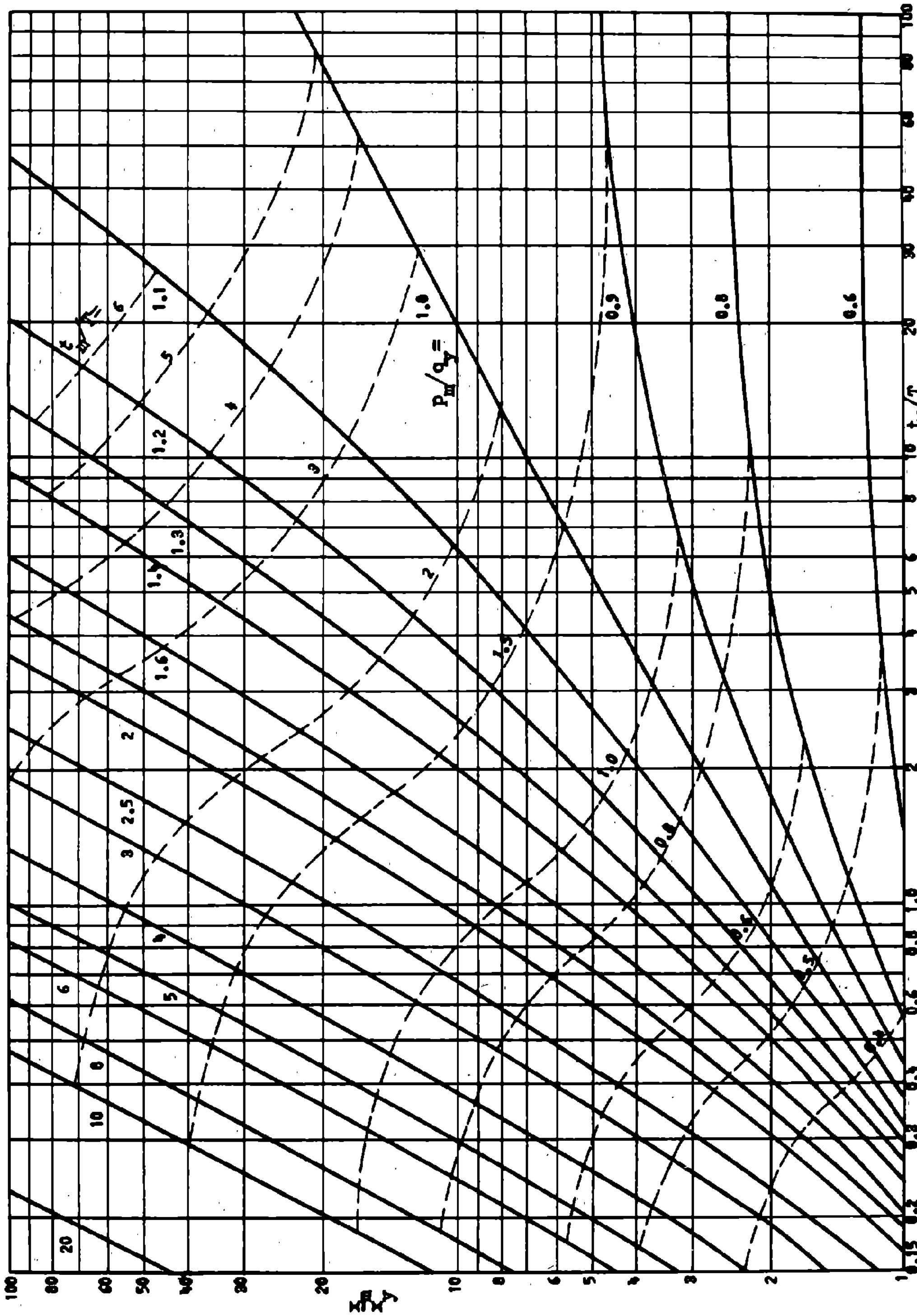

Fig. 4a. Maximum Response of Mass-Spring System to Initial-Peak Triangular Pulse; k=0, t_1/T=0

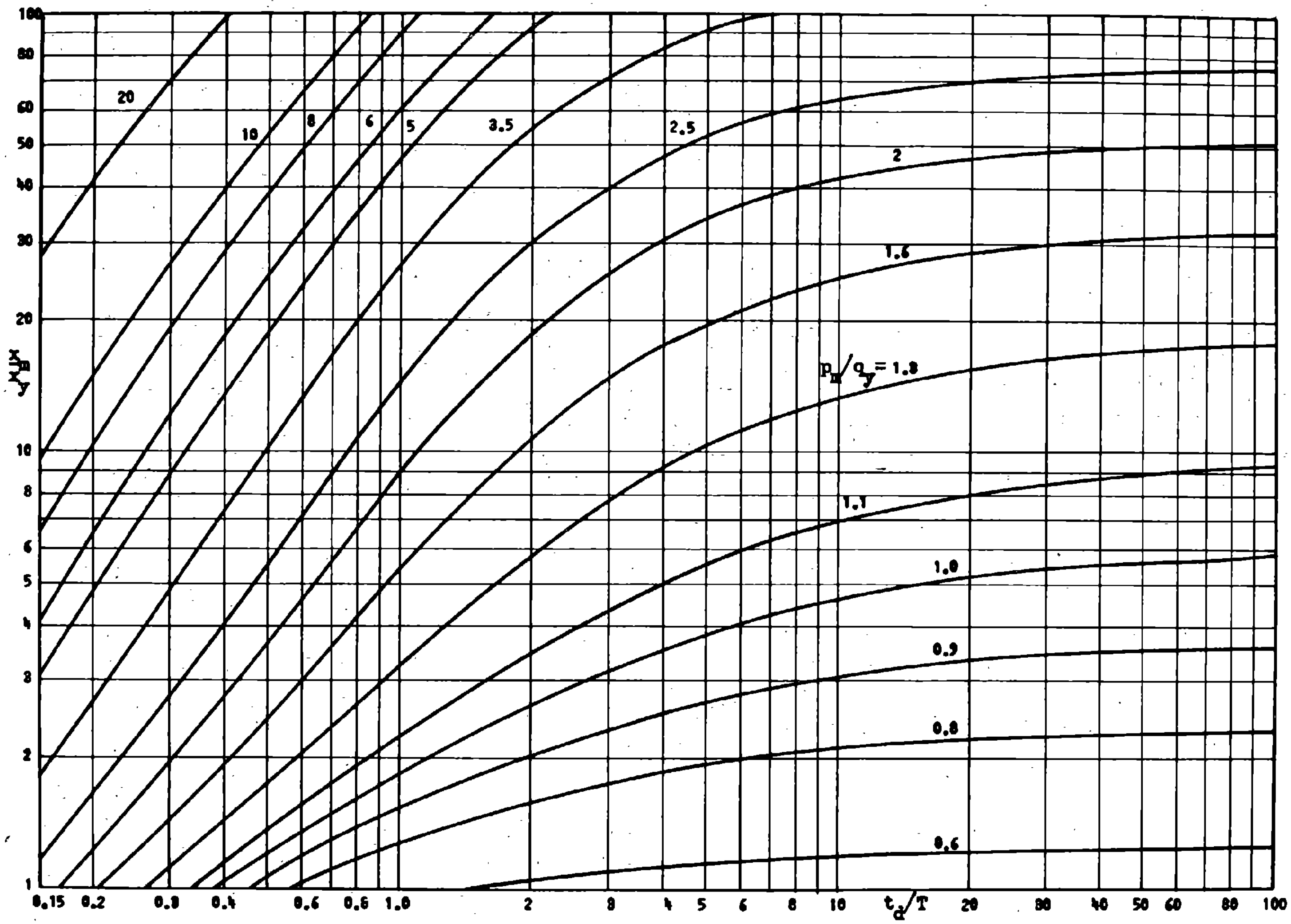

Fig. 4b. Maximum Response of Mass-Spring System to Initial-Peak Triangular Pulse; k=0.04, $t_1/T=0$

Figure 6-1 (continued)

Figure 6-1 (continued)

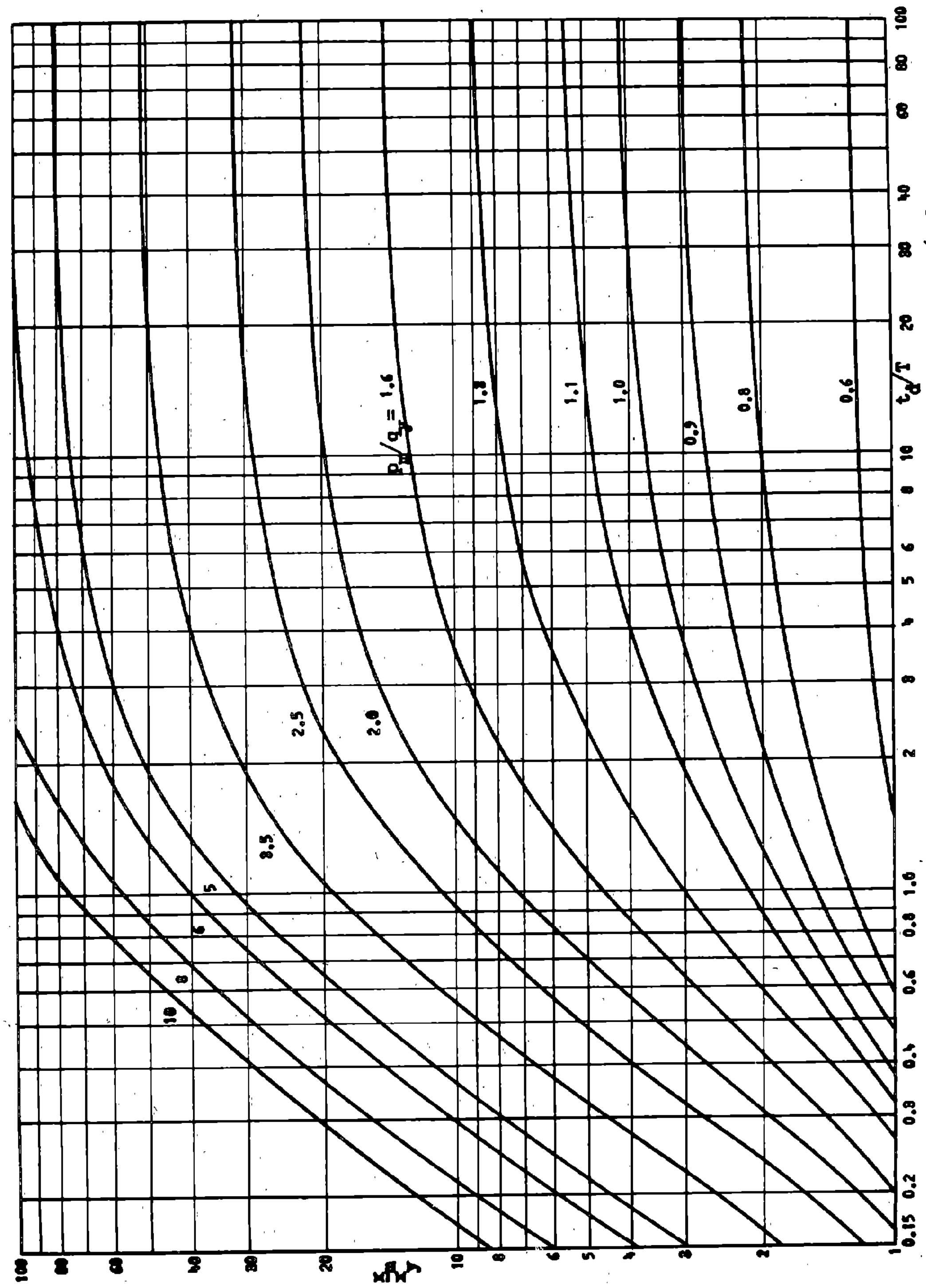

Fig. 4c. Maximum Response of Mass-Spring System to Initial-Peak Triangular Pulse; k=0.1, $t_1/T=0$

Figure 6-1 (continued)

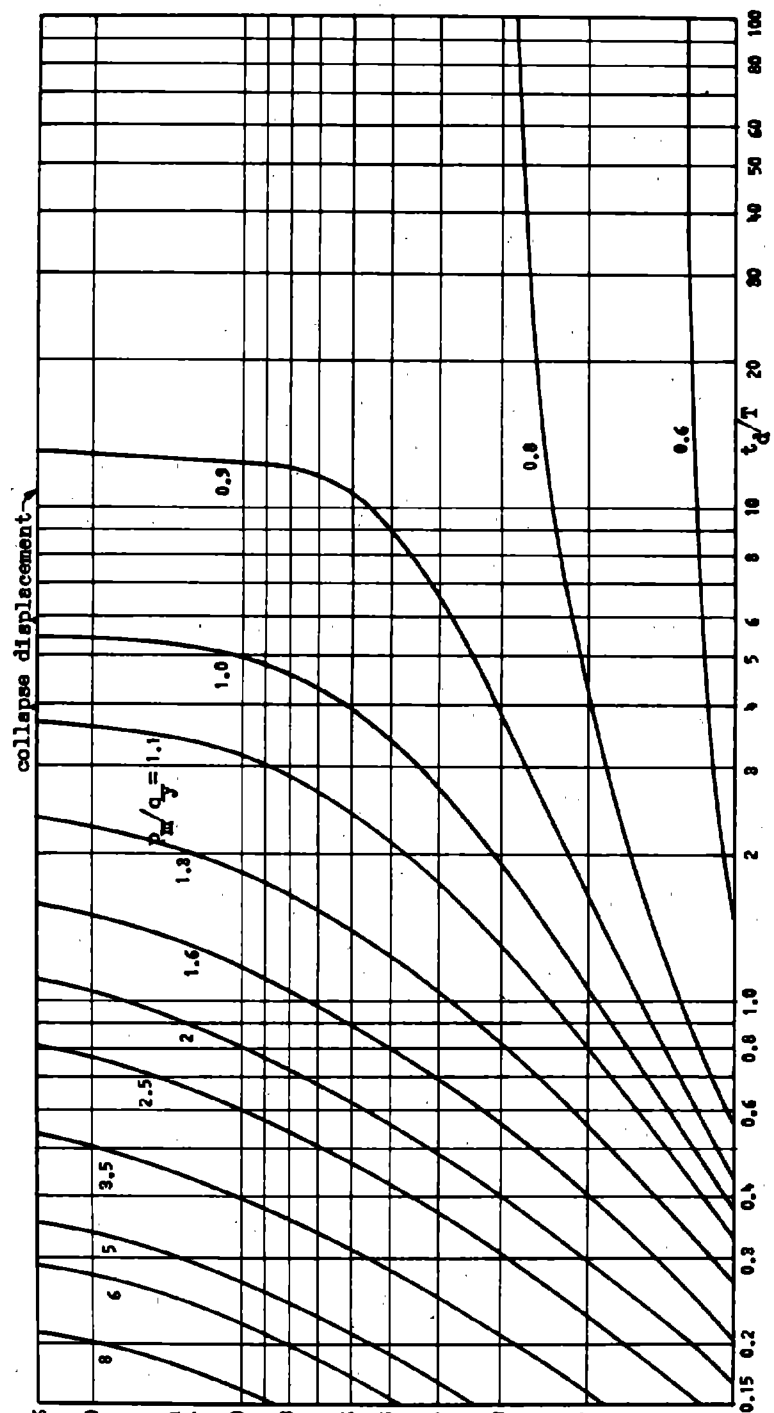

Fig. 4d. Maximum Response of Mass-Spring System to Initial-Peak Triangular Pulse; $k=-.04$, $t_1/T=0$

Figure 6-1 (continued)

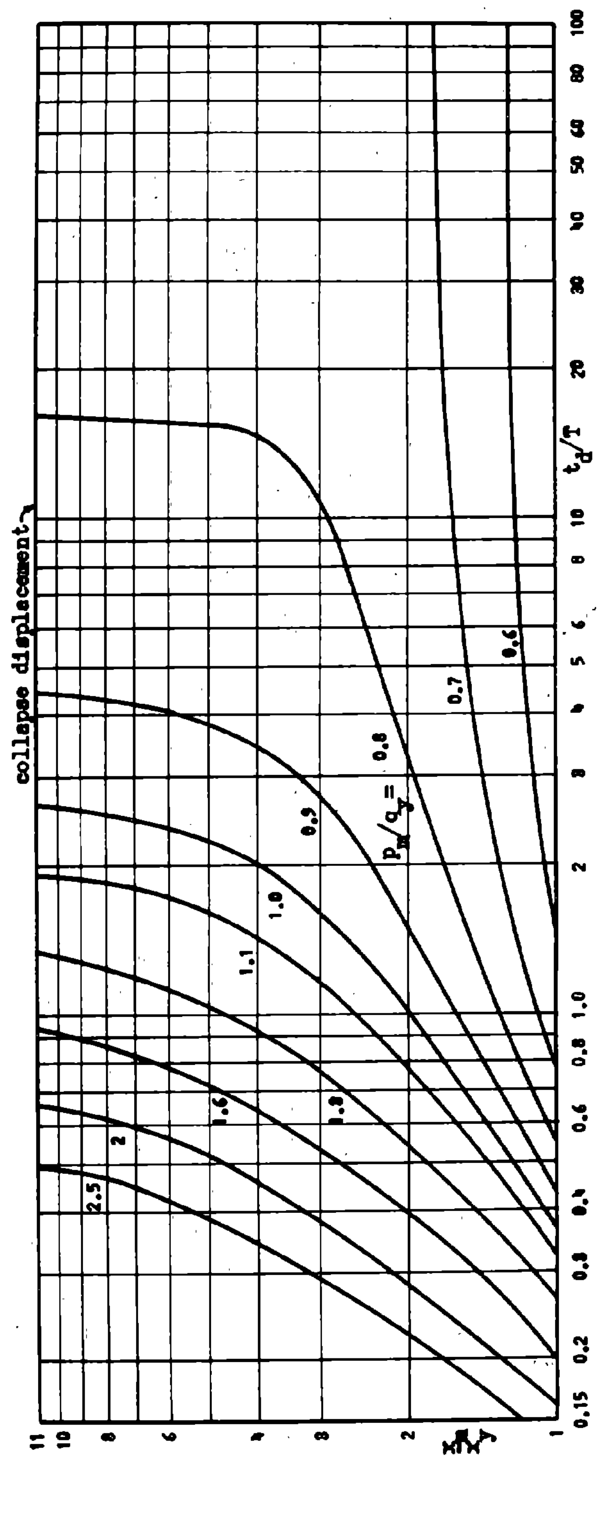

Fig. 4e. Maximum Response of Mass-Spring System to Initial-Peak Triangular Pulse; k=-.1, t_1/T=0

Figure 6-1 (continued)

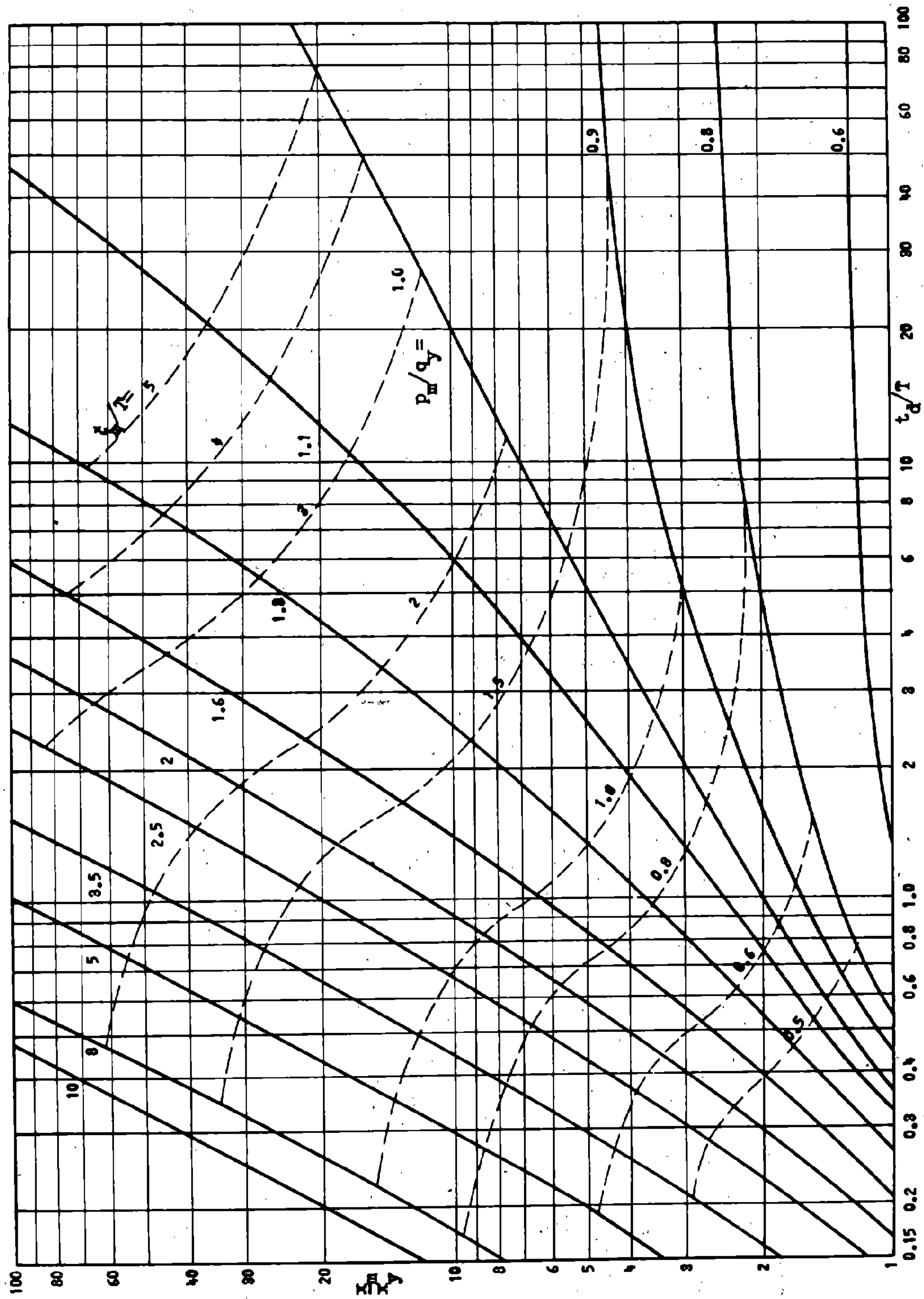

Fig. 5a. Maximum Response of Mass-Spring System to General Triangular Pulse; $k=0$, $t_1/T=0.1$

Figure 6-1 (continued)

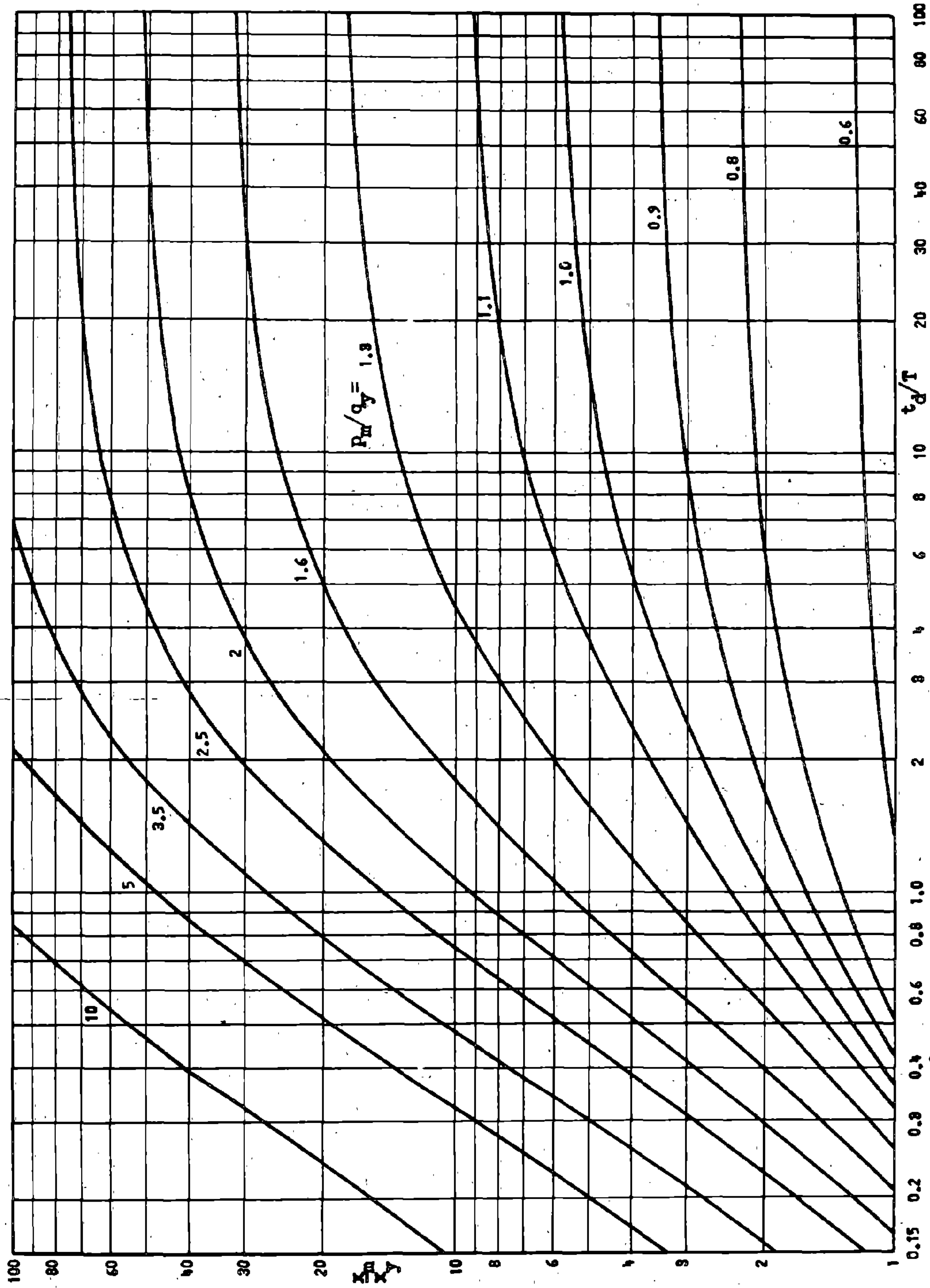

Fig. 5b. Maximum Response of Mass-Spring System to General Triangular Pulse; k=0.04, t_1/T=0.1

Figure 6-1 (continued)

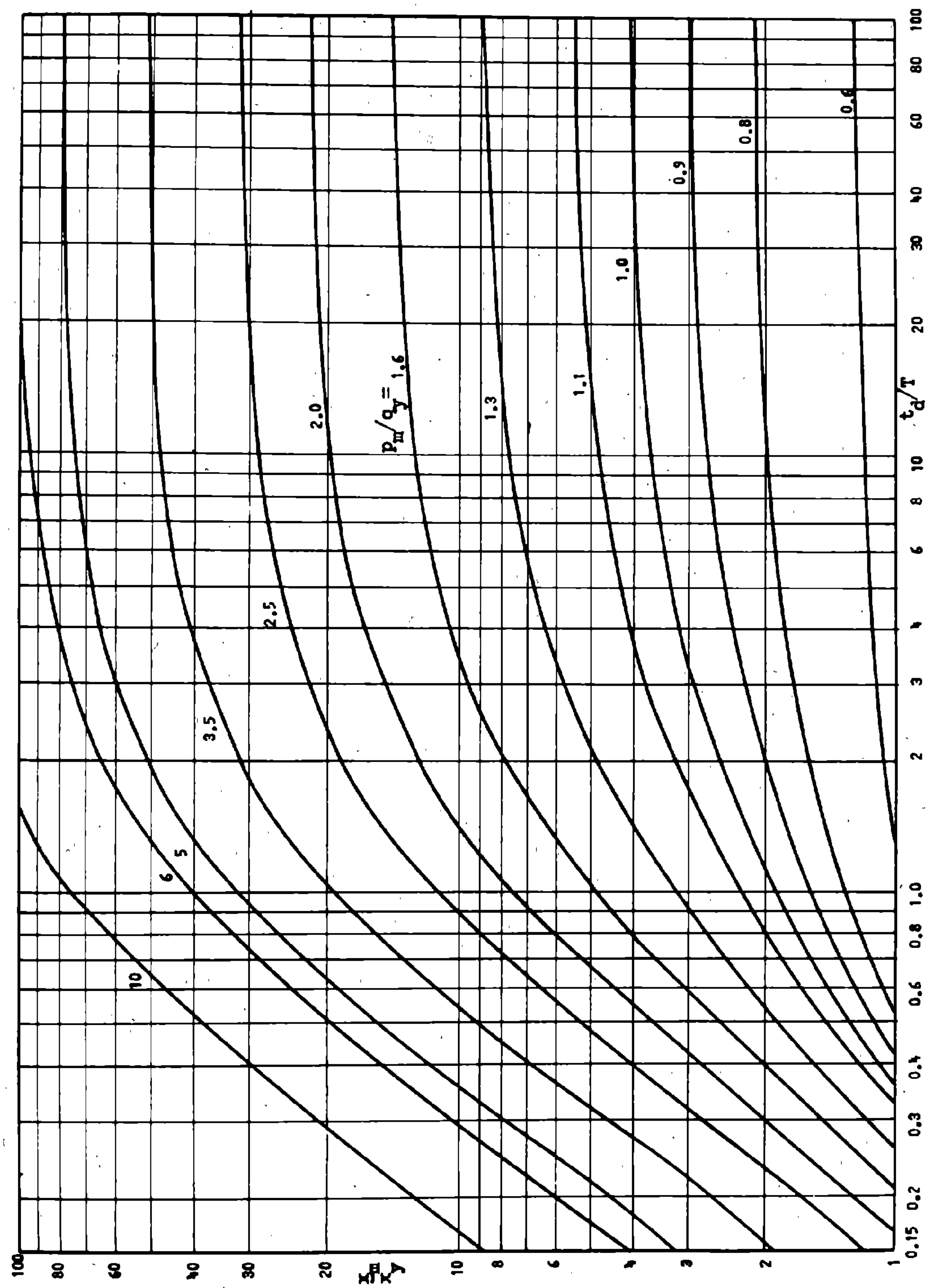

Fig. 5c. Maximum Response of Mass-Spring System to General Triangular Pulse; k=0.1, t_1/T=0.1

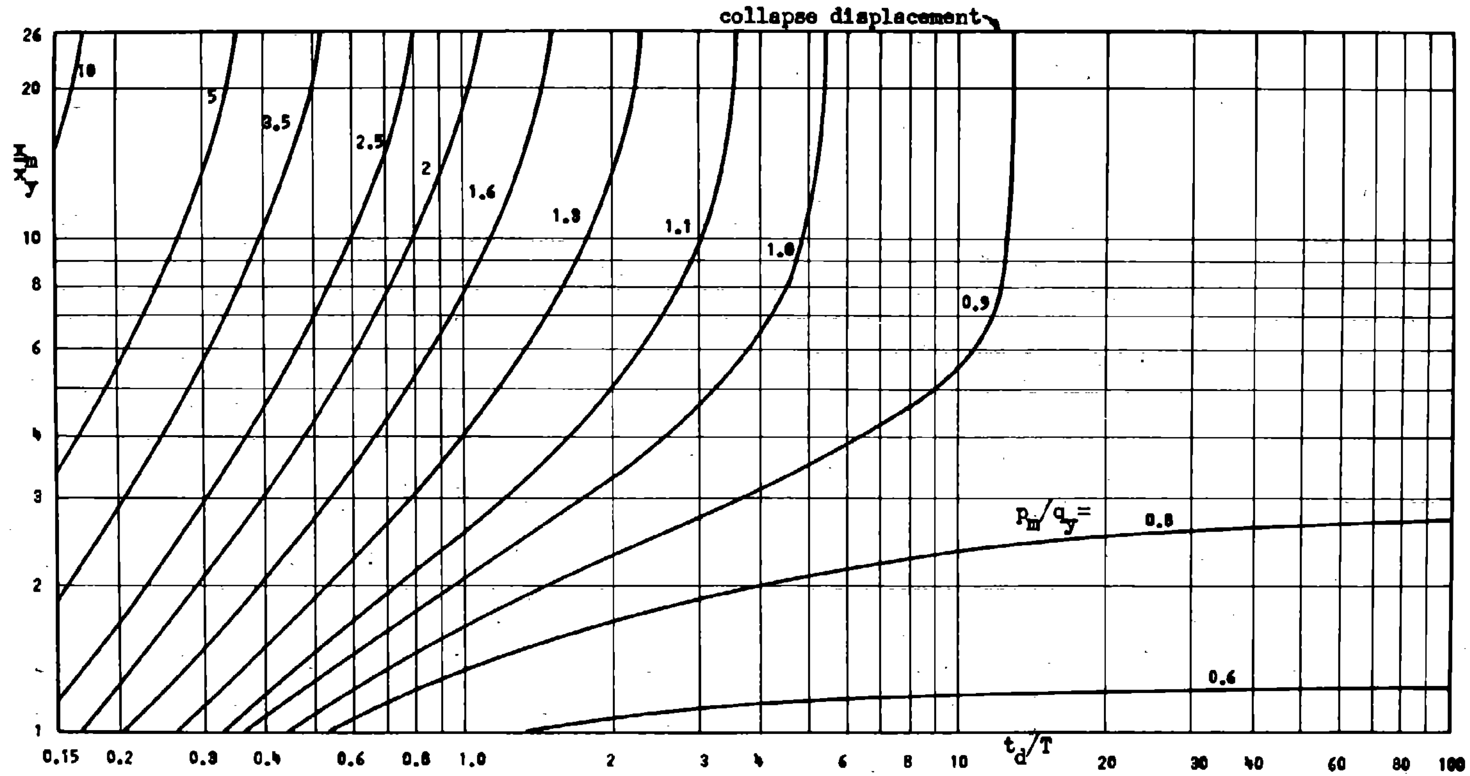

Fig. 5d. Maximum Response of Mass-Spring System to General Triangular Pulse; k=-0.04, $t_1/T=0.1$

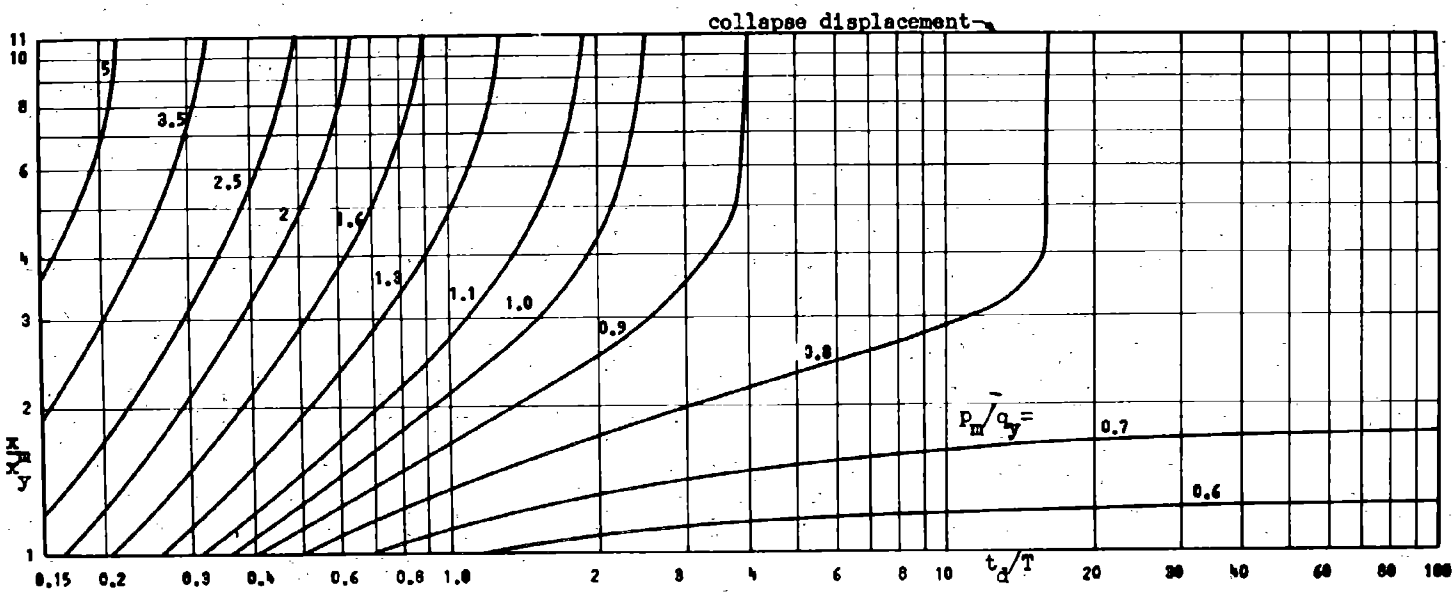

Fig. 5e. Maximum Response of Mass-Spring System to General Triangular Pulse; k=-0.1, t_1/T=0.1

Figure 6-1 (continued)

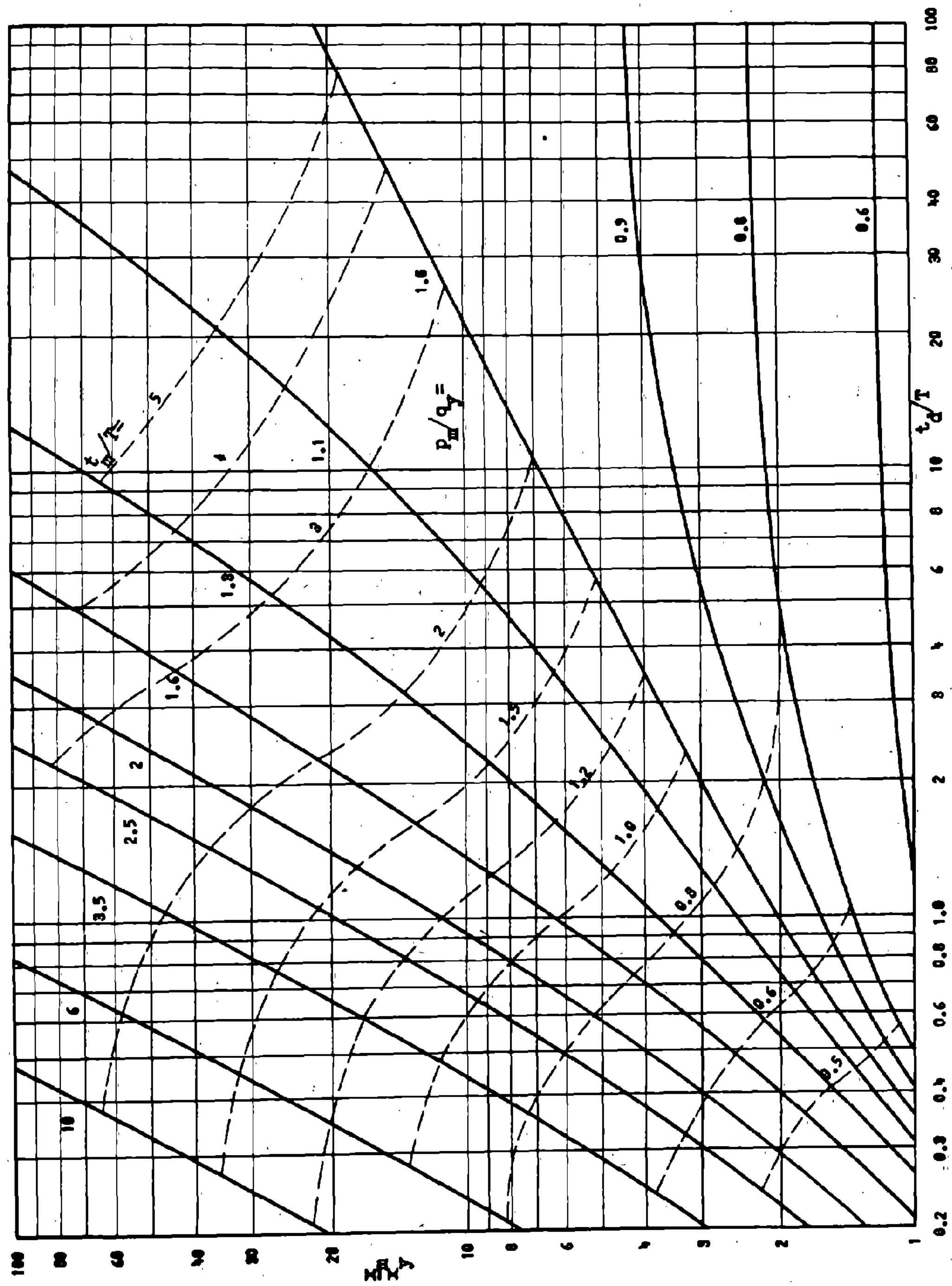

Fig. 6a. Maximum Response of Mass-Spring System to General Triangular Pulse; $k=0$, $t_1/T=0.2$

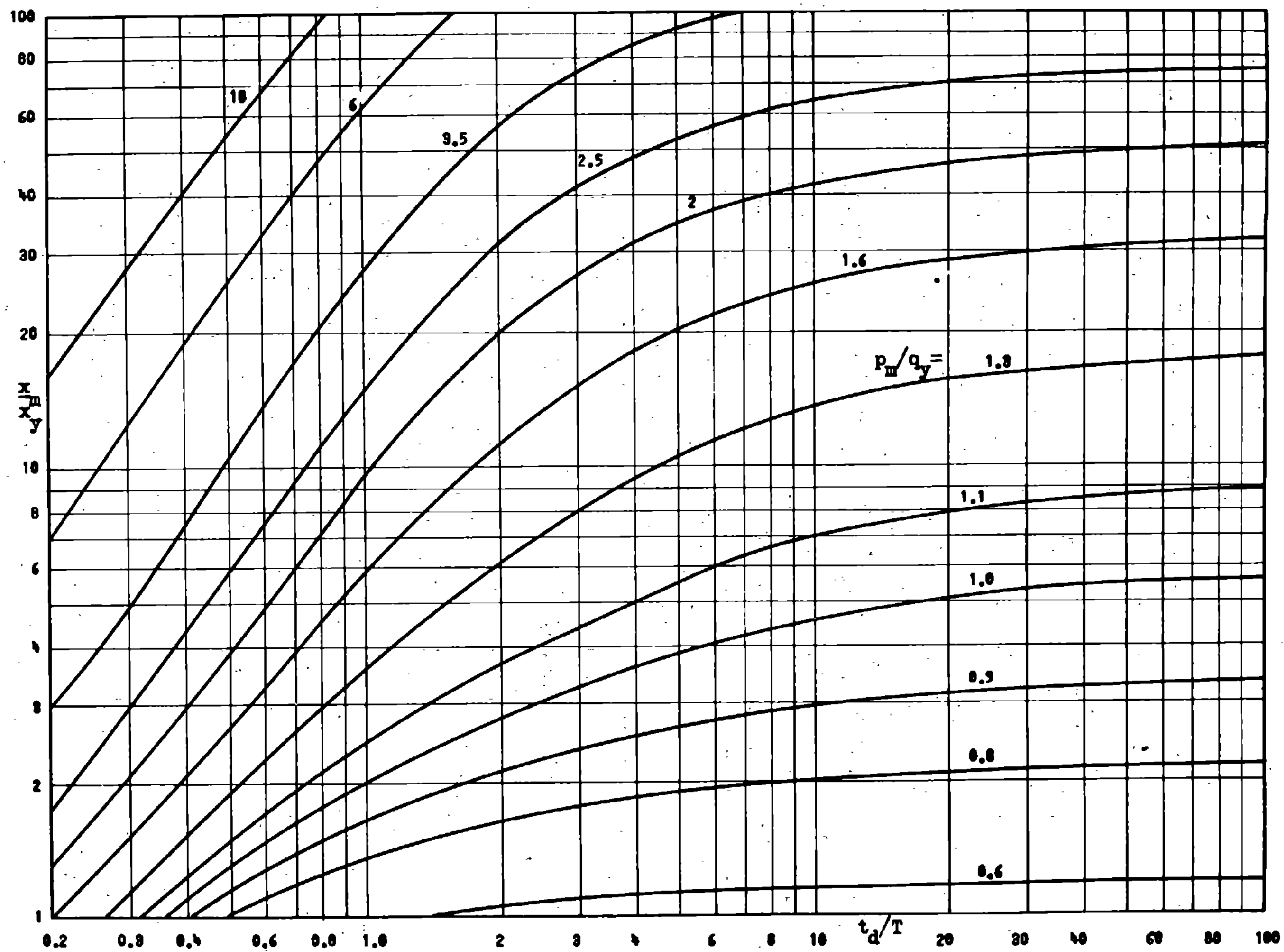

Fig. 6b. Maximum Response of Mass-Spring System to General Triangular Pulse; k=0.04, t_1/T=0.2

Figure 6-1 (continued)

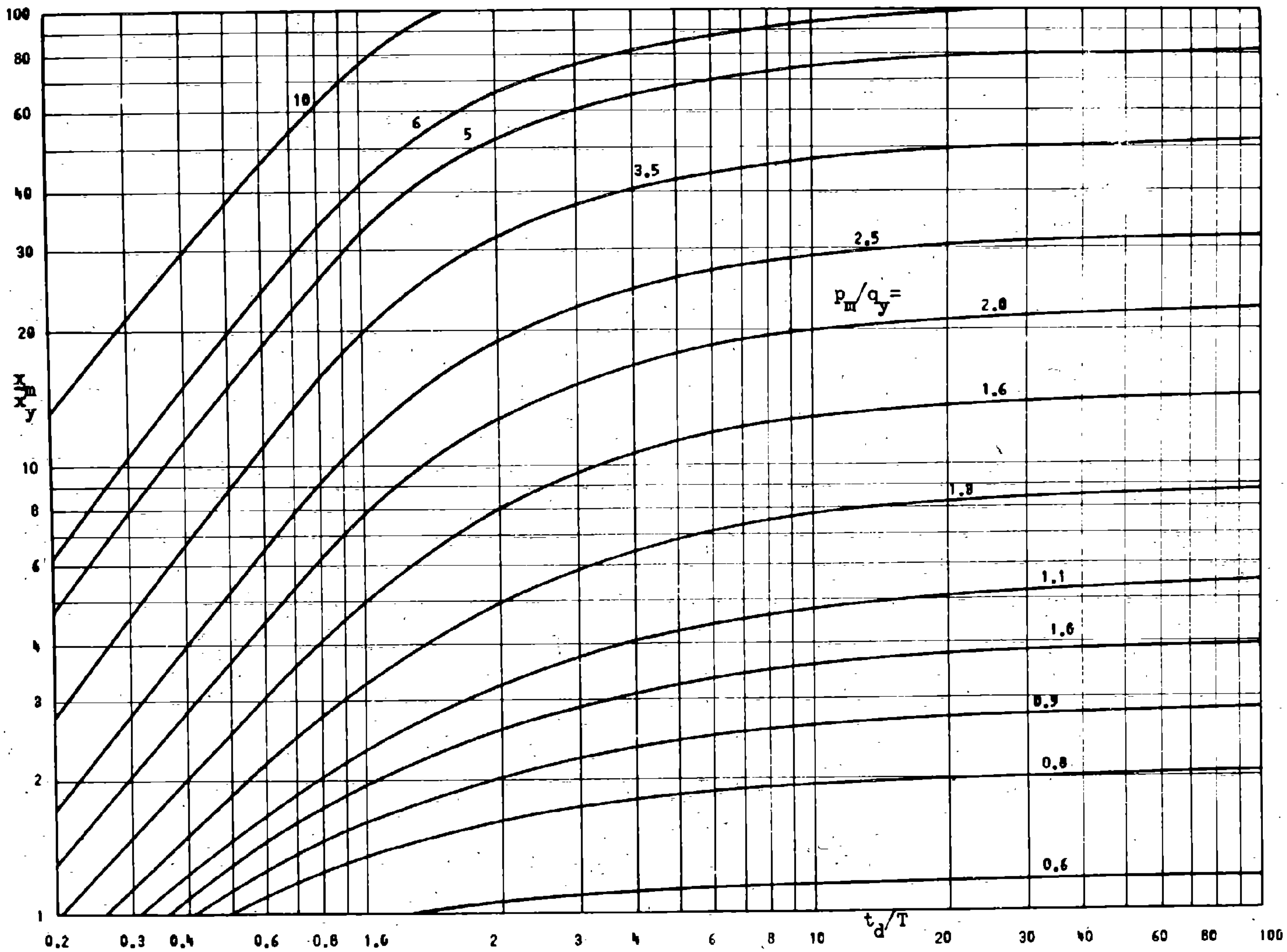

Fig. 6c. Maximum Response of Mass-Spring System to General Triangular Pulse; k=0.1, t_1/T=0.2

Figure 6-1 (continued)

Figure 6-1 (continued)

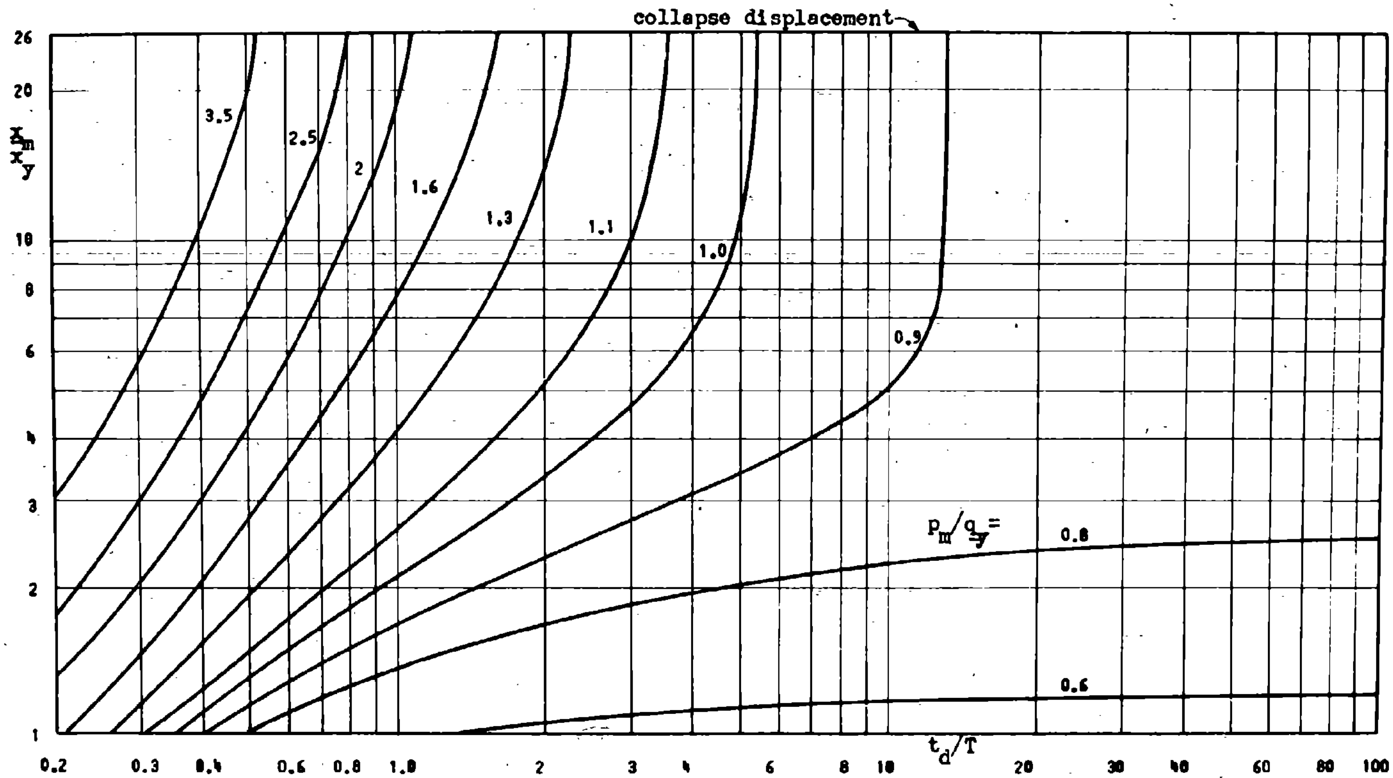

Fig. 6d. Maximum Response of Mass-Spring System to General Triangular Pulse; k=-0.04, t_1/T=0.2

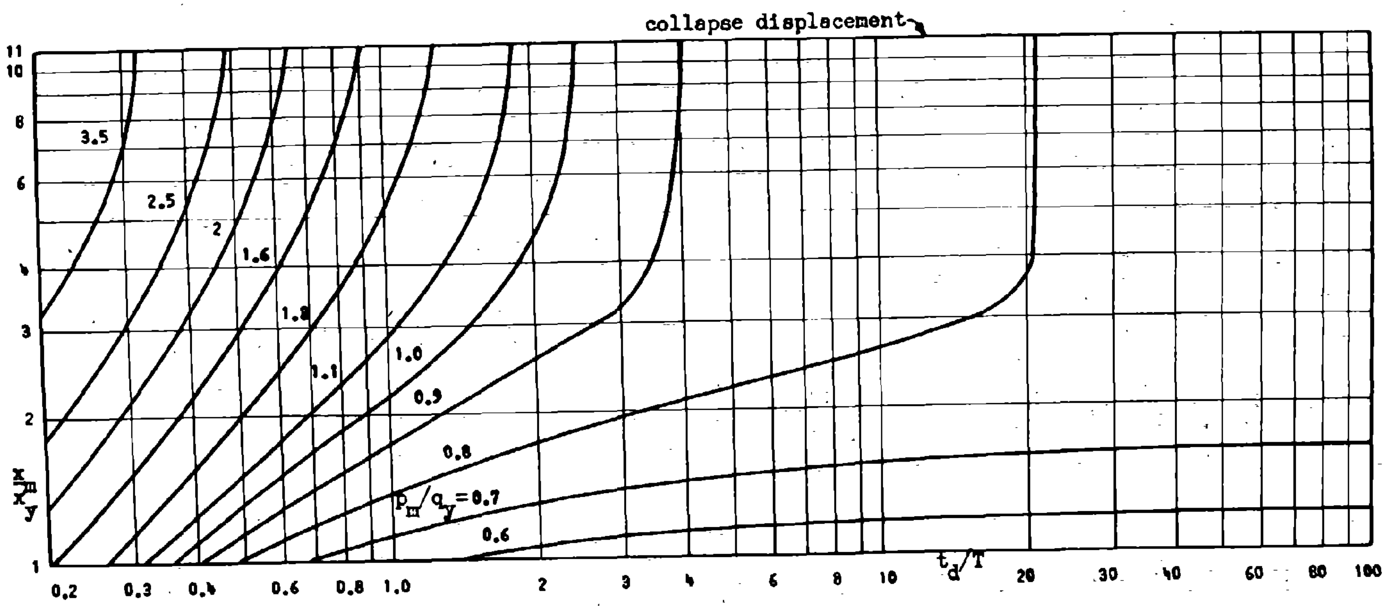

Fig. 6e. Maximum Response of Mass-Spring System to General Triangular Pulse; $k=-0.1$, $t_1/T=0.2$

Figure 6-1 (concluded)

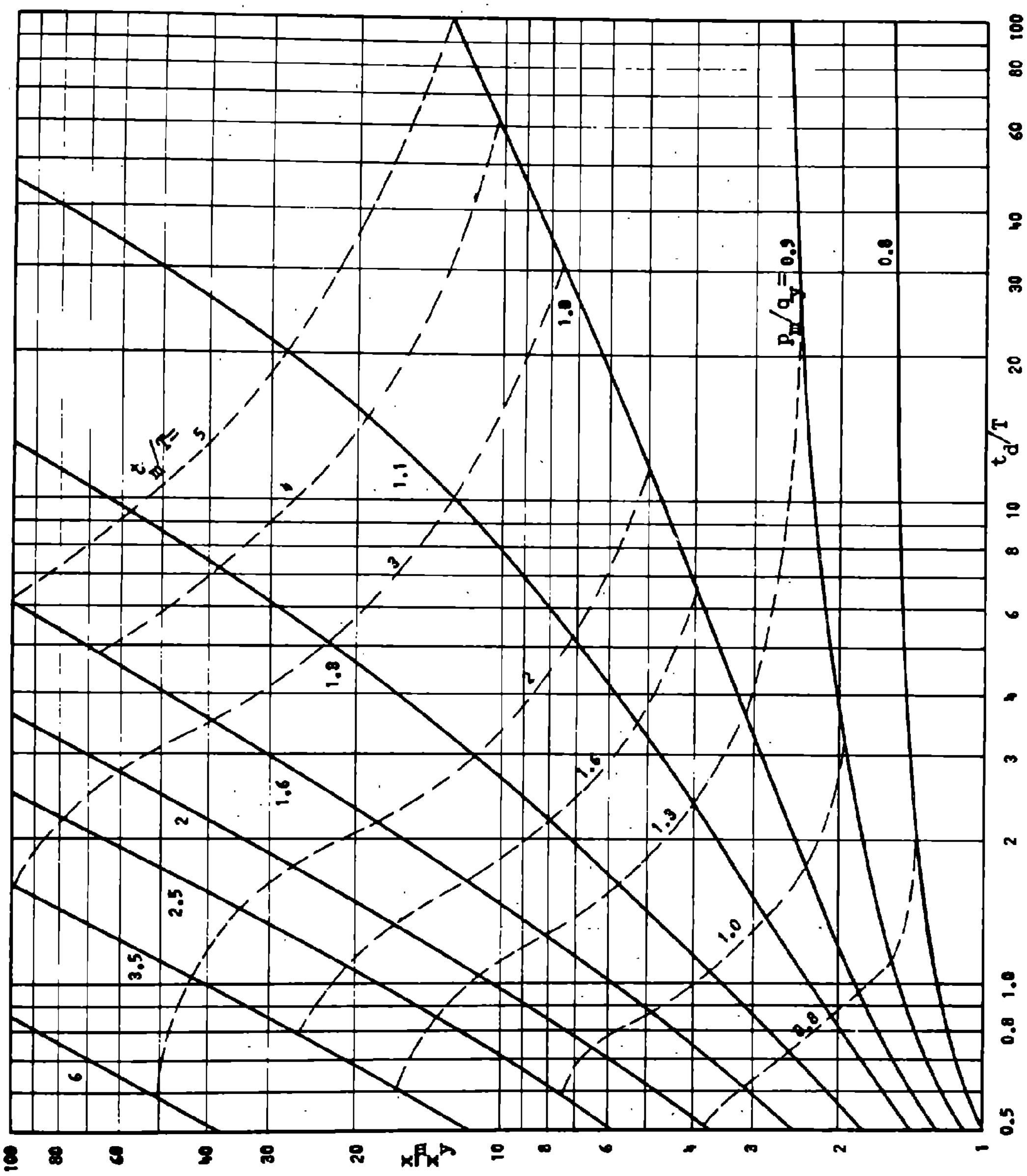

Fig. 7. Maximum Response of Mass-Spring System to General Triangular Pulse; k=0, $t_1/T=0.5$

Table 6.3

DYNAMIC DESIGN FACTOR TABLES[22]

Reproduced, without change, from Reference indicated.

6-10 DYNAMIC DESIGN FACTOR TABLES. The following tables are a complete tabulation of available dynamic design factors for use in the design procedures of this manual. Figure 6.3 and the following notation are placed conveniently to the tables for ready reference. The information in these tables is obtained from paragraphs 6-11 to 6-24 wherein detailed explanations of the different items are presented.

The general form of the resistance-deflection diagrams for structural elements is shown in figure 6.3. Further discussion of these functions and explanation of the figure are found in paragraph 6-14e.

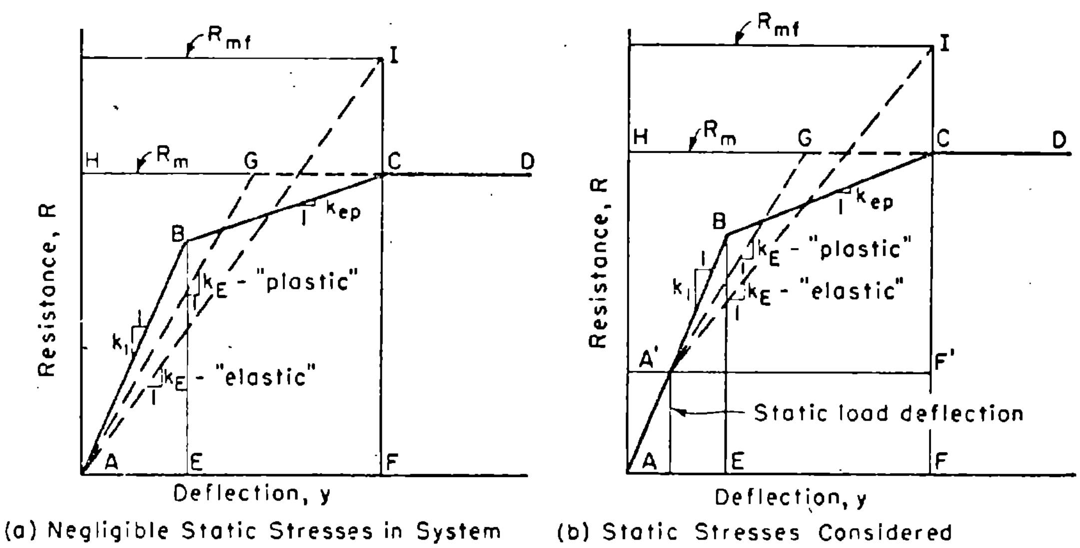

Figure 6.3. General resistance-deflection diagram for structural elements

Notation for Dynamic Design Factor Tables

a = Short side of rectangular slab, ft.

b = Long side of rectangular slab, ft.

E = Modulus of elasticity, kips/sq. in.

I = Moment of inertia.

I_a = Average of gross and transformed moments of inertia. (In two-way slabs, the average per unit width for short span).

M_P = Plastic resisting moment.

M_{Pm} = Plastic resisting moment at center line of beam or slab (kip-ft)

M_{Pfa} = The component (in a plane perpendicular to edge a), of the total plastic bending moment capacity along the fracture line boundary of one area A, or the total positive plastic bending moment capacity for a section parallel to edge a, kip-ft.

M_{Pfb} = The component (in a plane perpendicular to edge b), of the total plastic bending moment capacity along the fracture line boundary of one area B, or the total positive plastic bending moment capacity for a section parallel to edge b, kip-ft.

M_{Ps} = Plastic resisting moment at support (kip-ft).

M_{Psa} = Total plastic bending moment capacity along edge a, kip-ft.

M_{Psb} = Total plastic bending moment capacity along edge b, kip-ft.

M^O_{Pmb} = Plastic positive bending moment capacity per unit width in short span, kip-ft/ft.

M^O_{Psa} = Plastic negative bending moment capacity per unit width at center of edge a for long span kip-ft/ft.

M^O_{Psb} = Plastic negative bending moment capacity per unit width at center of edge b for short span, kip-ft/ft.

P = Total dynamic load on slab or beam, kips.

R = Total resistance of slab or beam, kips.

R_{mf} = Fictitious maximum resistance, kips (paragraph 6-14).

V_A = Total dynamic reaction along one edge a, kips.

V_B = Total dynamic reaction along one edge b, kips.

Table 6.3 (continued)

Table 6.1A

DYNAMIC DESIGN FACTORS
BEAMS AND ONE-WAY SLABS

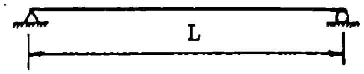

Simply-Supported

Loading Diagram	Strain Range	Load Factor K_L	Mass Factor K_M		Load-Mass Factor K_{LM}		Maximum Resistance R_m	Spring Constant k	Dynamic Reaction V
			Concen-trated Mass *	Uniform Mass	Concen-trated Mass *	Uniform Mass			
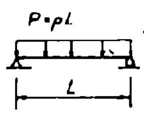	Elastic	0.64		0.50		0.78	$\frac{8M_P}{L}$	$\frac{384EI}{5L^3}$	0.39 R+0.11P
	Plastic	0.50		0.33		0.66	$\frac{8M_P}{L}$	0	$0.38R_m+0.12P$
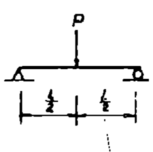	Elastic	1	1.0	0.49	1.0	0.49	$\frac{4M_P}{L}$	$\frac{48EI}{L^3}$	0.78 R-0.28P
	Plastic	1	1.0	0.33	1.0	0.33	$\frac{4M_P}{L}$	0	$0.75R_m-0.25P$
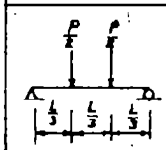	Elastic	0.87	0.76	0.52	0.87	0.60	$\frac{6M_P}{L}$	$\frac{56.4EI}{L^3}$	0.62 R-0.12P
	Plastic	1	1.0	0.56	1.0	0.56	$\frac{6M_P}{L}$	0	$0.75R_m-0.25P$

* Equal parts of the concentrated mass are lumped at each concentrated load.

Table 6.1B

BEAMS AND ONE-WAY SLABS

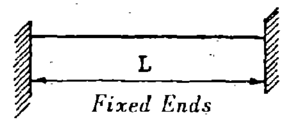

Loading Diagram	Strain Range	Load Factor K_L	Mass Factor K_M		Load-Mass Factor K_{LM}		Maximum Resistance R_m	Spring Constant k	Effective Spring Constant k_E		Dynamic Reaction V
			Concentrated Mass*	Uniform Mass	Concentrated Mass*	Uniform Mass			Elastic	Plastic	
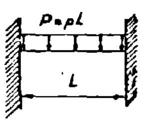	Elastic	0.53		0.41		0.77	$\frac{12M_{Ps}}{L}$	$\frac{384EI}{L^3}$	$\frac{264\ EI}{L^3}$	$\frac{307\ EI}{L^3}$	$0.36R+0.14P$
	Elasto-Plastic	0.64		0.50		0.78	$\frac{8}{L}(M_{Ps}+M_{Pm})$	$\frac{384EI}{5L^3}$	$R_{mf} = \frac{22M_P}{L}$		$0.39R+0.11P$
	Plastic	0.50		0.33		0.66	$\frac{8}{L}(M_{Ps}+M_{Pm})$	0			$0.38R_m+0.12P$
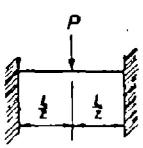	Elastic	1	1.0	0.37	1.0	0.37	$\frac{4}{L}(M_{Ps}+M_{Pm})$	$\frac{192EI}{L^3}$			$0.71R-0.21P$
	Plastic	1	1.0	0.33	1.0	0.33	$\frac{4}{L}(M_{Ps}+M_{Pm})$	0			$0.75R_m-0.25P$

* Concentrated mass is lumped at the concentrated load.

Table 6.3 (continued)

Table 6.1C

DYNAMIC DESIGN FACTORS
BEAMS AND ONE-WAY SLABS

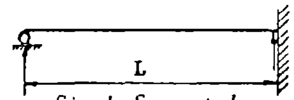

Simply-Supported and Fixed

Loading Diagram	Strain Range	Load Factor K_L	Mass Factor K_M		Load-Mass Factor K_{LM}		Maximum Resistance R_m	Spring Constant k	Effective Spring Constant k_E		Dynamic Reaction V
			Concentrated Mass*	Uniform Mass	Concentrated Mass*	Uniform Mass			Elastic	Plastic	
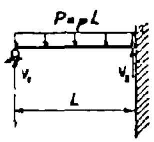	Elastic	0.58		0.45		0.78	$8M_{Ps}/L$	$185EI/L^3$	$\frac{153EI}{L^3}$	$\frac{160EI}{L^3}$	$V_1=0.26R+0.12P$ $V_2=0.43R+0.19P$
	Elasto-Plastic	0.64		0.50		0.78	$\frac{4}{L}(M_{Ps}+2M_{Pm})$	$\frac{384}{5}EI/L^3$	$R_{mf}=\frac{14.6M_P}{L}$		$V_1=V_2=0.39R+0.11P$
	Plastic	0.50		0.33		0.66	$\frac{4}{L}(M_{Ps}+2M_{Pm})$	0			$V_1=V_2=0.38R_m+0.12P$
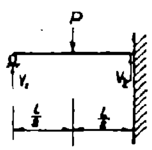	Elastic	1.0	1.0	0.43	1.0	0.43	$16M_{Ps}/3L$	$107EI/L^3$	$\frac{104EI}{L^3}$	$\frac{160EI}{L^3}$	$V_1=0.54R+0.14P$ $V_2=0.25R+0.07P$
	Elasto-Plastic	1	1.0	0.49	1.0	0.49	$\frac{2}{L}(M_{Ps}+2M_{Pm})$	$48EI/L^3$	$R_{mf}=\frac{6.63M_P}{L}$		$V_1=V_2=0.78R-0.28P$
	Plastic	1	1.0	0.33	1.0	0.33	$\frac{2}{L}(M_{Ps}+2M_{Pm})$	0			$V_1=V_2=0.75R_m-0.25P$
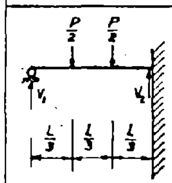	Elastic	0.81	0.67	0.45	0.83	0.55	$6M_{Ps}/L$	$132EI/L^3$	$\frac{117.5EI}{L^3}$	$\frac{122EI}{L^3}$	$V_1=0.17R+0.17P$ $V_2=0.33R+0.33P$
	Elasto-Plastic	0.87	0.76	0.52	0.87	0.60	$\frac{2}{L}(M_{Ps}+3M_{Pm})$	$\frac{56EI}{L^3}$	$R_{mf}=\frac{9.52M_P}{L}$		$V_1=V_2=0.62R-0.12P$
	Plastic	1	1.0	0.56	1.0	0.56	$\frac{2}{L}(M_{Ps}+3M_{Pm})$				$V_1=0.56R_m-0.25P$ $V_2=0.56R_m+0.13P$

* Equal parts of the concentrated mass are lumped at each concentrated load.

Table 6.2A

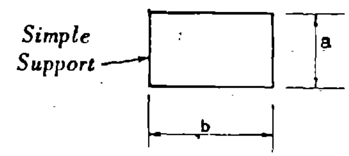

TWO-WAY SLABS: SIMPLE SUPPORTS, FOUR SIDES
UNIFORM LOAD

Strain Range	a/b	Load Factor K_L	Mass Factor K_M	Load-Mass Factor K_{LM}	Maximum Resistance	Spring Constant k	Dynamic Reactions V_A	Dynamic Reactions V_B
Elastic	1.0	0.45	0.31	0.68	$\frac{12}{a}(M_{Pfa}+M_{Pfb})$	$271\ EI_a/a^2$	0.07P+0.18R	0.07P+0.18R
	0.9	0.47	0.33	0.70	$\frac{1}{a}(12M_{Pfa}+11M_{Pfb})$	$248\ EI_a/a^2$	0.06P+0.16R	0.08P+0.20R
	0.8	0.49	0.35	0.71	$\frac{1}{a}(12M_{Pfa}+10.3M_{Pfb})$	$228\ EI_a/a^2$	0.06P+0.14R	0.08P+0.22R
	0.7	0.51	0.37	0.73	$\frac{1}{a}(12M_{Pfa}+9.8M_{Pfb})$	$216\ EI_a/a^2$	0.05P+0.13R	0.08P+0.24R
	0.6	0.53	0.39	0.74	$\frac{1}{a}(12M_{Pfa}+9.3M_{Pfb})$	$212\ EI_a/a^2$	0.04P+0.11R	0.09P+0.26R
	0.5	0.55	0.41	0.75	$\frac{1}{a}(12M_{Pfa}+9.0M_{Pfb})$	$216\ EI_a/a^2$	0.04P+0.09R	0.09P+0.28R
Plastic	1.0	0.33	0.17	0.51	$\frac{12}{a}(M_{Pfa}+M_{Pfb})$	0	$0.09P+0.16R_m$	$0.09P+0.16R_m$
	0.9	0.35	0.18	0.51	$\frac{1}{a}(12M_{Pfa}+11M_{Pfb})$	0	$0.08P+0.15R_m$	$0.09P+0.18R_m$
	0.8	0.37	0.20	0.54	$\frac{1}{a}(12M_{Pfa}+10.3M_{Pfb})$	0	$0.07P+0.13R_m$	$0.01P+0.20R_m$
	0.7	0.38	0.22	0.58	$\frac{1}{a}(12M_{Pfa}+9.8M_{Pfb})$	0	$0.06P+0.12R_m$	$0.10P+0.22R_m$
	0.6	0.40	0.23	0.58	$\frac{1}{a}(12M_{Pfa}+9.3M_{Pfb})$	0	$0.05P+0.10R_m$	$0.10P+0.25R_m$
	0.5	0.42	0.25	0.59	$\frac{1}{a}(12M_{Pfa}+9.0M_{Pfb})$	0	$0.04P+0.08R_m$	$0.11P+0.27R_m$

Table 6.3 (continued)

Table 6.3 (continued)

Table 6.2B (Sheet 1 of 2)

TWO-WAY SLABS: FIXED FOUR SIDES
UNIFORM LOAD

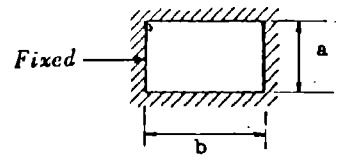

Strain Range	a/b	Load Factor K_L	Mass Factor K_M	Load-Mass Factor K_{LM}	Maximum Resistance	Spring Constant k	Dynamic Reactions V_A	Dynamic Reactions V_B
Elastic	1.0	0.33	0.21	0.63	$30.2\ M^o_{Psb}$	$870\ EI_a/a^2$	0.10P + 0.15R	0.10P + 0.15R
	0.9	0.34	0.23	0.68	$27.8\ M^o_{Psb}$	$798\ EI_a/a^2$	0.09P + 0.14R	0.10P + 0.17R
	0.8	0.36	0.25	0.69	$26.0\ M^o_{Psb}$	$757\ EI_a/a^2$	0.08P + 0.12R	0.11P + 0.19R
	0.7	0.38	0.27	0.71	$26.0\ M^o_{Psb}$	$744\ EI_a/a^2$	0.07P + 0.11R	0.11P + 0.21R
	0.6	0.41	0.29	0.71	$26.4\ M^o_{Psb}$	$778\ EI_a/a^2$	0.06P + 0.09R	0.12P + 0.23R
	0.5	0.43	0.31	0.72	$25.0\ M^o_{Psb}$	$866\ EI_a/a^2$	0.05P + 0.08R	0.12P + 0.25R
Elasto-Plastic	1.0	0.46	0.31	0.67	$\frac{1}{a}\left[12(M_{Pfa}+M_{Psa})+12(M_{Pfb}+M_{Psb})\right]$	$271\ EI_a/a^2$	0.07P + 0.18R	0.07P + 0.18R
	0.9	0.47	0.33	0.70	$\frac{1}{a}\left[12(M_{Pfa}+M_{Psa})+11(M_{Pfb}+M_{Psb})\right]$	$248\ EI_a/a^2$	0.06P + 0.16R	0.08P + 0.20R
	0.8	0.49	0.35	0.71	$\frac{1}{a}\left[12(M_{Pfa}+M_{Psa})+10.3(M_{Pfb}+M_{Psb})\right]$	$228\ EI_a/a^2$	0.06P + 0.14R	0.08P + 0.22R
	0.7	0.51	0.37	0.73	$\frac{1}{a}\left[12(M_{Pfa}+M_{Psa})+9.8(M_{Pfb}+M_{Psb})\right]$	$216\ EI_a/a^2$	0.05P + 0.13R	0.08P + 0.24R
	0.6	0.53	0.39	0.74	$\frac{1}{a}\left[12(M_{Pfa}+M_{Psa})+9.3(M_{Pfb}+M_{Psb})\right]$	$212\ EI_a/a^2$	0.04P + 0.11R	0.09P + 0.26R
	0.5	0.55	0.41	0.75	$\frac{1}{a}\left[12(M_{Pfa}+M_{Psa})+9.0(M_{Pfb}+M_{Psb})\right]$	$216\ EI_a/a^2$	0.04P + 0.09R	0.09P + 0.28R

Table 6.3 (continued)

Table 6.2B (Sheet 2 of 2)

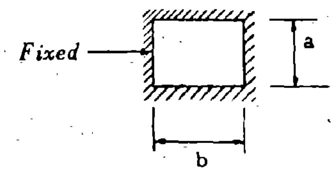

TWO-WAY SLABS: FIXED FOUR SIDES
UNIFORM LOAD

Strain Range	a/b	Load Factor K_L	Mass Factor K_M	Load-Mass Factor K_{LM}	Maximum Resistance	Spring Constant k	Dynamic Reactions V_A	Dynamic Reactions V_B
Plastic	1.0	0.33	0.17	0.51	$\frac{1}{a}\left[12(M_{Pfa}+M_{Psa})+12(M_{Pfb}+M_{Psb})\right]$	0	$0.09P+0.16R_m$	$0.09P+0.16R_m$
	0.9	0.35	0.18	0.51	$\frac{1}{a}\left[12(M_{Pfa}+M_{Psa})+11(M_{Pfb}+M_{Psb})\right]$	0	$0.08P+0.15R_m$	$0.09P+0.18R_m$
	0.8	0.37	0.20	0.54	$\frac{1}{a}\left[12(M_{Pfa}+M_{Psa})+10.3(M_{Pfb}+M_{Psb})\right]$	0	$0.07P+0.13R_m$	$0.10P+0.20R_m$
	0.7	0.38	0.22	0.58	$\frac{1}{a}\left[12(M_{Pfa}+M_{Psa})+9.8(M_{Pfb}+M_{Psb})\right]$	0	$0.06P+0.12R_m$	$0.10P+0.22R_m$
	0.6	0.40	0.23	0.58	$\frac{1}{a}\left[12(M_{Pfa}+M_{Psa})+9.3(M_{Pfb}+M_{Psb})\right]$	0	$0.05P+0.10R_m$	$0.10P+0.25R_m$
	0.5	0.42	0.25	0.59	$\frac{1}{a}\left[12(M_{Pfa}+M_{Psa})+9.0(M_{Pfb}+M_{Psb})\right]$	0	$0.04P+0.08R_m$	$0.11P+0.27R_m$

Table 6.2C (Sheet 1 of 2)

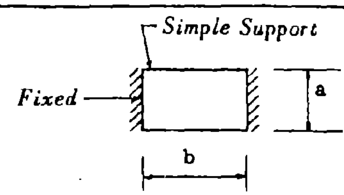

TWO-WAY SLABS: SIMPLE SUPPORTS, TWO LONG SIDES
FIXED SUPPORTS, TWO SHORT SIDES, UNIFORM LOAD

Strain Range	a/b	Load Factor K_L	Mass Factor K_M	Load-Mass Factor K_{LM}	Maximum Resistance	Spring Constant k	Dynamic Reactions V_A	Dynamic Reactions V_B
Elastic	1.0	0.39	0.26	0.67	$20.4\ M^o_{Psa}$	$575\ EI_a/a^2$	0.09P+0.16R	0.07P+0.18R
	0.9	0.41	0.28	0.68	$10.2\ M^o_{Psa} + \frac{11}{a} M_{Pfb}$	$476\ EI_a/a^2$	0.08P+0.14R	0.08P+0.20R
	0.8	0.44	0.30	0.68	$10.2\ M^o_{Psa} + \frac{10.3}{a} M_{Pfb}$	$396\ EI_a/a^2$	0.08P+0.12R	0.08P+0.22R
	0.7	0.46	0.33	0.72	$9.3\ M^o_{Psb} + \frac{9.7}{a} M_{Pfb}$	$328\ EI_a/a^2$	0.07P+0.11R	0.08P+0.24R
	0.6	0.48	0.35	0.73	$8.5\ M^o_{Psb} + \frac{9.3}{a} M_{Pfb}$	$283\ EI_a/a^2$	0.06P+0.09R	0.09P+0.26R
	0.5	0.51	0.37	0.73	$7.4\ M^o_{Psb} + \frac{9.0}{a} M_{Pfb}$	$243\ EI_a/a^2$	0.05P+0.08R	0.09P+0.28R
Elasto-Plastic	1.0	0.46	0.31	0.67	$\frac{1}{a}\left[12(M_{Pfa} + M_{Psa}) + 12(M_{Pfb})\right]$	$271\ EI_a/a^2$	0.07P+0.18R	0.07P+0.18R
	0.9	0.47	0.33	0.70	$\frac{1}{a}\left[12(M_{Pfa} + M_{Psa}) + 11(M_{Pfb})\right]$	$248\ EI_a/a^2$	0.06P+0.16R	0.08P+0.20R
	0.8	0.49	0.35	0.71	$\frac{1}{a}\left[12(M_{Pfa} + M_{Psa}) + 10.3(M_{Pfb})\right]$	$228\ EI_a/a^2$	0.06P+0.14R	0.08P+0.22R
	0.7	0.51	0.37	0.72	$\frac{1}{a}\left[12(M_{Pfa} + M_{Psa}) + 9.7(M_{Pfb})\right]$	$216\ EI_a/a^2$	0.05P+0.13R	0.08P+0.24R
	0.6	0.53	0.37	0.70	$\frac{1}{a}\left[12(M_{Pfa} + M_{Psa}) + 9.3(M_{Pfb})\right]$	$212\ EI_a/a^2$	0.04P+0.11R	0.09P+0.26R
	0.5	0.55	0.41	0.74	$\frac{1}{a}\left[12(M_{Pfa} + M_{Psa}) + 9.0(M_{Pfb})\right]$	$216\ EI_a/a^2$	0.04P+0.09R	0.09R+0.28R

Table 6.3 (continued)

Table 6.2C (Sheet 2 of 2)

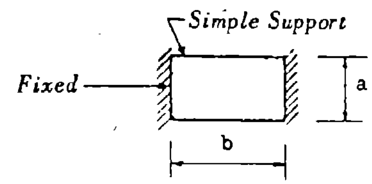

TWO-WAY SLABS: SIMPLE SUPPORTS, TWO LONG SIDES
FIXED SUPPORTS, TWO SHORT SIDES, UNIFORM LOAD

Strain Range	a/b	Load Factor K_L	Mass Factor K_M	Load-Mass Factor K_{LM}	Maximum Resistance	Spring Constant k	Dynamic Reaction V_A	Dynamic Reaction V_B
Plastic	1.0	0.33	0.17	0.51	$\frac{1}{a}\left[12(M_{Pfa} + M_{Psa}) + 12\ M_{Pfb}\right]$	0	$0.09P+0.16R_m$	$0.09P+0.16R_m$
	0.9	0.35	0.18	0.51	$\frac{1}{a}\left[12(M_{Pfa} + M_{Psa}) + 11\ M_{Pfb}\right]$	0	$0.08P+0.15R_m$	$0.09P+0.18R_m$
	0.8	0.37	0.20	0.54	$\frac{1}{a}\left[12(M_{Pfa} + M_{Psa}) + 10.3\ M_{Pfb}\right]$	0	$0.07P+0.13R_m$	$0.10P+0.20R_m$
	0.7	0.38	0.22	0.58	$\frac{1}{a}\left[12(M_{Pfa} + M_{Psa}) + 9.7\ M_{Pfb}\right]$	0	$0.06P+0.12R_m$	$0.10P+0.22R_m$
	0.6	0.40	0.23	0.58	$\frac{1}{a}\left[12(M_{Pfa} + M_{Psa}) + 9.3\ M_{Pfb}\right]$	0	$0.05P+0.10R_m$	$0.10P+0.25R_m$
	0.5	0.42	0.25	0.59	$\frac{1}{a}\left[12(M_{Pfa} + M_{Psa}) + 9.0\ M_{Pfb}\right]$	0	$0.04P+0.08R_m$	$0.11P+0.27R_m$

Table 6.3 (continued)

Table 6.2D (Sheet 1 of 2)

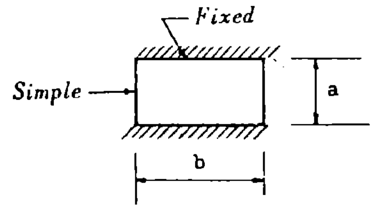

TWO-WAY SLABS: SIMPLE SUPPORTS, TWO SHORT SIDES
FIXED SUPPORTS, TWO LONG SIDES, UNIFORM LOAD

Strain Range	a/b	Load Factor K_L	Mass Factor K_M	Load-Mass Factor K_{LM}	Maximum Resistance	Spring Constant k	Dynamic Reactions V_A	Dynamic Reactions V_B
Elastic	1.0	0.39	0.26	0.67	$20.4\ M^o_{Psb}$	$575\ EI_a/a^2$	0.07P+0.18R	0.09P+0.16R
	0.9	0.40	0.28	0.70	$19.5\ M^o_{Psb}$	$600\ EI_a/a^2$	0.06P+0.16R	0.10P+0.18R
	0.8	0.42	0.29	0.69	$19.5\ M^o_{Psb}$	$610\ EI_a/a^2$	0.06P+0.14R	0.11P+0.19R
	0.7	0.43	0.31	0.71	$20.2\ M^o_{Psb}$	$662\ EI_a/a^2$	0.05P+0.13R	0.11P+0.21R
	0.6	0.45	0.33	0.73	$21.2\ M^o_{Psb}$	$731\ EI_a/a^2$	0.04P+0.11R	0.12P+0.23R
	0.5	0.47	0.34	0.72	$22.2\ M^o_{Psb}$	$850\ EI_a/a^2$	0.04P+0.09R	0.12P+0.25R
Elasto-Plastic	1.0	0.46	0.31	0.67	$\frac{1}{a}\left[12M_{Pfa} + 12(M_{Psb} + M_{Pfb})\right]$	$271\ EI_a/a^2$	0.07P+0.18R	0.07P+0.18R
	0.9	0.47	0.33	0.70	$\frac{1}{a}\left[12M_{Pfa} + 11(M_{Psb} + M_{Pfb})\right]$	$248\ EI_a/a^2$	0.06P+0.16R	0.08P+0.20R
	0.8	0.49	0.35	0.71	$\frac{1}{a}\left[12M_{Pfa} + 10.3(M_{Psb} + M_{Pfb})\right]$	$228\ EI_a/a^2$	0.06P+0.14R	0.08P+0.22R
	0.7	0.51	0.37	0.73	$\frac{1}{a}\left[12M_{Pfa} + 9.8(M_{Psb} + M_{Pfb})\right]$	$216\ EI_a/a^2$	0.05P+0.13R	0.08P+0.24R
	0.6	0.53	0.39	0.74	$\frac{1}{a}\left[12M_{Pfa} + 9.3(M_{Psb} + M_{Pfb})\right]$	$212\ EI_a/a^2$	0.04P+0.11R	0.09P+0.26R
	0.5	0.55	0.41	0.74	$\frac{1}{a}\left[12M_{Pfa} + 9.0(M_{Psb} + M_{Pfb})\right]$	$216\ EI_a/a^2$	0.04P+0.09R	0.09P+0.26R

Table 6.3 (continued)

Table 6.2D (Sheet 2 of 2)

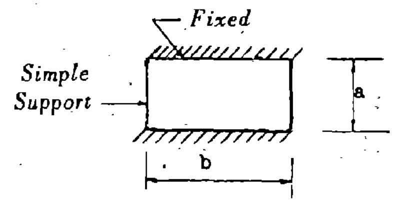

TWO-WAY SLABS: SIMPLE SUPPORTS, TWO SHORT SIDES
FIXED SUPPORTS, TWO LONG SIDES, UNIFORM LOAD

Strain Range	a/b	Load Factor K_L	Mass Factor K_M	Load-Mass Factor K_{LM}	Maximum Resistance	Spring Constant k	Dynamic Reactions V_A	V_B
Plastic	1.0	0.33	0.17	0.51	$\frac{1}{a}\left[12M_{Pfa} + 12(M_{Psb} + M_{Pfb})\right]$	0	$0.09P+0.16R_m$	$0.09P+0.16R_m$
	0.9	0.35	0.18	0.51	$\frac{1}{a}\left[12M_{Pfa} + 11(M_{Psb} + M_{Pfb})\right]$	0	$0.08P+0.15R_m$	$0.09P+0.18R_m$
	0.8	0.37	0.20	0.54	$\frac{1}{a}\left[12M_{Pfa} + 10.3(M_{Psb} + M_{Pfb})\right]$	0	$0.07P+0.13R_m$	$0.10P+0.20R_m$
	0.7	0.38	0.22	0.58	$\frac{1}{a}\left[12M_{Pfa} + 9.8(M_{Psb} + M_{Pfb})\right]$	0	$0.06P+0.12R_m$	$0.10P+0.22R_m$
	0.6	0.40	0.23	0.58	$\frac{1}{a}\left[12M_{Pfa} + 9.3(M_{Psb} + M_{Pfb})\right]$	0	$0.05P+0.10R_m$	$0.10P+0.25R_m$
	0.5	0.42	0.25	0.59	$\frac{1}{a}\left[12M_{Pfa} + 9.0(M_{Psb} + M_{Pfb})\right]$	0	$0.04P+0.08R_m$	$0.11P+0.27R_m$

Table 6.3 (concluded)

TABLE 6.5

DEEP BEAMS: UNIFORM LOAD, ELASTIC RANGE

$H/L > 2/5$

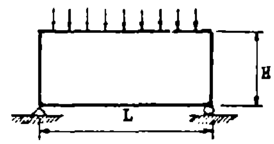

Support Condition	K_L	K_M	K_{LM}	Maximum Resistance, R_m Bending	Shear	δ_b	δ_s	Dynamic Reaction
Fixed	0.53	0.41	0.77	$\frac{12M_P}{L}$	$2V_u$	$\frac{L^3}{384E_cI_a}$	$\frac{L}{3E_cA_w}$	$V = 0.36R + 0.14P$
Simply-Supported	0.64	0.50	0.78	$\frac{8M_P}{L}$	$2V_u$	$\frac{5L^3}{384E_cI_a}$	$\frac{L}{3E_cA_w}$	$V = 0.39R + 0.11P$
Simply-Supported and Fixed	0.58	0.45	0.78	$\frac{8M_P}{L}$	$1.6V_u$	$\frac{L^3}{185E_cI_a}$	$\frac{15L}{48E_cA_w}$	$V_1 = 0.26R + 0.12P$ $V_2 = 0.43R + 0.19P$ (V_2 is at fixed end)

REFERENCES

1. Glasstone, S., editor, The Effects of Nuclear Weapons, U.S. Department of Defense and Atomic Energy Commission, February 1964 reprint (with changes) of 1962 edition, Superintendent of Documents, Washington, D.C.

2. Newmark, N. M., and J. D. Haltiwanger, Principles and Practices for Design of Hardened Structures, Air Force Design Manual, published by Air Force Special Weapons Center, Kirtland AFB, N. M., Rpt. No. SWC-TDR 62-138, December 1962 (AD-295 408).*

3. Manual of Steel Construction, 6th edition, American Institute of Steel Construction, Inc., New York, 1963; also 7th edition, 1970.

4. Building Code Requirements for Reinforced Concrete (ACI 318-63), American Concrete Institute, Detroit, June 1963. See also Ref. 60.

5. Uniform Building Code, 1967 edition, Vol. I, International Conference of Building Officials, Pasadena, Calif.

6. Southern Standard Building Code, 1965 edition, plus Amendments to Southern Standard Building Code, 1967 revision of 1965 edition, Southern Building Code Congress, Birmingham, Ala.

7. BOCA Basic Building Code, 4th edition, 1965, plus accumulative supplement, 1967, Building Officials Conference of America, Inc., Chicago.

8. The National Building Code, 1967 edition, American Insurance Association (successor to National Board of Fire Underwriters), New York.

9. Wiehle, C. K., Shelter Entranceways and Openings, prepared by Stanford Research Institute for the U.S. Office of Civil Defense, Washington, D.C., final report, September 1967 (AD-662 749).

10. Shelter Design and Analysis, Volume 1, Fallout Radiation Shielding, TR-20-(VOL. 1), U.S. Office of Civil Defense, July 1969, plus Changes 1 (July 1969) and 2 (Jan. 1970).

---

* Those references for which "AD-" numbers are shown are understood to be available for purchase from NTIS, Springfield, Virginia, 22151.

11. National Directory of Qualified Fallout Shelter Analysts, U.S. Office of Civil Defense, December 1969.

12. Murphy, H. L., "Fallout Shielding Analysis of Entranceways," Appendix 2 in final report by C. K. Wiehle, Shelter Entranceways and Openings, prepared by Stanford Research Institute for U.S. Office of Civil Defense, September 1967 (AD-662 749).

13. Suarez, M. A., A Method for Evaluation of Radiation Shielding Design, final report prepared by National Engineering Science Company for U.S. Office of Civil Defense, January 31, 1967.

14. Ultimate Strength Design Handbook, Vol. 1, Special Publication No. 17, American Concrete Institute, Detroit, Mich., 1967. See also Ref. 67.

15. Design Manual - AEC Test Structures, prepared by Holmes & Narver, Inc., Los Angeles, Calif., for U.S. Atomic Energy Commission Albuquerque Operations Office, 3 volumes, December 1961.

16. Anderson, F. E., Jr., R. J. Hansen, H. L. Murphy, N. M. Newmark, and M. P. White, Design of Structures to Resist Nuclear Weapons Effects, ASCE Manual of Engineering Practice No. 42, 1961, and Supplement 1963 (combined into a "1964 Edition").

17. Newmark, N. M., and W. J. Hall, Preliminary Design Methods for Underground Protective Structures, report for AFSWC, TDR-62-6, June 1962 (AD-330 059; now unclassified).

18. Murphy, H. L., Ground Motion Predictions for Nuclear Attack Area Studies, Stanford Research Institute Technical Report prepared for U.S. Office of Civil Defense, May 1967 (AD-690 208).

19. Eshbach, O. W., Handbook of Engineering Fundamentals, 2nd ed., Wiley.

20. Brooks, Nancy B., and N. M. Newmark, Development of Procedures for Rapid Computation of Dynamic Structural Response, U. of Illinois Civil Engineering Studies, Structural Research Series No. 83, final report for period July 1, 1953-June 30, 1954 to Physical Vulnerability Div., Directorate of Intelligence, USAF, Contract No. AF33(600)-24994, (formerly CONFIDENTIAL; UNCLASSIFIED as of February 3, 1958).

21. Newmark, N. M., "A Method of Computation for Structural Dynamics," Journal of the Engineering Mechanics Division, American Society of Civil Engineers, Proc. Paper 2094, July 1959; also ASCE Transactions, Vol. 127, Part I, Paper No. 3384, 1962.

22. Manuals-Corps of Engineers, U.S. Army, Engineering and Design, Design of Structures to Resist the Effects of Atomic Weapons, EM 1110-345-413 (July 1959), -414 to -416 (March 1957), -417 (January 1958), and -418 to -421 (January 1960), U.S. Government Printing Office, Washington, D.C. (AD-419 935 for -416).*

23. Newmark, N. M., Design of Openings for Buried Shelters, Report 2-67, U.S. Army Engineer Waterways Experiment Station, Vicksburg, Miss., July 1963.

24. Barksdale, B. H., Jr., and S. R. Wade, Methods of Shelter Cost Analysis, Hayes, Seay, Mattern and Mattern, Architects-Engineers, Washington D.C., for U.S. Office of Civil Defense, February 1967 (AD-646 847).

25. Wiehle, C. K., Shelter Entranceways and Openings, prepared by Stanford Research Institute for U.S. Office of Civil Defense, final report, September 1967 (AD-662 749).

26. Shelter Design and Analysis, Volume 3 - Environmental Engineering for Shelters, U.S. Office of Civil Defense, TR-20-(Vol. 3), May 1969.

27. "Survival Shelters," Chapter 15, ASHRAE Guide and Data Book - Applications, 1968, American Society of Heating, Refrigerating and Air-Conditioning Engineers, Inc., New York.

28. Baschiere, R. J., and M. Lokmanhekim, Shelter Forced Ventilation Requirements Using Unconditioned Air, GARD final report 1266, General American Transportation Corp., Niles, Mich., for U.S. Office of Civil Defense, February 1967.

29. Brode, H. L., A Review of Nuclear Explosion Phenomena Pertinent to Protective Construction, The RAND Corporation, Report R-425-PR, prepared for USAF Project RAND, May 1964 (AD-601 139). Brode has published a later version, "Review of Nuclear Weapons Effects," Annual Review of Nuclear Science, Vol. 18, 1968 (Annual Reviews, Inc., Palo Alto, Calif., 94306).

30. Manual of Standard Practice, 19th Edition, Concrete Reinforcing Steel Institute, Chicago, Illinois, and Western Concrete Reinforcing Steel Institute, Burlingame, California, 1968.

31. Discussions with project consultant, Professor W. J. Hall, University of Illinois.

32. Report of ASCE-ACI Joint Committee on Ultimate Strength Design, Structural Division, American Society of Civil Engineers, Proceedings Vol. 81, Paper No. 809, October 1955.

* Reprinted, without change, and redesignated; e.g., EM 1110-345-420 became Headquarters, Department of the Army, TM 5-856-8, and EM 1110-345-421 became TM 5-856-9.

33. Biggs, J. M., Introduction to Structural Dynamics, 1964 (McGraw-Hill).

34. Norris, C. H., et al., Structural Design for Dynamic Loads, 1959 (McGraw-Hill).

35. Newmark, N. M., and W. J. Hall, Preliminary Design Methods for Underground Protective Structures, U. of Ill. for USAF (contract AF 29(601)-1171), Dec. 1959 (declassified September 3, 1965); Appendix B. (Reference 17 is a later version, and is available from NTIS, Springfield, Virginia 22151.)

36. Hughes-Caley, F., and R. Kiang, Blast-Closure Valves, Stanford Research Institute Final Report for U.S. Office of Civil Defense, August 1965.

37. Vodvarka, F. J., Full Scale Burns in Urban Areas Shelter Experiments, IIT Research Institute Final Technical Report for U.S. Office of Civil Defense, June 1969.

38. Gurdjian, E. S., J. E. Webster, and H. R. Lissner, "Studies on Skull Fracture with Particular Reference to Engineering Factors," Am. Jour. Surgery, 78, 736, 1949.

39. White, C. S., I. G. Bowen, and D. R. Richmond, "A Comparative Analysis of Some of the Immediate Environmental Effects of Hiroshima and Nagasaki," Health Physics, Vol. 10, Pergamon Press, Oxford, 1964.

40. Recommended Practices for Welding Reinforcing Steel, Metal Inserts and Connections in Reinforced Concrete Construction, American Welding Society, AWS D12.1-61, 1961.

41. Rempel, J. R., Ground Shock and the Survival of the Contents of Personnel Shelters, Resistance of Human and Inanimate Contents of Hardened Shelters to Nuclear-Induced Ground Motion, Stanford Research Institute Technical Report prepared for OCD, November 1967, with Addendum, May 1968.

42. Building Exits Code for Life Safety from Fire, 19th ed., National Fire Protection Association, NFPA No. 101, Boston, 1963.

43. ASHRAE Handbook of Fundamentals, American Society of Heating, Refrigerating and Air-Conditioning Engineers, Inc., New York, 1967.

44. Bürgi, H., Lieutenant-Colonel, Fire Tests With Cars Parked in an Enclosed Car Park Building, reprint from the "Schweizerische Feuerwehr-Zeitung," No. 12/1970, Cerberus Ltd, CH-8708 Mannedorf ZH (Tests made on April 10, 1970 in Bern, Switzerland).

45. Guidelines for the Use of SI Units of Measurement in the Publications of the American Society of Civil Engineers (June 1972), A.S.C.E., New York, N.Y. (extracted from ASTM E380-70); ASTM E380-72, June 1972, was used for later conversion values.

46. Engineering News-Record, October 26, 1972, page 16.

47. ______, December 21, 1972, page 27.

48. Progressive Architecture, July 1972, page 96.

49. Smith, Paul D., P.E., Fire Protection and Life Safety for Underground Buildings, Gage-Babcock & Associates, Inc., letter report (unpublished), March 1972.

50. Murphy, H. L., Feasibility Study of Slanting for Combined Nuclear Weapons Effects (Revised), Stanford Research Institute Technical Report, for U.S. Office of Civil Defense (now Defense Civil Preparedness Agency), 2 vols., July 1971. (AD-734 831 and 2)*

51. Waterman, T. E., Fire Laboratory Test - Phase III, IIT Research Institute Final Technical Report for Defense Civil Preparedness Agency, February 1973.

52. Standard Grading Rules for West Coast Lumber, West Coast Lumber Inspection Bureau, Portland, Oregon, No. 16, Revised January 1, 1973 ($1).

53. 1970 Standard Grading Rules for Southern Pine Lumber, Southern Pine Inspection Bureau, Pensacola, Florida, including Supplements #1 and #2.

54. Timber Construction Manual, American Institute of Timber Construction, Washington, D.C., 1st ed., 1966 (Wiley); 2nd ed., 1974 is available.

55. Wood Handbook, Forest Products Laboratory, Forest Service, U. S. Department of Agriculture, Handbook No. 72, 1955; new edition is available, Revised August 1974, through the Supt. of Documents, Washington, D. C. 20402.

56. Gaylord, E. H. Jr., and C. N. Gaylord, editors, Structural Engineering Handbook, 1968, (McGraw-Hill); Section 16.

57. Merritt, F. S., editor, Standard Handbook for Civil Engineers, 1968 (McGraw-Hill); Section 11.

---

* Report contents are included herein - in this Consolidated Printing of Four Technical Reports - except portions superseded by later material in another of the four reports.

58. Merritt, J. L., and N. M. Newmark, Design of Underground Structures to Resist Nuclear Blast, U. of Ill., Civil Engineering Studies-Structural Research Series No. 149, Final Report for Office of Chief of Engineers, U. S. Army, April 1958 (Basic to AFDM, Ref. 2, per Dr. W. J. Hall, U. of Ill.)

59. Urquhart, L. C., editor-in-chief, Civil Engineering Handbook, 4th ed., 1959 (McGraw-Hill).

60. Building Code Requirements for Reinforced Concrete.(ACI 318-71), American Concrete Institute, Detroit, 1971. (See also Ref. 4)

61. Murphy, H. L., and J. E. Beck, Slanting for Combined Nuclear Weapons Effects: EXAMPLES WITH ESTIMATES, AND AIR BLAST ROOM FILLING, Stanford Research Institute Technical Report, for Defense Civil Preparedness Agency, June 1973. (AD-783 061)*

62. Murphy, H. L., and J. R. Rempel, Slanting for Combined Nuclear Weapons Effects: FIRE HAZARD REDUCTION, Stanford Research Institute Technical Report for Defense Civil Preparedness Agency, August 1972. (AD-763 472)*

63. Commentary on Building Code Requirements for Reinforced Concrete (ACI 318-71), American Concrete Institute, Detroit, Michigan, 1971.

64. "Bond Stress - The State of the Art," Reported by ACI Committee 408, Title No. 63-53, Journal of the ACI, Proceedings Volume 63, No. 11, November 1966; also published in ACI Manual of Concrete Practice, Part 2, 1973, American Concrete Institute, Detroit, Michigan.

65. Ferguson, P. M., Reinforced Concrete Fundamentals, with Emphasis on Ultimate Strength, 2nd ed., John Wiley & Sons, Inc., New York, N. Y., 1965.

66. Timoshenko, S. P., and J. M. Gere, Theory of Elastic Stability, 2nd ed., McGraw-Hill, New York, N. Y., 1961.

67. Design Handbook in Accordance with the Strength Design Method of ACI 318-71, VOLUME 1, 2nd ed., Publication SP-17(73), American Concrete Institute, Detroit, Michigan, 1973 [2nd (Corrected) Printing, March 1974]. See also Ref. 14.

* Report contents are included herein - in this Consolidated Printing of Four Technical Reports - except portions superseded by later material in another of the four reports.

68. Derivation of Equations, Ultimate Strength Design Handbook Volume 2, Columns, Supplement to SP-17A, American Concrete Institute, Detroit, Michigan (originally published as SP-7 until superseded by Ref. 70, but latter omits material now in this reference; available in xerographic reproduction from ACI).

69. Columns by Ultimate Strength Design Including Square Footings, Concrete Reinforcing Steel Institute, Chicago, Illinois, 1967.

70. Ultimate Strength Design Handbook, VOLUME 2, COLUMNS, Special Publication No. 17A, American Concrete Institute, Detroit, Michigan, 1970.

71. Rippstein, E. E., Reinforcing Bar Detailing, Concrete Reinforcing Steel Institute, Chicago, Illinois, 1970.

72. Manual of Standard Practice for Detailing Reinforced Concrete Structures (ACI 315-74), 6th ed., American Concrete Institute, Detroit, Michigan, 1974.

73. Godden, W. G., Numerical Analysis of Beam and Column Structures, 1965 (Prentice-Hall, Inc.); Chapters 1 and 3 (Reference 1.4 may be useful for source background).

74. Wiehle, C. K., Summary of the Dynamic Analysis of the Exterior Walls and Floor Systems of 50 NFSS Buildings, Stanford Research Institute Technical Report for U. S. Defense Civil Preparedness Agency, Washington, D. C., June 1974 (limited distribution; not in DDC).

75. DCPA Attack Environment Manual, Chapter 4, Research Directorate, Defense Civil Preparedness Agency, Washington, D. C. 20301, June 1972.

76. EMP Protection for Emergency Operating Centers, TR-61-A, May 1971, DCPA.

77. EMP Protective Systems, TR-61-B, November 1971, DCPA.

78. EMP and Electric Power Systems, TR-61-D, July 1973, DCPA.

79. Cohen, E., and E. B. Laing, "Perimeter Acquisition Radar Building at Safeguard Complex," ACI Journal, Spetember 1974, American Concrete Institute, Detroit, Michigan 48219.

80. Murphy, H. L., and J. E. Beck, Slanting for Combined Nuclear Weapons Effects: BLAST-RESISTANT DESIGN/ANALYSIS WITH EXAMPLES, Stanford Research Institute Technical Report, for Defense Civil Preparedness Agency, December 1974. (AD-A016 631)*

---

* Report contents are included in this Consolidated Printing of four reports.

BIBLIOGRAPHY

Merritt, J. L., and N. M. Newmark, Design of Underground Structures to Resist Nuclear Blast, U. of Ill., Civil Engineering Studies, Structural Research Series No. 149, April 1958. Suggested by Professor W. J. Hall (University of Illinois) as being basic to AFDM (Ref. 2).

Personnel Shelters & Protective Construction, NAVDOCKS P-81, Navy Bureau of Yards & Docks (now Naval Facilities Engineering Command), Washington, D.C., Sept. 1961; plus Change 1 (2/7/62) and Change 2 (7/9/62). Consider for effects data, structural and other analyses, etc., and review for slanting ideas.

Project Harbor report, about 1964 (not Little Harbor, a more recent report). Suggested by Professor Hall, particularly in connection with human tolerances.

Modification of Existing Buildings as Community Shelters, DRAFT for OCD Prof. Guide Series, Ammann & Whitney, Jan. 1965.

Suggested Building Code Provisions for Fallout Shelters, report prepared by Graves-Hill & Assoc., Architects, Lexington, Ky., for OCD, TR-36, May 1966. Contains review of various building codes.

Denton, D. R., A Dynamic Ultimate Strength Study of Simply Supported Two-way Reinforced Concrete Slabs, USA-WES Tech. Rpt. 1-789 prepared as final report for OCD, July 1967.

Janney, J. R., "Full-Scale Structural Testing and the New York World's Fair," Civil Engineering, ASCE, December 1968.

Raths, C. E., N. L. Scott, and J. R. Janney, Full-Scale Testing of New York World's Fair Structures, Volume I, The Bourbon Street Structure, Building Research Advisory Board, National Academy of Sciences, Washington, D.C., 1969.

The three bibliographic items above will be considered for floor slab analyses of structural resistance.

Heugel, W. F., and D. I. Feinstein, Shelter Evaluation Program, IITRI Technical Center Final Report, project M6088 to OCD (task 1614A), February 1967.

Longinow, A., Civil Defense Shelter Options for Fallout and Blast Protection (Dual-Purpose), IITRI Final Report for OCD, May 1967.

Longinow, A., et al., Civil Defense Shelter Options, IIT Research Institute Interim Report for OCD, November 1970.

OCD publications (several) and film/slides on Slanting (for fallout). Review for ideas translatable to slanting against combined effects.

Wiehle, C. K., and J. L. Bockholt, Existing Structures Evaluation, Part I: WALLS, Stanford Research Institute Technical Report prepared for OCD, November 1968 (AD-687 293).

Iverson, J. H., Existing Structures Evaluation, Part II; Window Glass and Applications, Stanford Research Institute Final Report prepared for OCD, December 1968 (AD-687 294).

Jensen, G. F., Existing Structures Evaluation, Part III: Structural Steel Connections, Stanford Research Institute Report prepared for OCD, December 1969 (AD-701 088).

Wiehle, C. K., and J. L. Bockholt, Existing Structures Evaluation, Part IV: Two-Way Action Walls, Stanford Research Institute Technical Report prepared for OCD, September 1970.

Allen, F. C., "Environmental Control Systems," Chapter VII, Parametric Study of Shelter System Costs by T. J. Logothetti et al, Stanford Research Institute report for U.S. Office of Civil Defense, Washington, D.C., January 1969.

The following ten reports were reviewed, seeking actual or potential changes in guidance affecting the design of footings to resist dynamic loads. Review results indicated no change, only support, of the guidance already provided by Reference 2 recommendations.

Carroll, W. F., Dynamic Bearing Capacity of Soils, Report 5; Vertical Displacements of Spread Footings on Clay: Static and Impulsive Loadings, U. S. Army Engineer Waterways Experiment Station, Vicksburg, Mississippi, Technical Report No. 3-599, Sept. 1963 (AD-450 619).

Jackson, J. G. Jr., and P. F. Hadala, Dynamic Bearing Capacity of Soils, Report 3; The Application of Similitude to Small-Scale Footing Tests, USAEWES Tech. Report No. 3-599, Dec. 1964 (AD-454 374).

N. M. Newmark and Associates, Design of Model Test Program for a Buried Field Shelter, USAEWES Contract Report No. 1-110, May 1965 (AD-465 567).

Hadala, P. F., Dynamic Bearing Capacity of Soils, Report 4; Investigation of a Dimensionless Load-Displacement Relation for Footings on Clay, USAEWES Tech. Report No. 3-599, June 1965 (AD-467 081).

Lysmer, J., Vertical Motion of Rigid Footings, USAEWES Contract Report No. 3-115, June 1965 (AD-469 600).

Poplin, J. K., Dynamic Bearing Capacity of Soils, Report 2; Dynamically Loaded Small-Scale Footing Tests on Dry, Dense Sand, USAEWES Tech. Report No. 3-599, Sept. 1965 (AD-623 516).

Drnevich, V. P., J. R. Hall, Jr., and F. E. Richart, Jr., Transient Loading Tests on a Rigid Circular Footing, USAEWES Contract Report No. 4-146, Feb. 1966 (AD-631 369).

Meyer, G. D. and W. J. Flathau, Static and Dynamic Laboratory Tests of Unreinforced Concrete Fixed-End Arches Buried in Dry Sand, USAEWES Tech. Report No. 1-759, Feb. 1967 (AD-650 851).

Kennedy, T. E. and J. T. Ballard, Dynamic Test of A Model Flexible-Arch-Type Protective Shelter, Report 1; Pilot Test, USAEWES Tech. Report No. 1-768, Apr. 1967 (AD-651 349).

Hadala, P. F. and J. G. Jackson, Jr., A Model Study of the Small Boy Footing Behavior, USAEWES Tech. Report No. 3-793, Aug. 1967 (AD-659 254).

Technical Reports
Consolidated Printing

VOLUME 2

SLANTING IN NEW BASEMENTS FOR COMBINED NUCLEAR WEAPONS EFFECTS: A Consolidated Printing of Four Technical Reports

October 1975

FEASIBILITY STUDY OF SLANTING FOR COMBINED NUCLEAR WEAPONS EFFECTS (Revised), Volumes 1 and 2 — *July 1971*

Slanting for Combined Nuclear Weapons Effects: FIRE HAZARD REDUCTION — *August 1972*

Slanting for Combined Nuclear Weapons Effects: EXAMPLES WITH ESTIMATES, AND AIR BLAST ROOM FILLING — *June 1973*

Slanting for Combined Nuclear Weapons Effects: BLAST-RESISTANT DESIGN/ANALYSIS WITH EXAMPLES — *December 1974*

For:

DEFENSE CIVIL PREPAREDNESS AGENCY
WASHINGTON, D.C. 20301

Contracts DAHC 20-67-C-0136 and 20-71-C-0292
DCPA Work Units 1154E and 1154H

STANFORD RESEARCH INSTITUTE
Menlo Park, California 94025 · U.S.A.

11-45

Technical Reports
Consolidated Printing

VOLUME 2

SLANTING IN NEW BASEMENTS FOR COMBINED NUCLEAR WEAPONS EFFECTS: A Consolidated Printing of Four Technical Reports

October 1975

By: H. L. Murphy, J. R. Rempel and J. E. Beck
Facilities and Housing Research

FEASIBILITY STUDY OF SLANTING FOR COMBINED NUCLEAR WEAPONS EFFECTS (Revised), Volumes 1 and 2 — *July 1971*

By: H. L. Murphy

Slanting for Combined Nuclear Weapons Effects: FIRE HAZARD REDUCTION — *August 1972*

By: H. L. Murphy and J. R. Rempel

Slanting for Combined Nuclear Weapons Effects: EXAMPLES WITH ESTIMATES, AND AIR BLAST ROOM FILLING — *June 1973*

By: H. L. Murphy and J. E. Beck

Slanting for Combined Nuclear Weapons Effects: BLAST-RESISTANT DESIGN/ANALYSIS WITH EXAMPLES — *December 1974*

By: H. L. Murphy and J. E. Beck

For:

DEFENSE CIVIL PREPAREDNESS AGENCY
WASHINGTON, D.C. 20301

Contracts DAHC 20-67-C-0136 and 20-71-C-0292
DCPA Work Units 1154E and 1154H

STANFORD RESEARCH INSTITUTE
Menlo Park, California 94025 · U.S.A.

CONTENTS

Volume 1

Preceding page blank

CONTENTS (Continued)

CONTENTS (Continued)

CONTENTS (Concluded)

TABLES

FIGURES

Preceding page blank

FIGURES (Continued)

FIGURES (Continued)

11-54

FIGURES (Concluded)

Appendix A

NUCLEAR WEAPONS EFFECTS

By J. H. Iverson

Appendix A

NUCLEAR WEAPONS EFFECTS

By J. H. Iverson

The purpose of this appendix is to describe the derivation of Figs. 2-1 through 2-8. In all but one case, these figures were based on Reference 1,* hereinafter referred to as ENW.

Figures 3.67a and 3.67b of ENW were used in the preparation of Table A-1. Heights-of-burst (HOB) were optimized to obtain the maximum range for each overpressure shown in the air burst portion of the table. HOB equal to zero was used to obtain the contact surface burst ranges.

Table A-1

DATA FOR A 1 kt WEAPON YIELD

Peak Overpressure (psi)	Air Burst Range (ft)	Air Burst HOB (ft)	Contact Surface Burst Range (ft)
6	2000	917	1367
8	1707	830	1133
10	1456	727	1021
15	1194	650	818
20	945	614	709
30	672	565	584
40	565	500	510
50	525	466	459

* References are listed at the end of this appendix.

Figure 2-1

The air burst curves were derived as follows:

1. The data in Table A-1 were used in ENW Figure 3.69 to obtain positive phase duration on the ground versus overpressure and versus dynamic pressure at eight pressures each.

2. The best least squares curve fit of six curve types was chosen and the positive phase duration was cube root scaled to 1 Mt.

3. Curves for overpressure and dynamic pressure were plotted, each versus positive phase duration. The equation of each curve is:

   a. For overpressure: $t = 1/(0.282831 + 0.009655p)$
   b. For dynamic pressure: $t = 3.71018 - 0.013855p$

   where t and p are positive phase duration and pressure, respectively.

The surface burst curves were derived as follows:

1. Ground distances were recorded from ENW Figure 3.69 at the point where each positive phase duration curve intersected HOB = 0.

2. These ground distances versus the positive phase duration values for overpressure and dynamic pressure were each subjected to a least squares curve fit of six different curves; the best fit in each case was:

   a. For overpressure: $t = d/(3110.49 + 1.07867d)$
   b. For dynamic pressure: $t = 0.419881 - (57.8975/d)$

   where d is the distance from ground zero for 1 kt.

3. The data shown in Table A-1 were then substituted into these equations, which resulted in eight relationships between overpressure and positive phase duration and eight relationships between dynamic pressure and positive phase duration.

4. The best least squares curve fit of six curve types was then obtained for both overpressure and dynamic pressure versus positive phase duration. The equations (scaled to 1 Mt) for the curves plotted are:

   a. For overpressure: $t = 6.03979p^{-0.398083}$
   b. For dynamic pressure: $t = 1/(0.258683 + 0.0016909p)$

   where t and p are positive phase duration and pressure, respectively.

Data obtained from Brode,[2]* Figs. 24 and 25, were also plotted on Fig. 2-1. Data points for positive phase duration versus peak overpressure were extracted from Brode for overpressure and dynamic pressure. Each set of data was subjected to a least squares curve fit of six different curves; the best fit in each case was:

a. For overpressure: $t = 5.03615\ p^{-0.430266}$

b. For dynamic pressure: $t = 1/(0.262811 + 0.0121185p)$

where t and p are positive phase duration and peak overpressure, respectively. The curves of these two equations were plotted on both parts of Fig. 2-1 since Brode indicates that positive phase duration for a given peak overpressure is independent of HOB.

Figures 2-2 Through 2-8

Figures 2-2 through 2-8 required that air burst slant range be calculated from the data in Table A-1 (for a contact surface burst, the slant range equals the range). Cube-root scaling provided the scaled, slant ranges shown in Table A-2 needed for the derivation of these figures.

Table A-2

SLANT RANGES FOR 200 kt AND 1 Mt

Overpressure	Air Burst				Contact Surface Burst			
	200 kt		1 Mt		200 kt		1 Mt	
(psi)	Yards	Miles	Yards	Miles	Yards	Miles	Yards	Miles
6	4290	2.44			2666	1.51	4560	2.59
8	3701	2.10			2211	1.26	3780	2.15
10	3173	1.80	5424	3.08	1989	1.13	3400	1.93
15	2651	1.51	4531	2.57	1597	0.91	2730	1.55
20	2197	1.25	3756	2.13	1381	0.78	2360	1.34
30	1712	0.97	2926	1.66	1141	0.65	1950	1.11
40	1471	0.84	2515	1.43	994	0.56	1700	0.96
50	1368	0.78	2340	1.33	895	0.51	1530	0.87

* Superscript numerals are related to the reference list at the end of this appendix.

Figure 2-2 depicts thermal energy as a function of peak overpressure. To prepare the air burst curves, the Table A-2 values were used in ENW Fig. 7.105 to obtain values of radiant exposure (thermal energy). These data were then scaled to 200 kt and 1 Mt by multiplying by 200 and 1000, respectively (ENW page 364). To prepare the surface burst curves, an existing computer program[3] was used to obtain data for plotting.

Figures 2-4 and 2-7, the free-field gamma radiation intensity curves, were derived by applying the data in Table A-2 to ENW Figs. 8.27a and 8.27b. The units of roentgens were changed to rads in accordance with note 9, ENW, page 579.

Figures 2-5 and 2-8 values were obtained as follows:

1. The integrated neutron flux, obtained by entering ENW Fig. 8.61 with the data in Table A-2, was multiplied by 1.8×10^{-9} rad to obtain dose in rads (ENW paragraph 11.90).

2. These data were scaled to 200 kt and 1 Mt by multiplying by 200 and 1000, respectively, as described in ENW paragraph 8.61.

Figure 2-3 is merely a summation of the data found in Figs. 2-4 and 2-5, and Fig. 2-6 is a similar summation of the data found in Figs. 2-7 and 2-8.

REFERENCES

1. Glasstone, S., editor, The Effects of Nuclear Weapons, U.S. Dept. of Defense and Atomic Energy Commission, February 1964 reprint (with changes) of 1962 edition (Supt. of Documents, Washington, D.C.).

2. Brode, H. L., A Review of Nuclear Explosion Phenomena Pertinent to Protective Construction, RAND Corp. rpt. R-425-PR, prepared for USAF Project RAND, May 1964 (AD-601 139). Brode has published a later version, "Review of Nuclear Weapons Effects," Annual Review of Nuclear Science, Vol. 18, 1968 (Annual Reviews, Inc., Palo Alto, Calif., 94306).

3. Martin, S., and S. Holton, Preliminary Computer Program for Estimating Ignition Ranges for Nuclear Weapons, USNRDL-TR-866, U.S. Naval Radiological Defense Laboratory, San Francisco, California, June 1965.

Appendix B

FIRE HAZARD REDUCTION

By R. G. Carroll and J. R. Rempel

8/72

Appendix B

FIRE HAZARD REDUCTION

By R. G. Carroll and J. R. Rempel*

PREFACE

This appendix demonstrates the extent to which architects and engineers can slant their building designs and otherwise provide for protection against the fire hazard to life during a nuclear weapons attack. The method chosen to carry out this goal has been to describe in some detail the nature of the hazard--as far as it is presently known--and then to set forth as explicitly as possible how the threat may be lessened or eliminated to the best of present understanding. This means that the appendix may be used as a prototype guide for architects and engineers wishing to learn about the fire threat accompanying weapon detonation and to do something to minimize it.

---

* Written originally by R. G. Carroll for the first (June 1969) combined nuclear weapons effects slanting report; revised by J. R. Rempel for this report. References 1 through 31 are associated with the original version; references 32-63 were added in this revision.

Preceding page blank

CONTENTS

FIGURES

TABLES

NOTATION

A	area of ventilation opening; smaller of two dimensions of equivalent radiator used in Law Method; empirical constant used to characterize fire progress
B	empirical constant used to characterize fire progress
C	separation distance between buildings according to Law Method; line of sight distance between elements of area on radiator and receiver
dA_1	infinitesimal element of surface area on thermal radiator
dA_2	infinitesimal element of surface area of thermal receiver
e	emissivity of thermal radiation
H	height of ventilation opening; height of equivalent radiator (used in Law Method)
I	intensity of thermal radiation
I_o	intensity of thermal radiation leaving radiator
L	length of equivalent radiator (used in Law Method)
N	ratio of larger equivalent radiator dimension to smaller (used in Law Method)
r	depth of recess in building facade (used in Law Method); burning rate
t	time, measured from ignition of fire
T	absolute temperature, degrees Kelvin
x	measure of fire progress, e.g., weight burned at time t
X	total fire progress at end of combustion, e.g., total weight of combustible material

α	scale factor used in adjusting fire progress
σ	Stefan-Boltzman constant = 1.36×10^{-12} cal/cm^2 sec degK
ϕ	configuration factor
θ_1	angle between normal to dA_1 and line of sight to dA_2
θ_2	angle between normal to dA_2 and line of sight to dA_1

ABBREVIATIONS

BTU	British Thermal Unit
C	degree Celsius
cal	calorie
cm	centimeter
F	degree Fahrenheit
fps	feet per second
ft	feet
hr	hour
in.	inch
K	degree Kelvin
kg	kilogram
kt	kiloton
lb	pound
m	meter
min	minute
mph	miles per hour
Mt	megaton
psf	pounds per square foot
psi	pounds per square inch
sec	second
sf	square foot

Appendix B

FIRE HAZARD REDUCTION

By R. G. Carroll and J. R. Rempel

Section 1 - Introduction

Fire may be brought to the shelter building by:

- Direct thermal radiation from the exploding nuclear weapon.*
- Windborne firebrands scattered into the air from fires burning elsewhere.
- Heat transfer (by radiation, convection, or both) from adjacent burning buildings or other nearby fires.
- Air blast effects on potential secondary fire sources within the building itself, such as heaters, fuel lines, fuel containers, and electrical equipment.

Under conditions of 6 to 12 miles visibility, air burst megaton weapons are capable of causing thermal ignitions of newsprint and similar tinder materials at a ground radius out to where the blast overpressure is approximately 2 psi.[1-3] Some types of fuel susceptible to ignition by thermal radiation are thin combustible materials (such as newspapers, dry grass and leaves) and window-exposed fuels (such as curtains and drapes). In general, the variables affecting the critical ignition energy (or the amount of thermal energy necessary to cause ignition) of tinder fuels are thickness, composition, color, and moisture content. Ignition of tinder fuels does not necessarily mean that a fire will develop. Other, heavier combustible materials must be in proximity to sustain combustion, and this condition is prevalent in residential and commercial buildings.[4] Therefore, it is probable that ignition of window fuels, i.e., drapes, shades, and curtains, would determine the range of sustained ignitions and multiple fires.

Variables that tend to mitigate the effects of the weapon thermal pulse are atmospheric obscuration and reduction of visibility,[3] lowered

---

* Single 1 Mt weapon air or surface burst is assumed (Chapter 1).

number or density of ignition points, fuel shielding from thermal radiation, window glass, and window screens. Ordinary, clean, single-pane window glass, for example, has a thermal transmittance in the range of 0.75.[5] Since thermal radiation is emitted within a few seconds (80% of total thermal energy within 8 seconds for a 1 Mt air burst[1]), window glass and screens would survive long enough before the arrival of the blast wave to be effective in attenuating the thermal radiation.

When all of these factors and variables are considered, the net effect is a decreased probable range of sustained ignition. As an example, for a condition of 6 to 12 miles visibility and a 1 Mt air burst, the ignition ground radius for beige cotton curtains shielded by window glass and screens is 2 to 3 miles[6] (8-15 psi range). As another approach, under the same conditions, Crowley et al.[7] estimate that for a completely exposed dwelling room, the probability of sustained room ignition is 50%. Therefore, it can be expected that sustained ignitions sufficient to cause rapid build-up of extensive fires would occur within the limits of the 5 psi radius, where blast damage is also likely to be intensive.

Blast/fire interactions are of two kinds: possible extinguishment by blast winds of primary fires (i.e., those caused by the weapon thermal pulse), and creation by blast of debris that is later exposed to fire. Although investigators have usually agreed that subsequent blast will not extinguish any substantial proportion of fires begun by the weapon thermal pulse[1(§7.54)], recent preliminary experiments suggest that small fires existing at the time of blast arrival tend to be suppressed by blast waves of 2.5 to 5 psi peak overpressure.[32] This is not true of fires in materials capable of supporting "smoldering" combustion, nor of blast waves of lower overpressure. In any case, fire suppression by blast winds will apply only to fires ignited by the radiant pulse from the weapon and not to fires ignited by firebrands or neighboring fires.

In some cases blast debris may be exposed to the final portion of the weapon thermal pulse, but only at extremely high overpressures will post-blast irradiance from the weapon be generally dangerous.[33]

In the regions beyond the 5 psi perimeter, the density of primary ignitions would diminish sharply with distance. Although large fires, even mass fires or conflagrations, may occur in scattered locations, the rate of build-up and firespread would be slow enough that sufficient time would be available for occupants of threatened shelters to take remedial action and, if necessary, to evacuate, hopefully to other shelters.

At all overpressure levels out to the 2 psi range, the fire-raising potential of the thermal pulse would be augmented by blast-induced, secondary fires. According to Moll,[8] secondary ignitions are estimated to have a frequency of 0.006 per 1,000 sf of total floor area that has sustained damage by overpressures of 2 psi or more. This corresponds to about one ignition per 100 houses.

Recent studies have demonstrated a significant potential for firespread in windborne embers or firebrands.[34,35] For example, an experimental, full-scale fire produced dangerous brands 600 to 800 ft downwind, depending on wind velocity. According to one investigator,[36] brands were the principal means of firespread in several large California suburban conflagrations between 1965 and 1970. In the California examples, transfer of heat between the small adjacent buildings by radiation seldom produced enough heating to cause ignition; brands falling on roofs or coming through windows were responsible for most of the firespread. Furthermore, brands are able to trigger actual ignition of material preheated by radiation and thus effectively lower the threshold for firespread between neighboring structures below that expected from considerations of radiative transfer alone. This effect has been reported[37] from the Rotterdam conflagration following the German attack of 1940, and Moysey and Muir have attempted to quantify it in the laboratory.[38]

Wind has other firespreading effects. From observations of test fires in full sized, all-wood, one-story buildings Wiersma and Martin[62] suggest that fire-heated air, driven by an ambient wind of 15 mph, may double the range (on the downwind side) within which exposed wood samples will be ignited over the ignition range with no wind. They note also that observed burning rate of a structure is increased by 30% when wind velocity is raised from 8 to 15 mph.

The phenomenon of firestorm* has been observed during certain large forest conflagrations, and occasionally as a result of World War II air raids on German and Japanese cities. For example, in Hamburg on July 27-28, 1943, British bomb loads of 50% high explosive and 50% incendiary bombs dropped on the city in a four-hour long attack started many individual, nearly simultaneous fire outbreaks over a wide area.[9] Because of the HE danger, and debris in the streets, and the enormous number

---

* Firestorms are of interest as an upper limit of fire severity, even though their likelihood of occurrence in the U.S. is considered to be negligible, as is discussed later herein.

of fires, fire fighters were helpless to prevent the individual fires from merging. The result was a classical firestorm characterized by centripetal fire-generated winds that sharply defined the geographical extent of destruction and by total destruction of everything flammable within the fire zone. Air temperatures in the streets were variously estimated to be as high as 1400 to 2400 F at the peak of the storm, which raged for 10 to 20 hours and was not approachable for approximately 48 hours.[39]

Even so, survival of a sheltered population in such a region is considered probable. Of some 280,000 people in the Hamburg firestorm, 85% survived and the majority of casualties were suffered by those in relatively primitive, basement-type shelters.[9] Of those people who occupied specially designed bunkers and splinter-proof shelters, 100% survived the firestorm. In Hamburg, bunkers were more or less isolated structures, many of which withstood direct HE bomb hits; they were sealed and ventilation was controllable. People perished in basement shelters under buildings that collapsed around them. In this way the fire could have been brought into direct contact with the shelter, and the ventilation have been either cut off altogether or the fresh air supply taken into the shelter through burning debris piles at the entrance and thus could have been dangerously contaminated with noxious gases.

This is not meant to suggest that firestorms are probable in the United States as a result of a nuclear attack. Rodden et al.[10] state that the optimum combination of the many conditions necessary to initiate a firestorm would be encountered infrequently. It should be kept in mind, however, that a single nuclear weapon with its great capacity for initiating primary and secondary fires simultaneously over a broad area as well as creating debris and fallout hazard, may be capable of causing firestorm, particularly within the 5 psi perimeter. In fact the fire resulting from the Hiroshima explosion of August 1945 is described as a firestorm,[1] which extended out to approximately the 4 psi range.[39] (Geographical conditions at the Nagasaki nuclear attack in 1945 prevented creation of a firestorm.) Furthermore, conditions in a small area during a heavy attack may for all practical purposes be indistinguishable from those existing in a true "firestorm."

No matter how fires are started, subsequent development and spread would be determined by the amount and distribution of combustible materials in the vicinity. Since measures would be taken to protect the slanted shelter building from direct thermal effects and blast induced fires, the primary concern is to minimize the probability of ignitions stemming from burning buildings adjacent to the shelter building. Studies have

shown that the probability of firespread depends, among other factors, on building density or "built-upness" of an area and therefore on the distance between buildings.[11]

Given that most buildings would not be equipped with protective window screens or other reflective devices and that the interior fire load of combustible furnishings and materials in all buildings would be sufficient to sustain combustion after ignition,[4] there is a possibility that structures and buildings adjacent to a shelter building would be on fire an hour or two after an attack. However, even though a shelter building may be equipped with thermal protection devices over all window openings, these would be blown away by the blast wave immediately subsequent to the thermal pulse. The shelter building would therefore be exposed to ignition by thermal radiation and convection from adjacent building fires. Since firespread by convection and brands requires at least modest horizontal winds and since spread by these means may be greatly enhanced by radiation, some protection of shelter buildings against radiant firespread should be considered by designers.

The laws governing radiant transfer of heat are well known; therefore, separation distances between buildings can be calculated to ensure a substantial degree of protection against radiant firespread from a burning building to a neighboring building.

Margaret Law[12] has provided a simplified procedure for such calculations, as described in the next section. Law's procedure is designed to reduce fire hazard from peacetime fires. It contemplates the eventual presence of professional firefighters at the scene and it does not contemplate firespread into a heavily blast-damaged environment. For this reason the siting techniques outlined in the next section must be supplemented by other structural countermeasures as described briefly in Section 4 below.

The Law method provides separation distances taking into account only thermal radiation emanating from the vertical wall openings of adjacent burning buildings; therefore, additional methods have been introduced to give consideration to the effects of flame and to bending of flames by wind. Exposure to the effects of convection currents has not been considered.

The harmful effects of fire on biological systems, particularly man, are discussed briefly in Section 3 below, as knowledge basic to all personal countermeasures against fire.

Finally, Section 5 mentions a few countermeasures shelter occupants might take for protection against harm by fire.

At the end of this appendix appear a reference list, including all references used in the preparation of this appendix; a bibliography, listing the most pertinent other literature reviewed; and Annex A, describing alternative methods for developing building separation distances.

Section 2 - Siting for Fire Hazard Reduction

Background

Two major factors enter into consideration when planning building separation distances:

- The level of radiation received from a fire in an adjacent building.
- The level of radiation that will ignite materials both on the outside of buildings and within rooms exposed by window openings.

The basis for determining these factors is oven-dry, unpainted wood, whose behavior has been shown by tests to be representative of most combustible materials. Spontaneous ignition of such wood occurs only at intensities of radiation above 0.8 cal/cm^2-sec. In the open, spontaneous ignition takes place rather quickly after exposure to radiation and either occurs within about 2 minutes or not at all.[12] Pilot ignition occurs when a secondary source of ignition is brought sufficiently near to ignite the gases emitted by a heated surface, but for pilot ignition to occur in the open, heating times as long as 10 minutes may be needed. Above an intensity of 0.3 cal/cm^2-sec, pilot ignition of wood from sparks or flying brands can take place.[12] Accordingly, 0.3 cal/cm^2-sec is taken as the upper limit of radiation exposure for determining separation distances.

Significant attenuation of incident radiation heat flux through window glass has been noted and measured.. However, for purposes of this guide, no credit for such attenuation can be taken for radiation heat flux emanating from adjacent burning buildings since all window glass is assumed to have been destroyed by the blast wave.

Intensity of Thermal Radiation

The intensity of thermal radiation, I, emitted by a radiator can be found from:

$$I = e \sigma T^4$$

where

e = emissivity = 1.0 for this guide

σ = Stefan-Boltzman constant

= 1.36×10^{-12} cal/cm^2-sec^1-deg. K^4

T = absolute temp. = (C + 273)

The temperature of a fire depends on the rate of burning, which classifies fires into two types:

- Those in which ventilation is restricted and the rate of burning depends on window size.

- Those in which the window area is 0.5 to 1.5 times the floor area, where the rate of burning depends on the fire load; these are considered to be fully ventilated fires.

Peak radiating intensities for test fires are shown in Fig. B-1 for a fully ventilated fire. From this figure, it is seen that the radiation intensity peaks at about 4 cal/cm^2-sec for all fire loads greater than 12 psf in cubical rooms; Law further stated that fully ventilated fire intensities vary little for ratios of window area to floor area of approximately one-half and greater. For the case of restricted ventilation, Fig. B-1A summarizes test results;[12] maximum fire temperature in this case depends on the quantity $A\sqrt{H}$, where A is the area of the ventilation opening (e.g., window) and H is the height or vertical dimension of the opening. The temperature is independent of fire load and room size. The figure shows temperature reaching 1100 F or radiation intensity reaching 4 cal/cm^2-sec at an abscissa of 5.5 m$^{5/2}$ or 107 ft$^{5/2}$; at higher values of the abscissa temperature is constant at 1100 F and thus has the same value as in a fully-ventilated fire. Law has argued that the assumption of a radiating intensity of 4 cal/cm^2-sec regardless of the ventilation introduces an error that is conservative for the purposes of fire protection and that in any case is small since, as will be seen below, a small opening can not pass a significant amount of radiation to neighboring buildings; therefore, Law recommended using 4 cal/cm^2-sec for all fire loads equal to or greater than 5 psf of floor area and 2 cal/cm^2-sec where fire loads are less than 5 psf.

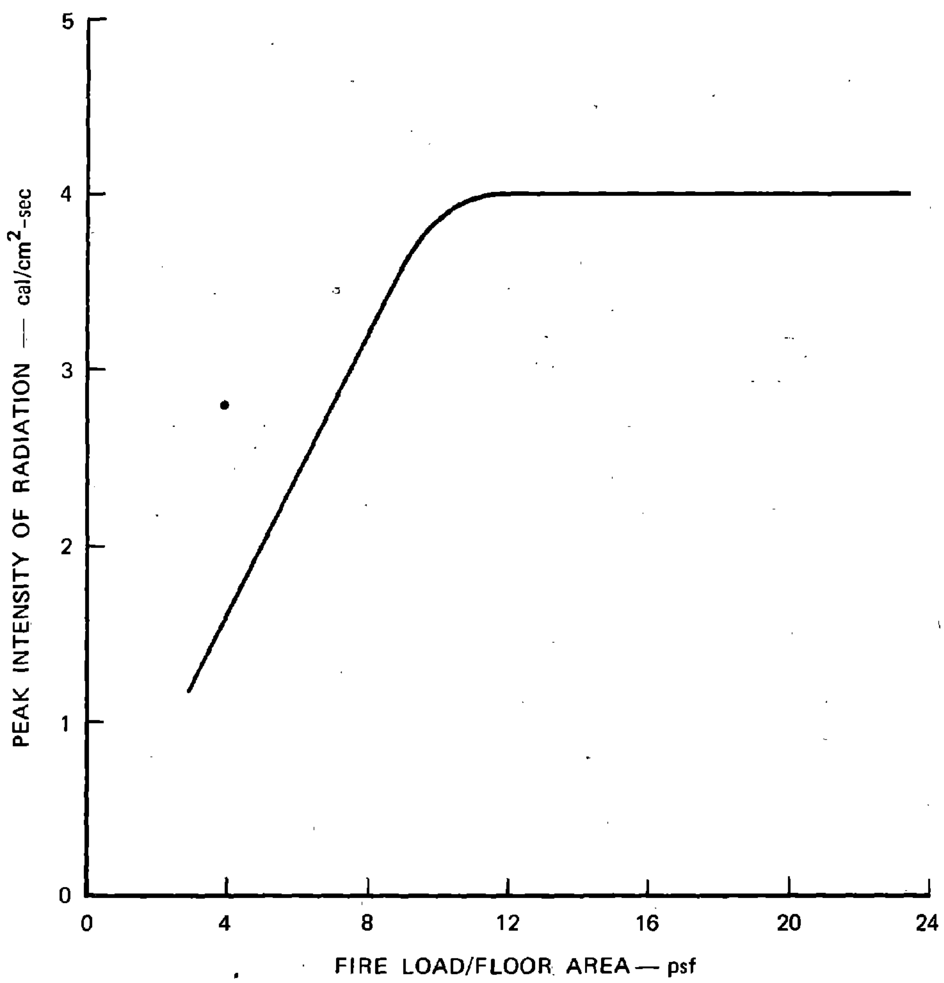

FIG. B-1 TEST FIRE RADIATION INTENSITIES FOR CUBICAL ROOMS[12] (Floor and window areas approximately equal)

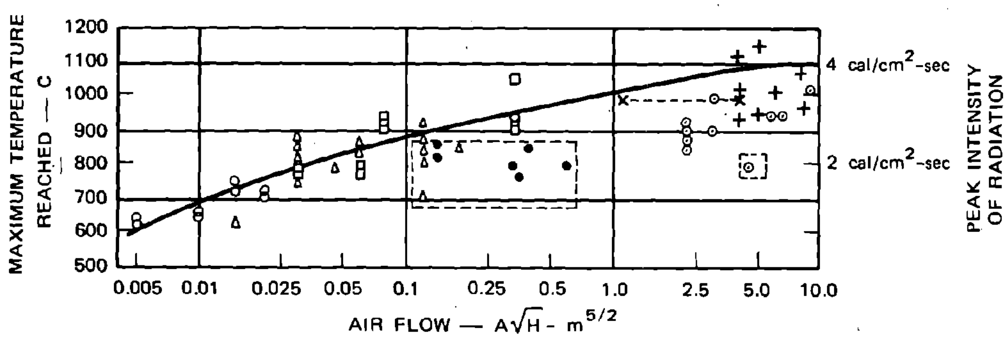

SOURCE	SCALE I FLOOR AREA 0.09 m^2	SCALE II FLOOR AREA 0.49 m^2	SCALE III FLOOR AREA 1 m^2	LARGE-SCALE FLOOR AREA 9 m^2
J.F.R.O.	○	△	□	+
Swedish Test				x---x
Kawagoe			•	⊙

FIG. B-1A MAXIMUM TEMPERATURE AND AIR FLOW.[12] Points within the broken lines are those where the fire load is less than 25 kg/m^2 (5 psf)

Configuration Factor

The intensity of radiation, I, on a receiving surface can be related to the intensity, I_o, emitted at the surface of a radiator by the expression.

$$I = \phi I_o$$

where ϕ is the configuration factor. This factor takes into account the geometry of the radiator as "seen" by the receiving surface and the separation distance between the radiator and the receiving surface. In the usual case, many openings in a burning building will be radiating; therefore, the above expression for n openings becomes

$$I = (\phi_1 + \phi_2 + \ldots\ldots\phi_n)I_o$$

Using 0.3 cal/cm^2-sec as the maximum tolerable I on a receiving surface, we have

$$\sum \phi_n = \frac{0.3}{I_o}$$

Thus the separation required becomes the distance where the maximum value of $\sum \phi_n$ is less than the ratio $\frac{0.3}{I_o}$. Since ϕ is proportional to S/C, where S = area of radiating surface and C = the separation distance to the receiving surface, it is possible, given the dimensions and configurations of windows and other openings, to compute the separation distance corresponding to the required value of $\sum \phi_n$. Except for simple radiator geometries, calculation of the magnitude of configuration factors is complicated. Nevertheless, circumstances may arise where the criteria for employing the simplified Law method to determine separation distance cannot be met, or perhaps greater precision in computing distances may be required. In this event, the only recourse is to determine separation distance as a function of ϕ of the radiation surface. Annex A presents two ways in which this may be accomplished: a computational method and an optical analog method.

Law's Method

On the premise that most cases will be accommodated if it is assumed that the radiator and receiving surface are parallel to each other, Law has developed a simplified method for determining separation distance.

This method embodies the concept of an "equivalent radiator," which is merely the area on the facade of a building that encloses all facade openings. As used herein, facade or wall openings refer to the area of openings, such as windows and combustible siding, that are capable of transmitting or emitting radiation from the wall of a burning building. Separation distances have been calculated for various percentages of wall openings and the dimension ratio of the equivalent radiator. These are shown in Figs. B-2 and B-3 for fire loads less than, and equal to or greater than, 5 psf. The dimension ratio, N, is a function of the length and height of the equivalent radiator. If the smaller of the two dimensions is designated "A," then N is the ratio of the larger dimension to A. Figure B-4 illustrates the derivation of A and N.

Entering Fig. B-2 or B-3 with the appropriate N and the percentage of wall openings in the equivalent radiator (as shown in Fig. B-4) a value of C/A can be read directly, and, C, the separation distance, is then easily calculated.

As an example using data from Fig. B-4 and assuming a fire load greater than 5 psf:

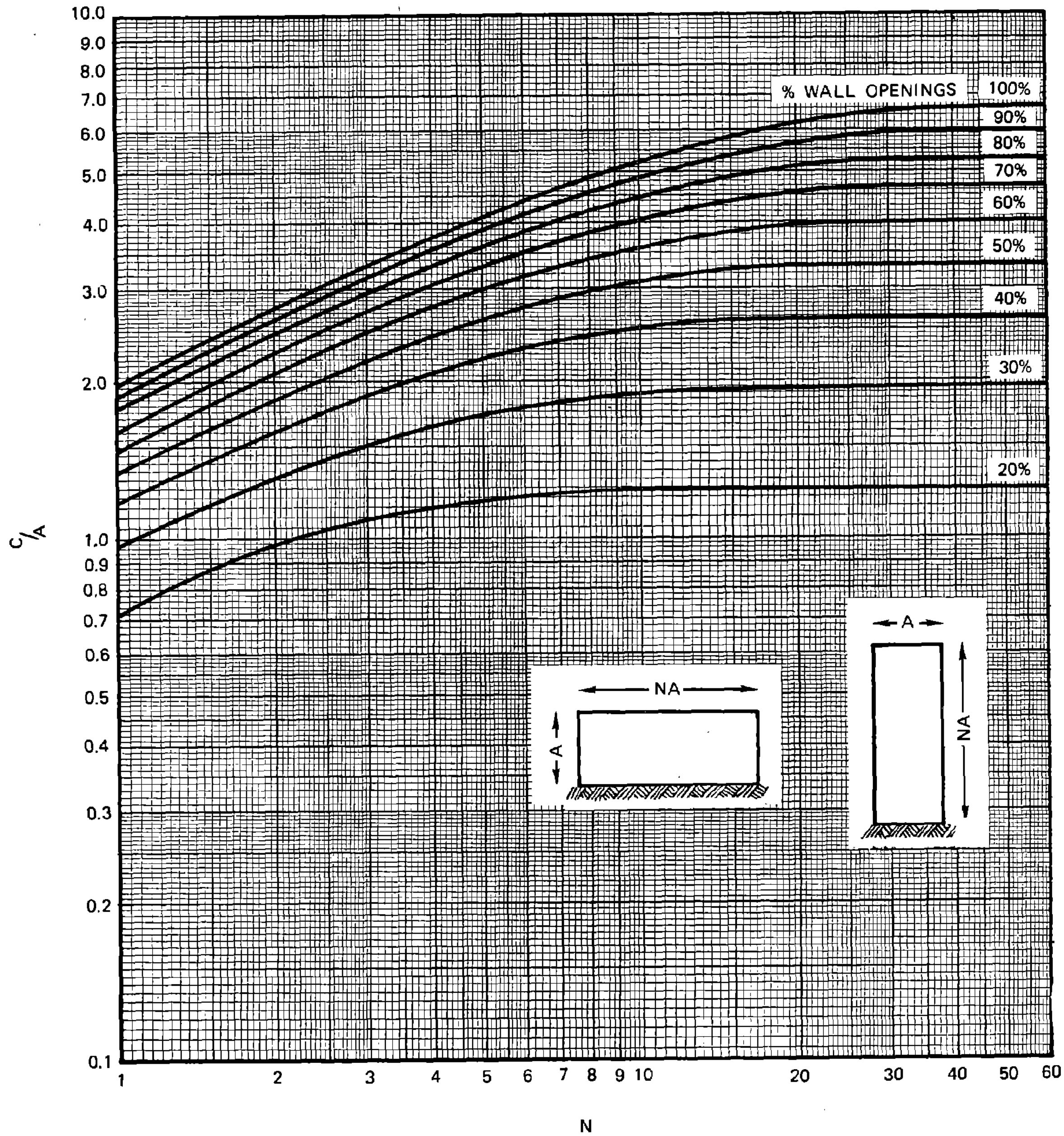

FIG. B-2 SEPARATION DISTANCE "C" FOR FIRE LOAD OF 5 PSF OR MORE[12]

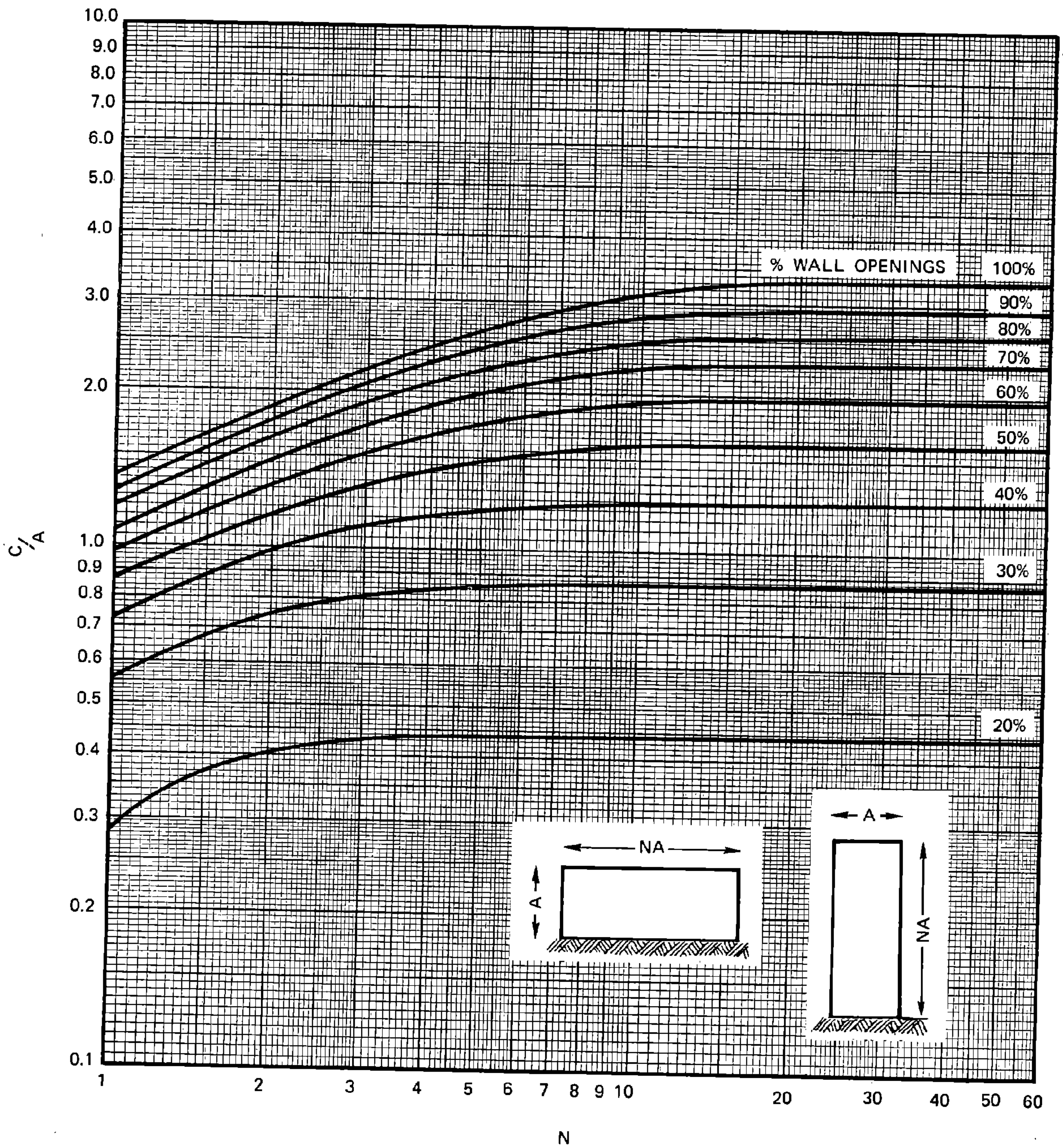

FIG. B-3 SEPARATION DISTANCE "C" FOR FIRE LOAD LESS THAN 5 PSF[12]

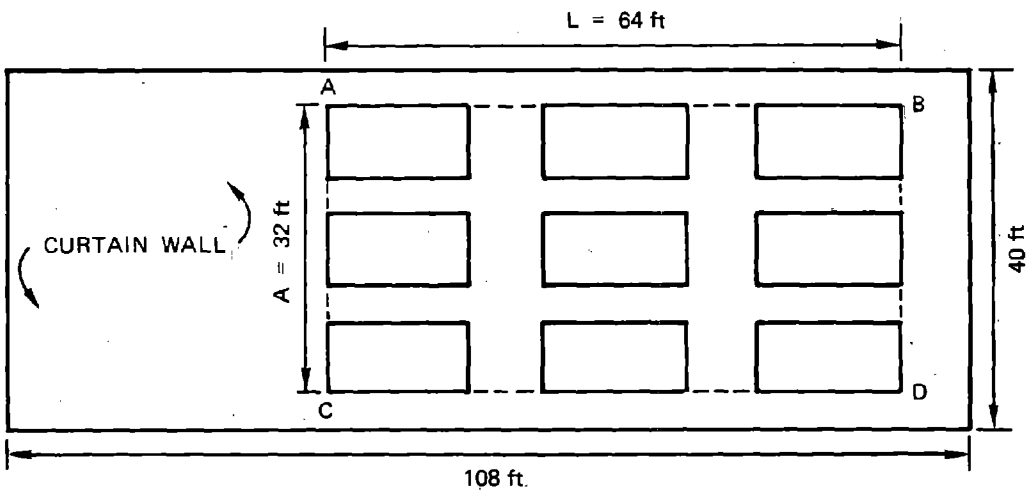

ELEVATION (Scale: 1" ≈ 20 ft)

- $H < L$, therefore $A = H = 32$ ft
- $L = 64$ ft
- $N = 64/32 = 2$
- Area ABCD = 2048 sf
- Area ABCD encloses all openings and is termed the "equivalent radiator."
- Area of openings (16 x 18) x 9 = 1152 sf
- $\frac{\text{Area of openings}}{\text{Area of ABCD}} = \frac{1152}{2048} = 56\%$

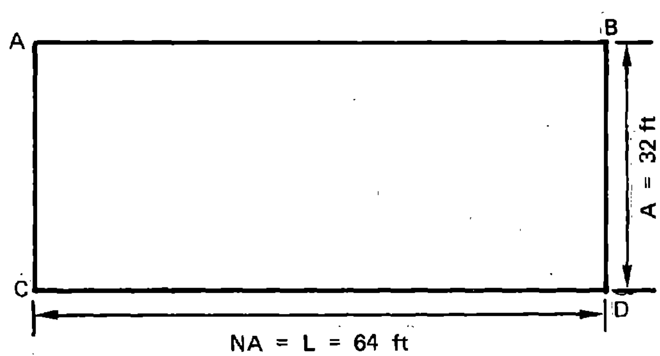

ELEVATION OF EQUIVALENT RADIATOR

FIG. B-4 DERIVATION OF DIMENSIONS FOR EQUIVALENT RADIATOR

- $N = 2.0$
- Percentage of openings = 56%
- Enter Fig. B-2 with N
- Read up to the 56% curve (interpolate)
- Then $C/A = 1.95$
- $C = (1.95)A = (1.95)32 = 62.4$ ft.

Building Facade Openings

a. Introduction

The separation distance, C, is very sensitive to the percentage of openings in the adjacent burning buildings. Obviously, the most conservative approach would be to assume that all buildings have 100% openings; this condition will probably prevail at those ground ranges within the 8 psi overpressure region and all framed buildings will probably have 100% openings within the 2 psi region. However, there are several reasons for not taking this conservative approach, which would lead to impractically large separation distances. These reasons are connected with the effects of blast wind upon existing fires and with certain assumptions made by Law in deriving building separation.

Moll[8] cites studies indicating that many incipient fires would be extinguished in fine fuels by blast winds with a peak velocity greater than 120 fps (associated with about 2.2 psi overpressure) and in thicker fuels at 150 fps velocities (3.0 psi overpressure). In addition, whereever curtain walls and windows are demolished, the extremely high blast wind would carry away and scatter the light ignition fuels. Admittedly, this is intuitive and a generalization, since in some cases building fuels may be concentrated within a building by blast and thereby aggravate the fire hazard.

The assumptions made by Law, which are perfectly suitable for peacetime fires but which are overly conservative for the conditions of nuclear attack, are:

(1) For fuel loads of 5 psf or greater, the thermal radiation intensity is 4 cal/cm^2-sec. This corresponds to a limiting fire temperature of about 1100 C (2000 F).

(2) The emissivity of the radiating building is constant at unity.

(3) Heat is being radiated simultaneously at the peak intensity from all openings in a building facade.

For purposes of fire protection in a nuclear attack environment, these assumptions are more restrictive than necessary. For example, thermal radiation is directly proportional to the fourth power of the absolute temperature of the radiating fire. Variations from the limiting fire temperature can cause significant differences in radiation intensity. Also, the emissivity of a building fire would generally be somewhat less than unity, and it would infrequently be the case when all wall openings are radiating heat of the same intensity in a multistory building. This is so because the combustible contents of buildings and the rate of burning will vary from room to room.

These circumstances suggest that, within the 2 psi region, the error caused by selection of building openings as solely the percentage of window and door openings in a facade, thereby ignoring openings caused by curtainwall collapse, would be offset in most cases by blast wind action on potential ignition points and by the conservative assumptions made by Law in her calculations.

If a mass fire occurred, it is possible that buildings adjacent to the shelter building could ignite and present burning facades that are one expanse of flame. The Law method, as cited herein, does not accommodate this eventuality.* Radiation from such an exposure would exceed the 4 cal/cm^2-sec used by Law as a maximum. However, these conditions would evolve and advance relatively slowly and permit evacuation of an exposed shelter building as an ultimate alternative.

Accordingly, it is recommended that, in the application of the Law method, determination of openings in exposing, adjacent building facades be limited to the ratio of the area of windows and combustible siding to the overall area of the facade (this represents a more hazardous fire situation than in the higher overpressure regions where walls have been destroyed but also where fuel loads have been blown away or reduced to debris or rubble).

---

* See, however, subsection entitled "Corrections for Flames" below.

b. Recessed Elevations

If a portion of the radiating building facade is set back, as in Fig. B-5, an adjustment in separation distance may be possible.

Generally two types of recesses will be found: (1) a recess with openings on all three sides and (2) a recess with openings only on the rear wall.

With openings on all three sides, the recess will appear as a radiating enclosure. In this case, the area of openings in the recess should be totaled and expressed as a percentage of the area of the aperture. If the total area of openings in the recess is equal to or greater than the area of the aperture, the aperture should be considered as a radiator with 100% openings. In either instance, the aperture is then treated simply as another element of the equivalent radiator representing the facade as a whole, and the corresponding separation distance is found as before. Figure B-5 includes an example problem.

When openings occur only on the rear wall of the recess, a reduction in separation distance is possible. First a value of the separation distance C_1 is found, assuming, as before, that all of the openings within the recess are radiating from the aperture. Then the area of openings in the recess are reduced by the factor

$$\left(\frac{C_1}{C_1 + r}\right)^2$$

where r is the depth of recess. The reduction in the area of openings is possible because of the apparent reduction when viewed from a point at the separation distance. Figure B-6 illustrates the rationale. With the reduction in the area of openings for the recess, a second distance, C_2, is found. An example problem is also given in Fig. B-6.

c. Elevation with Setback

As shown in Fig. B-7, when a part of a building is set back, there can be a corresponding adjustment in separation distance. First the separation distance is found assuming the elevation is in one plane. Then by constructing an equivalent radiator in the manner shown in Fig. B-7, a second separation line is drawn. The final line of separation is then traced as illustrated.

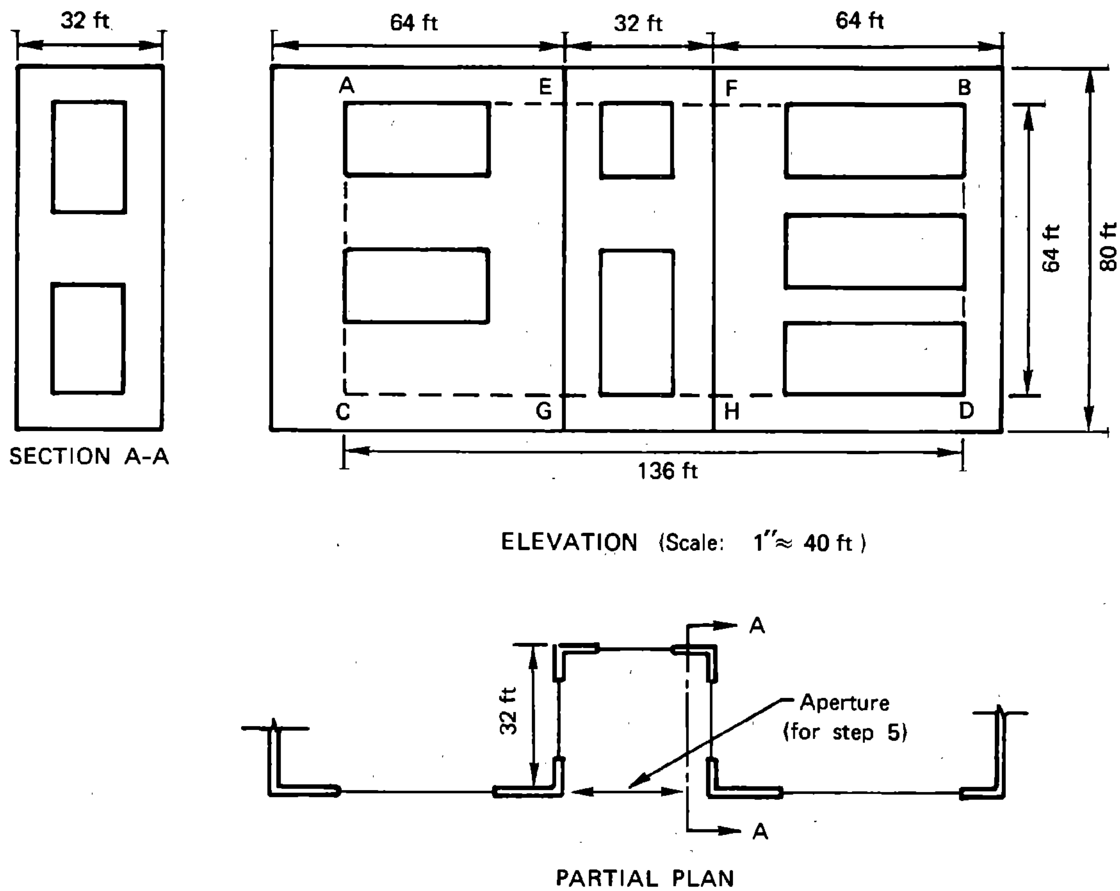

1. Area ABCD = 136 x 64 = 8704 sf
2. Area of openings in AECG = 1024 sf
3. Area of openings in FBHD = 1920 sf
4. Area of openings in recess = 2304 sf
5. Area of EFGH = 2048 sf which is less than 2304 sf of recess openings
6. Therefore EFGH = 100% openings
7. Total area of openings = items 2 + 3 + 5 = 4992 sf
8. Percentage openings = $\frac{\text{item 7}}{\text{item 1}} = \frac{4992}{8704} = 57\%$
9. A = 64 ft
10. $N = \frac{136}{64} = 2.13$
11. From Fig. B-2, C/A = 2.1
12. C = A x 2.1 = 64 x 2.1 = 134 ft

FIG. B-5 SEPARATION DISTANCE FOR RECESSED ELEVATION WITH OPENINGS ON ALL RECESS SIDES[12]

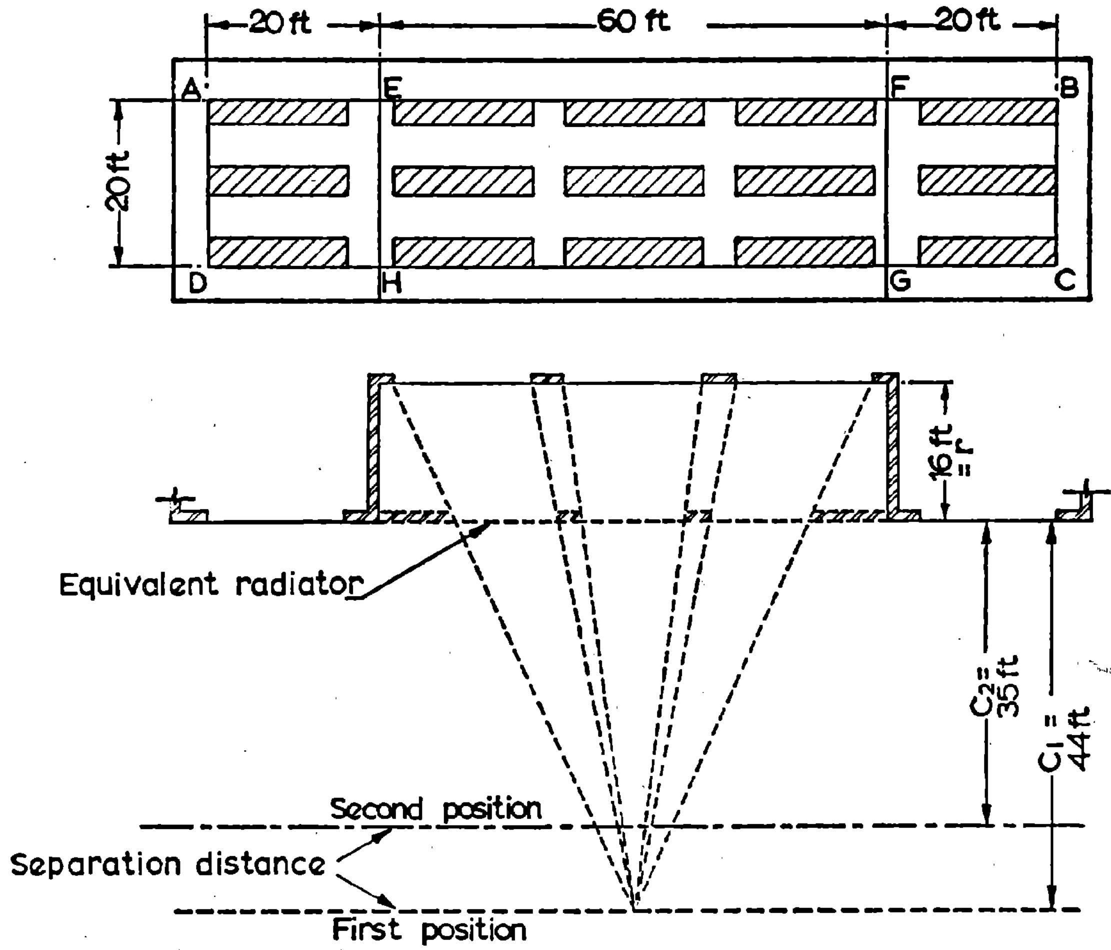

- Given a percentage of openings = 40% for areas AEDH, EFHG, and FBGC
- For the equivalent radiator ABCD, N = 5, A = 20
- From Fig. B-2, a 40% opening gives C_1 = 44 ft.
- Reduction factor = $\left[\dfrac{C_1}{C_1 + r}\right]^2 = \left[\dfrac{44}{60}\right]^2 = 0.54$
- Therefore EFGH has 0.54 x 40% = 22% opening
- Then for ABCD overall openings = 29%
- For N = 5, A = 20, from Fig. B-2, $C_2 \approx 35$ ft

FIG. B-6 SEPARATION DISTANCE FOR RECESSED ELEVATION WITH OPENINGS IN REAR WALL ONLY[12]

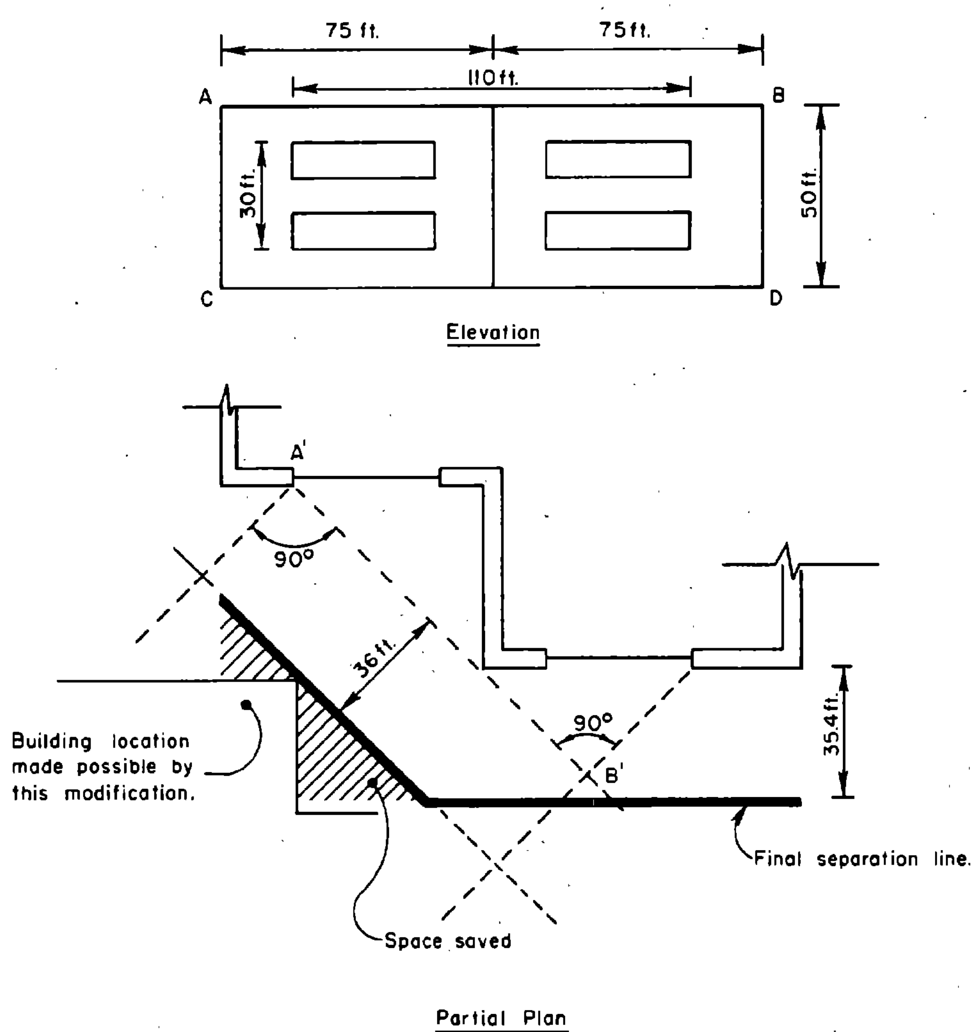

FIG. B-7 SEPARATION DISTANCE WITH SETBACK[12]

The computation for Fig. B-7 is:

- 21% openings
- $A = 30$
- More than 5 psf fuel load
- N for ABCD = 110/30 = 3.67
- From Fig. B-2, C/A = 1.18 and C = 35.4 ft
- N for equivalent radiator A'B' = 115/30 = 3.83
- From Fig. B-2, C/A = 1.20 and C' = 36 ft

The space saved is hatched in Fig. B-7.

d. Elevation with Widely Spaced Openings

If openings, or groups of openings, in a radiating facade are spaced widely apart, a point opposite one may receive a negligible contribution of radiation from the others. When this is true, the openings or groups should be considered separately.

The separation distance is calculated first for an equivalent radiator enclosing all openings in the facade. Then, if the horizontal distance between two groups of openings is greater than twice the calculated separation distance, they should be treated as separate radiators. An example is shown in Fig. B-8.

Factors Modifying Separation Distances

a. Windowless Facade in Shelter Building

Separation distances may be reduced for those facades of shelter buildings that have no openings and are constructed of noncombustible materials. In the extreme, the separation can be zero if a 3-hour fire wall exists between the two buildings.[13] The amount of reduction for other than fire walls is a matter of judgment. Phung[14] states that an examination of German cities suffering fire bombings indicates that a 10-foot separation between two brick buildings "had about a 50% chance of preventing fire spread."

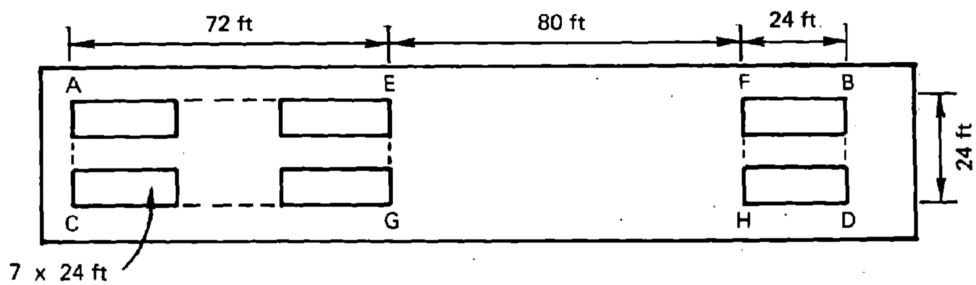

ELEVATION (Scale: 1" ≈ 40 ft)

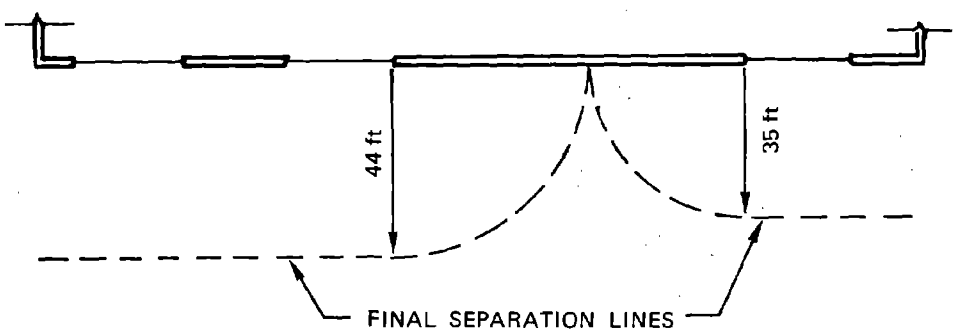

PARTIAL PLAN

- For equivalent radiator ABCD, Area = 176 x 24 = 4224 sf
- A = 24, N = $\frac{176}{24}$ = 7.3
- Area of each opening = 7 x 24 = 168 sf
- Area of all openings in ABCD = 1008 sf
- Percentage openings = $\frac{1008}{4224}$ = 24%
- From Fig. B-2 C/A = 1.45, C = 35 ft
- Since 80 ft is greater than twice 35 ft consider each area, AECG and FBHD, separately
- Area AECG has 39% openings, N = 3, A = 24. Then C from Fig. B-2 = 44 ft
- Area FBHD has 58% openings, N = 1, A = 24. Then C from Fig. B-2 = 35 ft

FIG. B-8 SEPARATION DISTANCE FOR BUILDING WITH WIDELY SPACED OPENINGS[12]

b. Exposing Building Taller Than Shelter Building

If exposing, adjacent buildings are one story or more taller than the shelter building, there would be a danger of exposing the shelter building roof to a dangerous level of heat radiation when the calculated separation distance is reduced. Obviously, judgment is required in this eventuality. If the exposed roof is Class A or B, as defined by the National Fire Code,[15] this hazard is nominal. However, for Class C, D, E, or F, danger of ignition is present.

Corrections for Flames

The remainder of this section deals with corrections, caused by the effects of flames, that can be applied to separation distances calculated in accordance with the foregoing Law method. Rigid application of these corrections could increase separation distances to the extent that an otherwise eligible slanting candidate might become ineligible. Therefore, it is recommended that, as a general rule, flame corrections should be applied only to the extent that candidacy (at least for more detailed consideration) is not obviated. The rationale for this recommendation lies in the fact that 100% protection from fire spread, e.g., by flying embers, on the basis of building separation distances, is neither practical nor possible in urban areas. Also, as previously stated, the objective of this appendix is to minimize the chance of firespread on the premise that shelter evacuation is reserved as the ultimate alternative in those instances where the shelter building is dangerously threatened by fire, even where a fallout radiation hazard exists.

a. Adjustment for Window Flames

Law's method does not consider the contribution to the total thermal radiation from a burning building made by flames emitted from windows and other openings. In those instances where an exposing building may have a high interior fuel load and a large percentage of wall openings, a fully involved fire in the building may present a single expanse of flames over 100% of the exposing facade. One way in which to account for this circumstance is to assume a greater percentage of wall openings in the exposing facade than actually exists.

b. Adjustment for Roof Flames

Adjustment for roof flames must be approached on a case-by-case basis. The type of roof construction, its age and condition, the number and type of roof openings, and the presence or absence of combustible roof structures--such as cooling towers--are all factors that must be considered.

It is suggested that recommendations of experienced fire department personnel be obtained where the combustibility of roofs may be an issue. Their suggestions as to potential flame height may be accounted for by increasing the area of a burning facade by an amount equal to average flame height multiplied by the horizontal dimension of the facade. The flame area would of course be incorporated into the equivalent radiator.

Cohn[11] recommends roof flame heights as follows:

• Flat or slightly peaked wood roofs	30 ft
• Medium peaked and bow-string roofs	45 ft
• High peaked roofs	60 ft

c. Bending of Flames Due to Wind

A rational method to account for the increased separation distance due to bending of flames has not been developed. However, it has been suggested[11] that exposure separation distances should be increased as follows:

- For "light" winds - no increase
- For "average" winds - add 25 feet to the separation distance for light winds
- For "higher" winds - add 40 feet to the separation distance for light winds.

Section 3 - Interior Fires and Associated Biological Hazards

Background

Fire hazards and behavior in a shelter building following an enemy attack must be regarded differently than in a non-shelter building fire under non-attack conditions. During peacetime, the rate of fire spread and smoke production assumes primary importance in terms of establishing a safe exit time for evacuation of building occupants. Furthermore, building component fire ratings imply that evacuation of the building is possible, organized fire-fighting forces are available, and an adequate water supply exists.[16,17]

On the other hand, evacuation of a shelter building would be hazardous following nuclear attack because of fallout. Since a shelter building fire may compel evacuation if left to grow unchecked, shelter occupants would have to be prepared to suppress incipient fires throughout the shelter building.

Fire Hazard Factors

The most pertinent biological fire hazard factors affecting shelter occupants are:

- Heat
- O_2 depletion; CO_2 and CO build-up
- Smoke

In considering these factors for purposes of this guide, the shelter area is assumed to be located in the basement of a multistory building.

a. Heat

In circumstances where a shelter wall or ceiling is exposed to a building fire, the hazard to shelter occupants from heat would depend on the fire intensity and duration and the diffusivity and thickness of the exposed shelter component. The most hazardous condition would occur when

the shelter ceiling, functioning as the floor slab of the first story, is exposed to a rubble fire.

Fuel, or fire loads in commercial, industrial, and public buildings commonly exceed 10 psf in a significant proportion of spaces.[4,17]

Leutz[18] states that with a building fire load of approximately 7 psf German investigations determined that it is possible for the debris from a building fire to maintain a temperature of 300-400 C (572-752 F) on a floor slab for periods of up to 5 to 6 hours. Under the assumption that temperatures in the debris will obtain <u>at the exposed surface of the floor slab</u>, Leutz states that modeling techniques indicate a temperature of 50 C (122 F) is reached on the underside of an 8-inch, reinforced concrete floor slab within 2 to 3 hours after a temperature of 300-400 C (572-752 F) is reached and sustained on the upper surface of the slab.

It is not known if the effect of ventilation on the underside of the exposed slab was considered by Leutz. Further, his assumption that temperatures inside a burning debris pile located on a concrete slab are also developed at the exposed surface of the slab may be overly conservative and needs to be tested by appropriate experiments. However, survival of shelter occupants under these conditions may depend heavily on adequate ventilation or other countermeasures such as removing or cooling off the burning debris on the exposed side of the slab.

Tests have been conducted by the National Bureau of Standards[17] in fire resistive buildings using various fire loads to simulate occupancy types. The time-temperature curves of these tests are plotted against the NBS Standard Time-Temperature Curve and are shown in Fig. B-9. Even for the lightest fire load tested, 8.5 psf, the "cooling out" rate after the peak of the fire gives a residual room temperature of 700 F after 1-1/2 hours, and a conservative extrapolation would still show a residual temperature in excess of 500 F after 2 hours.* However, if the burnout of a building were not accompanied by collapse of structural components, it is unlikely that sufficient heat would be developed in the floor slab to jeopardize shelter occupants. On the other hand, if burnout were accompanied by collapse of structural components, and an accumulation of hot rubble blanketed the floor slab over the shelter, countermeasures might have to be taken. Rubble fires may smolder for days at a time. A full scale building fire test conducted by the National Bureau of

---

* These temperatures were not measured at the surface of floor slabs but rather were taken at some intermediate level within the rooms involved in fire.

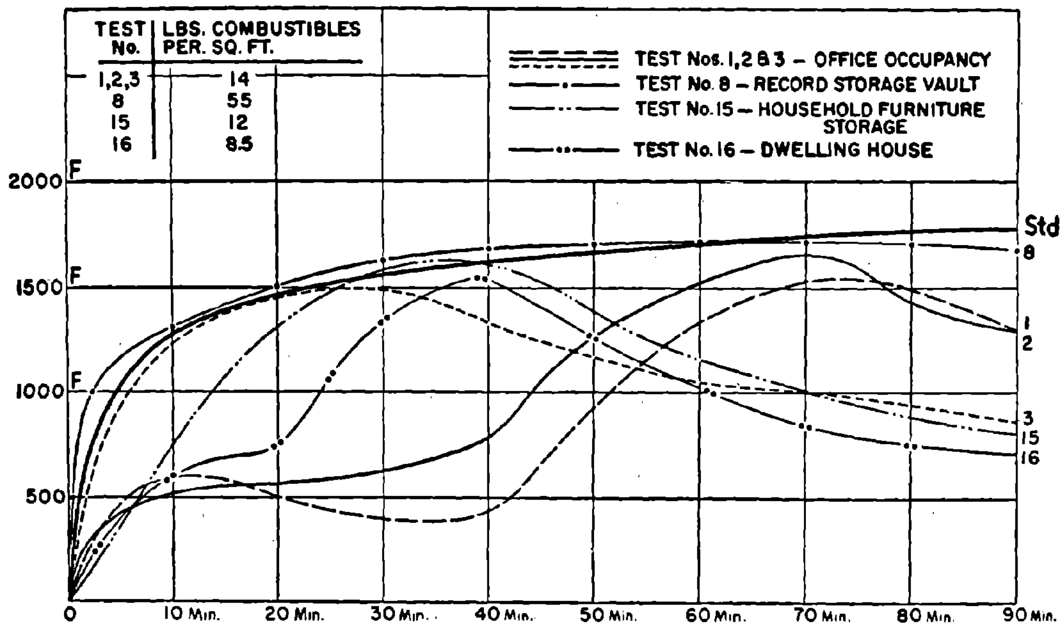

Actual time-temperature curves recorded in tests as compared with the Standard Time-Temperature Curve. This indicates the relative fire severity depending upon different fire loading. The Standard Time-Temperature Curve, while used as a convenient measure for general fire testing, actually represents a condition of high fire severity met in the early stages of actual fires only where combustible materials are of such a character as to favor rapid development of high temperatures.

FIG. B-9 TIME-TEMPERATURE TEST CURVES

Standards[15] measured temperatures in the rubble pile that persisted "in the vicinity of 1000 F for a period of 2 to 3 days."*

Table B-1 lists equivalent fire severities covering a wide range of fire loadings for "offices and light commercial occupancies."

Table B-1

ESTIMATED FIRE SEVERITY FOR OFFICES AND LIGHT COMMERCIAL OCCUPANCIES[17]
(Data for Fire Resistive Buildings with Combustible Furniture and Shelving)

Combustible Content Total, Including Finish of Floor and Trim (psf)	Heat Potential, Assumed† (Btu/sf)	Equivalent Fire Severity, Approximately Equivalent to that of Test Under Standard Curve for the Following Periods:
5	40,000	30 min
10	80,000	1 hr
15	120,000	1-1/2 hrs
20	160,000	2 hrs
30	240,000	3 hrs
40	320,000	4-1/2 hrs
50	380,000	7 hrs
60	432,000	8 hrs
70	500,000	9 hrs

† Heat of combustion of contents taken at 800 Btu/lb up to 40 psf, 7600 Btu/lb for 50 psf, and 7200 Btu/lb for 60 psf and more to allow for relatively greater proportion of paper. The weights contemplated by the tables are those of ordinary combustible materials, such as wood, paper, or textiles.

* Tests conducted by the U.S. Forest Service, Dept. of Agriculture, on a municipal building registered 1900 F in the rubble pile nearly 24 hours after the building was set on fire.[20] Slab surface temperatures were not reported.

Although no attempts have been made to simulate a holocaust for research purposes, several studies have recently been made of the effects on basement shelter stemming from a single realistic debris fire on the floor above.[40,41] This work is not complete, but results to date have shown that, without some sort of forced ventilation of cool air into the shelter, the fires degrade the habitability of the shelter spaces severely but are not likely to make them uninhabitable unless the load of combustible material burning on the slab over the basement is extremely large. This conclusion is well illustrated in Figs. B-10, B-11, and B-12, taken from Refs. 40-41. With debris burning on top of the reinforced concrete basement slab and with only natural air circulation within the basement space itself, the distribution of temperature in the basement as a function of time and distance below the ceiling is shown in Fig. B-10. The combustible load simulating that produced by a retail furniture store was 7.5 psf, and the load of noncombustibles in the simulated debris on the slab was 4.5 psf. Since air mixing within an occupied shelter would be greater than that achieved during these experiments, the results contained in Fig. B-11 are of more interest and are described below.

The total heat transmitted through a reinforced concrete slab into the basement from an experimental fire designed to simulate burning debris of a retail furniture store reached approximately 1200 BTU/sf by a time 40 hours after ignition (Fig. B-11); and the peak air temperature rises at 1 ft and 6 ft below the basement ceiling were 21 and 12 F, respectively (Fig. B-10). The temperature increases above ambient in the same locations 40 hours after ignition were still 50% of their peaks. However when the fire load over the basement was increased to 25.5 psf (simulating library debris), heat flux and temperature levels in the basement became unbearably high (Fig. B-12).

No forced ventilation was used in the basement during these experiments and outside apertures to the basement were closed but were not airtight. There were no people or other heat sources in the basement itself. The fire on the floor above the basement was confined to a room with concrete walls in which large openings were placed to simulate windows and doors blasted open by weapon effects.

The magnitude of the heat load added to the basement shelter by the fire on the concrete ceiling slab may be appreciated and the added ventilation requirements assessed, by considering that a man (weighing 154 lb; awake but sitting quietly) produces in metabolic heat about 400 BTU/hr.[20 (Chap. 7)] In other words, if the shelter area provides 10 sf per person, Fig. B-11 suggests that the time average effect over the life of

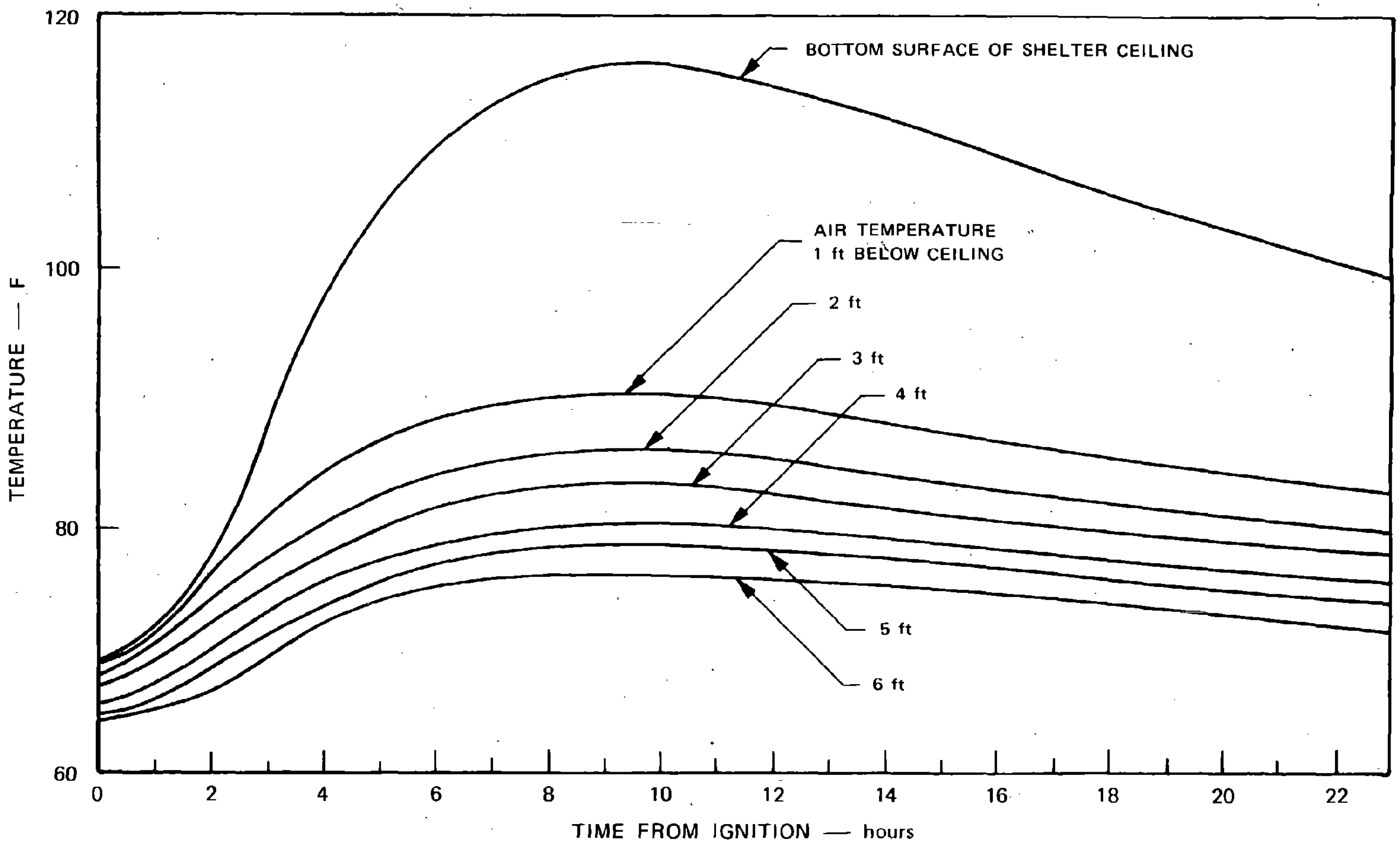

FIG. B-10 TEMPERATURES WITHIN THE SHELTER-RETAIL DEBRIS FIRE EXPOSURE[40] (FIRE LOAD 8.1 psf)

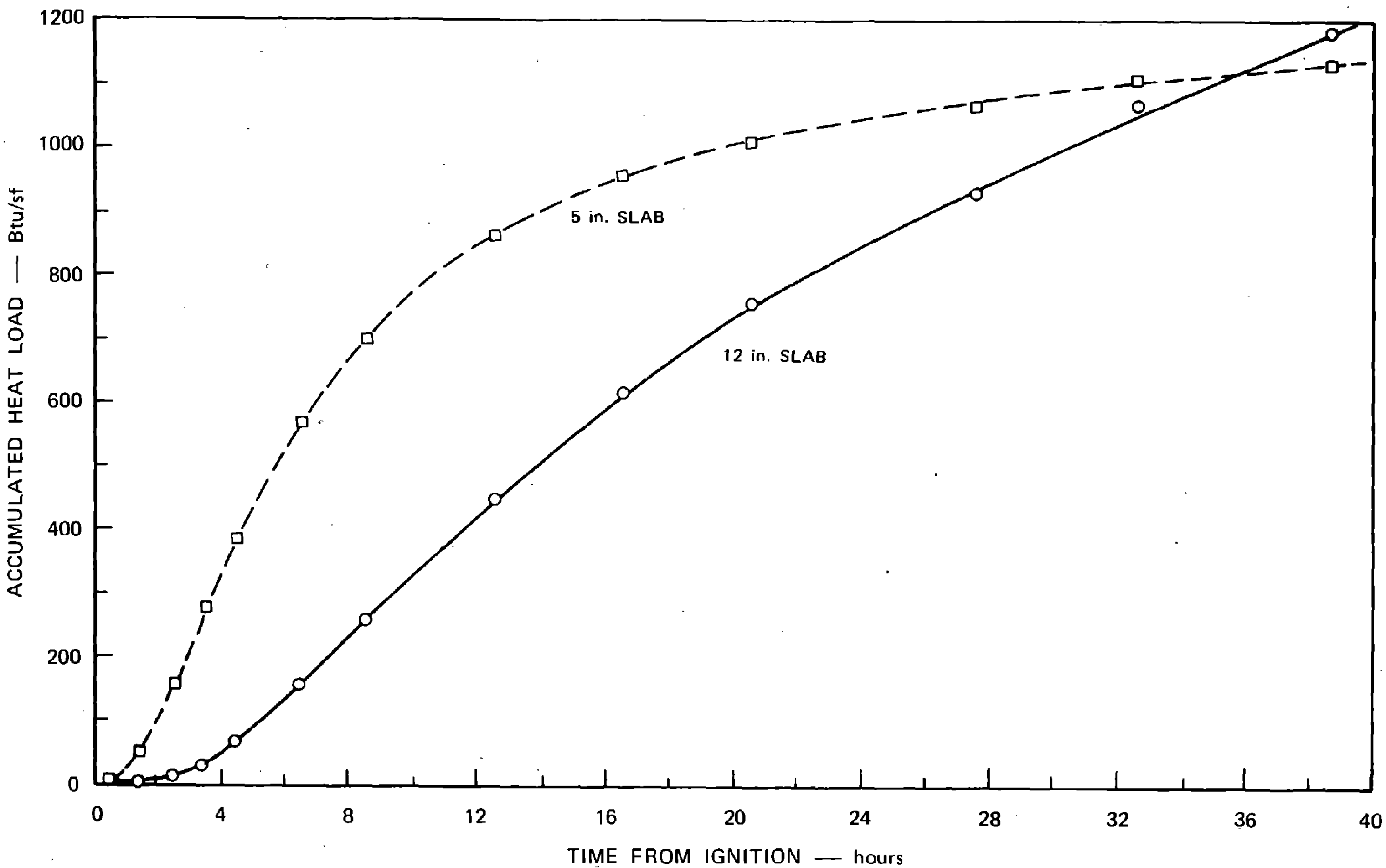

FIG. B-11 TOTAL ACCUMULATED HEAT LOAD PER SQUARE FOOT OF SHELTER CEILING FOR RETAIL DEBRIS FIRE (FIRE LOAD 8.1 psf)[40]

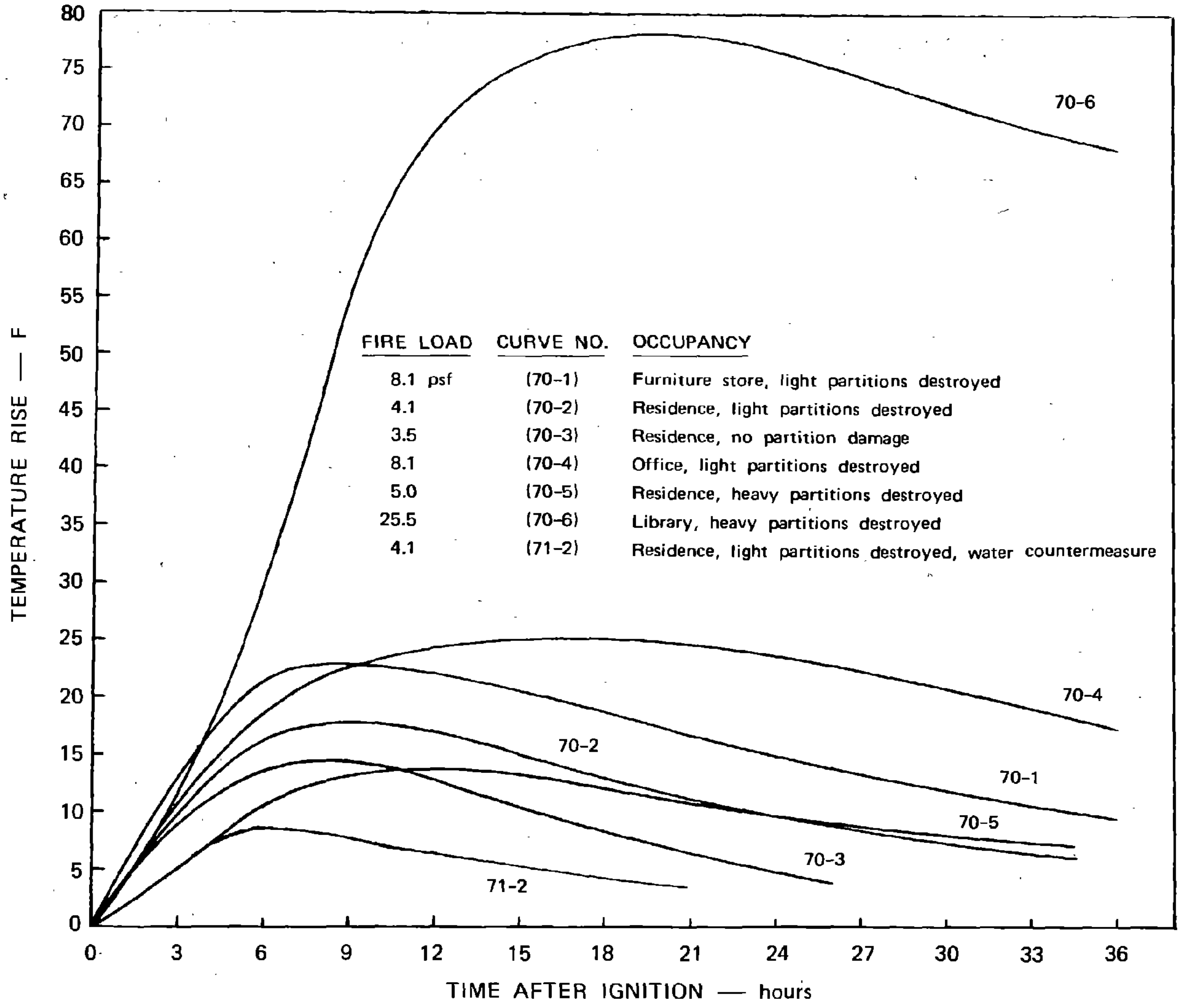

FIG. B-12 AIR TEMPERATURE RISE IN SHELTER, 1 FOOT BELOW CEILING[41]

the fire of the added heat load resulting from a retail debris fire is approximately equivalent to doubling the shelter population. The figure also suggests that, although the total added heat load may be independent of slab thickness, a concrete slab significantly less than about 12 in. thick may admit the fire heat as a pulse of relatively short duration but of a threatening magnitude; this is confirmed by Fig. B-13, which shows the heat flux into the basement as a function of time, based on the same data as Fig. B-11.

The bare concrete basement ceiling itself may reach temperatures between 100 and 200 F, becoming an uncomfortable source of radiation. Figure B-14, for example, shows ceiling temperatures of this magnitude measured during the experiments just mentioned. Nude men exposed to a wall at 200 F begin to experience body temperature elevation after 30 minutes.[30(Chap. 7)] Although clothing offers protection from radiation, a ceiling temperature of 200 F maintained for an hour or two may make the shelter highly uncomfortable. Slab thickness offers considerable protection against this radiant effect, as may be inferred from Fig. B-14. An insulating or reflective barrier may also be interposed to provide protection to shelterees.

According to Takata[42] a radiant flux of 0.08 cal/cm^2-sec causes pain to human flesh in 30 seconds; heat stroke can be expected to follow an exposure of several minutes to 1 hour at 0.002 to 0.030 cal/cm^2-sec, depending on ambient temperature and clothing. A concrete slab heated to a temperature between 100 and 260 F will produce radiation intensities in the range 0.01 to 0.03 cal/cm^2-sec (Stefan-Boltzman law, described under "Intensity of Thermal Radiation," Section 2 above).

Recent successes in calculational simulation of heat transfer through a concrete slab[41] make it possible in principle to relate slab thickness and fire parameters to the physical factors determining human hazard.

Safe exposure periods for humans at various combinations of temperature and relative humidity are given in Fig. B-15. If a shelter air temperature of 50 C (122 F) is assumed, it is readily seen that, even under moderate conditions of 30% relative humidity, those exposed could not be safe much beyond 3 hours. Of course, higher humidities can normally be expected in shelters, and, consequently, safe exposure periods would be considerably less than 3 hours unless special provisions for cooling were undertaken.

Figure B-15 is based on the average time required to raise pulse rate 50 beats per minute, from an initial rate of 75 to a final rate of 125, and to raise rectal temperature to 101 F from an initial temperature

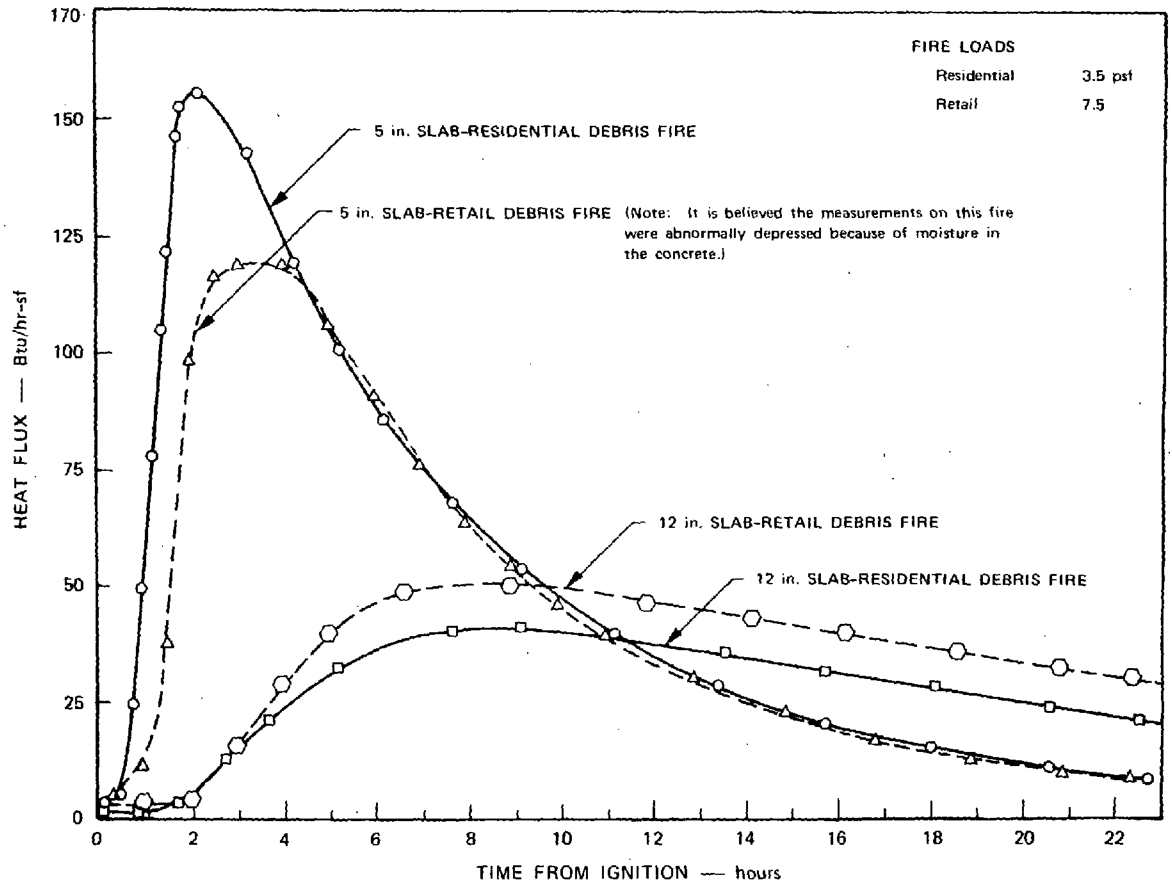

FIG. B-13 HEAT FLUX THROUGH SHELTER CEILING SLABS[40]

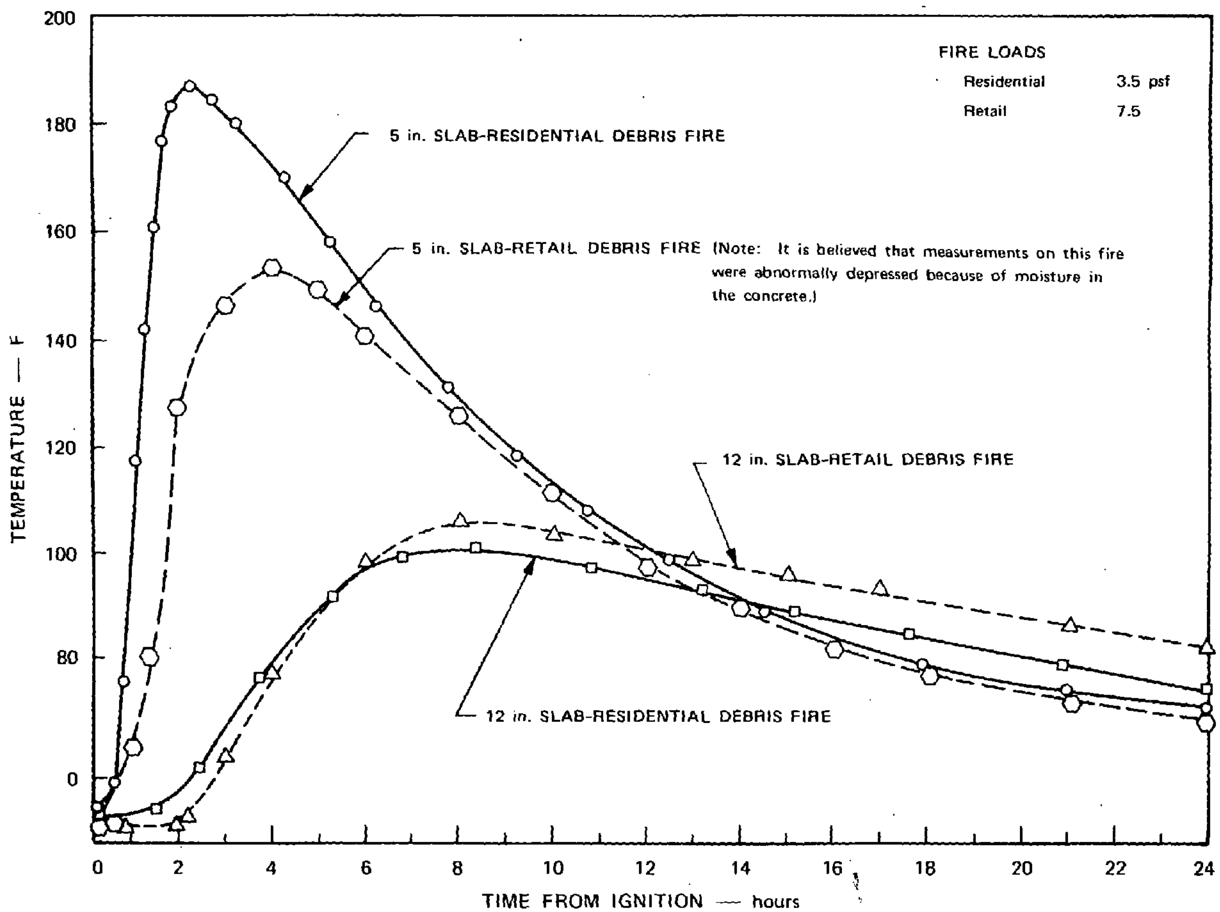

FIG. B-14 BOTTOM-SURFACE TEMPERATURES OF SHELTER CEILING SLABS[40]

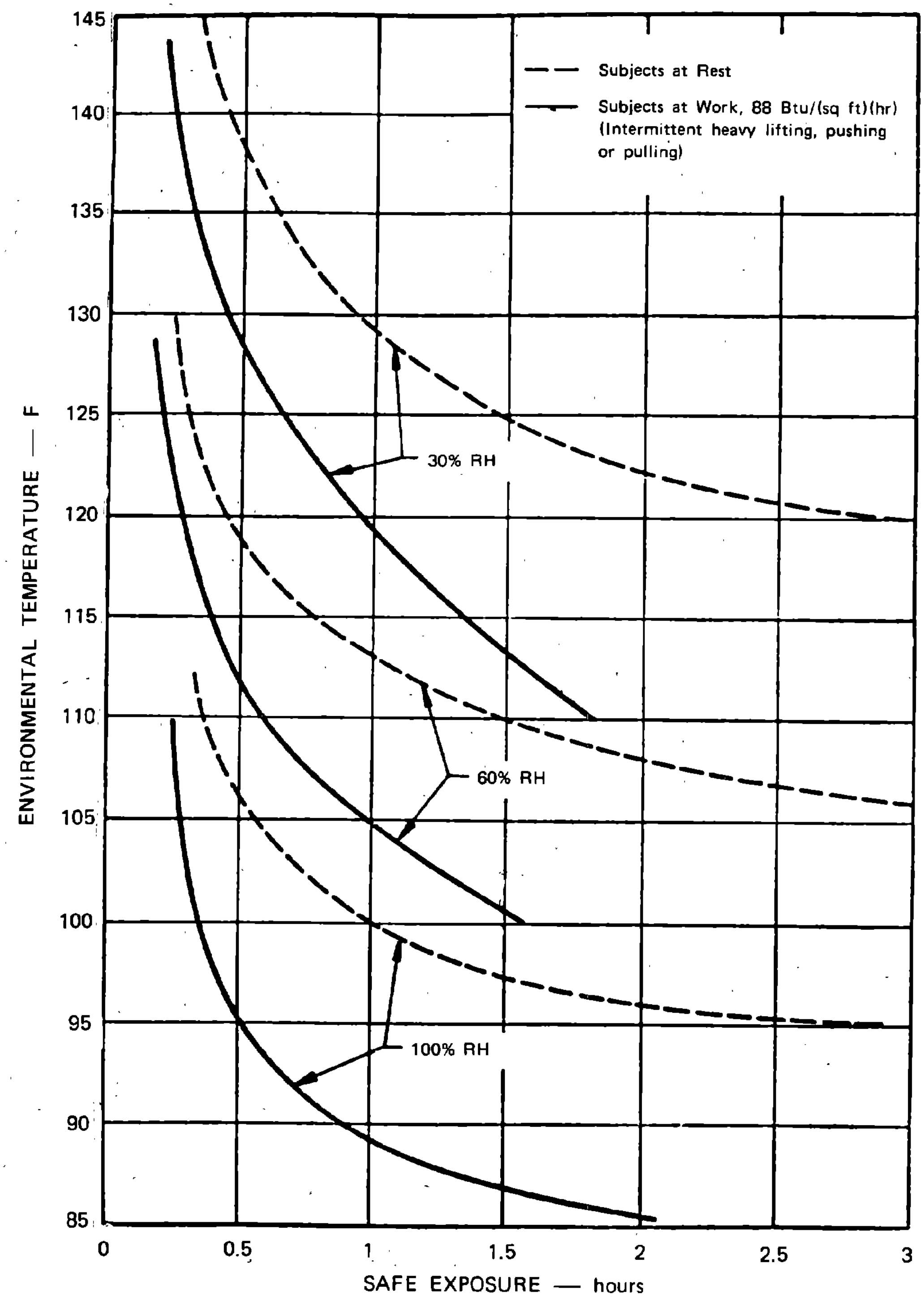

Reprinted by permission from ASHRAE Handbook of Fundamentals (1967)

FIG. B-15 SAFE PERIODS OF EXPOSURE FOR EXTREME ENVIRONMENTAL TEMPERATURES

between 98 and 99 F. Symptoms of heat distress do not appear until the pulse rate exceeds 130 and rectal temperature 101 F for more than one hour. Heat tolerance is highly individual and tests have shown some individuals can withstand conditions of even greater severity[19] than those shown in Fig. B-15. Temperature and humidity tolerances can be greatly increased if exposed individuals are regularly rested in a cool zone. Thus it is possible exposures to fallout radiation and heat from fires could be balanced against one another; that is, if a cool zone outside the shelter can be found, it may be preferable to expose periodically certain heat sensitive individuals (such as those required for heavy work) to fallout radiation in the cool zone. However, conditions of conflagration can easily be imagined such that a cool zone in the neighborhood of the shelter may not exist.

As safe exposure periods are exceeded, the physiological effects of heat are disastrous.[19] Body temperatures rapidly rise, metabolism increases, and heat stroke quickly follows.[19] The latter may well be fatal since help for the victim may not be available during a nuclear attack.

b. O_2 Depletion; CO_2 and CO Build-up

Dangerous depletion of oxygen and CO_2 build-up in a shelter in an external fire environment would be unlikely. On the other hand, there could be a danger from CO poisoning. During the Hamburg fire storm of World War II, occupants of bunker type shelters were compelled to shut down ventilation plants until the fire storm had subsided to avoid drawing in heat, smoke, and CO. Yet, in spite of gross overcrowding in the bunkers and extremely uncomfortable conditions, survival was nearly 100%. The bunkers were massive concrete structures and were gasproof, since they were fitted with air locks and gasketed doors. Occupants of the relatively primitive, neighborhood basement shelters were not so fortunate, and deaths from heat, smoke, and CO were common although even here more than 80% of shelter occupants survived.[19,21] Earp[22] concludes that:

> When the ventilating systems (including filtration) of public shelters were worked during incendiary raids and especially during fire storms, there was a danger of carbon monoxide being drawn in because it is not absorbed by the filters; nor does the gas mask protect against it. Hence in the Hamburg raids it was very fortunate for the shelter occupants that so many of the ventilating systems were closed down after a short time. Even when the ventilating plant was stopped, carbon monoxide might get in when doors were opened to admit people during a raid.

It can be concluded that there is a real danger of carbon monoxide poisoning both in shelters and in the streets. The calm appearance of the features and the natural position of many of the corpses found in the Hamburg shelters was a strong indication that death was due to carbon monoxide poisoning or to heat exhaustion.

Nevertheless, it is believed that fire storm conditions would not be reached in the United States, primarily because building densities in this country are substantially less than those in Hamburg during World War II.

Fires within a shelter building, however, would present a danger from O_2 depletion and CO_2 and CO build-up with the maximum hazard occurring when the fire was in the shelter. It is for this reason that shelter occupant countermeasures are so important.

Table B-2 summarizes the biological effects on man of various levels of concentration of O_2, CO_2, and CO. It should be noted that the effects of a varying proportion of each gas assumes an environment with normal concentrations of the other two gases. It is known that O_2 depletion when accompanied by increased levels of CO_2 and CO has a synergistic effect; however, quantification of these aggravated effects is lacking for man.[23]

A more recent compilation by Webb[43] of the human tolerance to CO_2 and CO is reproduced in Figs. B-16 and B-17. Webb's values for the CO effects versus time (Fig. B-16) agree with those presented in Table B-2 and show also that the CO_2 exposure duration is not of critical importance (Fig. B-17).* Fig. B-18* shows the effect of oxygen deprivation on the human body; again, after a time the body tends to adapt and effects are stabilized. The figure also shows the advantage of previous training or acclimatization to oxygen deficiency.

Pryor, Fear, and Wheeler[45] found striking synergistic effects in rats exposed to high temperature (hypothermia), excess CO_2, excess CO, and oxygen deprivation (anoxia). The deleterious effect of each of the

* In both Fig. B-17 and B-18, the proportion of the atmosphere along vertical scale is expressed in percentage by volume and in partial pressure. These quantitites are directly proportional to one another and volume percent may be obtained from partial pressure by dividing the latter by total atmospheric pressure under standard conditions, i.e., 760 mm Hg.

Table B-2

PHYSIOLOGICAL EFFECTS OF OXYGEN, CARBON DIOXIDE, AND CARBON MONOXIDE[24]

Effects of Oxygen Deficiency

Oxygen Content of Inhaled Air (percent)	Effects
20.9%	No effects; normal air.
15	No immediate effect.
10	Dizziness; shortness of breath; deeper and more rapid respiration; quickened pulse, especially on exertion.
7	Stupor sets in.
5	Minimal concentration compatible with life.
2-3	Death within one minute.

Effects of Carbon Dioxide

Carbon Dioxide Content of Inhaled Air (percent)	Effects
.04%	No effects; normal air.
2.0	Breathing deeper; tidal volume increased 30%.
4.0	Breathing much deeper; rate slightly quickened; considerable discomfort.
4.5-5	Breathing extremely labored, almost unbearable for many individuals. Nausea may occur.
7-9	Limit of tolerance.
10-11	Inability to coordinate; unconsciousness in about 10 minutes. Symptoms increase, but probably not fatal in 1 hour.
25-30	Diminished respiration; fall of blood pressure; coma; loss of reflexes; anesthesia. Death after some hours.

Table B-2 (concluded)

Effects of Carbon Monoxide

Carbon Monoxide Content of Inhaled Air (percent)	Effects
0.02%	Possible mild frontal headache after 2 to 3 hours.
0.04	Frontal headache and nausea after 1 to 2 hours. Occipital (rear of head) headache after 2-1/2 to 3-1/2 hours.
0.08	Headache, dizziness and nausea in 3/4 hour. Collapse and possible unconsciousness in 2 hours.
0.16	Headache, dizziness, and nausea in 20 minutes. Collapse, unconsciousness, and possible death in 2 hours.
0.32	Headache and dizziness in 5 to 10 minutes, unconsciousness and danger of death in 30 minutes.
0.64	Headache and dizziness in 1 to 2 minutes, unconsciousness and danger of death in 10 to 15 minutes.
1.28	Immediate effect. Unconsciousness and danger of death in 1 to 3 minutes.

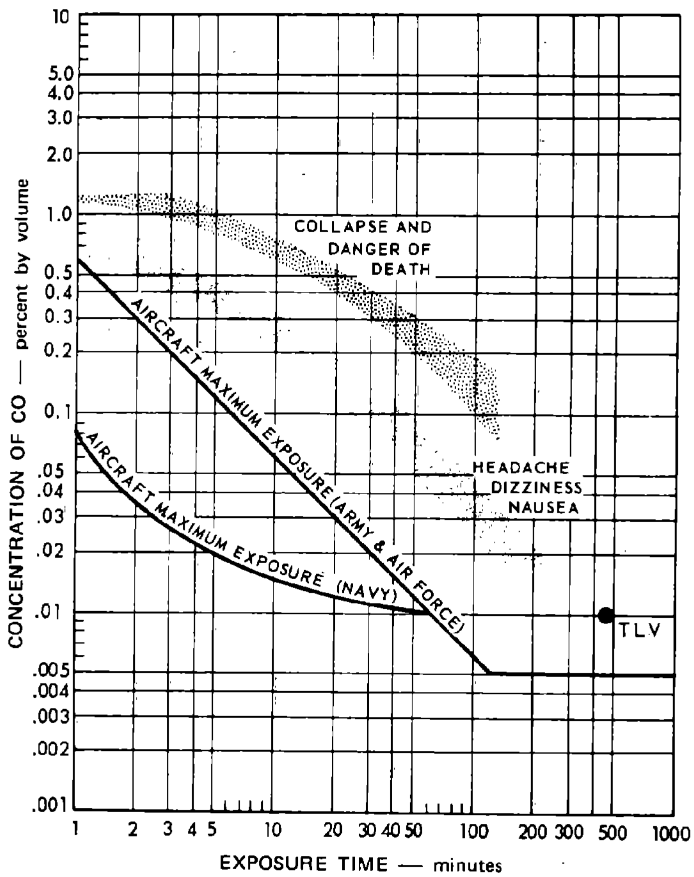

FIG. B-16 EFFECTS OF CARBON MONOXIDE UPON HUMANS[43]

The graph shows the effects of carbon monoxide on man as functions of concentration and exposure time. Milder effects are shown as a lightly shaded band of exposure times and concentrations, while dangerous or lethal times and concentrations are grouped in the heavily shaded band. The solid lines are the exposure limits set by the military services for aircraft. The point marked at 0.01% CO (100 ppm) and 480 minutes is the current Threshold Limit Value (TLV) for 8-hours-a-day exposure in industry.

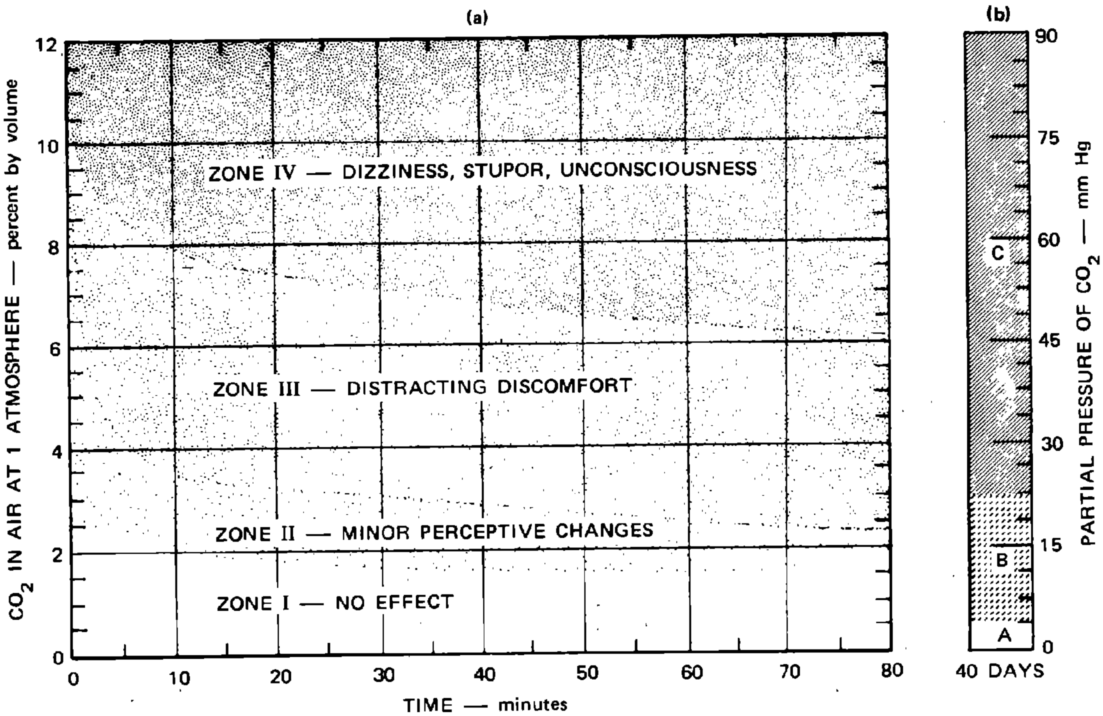

FIG. B-17 EFFECTS OF CARBON DIOXIDE UPON HUMANS[43]

The chart shows the general symptoms common to most subjects when exposed for the times indicated to mixtures of carbon dioxide in air at a total pressure of 1 atmosphere. In Zone I, no psychophysiological performance degradation, or any other consistent effect, is noted. In Zone II, small threshold hearing losses have been found and there is a perceptible doubling in depth of respiration. In Zone III, the zone of distracting discomfort, the symptoms are mental depression, headache, dizziness, nausea, "air hunger," and decrease in visual discrimination. Zone IV represents marked deterioration leading to dizziness and stupor, with inability to take steps for self-preservation. The final state is unconsciousness.

The bar graph at the right shows that for prolonged exposures of 40 days, concentrations of CO_2 in air of less than 0.5% (Zone A) cause no biochemical or other effects; concentrations between 0.5 and 3.0% (Zone B) cause adaptive biochemical changes, which may be considered a mild physiological strain; and concentrations above 3.0% (Zone C) cause pathological changes in basic physiological functions.

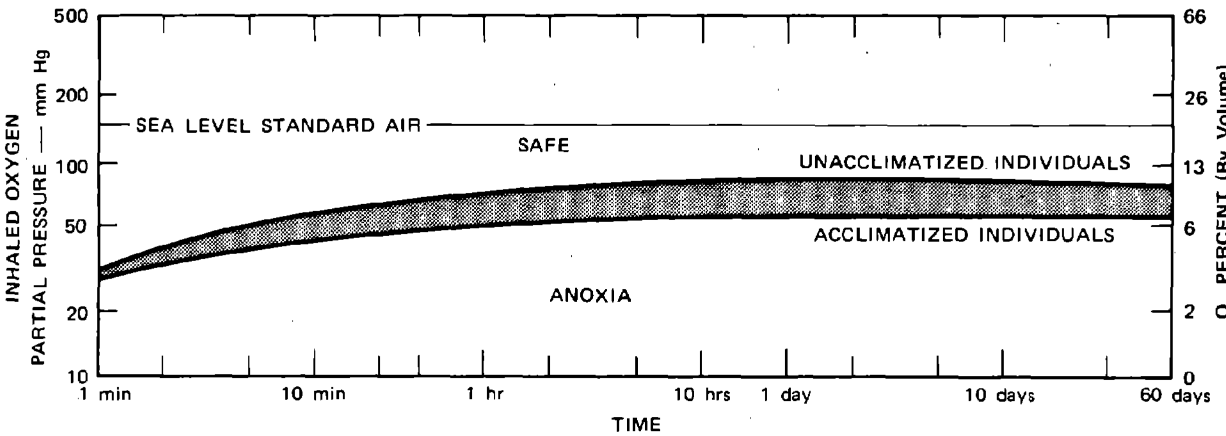

FIG. B-18 HUMAN TIME-TOLERANCES VERSUS OXYGEN PARTIAL PRESSURE[44]

four factors individually was established by a series of exposures of groups of 10 animals at escalating doses; for example, it was shown that, at 100 F maintained for 4 hours, 2 of 10 rats died. At 105 F nine out of 10 died. Time of death was also noted and provided an additional measure of lethalness. The four injurious factors were then combined in pairs and groups of 10 animals exposed to them. Minimum lethal doses of each factor were always less when applied in combination. The same effect was seen in aggravated form when three factors were applied in combination. In a later report, Pryor, Johnson, and Jackson[46] used the same experimental technique with an expanded list of deleterious factors, including exposures to HCN, SO_2 and NO_2 as well as the four primary factors used earlier. The results were the same: synergism, in all cases, was particularly strong when one of the three noxious gases (HCN, SO_2, and NO_2), was combined with one of the four primary factors. The authors speculated that the controlling mechanism of lethalness is essentially the same in the case of every factor; hence, the effects of several factors combined would be at least additive.

Pryor, Johnson, and Jackson[46] also found significant quantities of the toxic gases, HCN, SO_2 and NO_2, as combustion products of various materials likely to be present in an urban environment; in particular, hydrogen cyanide (HCN) appears in plentiful supply when wool is burned, but even the more common materials such as oak produce HCN to some extent. At the present time, however, experimental debris fire reports have not mentioned the presence or absence of these gases.

There is, however, ample evidence of the production of dangerous amounts of CO_2 and CO in structural fires. Some of the most recent data come from actual habitable structures burned by Butler[49] and by Wiersma and Martin.[61] This information clearly points to CO as the greatest life

threat among the three hazards: O_2 deprivation and CO_2 and CO poisoning. Butler has defined the "escape time" as the interval between ignition of the building and the first accumulation of a lethal concentration of CO (which he took as 0.05% by volume). In open rooms of burning buildings he reported escape times between 5 and 7 minutes. Clearly, substantial fire within the shelter itself is intolerable; but what are the effects on the shelter space gas content caused by fire elsewhere in the same or an adjoining building?

Sufficient experimentation to provide an adequate basis for analysis of the behavior of fire-generated gases within structures has not been performed. However, full scale experimental building burns conducted by Waterman[16] do give some specifics in this regard. Some of his conclusions were:

(1) Oxygen depletion in an active fire zone of a burning building will be reproduced throughout interconnecting spaces on the same or higher stories of a relatively "tight" structure or structural portion (unless very large volumes are being considered). Oxygen levels as low as 5% were measured (normal air has 20.9% O_2).

(2) In a burning building, shelters remote from the fire zone within that building--i.e., not exposed to a direct threat from thermal effects--and located on the same or higher floor level as the fire would be exposed to CO concentrations equal to 75% of those recorded in the fire zone. Since CO concentration in the fire zone attained a maximum of 3.3%, the shelters were exposed to levels up to 2.5% CO, well above the lethal limit of 1.28%.

(3) In fire resistive construction, downward movement of CO, emanating from fires on floors above a shelter, will probably not occur.

(4) However, wind pressures can drive fire gases into shelter spaces, even if fire-generated pressures are not sufficient to do so. Smoldering fires may produce significant infiltration of toxic gases by this means.

(5) Fire gases infiltrating a shelter having otherwise cool floor, walls, and ceiling do not significantly heat the shelter air space and would represent a hazard only because of toxicity or the ignition of combustibles within the shelter.

(6) Although much more data are needed on real fire environments and movement of fire gases through complex structures, the above conclusions lead to a further statement that fires within a "tight" envelope, such as a basement containing a shelter, cannot be tolerated and must be extinguished unless the barrier between the fire and the shelter is perfectly gas tight.

(7) A ventilating system equipped to maintain a slight overpressure (1/4 to 1/2 inch of water) in the shelter would normally ensure against infiltration of smoke and toxic gases from fires external to the shelter. (However, if outside fires were present, the ventilating system might have to shut down for a period anyway - a situation that did occur in the Hamburg fire storm. As an alternative to maintaining an in-shelter overpressure, toxic gas infiltration must be avoided by taking appropriate measures to seal all openings in the shelter.)

Later work by Takata and Waterman[41,47] has further substantiated Item (7) immediately above. Experiments show that migration of fire gases through specially prepared holes in basement ceiling slabs (to simulate possible blast produced cracks and fissures) constitutes no danger if the shelter space is not sealed or does not use recirculated air, but might be hazardous otherwise. In an experimental, full-scale building fire Vodvarka[48] kept the simulated shelter underneath the fire free of CO and CO_2 by pressurizing with a ventilating fan to a level of 0.05 to 0.03 inches of water during the initial 90 minutes following ignition, despite the presence of intentional holes through the ceiling slab.

Experiments demonstrate that ventilating air drawn into a basement over or through burning debris is extremely noxious, for example, the CO content in air drawn into a basement when a residential debris fire is burning outside the building rapidly rose to 0.35% at 40 minutes after ignition, and 2 hours later was still 50% of this peak value.[47] Other work with experimental fires confirms that dangerous levels of CO are generally present for significant periods in air drawn from a region in or near a fire.[24,49] Smoldering rubble fires, as well as active fires, can be strong sources of CO.[24] Because the peak flux of heat requires some time to pass through walls and ceilings into the shelter, it is often possible to shut down ventilation during periods of high toxic gas production, then return the ventilation system to operation later when it becomes necessary to protect the shelterees from the heat pulse.

Clearing debris from the area of the ventilation intake reduces the amount of CO brought into the basement; Takata and Waterman found in their experiments that clearing a 15 ft radius around the basement door was sufficient to reduce the CO content in the indrawn air below the lethal level, i.e., from 0.35% to a maximum of 0.04%.[47]

c. Smoke

Smoke is the most significant of the lesser understood hazard factors in a fire environment. Although each year many hundreds of casualties from smoke inhalation are reported, Lee[23] states that little is known about the actual biological mechanisms involved. This is primarily because smoke is such an ill-defined term. The generic term, "aerosol," defines smoke, fog, hazes, and fumes as a suspension of particles, liquid or solid, in a gaseous phase. However, the chemical constituents of these gaseous suspensions are difficult to evaluate. For example, smoke from the same sample of fuel will vary in the composition of the products or compounds in suspension depending on the rate at which it is heated and burned.

Although opinions vary, some observers state that true cases of fatalities from smoke inhalation are rare and that most casualties ascribed to smoke really are caused by asphyxiation or CO poisoning.[23] Nevertheless, a quantitative evaluation of the threat posed by smoke is not possible, in contrast with O_2 depletion and CO_2 and CO build-up, under the emergency conditions that would prevail in a shelter. Therefore, because of the high probability that smoke and fumes would be toxic, it must be assumed that all smoke and fumes are potentially lethal in the immediate environment of a shelter.[25]

Fire and safety engineers regard smoke as dangerous principally because it obscures the vision of those caught in a burning structure and because it induces panic.[50] It is also a lachrymator and an irritant. All three effects would have some importance to shelterees, particularly if it becomes necessary for them to leave the shelter to fight fires elsewhere in the building (see Section 5).

Section 4 - Design Countermeasures

Objectives

The objectives of design countermeasures against the threat of fires and countermeasure examples include:

- Minimize ignitions of the shelter building by radiation from the thermal pulse of a weapon and from adjacent burning buildings.
- Provide portable fire extinguishers for the use of shelter fire teams enabling them to extinguish incipient fires.
- Minimize spread of fire by appropriate construction directed to containment of fire on the floor of origin.
- Minimize downward spread of fires from the floor of origin.
- Prevent spread of smoke, toxic gases, and heat.
- Restrict shelter building candidates to those occupancies having moderate or lesser fire loadings.

Wherever the following criteria are exceeded by the National Building Code[13] for the type of fire-resistive construction and occupancy selected for the shelter buildings's primary use, that code or any other applicable codes should govern.

Thermal Radiation

Exterior wall openings, and roof openings such as skylights, should be provided with aluminized blinds or reflective drapes of noncombustible composition to provide protection from the thermal pulse of the weapon.[28,29] Ordinary painted metal venetian blinds, when closed, will also suffice, provided that they are hung with noncombustible tapes, even though the paint will char. As a minimum, shielding should be provided on the first floor of the shelter building.

Protection from thermal radiation from an adjacent burning building can also be provided by siting to obtain appropriate separation distances as described in Section 2 of this appendix.

Portable Fire Extinguishers

One 5-gallon stirrup pump type extinguisher with extra length hose (at least 6 feet long) should be provided for each 1,250 sf of shelter area with a minimum of 4 extinguishers per shelter. Also one 5-gallon stirrup pump type extinguisher should be provided for each 5,000 sf of nonshelter area.[29]

Structural Criteria

The minimum fire resistance ratings for structural components of shelter buildings should be those specified for "Ordinary Construction" as defined in Section 707 of the National Building Code,[13] except that separation distances calculated by the Law Method should govern where exposed facades (or walls) have window openings. Horizontal separation as defined by the National Building Code is not the same as the separation distance used by Law. Rather, under the Code, horizontal separation is established for each type of building, then the separation distance between two buildings becomes the sum of their respective horizontal separations. Furthermore, most code separations are designed only to stall the firespread until the fire department can arrive and would be inadequate in a nuclear attack.[51]

Table B-3 summarizes the fire resistance ratings for "Ordinary Construction."

Smoke and Toxic Gases

One alternative for protection of the shelter against infiltration of smoke and toxic gases would be to provide an independent, emergency shelter ventilation system designed to provide a positive pressure in shelter spaces[25] provided a source of uncontaminated air is available. Although interior pressures as low as 0.03 inches of water have been observed to prevent the migration of noxious gases into shelter spaces, pressurization between 0.25 and 0.50 inches of water may be necessary to turn back wind-driven fumes.

Table B-3

MINIMUM FIRE RESISTANCE RATINGS FOR ORDINARY CONSTRUCTION[13]

Component	Horizontal Separation (ft)	Maximum Percentage of Windows to Wall Area	Minimum Fire Resistance Rating
Exterior bearing walls*	0-3	0%	3 hours
	3-20	20	2 hours
	20-30	30	2 hours
	Over 30	40	2 hours
Exterior nonbearing walls*	0-3	0	3 hours
	3-20	30	2 hours
	20-30	40	1 hour
	Over 30	100	None required
Interior bearing walls*			2 hours
Interior partitions enclosing elevator shafts, stairways, and so forth, through floors of buildings four stories or more in height			2 hours
Interior partitions enclosing elevator shafts, stairways, and so forth, through floors of buildings fewer than four stories in height			1 hour
Roof structure			1 hour
Roof covering			Class A or B
Interior finish, maximum flame spread rating in nonshelter areas			75†
Interior finish, maximum flame spread rating in shelter areas			25†

* All exterior walls and interior load-bearing walls will be of approved noncombustible materials.

† Index based on ASTM E-84 Tunnel Test Method.

The other alternative is to attempt to seal the shelter against infiltration by means that will withstand blast loading. Penetrations of the shelter walls and ceilings by cables, pipes, and ducts should be grouted or equipped with sealants or gland seals to prevent infiltration. Ventilation ducts extending from the normal building ventilation system into the shelter should have vaportight fire dampers installed at the point of entrance to the shelter.[17] These should be automatic, heat-fused dampers capable of being operated manually by shelter personnel from inside the shelter.

The alternative chosen might depend on cost-effectiveness considerations, however, only the first alternative will remain effective after the shelter suffers the substantial cracks and other openings caused by blast.

Choice of interior finish materials with the goal of reducing smoke production is now receiving considerable study. Tests for smoke production capability of building materials are under development by the U.S. Forest Products Laboratory, the Underwriters Laboratories, Inc., and the National Research Council of Canada, but so far no single, adequate measure of the smoke hazard inherent in a material has appeared. There are currently more than a half dozen tests in use by various agencies.[50] *

Emergency Exits

Shelters in basements, particularly in buildings containing a high fire load, should be provided with emergency exits at some distance from the likely location of debris and fire. Tunnel exits may also serve as safe channels for ventilation air, except possibly for a few hours during the height of a local conflagration.

The Swiss Federal Office for Civil Defence has recommended that outlets from emergency exits and ventilation channels be placed a distance from the outer wall of the building containing the shelter equal to at least one half the height of the building.[60] This practice will reduce the likelihood the exit will be plugged with debris or the ventilation become contaminated with noxious, fire-produced gases.

In their commentary upon the West German Air Raid Protection Law, Zinkahn and Leutz[62] suggest that vertical shafts extending above possible debris be provided at the exit in those cases when it is not possible to remove the exit out of the debris zone altogether.

* including National Bureau of Standards

Combustible Contents

It is recommended that the maximum combustible fire load for any floor level posing a threat to the shelter should not exceed an average of 15 psf. Fire loads are composed of combustible furnishings, equipment, and structural components. Building occupancy generally governs the fire load. To select candidate shelter buildings, the proposed occupancy of a building can be checked against National Bureau of Standards data on the combustible contents of representative buildings by occupancy.

If candidate buildings are to be equipped with automatic sprinklers, to the extent that such sprinklers exceed the minimum requirements of the codes[13,30] a proportionate increase in the 15 psf maximum average fire load may be allowed provided that the building sprinkler system is served by a gravity tank system that may be expected to survive the air blast loading.

Together with the floor slab thickness and the effectiveness of the ventilation system, the combustible fire load carried by the floor immediately above a basement shelter determines the degree of protection from heat afforded the shelterees without effort on their part. For example, the work of Takata and Waterman[41] (reported in Section 3a above) suggests that a fire load of 15 psf on a slab 12 in. thick may be near the limit tolerable in the absence of artificial ventilation or personal countermeasures against fire (see Section 5 below).

To protect shelterees from the heat of fires the Swiss Federal Office for Civil Defence recommends shelter spaces be separated from the remainder of the building housing them by concrete ceilings or walls either 30 or 40 centimeters (11.8 or 15.7 inches) thick;[60] the greater thickness is required when the remaining structure is largely of wood or when combustible material such as wood or furniture is stored next to the shelter. Swiss regulations contemplate the possibility there will be a certain limited time during the attack when ventilation must be shut down due to the danger of carbon monoxide.

Section 5 - Shelter Occupant Countermeasures

Background

It is reasonable to assume that shelterees can be active in their own defense against fire. Given simple equipment and trained leadership, shelter occupants may to some extent control their own exposure to heat and noxious gases, even limit the spread of fire in their environment. It is this last task which is the most demanding.

Flying brands and embers would pose a continual threat during the entire time in shelter. The thermal radiation from a weapon threatens only for a few seconds and that from adjacent burning buildings no longer than the total burnout time of the buildings, a matter of a few hours to a half day under the worst conditions. However, flying brands emanating from fires elsewhere in the city could be carried great distances. They would become particularly prevalent and dangerous in conjunction with mass fires and conflagrations, which invariably develop large quantities of brands and embers. Usually the most serious threat is to roofs, but in a mass fire environment, wind and convection currents frequently develop a horizontal component sufficiently strong to carry brands into window openings. Fortunately, the threat from flying brands is amenable to control by fire watch teams, as discussed below.

Building codes commonly require Class A or B roof coverings within the fire limits of a city or wherever fire resistive building construction is involved.[17] Class C roof coverings are often specified in some cities as a minimum standard. All three classes "possess no flying brand hazard.[17] Nevertheless, the latent protection offered by these classes of roof coverings could be severely taxed in the vicinity of a mass fire, and monitoring and corrective action would have to be taken and should be anticipated by shelter personnel.

Fire countermeasures in a shelter building must be viewed as a purely local problem. Outside assistance could not be depended on. Detailed guidance in self help has been developed by IIT Research Institute in a report covering shelters in existing buildings.[29] The report is equally applicable to shelters in slanted buildings, and pertinent paragraphs therefrom have been incorporated in this section.

Organization

The shelter fire chief should be selected well before an emergency period and receive special shelter firefighting training. He should be chosen from the normal peacetime occupants of the building who are familiar with its interior layout, location of utility system controls, and characteristics of its occupancy. In addition, he should possess some firefighting or fire protection background. He should receive training covering all phases of fire prevention, detection, and extinguishment, including planning, equipping, and implementation techniques. He should also be responsible for the necessary equipment and be familiar with its use. In the attack period, he will be charged with staffing, instruction, and supervision of firefighting and fire watch teams, as well as other personnel engaged in fire prevention activities.

The successful suppression of all incipient fires that could occur within fallout shelter areas and other portions of shelter buildings would depend on the availability of sufficient personnel within each shelter who possess the ability to handle such fires utilizing only portable extinguishing appliances.

Fires of this nature could be effectively controlled by the use of two-man self-help teams, with each man equipped with an extinguisher and smoke mask. Therefore, the number of shelter firefighting personnel should be a multiple of the number of portable extinguishing appliances required for any given shelter building. It would appear reasonable to use a basis of three firefighters per extinguisher since this would allow for three 8-hour shifts and would also permit periodic rotation of firefighting personnel where required to limit total fallout radiation exposure.

All personnel should be given training that includes actual suppression of interior fires utilizing portable extinguishing appliances and smoke masks. In addition, basic instruction should be provided with reference to the types and mode of operation of various types of automatic sprinkler, standpipe and hose, and other extinguishing systems ensure their maximum utilization when available in shelter buildings.

Shelter Building Vulnerability

Initially, the shelter building should be surveyed to determine its vulnerability to fire and potential countermeasures. The survey should include:

- Identification of fire limiting areas capable of unsuppressed burnout.

- Determination of measures necessary to prevent spread of smoke and toxic gases into shelter areas.

- Potential hazard of fire exposure from adjacent buildings.

- Development of measures necessary to prevent primary ignitions from a weapon's thermal pulse.

- Determination of utility and process systems to be taken out of service in time of emergency.

- Inventory of fire control equipment and facilities.

The results of these surveys should be used by the fire chiefs and shelter managers to develop a fire control operational plan.

A quick, empirical method of assessing fire vulnerability of a shelter building, in terms of firespread potential, has been developed by Varley and Maatman.[29] It is limited to nonoperational, undamaged structures and may be used for an entire building or to draw conclusions about individual floors. Application of this method on an annual basis, and in conjunction with recommendations by professional firemen or fire engineers, would serve three valuable purposes: (1) forewarning the shelter staff of changed building conditions, e.g., fire load and structural modifications; (2) acquainting shelter staff with the building's firefighting facilities and their condition; and (3) orienting the staff's thinking within a framework of basic fire engineering principles.

Because the shelter building might sustain damage in a nuclear attack, contingencies might arise that could not be foreseen in advance. For example, fire walls, barriers, fire doors, and smoke vents could be damaged and rendered ineffective. For this reason, generalizations about fire behavior that may be inferred from a fire vulnerability survey should be avoided or, at the very least, they should be treated with circumspection. Some fire behavior generalizations to guard against are:

- "Downward movement of CO will probably not occur." This does not mean that such a condition cannot occur. In tests conducted by Waterman[26] fires generated gas pressures that caused CO to penetrate floor levels below the fire. Also Earp[22] states that:

"Thus it is quite likely that the occupants of basement shelters in Germany were poisoned by carbon monoxide in the smoke penetrating from the streets or burning buildings above."

- "A fire in the upper stories of a building will burn upwards" implies relative safety for the occupants on lower stories. In fact, if fire barriers are lacking or have been damaged, it is possible for fire to spread downwards.

- "Fire within a shelter space is only a problem of suppression since it will be discovered when incipient" is a dogmatic assumption and is highly dangerous. An "incipient" fire inside a shelter space may progress far enough to generate intolerable levels of CO_2 and CO if its discovery depends on chance observations by occupants. Furthermore, before a small fire can be extinguished, the smoke generated may become intolerable.

Consequently, the shelter manager should base planned remedial action on the somewhat subjective conclusion that (1) any fire on the floor levels above a shelter is potentially dangerous and (2) any fire on the same level as the shelter, either inside or outside, is potentially lethal. The nature of remedial action then becomes obvious - suppress fires as they occur.

Fire Control Plan

Both preattack and postattack operations must be covered in the fire control plan. As a minimum, the preattack plan should include a plan layout of each floor level of the building that indicates:

- Boundaries of fire limiting areas and location of fire control devices such as smoke vents, fire doors, fire walls, and barriers.

- Location of firefighting equipment including sprinkler system control valves and water flow alarm indicators.

- Location of all utility services controls.

- Supplementary instructions as required for operation of the building's utility services.

- Location of all emergency water supplies.

The postattack portion of the plan should provide for procedures to accomplish such tasks as the following:

- Extinguishment of ignitions that may have been caused by nuclear burst.
- Inspection of the entire shelter area for other possible ignitions.
- Assignment of shelter firefighting teams to survey the shelter building for the purpose of locating and extinguishing fires in nonshelter areas.
- Inspection of the entire shelter building for any other possible ignitions.
- Specific assignment of certain shelter firefighting teams to survey adjacent buildings for the purpose of locating and extinguishing fires.
- Where necessary to the long term shelter operation, restoration of the various utilities to service after examination of the potential safe operability of each.
- Where necessary, removal of any remaining combustibles to locations well away from exterior wall openings to reduce the possibility of their subsequent ignition from potential fires burning in adjacent buildings.
- Establishment of a fire watch routine to maintain the entire shelter building under constant surveillance.

It would be necessary during the postattack operations to coordinate the efforts of the various shelter firefighting teams and fire watch personnel with those of radiation monitoring personnel. This would be especially important for evaluating the potential safe operating periods available for any fire control and surveillance efforts that were attempted outside the fallout shelter area in the shelter building and in any of the surrounding buildings.

a. Equipment Required

- One 5-gallon stirrup pump extinguisher (with a hose at least 6 feet long) for each 1,250 sf of shelter area with a minimum of 4 extinguishers per shelter area.

- Smoke masks (U.S. Bureau of Mines approved type), together with spare canisters, provided in number equal to the allowance for stirrup pump extinguishers.

- Gloves and protective clothing for each member of the firefighting teams.

- Such tools as may be available in the shelter building, e.g., sledges, saws, chain falls, rope, and wrenches.

b. Postattack Fire Surveillance

With fire control activities limited to the self-help level, it is important to establish a continuing fire surveillance program for this period.

(1) Fire Watch in Nonshelter Areas. The problems of maintaining a fire watch tour under fallout radiation conditions could be met in two ways. With respect to personnel, cumulative dosages could be charted and appropriate rotation of fire watches could be accomplished. The other factor that would enhance the feasibility of firewatch tours is proper routing through irradiated areas. Routes could be designed to follow the most shielded portions of each area.

(2) Fire Watch in Shelter Areas. Discovery of a fire within a shelter cannot be left to chance. Because such fires could be potentially lethal, their discovery should be followed by immediate extinguishment. Given the prevalence of tension and apprehension, it would not be wise to relegate this important task to shelter occupants* since it would invite conditions of confusion if not outright panic.

In a buttoned-up shelter having no outside source of air, the effects of a fire could be critical. Posting of a continuous fire watch is suggested as the only measure that could adequately meet this situation.

* Other than those occupants specifically appointed for the purpose.

(3) Fire Watch Tour Schedules. Fire watch tours must be scheduled so that the time interval between successive tours would not allow a fire to develop beyond the stage at which it is extinguishable by self-help teams. Therefore, the various functional areas or spaces in the shelter building should be classified by fire hazard in terms of the time interval during which extinguishment is possible. The time interval for each area, i.e., the allowable fire build-up time, then would become the maximum time allowable between successive fire watch tours.

Table B-4 provides allowable fire build-up times for representative building functional areas. Since specific buildings may have unique functional conditions, the table is useful only as a baseline for on-site evaluation and refinement. In particular account must be taken of the fact that firespread in blast damaged structures is abnormally rapid.[49]

Build-up and Decay of Fires

a. Flashover

When a sustained ignition occurs in a room, there follows a period of heat build-up that eventually leads to total involvement of the room in flames. This is called a "flashover," and it is accompanied by a sudden and drastic surge in temperature. It essentially defines the point in time when firefighting efforts by self-help teams in the affected room become no longer possible and should be turned to halting the firespread to the next room.

Recent research[52,53] indicates that this significant time point, flashover, is the complicated product of many factors, but is strongly affected by size of existing fire in the room and size of room. Restricted ventilation usually hastens build-up of heat in the room, which is the essential prelude to flashover; however, once the existing fire becomes large, reducing ventilation can inhibit flashover, apparently by restricting the oxygen supply. In experimental fires in residential rooms, the time to flashover after a single flaming ignition of a major furniture item has been observed to be between 15 and 20 minutes.[26,63]

b. Automobile Fires

Highly realistic tests in England[54] and Switzerland[55] have demonstrated that fire among parked automobiles in a parking garage spread between automobiles slowly and with difficulty and that gasoline in the two-thirds full fuel tanks of the vehicles did not explode but burned slowly at the fuel tank filler cap. In some cases gas tank seams melted as the flames enveloped a burning car but never did the tank explode.

Table B-4

ALLOWABLE FIRE BUILD-UP FOR DORMANT AREAS LOCATED IN FIRE RESISTIVE BUILDINGS*

Area	Allowable Build-up Time (min)
Dining rooms	40
Flammable liquids	None
Heating and mechanical rm. (no combustibles)	120
Janitors' closets	60
Kitchens	12
Laundry rooms	30
Locker rooms (metal lockers)	60
Lodging rooms	30
Metal working areas	90
Motor vehicle areas	20
Offices (metal furniture)	120
Offices and schools (wood furniture)	75
Packing - unpacking	12
Paper (rolls, prints, patterns)	20
Paper (cutting, gluing, folding)	12
Repair shops	30
Sales areas	40
Sewing areas	20
Solid fuel storage (soft coal)	90
Solid fuel storage (wood, scraps, dust)	30
Stationery supplies	20
Theaters and auditoriums (stages without scenery)	60
Trash rooms	12
Wholesale storage (wood crates, wood patterns)	40
Wholesale storage (tight 10' piles, cartons, lt. crates)	30
Wholesale storage (loose 10' piles, cartons, lt. crates)	12
Wood working	30
Upholstering	20

* Values presume uncongested contents and structural surfaces having flame spread not greater than finished wood.[27]

Overhead sprinklers, when activated in these tests, failed to extinguish fires in automobile interiors, often spread the fire by floating burning gasoline to unburning automobiles and always created complete smoke obscuration of the fire site, making breathing without auxiliary breathing apparatus impossible.

c. Firespread and Fire Breaks

Following room flashover, the fire is capable of penetrating other rooms in a building. Horizontal and vertical firespread largely depends on a building's geometry and construction. The presence and integrity of firedoors and firewalls are important in suppressing the spread of the fire. In multistory buildings, the construction of the floors and ceilings is also important. Where they are made of noncombustible materials, vertical firespread will be limited to stairwells, elevator shafts, and other openings. Use of noncombustible materials can greatly contribute to the effectiveness of firefighting attempts. Other factors that affect the spread through the building are the fuel or fire loading, the position and compartmentalization of hallways, and the location of the initial ignition.

As McGuire[56] has pointed out, corridors (unlike most compartments in a structure) can be designed to contain little combustible material and thus can serve as interior firebreaks and means of access for firefighters. His full scale tests seem to show that the ceiling and upper portions of corridor walls are more important to fire propagation than the floor and floor covering. Waterman reports similar results.[64]

Under building conditions where the buoyant, hot gases of a fire are not confined, fires will usually spread to higher levels. Downward spread from the floor of ignition will usually occur only if structural failures expose lower floors to falling embers and debris. Thus downward spread depends on fire loading and structural fire resistance. Provided that the fire resistance ratings of structural components conform to the criteria in Table B-3, it is unlikely that downward spread of fire will occur.[25] (The structural strengths of some of the components listed in Table B-3 may have been reduced by air blast in which case their fire ratings will also be lowered.)

However, even with good fire resistive construction, fires should not be allowed to develop. Possible blast damage to fire doors and the threat presented by smoke and toxic gases would demand that fires be suppressed as soon as possible after ignition. Fortunately, studies have shown that small self-help teams of untrained men, using portable fire extinguishers, are effective in fighting room fires up to a point just before flashover.[27] After flashover, the only recourse is to attempt to seal off the rooms involved.

d. Empirical Fire Burning Rate

Wiersma and Martin[61] have reported times from ignition to flashover in each of the several rooms of test-burned former barracks. Their experiments were carried out in pairs of all-wood structures (spaced 20 ft between exterior walls) in which strong fires were deliberately kindled; consequently, some aspects of their results can not readily be generalized. The floor plan of one of their pairs of burned buildings along with the times between ignition and flashover in each room are reproduced in Table B-5. The approximate speed of advance of a similar test fire through a single example of these barracks has been given by Butler[49] as 12 fps. Because these buildings had attics through which fire spread rather quickly, it may be more realistic to regard them as containing essentially a single room and to consider the average of the entries in Table B-5 as approximately equal to flashover time for an all-wood room 40 x 50 x 10 ft, ignited by a vigorous fire in one corner.

Wiersma and Martin generalized the cumulative progress of their experimental burnings of six of these pairs of buildings by means of the equation

$$\frac{x}{X} = \frac{1}{1 + A\ t^{-B}}$$

where

x = total progress to time t

t = time measured from ignition

X = total progress at end of combustion, i.e., $X = \int_0^\infty \frac{dx}{dt}\, dt$ and A and B are empirical constants.

The quantities x and X must be consistent but may be radiant energy emitted, weight of combustibles in the structure consumed by time t, or other measure of fire progress. The averages of the values for the empirical constants reported by these authors are

$$B = 5.0$$

$$A = 1.0 \times 10^{8}$$

when time is measured in minutes.

Table B-5

TIMES OF ROOM FLASHOVER CAMP PARKS, 5 MARCH 1971[61]

Room Number	Time after Ignition to Flashover (min)
Building D	
Room 1	5
2	10
3	27
4	11
5	3
6	10
7	11
8	11
Building C	
Room 1	3
2	7.5
3	18
4	--
5	12
6	15
7	27
8	19

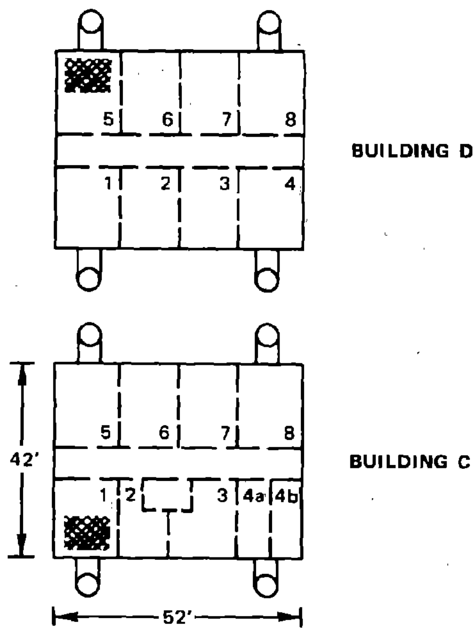

IGNITION ROOMS ARE C1 AND D5
CLOSED ROOMS ARE C7 AND D3

Differentiating the equation above with respect to time and substituting the average values of A and B, the rate of burning r = dx/dt is found to be:

$$\frac{r}{X} = \frac{1}{X}\frac{dx}{dt} = \frac{5.1 \times 10^{8}\ t^{-6}}{(1 + 1 \times 10^{8}\ t^{-5})^{2}}$$

The right hand side of this equation has been plotted in Fig. B-19 and shows the rate of burning r in these structures as a function of time. It is expected that the graph of the burning rate in any fuel-controlled fire will show the same shape but the time scale will vary widely, depending on the rate of firespread through the structure. The area under the curve of Fig. B-19 is unity; to find the numerical value of the rate r at any time t in minutes after ignition, the corresponding ordinate must be multiplied by the quantity X, that is, by a quantity proportional to the amount of material to be burned.

It is expected that after multiplying abscissa values by an appropriate factor α and dividing ordinate values by the same quantity α we may use the curve in Fig. B-19 to describe the progress of most normal fires. The value of α depends upon the firespread rate; if, for example, the fire intensity peaks 5 min. after ignition instead of 37 min. as shown in Fig. B-19, the $\alpha = 5/37$. Although rate of firespread depends in turn upon quantity to be burned, the dependence is not simple, even in structures of the same type.

For example, Butler[49] burned 1/6 and 1/16 scale models of the all-wood barracks buildings referred to above and reported rates of firespread as a function of horizontal linear dimension. His results are reproduced in Table B-6.

Table B-6

RATES OF FIRESPREAD IN BARRACKS AS A FUNCTION OF MODEL SIZE[49]

Scale	Rate of Spread (fps)	Horizontal Linear Dimension (ft)
full	12.0	45.0
1/6	1.1	7.5
1/16	0.14	2.8

Rate of spread is a function of the kind and distribution of combustibles as well as the quantity. Since the values in Table B-6 were drawn from experiments conducted in compact structures made almost entirely of wood, it is expected that those values probably constitute an upper limit among normal situations. However, if the structure is badly

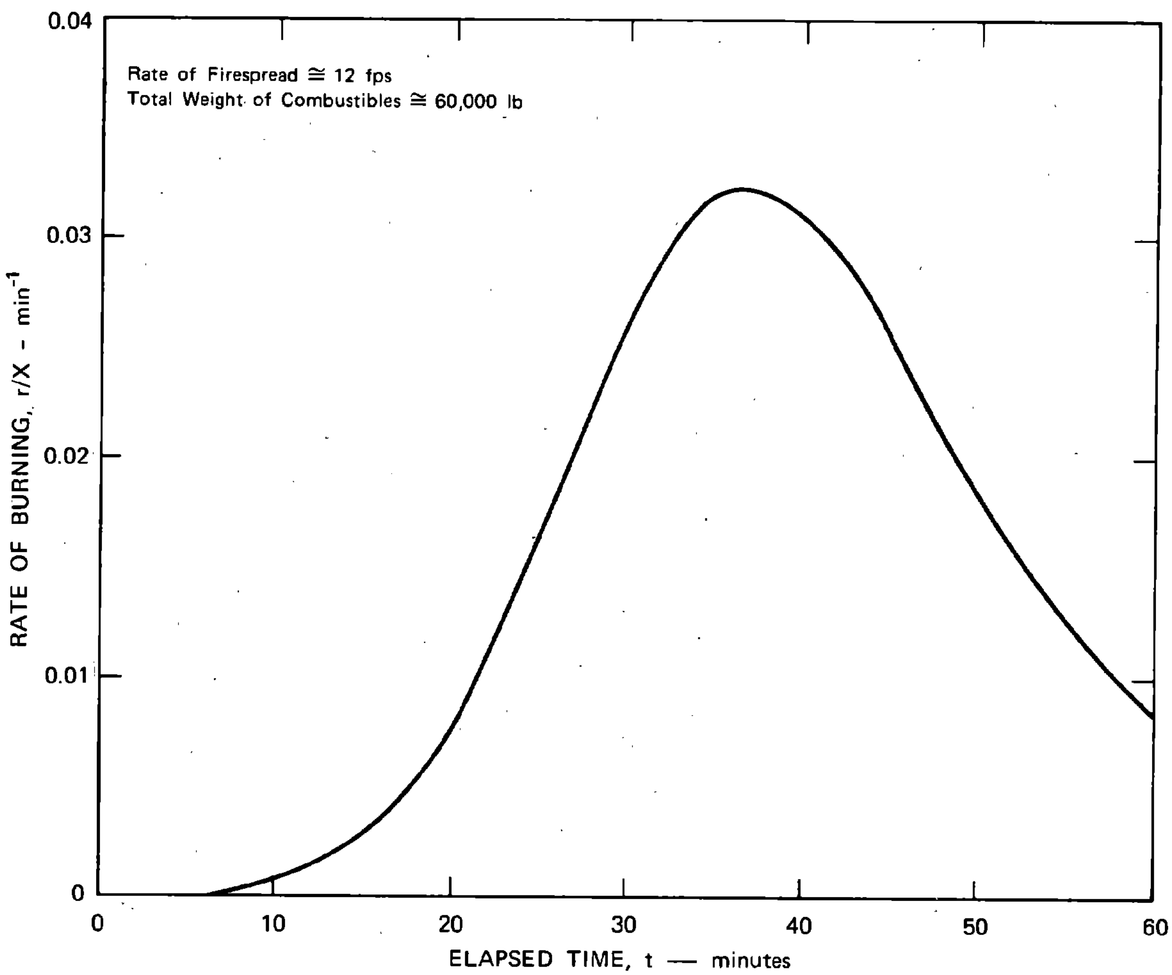

FIG. B-19 IDEALIZED RATE OF BURN

damaged (and in fact is essentially a pile of purely combustible debris), the firespread rate may be at least twice as high as it is in the intact structure.[49]

Fire Retardant Treatment (Thermal Hardening)

Significant, long-lasting fire-resistance protection in cellulosic materials, such as cotton and rayon, can be obtained by soaking them in solutions of certain fire retardant chemicals. Experiments have shown that subsequent exposure of these materials to thermal radiation (such as that from the weapon itself* or from a nearby fire) that would cause an untreated sample of the same substance to burst into sustained flame may either cause the treated sample to char or, at worst, to flame only during the period of irradiation.[57,58] The char tends to hold its structural form and may act as an inert absorber of subsequent radiation. Moll and McAuliffe[59] have recommended that treated draperies be closed over windows likely to be exposed to the thermal pulse of a nuclear weapon.

Table B-7 and B-8 list compositions of several effective flame retardants.[57,58] The tables also show the weight added to the material by the treatment. Since washing will remove these fire retardant materials, fabrics must be treated after each washing.

Emergency protection against the weapon thermal pulse may be found in almost any sort of coating over window glass and Moll and McAuliffe[59] have evaluated a number of handy substances that are suitable for the purpose, such as whitewash, white flour, mud, and others.

While covering openings with drapes or other materials will always decrease radiant thermal transmission through the opening, it should be noted that at extremely high intensities explosive evaporation of water content (decrepitation) and ablation may greatly reduce the effectiveness of a covering. Generally these extreme effects are apparent at distances from the burst within the radius corresponding to approximately 40 psi peak blast overpressure. For protection against radiant thermal pulses of this kind all metal shutters or blinds are necessary.

---

* By means of a carbon arc and shutter Wiltshire and Parker[58] exposed treated samples in the laboratory to radiant pulses very similar to those expected from weapons yielding 1 to 100 Mt at ranges corresponding to peak overpressures of 2.3, 3.0, and 5.0 psi.

Table B-7

PROVEN FLAME RETARDANTS[57]

Retardant	Solution Concentration (Percent)	Resultant Load (Percent)
$KHCO_3$	10	11.9
$KHCO_3$	2	2.72
Borax-Boric Acid*	10	12.7
Borax-Boric Acid*	2	2.76
Borax-Boric Acid*	0.2	0.29
$ALCL_3 \cdot 6\ H_2O$	2	2.77
$(NH_4)H_2\ PO_4$	2	2.74

* A mixture of 7% borax and 3% boric acid (N.F.P.A. Handbook, Retardant Formula Number 2).

Chapter VII of Ref. 1 points out two simple, effective steps toward greater fire resistance that may be taken in preparation for nuclear attack. Fresh, white paint applied to exposed wood surfaces will essentially make the wood incombustible under direct thermal radiation of 25 cal/cm^2 or less* and will under prolonged irradiation from a neighboring fire delay flashover enough to make firefighting feasible. A second recommended countermeasure is removal of easily ignitable material close to otherwise combustible structures; such material is kindling and its ignition leaves little opportunity for firefighting.

It should be noted again that the foregoing remarks and the suggestions contained in Tables B-7 and B-8 apply to cellusosic materials. Thermal hardening techniques for synthetic polymers can be quite different. Some examples of these can be found in compilations by Lyons [65] and Thiery. [66]

* Painted wood may burst into flame and be charred in a weapon thermal pulse of 25 cal/cm^2 but ignition is not sustained. A 30 kt weapon yields 25 cal/cm^2 at a range corresponding to approximately 4 psi peak overpressure.

Table B-8

FORMULAS FOR RETARDANT TREATMENTS[58]

Chemicals	A	B	C	D	B.B.P.
Borax	7 oz	6 oz	-	-	3 oz
Boric Acid	3 oz	-	-	-	1.5 oz
Diammonium Phosphate	-	6 oz	12 oz	-	-
Ammonium Sulfate	-	-	-	13 oz	-
Ammonium (mono) Phosphate	-	-	-	-	5 oz
Household Ammonia	-	-	-	Trace	-
Wetting Agent	Trace	Trace	Trace	Trace	Trace
Water	2 qt	2 qt	2 qt	2 qt	2 qt
Percent Add On (by weight)	11	9.3	7.5	13.2	10

Countermeasures Against Heat from Debris Fires

When the ceiling slab of a basement shelter is known to provide marginal thermal insulation, two simple countermeasures that might be planned ahead of time are water flooding and debris removal. Flooding could be accomplished remotely after the attack, provided that a secure water supply is made available and the slab is not too severely broken up. Preliminary experiments[47] demonstrate that addition of water in the amount of 1/3 gal/sf to the surface of the concrete slab reduces peak heat flux through the slab by approximately 20%, and removal of all debris (including ash) 1.5 hours after ignition lowers peak flux by 60 to 70%.

The combined countermeasures accomplish over 80% reduction in peak flux. Investigation of these countermeasures is understood to be continuing.

Annex A - Alternative Methods for Developing Building Separation Distances

Computational

The basic expression of the configuration factor ϕ can be obtained from the following diagram wherein dA_1 is an elemental radiator, dA_2 is an elemental receiver, and θ represents the angle between the line-distance, C, connecting the centroids of dA_1 and dA_2 and the normal to each area, respectively.

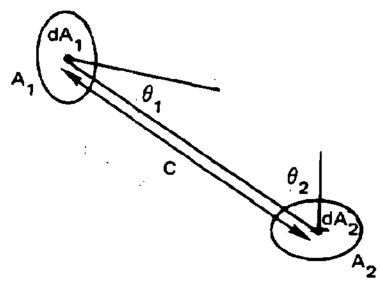

The intensity of radiation received at any point from a radiator is:

$$I = \phi I_o$$

and for our purposes (see Section 2 above):

$I = 0.3\ cal/cm^2$-sec as a maximum

$I = 4\ cal/cm^2$-sec for a fuel load equal to or greater than 5 psf

$I_o = 2\ cal/cm^{-2}$-sec for a fuel load less than 5 psf.

The energy received by unit area at dA_2 per unit time from dA_1 is:

$$\left(dA_1\right) \cdot \frac{I_o}{\pi} \left(\cos\ \theta_1\right) \left(\frac{\cos\ \theta_2}{C^2}\right)$$

and the intensity of radiation at dA_2 from the entire radiator is then:

$$I = \frac{I_o}{\pi} \int_{A_1} \frac{\cos \theta_1 \cos \theta_2}{C^2} dA_1$$

and since $\phi = I/I_o$:

$$\phi = \frac{1}{\pi} \int_{A_1} \frac{\cos \theta_1 \cos \theta_2}{C^2} dA_1$$

In our calculations the configuration factor Ø must be either $0.3/4 = 0.075$ (fuel load ≥ 5 psf) or $0.3/2 = 0.15$ (fueld load < 5 psf) and orientation angles can be measured; therefore, the distance C can be computed.

Optical Analog[31]

Figure B-20 indicates an optical analog that may be employed to determine the separation distance C. A model of the building facade (the radiator) is constructed of black photographic paper, covered with a diffusing material and then attached to the diffusing screen. The diffusing screen is uniformly illuminated. The interior of Section A is painted white to obtain high reflectivity. The interior of Section B is painted black to prevent reflected light from impinging the photocell. The cell has a sensitive area of about 1 cm^2 and is used together with a galvanometer to measure light intensity. The intensity of light emitted can be held constant by employing a constant voltage transformer. A calibrated scale attached to the galvanometer can then be used to read ϕ directly. Thus, when the photocell is placed close to the radiating area, the configuration factor will be unity, and when placed in the position of the receiving element, the configuration factor can be read directly from the scale. Should there be reflecting surfaces between the radiating surface and the point at which the measurement is to be made, these, with suitable reflectivity coefficients, would have to be included in the illuminated model. When the model of the radiating area is set up, the photo cell is backed off to read 0.15 or .075, depending on fuel load, and the proportional distance C is measured directly between the cell and the radiator.

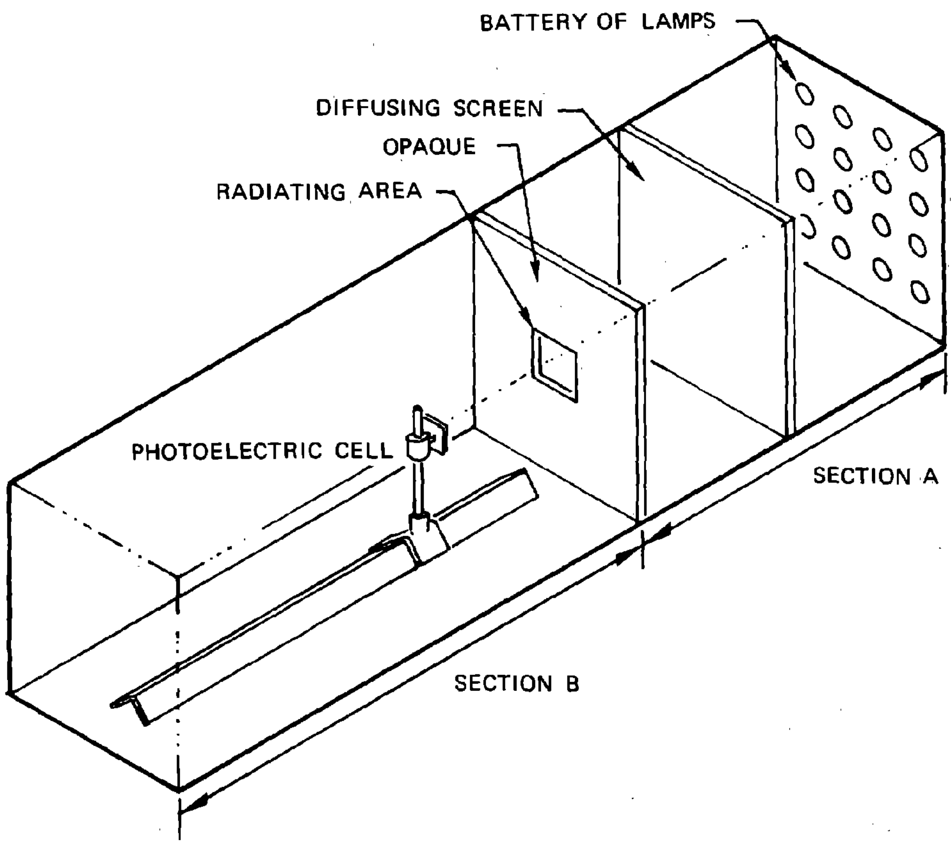

FIG. B-20 APPARATUS FOR DETERMINATION OF THE CONFIGURATION FACTOR[31]

B-72 BLANK

REFERENCES

1. Glasstone, S., Effects of Nuclear Weapons, U.S. Department of Defense and Atomic Energy Commission, 1962 edition (1964 reprinting), Superintendent of Documents, Washington, D.C.

2. Goodale, T. C., M. B. Harkins, and A. B. Willoughby, Feasibility of Active Countermeasures for Thermal Radiation Effects of Nuclear Weapons, Final Report, United Research Services, July 1963 (AD-412 733).*

3. Gibbons, Mathew G., Transmissivity of the Atmosphere for Thermal Radiation from Nuclear Weapons, U.S. Naval Radiological Defense Laboratory, San Francisco, California, August 12, 1966 (AD-641 481).

4. Combustible Contents of Buildings, Building Materials and Structures Report, U.S. Department of Commerce, July 25, 1957.

5. Bracciaventi, J., Window and Window Screens as Modifiers of Thermal Radiation Released in Nuclear Detonations, U.S. Naval Applied Science Laboratory, Brooklyn, N.Y., September 12, 1966 (AD-643 019).

6. Fire Aspects of Civil Defense, OCD TR-25, July 1968.

7. Crowley, J. W., et al., Development of Analytical Relationships and Criteria for Blast and Fire Vulnerability of Fallout Shelter Occupants, Systems Sciences Inc. Final Report for OCD Contract No. DAHC 20-67-C-0147, OCD Work Unit 1614B, October 1, 1967 (AD-842 356L).

8. Moll, Kendall, and John McAuliffe, Secondary Ignitions in Nuclear Attack, Stanford Research Institute Report Contract N228 (62479) 65701, OCD Work Unit 2534A, July 1965 (AD-625 173).

9. Brunswig, Hans, Practical Experiences of Fire Protection Services, A critical presentation of the organization technology and tactics of fire protection as employed by a civil defense organization during World War II in Germany, translated by C. E. Harvey and W. C. Truppner, OCD Work Unit No. 4315A, June 1966 (AD-652 618 & 619).

---

* AD numbers may be used to order report copies or microfiches from NTIS, Springfield, Virginia 22151.

10. Rodden, Robert M., Floyd I. John, and Richard Laurino, Exploratory Analysis of Fire Storms, Stanford Research Institute Report Contract N228 (62479) 65419, for U.S. Office of Civil Defense, May 1965 (AD-616 638).

11. Cohn, B. M., L. E. Almgren, and M. Curless, A System for Local Assessment of the Conflagration Potential of Urban Areas, Gage-Babcock and Associates report prepared for U.S. Office of Civil Defense (OCD-PS-64-74), March 1965 (AD-616 623).

12. Law, Margaret, Heat Radiation from Fires and Building Separation, Department of Scientific and Industrial Research and Fire Offices Committee, Joint Fire Research Organization, Fire Research Technical Paper No. 5, London, 1963.

13. The National Building Code, 1967 Edition, American Insurance Association, New York, N.Y., Chicago, Ill., and San Francisco, Calif.

14. Phung, P. V., and A. B. Willoughby, Prediction Models for Fire Spread Following Nuclear Attacks, URS Corporation, Final Report for OCD Contract No. OCD-PS-64-48, January 1965 (AD-613 359).

15. National Fire Code, Vol. 4, National Fire Protection Association, Boston, Mass., 1966-67.

16. Waterman, T. E., Shelter Habitability in Existing Buildings Under Fire Exposure, IIT Research Institute Report for U.S. Office of Civil Defense, Contract No. N228 (62479) 68355, June 1966 (AD-637 806).

17. Fire Protection Handbook, National Fire Protection Association, 12th ed., Boston, Mass., 1962.

18. Leutz, Herman, "Fireproof Shelters with Secured Ventilating Systems," Proceedings of the Symposium on Protective Structures for Civilian Populations, NAC-NRS, April 19-23, 1965.

19. Herrington, L. P., and J. D. Hardy, "Temperature and Humidity in Relation to the Thermal Interchange Between the Human Body and the Environment," Human Factors in Undersea Warfare, Panel on Psychology and Physiology, Committee on Undersea Warfare, National Research Council, Washington, D.C., 1949.

20. Handbook of Fundamentals, American Society of Heating, Refrigerating, and Air-Conditioning Engineers, Inc., New York, N.Y., 1967.

21. Bond, Horatio, "Fire Casualties of the German Attacks," Fire and the Air War, National Fire Protection Association, Boston, Mass., 1946.

22. Earp, Kathleen F., Deaths from Fire in Large Scale Air Attacks-With Special Reference to the Hamburg Fire Storm, Home Office, Scientific Advisors' Branch, Whitehall, S. W. 1, London, April, 1953.

23. Lee, William, et al., Design of Tests for the Effects of Mass Fires on Shelter Occupants, Isotopes Inc., Palo Alto, Calif., OCD Work Unit 1133B (Contract No. N00228-66-C-0917), September 26, 1966.

24. Broido, A., and A. W. McMasters, Effects of Mass Fires on Personnel in Shelters, Division of Forest Fire Research, Pacific Southwest Forest and Range Experiment Station, U.S. Forest Service, Department of Agriculture, for U.S. Office of Civil Defense (Contract No. DCM-SR-59-7), Technical Paper 50, August 1960.

25. Colvin, C. B., Shelter Remedial Actions Phase III Final Comprehensive Report, Appendix A, URS Corp. Report for Stanford Research Institute, EOSD Project 65-5, November 1967.

26. Waterman, T. E., et al., Prediction of Fire Damage to Installations and Built-up Areas from Nuclear Weapons - Phase III Experimental Studies - Appendices A-G, for National Military Command System Support Center (Contract No. DCA-8), November 1964.

27. Varley, R. B., and G. L. Maatman, Shelter Fire Vulnerability - Specific Fire Limiting Activities for Occupants, IIT Research Institute Report for U.S. Office of Civil Defense (Contract No. OCD-OS-62-210), September 9, 1964 (AD-449 386).

28. Laughlin, K. P., Thermal Ignition and Response of Materials, Project 31.5, Operation Teapot, Civil Effects Test Group, Office of Civil and Defense Mobilization, Battle Creek, Michigan, May 1955.

29. Varley, R. B., and G. L. Maatman, Shelter Fire Vulnerability - Survey and Analysis of Representative Buildings, IIT Research Institute Report for U.S. Office of Civil Defense (OCD-05-62-210), March 17, 1965 (AD-615 391).

30. Uniform Building Code, 1967 edition, International Conference of Building Officials, Pasadena, Calif.

31. Lawson, D. I., and D. Hird, "A Photometric Method of Determining Configuration Factors," British Journal of Applied Physics, 5, 72-4, 1954, Joint Fire Research Organization, Boreham Wood, England.

32. Goodale, Thomas, Effects of Air Blast on Urban Fires, URS Research Corporation Final Report, OCD Contract No. DAHC20-70-C-03730, December 1970 (AD-723 429).

33. Martin, S.B., R.W. Ramstad, T. Goodale, and C.A. Start, Effects of Air Blast on Urban Fire Response, URS Research Company Final Report for OCD, May 1969 (AD-695 383).

34. Waterman, T.E. and A.N. Takata, Laboratory Study of Ignition of Host Materials by Firebrands, IIT Research Institute Final Report for OCD, June 1969 (AD-697 270).

35. Vodvarka, F.J., Firebrand Field Studies, IIT Research Institute Final Report for OCD, September 1969 (AD-704 725).

36. Alger, Ray, Naval Ordnance Laboratory Group at Stanford Research Institute, personal communication, April 1971.

37. Miller, C.F., World War II German Fire Document Translations, Stanford Research Institute report to OCD, July 1967.

38. Moysey, E.B. and W.E. Muir, "Pilot Ignition of Building Materials by Radiation," Fire Technology, vol. 4, no. 1, pp 46-50, February 1968.

39. Pryor, A.J. and C.R. Yuill, Mass Fire Life Hazard, Southwest Research Institute Final Report for OCD, September 1966 (AD-642 790).

40. Waterman, T.E., Fire Laboratory Tests - Phase I, IIT Research Institute Final Report for OCD, September 1970 (AD-713 017).

41. Takata, A.N. and T.E. Waterman, Fire Protection for Basement Shelters in New Construction, IIT Research Institute Interim Technical Report for OCD, 29 June 1971.

42. Takata, A.N., A Review of Fire Hazard Distances, IIT Research Institute, April 1970 (AD-872 998).

43. Webb, P., editor, Bioastronautics Data Book, National Aeronautics and Space Administration, NASA SP-3006, 1964.

44. A Digest of Authoritative Opinion on the Limits of Human Exposure to Harmful Environmental Factors, Thomas A. Edison Research Laboratory, 22 August 1962.

45. Pryor, A.J., F.A. Fear, and R.J. Wheeler, Mass Fire Life Hazard, Southwest Research Institute, March 1968 (AD-672 035).

46. Pryor, A.J., D.E. Johnson and N.N. Jackson, Hazards of Smoke and Toxic Gases Produced in Urban Fires, Southwest Research Institute, September 1969 (AD-697 839).

47. Takata, A.N. and T.E. Waterman, Fire Protection for Basement Shelters in New Construction, IIT Research Institute Fourth Quarterly Report for OCD, 15 October 1971.

48. Vodvarka, F.J., Full Scale Burns in Urban Areas Shelter Experiments, IIT Research Institute, June 1969 (AD-697 271).

49. Bulter, C.P., Measurements of the Dynamics of Structural Fires, Stanford Research Institute, August 1970 (AD-716 327).

50. "The Control of Smoke in Building Fires - A State-of-the-Art Review", by the Task Group of Subcommittee IV of American Society of Testing and Materials Committee E-5, Materials Research and Standards, April 1971.

51. Ferguson, R.S., Principles of Fire Protection Applied in Part 3: Use and Occupancy, National Building Code of Canada, National Research Council of Canada, Division of Building Research, March 1970.

52. Waterman, T.E., "Room Flashover - Criteria and Synthesis", Fire Technology, 4, 25, 1968.

53. Waterman, T.E., Scaled Room Flashover, IIT Research Institute, April 1971 (AD-723 424).

4. Butcher, E.G., G.J. Langdon-Thomas, and G.K. Bedford, Fire and Car-Park Buildings, Fire Note Number 10, Ministry of Technology and Fire Offices' Committee, Joint Fire Research Organization, HM Stationery Office, London, 1968.

55. Bürgi, H., "Fire Tests with Cars Parked in an Enclosed Car Park Building," Scweizerische Feuer-Zeitung, No. 12, 1970.

56. McGuire, J.H., "The Spread of Fire in Corridors," Fire Technology, 4, 2, 103-108, 1968.

57. Alvares, N.J., and T.H. Anderson, Ignition Hardening of Cellulosic Materials, U.S. Naval Radiological Defense Laboratory, August 1967 (AD-663 086).

58. Wiltshire, L.L., and W.J. Parker, Ignition of Retardant Treated Cloth by Nuclear Weapon Thermal Pulses, U.S. Naval Radiological Defense Laboratory, August 1968 (AD-683 307).

59. Moll, K., and J. McAuliffe, Public Capabilities for Preventing and Extinguishing Ignitions from Nuclear Attack, Stanford Research Institute, November 1968; page 23, (AD-679 898).

60. Technische Weisungen für den Privaten Schutzraumbau, Federal Justice and Police Department, Federal Office for Civil Defense, Bern, Switzerland, 1966.

61. Wiersma, S.J., and S.B. Martin, Measurements of the Dynamics of Structural Fires, Stanford Research Institute report for OCD, August 1971 (AD-732 498).

62. Zinkahn, W. and H. Leutz, Commentary on the Law of Air Raid Protection, C.H. Beck, publisher, Munich and Berlin, 1956.

63. Vodvarka, F.J. and T.E. Waterman, Fire Behavior, Ignition to Flashover, IIT Research Institute report to OCD, June 1965

64. Waterman, T.E., Effects of Material Location and Area Coverage on Flame Spread in Corridors, IIT Research Institute technical report to Society of the Plastics Industry, Inc., April 1969

65. Lyons, J.W., The Chemistry and Use of Fire Retardants, John Wiley and Sons, Inc., New York, 1970

66. Thiery, P., Fireproofing, Chemistry, Technology and Applications, J.H. Goundry, translator, Elsevier Publishing Co., Ltd., New York, 1970

ANNOTATED BIBLIOGRAPHY

Standard Methods of Fire Tests of Building Construction and Materials, National Fire Protection Association Standard No. 251, May 1961, (ASTM-E-119).

- Provides methods for determining fire resistance ratings of materials.

Shorter, G. W., et al., "The St. Lawrence Burns," Quarterly of NFPA Vol. 50, No. 4, pp. 300-16, April 1960.

- Gives time-temperature readings from full scale tests in which residences were burned.

Thomas, P. H., "The Size of Flames from Natural Fires," Ninth Symposium on Combustion, New York and London, Joint Fire Research Organization, Boreham Wood, England, Academic Press, pp. 844-59, 1963.

- Flame height computations and graphs are given.

Fire Research 1961, Joint Fire Research Organization, Boreham Wood, England.

- General report that includes method for computation of flame heights emitted from windows.

Proceedings of the Symposium on Protective Structures for Civilian Populations, National Academy of Sciences, National Research Council, April 1965:

- Leutz, Herman, "Possibility of Occurrence of Area Conflagrations and Firestorm with Respect to Fuel Density," p. 31- . Describes method by which a fuel density index can be computed for specific areas and then tabulates values of indexes against probability of occurrence of fire spread, conflagration, or firestorm.

- Leutz, Herman, "Fireproof Shelters and Secured Ventilating Systems," p. 134- . Gives structural and mechanical criteria for the maintenance of tolerable conditions in the shelter when it is exposed to heating from adjacent fires, and ambient atmosphere is charged with CO, CO_2, and other gases of combustion. Note: Use of sand filter to act as heat sink is suggested.

- Smitt, Gosta, Fire Safe Shelter Design, p. 139- . Gives curves relating temperature development within shelters to varying degrees of shelter wall or ceiling heating from outside fires. Notes that slab temperature reached during fire exposures can have considerable effect on reinforcing steel strength. Cites strength reduction of 50% for 600 C, which is a temperature easily attained in a fire.

McGuire, J. H., "Fire and the Spatial Separation of Buildings," Fire Technology, National Fire Protection Association Quarterly, Vol. 1, No. 4, pp. 278-87, November 1965.

Fire Protection Engineering, NavDocks 2068 (Rev. 9-61), U.S. Naval Facilities Engineering Command, Washington, D.C.

- Fire protection engineering criteria for design, construction, maintenance and operation of buildings, structures, and facilities. Includes building separation curves for combustible and non-combustible buildings.

Takata, A. N. and T. E. Waterman, Fire Laboratory Tests - Phase II - Interaction of Fire and Simulated Blast Debris, IIT Research Institute report for OCD, February 1972.

- Latest summary of research into heat conduction and gas migration through concrete ceiling slab into closed basement shelter and possible countermeasures against them.

Hedge, J. C. and T. E. Waterman, Fire Test Ratings for Shelter Components, IIT Research Institute Final Technical Report for OCD, 15 May 1969.

- Discusses values of physical parameters used in calculations of heat flow through concrete slabs and presents results of a number of these calculations.

- Discusses designs for heat-and gas-proof shelter doors and presents some results of tests of them.

Wiersma, S. J., Measurements of the Dynamics of Structural Fires, Stanford Research Institute Annual Report for Defense Civil Preparedness Agency, August 1972.

- Probably the definitive work on the measurement of the empirical burning rate of full-size, all-wood barracks buildings described on page B-62 above. (Published too late for inclusion of the findings in this Appendix.)

The two references below pertinent to the subject of fires in large buildings came to the attention of the authors too late for incorporation of their information in this Appendix:

Fire Problems in High-Rise Buildings, prepared by the Bureau of Industrial Education, California State Department of Education, 1971.

Proceedings: Reconvened International Conference on Firesafety in High-Rise Buildings, Public Buildings Service, General Services Administration, October 5, 1971.

Appendix C

INITIAL RADIATION CALCULATIONS FOR ENTRANCEWAYS

By C. K. Wiehle

Reproduced, without change, from: Wiehle, C. K., Shelter Entranceways and Openings, prepared by Stanford Research Institute for OCD, final report, September 1967. (AD-662 749)

NOTE: While fully outside entranceways are illustrated, the analysis techniques are useful for all entranceway configurations. No one type should be inferred as the recommended type for all applications.

Appendix C

INITIAL RADIATION CALCULATIONS FOR ENTRANCEWAYS

By C. K. Wiehle

Introduction

Although there are many unknowns concerning both the attenuation of radiation through entranceways and its distribution within the structure, the simplified procedures presented in Refs. 5 and 6 were felt to be adequate for the designs prepared here. Basically, there are three problems associated with the analysis of an entranceway for the initial nuclear radiations. These are the determination of the free-field initial radiation intensities, the maximum permissible dose, and the entranceway attenuation of the radiation. The methods used to calculate these quantities, together with an illustrative example, are given in the following subsections.

Initial Nuclear Radiation

The initial nuclear radiation is defined in Ref. 1 as the radiation emitted within one minute after the detonation of a nuclear weapon, including the prompt radiation. For the purpose of this study, Ref. 1 was used to obtain the intensities of the free-field gamma and neutron radiation at the entranceway opening. Because of the yield-range-dose relationships, it is necessary to specify a yield, range, and HOB (height of burst) before the radiation intensity in the free-field can be calculated. However, even with precise yield-range data, Ref. 1 cautions that any calculation of radiation exposure dose is subject to wide fluctuation in reliability due to variation in weapon design and characteristics. Only the 20 psi overpressure level from a 200-kt weapon yield was considered for the radiation intensity calculations in this study.

Maximum Permissible Radiation Dose

The establishment of a total permissible dose for shelter occupants, although beyond the scope of this study, is a primary factor in the design and cost of entranceways. Even at the modest overpressure level of 20 psi examined in this study, the initial radiation requirement increased the cost of the blast shelter entranceways. The total dose in the shelter

is composed of the initial radiation and residual fallout radiation that penetrates both the entranceway and the shelter proper. For a specific shelter design problem, the relationship between the contributions of the radiation from these two sources can be studied to obtain an economical compromise for the entranceway and shelter design. However, for a study of only the entranceway portion of the shelter system, it is necessary first to establish a permissible dose and then to estimate the entranceway contribution for both initial and residual radiation. For the purposes of this study, it was sufficient to adopt the criterion presented in Ref. 5. Essentially, this limited the total radiation dose in the shelter to 40 rads, with the assumption that the permissible dose was divided equally at 20 rads each for the entranceway and the shelter proper. Further, the entranceway portion was divided equally between initial and fallout radiation, which resulted in a permissible initial radiation dose of 10 rads through the entranceway. To adhere to the criterion mentioned above for a specific shelter would require assuming an accumulated total dose for the free-field fallout radiation and determining its attenuation through the entranceway. However, as noted in the fallout radiation analysis in Appendix 2,* for a study of entranceways only, it was believed sufficient to determine the PF for the blast entranceways in the usual manner (Ref. 20) at a detector point 3 ft inside the shelter entry without calculating the actual radiation dose.

Another factor that is important in describing the permissible radiation dose received by shelterees is the exposed and absorbed dose of nuclear radiation. To describe the effects of nuclear radiation on a biological system adequately, it is necessary to express the free-field radiation exposure dose as an absorbed dose. This has been accomplished by introduction of the rad, which is defined as the absorbed dose of any nuclear radiation that is accompanied by the liberation of 100 ergs of of energy/gram of absorbing material (Ref. 1). Because of the uncertainty of determining the biological effect of nuclear weapons and to simplify the radiation analysis, the absorbed dose in rads was used in this study to judge the adequacy of the entranceways for providing initial radiation protection.

Entranceway Radiation Attenuation

The attenuation of the free-field nuclear radiation intensities through an entranceway can conveniently be separated into three phases for purposes of analysis: the entrance reduction factor, entranceway bend and corridor attenuation, and barrier attenuation.

---
* Appendix D herein.

Entrance Reduction Factor

The important factors in determining the initial radiation dose within the entranceway are the orientation of the entrance opening relative to the burst point, the entranceway geometry, and the free-field radiation intensity. In general, Refs. 5 and 6 both conclude that the hazard from radiation streaming into the entrance opening would be maximum for a line-of-sight direction along the longitudinal axis of the entrance section between a detector located in the entranceway, usually at the first bend, and the burst point. This would result from the fact that the higher energy gamma rays and neutron particles are more likely to come from a line-of-sight direction than from a scattered direction. Although the effect on radiation dose of the angle between the line-of-sight and the burst point was not investigated, it was possible to examine limited burst positions on the vertical plane through the longitudinal axis of the entrance section. The locations were on the line-of-sight from the detector approximately along the longitudinal axis of the entrance section, on the grazing line-of-sight between the detector and the first step of the entranceway, and for a surface burst location. It was found that the most critical location was for the grazing line-of-sight. In general, as the HOB is increased, the range for a given yield and overpressure also increases to a maximum for some optimum HOB. Since the initial radiation dose is range dependent, it would decrease to a minimum at the optimum HOB for a given yield and overpressure. Although the magnitude of the entrance reduction factor is dependent on the angular deviation from the line-of-sight orientation, the reduction of this factor for the grazing line-of-sight is more than offset by the increase in free-field radiation intensity due to the decreased range; this was not the case for the surface burst location. It may well be that some intermediate angle between those selected may produce a greater entrance section radiation dose, but it was felt sufficient for the purposes of the entranceway designs and cost estimates in this study to use the grazing line-of-sight for the initial radiation analysis.

To determine the fraction of the free-field radiation that would penetrate the entrance section, it is necessary to compute the solid angle fraction subtended by the entrance opening and the detector location. Figure 1-1, obtained from Ref. 20, can be used to calculate the solid angle fraction for rectangular openings. To calculate the entrance reduction factor, R_{fe} for both gamma and neutron radiation, the solid angle fraction is used to enter Figure 1-2, which was obtained from Ref. 6.

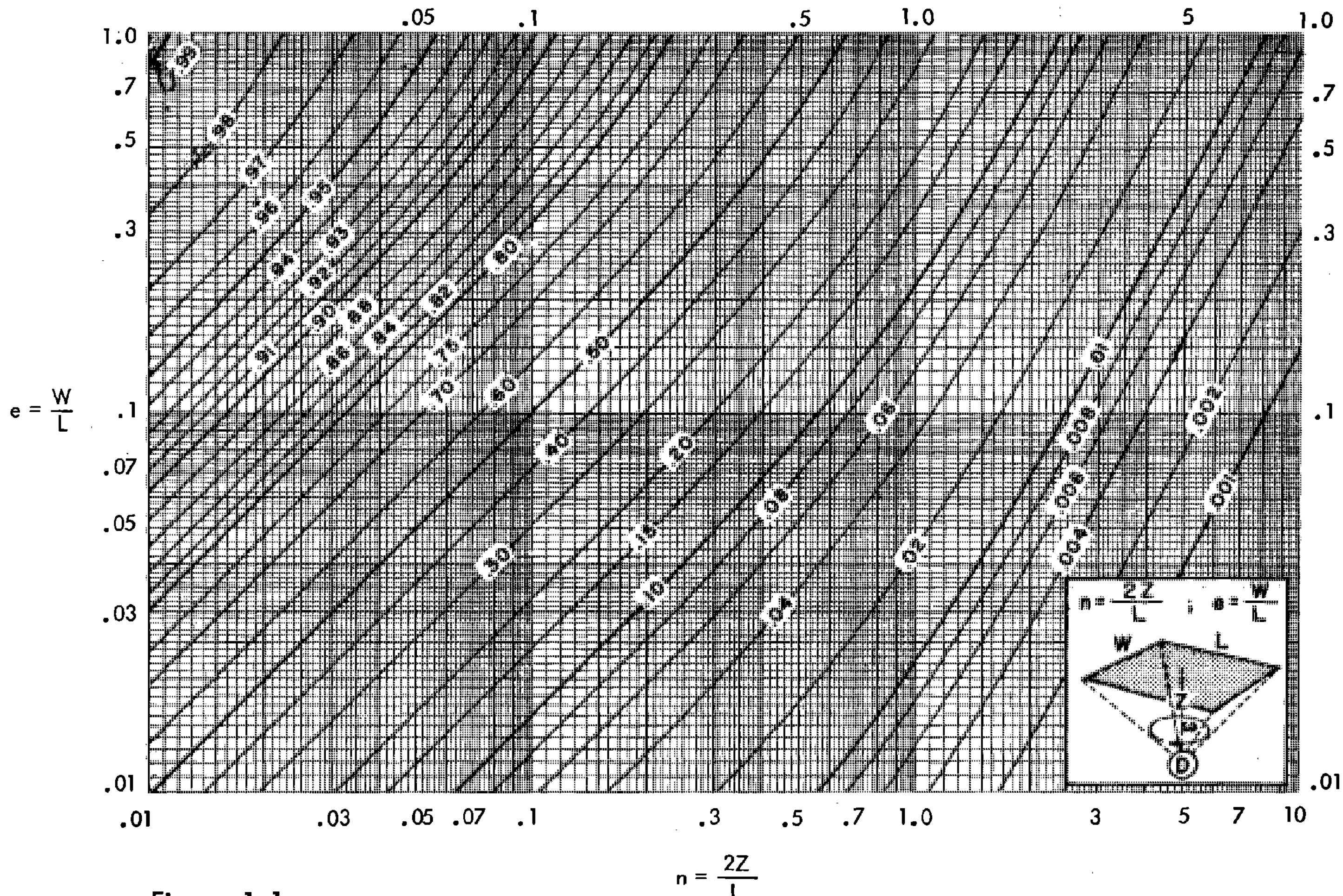

Figure 1-1

VALUES OF SOLID ANGLE FRACTION, ω

SOURCE: Ref.20

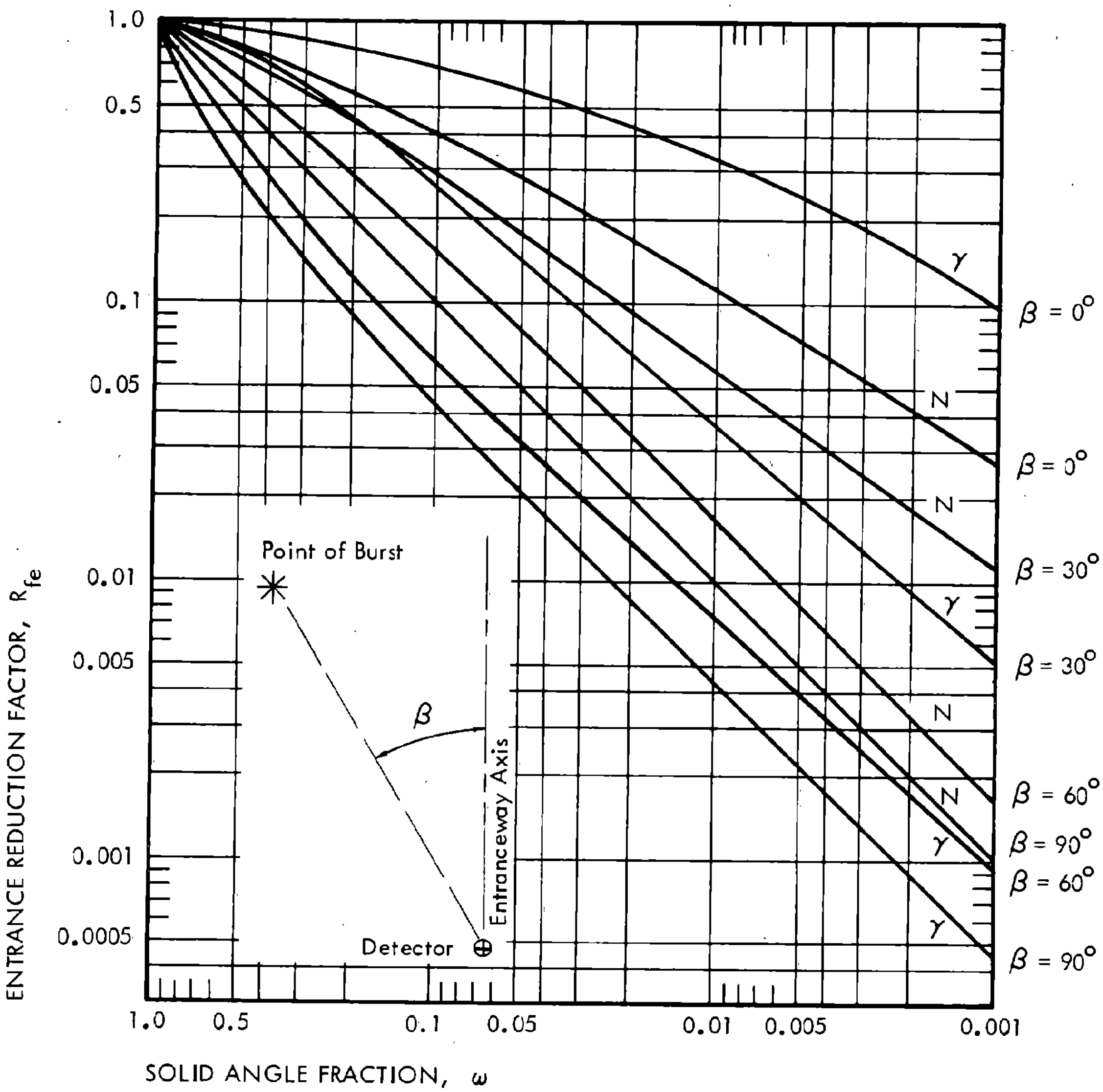

Figure 1-2

ENTRANCE REDUCTION FACTOR FOR INITIAL NUCLEAR RADIATION VERSUS SOLID ANGLE FRACTION AND BURST POINT

SOURCE: Ref. 6.

Entranceway Bend and Corridor Attenuation

Gamma Radiation

As noted in Refs. 15-19, even though considerable analytical and experimental effort has been expended in recent years to study the transmission of gamma radiation through tunnels and bends, detailed calculations for the initial nuclear gamma radiations are both tedious and of uncertain accuracy. For the purposes of this project, the following simplified method presented in Ref. 5 was therefore felt to be adequate. The reduction factor, R_f, for the first 90° bend beyond the entrance section is given by

$$R_{f_1} = 0.1\omega_1$$

where ω_1 = solid angle fraction subtended by the corridor section at the next point of interest

For the second and subsequent 90° bends, the reduction factor is given by

$$R_{f_n} = 0.5\omega_n$$

for n = 2, 3...

Neutron Radiation

Because of the lack of theoretical and experimental information on neutron attenuation in entranceways, it was sufficient for this study to use the simplified procedures presented in Refs. 5 and 6 to determine the length of corridor required for neutron radiation attenuation. The method is based on the concept of the length of corridor required to reduce the neutron dose by one-half. Since neutron attenuation occurs by neutron collision with the corridor walls, it is assumed that the attenuation is a function of the average cross-sectional dimensions of the corridor and not of the bends in the corridor. The experimental evidence indicates that the corridor half-length increases with the neutron energy, although information is lacking for the higher energy levels associated with nuclear weapons. This is accounted for in the method by neglecting any neutron radiation attenuation by wall interaction in the first section of the entranceway and by assuming that most of the higher energy neutrons are not transmitted past the first corridor bend.

It is assumed that the neutron half-length for the corridor beyond the first bend is given by

$$L_{1/2} = 1/2\ K\ (H + W) = 0.366\ (H + W)$$

where $L_{1/2}$ = half length of entranceway corridor, ft

K = 0.732, experimentally determined ratio

H = height of corridor, ft

W = width of corridor, ft

The number of neutron half-lengths for the corridor is given by

$$n = \frac{L}{L_{1/2}}$$

n = number of corridor half-lengths

L = total length of corridor beyond first bend to point of interest, ft

The reduction factor, R_{fc}, for neutron radiation for the corridor beyond the first bend is given by

$$R_{fc} = \frac{1}{(2)^n}$$

Because of a lack of adequate information, the method above does not specifically include a factor for secondary gamma rays resulting from the absorption of thermal neutrons in the corridor walls. In Ref. 5, it is stated that the present degree of conservatism in design should help reduce this hazard.

Barrier Attenuation

Barrier at Entrance

To determine the barrier reduction factor, B, at the outside entrance, Figures 1-3 through 1-5 have been reproduced from Ref. 5. Figure 1-3 shows the barrier reduction factor in relationship to the mass thickness of the shielding material and the angle of incidence for nitrogen capture gamma radiation. The use of nitrogen capture gamma

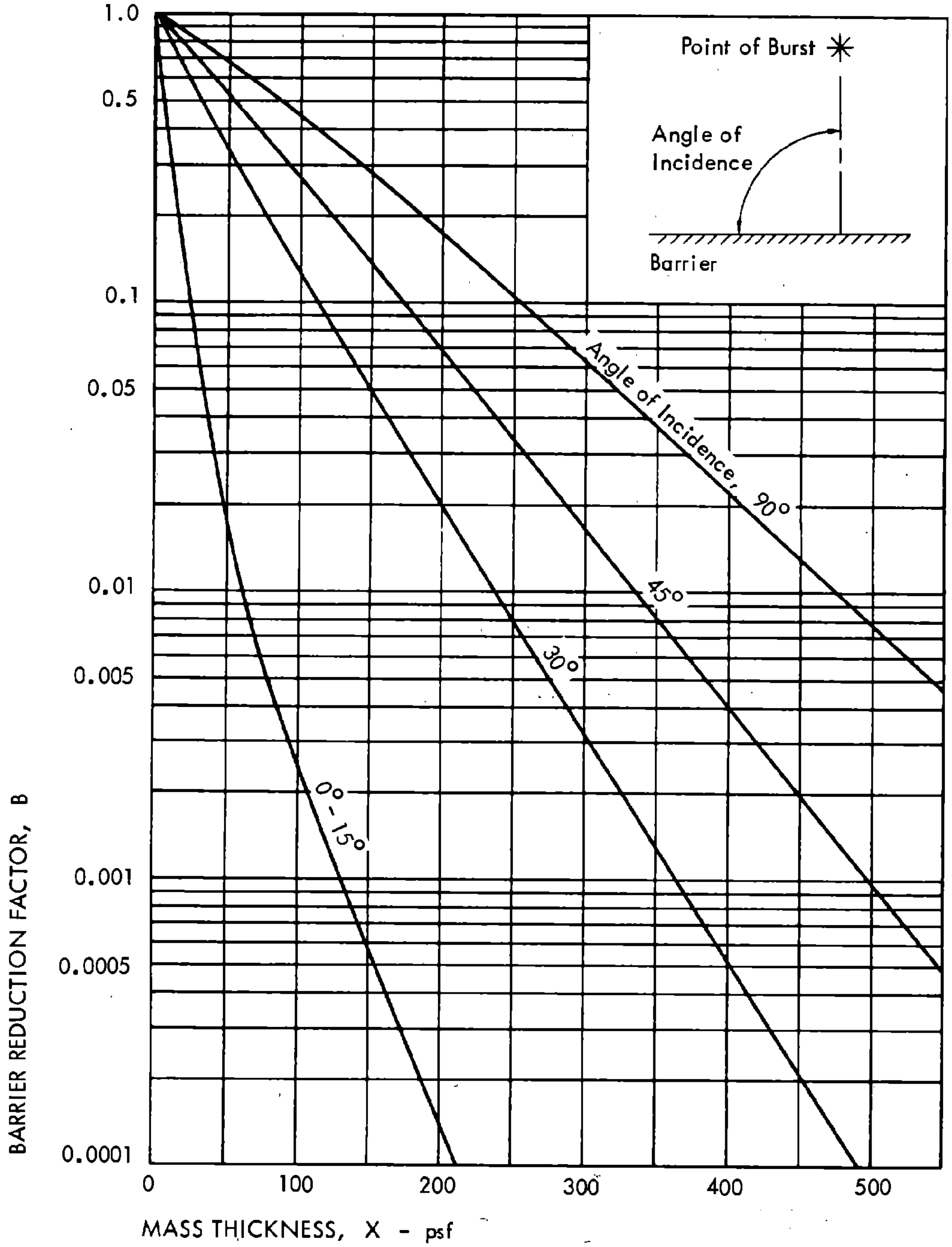

Figure 1-3

BARRIER REDUCTION FACTOR VERSUS MASS THICKNESS FOR NITROGEN-CAPTURE GAMMA RADIATION

SOURCE: Ref. 5

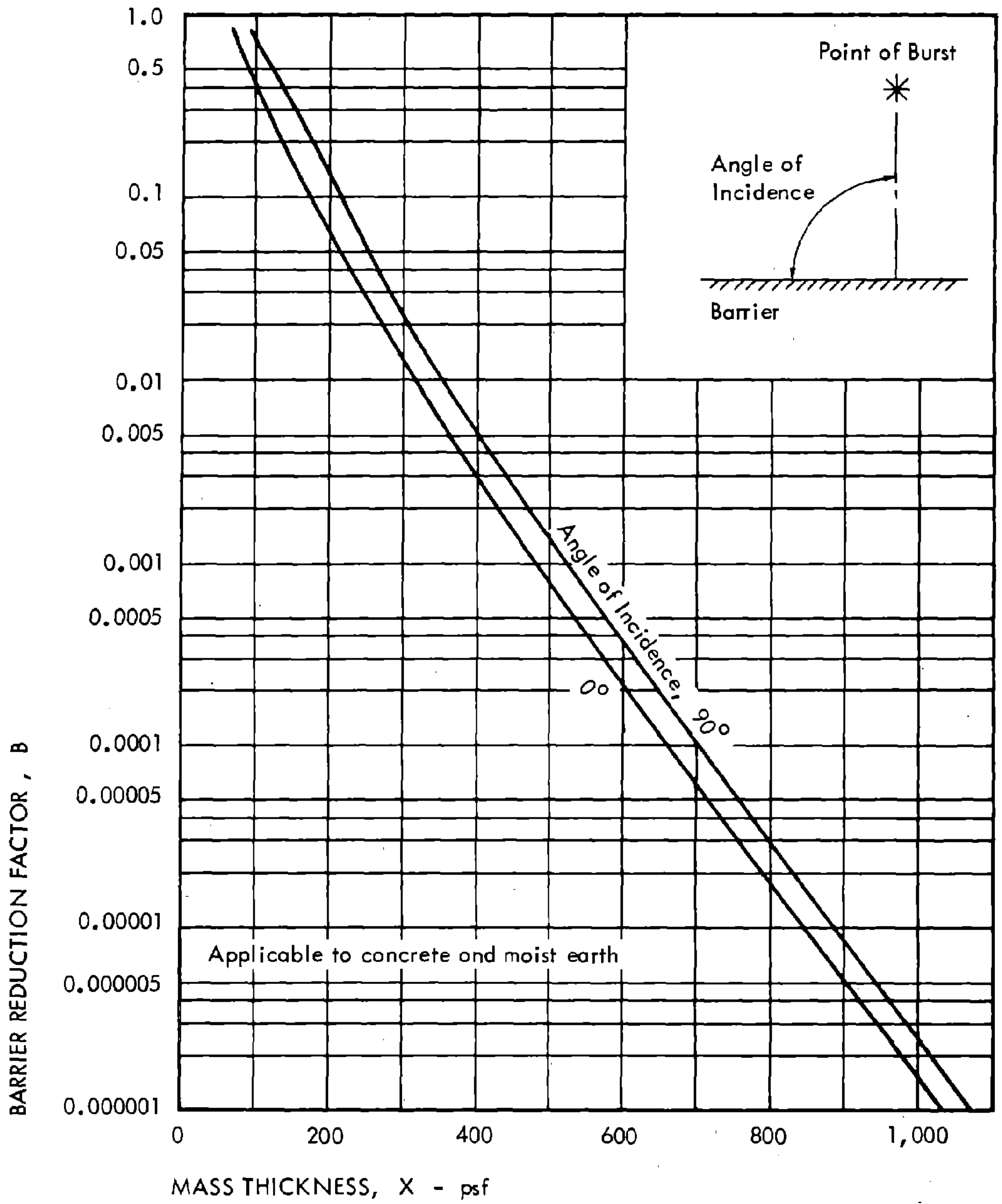

Figure 1-4

BARRIER REDUCTION FACTOR VERSUS MASS THICKNESS FOR 14 Mev NEUTRONS

SOURCE: Ref. 5.

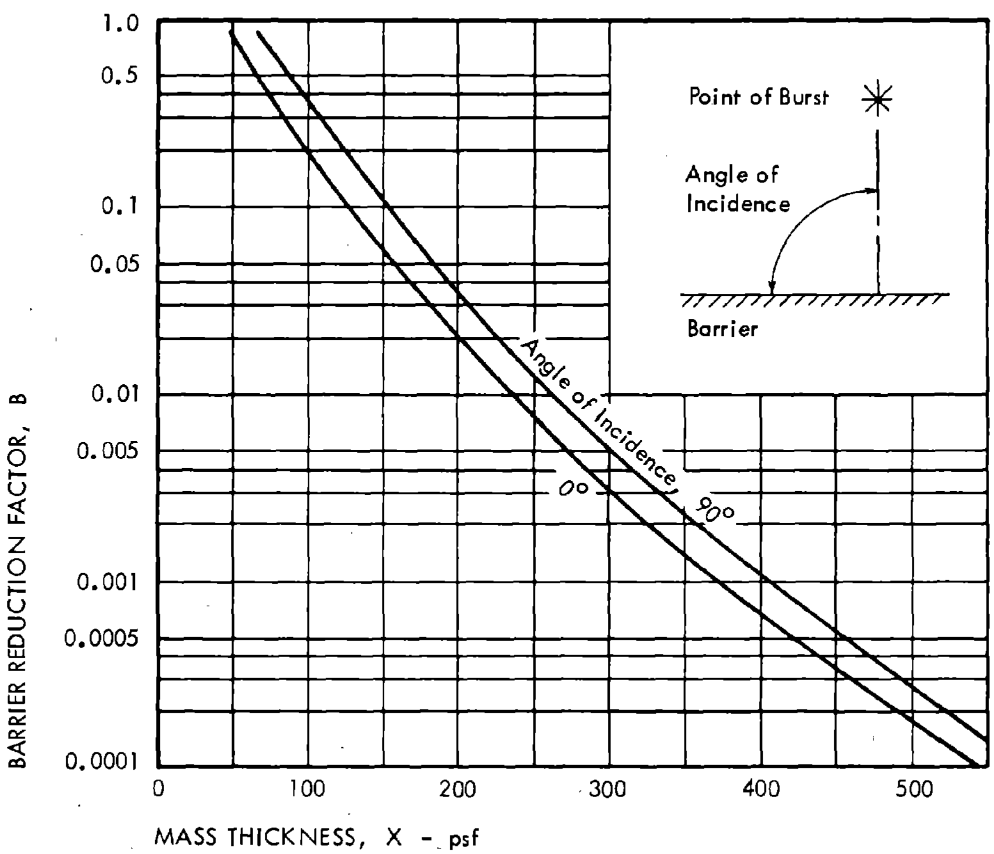

Figure 1-5

BARRIER REDUCTION FACTOR VERSUS MASS THICKNESS FOR 2.5 Mev NEUTRONS

SOURCE: Ref. 5.

radiation for shielding analyses is justified since it is the primary component of the initial gamma radiation at the ranges of interest in this study, and it is recommended as being on the conservative side in Ref. 1. A degree of conservatism for the barrier reduction factor is probably warranted for entranceways due to the previously mentioned neglect of the secondary gamma rays. Figures 1-4 and 1-5 show the barrier reduction factors for fusion yield neutrons ($\sim$ 14 Mev) and fission yield neutrons ($\sim$ 2.5 Mev), respectively.

Barriers Beyond First Corridor Bend

Gamma Radiation. The energy level of gamma radiation, which has been scattered through an angle of 90°, cannot be greater than 0.51 Mev, regardless of the initial energy. Therefore, the recommendation in Ref. 5 that Figure 1-6 be used for gamma ray barrier shielding beyond the first corridor bend, was adopted for this study.

Neutron Radiation. As recommended in Ref. 5, the reduction factors for neutron attenuation through barriers located beyond the first bend were obtained from Figure 1-5 for 2.5 Mev neutrons. The use of the lower average neutron energy level for interior barriers seems justified on the basis of the degradation of the free-field energy level beyond the first 90° corridor bend (Refs. 5 and 19).

Illustrative Example

To obtain the cost data presented in this report, it was necessary to perform an analysis of the attenuation of the initial radiation for the six blast entranceways (Types J and K). To demonstrate the method outlined in the previous sections, a typical initial radiation analysis is presented for entranceway J-1 in Figures 1-7 and 1-8.

Solid Angle Fractions

The solid angle fractions subtended at the various points shown on Figures 1-7 and 1-8 are given in the following tabulation. The values

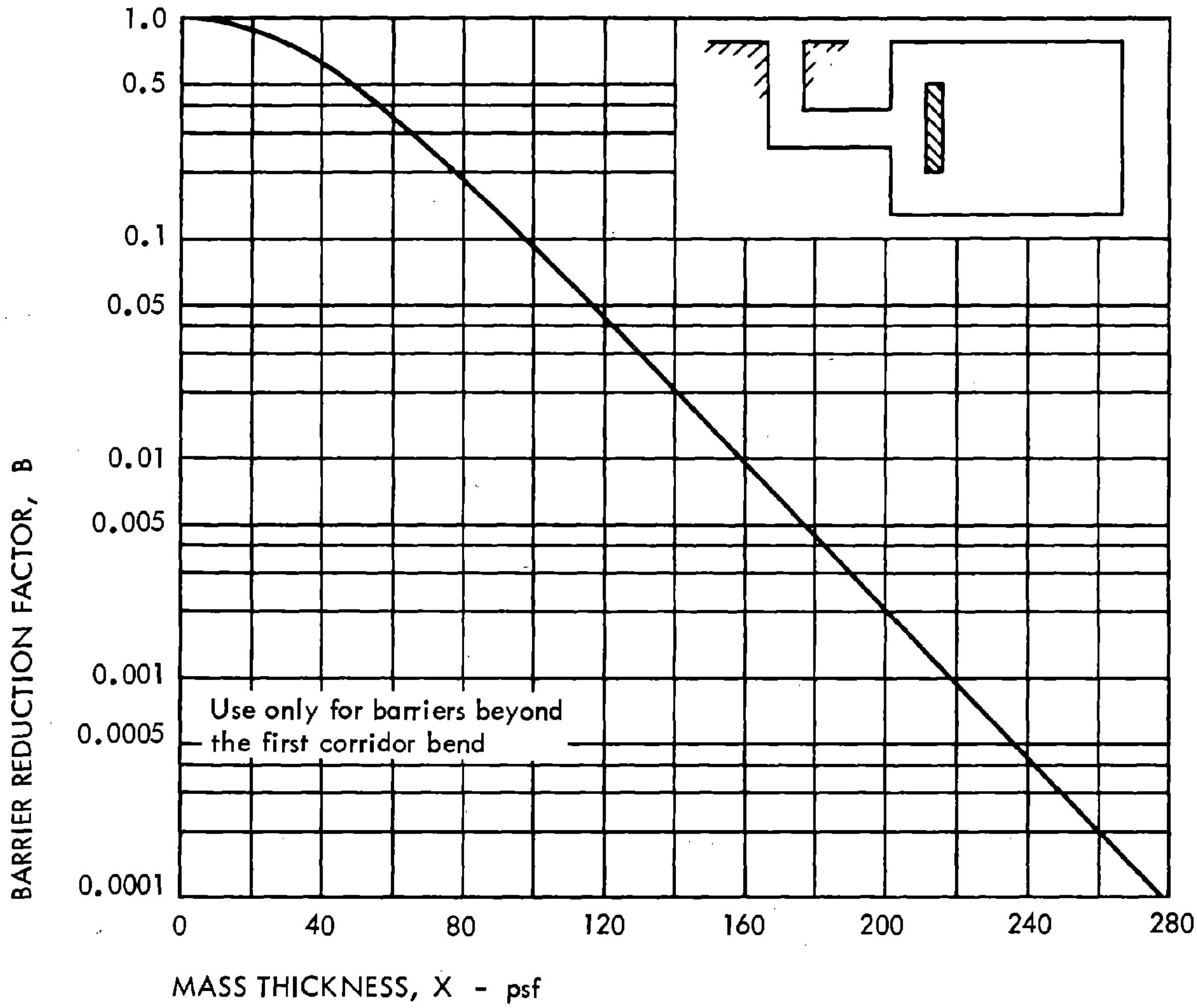

Figure 1-6

BARRIER REDUCTION FACTOR VERSUS MASS THICKNESS
FOR 0.51 Mev GAMMA RAY PHOTON

SOURCE: Ref. 5.

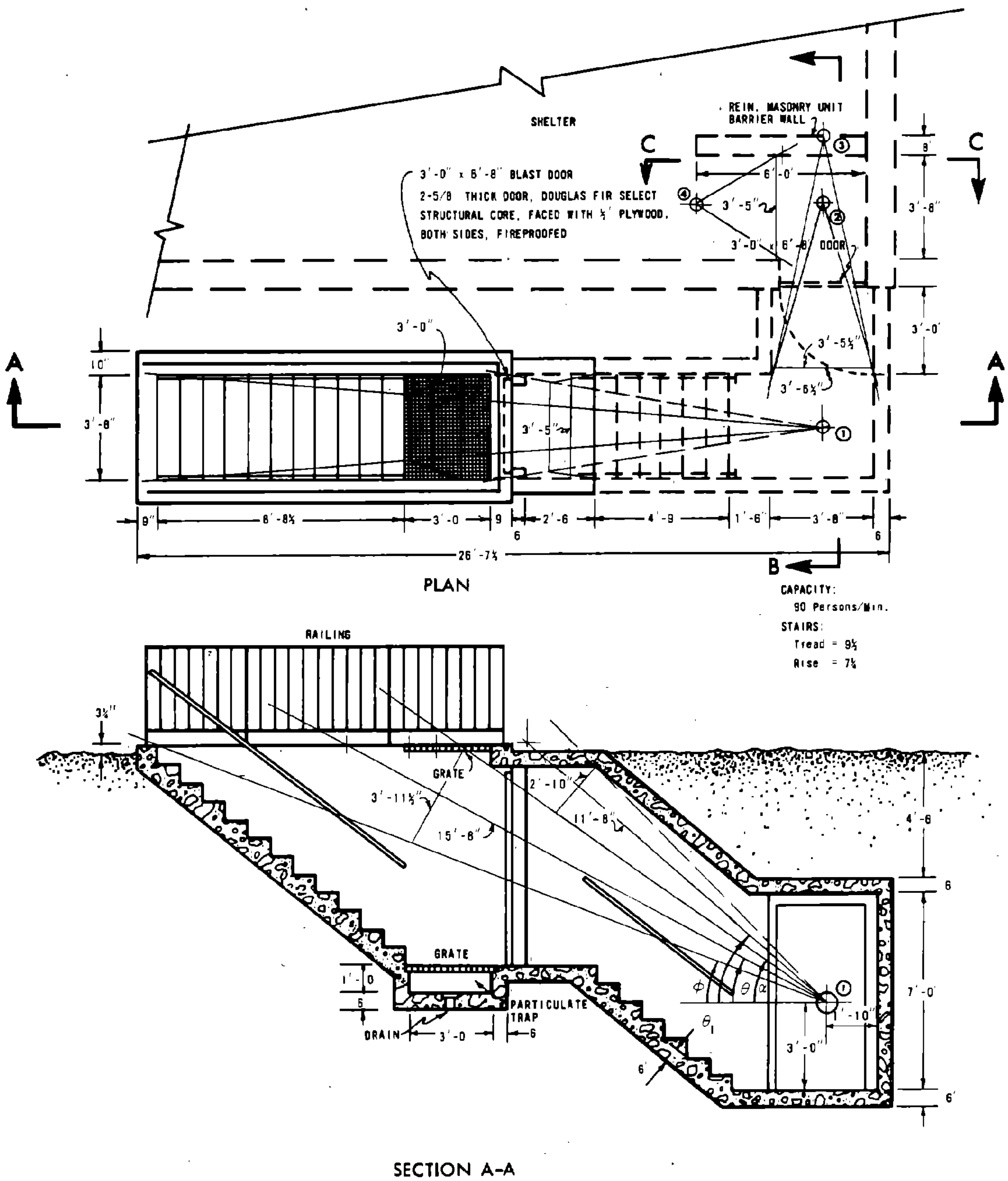

Figure 1-7

UNDERGROUND BLAST SHELTER ENTRANCEWAY, J-1

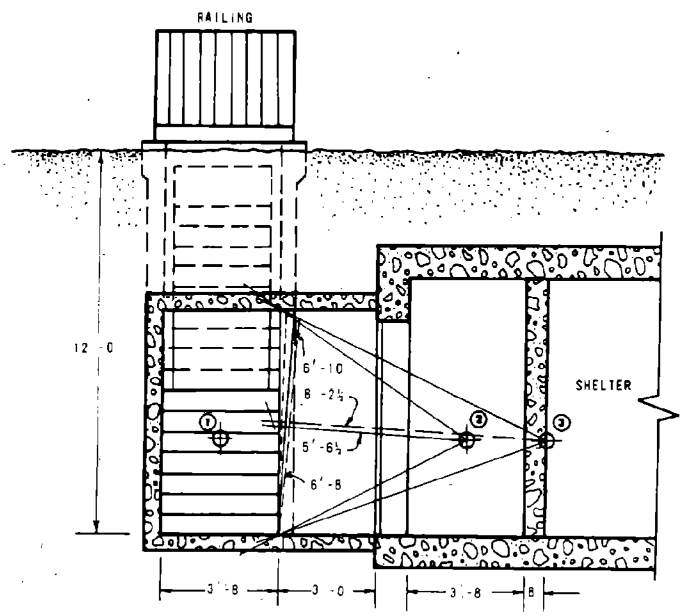

SECTION B-B

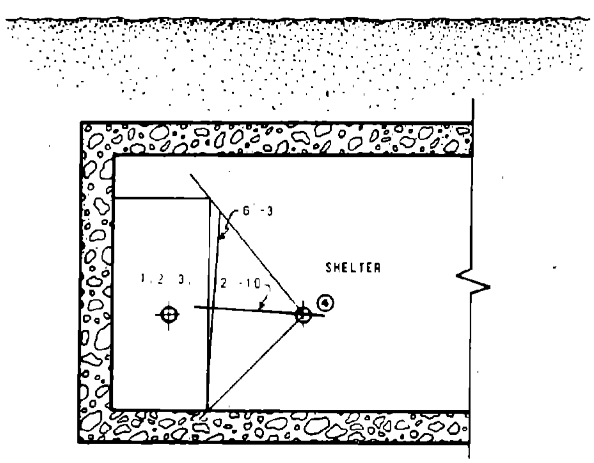

SECTION C-C

Figure 1-8

ENTRANCEWAY J-1, SECTIONS B-B AND C-C

of W, L, and Z were determined graphically as noted on the figures and used to obtain the solid angle fractions, ω, from Figure 1-1:

Point	W	L	Z	e	n	ω
1	3.00	3.96	15.67	0.76	7.91	0.008
2	3.46	6.67	5.54	0.52	1.66	0.10
3	3.54	6.83	8.21	0.52	2.40	0.055
4	3.42	6.25	2.83	0.55	0.91	0.25

where W, L = dimensions of the entrance opening projected on the plane normal to the selected line-of-sight, ft

Z = distance from detector to plane of W and L, ft

$$e = \frac{W}{L}$$

$$n = \frac{2Z}{L}$$

Assumed Weapon Parameters

Peak overpressure, P_{so} = 20 psi
Weapon yield, W = 200 kt
$W^{1/3}$ = 5.85

Free Field Initial Radiation

As noted previously, the worst case orientation for radiation streaming in the entranceways in this study, was found to be for the grazing line-of-sight ϕ, as shown on Figure 1-7.

Slant Range

Knowing the peak overpressure and the angle ϕ, the horizontal range, R, to the shelter entranceway can be determined from Ref. 1 (Para. 3.67):

$$R = 780\ W^{1/3} = (780)(5.85) = 4560 \text{ ft}$$

and the slant range, R_s, is

$$R_s = \frac{4560}{\cos \phi} = 4900 \text{ ft} = 1630 \text{ yd}$$

Free-Field Initial Radiation

Using the appropriate figures and scaling factors from Ref. 1 (Para. 8.27, 8.61, and 11.90), the free-field initial radiation dose can be determined for a 200 kt weapon yield at the slant range of the entranceway as follows:

Gamma radiation = 4500 rads
Neutron radiation = 580 rads

Entranceway Reduction Factors

Gamma Radiation

At Point 1*

From Figure 1-2, for $\omega_1 = 0.008$ and $\beta = (\theta - \phi) = 7^{\circ}$

$$R_{fe} = 0.15$$

At Point 2

$$R_f = R_{fe} \; (0.1\omega_2)$$

$$R_f = (0.15)(0.1)(0.10) = 0.0015$$

At Point 3

$$R_f = R_{fe} \; (0.1\omega_3)B$$

From Figure 1-6, for $X = \frac{8}{12}(150) = 100$ psf

$$B = 0.1$$

$$R_f = (0.15)(0.1)(0.055)(0.1) = 0.00008$$

At Point 4

$$R_f = R_{fe} \; (0.1\omega_2)(0.5\omega_4)$$

$$= (0.15)(0.1)(0.10)(0.5)(0.25) = 0.00019$$

---

* The barrier reduction factor for the wood blast and entry doors is insignificant and is therefore not included.

Neutron Radiation

At Point 1

From Figure 1-2, for $\omega_1 = 0.008$ and $\beta = 7^\circ$

$R_{fe} = 0.08$

At Point 2

$L_{1/2} = 0.366\ (H+W)$

$= 0.366\ (7.00 + 3.67) = 3.90'$

$L = 7.67'$

$n = \frac{L}{L_{1/2}} = \frac{7.67}{3.90} = 1.97$

$R_{fc} = \frac{1}{(2)^n} = 0.255$

$R_f = R_{fe} \times R_{fc}$

$R_f = (0.08)(0.255) = 0.020$

At Point 3

From Figure 1-5, for X = 100 psf and angle of incidence = 90°

$B = 0.35$

$R_f = (0.08)(0.255)(0.35) = 0.0071$

At Point 4

$L_{1/2} = 0.366\ (7.65 + 3.67)$*

$= 4.14'$

$L = 11.84'$

$n = \frac{11.84'}{4.14} = 2.86$

* Average for corridor in entranceway and shelter

$R_{fc} = \frac{1}{(2)^n} = 0.138$

$R_f = R_{fe} \times R_{fc}$

$R_f = (0.08)(0.138) = 0.011$

Initial Gamma Radiation Dose

Through Entranceway

Dose at Point 2

$R_f = 0.0015$

$D_2 = R_f \times D_o$

where D_o = outside radiation dose

D_i = inside radiation dose

$D_2 = (0.0015)\ (4500) = 6.8$ rads

Dose at Point 3

$R_f = 0.00008$

$D_3 = (0.00008)(4500) = 0.4$ rad

Dose at Point 4

$R_f = 0.00019$

$D_4 = (0.00019)(4500) = 0.9$ rad

Through Entrance Roof Slab

Dose at Point 2

From Figures 1-7 and 1-8, $W = 2.17'$, $L = 3.42'$, $Z = 11.67'$

From Figure 1-1, for $e = 0.64$, $n = 6.82$

$\omega_{1A} = 0.009$

From Figure 1-2, for $\omega_{1A} = 0.009$ and $\beta = \theta_1 = \phi = 20^\circ$

$R_{fe} = 0.07$

From Figure 1-3, for $X = 1/2\ 150 = 75$ psf, and angle of incidence = $\phi = 21^{\circ}$

$B = 0.06$

$R_f = R_{fc}\ (0.1\omega_2)\ B$

$R_f = (0.07)(0.1)(0.10)(0.06) = 0.000042$

$D_2 = R_f \times D_o$

$D_2 = (0.00004)(4500) =$ negligible

Dose at Point 4

$R_f = R_{fe}\ (0.1\omega_2)(0.5\omega_4)\ B$

$R_f = (0.07)(0.1)(0.10)(0.5)(.25)(0.06) = 0.000005$

$D_4 =$ negligible

Through Roof Slab over Point 1

Dose at Point 2

$X = (\frac{150}{2}) + (4.5 \times 100) \approx 525$ psf*

From Figure 1-3, for $X = 525$ psf and angle of incidence = 21°

$B \ll 0.0001$

$R_f = B\ (0.1\omega_2)$

$R_f \ll (0.0001)(0.1)(0.10) \ll 0.000001$

$D_2 =$ negligible

Therefore gamma radiation dose through roof slab over point 1 is negligible at all points of interest

* Assumes an infinite plane barrier with no geometry reduction

Through Entranceway Walls

Dose at Point 4

$X = (1.5 \times 150) + (2.5 \times 100) = 475$ psf

From Figure 1-3, for X = 475 psf and angle of incidence = 0 - 15°

D_4 = negligible

Initial Neutron Radiation Dose

Through Entranceway

Dose at Point 2

$R_f = 0.020$

$D_2 = R_f \times D_o$

$D_2 = (0.020)(580) = 11.6$ rads

Dose at Point 3

$R_f = 0.0071$

$D_3 = (0.0071)(580) = 4.1$ rads

Dose at Point 4

$R_f = 0.011$

$D_4 = (0.011)(580) = 6.4$ rads

Through Entrance Roof Slab

Dose at Point 2

From Figure 1-2, for $\omega = 0.009$ and $\phi = 20^\circ$

$R_{fe} = 0.07$

From Figure 1-4, for X = 75 psf and angle of incidence = $\phi = 21^\circ$

$B = 0.8$

$R_f = R_{fe} \times B \times R_{fc}$

$R_f = (0.07)(0.8)(0.255) = 0.014$

$D_2 = R_f \times D_o$

$D_2 = (0.014)(580) = 8.1$ rads

Dose at Point 3

$R_f = R_{fe} \times B \times R_{fc} \times B$

$R_f = (0.07)(0.8)(0.255)(0.35) = 0.0050$

$D_3 = (0.0050)(580) = 2.9$ rads

Dose at Point 4

$R_f = R_{fe} \times B \times R_{fc}$

$R_f = (0.07)(0.8)(0.138) = 0.0077$

$D_4 = (0.0077)(580) = 4.5$ rads

Through Roof Slab Over Point 1

Dose at Point 2

From Figure 1-4, for X = 525 psf and angle of incidence = 21°

$B = 0.0007$

$R_f = B \times R_{fc}$

$R_f = (0.0007)(0.255) = 0.00018$

$D_2 = (0.00018)(580) =$ negligible

Therefore, neutron radiation dose through roof slab over Point 1 is negligible at all points of interest

Through Entranceway Walls

Dose at Point 4

From Figure 1-4, for X = 475 psf and angle of incidence = 0^{o} *

B = 0.001

D_4 = (0.001)(580) = 0.6 rads

Summary

The tabulation below summarizes the initial radiation dose.

Source	Type of Radiation	Dose in Rads Point 2	Point 3	Point 4
Entranceway	Gamma	6.8	0.4	0.9
Entranceway	Neutron	11.6	4.1	6.4
Entrance roof slab	Gamma	0	0	0
Entrance roof slab	Neutron	8.1	2.9	4.5
Roof slab at Point 1	Gamma	0	0	0
Roof slab at Point 1	Neutron	0	0	0
Entranceway walls	Gamma	--	--	--
Entranceway walls	Neutron	--	--	0.6
Total radiation dose		27	7	12

From the above tabulation, it is apparent that to reduce the 27 rad dose at Point 2 to a tolerable level in the shelter would require either lengthening the corridor or adding a barrier wall at the shelter entrance. The addition of a 6-ft long barrier wall reduces the dose to 7 rads at the interior face of the wall and to 12 rads at the entrance to the shelter proper. In view of the uncertainties in calculating the free-field nuclear radiation quantities and in the radiation analysis method, the entranceway design is considered adequate for the cost analysis performed

* This assumes the walls are infinite in extent. If the geometry were considered, the reduction factor would be decreased.

in this study. If desired, it would be relatively inexpensive to reduce the radiation dose further by increasing the thickness of the entrance slab, by increasing the length of the barrier wall, or by increasing the length of the corridor between Points 1 and 2. For instance, increasing the thickness of the entrance slab from 6 in. to 9 in. would reduce the radiation dose for Point 4 at the shelter entrance from 12 to approximately 8 rads, but would not significantly increase the total cost of the entranceway.

C-26 BLANK

REFERENCES

1. Glasstone, S., ed., The Effects of Nuclear Weapons, Department of Defense and Atomic Energy Commission, Washington, D.C., February 1964.

5. Newmark, N. M., Design of Openings for Buried Shelters, Contract Report No. 2-67, U.S. Army Engineer Waterways Experiment Station, Vicksburg, Mississippi, July 1963.

6. Stevenson, J. D., and J. A. Havers, Entranceways and Exits for Blast-Resistant Fully-Buried Personnel Shelters, Illinois Institute of Technology Research Institute (for Office of Civil Defense), Chicago, Illinois, September 1965.

20. Office of Civil Defense, Shelter Design and Analysis, TR-20 (Vol. 1), Washington, D.C., May 1964.

Appendix D

FALLOUT SHIELDING ANALYSIS OF ENTRANCEWAYS

By H. L. Murphy

Reproduced, without change, from original publication as Appendix 2 to: Wiehle, C. K., Shelter Entranceways and Openings, prepared by Stanford Research Institute for OCD, final report, September 1967. (AD-662 749)

NOTE: While fully outside entranceways are illustrated, the analysis techniques are useful for all entranceway configurations. No one type should be inferred as the recommended type for all applications.

Appendix D

FALLOUT SHIELDING ANALYSIS OF ENTRANCEWAYS

By H. L. Murphy

The entranceways developed in the project were examined for shielding capability against fallout contaminant from a nuclear detonation, as stated earlier. This somewhat repetitive FSA (fallout shielding analysis) work led to an approach that is presented in this appendix. Entranceways A-2 and C-1 are used for demonstration.

Entranceway pencil drawings to scale were used, since their use permits direct measurement of the many dimensions needed in FSA and thereby saves much working time over a method requiring any calculation of dimensions.

The basic tool was that whose use is currently taught in Office of Civil Defense FSA courses for practicing engineers and architects (Ref. 20). Therein, a careful comparison of Figure 4.6, used for cleared (or contaminated) finite circular areas, with the roof chart (Chart 4) values for a zero mass thickness roof showed identical results for the same solid angle fractions; however, Chart 4 with its entering argument of solid angle fraction (ω) is better suited to entranceway FSA purposes.

Certain assumptions are necessary in entranceway FSA. Some used in this project were:

1. Contamination factors: Fallout contaminant enters the entranceway portal at the "standard" (outdoor) rate per unit (horizontally projected) area, and this is then spread uniformly over all horizontal areas of the entranceway but not beyond the first turn. Using entranceway A-2 (see Figure 2-1) as an example, the contamination factor would be the area of the portal (3.67 $\times$ 9.5 ft) divided by the total area of steps and particulate trap under the grating (3.67 $\times$ 19.42 ft), or 0.489. To assume that the contaminant would only fall straight down into the entranceway would be nonconservative in PF (protection factor) results and would be assuming zero wind conditions. At the other end, it might be assumed that most if not all of the contaminant would accumulate

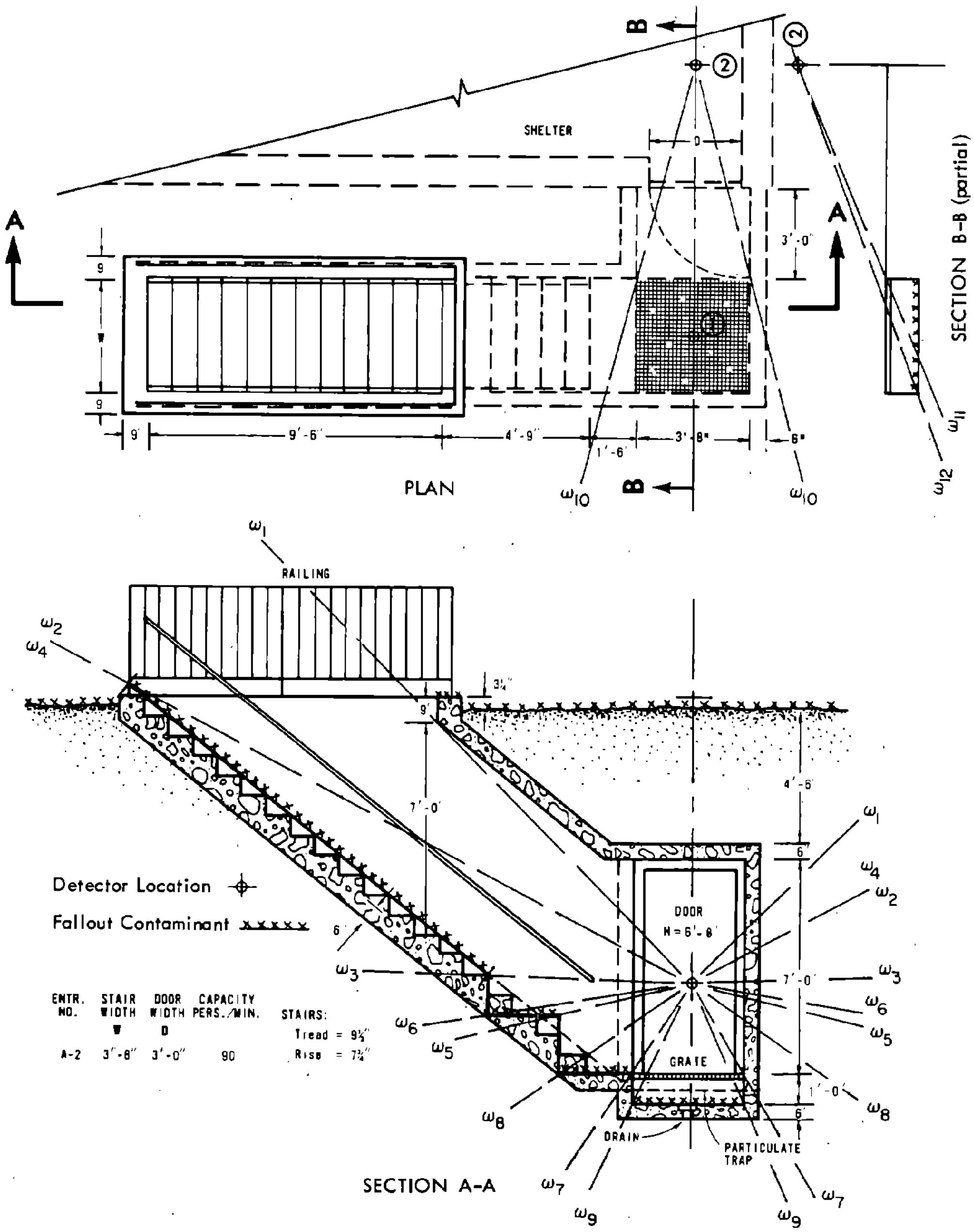

ENTR. NO.	STAIR WIDTH W	DOOR WIDTH D	CAPACITY PERS./MIN.
A-2	3'-8"	3'-0"	90

STAIRS:
Tread = 9½"
Rise = 7¾"

Figure 2-1
WORKED-OUT EXAMPLE 1

on the step at the level of the grating and on the trap under the grating. This assumption is conservative but was not used because shelter occupants could readily sweep the step contaminant through the grating or flush down both step and trap to get rid of the contaminant entirely.

This assumption was modified in entranceways such as B-5 as follows: Each side of the entranceway was separately handled as described for entranceway A-2 down to and including the grating, resulting in a doubling of the assumed contamination under the grating.

Another contamination factor was used in dealing with the steps located above the horizontal plane of the detector; it is discussed in the Worked-Out Example 1.

2. Steel gratings hold no falling contaminant and provide negligible shielding.

3. Doors of ordinary wood or hollow metal construction provide negligible shielding.

4. Detector location is a point although the human body is not.

5. For stairs located above the detector horizontal plane, neither the stairs nor stair nosings, if any, provide significant shielding. This assumption is demonstrated by the examples.

6. Where a contaminated area could both be "seen" (at least partially) by the final detector location and was in a tunnel-like location--for example, the trap under the grating, entranceway A-2--contributions were included for both (a) the contaminated area directly to the final detector location and (b) for the same contaminant being "seen" at a detector location directly above the contaminant, and then through a right-angle (tunnel) turn to the final detector location. This assumption was termed the "tunnel effect" for use in this study. It was sometimes applied as just described; sometimes only the larger of the two contributions (a) and (b) was used; or, for a relatively open entranceway (for example, entranceway D-4), only contribution (b) was used. The rationale was based on the likelihood of gamma radiation scattering off walls in a somewhat long and narrow, relatively confined, tunnel-like situation.

Entranceway A-2 fallout shielding analysis was made using a pencil scale drawing illustrated by Figure 2-1. The computational steps shown in Table 2-1 are explained following the table.

Table 2-1

COMPUTATIONS FOR WORKED-OUT EXAMPLE 1

	ω	W	L	Z	ω	Multipliers	C_o
1.	ω_1	3.67	18	9.3	.0860	-0.5/0.489	-.0036
2.	ω_2	3.67	35.2	9.3	.1095	0.5/0.489	.0046
3.	ω_3	3.67	10.4	3.9	.2213	-0.5 X 0.85	-.0186
4.	ω_4	3.67	40.6	3.9	.2746	0.5 X 0.85	.0238
5.	ω_5	3.67	8.3	1.1	.6223	-0.5	-.0791
6.	ω_6	3.67	13	1.1	.6416	0.5	.0827
7.	ω_7	3.67	3.67	3	.1755	-0.5	-.0169
8.	ω_8	3.67	8.3	3	.2780	0.5	.0284
9.	ω_9	3.67	3.67	4	.1112	1	.0207
10.							C_1 = .0472
11.	ω_{10}	3.67	7	7	.0723	$0.2C_1\omega_{10}$	.0007
12.	ω_{11}	3.67	18.7	4	.2505	-0.5	-.0252
13.	ω_{12}	3.67	21.33	4	.2553	0.5	.0257

C_t = .0012 X 0.489

= .0006

PF ≈ 1700

Lines 1-2: Core and peripheral area of a decontaminated, zero mass roof (Chart 10, Case 3). Dividing this one item by the contamination factor permits applying the factor to the overall total contribution, rather than to each step, because it applies to all other contributions except this one.

Lines 3-on: Roof contributions all taken from Chart 4, zero mass thickness.

Lines 3-4: Steps changed to a plane, which is then treated as if horizontal; second contamination factor enters here, in that the plane used has a greater area than the horizontal area of the steps, thus the 0.85 multiplier.

Lines 5-8: Steps below detector horizontal plane, simplified into two steps.

Line 9: Particulate trap contribution to detector location 1.

Line 11: Converts total contribution to detector location 1 through a turn and solid angle fraction into a contribution to detector location 2.

Lines 12-13: Contribution from portion of trap seen from detector location 2.

An entranceway C-1 FSA was made, also using a pencil scale drawing illustrated by Figure 2-2. The computational steps shown in Table 2-2 are explained below.

Table 2-2

COMPUTATIONS FOR WORKED-OUT EXAMPLE 2

	ω	W	L	Z	ω	Multipliers	C_o
1.	ω_1	3.7	4	9	.0278	+0.5 [X_o=75]	.0011
2.	ω_2	3.7	23.5	9	.1022	+0.5 [X_o=75]	.0040
3.							C_1 = .0051
4.	ω_3	3	6.8	3.5	.1770	$0.2C_1\omega_3$	C_{T_A}= .0002
							$PF_A \approx$ 5000
5.	ω_4	3.67	12	6.4	.1207	$0.7\omega_5$ [X_o=100]	.0006
6.	ω_5	2.5	6.67	3.5	.1491		--
7.	ω_6	3.67	17.2	9.3	.0839	0.5 [X_o= 100]	.0021
							C_{T_B} = .0027 x 0.571 = .0015
							$PF_B \approx$ 670

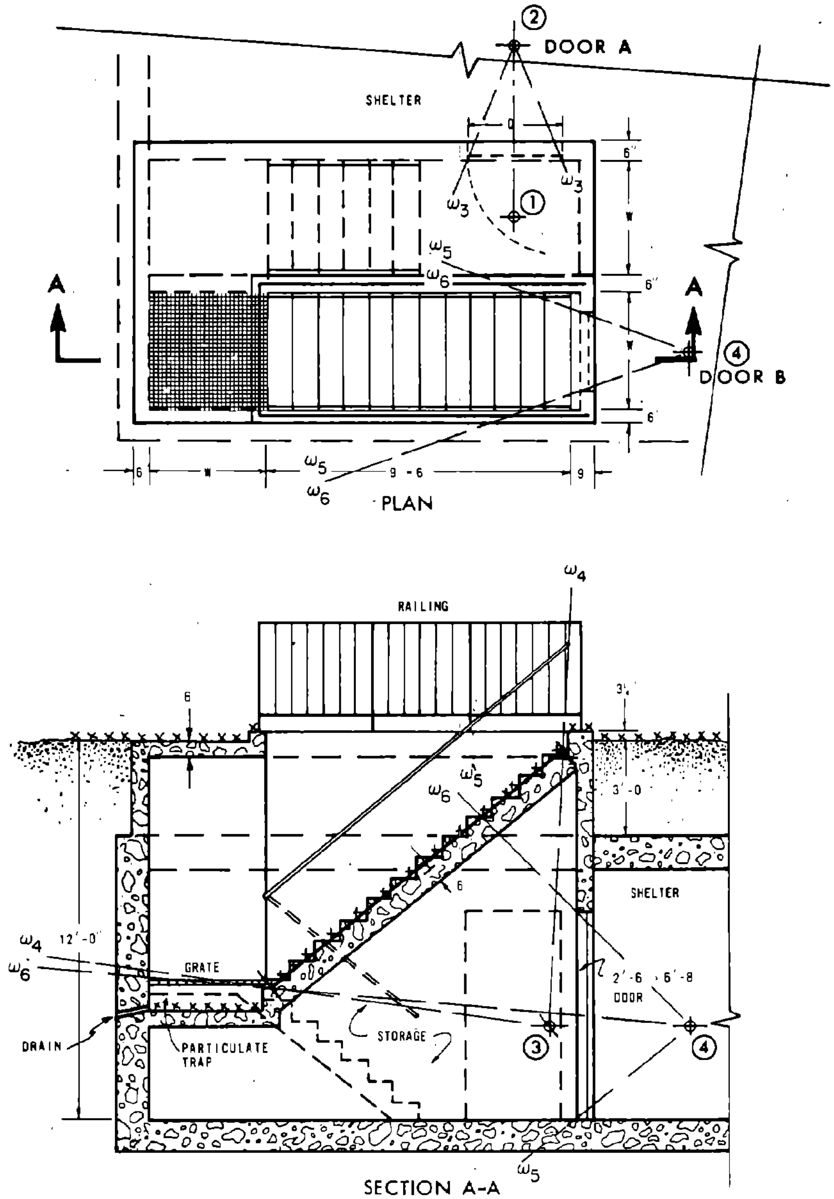

ENTR. NO.	STAIR WIDTH W	DOOR SIZE D	CAPACITY PERS./MIN.	STAIR
C-1	3'-8	3'-0 × 6'-8	90	TREAD 9½

Figure 2-2

WORKED-OUT EXAMPLE 2

Door A

General: Radiation from contamination on stairs must come through the concrete steps, a 6-in. concrete wall acting like an interior partition, and the doorway restriction, <u>or</u> must be reflected through three turns, in either case making this contribution negligible. Similar thinking may be applied to the trap under the grating. Thus, the only contribution left to be considered is that from the contaminated roof above the room where detector location 1 is shown, an ordinary off-center detector location problem. Contributions were all taken from Chart 4.

Lines 1-2: Roof above off-center detector location 1 (ω_1 and ω_2 not shown in Figure 2-2).

Line 4: Turn and solid angle fraction from 1 to 2.

Door B

General: Stairs simplified as in Worked-Out Example 1. Because of tunnel effect, contributions taken directly to detector location 4, and via 3 to 4; that direct to 4 restricted to portion seen through doorway, because any other must come through concrete stairs (used 8-in. or 100 psf, for mass) and through 6-in. more concrete in lintel, thereby becoming negligible. Any contribution from trap under grating is negligible because of both geometry and barriers. Contribution from roof over detector location 1 must come through several heavy barriers, so it is negligible. Contamination factor for steps and trap under grating amounts to 9.5/13.17 and must be combined with a factor for the simplified stairs amounting to 9.5/12, giving a combined factor of 0.571. Contributions were all taken from Chart 4.

Line 5: First right-angle turn is 0.2 and no turn is 1; for this partial turn, 0.7 was used.

Line 7: Ray from stairs to detector location 4 treated as normal to the simplified stairs, thus solution is for a half-roof.

Some of the values in Tables 2-1 and 2-2 are shown to an unwarranted number of decimal places. They are shown that way, however, because (1) all solid angle fractions and all zero mass roof contributions were computer-calculated so that no extra work was involved and (2) such might be useful to anyone trying to check through the computations, for understanding or other reasons.

Near the end of this work, two simplifications used (as in the first example problem solution herein) were subjected to more detailed examination. Computer programs were used for computing solid angle fractions and for computing radiation contributions, both to save professional working time and, more specifically, to carry values out to several decimal places, take differences, and then round off the total to fewer decimal places, all aimed at reducing round-off values wherein "roof" cores were continually subtracted from larger "roof" values. Simplifications examined were:

1. Simplification of the stairs located below the detector horizontal plane to fewer stairs. In Figure 2-1, the total contribution from the actual steps below the detector horizontal plane, including the step at the level of the grating, amounted to 0.0164.* In Worked-Out Example 1 the contribution based on the simplification amounted to 0.0151,* or an error of -8 percent in this one item. In carrying this nonconservative error forward, however, the tunnel turn reduces its effect so much as to leave the overall total contribution unchanged.

2. Simplification of the stairs located above the detector horizontal plane to a sloping, plane, smooth, contaminated surface, then analyzed by rotating the plane of the detector. Each step in Figure 2-1 was analyzed by considering it in five "roof" increments as indicated in the sketch, but the same Z distance was used for each step, as shown by the sketch arrow. The mass thickness of each increment was determined from its scaled thickness (on a scale drawing at 1"=0.1'), using reinforced concrete at 150 pcf. With a core and peripheral roof calculation for each of five increments and for each of 15 steps, 150 roof contributions were calculated. In Worked-Out Example 1, the contribution from the simplification of the stairs above the detector horizontal plane was 0.0052.* The results from the 150 roof calculations was 0.00524,* indicating an error of < 1 percent. Table 2-3 gives

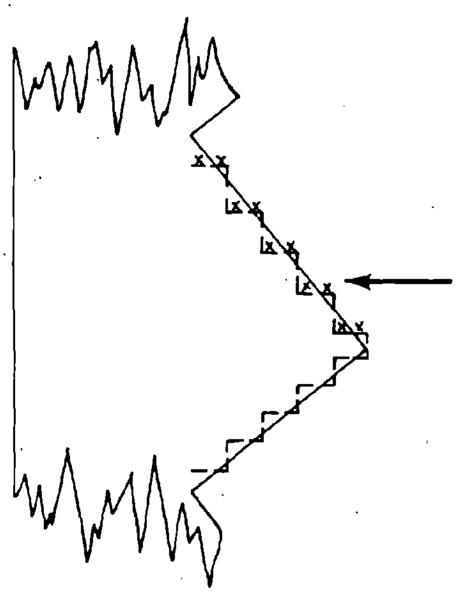

* Value before applying general contamination factor, 0.489.

values obtained for stair widths of 22, 44, and 66 in., and shows gross errors ranging from -9 percent to +10 percent in using the sloping plane approximation. Such errors would be indeed negligible after the radiation contribution values were multiplied by 0.489 (contamination factor), 0.2 (first tunnel turn), and 0.0723 (tunnel solid angle fraction), or a combined multiplier of 0.00707. Unfortunately, time was not available for detailed calculations varying other parameters than stair width.

Table 2-3

CONTRIBUTIONS FOR VARIOUS STAIR WIDTHS

	Detailed Computations		Sloping Plane Approximation		
Stair Width	C_T	$\left[\frac{9.5''}{6''}\right] C_T$	C_o	$0.85\ C_o$	Error
22"	.00166	.00263	.0028	.0024	-9%
44"	.00331	.00524	.0061	.0052	-1%
66"	.00487	.00771	.0100	.0085	+10%

The matter of stair nosings was reviewed briefly during the work. Nosings are required by some building codes, for the particular tread-rise values used. One standard nosing detail, shown in Ref. 38, is a simple one requiring only the sloping of the riser, the effect of which is to increase the tread by 1 in. Such a change would have only a trivial effect on the computations herein; e.g., use of this nosing in the examples in this appendix would mean only that each nosing would move the contaminant out 1 in. from the back of the tread below, leaving the same amount of tread contaminated as was assumed.

D-12 BLANK

REFERENCES

20. Office of Civil Defense, Shelter Design and Analysis, TR-20 (Vol. 1), Washington, D.C., May 1964

38. American Concrete Institute, Manual of Standard Practice for Detailing Reinforced Concrete Structures, ACI 315-51 (Drg. 30), Detroit, Michigan, Jan. 1952

Technical Reports
Consolidated Printing

VOLUME 3

SLANTING IN NEW BASEMENTS FOR COMBINED NUCLEAR WEAPONS EFFECTS: A Consolidated Printing of Four Technical Reports

October 1975

FEASIBILITY STUDY OF SLANTING FOR COMBINED NUCLEAR WEAPONS EFFECTS (Revised), Volumes 1 and 2 — *July 1971*

Slanting for Combined Nuclear Weapons Effects: FIRE HAZARD REDUCTION — *August 1972*

Slanting for Combined Nuclear Weapons Effects: EXAMPLES WITH ESTIMATES, AND AIR BLAST ROOM FILLING — *June 1973*

Slanting for Combined Nuclear Weapons Effects: BLAST-RESISTANT DESIGN/ANALYSIS WITH EXAMPLES — *December 1974*

For:

DEFENSE CIVIL PREPAREDNESS AGENCY
WASHINGTON, D.C. 20301

Contracts DAHC 20-67-C-0136 and 20-71-C-0292
DCPA Work Units 1154E and 1154H

STANFORD RESEARCH INSTITUTE
Menlo Park, California 94025 · U.S.A.

Technical Reports
Consolidated Printing

VOLUME 3

SLANTING IN NEW BASEMENTS FOR COMBINED NUCLEAR WEAPONS EFFECTS: A Consolidated Printing of Four Technical Reports

October 1975

By: H. L. Murphy, J. R. Rempel and J. E. Beck
Facilities and Housing Research

FEASIBILITY STUDY OF SLANTING FOR COMBINED NUCLEAR WEAPONS EFFECTS (Revised), Volumes 1 and 2 — *July 1971*

By: H. L. Murphy

Slanting for Combined Nuclear Weapons Effects: FIRE HAZARD REDUCTION — *August 1972*

By: H. L. Murphy and J. R. Rempel

Slanting for Combined Nuclear Weapons Effects: EXAMPLES WITH ESTIMATES, AND AIR BLAST ROOM FILLING — *June 1973*

By: H. L. Murphy and J. E. Beck

Slanting for Combined Nuclear Weapons Effects: BLAST-RESISTANT DESIGN/ANALYSIS WITH EXAMPLES — *December 1974*

By: H. L. Murphy and J. E. Beck

For:

DEFENSE CIVIL PREPAREDNESS AGENCY
WASHINGTON, D.C. 20301

Contracts DAHC 20-67-C-0136 and 20-71-C-0292
DCPA Work Units 1154E and 1154H

STANFORD RESEARCH INSTITUTE
Menlo Park, California 94025 · U.S.A.

CONTENTS

Volume 1

CONTENTS (Continued)

CONTENTS (Continued)

CONTENTS (Concluded)

Volume 2

Volume 3

TABLES

FIGURES

FIGURES (Continued)

FIGURES (Continued)

FIGURES (Concluded)

Appendix E

ROOM FILLING FROM AIR BLAST

By J. R. Rempel

PREFACE

This appendix is intended to serve both as a source of immediately applicable methodology and as a guide to the underlying gas dynamic theory. Those interested more in applying the methodology than in derivations and comparisons of calculated and observed results will find the following parts of this appendix of particular importance:

Location	Description
Section IIA	The simplest and fastest method of estimating average pressure in a room as a function of time; adequate for many purposes. The room may have one or more openings to the outside pressure source or sources.
Section IIB3	Two different methods for a step-by-step, hand calculation providing average room pressure, as well as dynamic pressure in the opening; valid for all flows through a single opening into a single room when the outside pressure is known as a function of time. Either method may be used but Method F is recommended for inflow, Method D for outflow.
Section IIC	General formulas describing geometric extent of the jet created inside the room by inflowing air and for dynamic pressure distribution within the jet. Provides basis for calculation of jet distribution in Table E-3.
Table E-3	A computer program to calculate average pressure within a single room, as well as dynamic pressure distribution around as many as eight openings as functions of time when the single room has openings into several different pressure fields (e.g., a room with front, rear, and side windows struck by a blast on the front wall). If desired, follows translation of objects caught in jet.

Location	Description
Section IVB	A specific numerical example using one of the step-by-step procedures set forth in Section IIB3 for the calculation of average room pressure, as well as dynamic pressure in each opening, during filling of a single room through two openings into separate pressure fields. Also illustrates the calculation of certain nuclear blast wave parameters.

The Notation section near the end of this Appendix defines the symbols used in the methodologies just described; the computer program versions of some of these symbols appear also in the Notation section. Subscripts not explained there refer to physical spaces, i.e., subscript 1 indicates quantity is measured outside the room; other odd-numbered subscripts refer to interior of rooms and even-numbered subscripts refer to connecting ducts or openings.

CONTENTS

FIGURES

TABLES

Appendix E

ROOM FILLING FROM AIR BLAST
By J. R. Rempel

I Introduction

When a blast wave strikes a building, even should the structure withstand the initial impact, the resulting inflow of air through windows and other openings can be critical in determining the safety of any people sheltered by the structure and in determining the response of the structure itself to the blast impact. Although the physical laws obeyed by moving gases are well known and the course of the inflow in filling the building can in principle be calculated completely, any such calculation is far too lengthy to be practical for most purposes; fortunately, simplifications can be introduced which greatly shorten the labor of estimating effects of the blast inside the building and which give results in good to fair agreement with experiments done with small models. In general, the effect of the inflow is to provide a stream of fast moving air in the shelter space which may (1) endanger shelterees by hurling them against large relatively fixed objects or by hurling objects against them, (2) provide a back pressure on the inner surfaces of outside structure walls countering the blast pressures on their outer surfaces, and (3) provide pressure against interior walls.

Several factors enter into the calculation: the pressure outside each wall with openings and the time each opening becomes available, the area occupied by each opening and the volume of each room, the number of connected rooms and the area of each connection, and the ambient pressure and temperature in the building before the blast strikes. Perhaps the first of these to consider is what proportion of the wall exposed to the blast is open. If this fraction is greater than one half, the shock front leading the blast wave will pass into the building only slightly weakened and subsequent inside pressure should be estimated from a knowledge of shock pressure and the laws of shock reflection. Methods appropriate to this case are only touched upon here. On the other hand, should the fraction be less than one tenth, clearly the filling is not a shock process and the methods treated here are quite pertinent. Unfortunately, in many applications the fraction of open area will lie between these two extremes and, in these cases after the room filling calculation has been completed according to the methods suggested here, some thought must be given independently to the influence of the entering shock front.

When the source of the blast wave is an explosion and the location of the building in relation to the point of explosion is known or postulated, "free-field" pressure histories at the building site can be found in standard references,[1,2,15*] and from these histories well-known methods[1,3] are available to derive approximate histories on the outside of the walls of the building. Briefly, these methods account for a short-lived peak of pressure created by the impact of the front upon the wall nearest the explosion, the relatively fast erosion of this high pressure to a level which is the sum of the free field pressure plus a drag pressure on the wall due to the high winds behind the blast front. This quasi-steady pressure then decays slowly to zero as the blast wave moves onward past the structure.

Ordinary window glass breaks rather quickly, i.e., within 8 ms (milliseconds) or less when struck by blast overpressure of 1 psi (pound per square inch) or more.[4] Doors may withstand outside pressure longer, or even altogether. The time an opening becomes available with respect to the first impact of the blast upon the building becomes, then, the breaking time plus the time required by the wave to travel from the wall nearest the explosion to the opening. If the opening is in the wall nearest the explosion, travel time is of course zero. Strictly, the decay of the blast wave overpressure which occurs during this time must be taken into account, but when the blast arises from a nuclear explosion of yield greater than a few kt (kilotons), this decay is slight and negligible; that is, a single "free-field" pressure history for all openings may be assumed.

The methods given here are simplified and their use leads only to estimates. They are intended to provide: (1) calculations applicable to hand computation by those untrained in gas dynamics and (2) approximate results useful until more careful calculations are made. Only in the case of the simplest structural configurations and the simplest pressure history shapes can limits of error be suggested for these results. Such cases are the subject of the discussion immediately below.

II Classical Nuclear Blast Wave Incident upon a Single Room with Openings into Single Pressure Field

A. Estimation of Inside Pressure History

The "classical" blast wave from nuclear explosions consists of a steep pressure front or rise followed by a long-lasting decay phase, during which the pressure in the wave falls to zero. It is accompanied by high winds giving rise to dynamic pressure against objects in the stream. Striking a wall at normal or near normal incidence, it creates a high-pressure

* References for Appendix E are listed at the end of the appendix.

zone at the surface, which however is rapidly eroded as relief waves move across the wall face from the edges. As a first approximation in the calculation of room filling, this reflected phase can usually be neglected. Following the decay of the high reflected pressure, the quasi-steady pressure (free field plus drag) remains against the wall for hundreds of milliseconds to several seconds, depending on explosive yield. Generally filling is complete before this quasi-steady pressure has fallen more than a few percent; hence, as a first approximation the outside pressure may often be considered constant and, if only a single wall with opening is exposed to the blast, the time ΔT (in milliseconds) to complete filling may be computed as the ratio $\frac{V}{2A}$, where V is room volume in cubic feet and A is area of opening in square feet.* The average room pressure at any time t during the filling process is then simply the fraction of the quasi-steady outside pressure given by the ratio $\frac{t}{\Delta T}$. For the purposes of this calculation, areas of several openings in the same wall should be added together to form the quantity A.†

In case there are two or more walls with openings exposed to the blast and each such wall sustains a different outside pressure history (as will happen, for example, when the drag coefficient is different for two walls), the calculation is more complicated but first estimates of filling time and average inside pressure during filling can be found by adding interior pressures calculated as if each wall alone were exposed. As an example, consider a room of volume 30'x10'x10' = 3000 ft^3 in which the front wall has total openings of 36 sf and side walls have total openings of 60 sf. The ratios $\frac{V}{2A}$ for the front and side walls are 41.7 and 25 ft, respectively. If the quasi-steady overpressure on the front wall is 10 psig (pounds per square inch - gauge) and on the side wall 8 psig and if, further, the side wall opening becomes available 10 ms after the first blast impact, then the average inside pressure will be approximately as shown in Figure E-1 by the heavy line OAFG. In other words the room will fill in approximately 24 ms. Lines OAC and DE represent filling rates through front and side walls, respectively; and ordinates of OAC and DE are added to form the line OAF. Of course after the average inside pressure exceeds 8 psi there will be outflow through the side wall; to allow for this loss, the line FG has been placed between the outside pressure at the side wall (8 psig) and the outside pressure at the front wall (10 psig). The ordinate at FG is closer to 8 psig than to 10 psig because the area of the opening in the side wall is greater than that in the front wall. The line FG is intended to represent the final quasi-equilibrium pressure in the room. As outside pressure slowly falls to normal, room pressure will follow it.

---

* Empirical relationship, dimensionally inconsistent. Meanings of symbols as used in this Appendix are defined as introduced and under "Notation" at end of Appendix.

† The experimental justification of most of the procedures described in this section is demonstrated later in Figures E-4, E-5, E-6 and E-8.

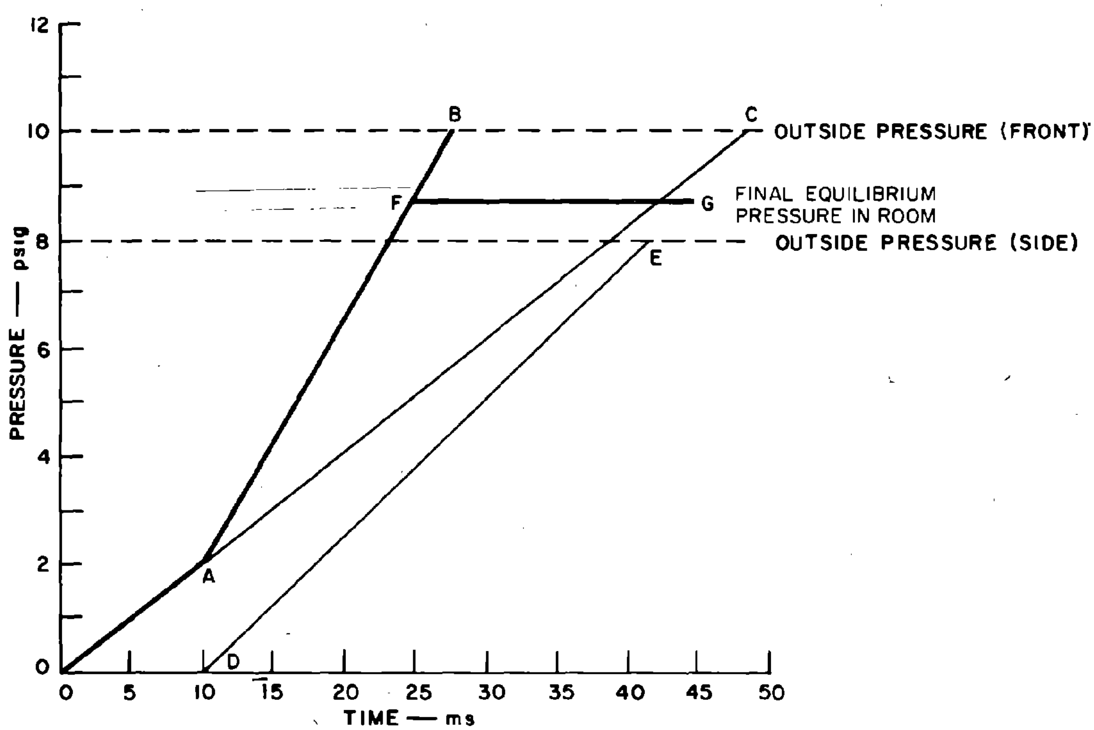

FIGURE E-1 APPROXIMATE FILLING RATE THROUGH TWO WALLS

These simple calculations do not apply when the reflected pressure lasts an appreciable length of time, or when the wave is nonclassical, such as it would be were a precursor present. Under these conditions the more detailed methods set forth below must be followed.

A theoretical justification due to Kriebel[24] of the approximate filling time $\Delta T = V/2A$ appears below in Section IIB1.

B. Detailed Calculation of Inside Pressure History

Confidence in the simple method noted above rests upon experience with a step-by-step calculation and comparison of its results with experiments. This calculation applies the principles of steady isentropic flow in ducts in successive, small time intervals. Conditions computed for the end of one time step become initial conditions for the next step. Conservation of energy, momentum and mass, along with the assumption that the air behaves as a perfect gas with constant specific heats, determine the thermodynamic variables, pressure, temperature and density, as well as the wind speed through the opening. Unique expressions lending themselves to simple calculation cannot be given for the laws of conservation of energy and momentum, so alternative forms leading to somewhat different results will be stated. All such expressions rely upon certain approximations to the conservation laws, and these approximations usually introduce errors into the results in comparison with which the approximations arising in the assumptions of isentropy, perfect gas behavior, and constant specific heats are negligible.

1. Inflow. Figure E-2 shows the idealized room with a single opening struck head-on by a blast wave. Three regions are noted: the outside ①, the doorway ②, which serves as a duct connecting the outside with the room ③. In order to make the calculations tractable, uniformity of conditions in each of the two regions ① and ③ and over the cross section of region ② is assumed; furthermore, during each small time interval Δt, steady conditions are assumed in each region. During the aforementioned quasi-steady state outside the building, these assumptions are probably valid for region ① but they clearly introduce error if the reflection or diffraction phase lasts an appreciable time, for during that episode relief waves are moving into the region from the edges of the building as well as from the doorway itself causing rapid fluctuations in wind speed and pressure. (Some account is taken of changes in pressure during the diffraction episode by the standard techniques of estimating outside pressure.) Similar remarks can be made concerning regions ② and ③, but if we are content to deal with "average" pressure and speed in those two regions, we may apply the step-by-step isentropic analysis. However, our present methods do not provide for any apportionment of gaseous energy in region ③ between streaming kinetic energy and internal energy; for simplicity of calculation it will be treated as entirely internal at all times, which will cause overestimation of pressure and neglect of winds within the chamber. In evaluating the wind threat, the speed and dynamic pressure in the duct ② must be regarded as the upper bounds on wind speed and dynamic pressure in region ③. Later, methods will be given for estimating change in dynamic pressure as the wind moves into the room.

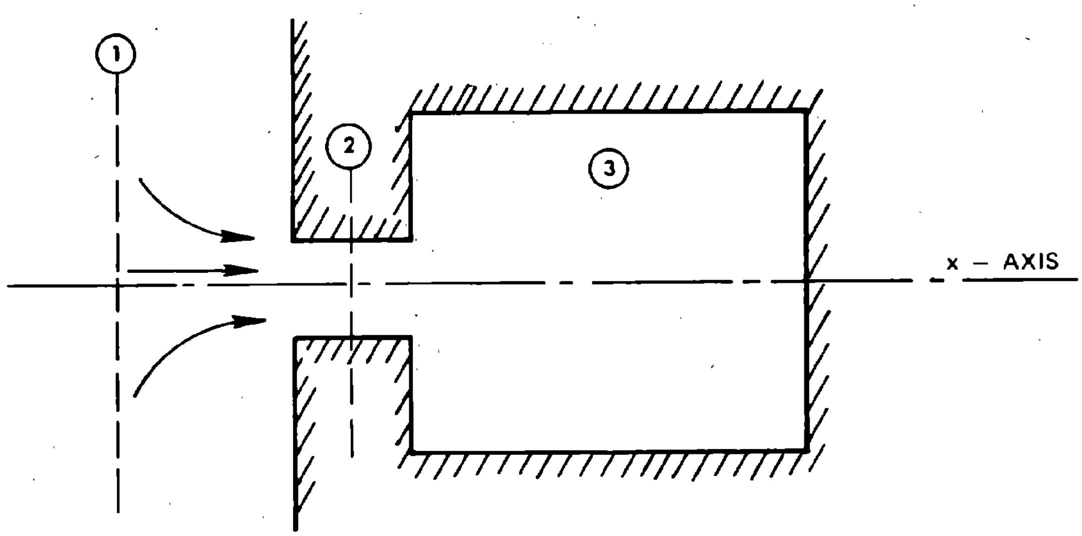

FIGURE E-2 THE FILLING CHAMBER

In writing the conservation equations, two views can be taken of conditions in region ①. On the one hand, pressure, density and wind speed may be those of the free field behind the blast front or, on the other hand, the air upstream of the opening may be treated as stagnate at a pressure above free field, either by the amount of the reflected pressure or by the amount of the product of the drag coefficient and dynamic pressure. Provided drag coefficients are known, the second view is more simply applied, especially when the blast front does not meet the wall head-on. In what follows, the pressure, P_1, and density, ρ_1, in region ① will be those of stagnate air outside the wall. The work done in moving a mass element Δm in region ① through a small distance Δx toward region ② is:

$$P_1 A_1 dx = P_1 \Delta V_1 = P_1 \cdot \frac{\Delta m}{\rho_1}$$

where A_1 is the cross sectional area, and ΔV is the volume occupied by Δm in region ①. The mass element carries with it the internal energy it had in region ①, i.e.,

$$\frac{1}{\gamma - 1} \cdot \frac{P_1}{\rho_1} \cdot \Delta m$$

where γ is the ratio of specific heat at constant pressure to the specific heat at constant volume. (The perfect gas equation of state is assumed; see Ref. 5.) If the flow into the room is steady, energy conservation requires that the same total energy, specifically, the sum

$$\frac{1}{\gamma - 1} \cdot \frac{P_1}{\rho_1} \cdot \Delta m + \frac{P_1}{\rho_1} \cdot \Delta m = \frac{\gamma}{\gamma - 1} \cdot \frac{P_1}{\rho_1} \cdot \Delta m$$

be given up within region ② during the same time interval. Furthermore, mass conservation asserts that the mass element moving through region ② toward region ③ equal Δm. The work done in region ② in pressing the mass element toward region ③ is

$$\frac{P_2}{\rho_2} \cdot \Delta m$$

and the internal energy in the element is

$$\frac{1}{\gamma - 1} \cdot \frac{P_2}{\rho_2} \cdot \Delta m$$

where the subscript 2 denotes conditions in region 2. Since the air is flowing into the room, however, the element in 2 also carries (streaming) kinetic energy of amount

$$\frac{1}{2} u_2^{\ 2} \ \Delta m$$

where u designates particle or material speed. Thus, if conditions are not changing too fast, we can write (cancelling out the factor Δm):

$$\frac{\gamma}{\gamma - 1} \cdot \frac{P_1}{\rho_1} = \frac{\gamma}{\gamma - 1} \cdot \frac{P_2}{\rho_2} + \frac{1}{2} u_2^2 \qquad (1)$$

To apply conservation of linear momentum we consider a control surface, shown dashed in Figure E-3, enclosing an arbitrarily shaped volume outside the room and a portion of the entry duct (or doorway). Thus, a part of the control surface spans the duct throat where the air is moving rapidly into the room and consequently the air pressure P_2 is much lower

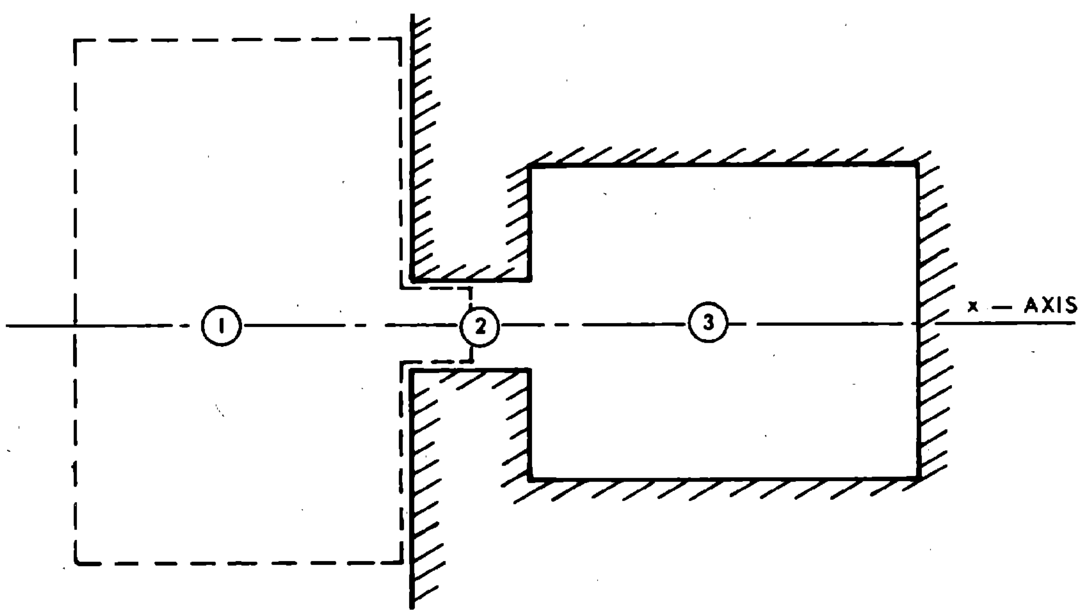

FIGURE E-3 FIRST CONTROL SURFACE

than the air pressure P_1 elsewhere within and on the control surface.* Newton's second law of motion states the net force in any direction on the air mass within the surface must equal the time rate of change of momentum in the same direction within the surface. Because of symmetry there is no net force in any but the x-direction; the net force (neglecting friction and viscous effects) in the x-direction is the difference between the high outside air pressure and the low duct air pressure integrated over the duct throat, i.e., the net force is:

$$\left(P_1 - P_2\right) A_2$$

This net force is balanced by a rate of change in momentum, which arises from two sources: (1) an acceleration of air within the control surface toward the open duct and (2) the high speed flow of air through the duct and out of the volume enclosed by the control surface altogether. After the initial diffraction of the shock wave through the doorway and after jet flow has been established into the room,† the second of these sources is the more important and we neglect the first in our calculation. The rate of flow of mass through the duct is:

$$\rho_2 u_2 A_2$$

hence, the rate of change of momentum (product of mass and speed) is:

$$\rho_2 u_2^2 A_2$$

Conservation of momentum (Newton's second law of motion) then implies:

$$\left(P_1 - P_2\right) A_2 = \rho_2 u_2^2 A_2$$

Canceling the factor A_2, we find:

$$P_1 - P_2 = \rho_2 u_2^2 \qquad (2)$$

---

* Pressure on the walls will be less than P_1, around the entrance to the duct, but the mass flow rate is not highly sensitive to corrections made for this effect; to simplify calculation, uniform pressure P_1 is assumed everywhere in 1. This assumption is conservative in assessing protective capability.

† See Section IIC.

Finally we note that, even in the presence of moderately strong or weak shocks, the isentropic equation of state of a perfect gas is accurate enough for this approximate calculation; hence,

$$\rho_2 = \rho_1 \left[\frac{P_2}{P_1}\right]^{1/\gamma} \tag{3}$$

(See Ref. 7).

Given P_1 and ρ_1, Eqs. (1), (2), and (3) may be solved for P_2, ρ_2, and u_2.* The result can be written as:

$$\frac{2\gamma}{\gamma + 1} \left[\frac{P_2}{P_1}\right]^{1/\gamma} = \frac{P_2}{P_1} + \frac{\gamma - 1}{\gamma + 1} \tag{4}$$

which is independent of ρ_1. If $y = \frac{P_2}{P_1}$, $A_o = \frac{\gamma - 1}{\gamma + 1}$

and $B = \frac{2\gamma}{\gamma + 1}$, Eq. (4) can be put in the form

$$By^{\frac{1}{\gamma}} = y + A_o \tag{5}$$

When A_o and B have the values stated above, Eq. (5) has two solutions, one of which is $y = 1$ and the other is $y = 0.1912$. The second solution is the only one of interest here and will be designated y_o.

To continue the calculation ρ_1 must be known. This value can be found from the Rankine-Hugoniot relations and knowledge of the strength and angle of incidence of the original shock front (Ref. 1,2), or it can, with enough accuracy for incident shock strengths less than 15 psi, be computed from standard conditions† using the isentropic equation of state, i.e.,

---

* For diatomic gases like air, γ=1.4; see Ref. 8.

† Standard conditions (atmospheric) are defined in Table 6.1, Chapter 6, Volume 1 of the present work.

$$\rho_1 = \rho_o \left[\frac{P_1}{P_o} \right]^{1/\gamma} \tag{6}$$

where P_o and ρ_o are standard pressure and density, respectively. With ρ_1 known, air density and pressure in the opening can be calculated from:

$$\rho_2 = \rho_1 \, y_o^{\;1/\gamma} \tag{7}$$

$$P_2 = y_o \, P_1 \tag{8}$$

from which wind speed becomes:

$$u_2 = \left[\frac{P_1 - P_2}{\rho_2} \right]^{\frac{1}{2}} = \left[\frac{P_1 \, (1 - y_o)}{\rho_1 \, y_o^{\,1/\gamma}} \right]^{\frac{1}{2}} \tag{9}$$

The mass flow into the room 3 can be written

$$\Delta m = \rho_2 \, u_2 \, A_2 \Delta t$$

$$= \left[P_1 \, (1 - y_o) \, y_o^{\frac{1}{\gamma}} \, \rho_1 \right]^{\frac{1}{2}} A_2 \, \Delta t \tag{10}$$

If, V_3 is the volume of the room and the prime is used to denote conditions in the room at the beginning of time step Δt, then average density in the room ρ_3 at the end of Δt can be written as:

$$\rho_3 = \rho_3{}' + \frac{\Delta m}{V_3} \tag{11}$$

To find pressure in the room at the end of the time step we assume that all the energy lost in region 1 appears as an increase of internal energy of the gas in the room, i.e.,

$$\frac{\gamma}{\gamma - 1} \cdot \frac{P_1}{\rho_1} \cdot \Delta m = \frac{1}{\gamma - 1} \cdot \left(P_3 - P_3{}' \right) \; V_3$$

which can be solved to give P_3 in terms of known quantities:

$$P_3 = \frac{\gamma P_1}{\rho_1} \cdot \frac{\Delta m}{V_3} + P_3{}' \tag{12}$$

At any time air temperature T_3 within the room can be calculated from the perfect gas law:

$$T_3 = \frac{P_3}{R\rho_3}$$

where R is the gas constant[5] for air in the appropriate units (e.g., in English units R = 2.329 Btu/slug-F). The quantity T_3 can reach high values as a result of the compression existing behind the shock and within the room; however, if airflow to the outside (outflow) is maintained, the relaxation of pressure following the passage of the front will return room gas temperatures to safe levels before injury to occupants is likely. Only the long-lasting increase in room temperature resulting from fires will normally be a threat to the shelterees.

Numerical Example No. 1 (Inflow by Method F). The rate of pressure rise in a room of volume $V_3 = 15.0 \times 33.3 \times 8.0 = 4000$ cf containing openings into a single pressure field of total area $A_2 = 3 \times 7 = 21$ sf that faces side-on blast wave overpressure of 15 psi is calculated by taking the term P_3' to the left side of the Eq. (12) so that the equation reads:

$$P_3 - P_3' = \frac{\gamma P_1}{\rho_1} \cdot \frac{\Delta m}{V_3}$$

Substituting for Δm, from Eq. (10) and dividing both sides by Δt, we find:

$$\frac{P_3 - P_3'}{\Delta t} = \frac{\gamma P_1}{\rho_1 V_3} \cdot A_2 \; P_1(1-y_o) \; \rho_1 y_o{}^{1/\gamma} \; {}^{0.5}$$

In the limit of small Δt, this expression becomes the rate of pressure rise in the room, viz.,

$$\frac{P_3 - P_3'}{\Delta t} \longrightarrow \frac{dP_3}{dt}$$

Assuming that ambient pressure before blast arrival is the standard value i.e., $P_o = 14.7$ *psi, an outside overpressure of 15 psi means that*

$$P_1 = 15 + 14.7 = 29.7 \text{ psi}$$

We approximate outside air density from Eq. (6) viz.:

$$\rho_1 = \rho_o \left[\frac{P_1}{P_o} \right]^{1/\gamma}$$

and (from Table 6.1 of Volume 1 of the present work) find the standard density of dry air at 14.7 psi and 59.0 F to be 0.002378 lb-sec^2*/ft*^{4} *(or slug/cf). Choosing this value as ambient (i.e.,* ρ_o*), we calculate:*

$$\begin{aligned}\rho_1 &= 0.002378\ (29.7/14.7)^{1/1.4} \\ &= 0.003930 \text{ lb-sec}^2/\text{ft}^4 \text{ (slug/cf)}\end{aligned}$$

From page E-19

$$y_o = 0.1912$$

Hence, the initial rate of pressure increase in the room is:

$$\begin{aligned}\frac{dP_3}{dt} &= \frac{1.4 \times 29.7}{0.00393 \times 4000} \left[29.7(1-0.1912)(0.1912)^{1/1.4}\ (0.00393)144. \right]^{0.5} 21. \\ &= 231.5 \text{ psi/sec}\end{aligned}$$

and this rate will remain constant as long as P_1 *and* ρ_1 *are unchanging. If* P_1 *and* ρ_1 *do not change, then filling time* ΔT *becomes:*

$$\begin{aligned}\Delta T &= \frac{P_1 - P_o}{\frac{dP_3}{dt}} = \frac{15.0}{231.6} = 0.06476 \text{ sec} \\ &= 64.8 \text{ ms}\end{aligned}$$

An estimate by the simple method of Section IIA leads to a Value:

$$\Delta T = \frac{V}{2A} = \frac{4000}{2 \times 21} = 95.2 \text{ ms}$$

Conditions existing in the chamber at the beginning of a time step are used in the foregoing calculations only in Eqs. (11) and (12) and do not influence duct parameters because transients have been omitted from consideration. Transient phenomena, for example, determine the direction of flow; that is, if $P_1 > P_3$, flow is inward as discussed above, but otherwise flow is outward. Repeated neglect of signals originating from the room leads to an accumulation of error in the calculation of average pressure as can be seen from comparisons between calculation as above and measurement shown in Figures E-4, E-5, and E-6. The experiments[9] were carried out in a 24-inch shock tube; the configuration of each model chamber is shown in an inset in the figure; and the foregoing calculation produces Curve F of the figures. The curves in Figures E-5 and E-6 labelled "external history (A)" are measurements in the free stream by means of a pitot tube oriented with respect to the stream to conform with the orientation of the opening in the model room; "external history" in Figure E-4 is side-on overpressure in the unobstructed shock tube.[9] In each case the calculation initially yields pressure in agreement with observation but eventually shows room pressure during filling in excess of measurement, although the maximum difference is 20% or less. Magnitude of Δt for these calculations was one-quarter the transit time of a sound signal across the room.

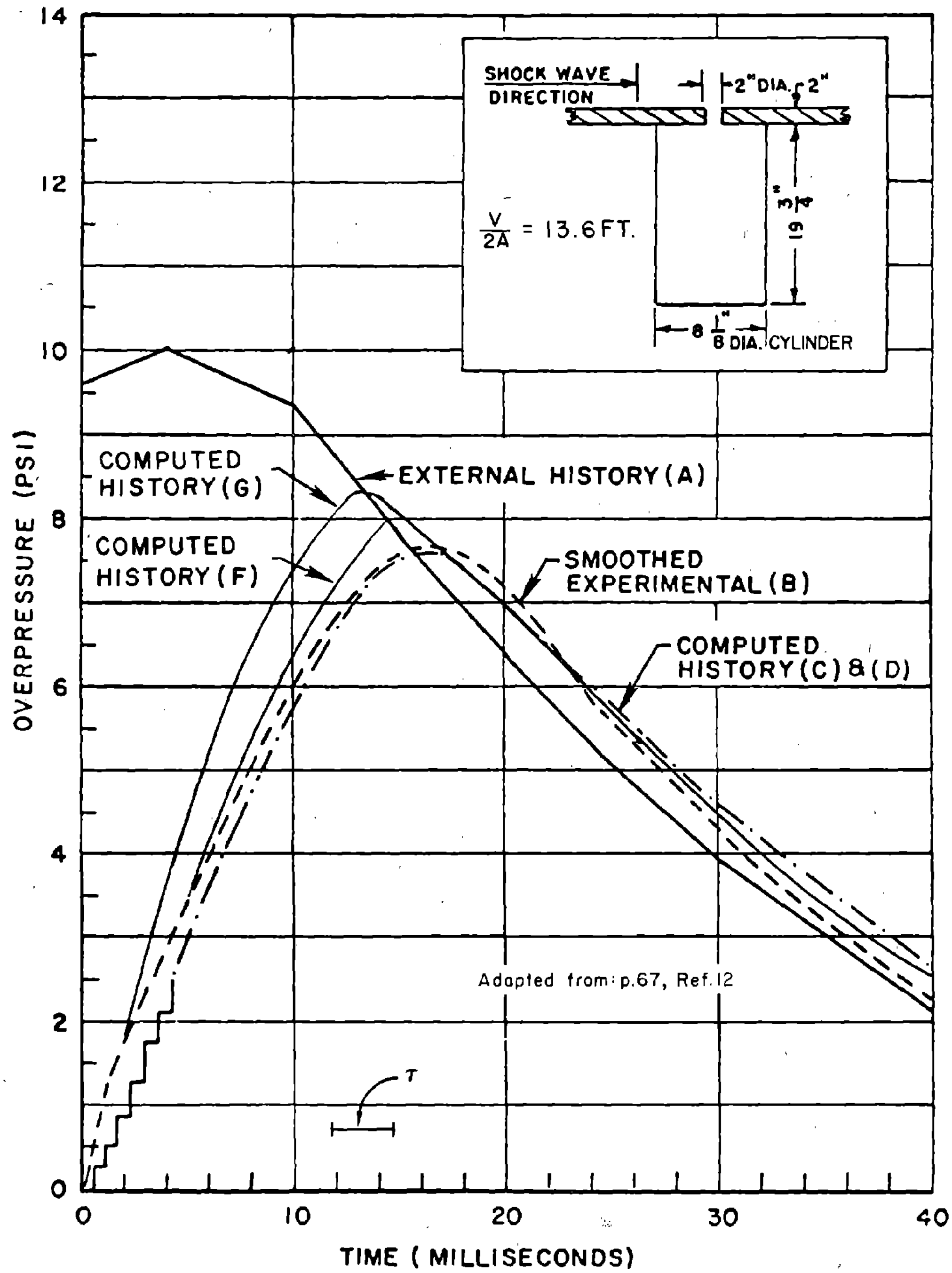

FIGURE E-4 FILL HISTORIES FOR SIDE-ON INCIDENCE

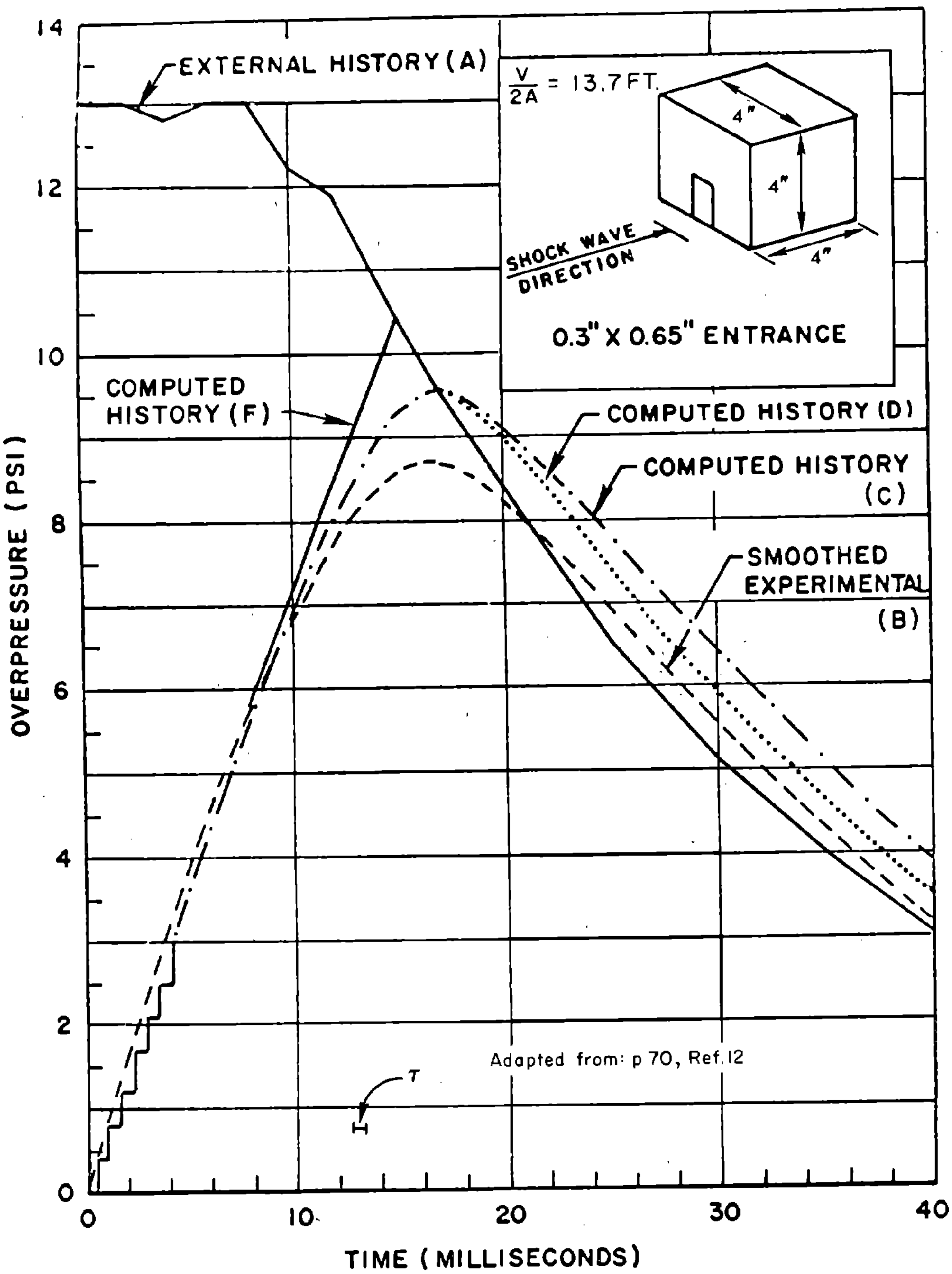

FIGURE E-5 FILL HISTORIES FOR A FACE-ON MODEL

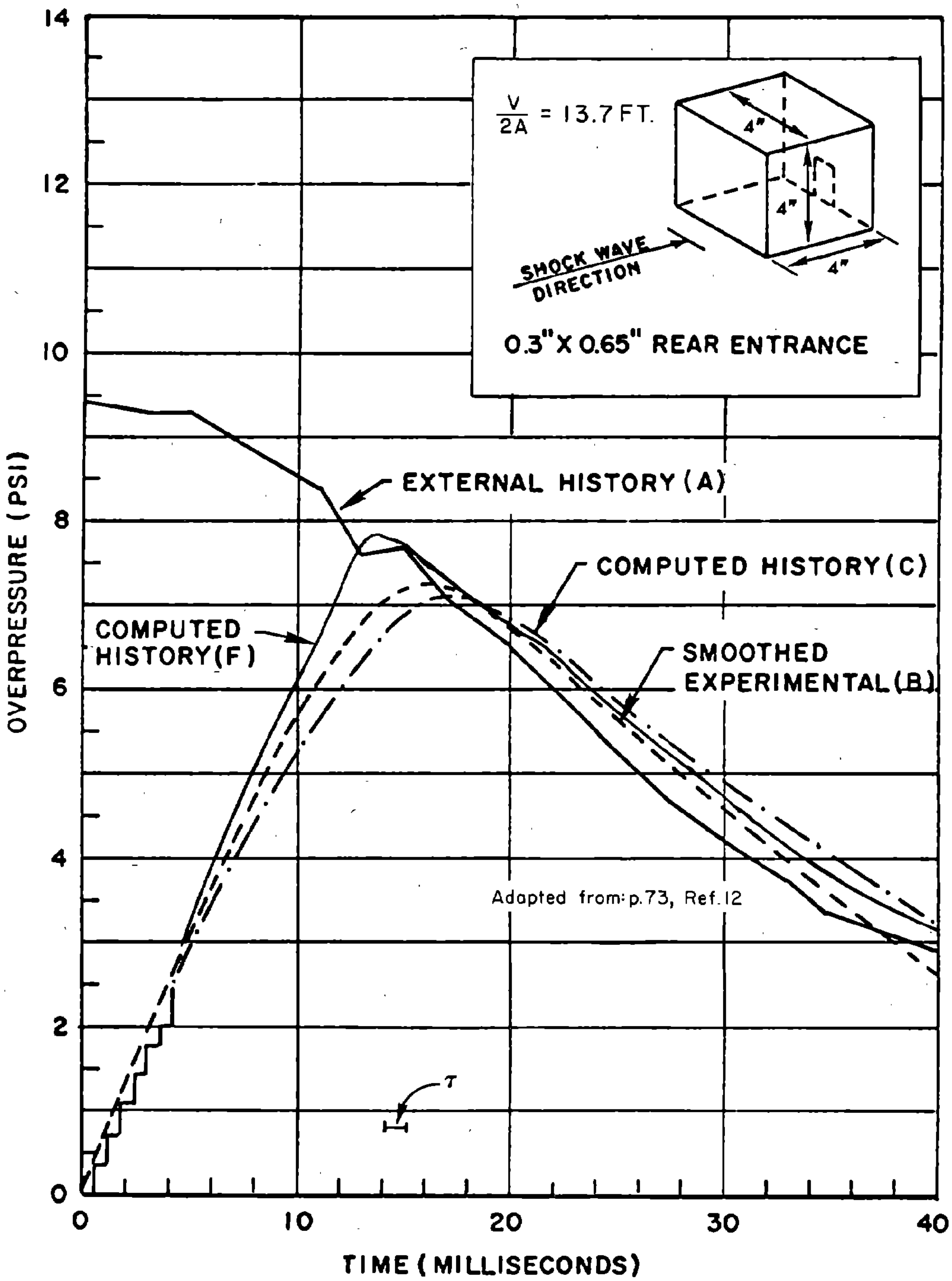

FIGURE E-6 FILL HISTORIES FOR A REAR FILL MODEL

Choice of the size of Δt is somewhat arbitrary except that (1) values much greater than sound transit time will give a false idea of the degree of irregularity in the fill process and (2) enough steps should be taken to make it possible for the influence of variations in P_1 to be shown in the results. The length of the bar labelled "τ" in Figures E-4, E-5, and E-6 represents the sound transit time across the longest room dimension.

A similar degree of comparison between calculation and measurement is found in the results shown in Figure E-8 stemming from a 27 cf model exposed to a large chemical explosion, except that the transient fluctuations associated with the entering shock front are more easily discerned in the larger model than in the small shock tube models. The parameter values used in the calculations summarized in Figure E-8 were:

P_o = 13.58 psia	ambient pressure
ρ_o = 0.00209 slug/cf	ambient density
γ = 1.4	ratio of specific heats
A_2 = 0.821 sf	area of opening
V_3 = 27.0 cf	volume of model room

The fraction of the impacted wall area occupied by the opening is slightly less than one-tenth.

From the results shown in Figures E-4, E-5, E-6, and E-8, some estimate can be made of the validity of the greatly simplified method of computing pressure rise in a filling room set forth in Section IIA. In each figure, the value of V/2A in feet has been entered. A constant pressure rise from zero time and zero overpressure to a pressure equal to outside pressure at a time equal to V/2A msec overestimates the fill pressure and underestimates the fill time in the small models but seems to give results in good agreement with both calculation and measurement in the three-foot cube model reported in Figure E-8, although the presence of important oscillations (caused by shock waves) in the pressure record in the large model makes clear assessment difficult. It should be noted also that the fraction of the wall struck by the blast that is occupied by the opening (opening fraction) is over 9 percent in the large model while only 1.2 percent in the small 4-inch cube models. The straight-line estimate explained in Section IIA would appear to be good also in Figure E-4 for which model size is intermediate and opening fraction is almost 6 percent.

The data from the models suggest that the simplified method of estimating pressure rise in a room, set forth in Section IIA, is adequate when outside pressure decay is slow as in a free-field nuclear blast wave. As will be noted later, when there exists an important diffraction phase in

the blast wave interaction with the structure, more sophisticated methods may be justified.

The existence of significant theoretical errors in our treatment of flow into a room by quasi-steady analysis is clearly revealed by considering the single control surface formed by superposition of that shown in Figure E-3 and that indicated with dashed lines in Figure E-7. Such a surface coincides with the inner surfaces of the room and passage and extends into quiescent air outside. Under our hypotheses there is no flow through this surface anywhere and no change of momentum within it, yet the surface integral of the x-component of pressure over the boundaries does not vanish.

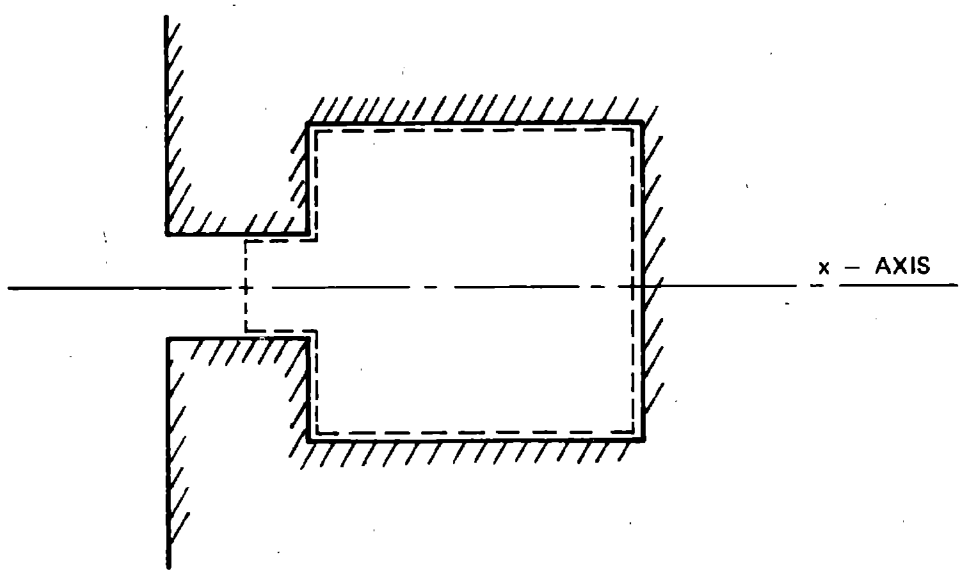

FIGURE E-7 SECOND CONTROL SURFACE

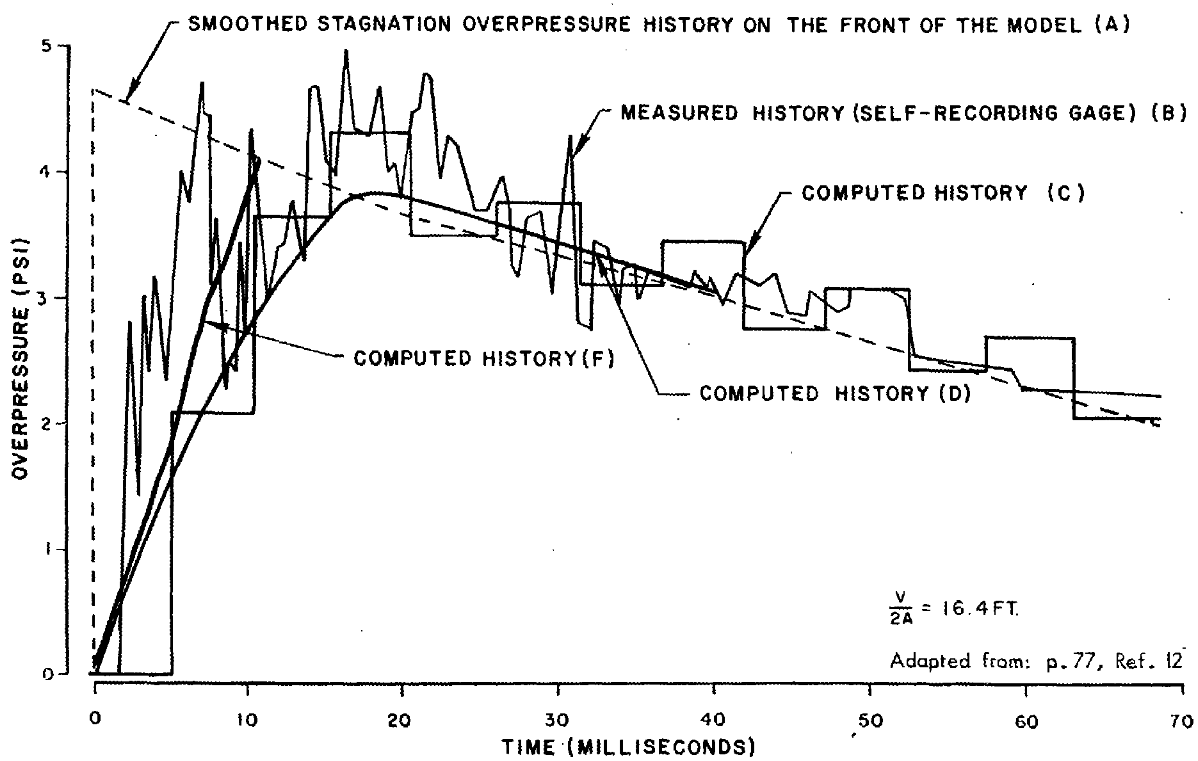

FIGURE E-8 COMPARISON OF THE COMPUTED VERSUS THE EXPERIMENTAL FILL HISTORY OF THE MODELED CHAMBER TESTED IN PROJECT DISTANT PLANE

This absurdity can be avoided in one or both of two ways. A term may be added to the right side of Eq. (2) to account for the changing flow pattern within the control surface shown in Figure E-3 or a term may be added to the left side of Eq. (2) to account for the possible nonuniformity of pressure over the boundaries of the surface. As the room begins to fill, a rarefaction wave moves back into the high pressure gas outside the first doorway bringing more and more gas into motion toward the opening. In other words, the neglect of the rate of change with time of the momentum within the control surface outside the room may be at least one cause of the contradiction noted above. Any attempt to calculate a correction for this effect would certainly add to the complexity of these simplified procedures; furthermore, the degree of agreement between observations and theory of Method F (shown in Figures E-4, E-5, and E-6) suggests that the added effort to account for the rarefaction wave may not be needed to achieve the desired degree of accuracy. Nevertheless, it is worthwhile to consider another method of estimating average pressure in a filling room.

Some writers[10,11,12,17] use the equation

$$P_2 = P_3' \tag{13}$$

instead of Eq. (2). Justification for Eq. (13) is based on analogy with the treatment of flow into a large chamber steadily being evacuated.[13] Equation (13) of course provides continual coupling between flow conditions and conditions in the room.

Using Eq. (13) we derive the pressure buildup inside the room in the following way. Substituting Eq. (3) into Eq. (1), then replacing P_2 with P_3' according to Eq. (13) and solving the resulting equation for u_2, we find:

$$u_2 = \left[\frac{2\gamma}{\gamma-1} \cdot \frac{P_1}{\rho_1} \left(1 - \left(\frac{P_3'}{P_1} \right)^{1-1/\gamma} \right) \right]^{1/2} \tag{14}$$

from which we calculate the mass inflow in the time increment Δt:

$$\begin{aligned} \Delta m &= K\, \rho_2\, u_2\, A_2\, \Delta t \\ &= K\, \rho_1 \left(\frac{2\gamma}{\gamma-1} \cdot \frac{P_1}{\rho_1} \right)^{1/2} \left(\frac{P_3'}{P_1} \right)^{1/\gamma} \left[1 - \left(\frac{P_3'}{P_1} \right)^{1-1/\gamma} \right]^{1/2} A_2\, \Delta t \end{aligned} \tag{15}$$

Whenever Eq. (13) is employed, empirical corrections are made to reduce the calculated inflow rate; the simplest correction is the discharge coefficient,[14] represented by the factor K in Eq. (15). Investigators at the IIT Research Institute[17] have found it necessary to use the value K=0.7 to reconcile computed pressure rises in small models with those measured; Curves D in Figures E-4 and E-5 have been produced by a calculation based on Eq. (13), with K=0.7 during inflow and K=1.00 during outflow.

The value of the discharge coefficient is usually discussed in connection with boundary layer thickness and the Reynolds number.[13] The relatively good agreement between the observed room pressures and Curves D was obtained in very small models, not in full-sized rooms. To estimate the influence of the value of K on calculated pressure rise, Curve G, based on the value of K=1.00 during both outflow and inflow, has been entered in Figure E-4. Presumably, the Reynolds number will be larger in the flow into full-sized rooms, and the discharge coefficient more nearly equal to 1.00 than in the flow into small models.

Finally, the pressure increment during the interval Δt is found by substitution of Eq. (15) into Eq. (12):

$$P_3 - P_3' = K\,\gamma\,P_1\left[\frac{2\gamma}{\gamma-1}\cdot\frac{P_1}{\rho_1}\right]^{\frac{1}{2}}\left(\frac{P_3'}{P_1}\right)^{\frac{1}{\gamma}}\left[1-\left(\frac{P_3'}{P_1}\right)^{1-\frac{1}{\gamma}}\right]^{\frac{1}{2}}\frac{A_2\,\Delta t}{V_3} \qquad (16)$$

Melichar[11,12] omits both the factors K and γ before the right-hand side of Eq. (16), which is equivalent numerically to making $K=0.7$ and $\gamma=1.4$. He attempts to justify this procedure on theoretical grounds unconnected with boundary layer theory.[12] Some of his numerical results are shown as Curves C in Figures E-4, E-5, E-6, and E-8. Melichar employs a value of Δt equal to the transit time of sound across the room.

Numerical Example No. 2 (Inflow by Method D). *We will apply Eq. (16) with $K = 0.7$ to the filling room considered in Numerical Example No. 1. The initial rate of pressure increase will be calculated by substituting $P_3' = 14.7$ psi, $P_1 = 29.7$ psi, and $\rho_1 = 0.003930$ slug/cf:*

$$\frac{dP_3}{dt} = 0.7 \times 1.4 \times 29.7 \left[\frac{2.8}{0.4}\,\frac{29.7\times 144}{0.003930}\right]^{0.5} \left(\frac{14.7}{29.7}\right)^{1/1.4}$$

$$\times \left[1 - \left(\frac{14.7}{29.7}\right)^{1-1/1.4}\right]^{0.5} \frac{21}{4000} = 108.9 \text{ psi/sec}$$

Had we assumed $K=1$, then $\frac{dP_3}{dt} = 155.5$ psi/sec

Thus the initial pressure rise calculated under the assumptions $P_2 = P_3'$ and $K \le 1$ is lower than the rate calculated in the previous numerical example by Method F. However, the rate by Eq. (16) is not constant; it falls slowly from its initial value, so that in the conditions postulated in these examples Method F forecasts a markedly shorter fill time than does Eq. (16).

Pursuing the analogy between room filling and steady flow into a chamber held at constant pressure, we expect to encounter the phenomenon of choking as the ratio of room pressure to outside pressure drops below the critical value.[13] Choking limits the rate at which mass flows into the room; hence, when inflow is choked, the rate of pressure rise dP_3/dt and wind speed u_2 in the entry will be limited.

For a given set of reservoir conditions, i.e., for each pair of values P_1 and ρ_1, the critical pressure ratio is that for which isentropic flow into the room achieves the maximum mass rate and for which the flow speed equals local sound speed. Therefore, to find this critical ratio, we can differentiate Eq. (15) with respect to P_3'/P_1, set the result equal to zero, and solve for $(P_3'/P_1)_{crit}$, which yields:

$$\left(\frac{P_3'}{P_1}\right)_{crit.} = \left(\frac{2}{\gamma+1}\right)^{\frac{\gamma}{\gamma-1}}$$

For every value of P_3' below the critical value as given above, mass flow into the room will be that obtained by substituting the critical ratio into Eq. (15), i.e.:

$$(\Delta m)_{\text{choked}} = K\left[\gamma\,\rho_1\,P_1\left(\frac{2}{\gamma+1}\right)^{\frac{\gamma+1}{\gamma-1}}\right]^{\frac{1}{2}} A_2\,\Delta t \qquad (17)$$

Because the mass flow rate is limited in this way independently of the value of P_3' it is called "choked" flow. Flow obeying Eq. (15) is called "unchoked" or "subsonic." Numerically, when $\gamma = 1.4$ the critical ratio equals 0.5283; thus, assuming ambient pressure is 14.7 psia,* the critical outside pressure is

$$\frac{14.7}{0.5283} = 27.83 \text{ psia or } 13.13 \text{ psig}$$

In none of the experiments reported in Figures E-4, E-5, and E-6 did peak overpressure rise above 13.13 psig; hence, according to the foregoing theory, choked flow should not have occurred.

<u>Numerical Example No. 3 (Choked Inflow)</u>. When inflow is choked, Eq.(17) replaces Eq. (15). Rate of pressure rise dP_3/dt is then found by substituting Eq. (17) into Eq. (12) and the wind speed u_2 is found by substituting into Eq. (14) the critical pressure ratio $(P_3/P_1)_{crit}$ as shown in the numerical example that follows.

Consider a 4000-cf room filling side-on from a 20 psi overpressure blast wave through an opening 21 sf in area. Since the incident overpressure is greater than critical, viz., 13.13 psig, inflow is choked, and Eq. (17) applies until the difference between inside and outside pressures falls below critical.

The initial rate of pressure rise within the room depends on the following values:

$\gamma = 1.4$

$P_1 = 14.7 + 20 = 34.7$ psi

$K = 0.7$

$A_2 = 21$ sf

* Pounds per square inch, absolute.

Outside air density ρ_1 *can be approximated by using the isentropic equation of state, Eq. (6), and standard conditions:*

$$\rho_1 = \rho_o \left(\frac{P_1}{P_o}\right)^{1/\gamma} = 0.002378 \left(\frac{34.7}{14.7}\right)^{1/1.4}$$

$$= 0.004397 \text{ slugs/cf}$$

(According to p. 3.49 of Ref. 1 the air density ρ_1 *behind a shock front of overpressure equal to p moving through air at pressure* P_o *and density* ρ_o *is:*

$$\rho_1 = \rho_o \frac{7P_o+6p}{7P_o+p}$$

Substituting the values given, for ρ_o *and* P_o*, we calculate:*

$$\rho_1 = 0.002378 \frac{7\times14.7 + 20\times6}{7\times14.7 + 20}$$

$$= 0.004313 \text{ slug/cf}$$

Thus, the approximation based on the isentropic equation of state, Eq. (6), is only 2% higher than the correct value 0.004313 slug/cf.)

We now know everything necessary to compute the initial rate of pressure increase within the room. From Eqs. (17) and (12):

$$\frac{\Delta m}{\Delta t} = 0.7 \left[1.4 \times 0.004313 \times 34.7 \times 144 \left(\frac{2}{1.4+1}\right)^{\frac{1.4+1}{1.4-1}}\right]^{0.5} 21$$

$$\frac{dm}{dt} = 46.73 \text{ slug/sec}$$

Rewriting Eq. (12) in differential form:

$$\frac{dP_3}{dt} = \frac{\gamma P_1}{\rho_1 V_3} \frac{dm}{dt}$$

we calculate:

$$\frac{dP_3}{dt} = \frac{1.4 \times 34.7 \times 46.73}{0.004313\times4000} = 131.6 \text{ psi/sec}$$

Assuming P_1 remains constant, we can find the time $\Delta T'$ required to fill the room to the extent that flow is no longer choked as follows:

$$\Delta T' = \frac{20-13.13}{131.6} = 0.05220 \text{ sec}$$
$$= 52.0 \text{ ms}$$

After time $\Delta T'$, inflow is no longer choked and further pressure increase is calculated in time steps by Eq. (16) as follows:

We assume P_3' is constant during a small time increment $\Delta t = 5$ ms and, noting that $P_3' = 20-13.13+14.7 = 21.57$ psia, we calculate from Eq. (16):

$$P_3 = P_3' + 0.7 \times 1.4 \times 34.7 \left[\frac{2\times 1.4}{0.4} \cdot \frac{34.7 \times 144}{.004313}\right]^{0.5} \left(\frac{21.57}{34.7}\right)^{1/1.4}$$
$$\times \left[1 - \left(\frac{21.57}{34.7}\right)^{1-1/1.4}\right]^{0.5} \quad \frac{21 \times .005}{4000}$$

$$P_3 = 21.57 + 0.6451 = 22.215 \text{ psig}$$

The calculation is now repeated with $P_3' = 22.215$ and a new value of P_3 found, which becomes P_3' in the next time step. The procedure is repeated until $P_3 > P_1$, at which time the room is considered filled.

For the case of choked inflow, Eq. (17), the simple estimate in Section IIA of rate of pressure rise and of filling time ΔT may be theoretically justified as follows.[24] Combining Eqs. (12) and (17), we find

$$\frac{P_3 - P_3'}{\Delta t} = \frac{dP_3}{dt} = \frac{\gamma P_1}{\rho_1 V_3} \frac{dm}{dt} = \frac{A_2 K \gamma^{1.5}}{V_3} \frac{P_1^{1.5}}{\rho_1^{0.5}} \left(\frac{2}{\gamma+1}\right)^{\frac{\gamma+1}{2(\gamma-1)}} \tag{18}$$

If P_1 remains constant and the inflow remains choked during most of the filling time, then

$$\Delta T \approx \frac{P_1 - P_o}{\frac{dP_3}{dt}} = \frac{V_3}{KA_2} \frac{1}{\gamma^{1.5}} \left(\frac{\gamma+1}{2}\right)^{\frac{\gamma+1}{2(\gamma-1)}} \left(\frac{\rho_o}{P_o}\right)^{0.5} \left(\frac{P_o}{P_1}\right)^{0.5} \left(\frac{P_1}{P_o}\right)^{\frac{1}{2\gamma}} \left(1 - \frac{P_o}{P_1}\right)$$

Taking $P_o = 14.7$ psi, $\rho_o = 0.002378$ slugs/cf, $\gamma = 1.4$ and $K = 1$, we find the factor

$$\frac{1}{K\gamma^{1.5}} \left(\frac{\gamma+1}{2}\right)^{\frac{\gamma+1}{2(\gamma-1)}} \left(\frac{\rho_o}{P_o}\right)^{0.5}$$

takes on the value

$$\frac{1}{1.0\ (1.4)^{1.5}} \quad (1.2)^{3.0} \left(\frac{0.002378}{14.7} \quad \frac{\text{lb-sec}^2}{\text{ft}^4} \ \frac{\text{in}^2}{\text{lb}} \quad \frac{\text{ft}^2}{144\ \text{in}^2}\right)^{0.5}$$

$$= 0.001105 \text{ sec/ft}$$

$$= 1.10 \text{ ms/ft}$$

Hence,

$$\Delta T \approx 1.10 \quad \frac{V_3}{A_2} \left(\frac{P_o}{P_1}\right)^{0.5} \left(\frac{P_1}{P_o}\right)^{\frac{1}{2\gamma}} \left(1 - \frac{P_o}{P_1}\right) \quad \text{ms/ft}$$

Evaluating this expression numerically, we find that in the range

$$0.528 \geq \frac{P_o}{P_1} \geq 0.25$$

the variation of ΔT is within

$$\frac{1}{2.11} \ \frac{V_3}{A_2} \geq \Delta T \geq \frac{1}{1.48} \quad \frac{V_3}{A_2}$$

It turns out that when the inflow is unchoked, the simple estimate in Section IIA for filling time ΔT can also be shown, as follows, to be approximately true, at least until

$$\frac{P_o}{P_1} \geq 0.8$$

Substitution of Eq. (15) into Eq. (12) results in the expression for rate of pressure rise.

$$\frac{dP_3}{dt} = \frac{P_1 A_2 K}{\rho_1 V_3} \gamma \left(\frac{2\gamma}{\gamma-1}\right)^{0.5} \left(\rho_1 P_1\right)^{0.5} \left(\frac{P_3}{P_1}\right)^{\frac{1}{\gamma}} \left[1 - \left(\frac{P_3}{P_1}\right)^{\frac{\gamma-1}{\gamma}}\right]^{0.5}$$

Substituting the isentropic equation of state, Eq. (6), we find:

$$\frac{dP_3}{dt} = \frac{A_2 P_o^{1.5} K}{V_3 \rho_o^{0.5}} \left(\frac{P_o}{P_1}\right)^{\frac{1-3\gamma}{2\gamma}} \left(\frac{P_3}{P_1}\right)^{\frac{1}{\gamma}} \left[1 - \left(\frac{P_3}{P_1}\right)^{\frac{\gamma-1}{\gamma}}\right]^{0.5} \quad (19)$$

When P_o is substituted for P_3 on the right-hand side, this becomes the expression for the initial rate of pressure rise; furthermore, if this rate is assumed constant (as seems to be nearly true from the experimental observations), then

$$\Delta T = \frac{P_1 - P_o}{\left(\frac{dP_3}{dt}\right)} = \frac{V_3}{A_2 K} \frac{1}{\gamma} \left(\frac{\gamma-1}{2\gamma}\right)^{0.5} \left(\frac{\rho_o}{P_o}\right)^{0.5} \frac{\left(\frac{P_o}{P_1}\right)^{\frac{3\gamma-1}{2\gamma}} \left(\frac{P_1}{P_o} - 1\right)}{\left[1 - \left(\frac{P_o}{P_1}\right)^{\frac{\gamma-1}{\gamma}}\right]^{0.5}}$$

Evaluating the factor

$$\frac{1}{K\gamma} \left(\frac{\gamma-1}{2\gamma}\right)^{0.5} \left(\frac{\rho_o}{P_o}\right)^{0.5}$$

using the values K = 1.0, $\gamma = 1.4$, $P_o = 14.7$ psi and $\rho_o = 0.002378$ lb-sec^2/ft^4 we can write:

$$\Delta T = \frac{1}{1.4}\left(\frac{0.4}{2.8}\right)^{0.5}\left(\frac{0.002378}{(14.7)(144)}\right)^{0.5}\frac{V_3}{A_2}\frac{\left(\frac{P_o}{P_1}\right)^{\frac{3\gamma-1}{2\gamma}}\left(\frac{P_1}{P_o}-1\right)}{\left[1-\left(\frac{P_o}{P_1}\right)^{\frac{\gamma-1}{\gamma}}\right]^{0.5}}$$

$$= 0.286\ \frac{V_3}{A_2}\frac{\left(\frac{P_o}{P_1}\right)^{\frac{3\gamma-1}{2\gamma}}\left(\frac{P_1}{P_o}-1\right)}{\left[1-\left(\frac{P_o}{P_1}\right)^{\frac{\gamma-1}{\gamma}}\right]^{0.5}}\quad \text{ms/ft}$$

Over the interval $0.528 \le P_o/P_1 \le 0.8$, the calculated filling time ΔT according to the above formula lies between two values, viz:

$$\frac{1}{2.10}\frac{V_3}{A_2} \ge \Delta T \ge \frac{1}{3.83}\frac{V_3}{A_2}$$

The rate of pressure rise during choked inflow is of course independent of room pressure, Eq. (18), but even when the inflow is or becomes unchoked the rate is only weakly dependent on room pressure P_3, as we see by evaluating the last two factors on the right side of Eq. (19), viz:

$$\left(\frac{P_3}{P_1}\right)^{\frac{1}{\gamma}}\left[1-\left(\frac{P_3}{P_1}\right)^{\frac{\gamma-1}{\gamma}}\right]^{0.5}$$

and plotting the result as a function of P_3/P_1 in Figure E-9 The figure shows that rate of pressure rise varies between limits of ±10% as long as P_3/P_1 is within the bounds: $0.2 < P_3/P_1 < 0.8$.

The equations, derived from quasi-steady analysis, neglect the inertia of the inflowing column of air; therefore, we might expect a tendency for the rate of pressure rise to continue at the level established earlier to compete with a tendency to fall as forecast by the equations.

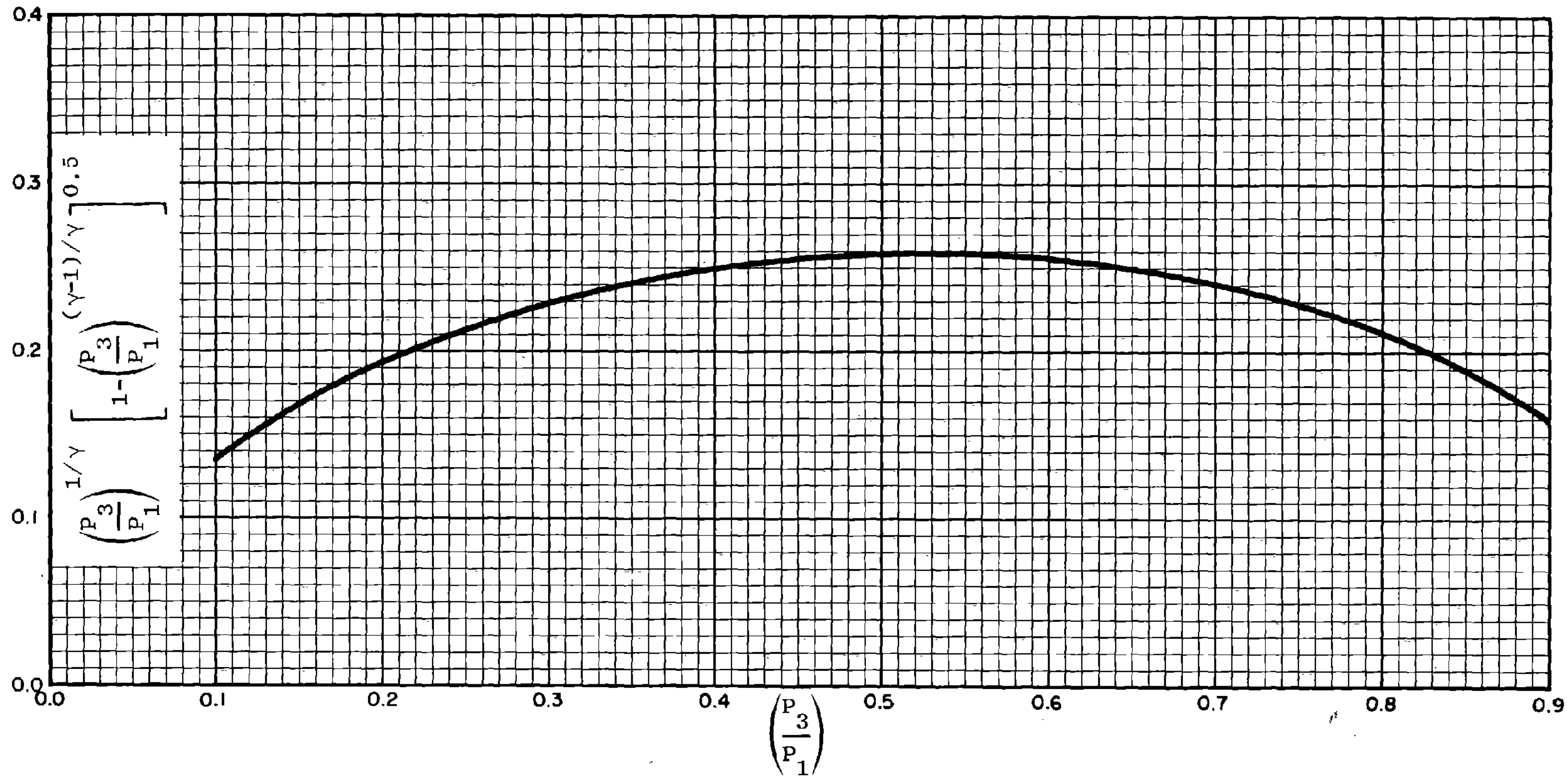

FIGURE E-9 VARIATION OF PRESSURE RATE DURING UNCHOKED FLOW (γ = 1.4)

Summary. Several distinct methods have been presented for estimating the rate of pressure rise in a room filling from a nuclear-induced air blast wave. All the methods are based on an analogy with steady flow in ducts and none applies to a room in which more than half of its exterior wall area is open to the blast. The simplest of the methods, given in Section IIA, demands only a knowledge of the room volume, the areas of the openings through which the blast enters, and the outside pressure against each opening during the filling. Should this outside pressure vary greatly during the filling, the methods of Section IIA will not in general be accurate.

A slightly more complicated method of calculating the rate of pressure rise takes into account the variation of outside pressure but not the resultant rise of inside pressure. This technique (Method F) uses Eqs. (9), (10) and (12). Despite their relative simplicity, both this method and the one outlined in Section IIA appear to give results in good agreement with observations in small and intermediate models.

The most sophisticated method of estimating rate of pressure rise within a room filling from an air blast and the wind speed in the entry comes from Eqs. (14), (16) and (17) (Method D) and makes use of the instantaneous pressures in the room and outside and requires the determination of whether the flow is choked as well as knowledge of an empirical discharge coefficient.

These methods are outlined in equation form in Section IIB3.

2. Outflow. All the experimental data discussed so far show that room pressure eventually exceeds outside pressure by a small amount. If all openings are into the same outside pressure field and if the fall of outside pressure is steady and slow, this "overshoot" is not likely to be of practical importance. However, as will be seen later, if a room has openings that are affected by different outside pressure histories, a significant outward pressure may develop on one or more walls of the room. To calculate this pressure, the rate of outflow of air through each opening must be found.

To compute inflow we treated the exterior atmosphere and the aperture leading into the room as parts of a system of ducts through which quasi-steady flow was maintained. Pressure increase within the room was computed as resulting from the transfer of mass and energy from the large outside reservoir into the room. Outflow may be treated in the same way, except that the direction of flow is reversed. For outflow, Eqs. (1) and

(2) still apply, but the air in the "duct" now originates in the room, and the adiabatic expansion law, Eq. (3), must be replaced by

$$\rho_2 = \rho_3' \left[\frac{P_2}{P_3'}\right]^{1/\gamma} \tag{20}$$

Equations (1), (2), and (20) can be combined to form an equation identical to Eq. (5) except that now

$$B = \frac{2\gamma}{\gamma + 1} \cdot \frac{\rho_3'}{\rho_1} \left[\frac{P_1}{P_3'}\right]^{1/\gamma} \tag{21}$$

But, as before,

$$y = \frac{P_2}{P_1} \qquad \text{and} \qquad A = \frac{\gamma - 1}{\gamma + 1} \tag{22}$$

In this form, Eq. (5) has two solutions in the range $0 \leq y \leq 1$ whenever $\gamma = 1.4$ and

$$\frac{\rho_3'}{\rho_1} \left[\frac{P_1}{P_3'}\right]^{1/\gamma} > 1$$

or

$$\frac{P_1}{\rho_1^{\gamma}} > \frac{P_3'}{\rho_3'^{\gamma}} \tag{23}$$

These two solutions merge into a single solution at $y = \left[\frac{B}{\gamma}\right]^{\frac{\gamma}{\gamma - 1}}$

if

$$\frac{P_1}{\rho_1^{\gamma}} = (0.9094) \quad \frac{P_3'}{\rho_3'^{\gamma}}$$

Furthermore, if $\gamma = 1.4$, Eq. (5) has only one solution in the range of $0 \leq y \leq 1$ whenever

$$\frac{P_3'}{\rho_3'^{\gamma}} \geq \frac{P_1}{\rho_1^{\gamma}} > (0.9094) \quad \frac{P_3'}{\rho_3'^{\gamma}} \tag{24}$$

Also, if

$$\frac{P_1}{\rho_1^{\gamma}} < (0.9094) \quad \frac{P_3'}{\rho_3'^{\gamma}} \tag{25}$$

no solution to Eq. (5) exists.

Since the quantity P/ρ^{γ} is constant along an isentrope and increases with entropy, the truth of Inequality (25) implies that at the end of inflow specific entropy (i.e., entropy per unit mass) outside is less than approximately 0.9 the specific entropy within the room. Thus, in order to establish the existence of a solution to Eq. (5) during outflow, we must calculate the increase in specific entropy within the room during inflow and compare it with the increase in entropy through the shock front.

The increase in specific entropy in the room at any time during filling can be formally calculated as follows. First, we note that temperature of air in the room rises during the whole inflow period, as can be seen by treating Δm as a true differential and writing Eq. (12) as:

$$dP_3 = \frac{\gamma P_1}{\rho_1 V_3} \cdot dm$$

From the perfect gas law

$$P_3 = \frac{m_3 R T_3}{V_3}$$

where m_3 is the mass of air in the room, and R the gas constant for air, we write

$$dP_3 = \frac{R T_3}{V_3} \cdot dm + \frac{m_3 R}{V_3} \cdot dT_3$$

$$dP_3 = \frac{P_3}{m_3} \cdot dm + \frac{m_3 R}{V_3} \cdot dT_3 = \frac{\gamma P_1}{\rho_1 V_3} \cdot dm$$

Noting that $m_3 = \rho_3 V_3$ and collecting terms, we find

$$\frac{1}{V_3}\left[\frac{\gamma P_1}{\rho_1} - \frac{P_3}{\rho_3}\right] dm = \frac{m_3 R}{V_3} \cdot dT_3$$

Multiplying both sides of the equation by V_3/R and using the perfect gas law in the form $P/(R\rho) = T$, we find the following relation between inside and outside temperatures during filling:

$$\left[\gamma T_1 - T_3\right] \quad dm = m_3 \quad dT_3 \tag{26}$$

Clearly, at the start of filling $T_1 > T_3$; hence, at the start $dT_3 > 0$. Moreover Eq. (26) shows that T_3 can increase above T_1 while $dm > 0$ until T_3 approaches $\gamma\, T_1$. Thus as temperature outside (T_1) falls due to the adiabatic relaxation behind the shock front, inflow and rising inside temperature continue.

Second, we can find a simple relation between the actual temperature increase within the room and a temperature increase in an isentropic process resulting in the same density increase.

In an isentropic process involving a certain mass of ideal gas the quantity $\rho/T^{1/(\gamma-1)}$ is constant; or taking differentials,

$$\frac{d\rho}{\rho} = \frac{dT}{\gamma T - T}$$

Rewriting Eq. (26) as

$$\frac{dm}{m_3} = \frac{dT_3}{\gamma T_1 - T_3}$$

then dividing (left-side) numerator and denominator by V_3 and noting that density $\rho_3 = m_3/V_3$, we find

$$\frac{d\rho_3}{\rho_3} = \frac{dT_3}{\gamma T_1 - T_3}$$

In other words the process of room filling during the time period t to t + dt results in a temperature increase dT_3 that bears the relation

$$\frac{dT_3}{(dT_3)_{isentropic}} = \frac{\gamma T_1 - T_3}{\gamma T_3 - T_3}$$

to the temperature increase in an isentropic process providing the same density increase. When $T_1 > T_3$, $\dfrac{dT_3}{(dT_3)_{isentropic}} > 1$

Finally, the entropy increase within the room is calculated from the specific heat at constant volume (or density).

$$dS = \frac{c_v dT}{T}$$

where c_v is specific heat at constant volume. If we imagine a return to the isentrope (after an increment of filling) by a process at constant density or volume, the specific entropy change within the room resulting from the filling increment becomes

$$dS_3 = \frac{c_v}{T_3} \left[dT_3 - (dT_3)_{isentropic} \right]$$

or,

$$dS_3 = \frac{c_v \gamma}{T_3} \left[\frac{T_1 - T_3}{\gamma T_1 - T_3} \right] dT_3 \tag{27}$$

which on substitution of the quantity dT_3 from Eq. (26), becomes

$$dS_3 = \frac{c_v \gamma}{T_3 m_3} (T_1 - T_3) dm \tag{28}$$

Therefore, during inflow (i.e., when $dm > 0$) specific entropy within the room will increase until $T_3 = T_1$ or $P_3 = P_1$, whichever occurs first.

Because of the passage of the shock front, air outside has greater than normal specific entropy. Hence, initially before inflow begins

$$\frac{P_1}{\rho_1^\gamma} > \frac{P_3}{\rho_3^\gamma}$$

however, Eq. (28) shows that the inflow process, according to the theory applied here, creates entropy within the room. Should enough entropy be so created, Inequality (25) may eventually be satisfied and solution of the outflow equations presented here may be impossible. The rise in specific entropy within the room as a result of inflow is:

$$\Delta S_3 = c_v \gamma \int_{t=0}^{P_3 = P_1} \frac{T_1 - T_3}{T_3 m_3} \frac{dm}{dt} dt$$

where t = time and T_1, T_3, and m_3 are functions of time. From Eq. (26) we know that T_3 rises asymptotically toward γT_1 until $P_1 = P_3$; thus, T_3 may be larger than T_1. For a given function $P_1(t)$ [which determines $T_1(t)$, $T_3(t)$, and $m_3(t)$], the maximum specific entropy within the room will be reached when

$$T_3 = T_1$$

If we assume that at this time inflow is still under way, then

$$P_1 > P_3$$

which implies, when $\gamma > 1$, that

$$P_1^{1-\frac{1}{\gamma}} > P_3^{1-\frac{1}{\gamma}}$$

or

$$P_1^{\frac{1}{\gamma}-1} < P_3^{\frac{1}{\gamma}-1}$$

Now from the equality of the temperatures at this time, the perfect gas law implies

$$\frac{P_1}{\rho_1} = \frac{P_3}{\rho_3}$$

Multiplying both sides by the last inequality above, we find

$$\frac{P_1^{1/\gamma}}{\rho_1} < \frac{P_3^{1/\gamma}}{\rho_3}$$

or

$$\frac{P_1}{\rho_1^{\gamma}} < \frac{P_3}{\rho_3^{\gamma}}$$

Hence, in general, the possibility may not be ruled out that Inequality (25) will be satisfied. Whether the outflow equations as presented here have a solution will depend on the nature of the function $P_1(t)$. If outflow is to be calculated, then to provide an initial disparity between specific entropy outside and inside, the inflow period must be treated using the initial density behind the shock front and computed from the Hugoniot relation:[1]

$$\rho_{1o} = \rho_o \frac{(\gamma+1)P_{1o} + (\gamma-1)P_o}{(\gamma-1)P_{1o} + (\gamma+1)P_o} \tag{29}$$

Subsequent outside air densities may be calculated from the adiabatic law:

$$\rho_1 = \rho_{1o} \left[\frac{P_1}{P_{1o}} \right]^{1/\gamma} \tag{30}$$

In Eqs. (29) and (30), ρ_{1o} and P_{1o} refer to the air density and absolute pressure immediately behind the shock front. When peak pressure at an opening is reached by reflection of an incident shock wave from a wall, Eq. (30) is not correct regardless of whether P_{1o} is taken as peak incident absolute pressure or peak reflected absolute pressure, but the error in using Eq. (30) is small. We will arbitrarily consider ρ_{1o} and P_{1o} as representing conditions behind the free-field shock front. Use of Eqs. (29) and (30) may make it possible to satisfy the reverse of Inequality (25).

The outflow method discussed above and contained in Eqs. (5), (21) and (22) is analogous to Method F discussed in Section IIB1 for inflow. Should Inequality (25) be satisfied; other calculational methods must be used for the outflow phase, such as that proposed by Melichar[11,12] or that reported by IIT Research Institute.[17] These methods equate duct pressure P_2 with outside pressure during outflow; the IIT investigators then fit observed outflow pressure data by choosing values for the discharge coefficient and for the ratio of inside to outside pressure at the time of flow reversal. These methods are analogous to Method D discussed under Inflow in Section IIB1 and are treated in detail in the next subsection as a part of Method D.

3. Outline of Hand Calculation.* In constructing from the foregoing equations a calculational scheme for estimating the parameters of flow into and out of a single room with a single opening we start with a series of values of P_1, one for each time step. These may be obtained by linear interpolation from a given table of outside pressure as a function of time and each value should pertain to the center of the time interval. The size of the time interval, Δt, itself is arbitrary, but it should be no greater than the quantity τ; presumably up to a limit, greater accuracy results from smaller values of Δt. The size of Δt may be changed during the calculation when the rate of change of flow parameters changes. We also need values for ambient pressure P_o and density ρ_o.

* If the outside pressure is the result of a classical nuclear blast wave, the computer program described in Section V will perform this calculation.

As a general rule, Δt may be chosen to be one-tenth of γ. Certain tests incorporated into the calculation below will indicate when the value of Δt must be reduced.

Two methods of calculation are shown below. The first is that used to produce Curves F in Figures E-4, E-5, E-6, and E-8, namely, that based on Eqs. (1), (2) and (3) for inflow or Eqs. (1), (2) and (30) for outflow, and in the outline below it is called Method F. This method has the advantage of great simplicity and of not requiring knowledge of empirical constants; however, as will be explained later, values of wind speed and dynamic pressure computed by it are subject to doubt in some cases and for that reason a method given by IIT Research Institute is included also. The latter (and our second) method is responsible for Curves D in the Figures E-4, E-5, and E-8 and, therefore, in the outline below it is called Method D. As noted earlier, Method D for the unchoked flow case is numerically equivalent to the calculation used by Melichar[11,12] (Curves C in Figures E-4, -5, -6 and -8).

Average pressure inside a room and dynamic pressure in the single opening to an outside reservoir whose pressure variation in time is known may be calculated as functions of time by the sequential application of the steps stated below. Each cycle through a series of steps completes the calculation for one time interval. The first three steps are executed only during the first cycle; subsequent passes begin with step (4), as indicated in the outline. Step (5) is a branch point to separate sequences for inflow and outflow, chosen according to a criterion given in step (5). There are further branches: (a) to Method D or F, chosen at the discretion of the user at each time; and (b) under Method D to choked or unchoked flow, determined by stated criteria. Throughout the outline, the quantity γ has been set equal to 1.4.

(1) Set $P_3' = P_o$ and $\rho_3' = \rho_o$ and $t = 0$.

(2) Compute

$$\rho_{1o} = \rho_o \frac{6P_{1o} + P_o}{P_{1o} + 6P_o}$$

where P_{1o} is the absolute pressure immediately behind the shock front, and ρ_{1o} is the associated air density.

(3) Choose value of Δt (see opening paragraph of this Section IIB3).

(4) Determine outside pressure at the current time; i.e., determine P_1, from the known reservoir pressure history (pressure variation with time). During first time interval $P_1 = P_{1o}$.

If the current value of P_1 differs from the immediately preceding value by more than 5% of itself, return time value to previous step (i.e., subtract Δt from current time), reduce Δt by half, and repeat preceding pass through this outline

(5) Determine direction of flow; i.e., if $P_1 > P_3'$, flow is inward; go to step (6). Otherwise flow is outward; go to step (28).

Inflow

(6) Compute

$$\rho_1 = \rho_{1o}\left[\frac{P_1}{P_{1o}}\right]^{0.7143}$$

Branch to selected Method below for step number (7D) (Method D) or step (7F) (Method F).

Method D (Inflow)

(7D) If $P_3'/P_1 \leq 0.5283$ inflow is choked; go to step (8D). Otherwise inflow is unchoked; go to step (18D).

Choked Inflow

(8D) $$\Delta m = K\left[1.4\,\rho_1\,P_1\left(\frac{2}{2.4}\right)^{\frac{2.4}{0.4}} F^*\right]^{1/2} A_2\,\Delta t$$

$$= 0.6847\;K\;[\rho_1\,P_1\,F]^{1/2}\;A_2\;\Delta t$$

Using the recommended value[17] of K = 0.70 this becomes

$$\Delta m = 0.4793\,[\,\rho_1\,P_1\,F]^{1/2}\,A_2\,\Delta t$$

The quantity A_2 is the sum of the areas of all openings into the pressure P_1.

(9D) $P_2 = P_3'$

(10D) $$\rho_2 = \rho_1\left[\frac{P_2}{P_1}\right]^{0.7143}$$

* The factor F is often necessary for consistency of units. For example, if u_2 is in ft/sec and P_1 is in lb/in^2 and ρ_1 in lb/cf, then F = 32. X 144. = 4,608.

(11D) $u_2 = \frac{\Delta m}{\Delta t \; A_2 \rho_2 K}$

(12D) $P_3 = P_3' + 1.4 \frac{P_1}{\rho_1} \frac{\Delta m}{V_3}$

(13D) Go to step (23D)

Unchoked Inflow

(18D) $P_2 = P_3'$

(19D) $\rho_2 = \rho_1 \left[\frac{P_2}{P_1} \right]^{0.7143}$

(20D) $u_2^2 = 7 \left[\frac{P_1}{\rho_1} - \frac{P_2}{\rho_2} \right] F$

(21D) $\Delta m = \rho_2 u_2 A_2 \; \Delta t$

(22D) $P_3 = P_3' + 1.4 \frac{P_1}{\rho_1} \frac{\Delta m}{V_3}$

If $|P_3 - P_3'| > .05 \, P_3'$ return to immediately preceding time (i.e., subtract Δt from current time), reduce Δt by one-half, and return to step (4).

(23D) $\rho_3 = \rho_3' + \frac{\Delta m}{V_3}$

(24D) If desired, dynamic pressure, q_2, in the opening can be found from:

$$q_2 = \frac{1}{2} \frac{1}{A_2^2 \rho_1} \left(\frac{\Delta m}{\Delta t} \right)^2 \frac{1}{F} \left(\frac{P_1}{P_3'} \right)^{1/\gamma} \quad \text{(See Section IIC)}$$

(25D) $P_3' = P_3$

(26D) $\rho_3' = \rho_3$

(27D) Advance time by amount Δt and return to step (4).

Method F (Inflow)

(7F) $P_2 = 0.1912\ P_1$

(8F) $\rho_2 = \rho_1 \left[\frac{P_2}{P_1}\right]^{0.7143} = 0.3067\ \rho_1$

(9F) $u_2^2 = 7 \left[\frac{P_1}{\rho_1} - \frac{P_2}{\rho_2}\right] F = 2.637 \left[\frac{P_1}{\rho_1}\right] F$

(10F) $\Delta m_3 = u_2\ \rho_2\ A_2\ \Delta t = 0.498\ (P_1\ \rho_1\ F)^{1/2}\ A_2 \Delta t$

(11F) $P_3 = P_3' + 1.4\ \frac{P_1}{\rho_1}\ \frac{\Delta m_3}{V_3}$

(12F) $\rho_3 = \rho_3' + \frac{\Delta m_3}{V_3}$

(13F) If desired, the dynamic pressure, q_2, in the doorway can be calculated:

$$q_2 = \frac{1}{2A_2^2 \rho_1} \left(\frac{\Delta m}{\Delta t}\right)^2 \frac{1}{F} \left(\frac{P_1}{P_3'}\right)^{1/\gamma}$$ (See Section IIC)

(14F) $\rho_3' = \rho_3$

(15F) $P_3' = P_3$

(16F) Advance time by amount Δt and return to step (4).

Outflow

(28) Branch to selected Method below for step (29D) (Method D) or step (29F) (Method F).

Method D (Outflow)

(29D) If $P_1/P_3' \le 0.5283$, outflow is choked; go to step (30D). Otherwise outflow is unchoked; go to step (39D).

Choked Outflow

(30D) $$\Delta m = -0.6847\ K\ [\rho_3'\ P_3'\ F]^{1/2}\ A_2 \Delta t$$

Using the recommended value[17] K = 1.0 for outflow this becomes

$$\Delta m = -0.6847\ [\rho_3'\ P_3'\ F]^{1/2}\ A_2 \Delta t$$

(31D) $$P_2 = P_1$$

(32D) $$\rho_2 = \rho_3' \left[\frac{P_2}{P_1} \right]^{0.7143}$$

(33D) $$u_2 = \frac{\Delta m}{\Delta t\ A_2\ \rho_2\ K}$$

(34D) $$P_3 = P_3' + 1.4\ \frac{\Delta m}{V_3}\ \frac{P_3'}{\rho_3'}$$

(35D) $$\rho_3 = \rho_3' + \frac{\Delta m}{V_3}$$

(36D) $$P_3' = P_3$$

(37D) $$\rho_3' = \rho_3$$

(38D) Advance time by amount Δt and return to step (4).

Unchoked Outflow

(39D) $$P_2 = P_1$$

(40D) $$\rho_2 = \rho_3' \left[\frac{P_2}{P_3'} \right]^{0.7143}$$

(41D) $$u_2^2 = 7 \left[\frac{P_1}{\rho_1} - \frac{P_2}{\rho_2} \right] F$$

(42D) $\Delta m = -\rho_2 u_2 A_2 \Delta t$

(43D) $P_3 = P_3' + 1.4 \frac{\Delta m}{V_3} \frac{P_3'}{\rho_3'}$

If $P_3 - P_3' > .05 P_3'$ return to immediately preceding time (i.e., subtract Δt from current time), reduce Δt by one-half, and return to step (4).

(44D) Go to step (35D)

Method F (Outflow)

(29F) If $P_1/\rho_1^\gamma < (0.9094)(P_3'/\rho_3^\gamma)$, Method F cannot be used. Go to step (29D).

(30F) $B = \frac{7}{6} \frac{\rho_3'}{\rho_1} \left[\frac{P_3'}{P_1}\right]^{0.7143}$, $A = \frac{\gamma-1}{\gamma+1}$

(31F) Solve $By^{0.7143} = y + A$ for y.

(32F) $P_2 = yP_1$

(33F) $\rho_2 = \rho_3' \left[\frac{P_2}{P_3'}\right]^{0.7143}$

(34F) $\Delta m = -\rho_2 u_2 A_2 \Delta t$

(35F) $P_3 = P_3' + 1.4 \frac{P_1}{\rho_1} \frac{\Delta m}{V_3}$

If $P_3 - P_3' > .05 P_3'$ return to immediately preceding time (i.e., subtract Δt from current time), reduce Δt by one-half, and return to step (4).

(36F) $\rho_3 = \rho_3' + \frac{\Delta m}{V_3}$

(37F) $P_3' = P_3$

(38F) $\rho_3' = \rho_3$

(39F) Advance time by amount Δt and return to step (4).

C. Wind Speed and Dynamic Pressure (Jet Effect)

Should it become clear the shelter structure will withstand the pressure stemming from the shock wave and filling of interior spaces, interest will shift to the dynamic effects on the shelter contents of the filling stream itself, i.e., on the wind speed and, particularly, the dynamic pressure within the jet of air moving into the shelter space.

Unfortunately, direct measurements of wind speed and dynamic pressures in rooms filling from shock waves are even fewer than observations of room pressure. The differences among the predictions of speed of the several calculational methods are large, but the values of dynamic pressure are often in fair agreement. For estimates of the acceleration of objects in the stream, the dynamic pressure and wind direction are the only pertinent parameters.

1. Quantitive Description. Our recommended procedures for estimating dynamic pressures within a room consist of two parts: (1) calculation of core dynamic pressure, viz., that immediately inside the entry, and (2) quantitative description of the spread of the jet through the room.

Since the calculation of average pressure rise within the room are reasonably successful, especially by Methods D and F, our recommended procedures for estimating core dynamic pressure are derived from expressions for mass flow. Specifically, we define core dynamic pressure as

$$q_{core} = \frac{1}{2} \rho_{core} u_o^2$$

where ρ_{core} is air density in the jet core and u_o is wind speed just inside the entry. Now if we assume the core of the incoming jet just fills the doorway, we can express the mass rate of flow as:

$$\frac{\Delta m}{\Delta t} = \rho_{core} u_o A_2$$

After rearrangement, this becomes:

$$u_o = \frac{1}{\rho_{core} A_2} \left(\frac{\Delta m}{\Delta t}\right) \tag{25}$$

Substituting this expression for u_o in the defining equation for core dynamic pressure, we find:

$$q_{core} = \frac{1}{2 \rho_{core} A_2^2} \left(\frac{\Delta m}{\Delta t}\right)^2 \tag{26}$$

Air density in the jet core is related to air density outside the room by the isentropic equation of state, Eq. (3), in which P_2 and ρ_2 are replaced by P_{core} and ρ_{core}, respectively.

Thus,

$$\rho_{core} = \rho_1 \left(\frac{P_{core}}{P_1}\right)^{1/\gamma} \tag{27}$$

However, it is a good approximation to assume*

$$P_{core} = P_3 \tag{28}$$

i.e., core pressure equals room pressure.

Substituting Eqs. (27) and (28) into Eq. (26), we find:

$$q_{core} = \frac{1}{2\rho_1 A_2^2} \left(\frac{P_1}{P_3}\right)^{1/\gamma} \left(\frac{\Delta m}{\Delta t}\right)^2 \tag{29}$$

Thus any of our previously developed expressions for mass flow rate $\Delta m/\Delta t$ (cf. Eqs. (10), (15), or (17) can be used in Eq. (26) to compute core dynamic pressure q_{core}. This calculation is not exact, because the area of the core will not in fact equal A_2, particularly when outside pressure is high (viz., inflow is choked according to Method D).

For information on the spread and attenuation of the jet within the room, we have relied on the steady jet characterized in such detail by Ambramovich[20] and illustrated in Figure E-10, where air is considered to be flowing from a reservoir at high pressure on the left through the aperture into the region of low pressure (i.e., the interior of the shelter) on the right. In the theory, the entry aperture may be slit of essentially infinite length and width b_o or it may be a circular opening of diameter b_o. Although the description of the jet is different for the slit than for the circle, the difference is not important here. Since most actual openings will be somewhere between the two, we assume that any actual opening has been approximated by a slit or by a circle and only one set of formulas is given. As shown in Figure E-10, inflowing air generally fans out into the receiving reservoir, slowing down after passing through a conical or wedge-shaped "core." Wind speed is constant everywhere within the core. The jet consists of the core and the surrounding fan, known as the mixing zone.

---

* It is also a good approximation at low overpressures to assume $\rho_{core} = \rho_3$.

Abramovich characterizes the jet by three parameters: width of the opening b_o; wind speed u_o in the axial direction at the initial cross section of the jet; and ratio θ between temperature in the core and that in the receiving reservoir (i.e., the shelter space). The flow is driven by a pressure difference between the two reservoirs, but it appears to be a fact that pressure everywhere within the usual subsonic jet itself is uniform and equal to that in the receiving reservoir. In other words, pressure equilibrium is quickly established between the jet and the air already in the reservoir. In most cases of room filling the ratio θ will be nearly 1, which implies that air density in the jet core nearly equals air density in the room; i.e.,

$$\rho_{core} \approx \rho_3$$

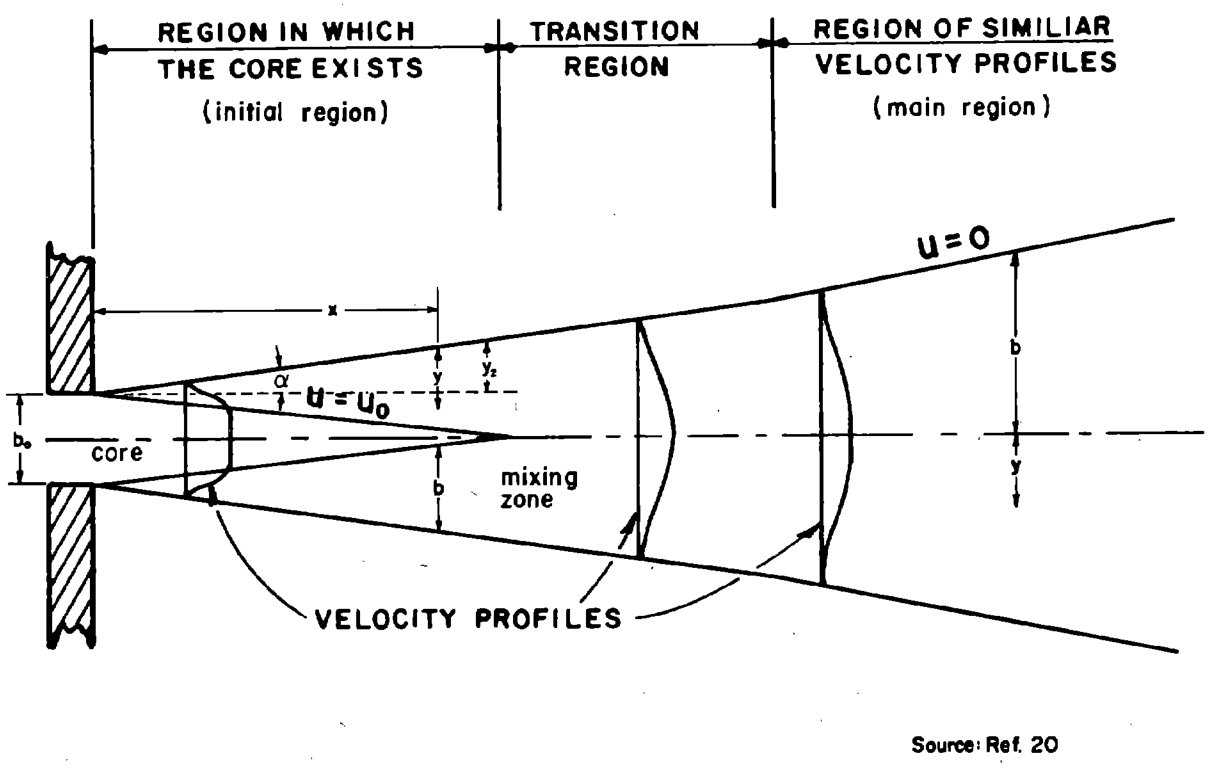

FIGURE E-10 SCHEMATIC OF JET FLOW

The description appearing below of the fully developed jet hinges on the value u_o of wind speed in the core, and calculations of the translation of objects on shelter floors by incoming air are based on values of q_{core} along with estimates of drag acceleration coefficients, as described further in Section IIC1. As in the treatment in Section IIB1 of the build-up of pressure within the shelter space, the parameters of the jet are here calculated quasi-statically. This procedure fails in the early stages and again in the late stages of room filling.

Before quasi-steady jet behavior is observed, air motion in the neighborhood of the opening is governed by the laws of shock waves. At that time, particle speed is relatively slow but as the diffracted waves reverberate in the opening, conditions for jet-like flow are established. This build-up of flow through the opening lasts a length of time

$$t_1 \approx \frac{4b_o}{c} \tag{30}$$

where c is the speed of sound in the opening. If this time interval is long enough to be important, it is recommended that mass flow rate in the opening be treated as varying linearly with time during t_o, from an initial value equaling that behind the incident shock:

$$\frac{\Delta m}{\Delta t} = \rho_s \dot{u}_s A_2 = \rho_s \left(P_s - P_o\right)^{1/2} \left(\frac{1}{\rho_o} - \frac{1}{\rho_s}\right)^{1/2} A_2 \tag{31}$$

to that in the fully developed jet at time t_1. In Eq. (31) the subscript s designates conditions behind the incident shock, which may not be the same as conditions in the stagnated air outside the shelter, i.e., in that volume of air designated 1 in Figure E-3. This method of interpolating between shock or transient conditions and true quasi-steady conditions is used in the room filling computer program described in Section IVA.

The cessation of jet inflow at the conclusion of room filling shows a similar inertia. In confined spaces, inflow tends to establish a swirling pattern, which persists even after pressure equilibrium is reached between inside and outside environments.

The fully developed steady subsonic jet is described by the following three sets of formulas, each set valid in one of the three regions shown in Figure E-10. Only wind speed in the axial direction is calculated, since the horizontal speed exerts a comparatively negligible drag force.

Initial Region. The speed u in the mixing zone outside the core decreases with increasing distance from the core. At the jet boundary u = 0 and at the core boundary $u = u_o$. At a point in any plane at right angles to the jet axis and within the mixing zone

$$u = u_o \left\{ 1 - \left[1 - \eta^{1.5} \right]^2 \right\} \tag{32}$$

where $\eta = y/b$, y is the distance from the jet boundary (measured in a direction perpendicular to the jet axis) to any point outside the core, and b is the mixing zone half width also measured perpendicularly to the axis, both as shown in Figure E-10 (e.g., at the core boundary y = b and at the jet boundary y = 0). The quantity b varies linearly with distance x from the opening, i.e.,

$$b = 0.27x \tag{33}$$

or, equivalently, the slope of the outer jet boundary (where u = 0) can be written

$$\tan \alpha = 0.158 \quad \text{or} \quad \alpha \approx 9^{\circ}$$

the length of the initial region (and the length of the core) is approximately $4.5b_o$.

Transition Region. Formulas valid for the transition region can be written, but they are not necessary for present purposes. If desired, values of quantities in this region may be interpolated between the initial and main regions. The length of the transition region, however, may be required and is approximately $2.2b_o$.

Main Region. Here, as in the transition region, there is no core: The jet is entirely mixing zone but the slope of the jet boundary is greater than in the initial region, i.e.,;

$$\alpha \approx 12.5^{\circ}$$

and the half-width of the jet is:

$$b = x \tan \alpha \approx 0.22\,x \tag{34}$$

In any cross section of the jet made normal to its axis, wind speed is a maximum at the axis and falls to zero at the jet boundary. However, wind speed u_m along the axis decreases with distance from the opening;

$$u_m = u_o \frac{6.2b_o}{x}$$

Now the variation in any cross section at a distance $y < b$ from the axis is:

$$u = u_m \left(1 - \eta^{1.5}\right)^2$$

where $\eta = y/b$ as shown before, except that y and b have slightly different meanings (Figure E-10). Hence, the dependence on both x and y is found by combining the last two expressions:

$$u = u_o \frac{6.2b_o}{x} \left(1 - \eta^{1.5}\right)^2 \tag{35}$$

Since density is nearly uniform throughout the jet, we can relate the dynamic pressure in the main region to that in the core by multiplying core dynamic pressure by the square of the ratio of wind speeds:

$$q = q_{core} \left(\frac{6.2b_o}{x}\right)^2 \left(1 - \eta^{1.5}\right)^4 \tag{36}$$

<u>Numerical Example No. 4 (Jet Dynamic Pressure)</u>. Consider the room described in the numerical example of choked inflow on page E- 33. We will calculate the furthest extent of the jet core, the initial core dynamic pressure and the initial dynamic pressure in the established jet at a point 25 ft inside the door and 5 ft off the center line through the door.

Shock arrival at the door is followed by the diffraction phase, during which time the jet emerging from the doorway into the room is

established. If we consider the door as approximately circular, its radius will be

$$b_o \approx \left(\frac{21}{\pi}\right)^{0.5} = 2.58 \; ft.$$

Since its area is 21 sf. to calculate the period of jet buildup using Eq. (30), we need a value for sound speed in the doorway, where initially the pressure is intermediate between that outside and that inside. As an approximation we can base our value of sound speed on initial conditions in the room (viz., pressure P_o = 14.7 psi and density ρ_o = 0.002378 slugs/cf) and apply the formula on page 10-38 of Ref. 5 viz.,

$$c = \left(\frac{\gamma P_o}{\rho_o}\right)^{0.5} = \left(\frac{1.4 \times 14.7 \times 144}{0.002378}\right)^{0.5}$$

$$= 1116. \; fps$$

Thus $$t_1 = \frac{4 \times 2.58}{1116} = 0.00914 \; sec$$

Since the duration of choked inflow is 52.0 ms (which is greater than t_1) the initial mass inflow rate after establishment of the jet will be (from Numerical Example No. 3):

$$\frac{dm}{dt} = 46.7 \; slug/sec$$

and from Eq. (29) the initial core dynamic pressure becomes:

$$q_{core} = \frac{(46.7)^2}{2 \times 0.004397 \times (21)^2 \times 144} \left(\frac{34.7}{14.7}\right)^{1/1.4}$$

$$= 7.21 \; psi$$

This core pressure reaches approximately

$$4.5 \; b_o = 4.5 \times 2.58 = 11.6 \; ft$$

in the room along the jet axis. Immediately following the core is the transition region extending a distance $2.2 \; b_o = 2.2 \times 2.58 = 5.68$ ft

further into the room. The main region of the jet begins, then, at a point 11.6 + 5.68 = 17.3 ft inside the doorway. On the jet axis (y = o) at a distance 25 ft from the door x = 25 and Eq. (36) gives the dynamic pressure as:

$$q = 7.21 \left(\frac{6.2 \times 2.58}{25}\right)^2 = 2.96 \text{ psi}.$$

The half width of the mixing zone at this distance from the door is by Eq. (34):

$$b = 0.22 \times 25 = 5.5 \text{ ft}$$

so that at a point 5 ft off the axis $\eta = \frac{5}{5.5} = 0.909$ *and Eq. (36) gives the dynamic pressure as:*

$$q = 2.96 \left[1 - (0.909)^{1.5}\right]^4$$
$$= 0.000936 \text{ psi} \approx 0.0$$

2. <u>Countermeasures Against the Jet</u>. Obstacles to flow, such as corners or barriers, may be found in a shelter or can be deliberately designed into the structure. Coulter[21] has reportedly increased protection against the threat of the jet by placing a simple baffle inside the doorway to a small model of a shelter space, as illustrated in Figure E-11. Entry barriers or mazes certainly have the effect of increasing the duration of the diffraction phase, viz., the time during which the jet is building up to full intensity. Thus, if the driving pressure is of short duration or is rapidly decreasing, the average intensity of the jet flowing into the shelter can be reduced by the presence of a barrier at the entry. When the weapon yield is very small, i.e., a few kilotons, and peak overpressure larger than 1 psi, the delay in establishment of the jet resulting from the presence of a baffle or maze may have a measurable effect on the jet, but durations of moderate overpressures (1 to 15 psi) caused by megaton weapons are so long that the relatively brief delays offered by simple baffles are of little use in reducing the jet hazard. Another feature of baffles or mazes is the additional wall friction that might impede jet flow. Generally, to make friction effective at the high Reynolds numbers usually found in cases of blast room-filling, the length of constrained flow must be so great as to leave little space for shelter, as we shall see later in this section.

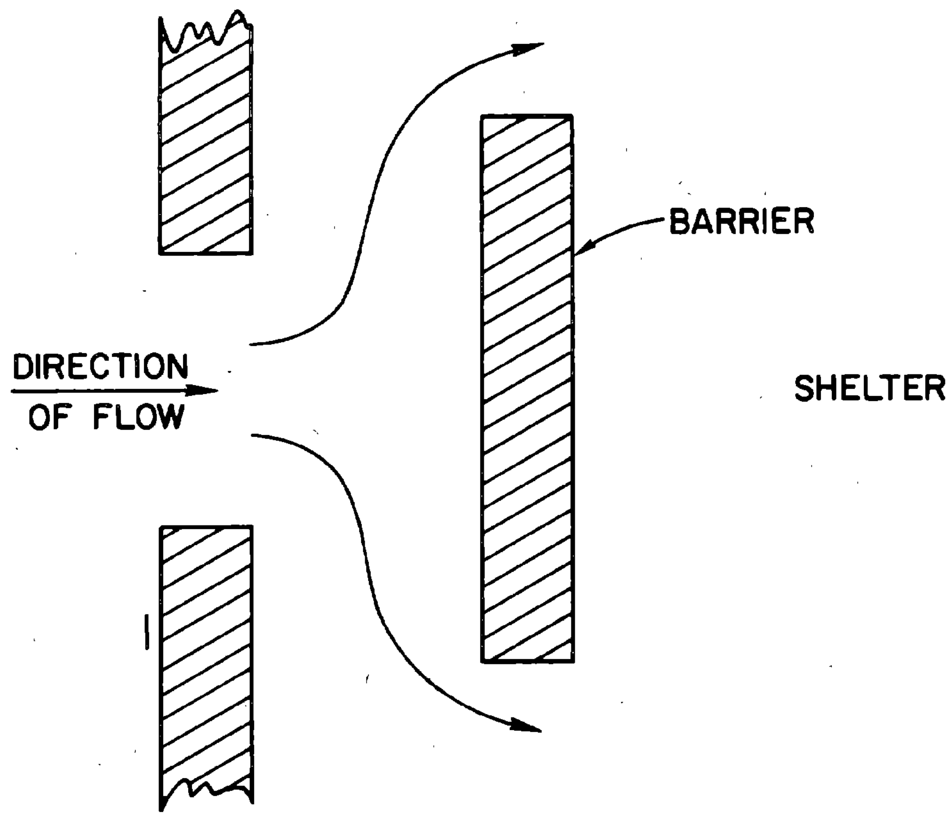

FIGURE E-11 SIMPLE BARRIER AT SHELTER ENTRY

Floor space usable for shelter might be increased by deliberate diffusion of the flow throughout the room, as suggested by the sketch in Figure E-12. In this case, the area A_2 appearing in the denominator of Eq. (29) may effectively be much greater than the area of the entry and the peak dynamic pressure in the room reduced below the danger level everywhere. A diffuser should also reduce vorticity, the presence of moving centers of high speed rotational flow extending over very limited areas at any one time. A vortex may be dangerous to human bodies in its path since wind speeds within the vortex may be considerably greater than in the jet core. Diffusion should not be considered unless the maximum or choked* flow rate $(\Delta m/\Delta t)_{choked}$ can be shown to be safe† when diffused

* See page 32.

† The general subject of hazard to shelterees in open shelter is discussed in Volume 1, pages 8-67 to 8-71, of the present work. The technical background necessary to calculation of the hazard is presented later in this section.

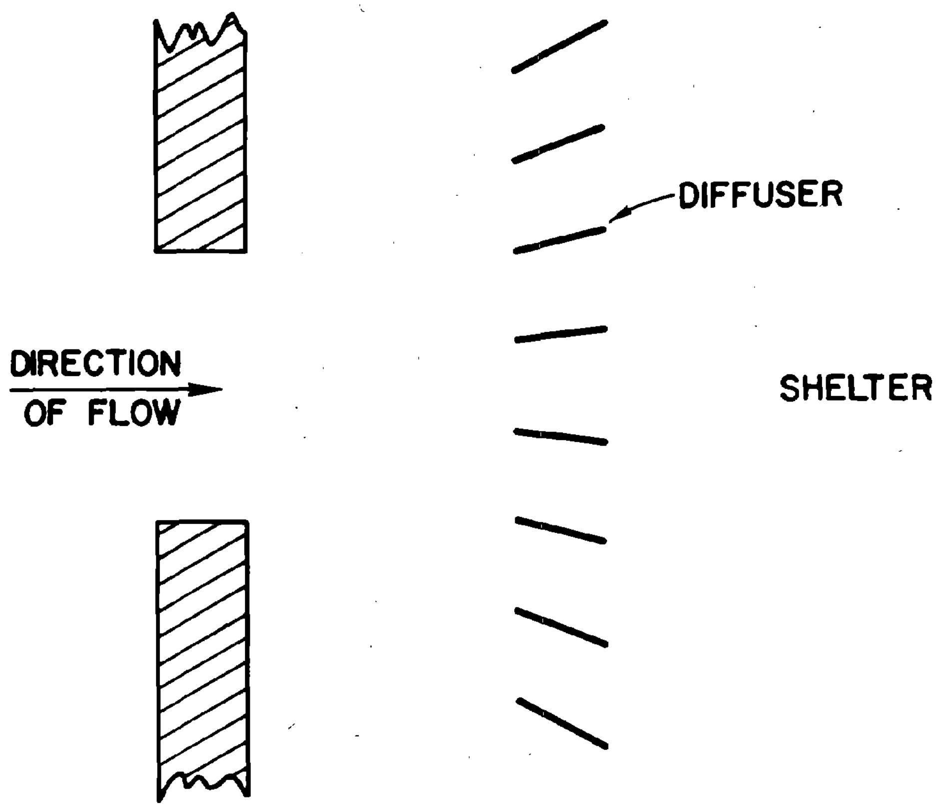

FIGURE E-12 DIFFUSER-BAFFLE SCHEME AT ENTRY

over a broad area at the entrance. Possibilities offered by deliberate diffusion are under study. The diffuser shown in Figure E-12 is schematic only and is not meant to suggest an actual device.

One kind of barrier that might reduce the jet intensity flowing over prone shelterees is a ramp to deflect part of the incoming stream toward the ceiling. No device of this kind has been studied.

Another seemingly useful characteristic of steady flow through pipes (and presumably of steady flow and quasi-steady flow through entry mazes) is a certain loss of momentum (or average wind speed) with distance traveled.[27] While it seems likely that, other things being equal, the loss through an entry maze would be greater than the loss through a pipe, the known loss rate through pipes of certain regular cross-sectional shapes

(with both rough and smooth walls) appears so slight that we are led to the belief that an entry maze effective for the protection of shelterees from translational hazard must be unreasonably long or that we must seek other protective mechanisms in the maze not found in pipes.

In order to demonstrate the frictional loss rate quantitatively we calculate it here for a pipe, which we imagine is serving as an entry to a shelter. The nondimensional coefficient of resistance λ is defined by the equation:[27]

$$\frac{dP}{dl} = \frac{\lambda}{d} q \tag{37}$$

where dP/dl is the loss of pressure head per unit length of travel
d is the pipe diameter
q is the mean dynamic pressure in a cross section.

In smooth pipes the coefficient λ is a function only of the non-dimensional group called the Reynolds number[5] Re which is a function of a linear dimension (in this case, the diameter d of the pipe), wind speed u, air viscosity η and air density ρ; i.e.,

$$Re = \frac{du\rho}{\eta}$$

Air viscosity is a function is a function of temperature, but in the range of our interest it can be taken[5,26] as approximately 4.0×10^{-5} lb sec/ft^2. If we assume that the pressure differential between inside and outside equals 10 psi, inside pressure P_3' is standard atmospheric* or 14.7 psi, air density in the entry and room is also standard* or 0.002378 slug/cf and $\gamma = 1.4$; then Eqs. (13) and (14) give the value of wind speed u_2 in the entry, i.e., $u_2 = 998$ fps. Also dynamic pressure, $q = (\rho u^2)/2 = 8.23$ psi. Hence, for the flow in our hypothetical pipe entry:

$$Re = 2.38 \times 10^5$$

where we have assumed a pipe diameter d of 4 ft.

Figure E-13 shows the dependence of frictional resistance λ on Re. The pronounced change in slope of the curve between RE = 2000 and Re = 4000 corresponds to the transition from laminar to turbulent flow.[27,28] Unfortunately, a 10-psi pressure differential across our hypothetical pipe entry leads to turbulent flow, where the value of λ is generally less than for laminar flow.

* See page 6-8 of Volume 1 of the present work.

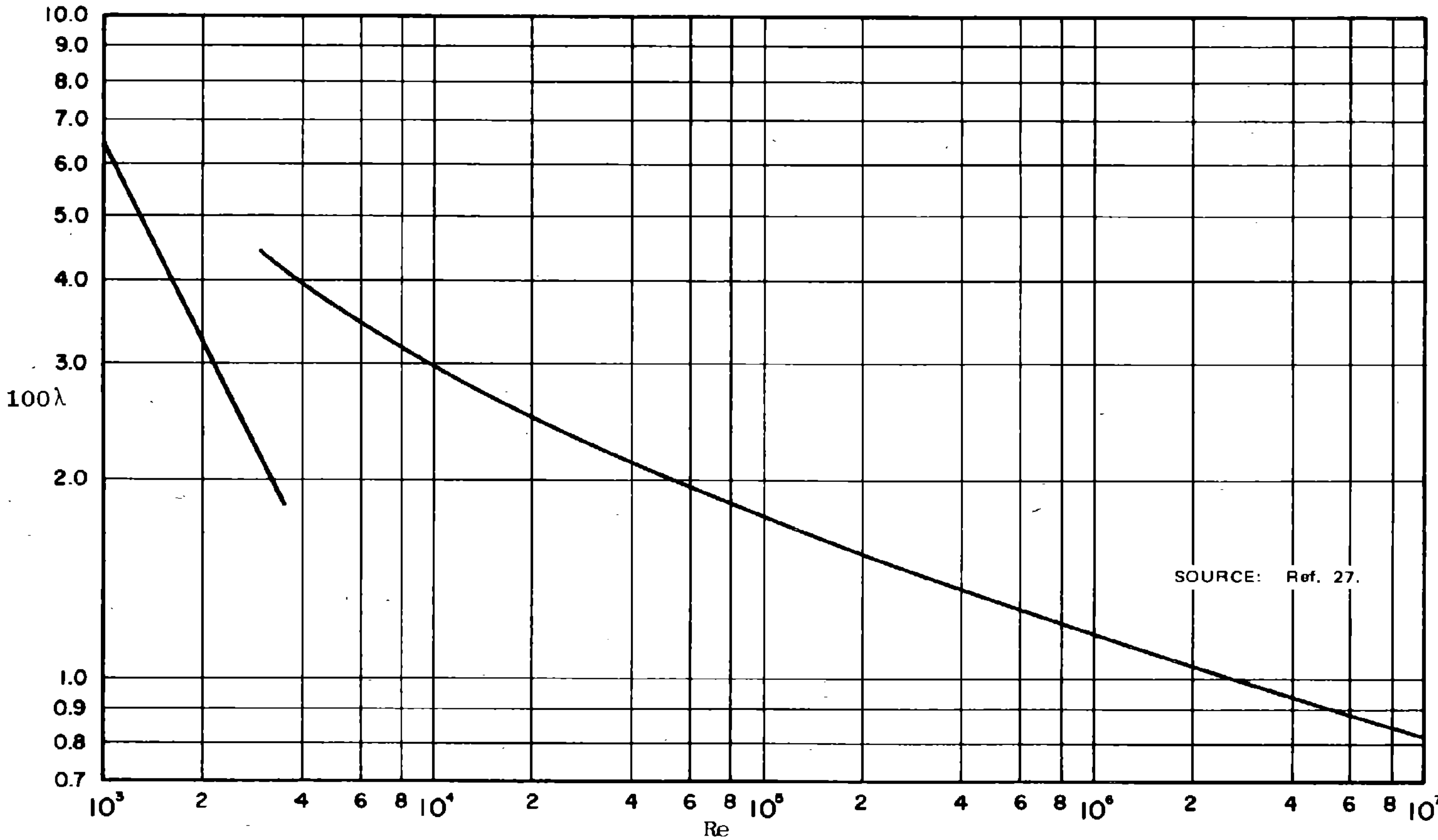

FIGURE E-13 FRICTIONAL RESISTANCE IN A SMOOTH PIPE

Reading Figure E-13 we expect the coefficient of resistance to be:

$$\lambda \approx 0.015$$

and Eq. (37) tells us immediately that the initial rate of loss of head is small. However, we can continue the quantitative estimate as follows.

Equation (1) can be written for any cross section in the pipe, which is another way of saying that the quantity

$$\frac{\gamma}{\gamma-1}\ \frac{P}{\rho} + \frac{1}{2}\ u^2 = c$$

is a constant along the length of the pipe. Since we know the values of the flow parameters at the intake cross section, we can evaluate this constant; i.e.,

$$c = \frac{\gamma}{\gamma-1}\ \frac{P_1}{\rho_1} + \frac{1}{2}\ u_1^2 \tag{38}$$

where the subscripts refer to the initial cross section. Multiplying both sides of Eq. (38) by ρ and differentiating, we find:

$$-c\ d\rho + \frac{\gamma}{\gamma-1}\ dP + dq = 0 \tag{39}$$

In steady flow another equation is available, since the mass passing through a cross section per unit time is the same everywhere along the pipe, or

$$\rho u = M,\text{ a constant} \tag{40}$$

Squaring both sides of Eq. (40) and dividing by 2ρ, we can write:

$$\frac{1}{2}\ \rho u^2 = \frac{M^2}{2\rho}$$

Noting the definition, $q = (\rho u^2)/2$, and rearranging terms, we discover:

$$\rho = \frac{M^2}{2q}$$

After differentiation, this becomes:

$$d\rho = -\frac{M^2}{2q^2}$$

The last relation can be used in Eq. (39) to eliminate the density, so that we can rewrite Eq. (39) as follows:

$$dP = -\frac{\gamma-1}{\gamma}\left(1 + \frac{CM^2}{2q^2}\right) dq$$

To find the rate of change of dynamic pressure with distance of flow through the pipe, we substitute this expression for dP into the defining equation for λ, Eq. (37):

$$\frac{dq}{d\ell} = -\frac{\gamma}{1-\gamma} \frac{1}{1 + \frac{CM^2}{2q^2}} \frac{\lambda}{d} q$$

$$\left(\frac{1}{q} + \frac{CM^2}{2q^3}\right) dq = -\frac{\gamma}{1-\gamma} \frac{\lambda}{d} d\ell$$

This differential equation is easily integrated to give the relation we seek between the distance of travel ℓ and dynamic pressure q:

$$\ell n \frac{q_1}{q} + \frac{CM^2}{4}\left(\frac{1}{q^2} - \frac{1}{q_1^2}\right) = \frac{\gamma}{1-\gamma} \frac{\lambda}{d} \ell$$

Here q_1 is the dynamic pressure in the initial cross section. The constants C and M can be evaluated for our hypothetical pipe entry by using the previously calculated initial values of the flow parameters as follows:

$$P_1 = 14.7 + 10.0 = 24.7 \text{ psi}$$

$$\rho_1 = \rho_o \frac{7P_o + 6p^*}{7P_o + p}$$

$$= 0.002378 \text{ slug/cf } \frac{7 \times 14.7 + 6 \times 10}{7 \times 14.7 + 10}$$

$$= 0.00343 \text{ slug/cf}$$

$$u_1 = 998. \text{ fps}$$

$$\gamma = 1.4$$

Substituting these values in Eq. (38), we find:

$$c = 4.13 \times 10^6 \text{ ft}^2/\text{sec}^2$$

Equation (40) yields:

$$M = 3.42 \frac{\text{lb sec}}{\text{ft}^3}$$

Hence,

$$\frac{CM^2}{4} = 582 \text{ psi}^2$$

As noted above, the value of λ is initially 0.015; however as friction reduces wind speed, the Reynolds number will decrease and λ increase. However, the change in λ corresponding to a tenfold decrease in wind speed is less than a factor of 2, as is clear from Figure E-13. To find the length of flow required to reduce q to a value q/2, we will use Eq. (41) and assume λ is constant and equal to 0.02. Hence,

$$\ell n\, 2 + \frac{582}{(8.23)^2} \times 3 = \frac{7}{2}\, 0.002\, \frac{\ell}{d}$$

or,

$$\frac{\ell}{d} = 9820$$

---

* This is the air density behind a shock front of overpressure p in a standard atmosphere. See page 122 of Ref. 1. See page 6-8, Volume 1, of the present work for characteristics of the standard atmosphere.

In other words, a flow distance of nearly 10,000 diameters is needed to reduce the dynamic pressure in our hypothetical pipe entry to one-half its initial value.

Since increasing the value of λ tenfold, or even one hundredfold, would not make the results of our calculation significantly more optimistic, it appears doubtful that any sort of pipe friction in an entry maze will be of practical help in the design of open shelter. In fact, resistance in pipes of triangular and rectangular cross section is only slightly greater than in pipes of circular cross section.* Roughening the inside walls of pipes with sand increases λ no more than four times.†

It may be possible to increase the flow into a shelter (and thus reduce drag time) in a way not threatening to shelterees by using a porous wall; that is, admit the shelterees through a relatively small open doorway and fill the room with air from the blast wave through countless tiny ducts placed in an entire wall or walls. Such a method is a variation on the diffuser pictured in Figure E-12.

Within the shelter, friction will be important wherever the flow is caused to pass a corner, where the boundary layer will generally separate from the wall and a zone of turbulence will be created. Flow turning an inside corner, for example, will avoid the wall and pass outside a turbulent vortex zone, as sketched in Figure E-14. Flow past an outside corner, as in Figure E-15, will also be associated with a turbulent vortex zone, but there is no guarantee the zone will remain in one place as the room fills. In fact, the vortices may be shed from the corner and objects within the room buffeted as the very high speed winds within the vortices pass over them.

3. Calculation of the Drag Force on Objects. A still object in a stream of moving air is accelerated according to the formula

$$\frac{dv}{dt} = \frac{C_d A}{M} q \qquad (42)$$

where C_d = drag coefficient of object
A = cross sectional area of object normal to flow
M = mass of object
q = dynamic pressure of moving air

---

* See Figure 20.12, page 517, Ref. 27

† See Figure 20.18, page 521, Ref. 27.

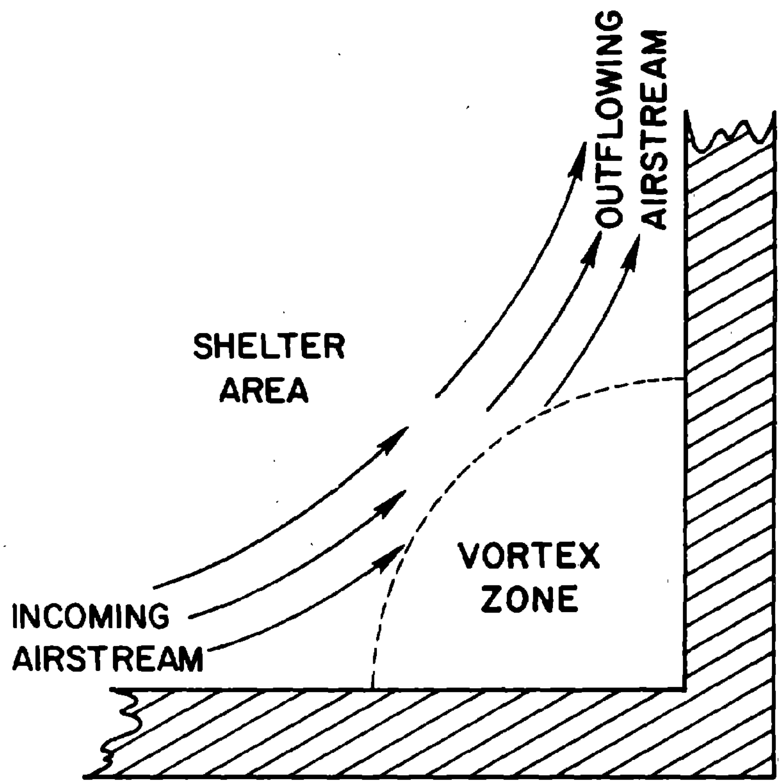

FIGURE E-14 DEFLECTION OF AIRSTREAM IN CORNER

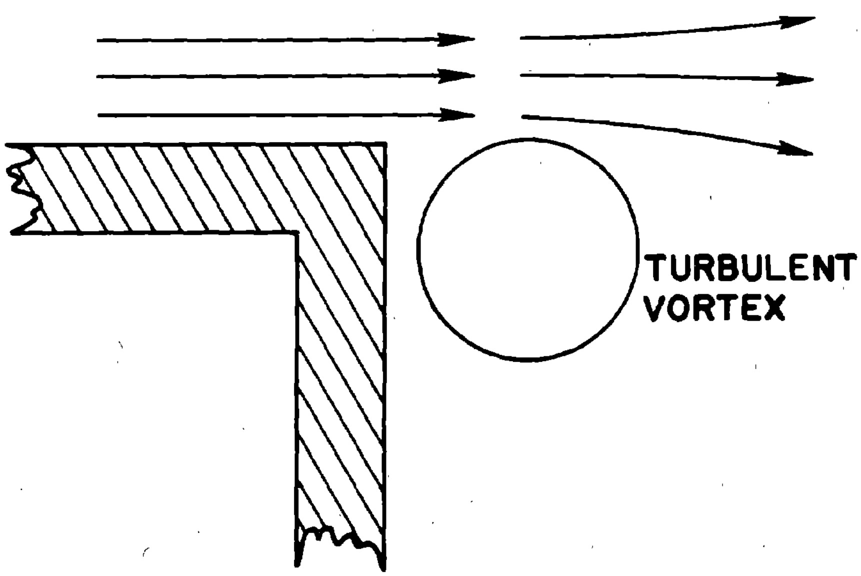

FIGURE E-15 FLOW PAST OUTSIDE CORNER

The drag coefficient C_d is a function of object shape and Reynolds number, Re, which is a dimensionless group depending on object size, L, wind speed, u, air viscosity, η, and air density, ρ:

$$Re = \frac{Lu\rho}{\eta} \qquad (43)$$

Viscosity is a function of temperature but in the range of our interest it can be taken[5,26] as approximately 4.0×10^{-5} lb sec/ft^2.

Actually, there are two kinds of drag force exerted by moving air on a body: skin friction drag and pressure drag. Friction drag is important only when Re < 10, otherwise, only pressure drag need be considered. Both kinds of drag force are expressed by Eq. (42).

For pressure drag and for the spherical and cylindrical shapes, the coefficient C_d varies with Reynolds number as shown in Figures E-16 and E-17. The data in Figure E-17 apply to a cylinder whose axis is normal to the wind. Friction drag will not generally be important in blast filling of rooms. Since the Reynolds numbers corresponding to hazardous flows will usually be above 100, Figs. E-16 and E-17 show that the drag coefficient may conservatively be assumed constant at the value of 1. (The discontinuity shown near the value Re = 10^6 is associated with the onset of turbulence.)

Most of the measurements of dynamic pressure have been made indirectly by observing the motion of object accelerated by the drag force of an air jet. For example, Coulter has reported the acceleration of an 1/8-inch diameter nylon ball placed in the doorway of a small model room struck head-on by a weak shock wave[9]; in another series of experiments, Coulter has observed the motion of cylinders in a model basement filling from a shock wave.[25]

As illustrations of the calculation of acceleration of objects in a jet, we will attempt to account for Coulter's observations.

Our procedure will be as follows:

(1) Show the negligibility of any acceleration ascribable to the differential force on the object while the shock wave is still passing across the object.

(2) Estimate the acceleration of the object in the flow immediately behind the shock front. This will require knowledge of flow characteristics from articles 3.47 through 3.50 of Ref. 1, viz., wind speed, air density and dynamic pressure.

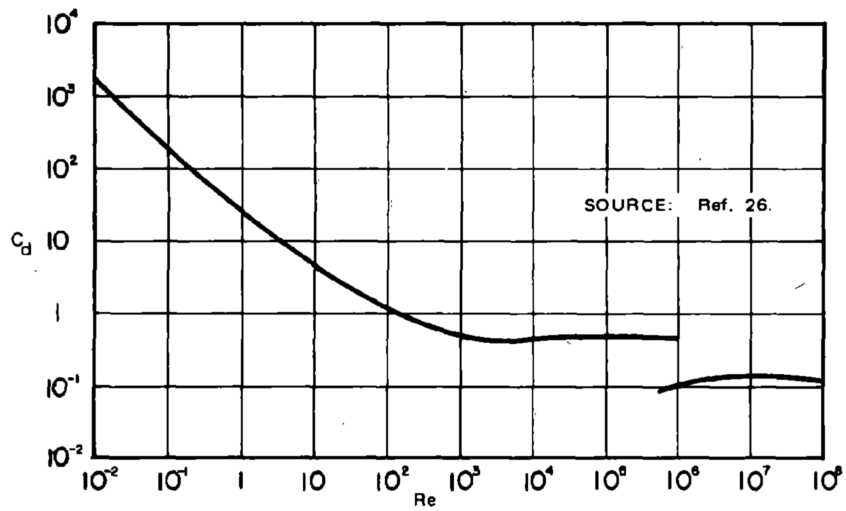

FIGURE E-16 EXPERIMENTAL DRAG COEFFICIENTS OF SPHERE

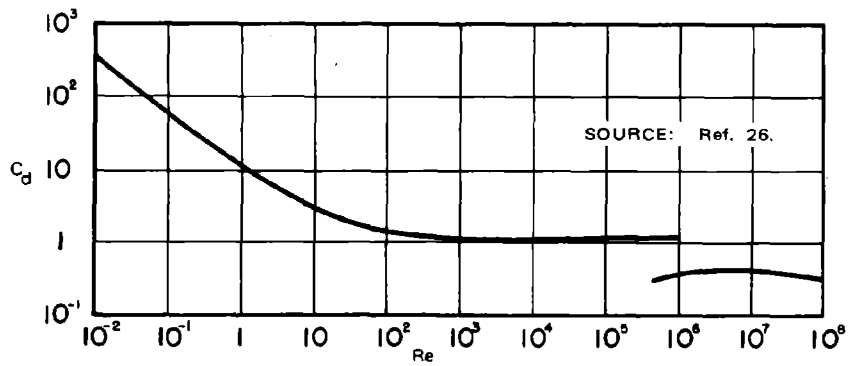

FIGURE E-17 DRAG COEFFICIENT OF CIRCULAR CYLINDER IN FLOW NORMAL TO AXIS (BETWEEN WALLS)

(3) Estimate duration of jet buildup from Eq. (30).

(4) Calculate acceleration of the object in the fully established jet using Eqs. (29) and (42).

(5) From the results of steps (2) and (4), approximate the speed gained during the buildup phase.

(6) Calculate the speed gained and distance travelled during the remainder of the room filling; hence, find the final speed and displacement of the ball to compare with observation.

Step (1) is accomplished by finding an upper bound to the impulse given to the ball by the pressure differential in the shock front during its passage across the ball diameter. The duration of the unbalanced shock pressure on the ball is less than the time of passage, T, of a sound signal across the ball diameter, D, i.e., $T = D/c_o$. The impulse, I, must be less than the overpressure $(P - P_o)$ times the ball cross sectional area $\pi D^2/A$ times T or:

$$I < (P - P_o)\,\frac{\pi D^2}{4}\,T = (P - P_o)\,\frac{\pi D^3}{4c_o}$$

If the specific gravity* of nylon is approximately unity, then the mass of the ball will be

$$M = \frac{\pi}{6} D^3 \rho_w$$

where ρ_w stands for the density of water. The speed, v, imparted to mass, M, by the impulse, I, can therefore not be greater than:

$$v = \frac{I}{M} < \frac{(P-P_o)\,\pi\,\frac{D^3}{4}}{\frac{\pi}{6} D^3 \rho_w c_o} = \frac{3}{2}\,\frac{P-P_o}{\rho_w c_o}$$

$$v < 0.488 \text{ fps}$$

where we have taken the density of water as 1.94 slugs/cf (page 6-04 of Ref. 5).

---

* See p. 13-48, Ref. 5, for a definition of specific gravity.

Thus the acceleration attributable directly to the shock is in this case and in most other cases completely negligible. As we will see, the drag force resulting from the wind immediately behind the shock front causes more acceleration than the front itself and the acceleration owing to the fully developed jet causes still greater acceleration

To begin step (2) we must write an expression for sound speed as a function of pressure and density. From Eq. (5) of Chapter 20 in Ref. 5, sound speed, c, can be written:

$$c = \left(\frac{\gamma P}{\rho}\right)^{0.5} = \left(\frac{1.4P}{\rho}\right)^{0.5}$$

where we have substituted the value $\gamma = 1.4$.

Then (from page 122 of Ref. 1) wind speed behind the shock of pressure, P, is

$$u = \frac{5}{7}\,\frac{P-P_o}{P_o}\,\frac{c_o}{\left[1 + \left(\frac{6\left(P-P_o\right)}{7P_o}\right)\right]^{0.5}}$$

where P_o = pressure ahead of shock front and

c_o = sound speed ahead of front.

From the same reference, density behind the front can be expressed as:

$$\rho = \frac{7 + \frac{6\left(P-P_o\right)}{P_o}}{7 + \frac{\left(P-P_o\right)}{P_o}}\,\rho_o \tag{44}$$

and dynamic pressure (from Eq. (3.49.1) of Ref. 1) is

$$q = \frac{5}{2}\,\frac{\left(P-P_o\right)^2}{6P_0+P} \tag{45}$$

In his experiment with the nylon ball, Coulter allowed a shock front of overpressure equal to 4.89 psig to strike a reflecting plate in which an entrance 1 x 4 inches was cut. Since the chamber behind the opening had a volume-to-opening area ratio (V/A) equal to 1.33, filling was essentially complete in 1.33/2 = 0.667 ms, during which time there was little or no decay of the incident wave. Hence, $P - P_o = 4.89$ psi, Table 6.1 on page 6-9 of Volume 1 of the present work gives standard atmospheric air density ρ_o at sea level and temperature of 59F as 0.002378 $\text{lb-sec}^2/\text{ft}^4$; and if we assume $P_o = 14.7$ psi, then air density behind the shock becomes:

$$\rho = 0.002917 \ \text{lb-sec}^2/\text{ft}^4$$

and dynamic pressure

$$q = 0.5546 \ \text{psi}$$

and sound speed, c_o, in standard air

$$c_o = 1116. \ \text{fps}$$

Under these conditions, wind speed becomes:

$$u = 233.9 \ \text{fps}$$

From these values of wind speed and air density we calculate the Reynolds number , Eq. (43), for the nylon ball caught in the wind immediately behind the shock:

$$Re = \frac{Lu\rho}{\eta} = \frac{(1/8) \times (1/12) \times 233.9 \times 0.002917}{4.0 \times 10^{-5}}$$

$$= 177.7$$

Finally, Figure E-16 suggests for Re = 178 a value of C_d near 0.9. We can now use Eq. (42) to calculate the initial acceleration of the nylon ball:

$$\frac{dv}{dt} = \frac{C_d A}{M} \ q = \frac{0.9\pi D^2/4}{\frac{\pi}{6} D^3 \rho_w} \ q = \frac{1.35}{D\rho_w} \ q$$

$$\frac{dv}{dt} = 5345. \ \text{ft/sec}^2$$

For step (3) we estimate the duration t_o of the jet buildup from Eq. (30)

$$t_1 \sim \frac{4b_o}{c}$$

Here c should be the sound speed behind the shock front, where we have found air density to be

$$\rho = 0.002917 \text{ lb-sec}^2/\text{ft}^4$$

and where P = 14.7 + 4.89 = 19.6 psi;
hence,

$$c = \left(\frac{1.4P}{\rho}\right)^{0.5} = 1164.\ \text{fps}$$

Taking b_o = 1 inch, the width of the opening, we find

$$t_1 = \frac{4 \times 1}{12 \times 1164} = 0.286 \text{ ms}$$

Since the filling time of the model, estimated by the simple rules of Section IIA, is approximately 0.667 ms, the buildup time t_1 is significant and we must consider the effect of the shock drag force on the object.

Step (4) begins with the calculation of reservoir conditions outside the entry to the model. Reflection at normal incidence of a 4.89-psig shock produces a reflected overpressure (cf. Eq. (3.50.1) of Ref. 1) equal to

$$P_1 = 2\ P\text{-}P_o + (\gamma+1)\ q$$

Substituting γ = 1.4 and q = 0.555 psi

$$P_1 = 25.8 \text{ psia}$$

Air density in the reservoir can be found from a second application of Eq. (44), where now ρ_o and P_o are the density and overpressure behind the incident shock and $P = P_1$. Hence,

$$\rho_1 = \frac{7 + \frac{6}{19.6}\ (25.8-19.6)}{7 + \frac{25.8-19.6}{19.6}} \quad 0.0029717$$

$$\rho_1 = 0.003548 \text{ lb-sec}^2/\text{ft}^4$$

(We might have with enough accuracy found ρ_1 by using Eq. (6) and taking P_o = 14.7 psi and ρ_o = 0.002378 lb-sec^2/ft^4, the values in a normal atmosphere at sea level and temperature 59F.)

These reservoir conditions remain constant during the whole filling time.

From a knowledge of reservoir conditions alone, we can calculate mass inflow rate by Method F; specifically, from Eq. (10) we write:

$$\frac{\Delta m}{\Delta t} = \left[P_1 \ (1-y_o)\ y_o^{1/\gamma}\ \right]^{0.5} A_2$$

(Alternatively , we could use Method D and either Eq. (15) or Eq. (17).) The above expression for $\Delta m/\Delta t$ becomes upon substitution of numerical values for ρ_1 and P_1:

$$\frac{\Delta m}{\Delta t} = 1.809\ A_2 \text{ slugs/sec-ft}^2$$

Core dynamic pressure, then, comes from Eq. (29):

$$q_{core} = \frac{(1.809)^2}{2 \times 0.003548 \times 144}\left(\frac{P_1}{P_3}\right)^{0.7143} \quad \text{psi}$$

$$= 3.202\left(\frac{P_1}{P_3}\right)^{0.7143} \quad \text{psi}$$

As an approximation, we will use a mean value for the pressure ratio

$$\frac{P_1}{P_3} \approx \frac{25.8}{\frac{25.8 + 14.7}{2}} = 1.274$$

Hence,

$$q_{core} \approx 3.81 \text{ psi}$$

(Since $P_1 < 13.13$ psig, were we to use Method D, inflow would be unchoked and Eq. (15) would apply. Initially $P_3' = 14.7$ psi so that by Method D initial mass inflow rate for the same reservoir conditions becomes:

$$\frac{\Delta m}{\Delta t} = 1.733 \; A_2 \text{ slugs/sec-ft}^2$$

which compares fairly well with the mass inflow rate computed by Method F above.)

In order to find a value for the drag coefficient C_d in Figure E-16, we must determine the wind speed u from the mass flow rate and room air density. Again, taking a value for the density that is the mean between initial and final density in the chamber:

$$u = \frac{1}{\rho_3 A_2} \quad \frac{\Delta m}{\Delta t} = \frac{1.809}{\dfrac{0.002378 + 0.003548}{2}}$$

$$\approx 610. \text{ fps}$$

from which we calculate the Reynolds number to be:

$$Re = \frac{Lu\rho}{\eta} = \frac{\frac{1}{8} \times \frac{1}{12} \times 610 \times 0.002963}{4 \times 10^{-5}}$$

$$= 472$$

From Figure E-16, C_d for the 1/8-inch sphere in such a flow is approximately 0.56. Combining these values in Eq. (42):

$$\frac{dv}{dt} = \frac{C_d A}{M} \; q_{core} = \frac{3}{2} \; \frac{C_d}{D\rho_w} \; q_{core}$$

$$= 22950 \text{ ft/sec}^2$$

Comparing this result with that of step (2), we see that acceleration in the fully established jet is four times greater than that immediately behind the incident shock front.

(The combination of constants $C_d A/M$ is sometimes known as the "acceleration coefficient."[14] Over a wide range of Reynolds numbers it is characteristic only of the object being dragged. The interactive computer program listed in Table E-3 will ask the operator to enter a value for the acceleration coefficient before calculating slide trajectories.)

For step (5) we estimate the speed gain during the establishment of the jet by averaging the acceleration at the beginning of filling (viz., 5345 fps) and that in the fully established jet (viz., 22950 fps). Hence the speed gain Δv_1 during the time $t_o = 0.286$ ms becomes:

$$\Delta v_1 = \int_o^{t_o} \overline{\frac{dv}{dt}} \quad dt$$

$$\Delta v_1 = \frac{5345 + 22950}{2} \times 0.000286 \quad \text{fps}$$

$$\Delta v_1 = 4.05 \text{ fps}$$

Finally, in Step (6) we compute the additional speed gain Δv_2 from the fully established jet. For estimating an upper bound to this gain we can assume the drag force remains constant during the interval between t_o and the completion of filling, i.e., during a time 0.667 - 0.286 = 0.381 ms. In that case

$$\Delta v_2 < 22950 \times 0.000381 = 8.74 \text{ fps}$$

or the total speed $v = \Delta v_1 + \Delta v_2 < 8.74 + 4.05 = 12.8$ fps.

The distance moved s is bounded by the value:

$$s = \iint \frac{dv}{dt} \quad dt \ dt$$

$$s < 0.5 \times 22950 \times (0.381)^2 \times 10^{-6} \times 0.000381$$

$$s < 0.0385 \text{ inch}$$

From this calculation we concluded that the ball stayed in the jet core until filling was complete.

Coulter, however, reported terminal speed of the nylon ball (after 0.700 ms) as 29.8 fps. The cause of the discrepancy between our upper bound $v < 12.8$ fps and Coulter's observation is not known. Had we postulated immediate jet establishment (that is, had we assumed $t_1 = 0$), we would calculate an upper bound on v somewhat larger than 12.8 fps as follows:

$$v < 22950 \times 0.000667 = 15.3 \text{ fps}$$

however, this upper bound is still only half as large as the speed reported.

In Eq. (42) the dynamic pressure q is a function of the time after shock arrival and of the position of the ball as it moves with the wind. (It is also a function of the ball speed, since drag force depends only on the difference between ball speed and wind speed. This dependence is not important when the ball speed is negligibly smaller than wind speed, as is the case in the example of the nylon ball.) By integrating Eq. (42) numerically the time and position dependence of dynamic pressure q can be taken into account, and in the case of a large room filling through a small opening time and position dependence of q must be taken into account. For example, Coulter[25] has observed the filling of a model basement from 5-, 10-, and 20-psig shock waves. Filling time was observed to be approximately 14 ms and jet establishment required between 1 and 2 ms. In these basement models, the room-filling wind swept over model barrels resting upright on the floor and simulating shelter supplies. The barrels moved the length of the room and their final speeds were measured approximately from motion pictures. Using a drag coefficient $C_d = 0.47$ (i.e., assuming an approximately spherical shape for the barrel) in a stepwise integration of Eq. (42), we calculate in the case of the 5-psig wave a final speed of 7.1 fps. Coulter measured a final speed equal to 7.5 fps. In this case then of relatively rapid jet establishment our calculation of drag acceleration of an object in a room-filling wind was fairly successful.

III. Multiple Rooms

A. Inflow

Although the algebra becomes increasingly cumbersom as rooms are added, the foregoing principles of calculation can be applied to a series of connected rooms. For example, two rooms are represented in Figure E-18 for which two control surfaces* can be employed. In the figure the

* The concept of control surfaces is explained in Section IIB1 above.

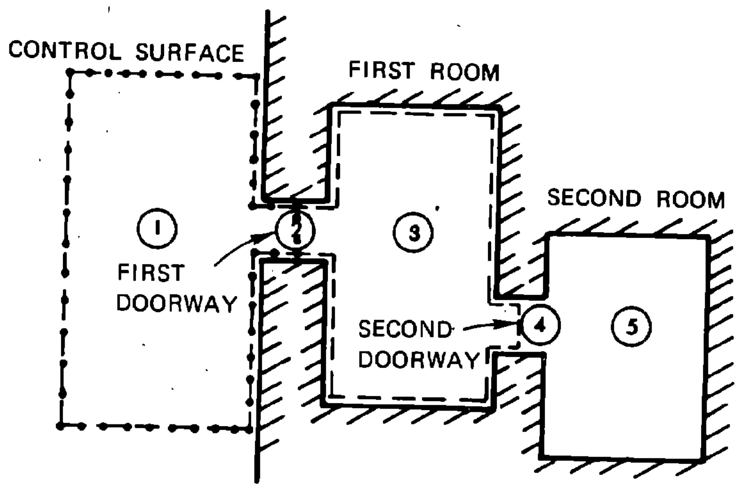

FIGURE E-18 CONTROL SURFACE USED IN CALCULATING FLOW INTO SECOND ROOM

larger control surface, shown dashed, includes the first or outer room as well as an arbitrary volume outside and the doorway between them. The smaller, shown dotted, embraces only the outside volume and the first doorway. In this section only inward flow through these surfaces will be considered; outflow, as well as inflow through one doorway combined with outflow in another, will be treated in the following section. Through the smaller surface the momentum flux is due to flow through the first doorway and the resulting conservation of momentum equation can be written exactly as in Eq. (2). In addition, conservation of energy, Eq. (1), and the isentropic equation of state, Eq. (3), both apply without change to the filling of the first or outer of two connected rooms from an outside blast wave. Equations (1), (2), and (3) constitute a solution by Method F. If Method D or G* is preferred, Eq. (13) replaces Eq. (2). In other words, within the accuracy of our approximation, the mass flow rate and wind speed through the first or outer doorway does not depend on the presence or absence of an inner room. Average pressure in the outer room, of course, is different when an inner room is present from what it is when an inner room is absent.

Calculation of the flow into the second or inner room by Method D or G requires obvious extensions of the foregoing set of equations. We may write conservation of energy as follows:

$$\frac{\gamma}{\gamma-1} \cdot \frac{p_3'}{\rho_3'} + \frac{1}{2} u_3^2 = \frac{\gamma}{\gamma-1} \cdot \frac{P_4}{\rho_4} + \frac{1}{2} u_4^2 \qquad (46)$$

where u_3 is the wind speed through the outer room. The analog of Eq. (13) in the inner room is:

$$P_4 = P_5' \qquad (47)$$

Conservation of mass implies the relation:

$$\rho_3 u_3 A_3 = \rho_4 u_4 A_4 \qquad (48)$$

where A_3 is an effective cross-sectional area of the outer room serving as a duct for flow into the inner room. Finally, we can write the isentropic equation of state for air in the second doorway:

---

* See Section IIB1 above. Method G is identical to Method D (described by Eqs. (16) and (17) above) except the discharge coefficient K is assumed to be unity.

$$\rho_4 = \rho_3' \left(\frac{P_4}{P_3'}\right)^{\frac{1}{\gamma}} \tag{49}$$

We thus have four equations - Eqs. (46), (47), (48), and (49) - to solve for four unknowns: ρ_4, u_4, P_4 and u_3. The mass flow through the second doorway can then be found from the equation:

$$\Delta m_5 = K_4 \rho_4 u_4 A_4 \Delta t \tag{50}$$

where K_4 is the discharge coefficient for the second or inner doorway. Flow will be choked* when the ratio $r = P_5'/P_3'$ reaches the critical value, determined by the vanishing of the derivative $d(\Delta m_5)/dr$.

Solving Eqs. (46) through (49) for u_4^2, we find

$$u_4^2 = \frac{2\gamma}{\gamma-1} \frac{P_3'}{\rho_3'} \left[- \left(\frac{P_5'}{P_3'}\right)^{1-1/\gamma} + 1 \right] \frac{1}{-\left(\frac{P_5'}{P_3'}\right)^{2/\gamma} \frac{A_4^2}{A_3^2} + 1}$$

Taking the square root and substituting this expression in Eq. (50), the analog to Eq. (15) is found to be:

$$\Delta m_5 = K_4 \left(\frac{2\gamma\rho_3' P_3'}{\gamma-1}\right)^{0.5} \left(\frac{P_5'}{P_3'}\right)^{1/\gamma} \left[-\left(\frac{P_5'}{P_3'}\right)^{1-1/\gamma} +1 \right]^{0.5} \frac{A_4 \Delta t}{\left[-\left(\frac{P_5'}{P_3'}\right)^{2/\gamma} \left(\frac{A_4}{A_3}\right)^2 + 1 \right]^{0.5}} \tag{51}$$

Except for the final factor on the right side, Eq. (51) is equivalent to Eq. (15) with the substitutions $K \rightarrow K_4$, $\rho_1 \rightarrow \rho_3'$, $P_1 \rightarrow P_3'$, and $P_3' \rightarrow P_5'$. If we make the reasonable assumptions that $A_4 \ll A_3$ and $P_5' < P_3'$, then the final factor becomes unity and the similarity is exact. In this case,

---

* See Section IIB1 for a discussion of choking.

calculation of filling in the second room can be carried out by Method D or G as if the first room served as an outside reservoir for the second room treated as a single room. At each time step the pressure rise in the first room is found from Eq. (12), in which

$$\Delta m = \Delta m_3 - \Delta m_5$$

where Δm_3 is the mass increment flowing through the first doorway, calculated from Eqs. (1), (3) and (13).

Method F can be used to calculate pressure rise in the second room, but because of the logical absurdity mentioned in Section IIB1 provision must be made in the analysis for one or more correction terms Δ in equations expressing conservation of momentum.

To write conservation-of-momentum equations useful in solving for the flow into the second or inner room, we consider again the larger of the two control surfaces shown in Figure E-18, which embraces the same volume as the superposition of the two control surfaces drawn in Figures E-3 and E-7. Were the second doorway not present, the momentum flux through the surface would be zero; yet, the usual assumption of uniform pressure within the first room leaves us with a nonvanishing component of force in the x-direction after integration over the control surface. This is the logical absurdity presented in Section IIB1 above. To correct this inconsistency, we postulate the existence of a force symbolized by Δ_3 on the wall of the first room directly opposite the doorway; thus, when the second doorway is absent, the momentum balance becomes:

$$\left(P_1 - P_3'\right) A_2 + \Delta_3 = 0$$

Solving this equation for Δ_3, we find:

$$\Delta_3 = -\left(P_1 - P_3'\right) A_2 \tag{52}$$

Now in writing the momentum balance with the second doorway present we include the term Δ_3, as follows:

$$\left(P_1 - P_3'\right) A_2 + \Delta_3 + \left(P_3' - P_4\right) A_4 = \rho_4 u_4^2 A_4 \tag{53}$$

After substitution of the value of Δ, this equation reduces to:*

$$\left(P_3' - P_4\right) A_4 = \rho_4 u_4^2 A_2 \tag{54}$$

Combining Eqs. (46), (48), (49) and (51) we can solve for the four unknowns: u_3, P_4, ρ_4, and u_4.

The resulting solution for P_4 can be put in a form similar to that used in computing P_2 in Eq. (5)[4]:

$$\frac{2\gamma}{\gamma + 1}\left(\frac{P_4}{P_3'}\right)^{1/\gamma} = \frac{P_4}{P_3'} + \frac{\gamma - 1}{\gamma + 1}\left[1 - \left(\frac{A_4}{A_3}\right)^2\left(\frac{P_4}{P_3'}\right)^{2/\gamma}\right] + \frac{\gamma - 1}{\gamma + 1}\left[\frac{A_4}{A_3}\left(\frac{P_4}{P_3'}\right)^{1/\gamma}\right]^2 \frac{P_4}{P_3'} \tag{55}$$

If $y = \dfrac{P_4}{P_3'}$

$$A_o = \frac{\gamma - 1}{\gamma + 1}\left\{\left[1 - \left(\frac{A_4}{A_3}\right)^2\left(\frac{P_4}{P_3'}\right)^{2/\gamma}\right] + \left[\frac{A_4}{A_3}\left(\frac{P_4}{P_3'}\right)^{1/\gamma}\right]^2 \frac{P_4}{P_3'}\right\}$$

---

* The use of Eq. (51) is equivalent to neglecting the possibility of continuous flow through the "maze" or pipe consisting of the first doorway, the first room, and the second doorway, such as was considered in Section IIC2 above. Presumably, were the first room small enough, such continuous pipe-like flow would be established, making it more sensible to treat the two connected rooms as a single room of volume equaling the sum of the volumes of its two components. The means of calculating which of the two analytical treatments (viz., analysis as two connected rooms, or as a single room) is appropriate are not available. As we shall see in a numerical calculation later (cf. Figure E-19), treatment as two connected rooms may reveal no significant pressure difference between the two rooms and yield essentially the same pressure history in the blast-filled volume as does treatment as a single room.

and $B = \frac{2\gamma}{\gamma + 1}$

then Eq. (43) can be written in the same form as Eq. (5); viz.,

$$B\, y^{1/\gamma} = y + A_o$$

Since $P_4 \leq P_3'$ and usually $A_4 \ll A_3$,

$$A_o \cong \frac{\gamma-1}{\gamma+1} \tag{56}$$

Use of Eq. (56) is equivalent to neglecting the average wind speed in the first room; i.e., if $u_3 = o$ is substituted in Eq. (46), Eq. (56) is exact.

After the duct parameters, i.e., ρ_2, P_2, u_2, ρ_4, u_4, and, if desired, u_3, have been found from the foregoing equations, then the new room pressures P_3 and P_5 and densities ρ_3 and ρ_5 are calculated as follows:

$$\Delta m_5 \left(\frac{\gamma}{\gamma-1} \cdot \frac{P_3'}{\rho_3'} + \frac{1}{2} u_3^2 \right) = \frac{1}{\gamma-1} (P_5 - P_5') V_5 \tag{57}$$

where $\Delta m_5 = u_4 \rho_4 A_4 \Delta t$, mass increment in second room

$$\frac{\gamma}{\gamma-1} \cdot \frac{P_1}{\rho_1} \cdot \Delta m = \frac{1}{\gamma-1} (P_3 - P_3') V_3 + \frac{1}{\gamma-1} (P_5 - P_5') V_5 \tag{58}$$

where $\Delta m = u_2 \rho_2 A_2 \Delta t$, mass increment in first room;

$$\rho_5 = \rho_5' + \frac{\Delta m_5}{V_5} \tag{59}$$

and

$$\rho_3 = \rho_3' + \frac{\Delta m - \Delta m_5}{V_3} \tag{60}$$

Numerical Example No. 5 (Flow into Two Connected Rooms). Assume that the room considered in Numerical Example No. 3 has within it a small storage compartment of 800 cf volume opening onto the main room through a small passage 10 sf in area. We compute the pressure rise in both portions of the 4000-cf volume in the first time increment $\Delta t = 5$ ms.

Before making the detailed calculations however, we can see from the simple rule in Section IIA that there will never be significant pressure difference between the two volumes. The approximate filling time of the larger volume is:

$$\Delta T_1 = \frac{4000 - 800}{2 \times 21} = 76.2 \text{ ms}$$

and for the smaller volume:

$$\Delta T_2 = \frac{800}{2 \times 10} = 40.0 \text{ ms}$$

The fact that $\Delta T_2 < \Delta T_1$ means that the smaller volume will keep pace with the larger volume in filling, as we can understand from the detailed calculation below by Method D.

The initial mass flow rate through the outer doorway (calculated in Numerical Example No. 3) is:

$$\frac{dm}{dt} = 46.73 \text{ slug/sec}$$

which means that in the first time increment

$$\Delta m_3 = 46.73 \times 0.005 = 0.2336 \text{ slug}$$

Such a mass increment means, according to Eq. (12), that the average pressure rise in the outer room without flow into the inner room will be:

$$\Delta P_3 = P_3 - P_3' = \frac{1.4 \times 34.7 \times 0.2336}{0.004313(4000-800)} = 0.8222 \text{ psi}$$

In applying Eq. (51) we use the values $P_5' = 14.7$ psi, $K_4 = 0.7$, and provisionally assume $P_3' = 14.7 + 0.822 = 15.51$ psi. Also by Eq. (11) the provisional value of outer room density is:

$$\rho_3' = 0.002378 + \frac{0.2336}{3200} = 0.002451 \text{ slug/cf.}$$

Hence,

$$\Delta m_5 = 0.7 \left(\frac{2 \times 1.4 \times 0.002451 \times 15.52 \times 144}{1.4 - 1}\right)^{0.5} \left(\frac{14.7}{15.52}\right)^{1/1.4}$$

$$\times \left[1 - \left(\frac{14.7}{15.52}\right)^{1-1/1.4}\right]^{0.5} \frac{10 \times 0.005}{\left[1 - \left(\frac{14.7}{15.52}\right)^{2/1.4} \left(\frac{10}{21}\right)^2\right]^{0.5}}$$

$$= 0.02910 \text{ slug}$$

The mass remaining in the main room then is:

$$\Delta m = 0.2336 - 0.02910 = 0.2045 \text{ slug}$$

and the corrected density in the main room at the end of the first time step is:

$$\rho_3 = 0.002378 + \frac{0.2045}{3200} = 0.002442 \text{ slug/cf}$$

and in the small room:

$$\rho_5 = 0.002378 + \frac{0.02910}{800} = 0.002414 \text{ slug/cf}$$

Corrected pressure in the main room at the end of the first time step is by Eq. (12):

$$P_3 = 14.7 + \frac{1.4 \times 34.7 \times 0.2045}{0.004313 \times 3200} = 15.42 \text{ psi}$$

and using an analogy to Eq. (12) in which P_1 and ρ_1 have been replaced by P_3' and ρ_3', respectively, we calculate the pressure in the small connected volume to be:

$$P_5 = 14.7 + \frac{1.4 \times 14.7 \times 0.02910}{0.002378 \times 800} = 15.01 \text{ psi}$$

For the second time increment time is advanced to $t = 0.005$ sec and any change in outside conditions must be reflected in the values of P_1 and ρ_1. If we assume P_1 and ρ_1 are unchanged during the first time step, then dm/dt through the outer doorway is the same as it was initially; the preliminary increases in P_3 and ρ_3 are the same, i.e.,

$$P_3' = 15.42 + 0.8222 = 16.24 \text{ psi}$$

and

$$\rho_3' = 0.002442 + \frac{0.2336}{3200} = 0.002515 \text{ slug/cf}$$

Again applying Eq. (51) we find:

$$\Delta m_5 = 0.7 \left(\frac{2.8 \times 0.002515 \times 16.24 \times 144}{0.4}\right)^{0.5} \left(\frac{15.01}{16.24}\right)^{1/1.4}$$

$$\left[1 - \left(\frac{15.01}{1624}\right)^{1-1/1.4}\right]^{0.5} \frac{}{\left[\left(\frac{15.01}{16.24}\right)^{1/0.7} \left(\frac{10}{21}\right)^{2}\right]^{0.5}}$$

$$= 0.03546 \text{ slug}$$

The net increase in the main room is then:

$$\Delta m = 0.2336 - 0.03546 = 0.1981 \text{ slug}$$

So that at the end of the second time increment:

$$P_3 = 15.42 + \frac{1.4 \times 34.7 \times 0.1981}{0.004313 \times 3200} = 16.12 \text{ psi}$$

$$P_5 = 15.01 + \frac{1.4 \times 16.24 \times 0.03546}{0.002515 \times 800} = 15.41 \text{ psi}$$

$$\rho_3 = 0.002515 + \frac{0.1981}{3200} = 0.002577 \text{ slug/cf}$$

$$\rho_5 = 0.002414 + \frac{0.03546}{800} = 0.002458 \text{ slug/cf}$$

As we forecast, the pressure differential between the two connected volumes is decreasing in time and will remain small.

B. Outflow

The foregoing section considered inward flow through both doorways. The principles for studying outflow through one or both doorways are the same but certain equations must be rewritten. Two statements can be made:

First, outflow (like inflow) through the first or outer doorway can be calculated exactly as set forth for a single room. In the case of outflow, Eqs. (1), (2), and (20) are required, as explained in Section IIB2.

Second, both inflow and outflow through the second or inner doorway are affected by the direction of flow through the first doorway. There are therefore three cases remaining to be treated in discussing flow

through the second doorway: (1) flow through the second doorway is outward while flow through the first is inward, (2) flow through the second doorway is outward while flow through the first is outward, and (3) flow through the second doorway is inward while flow through the first is outward. The case of inward flow through both doorways has been treated in the preceding section.

In Case (1), $u_3 = 0$ and Eq. (46) simplifies to:

$$\frac{\gamma}{\gamma-1} \cdot \frac{P_3'}{\rho_3'} = \frac{\gamma}{\gamma-1} \cdot \frac{P_4}{\rho_4} + \frac{1}{2} u_4^2 \tag{61}$$

but a momentum balance such as Eq. (53) must contain two correction terms, Δ_3 and Δ_5, to account for excess force against the righthand and lefthand walls, respectively, of the first room; Δ_3 is given by Eq. (52) and by analogy we can write:

$$\Delta_5 = (P_5' - P_3')\ A_4 \tag{62}$$

Hence, writing the momentum balance as follows:

$$(P_1 - P_3')\ A_2 + \Delta_3 + (P_3' - P_4)\ A_4 + \Delta_5 = \rho_4 u_4^2\ A_4 \tag{63}$$

and substituting for Δ_3 and Δ_5, we find:

$$P_5' - P_4 = \rho_4\ u_4^2 \tag{64}$$

To the outflow through the second or inner doorway we can apply the isentropic equation of state in analogy with Eq. (6):

$$\rho_4 = \rho_5' \left(\frac{P_4}{P_5'}\right)^{1/\gamma} \tag{65}$$

Combining Eqs. (61), (64), and (65), we find:

$$By^{1/\gamma} = y + A_o$$

where

$$y = \frac{P_4}{P_5'} \tag{66}$$

$$B = \frac{2\gamma}{\gamma+1} \cdot \frac{\rho_5'}{\rho_3'} \cdot \frac{P_3'}{P_5'} \tag{67}$$

$$A_o = \frac{\gamma-1}{\gamma+1} \tag{68}$$

In Case (2), there is net flow through the first room (i.e., $u_3 \neq 0$); Eq. (46) is unchanged but the analog of Eq. (53) is:

$$(P_1 - P_3') A_2 + (P_3' - P_4) A_4 + \Delta_5' = \rho_4 u_4^2 A_4 \tag{69}$$

where
$$\Delta_5' = (P_5' - P_3') A_4 - (P_1 - P_3') A_2 \tag{70}$$

This value of Δ_5' is computed by noting that the momentum flux through a control surface embracing both rooms and the outside reservoir is zero, i.e.:

$$(P_5'-P_3') A_4 - \Delta_5' + (P_3'-P_1) A_2 = 0$$

Combination of Eqs. (69) and (70) leads again to Eq. (64).

Solving Eqs. (46), (48), (64), and (65), we find again that

$$By^{1/\gamma} = y + A_o$$

where x and B are given by Eqs. (66) and (67), but now

$$A_o = \frac{\gamma+1}{\gamma-1} \left\{ (1-\alpha^2) \left[\frac{P_1 - P_3'}{P_5'} \cdot \frac{A_2}{A_4} + \frac{P_3' + \Delta_5'}{P_5'} \right] + \alpha^2 y \right\} \tag{71}$$

and
$$\alpha = \frac{A_4}{A_3} \cdot \frac{\rho_5'}{\rho_3'} \cdot y^{1/\gamma} \tag{72}$$

$$A_o = \frac{\gamma-1}{\gamma+1} \{(1-\alpha^2) + \alpha^2 y\} \tag{73}$$

Since, ordinarily, $A_3 \gg A_4$, and $y < 1$, $\alpha^2 \ll 1$, from which we conclude:

$$A_o \approx \frac{\gamma-1}{\gamma+1} \tag{74}$$

An alternative expression for A in Case (2) can be found by writing the excess force on the wall against which the outflow from the second room is directed as the pressure differential across the duct times the duct area:

$$\Delta''_5 = (P'_5 - P'_3)\, A_4 \tag{75}$$

Substituting Δ''_5 from Eq. (75) for Δ'_5 in Eq. (71), we compute for the constant term

$$A_o = \frac{\gamma-1}{\gamma+1}\left\{(1-\alpha^2)\left[\frac{P_1 - P'_3}{P'_5}\cdot\frac{A_2}{A_4} + 1\right] + \alpha^2\, y\right\} \tag{76}$$

which for small α becomes

$$A_o = \frac{\gamma-1}{\gamma+1}\left[\frac{P_1 - P'_3}{P'_5}\cdot\frac{A_2}{A_4} + 1\right] \tag{77}$$

In Case (3), namely, outflow through the first doorway combined with inflow through the second, conditions in the second doorway are computed by solving Eq. (46) with $u_3 = 0$, Eq. (49) and

$$(P_1 - P'_3)\, A_2 + (P'_3 - P_4)\, A_4 = \rho_4\, u_4^2\, A_4$$

(There is no excess force on the walls of the first room hence no correction terms appear in Eq. (78).

These equations lead to Eq.(5), in which

$$y = \frac{P_4}{P'_3}$$

$$B = \frac{2\gamma}{\gamma+1}$$

$$= \frac{\gamma-1}{\gamma+1}\left[\left(\frac{P_1}{P'_3} - 1\right)\frac{A_2}{A_4} + 1\right]$$

In summary then we see that in every case an equation of the form $By^{1/\gamma} = y + A$ must be solved for y. This equation is encountered also in the first doorway if Method F is used. In Table E-1 the meanings of y, A, and B for each case are listed. Since conditions in the first doorway under Method F are independent of conditions inside, the definitions for the first duct appear separately.

Table E-1

MEANINGS OF y, A_o, AND B IN THE EQUATION $By^{1/\gamma} = y + A_o$ WHEN METHOD F IS USED

First doorway

Inflow

$$y = \frac{P_2}{P_1}$$

$$B = \frac{2\gamma}{\gamma + 1}$$

$$A_o = \frac{\gamma - 1}{\gamma + 1}$$

Outflow

$$y = \frac{P_2}{P_3'}$$

$$B = \frac{2\gamma}{\gamma + 1} \cdot \frac{\rho_3'}{\rho_1} \cdot \frac{P_1}{P_3'}$$

$$A_o = \frac{\gamma - 1}{\gamma + 1} \cdot \frac{P_1}{P_3'}$$

Second doorway

Inflow Both Doorways

$$y = \frac{P_4}{P_3'}$$

$$B = \frac{2\gamma}{\gamma + 1}$$

$$A_o = \frac{\gamma - 1}{\gamma + 1}\left[1 - \left(\frac{A_4}{A_3} y^{1/\gamma}\right)^2 (1 - y)\right]$$

Outflow Both Doorways

$$y = \frac{P_4}{P_5'}$$

$$B = \frac{2\gamma}{\gamma + 1} \cdot \frac{\rho_5'}{\rho_3'} \cdot \frac{P_3'}{P_5'}$$

$$A_o = \frac{\gamma - 1}{\gamma + 1}\left[1 - \alpha^2 (1 - y)\right]$$

$$\alpha = \frac{A_4}{A_3} \cdot \frac{\rho_5'}{\rho_3'}\, y^{1/\gamma}$$

or alternatively

$$A_o = \frac{\gamma - 1}{\gamma + 1}\left\{(1 - \alpha^2)\left[\frac{P_1 - P_3'}{P_5'} \cdot \frac{A_2}{A_4} + 1\right] + \alpha^2 y\right\}$$

Inflow First Doorway/Outflow Second Doorway

$$y = \frac{P_4}{P_5'}$$

$$B = \frac{2\gamma}{\gamma + 1} \cdot \frac{\rho_5'}{\rho_3'} \cdot \frac{P_3'}{P_5'}$$

$$A_o = \frac{\gamma - 1}{\gamma + 1}$$

Outflow First Doorway/Inflow Second Doorway

$$y = \frac{P_4}{P_3'}$$

$$B = \frac{2\gamma}{\gamma + 1}$$

$$A_o = \frac{\gamma - 1}{\gamma + 1}\left[\left(\frac{P_1}{P_3'} - 1\right)\frac{A_2}{A_4} + 1\right]$$

In Figure E-19 results of a calculation carried out by Method F for two rooms are compared with measurement[23] of average pressure in the first room. The two rooms consisted of two small models such as those illustrated in Figures E-5 and E-6 placed back to back with a connecting door exactly like the outside door. The experiment was performed in a shock tube in which the wave struck the first doorway head-on. Also in Figure E-19 appears the result of a calculation treating the whole volume of the two model rooms as if it were in a single room. In Figure E-20 measured and calculated results for the second room in the model appear. At least in this one example, all three calculated pressure rises, i.e., in the first room, in the second room, and in the whole volume of both rooms treated as a single room, are quite similar and there appears to be no advantage in using the complicated procedures for computing the fill of two connected rooms.

The calculated histories shown in Figures E-19 and -20 have not been carried beyond the time of equilibrium between inside and outside pressures.

Figure E-21 shows pressure history calculated by Method D ignoring the wall between rooms. For this calculation the discharge coefficient has been set equal to 0.7 on inflow and 1.0 for outflow.*

The outside pressure, in Figures E-19, E-20, and E-21, labeled "input history," was measured as a pressure on the front face of the model simultaneously with the measurements of interior pressures. The short-lived reflected wave does not appear in these external histories.

IV Openings into Different Pressure Fields

The detailed calculations of inside pressure history considered in Section IIB above can easily be extended to the case of simultaneous flow into a single room through several openings, each of which is exposed to a separate outside pressure history. This situation will arise, for example, when a nuclear blast wave sweeps over a building, striking one of the four walls head-on, two side-on and exposing the fourth to the wake of the wave. If the burst is above the ground and the roof is in the regular reflection region,† the roof will be struck partly head-on; otherwise, it will be struck side-on. Head-on impact produces a strong but brief reflected wave followed by a quasi-steady wind and an associated

---

* CAVFIL, a FORTRAN program written at IIT Research Institute, was used to make the computation

† See pages 109-115, Ref. 1.

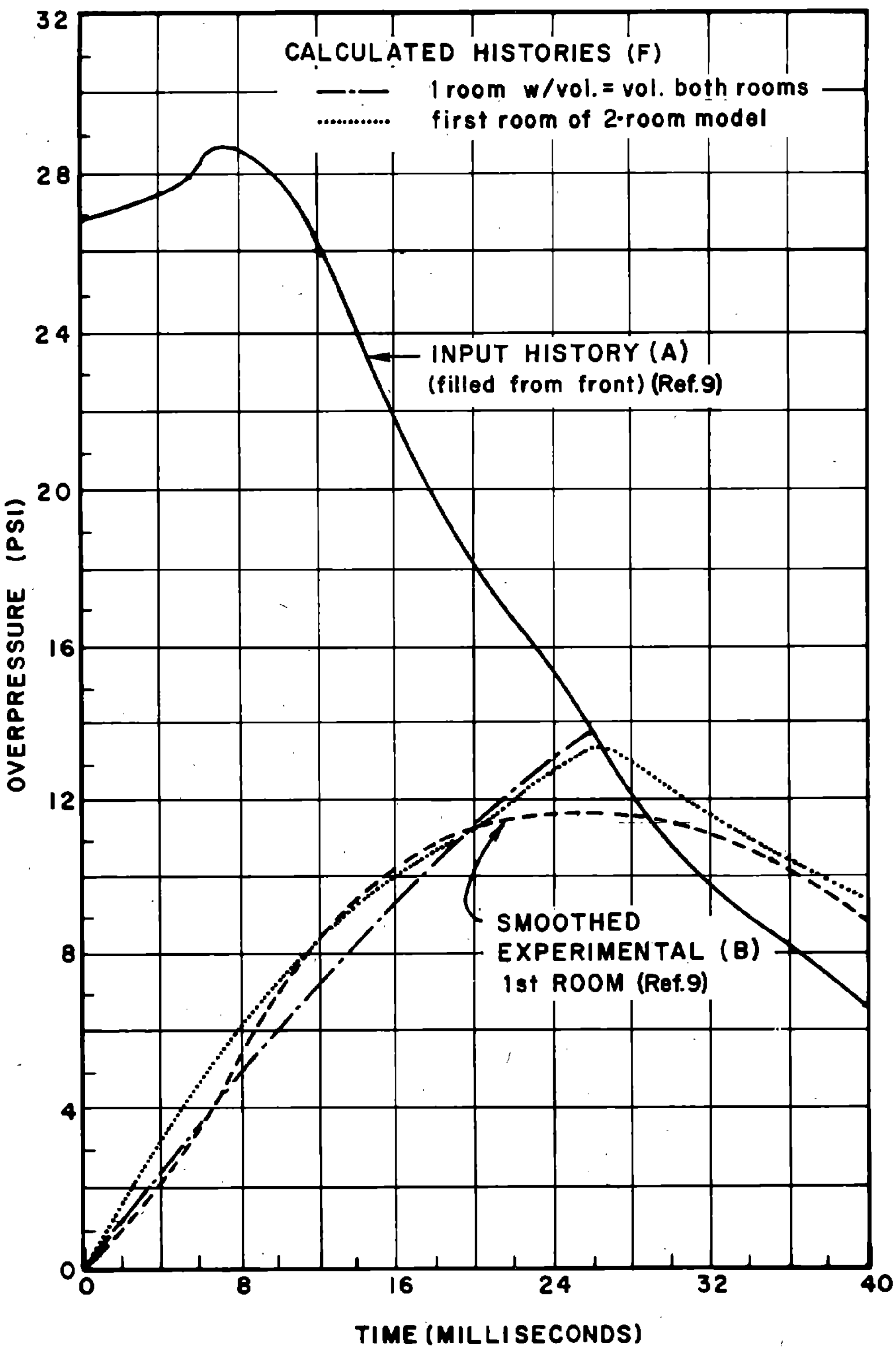

FIGURE E-19. COMPARISON OF OBSERVATIONS IN THE FIRST ROOM OF A TWO-ROOM MODEL WITH CALCULATIONS BY METHOD F

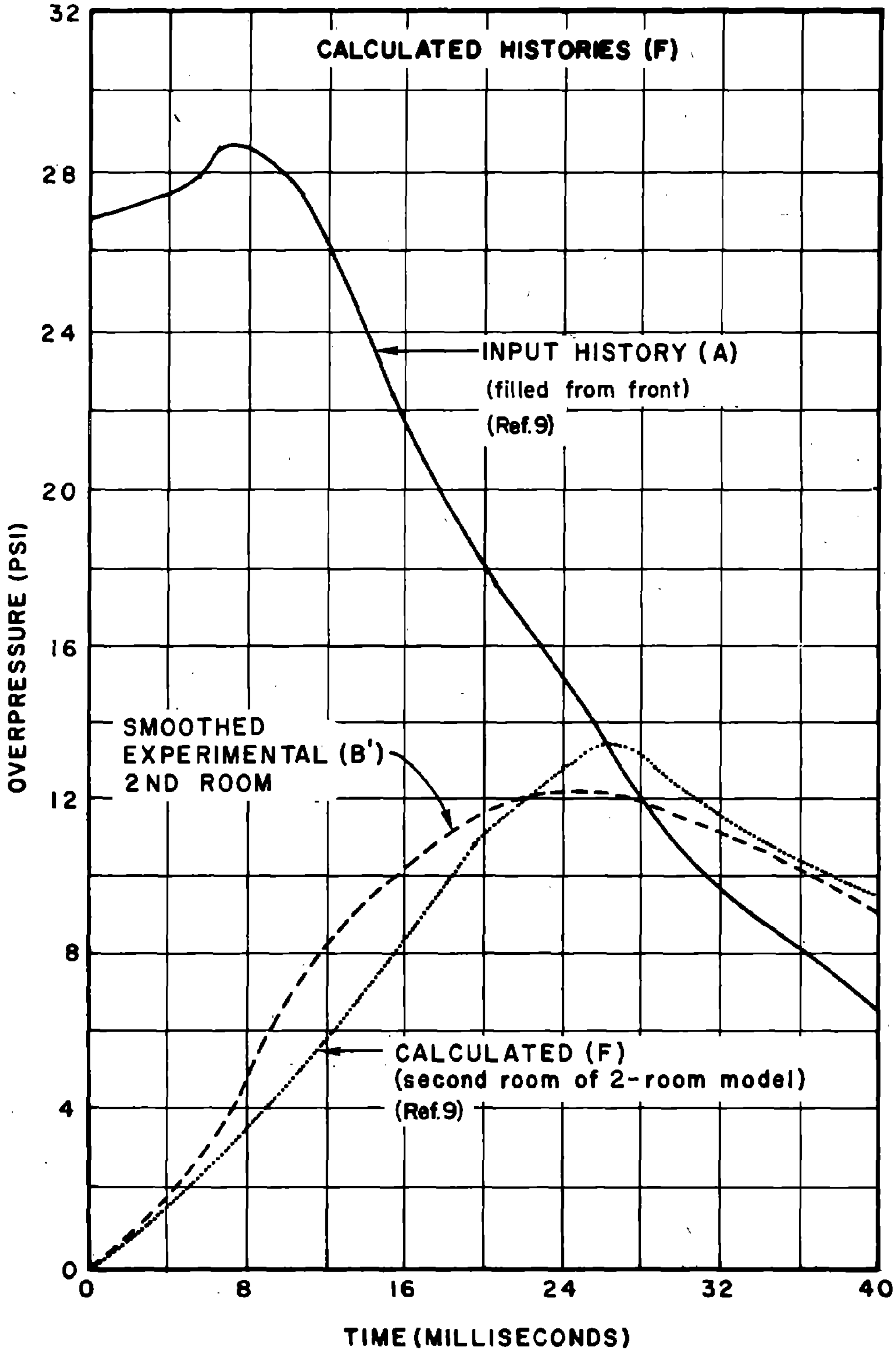

FIGURE E-20 COMPARISON OF OBSERVATIONS IN THE SECOND ROOM OF A TWO-ROOM MODEL WITH CALCULATIONS BY METHOD F

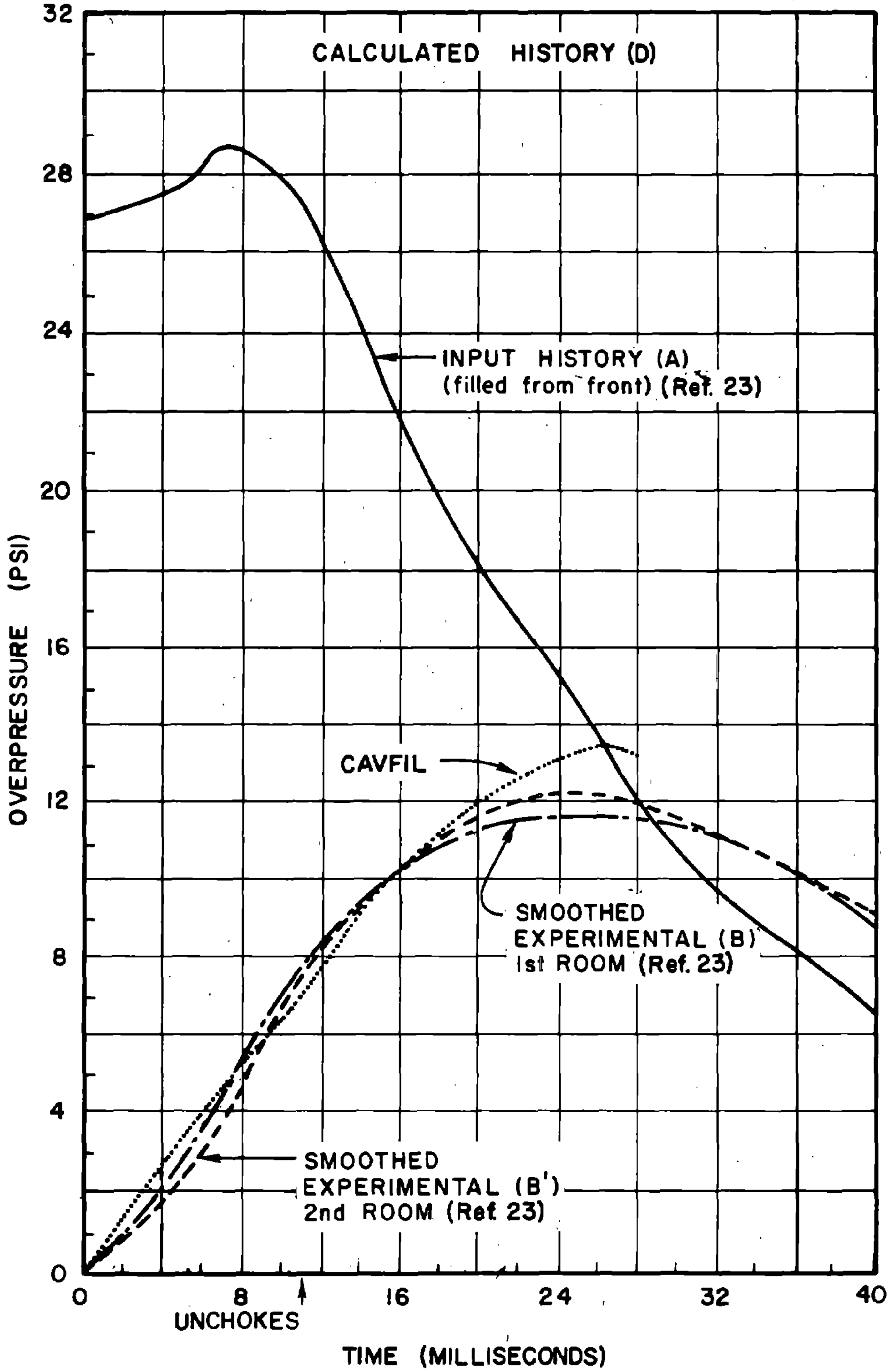

FIGURE E-21 COMPARISON OF OBSERVATIONS IN TWO-ROOM MODEL WITH CALCULATIONS BY METHOD D

strong drag force superimposed upon the free-field overpressure. When impact is not head-on, only the drag and free-field overpressures are ordinarily taken into account. References 1 and 3 contain discussions of methods of estimating outside pressure in these cases. (Reference 2 of Volume 1 of the present work gives detailed information about the drag forces exerted by wind.)

A head-on blast or shock wave striking a wall is first reflected at the surface to a peak overpressure 2 to 8 times as great as the incident. This high pressure lasts a relatively short time as rarefactions from regions of low pressure at the sides of the wall erode the reflected pressure; the erosion takes a length of time called the "clearing time." At the conclusion of clearing, pressure against the wall is the sum of free-field pressure plus a "drag" arising from the flow pattern, which has by now been established around the wall.

A wall oriented side-on to the shock front experiences no reflected pressure; and sometimes the free-field pressure against the wall is reduced by the flow past the wall. This reduction may be accounted for by assigning the wall a negative "drag" coefficient (although true drag is of course exerted in a direction parallel to the flow and is completely negligible for a more or less smooth wall). In our numerical example to follow we assume the drag coefficient of the wide walls to be zero. The pressure against walls struck completely side-on is the free-field pressure.

The wall of a rectangular building opposite to the wall struck head-on (we will call it the rear wall) will always feel a pressure less than free-field pressure, as long as the front wall stands to shield it. Here again, the drag force and drag coefficient are negative.

These principles are illustrated quantitatively in the numerical example below.

<u>Numerical Example No. 6</u>. As an indication of how the foregoing general procedures may be modified to account for several openings a brief numerical example is presented here.

Consider a volume contained in two rooms connected to each other by an open doorway and consider each room connected to the outside by a single doorway, as shown in Figure E-22. The blast wave that sweeps over the structure will be characterized by a free-field overpressure of 10 psig, head-on incidence upon the opening to the larger room, and

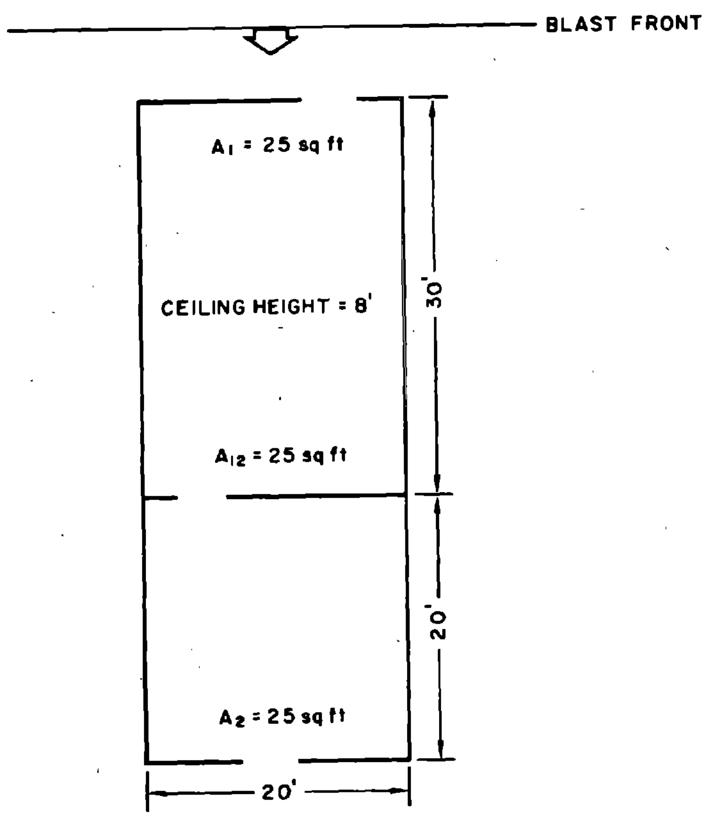

FIGURE E-22 SKETCH ILLUSTRATING NUMERICAL EXAMPLE

positive phase duration of 1 sec. Standard conditions will be assumed, i.e., $P_o = 14.7$ *psia and* $\rho_o = 0.0761\ lb/ft^3$. *In the front wall the opening area is 25* sf^2 *and there is a like opening in the rear wall. Because the door between the rooms has an area comparable to the area of each of the outside doors, the presence of the partition will be ignored and the volume to be filled taken as*

$$V_3 = 50 \times 20 \times 8 = 8000\ cf$$

As a first step the pressure histories outside the two doors will be calculated, according to the procedures recommended by Ref. 1. Since the first window is struck head-on, there will be no time delay there and the peak pressure will be the reflected pressure P_R, *which is calculated as:*

$$P_R = 2\ P_{so} \cdot \frac{7\ P_o + 4\ P_{so}}{7\ P_o + P_{so}}$$

Here

$$P_{so} = 10\ psi \text{ and } P_o = 14.7\ psi; \text{ hence}$$

$$P_R = 25.3\ psi$$

This reflected pressure will be felt in declining strength for the duration of the clearing time, t_c, *which is estimated as*

$$t_c = \frac{3s}{c}$$

where s is a dimension of the wall undergoing pressure clearing and c is sound speed. In this case

$$c = (\gamma\ P_o/\rho_o)^{1/2} = (1.4 \times 14.7 \times 32 \times 144/0.076096)^{1/2} = 1116\ ft/sec$$

and $s = 20$

so that

$$t_c = 53.7\ ms$$

As an approximation, the decline of reflected pressure during the interval

$$0 \le t \le t_c$$

is treated as linear; that is, at $t = t_c$ *the pressure* P_c *on the first wall is simply the sum of the free-field overpressure* P_{sc} *and the drag* P_{dc} *arising from the winds behind the shock front. Since during the time* t_c *free-field pressure has fallen exponentially*[1] *from* $P_{so} = 10$ *psi:*

$$P_{sc} = P_{so} \left(1 - \frac{t_c}{t_o}\right) e^{-t_c/t_o}$$

where t_o *is the free-field duration of positive overpressure; in this case* $t_o = 1$ *sec so that*

$$P_{sc} = 8.97 \text{ psi}$$

Peak drag pressure P_{do} *is computed from the formula*

$$P_{do} = \frac{5}{2} \cdot \frac{(P_{so})^2}{7\ P_o + P_{so}} = \frac{5}{2} \cdot \frac{100}{7 \times 14.7 + 10} = 2.21 \text{ psi}$$

so that drag pressure at $t = t_c$ *is:*[1]

$$P_{dc} = P_{do} \left(1 - \frac{t_c}{t_o}\right)^2 e^{-2\ t_c/t_o}$$

Numerically, this is

$$P_{dc} = 1.78 \text{ psi}$$

Therefore the pressure outside the first opening at $t = t_c$ *is:*

$$P_c = P_{sc} + P_{dc} = 8.97 + 1.78 = 10.75$$

and, assuming a linear fall from P_{so} *to* P_c*, for* $0 \le t \le t_c$*, pressure* P_1 *outside first wall as a function of time becomes:*

$$P_1 = P_c + \frac{(t_c - t)}{t_c} \quad (P_R - P_c) \tag{79}$$

For the remainder of the positive phase duration, outside pressure at the first opening is simply the sum of the decayed side-on pressure

$$P_s = P_{so} \left(1 - \frac{t}{t_o}\right) e^{-t/t_o} \tag{80}$$

and decayed dynamic pressure

$$P_d = P_{do} \left(1 - \frac{t}{t_o}\right)^2 e^{-2t/t_o} \tag{81}$$

so that for $t_o > t > t_c$

$$P_1 = P_s + P_d \tag{82}$$

For the first wall a drag coefficient equal to + 1.0 has been tacitly assumed above but for the second opening this coefficient will be different from 1, and according to Ref. 1, a value of -0.4 can be assumed. At the rear opening there is no reflected pressure and the delay is equal to the time taken by the front to traverse the building (assuming that the opening is already open upon blast arrival or that it is immediately forced open by the blast). Blast front speed can be found from the formula[1]

$$U = c_o \left(1 + \frac{\gamma + 1}{2} \cdot \frac{P_{so} - P_o}{P_o}\right)^{1/2}$$

where c_o *= sound speed in ambient air, i.e.,*

$$c_o = \left(\gamma\ P_o\ 32 \times 144/\rho_o\right)^{1/2} = 1116\ ft/sec$$

Hence,

$$U = 1116 \times \left(1 + \frac{2.4}{2.8} \times \frac{10}{14.7}\right)^{1/2} = 1148\ ft/sec$$

so that delay at the rear entrance is $\frac{50}{1148} = 43.5$ *ms.*

Beginning at t = 43.5 ms the room starts to fill through the rear opening. (Outflow through openings other than the first can ordinarily be neglected during the delay period: either the other openings are closed to the blast for a certain period or, if not, the blast travel time to them is much shorter than the time required to start outflow through them.)

Filling through the rear opening takes place however from a reservoir at lower pressure than that outside the front opening, i.e., outside pressure P_{1r} at the rear is:

$$P_{1r} = P_s - 0.4\ P_d \tag{83}$$

The decline in P_{so} and P_{do} that occurs while the blast front travels from front to rear opening is negligibly small and can be safely neglected for buildings of ordinary size.

For this sample case, the quantities P_1 (pressure outside the front opening) and P_{1r} (pressure outside the rear opening) have been calculated as functions of time and plotted in Figure E-23. The figure shows the discontinuity in the derivative of P_1 with respect to time at the point (t_c, P_c) when the reflected pressure is assumed to disappear and the outside pressure takes on its quasi-steady value.

Also plotted in the figure are inside pressure histories P_3 calculated by two methods: the greatly simplified procedure given in Section IIA of this report and the step-by-step Method F explained in Section IIB. In the first of these two procedures, the estimated history is given by the line segments ODFG obtained as follows. When the blast arrives at the front opening, filling immediately begins along line OA, where point A is the intersection of the outside pressure history and the abscissa

$$t = \frac{V_3}{2A_1} = \frac{8000}{2 \times 25} = 160 \text{ ms}$$

Line BC is a similar line representing filling through the rear opening, beginning after the delay time of 43.5 ms. Ordinates under the line BC have been added to ordinates of OA to produce the line DE. Since areas of both openings are equal, the point F is placed halfway between current outside pressures outside the front and rear openings and the decline of P_3 represented schematically by the line FG.

The step-by-step calculation results in the curve labelled "Method F" in Figure E-23. Because of the high reflected pressure during the interval $0 \leq t \leq t_c$ (which does not influence the results of the simplified method in this example), the more careful calculation shows a faster build-up of

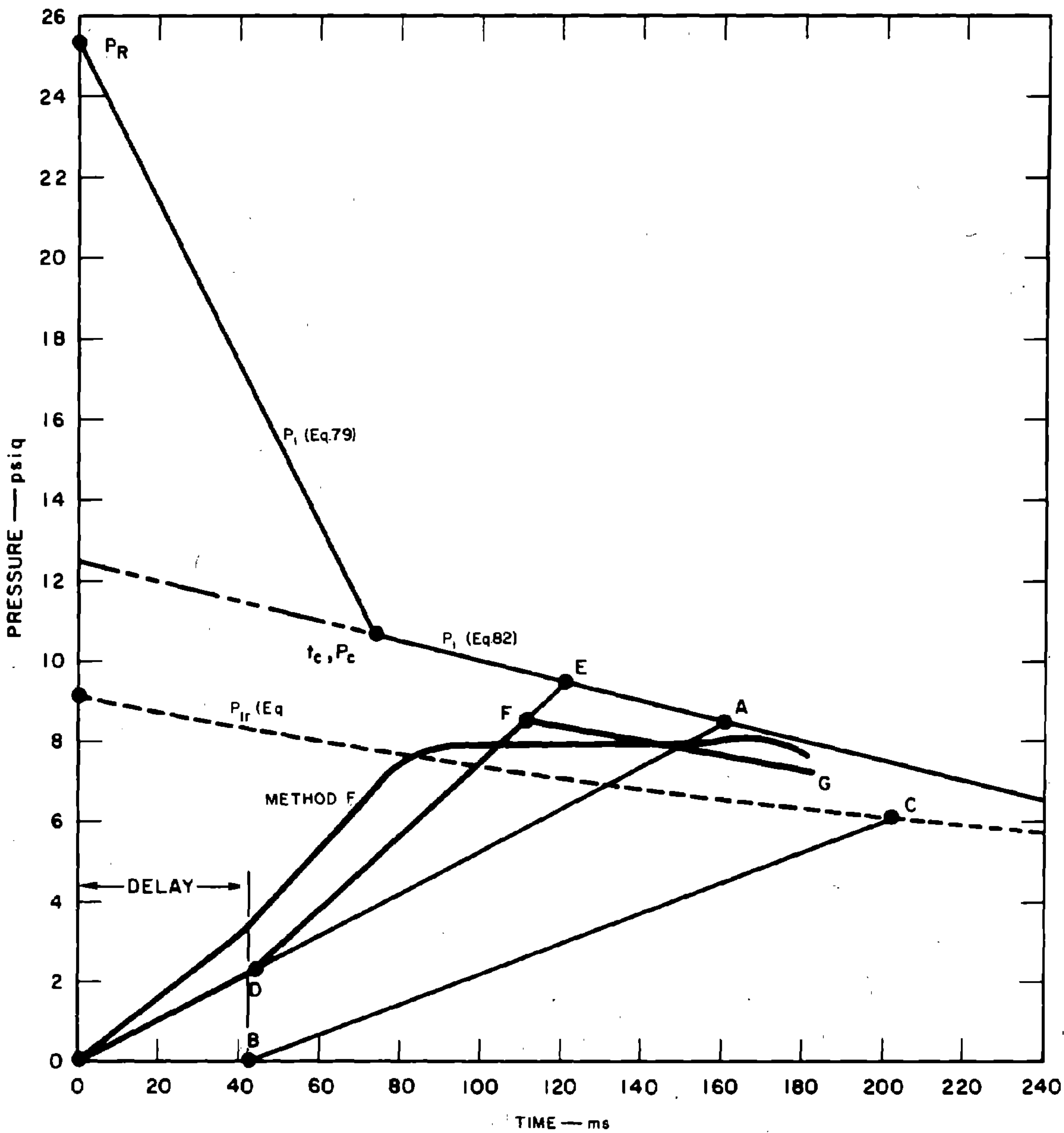

FIGURE E-23 ILLUSTRATIVE EXAMPLE

room pressure than the line ODF. To demonstrate the method the first step of the stepwise solution will be calculated below. In this sample calculation the reverberation time t_1 (Eq. (30)) is assumed to be zero for simplicity.

Since the least sound transit time across the room is approximately 20 ms we will choose a value of Δt = 5 ms. At t = 0 there is only one opening, that in the front wall. Outside pressure there at that time is P_R = 25.3 psig. Inside pressure $P_3' = P_o$ = 14.7 psia and density is $\rho_3' = \rho_o$ = 0.002378 slug/cf.

1. $P_1 = 25.3 + 14.7 = 40.0$ psia.

2. $\rho_1 = \left(\frac{P_1}{P_0}\right)^{1/\gamma} \rho_o = \left(\frac{40.0}{14.7}\right)^{1/1.4} (0.002378) = 0.004861$ slug/cf

3. $P_2 = 0.1912 \quad P_1 = (0.1912) \times (40.0) = 7.65$ psia

4. $\rho_2 = \left(\frac{P_2}{P_1}\right)^{1/\gamma} \rho_1 = (0.307) \times (0.004861) = 0.001492$ slug/cf

5. $u_2^2 = \frac{2\gamma}{\gamma - 1}\left(\frac{P_1}{\rho_1} - \frac{P_2}{\rho_2}\right) = \frac{2.8}{0.4}\left(\frac{40.0}{0.004861} - \frac{7.65}{0.001492}\right) \times 144 = 3.13 \times 10^6 \frac{ft^2}{sec^2}$

6. Since $P_1 > P_3'$: $u_2 > 0$, i.e., flow is inward. Were $P_3' > P_1$, u_2 would be negative.

7. $\Delta m_{31} = u_2 \ \rho_2 \ A_1 \ \Delta t = 0.3298$ slug.

8. $q_{core} = \left(\frac{\Delta m_{31}}{\Delta t}\right)^2 / \, 2 \rho_3' \ A_1^2 \ (144) = 10.0$ psi

9. $\Delta w_{31} = \frac{P_1 \ \Delta m_{31}}{\left(\frac{\gamma - 1}{\gamma}\right) \rho_1} = \frac{(40.0)(0.3298)}{\frac{0.4}{1.4}(0.004861)} \times 144 = 1.36 \times 10^6$ ft lb

10. *Since the rear opening is closed at this time:*

$$\Delta m_{32} = \Delta w_{32} = 0$$

Were the second opening available, Steps 1 - 9 would be repeated using initial outside pressure at rear opening to calculate Δm_{32} *and* Δw_{32}

11. $\Delta m_3 = \Delta m_{31} + \Delta m_{32} = 0.3298$ *slug*

12. $\Delta w_3 = \Delta w_{31} + \Delta w_{32} = 1.36 \times 10^6$ *ft lb*

13. $P_3 = P_3' + \dfrac{(\gamma - 1)\ \Delta w_3}{V_3} = 14.7 + \dfrac{(0.4)(1.36 \times 10^6)}{8000 \times 144} = 15.17$ *psia* *(room pressure)*

14. $\rho_3 = \rho_3' + \dfrac{\Delta m_3}{V_3} = 0.002378 + \dfrac{0.3298}{8000} = 0.002419$ *slug/cf (air density in room)*

15. P_3' *equal to* P_3

    and ρ_3' *equal to* ρ_3 *and return to Step 1 with value of*

    P_1 *at* $t = \Delta t = 5$ *ms*

V. Computer Program

The time-sharing computer program listed in Table E-2 will calculate and report average pressure inside an open room exposed to a nuclear blast wave. Dynamic pressures of winds entering the room and translation speeds of objects caught in a jet(s) may be obtained also. The program is interactive or conversational, that is, the user provides necessary input data by typing responses to questions. A sample input and output listing is shown in Table E-3. The user's responses are underlined.

Provision is made in the program for a maximum of eight openings into the room from the outside; delay times between wave front arrival (at the blastward face of the room) and the start of flow through the opening must be applied. Delays will be caused by shock travel time

Table E-2
COMPUTER PROGRAM

```
C INTERACTIVE FØRTRAN PRØGRAM TØ CØMPUTE HISTØRY ØF AVERAGE PRESSURE
C AND DYNAMIC PRESSURE DISTRIBUTIØN WITHIN A SINGLE RØØM WHICH IS
C FILLING FRØM A NUCLEAR BLAST WAVE THRØUGH AS MANY AS EIGHT
C ØPENINGS IN ANY WALL ØR WALLS ØF RØØM. IF DESIRED, PRØVIDES
C SØME TRANSLATIØNAL EFFECTS ØN AN ØBJECT CAUGHT IN JET.
C USES METHØD F. CANNØT CØMPUTE BEYØND END ØF PØSITIVE PHASE.
      CØMMØN G2,G3,L3,Q(500,8),T(500),A(8,2),NWIN,NT1,C,AB
      LØGICAL L1,L2,L3,L4,L5,L6,L7,L8
      DIMENSIØN P(500),N(8),Q2(8),PØUT(8)
      DIMENSIØN Q3(8),DREV(8),TREV(8)
      PRINT,"AMBIENT AIR PRESSURE (PSIA)"
      INPUT,PØ
      PRINT,"AMBIENT AIR DENSITY (SLUGS/CF)"
      INPUT,RHØØ
      PRINT,"RØØM VØLUME (CF)"
      INPUT,V3
      PRINT,"NUMBER ØF ØPENINGS (NØT MØRE THAN 8)"
      INPUT,NWIN
      PRINT,"AREAS ØF EACH ØPENING (SF)"
      INPUT,(A(I,1),I=1,NWIN)
      PRINT,"LØCATIØN CØDE FØR EACH ØPENING"
      INPUT,(N(I),I=1,NWIN)
      PRINT,"DELAY IN ENTRY AT EACH ØPENING (MS)"
      INPUT,(A(I,2),I=1,NWIN)
      PRINT,"CØMMUNICATIØN DISTANCE (FT) FØR EACH ØPENING"
      INPUT,(DREV(I),I=1,NWIN)
      PRINT,"CLEARING TIME (MS)"
      INPUT,TC
      PRINT,"DRAG CØEFFS FØR LØCATIØN CØDES 1, 2 AND 3"
      INPUT,CDFF,CDFS,CDFR
      PRINT,"PEAK FREE FIELD ØVERPRESSURE (PSIG)"
      INPUT, PSØ
      PRINT, "DURATIØN ØF PØSITIVE PHASE (SEC)"
      INPUT, TO
      TC=TC/1000.
      PRINT,"WANT PEAK VALUES ØNLY (.TRUE. ØR .FALSE.)"
      INPUT,L1
      IF(L1)GØ TØ 3
      PRINT,"INTERVAL BETWEEN VALUES ØF ØUTPUT (MS)"
      INPUT,TI
      TI=TI/1000.
      PRINT,"WANT  DECLINE ØF RØØM PRESSURE (.TRUE. ØR .FALSE.)"
      INPUT,L2
      GØ TØ 5
    3 TI=TO/99.
      L2=.FALSE.
    5 L3=.FALSE.
      L7=.FALSE.
      PRINT,"WANT ØUTSIDE PRESSURE (.TRUE. ØR .FALSE.)"
      INPUT,L5
      PRINT,"WANT DYNAMIC PRESSURES (.TRUE. ØR .FALSE.)"
      INPUT,L4
      PRINT,"WANT TRANSLATIØN EFFECTS (.TRUE. ØR .FALSE.)"
      INPUT,L6
      IF(.NØT.L6)GØTØ 6
      PRINT,"ACCELERATIØN CØEFFICIENT (SF/SLUG)"
      INPUT,AB
    6 IF(L5)PRINT 26
      PR=2.*PSØ*(7.*PØ+4.*PSØ)/(7.*PØ+PSØ)
      PDØ=2.5*PSØ*PSØ/(7.*PØ+PSØ)
      PSC=PSØ*(1.-TC/TO)*EXP(-TC/TO)
      PDC=PDØ*(1.-TC/TO)*(1.-TC/TO)*EXP(-2.*TC/TO)
      PC=PSC+PDC
      NT=TO/TI+1
      NT1=NT
      IF(NT.LE.500)GØTØ 13
      TMAX=500.*TI
      PRINT,"***VECTØR ØVERLØADED - TIME INTERVAL TRUNCATED"
      PRINT,"MAX. TIME= ",TMAX," (SEC)"
      NT1=500
   13 G=1.4; G2=1./G ; G3=1.-G2 ; G4=2./G3
      G5=G+1.; G6=2.*G/G5; G7=(G-1.)/G5
      G9=.1912**G2
      GPØ=2.*G*PØ ; GPS=2.*G*(PSØ+PØ)
      PCRIT=(2./G5)**(G/(G-1.))
      RHØ1Ø=RHØØ*(GPØ+G5*PSØ)/(GPØ+(G-1.)*PSØ)
      RHØ11=RHØ1Ø*(GPS+G5*(PR-PSØ))/(GPS+(G-1.)*(PR-PSØ))
      C=SQRT(G*PØ*144./RHØØ)
      DØ 7 I=1,NWIN
      TREV(I)=4.*DREV(I)/C
      Q2(I)=0.
      A(I,2)=A(I,2)/1000.
    7 CØNTINUE
      DØ 8 I=1,NWIN
      DØ 8 J=1,NT1
    8 Q(J,I)=0.0
      I2=0
      P3Ø=PØ ; RHØ3Ø=RHØØ
      TT=0. ; TØ=0.
      TAU=2.*(V3**(1./3.))/C
      DT=TAU/10.
      DDT=DT
    9 IF(TI-2.*DDT)10,11,11
   10 DDT=DDT/2.
      GØ TØ 9
   11 IF(DDT-.0005*TO)31,32,32
   32 DDT=DDT/2.
      GØ TØ 11
   31 ISTØP=TI/DDT+1
      DDT=TI/ISTØP
       MC=-1
       DØ 990 J=1,NT1
       IF(J.GT.500)GØTØ 992
       DØ 99 I=1,ISTØP
       MC=MC+1
       MD=2 ; II=I
       IF(MC.NE.0)GØ TØ 62
       II=I-1 ; MD=1
```

```
 62   TT=TØ+II*DDT
      IF(TT.GT.TO)GØ TØ 99
      R=TT/TO ; RR=1.-R
      PD=PDØ*RR*RR*EXP(-2.*R)
      PS=PSØ*RR*EXP(-R)
      DM=0. ; W=0.
      DØ 500 K=1,NWIN
      M=N(K) ; DLY=A(K,2)
      IF(DLY.GT.TT)GØ TØ 500
      PS1=PSØ+PØ
      RHØ12=RHØ1Ø
      GØ TØ (15,16,17),M
 15   CDF=CDFF
      IF(TC.EQ.0.)GØ TØ 21
      IF(TT-TC)20,20,21
 20   P11=(TC-TT)*(PR-PC)/TC+PC
      RHØ12=RHØ11
      PS1=PR+PØ
      GØ TØ 30
 16   CDF=CDFS
      GØ TØ 21
 17   CDF=CDFR
 21   P11=PS+CDF*PD
 30   PØUT(K)=P11
      P11=P11+PØ
      RHØ1=RHØ12*((P11/PS1)**G2)
      L8=.FALSE.
      US=0.
      DDM1=0.
      IF(TT.GE.TREV(K))GØTØ 1
      US=(C*PS/(G*PØ))/SQRT(1.+PS/(G6*PØ))
      DDM1=RHØ1*US
      L8=.TRUE.
  1   IF(P11-P3Ø)36,35,37
 35   U22=0.
      GØ TØ 39
 36   JSIGN=-1
      AA=G7*P11/P3Ø
      BB=G6*RHØ3Ø*P11/(RHØ1*P3Ø)
      Z=P11/(RHØ1**G)
      Y=.9094*P3Ø/(RHØ3Ø**G)
      IF(Y.GT.Z)GØ TØ 60
      CALL EQ(AA,BB,P2)
      IF(.NØT.L3)GØ TØ 303
      NT1=J
      GØ TØ 19
 60   X=P3Ø/RHØ3Ø
      Y=P11/P3Ø
      IF(Y.GT.PCRIT)Y=PCRIT
      RHØ2=RHØ3Ø*(Y**G2)
      P2=P11
      IF(I2.EQ.0) PRINT, "Y.GT.Z, METHØD D USED IN SØME CALCULATIØNS"
      I2=1
      GØ TØ 44
303   RHØ2=((P2)**G2)*RHØ3Ø
      P2=P2*P3Ø
      X=P3Ø/RHØ3Ø
      GØ TØ 38
 37   JSIGN=+1
      P2=.1912*P11
      RHØ2=G9*RHØ1
      X=P11/RHØ1
 38   U22=G4*(X-P2/RHØ2)*144.
 44   CØNTINUE
      IF(U22)40,39,39
 40   PRINT,"U22 NEGATIVE",U22
      PRINT,"JSIGN=",JSIGN
      GØ TØ 999
 39   U2=SQRT(U22)*JSIGN
      Q2(K)=0.
      GØ TØ (500,65),MD
 65   DDM=U2*RHØ2
      IF(L8)GØTØ 4
      Q2(K)=JSIGN*DDM*DDM/(2.*RHØ1*144.*((P3Ø/P11)**G2))
      DDM=DDM*A(K,1)*DDT
      GØTØ 2
  4   DDM=DDM1+(DDM-DDM1)*TT/TREV(K)
      Q2(K)=JSIGN*DDM*DDM/(2.*RHØ1*144.*((P3Ø/P11)**G2))
      DDM=DDM*A(K,1)*DDT
      GØTØ 2
  2   DM=DM+DDM
      W=W+P11*DDM/(G3*RHØ1)
500   CØNTINUE
      P3A=P3Ø
      RHØ3Ø=RHØ3Ø+DM/V3
      P3Ø=P3Ø+(G-1.)*W/V3
      IF(.NØT.L2.AND.P3Ø.LT.P3A)GØTØ 80
      GØ TØ (19,99),MD
 80   L7=.TRUE.
      NT1=J
      P3Ø=P3A
      TT=TT-II*DDT
      GØ TØ 19
 99   CØNTINUE
 19   TØ=TT
      P(J)=P3Ø-PØ
      T(J)=TT
      IF(L5)PRINT 27,J,(PØUT(K),K=1,NWIN)
      DØ 18 L=1,NWIN
      IF(Q2(L))41,42,42
 41   Q(J,L)=0.
      GØTØ 43
 42   Q(J,L)=Q2(L)
      IF(L7) Q(J,L)=Q3(L)
 43   Q2(L)=0.
 18   CØNTINUE
      IF(L3)GØ TØ 992
      IF(L7)GØTØ 800
990   CØNTINUE
```

```
800   IF(L1)GØTØ 991
      GØ TØ 992
991   PRINT 50,T(NT1),P(NT1),(Q(2,K),K=1,NWIN)
50    FØRMAT(1H0,30X,11HPEAK VALUES//1H 6HTIME= ,E11.4,1X,
      &3HSEC,4X,10HPRESSURE= ,E11.4,1X,4HPSIG//
      &18H DYNAMIC PRESSURES,1X,5H(PSI)/8(1H E11.4/))
      STØP
992   PRINT 22
      DØ 993 I=1,NT1
      PRINT 51,I,T(I),P(I)
993   CØNTINUE
22    FØRMAT(1H-///14H TIME STEP NØ.,3X,9HTIME(SEC),7X,7HINSIDE
&     15HPRESSURE (PSIG)//)
51    FØRMAT(1H ,I10,5X,E11.4,5X,E11.4)
      PRINT," "
      IF(.NØT.L4)GØ TØ 995
      PRINT 23
      DØ 994 I=1,NT1
      PRINT 24,T(I),(Q(I,K),K=1,NWIN)
994   CØNTINUE

995   IF(L6)CALL SLIDE
23    FØRMAT(1H-///1H 15X,40HCØRE DYNAMIC PRESSURES (PSI) AT EACH ØPE
&     ,4HNING//12H ØPENING NØ.,2X,1H1,7X,1H2,7X,1H3,7X,1H4,7X,1H5,7X,
&     1H6,7X,1H7,7X,1H8//10H TIME(SEC)//)
24    FØRMAT(1H F7.3,1X,8F8.2)
26    FØRMAT(1H0,14X,40HØUTSIDE PRESSURES (PSIG) AT EACH ØPENING//
&     12H ØPENING NØ.,5X,1H1,6X,1H2,6X,1H3,6X,1H4,6X,1H5,6X,1H6,
&     6X,1H7,6X,1H8/14H TIME STEP NØ.//)
27    FØRMAT(1H ,I6,7X,8(F6.2,1X))
999   STØP
      END
      SUBRØUTINE EQ(A,B,X)
C SØLVES THE EQUATIØN B*(X**G2)=X+A FØR X
      CØMMØN G2,G3,L3
      LØGICAL L3
      XØ=(B*G2)**(1./G3)
      F1=XØ+A
      F2=B*(XØ**G2)
      IF(F1-F2)1,2,3
3     PRINT,"NØ SØLN IN EQ"
      L3=.TRUE.
      RETURN
2     IF(XØ-1.)4,5,5
5     PRINT,"NØ SØLN IN EQ LT 1"
      L3=.TRUE. ; RETURN
4     X=XØ ; RETURN
1     N=0
      IF(XØ-1.)8,42,7
7     N=1
8     F1=1.+A
      IF(F1-B)9,10,11
9     N=N+3 ; GØ TØ 12
10    N=N+1 ; GØ TØ 12
11    N=N+5
12    GØ TØ (40,5,40,42,39,5),N
39    XU=1. ; XL=XØ ; GØTØ 21
40    XU=XØ ; XL=0. ; GØ TØ 21
42    XU=1. ; XL=0. ; GØ TØ 21
21    XM=(XU+XL)/2.
      R=(XU-XL)/XU
      IF(R-0.001)22,23,23
23    F1=XM+A
      F2=B*(XM**G2)
      IF(F1-F2)24,22,25
24    XU=XM
      GØ TØ 21
25    XL=XM ; GØ TØ 21
22    X=XM
99    RETURN
      END
      SUBRØUTINE SLIDE
      CØMMØN G2,G3,L3,Q3(500,8),T(500),A(8,2),NWIN,NT,C,AA
      PRINT 7
3     FØRMAT(1H ////)
      PRINT 4, AA
      AA=AA*144.
4     FØRMAT(1H-,22X,27H***TRANSLATIØN ØF ØBJECT***//
&     27H ACCELERATIØN CØEFFICIENT =,F9.4,2X,9H(SF/SLUG)/
&     32H CØØRDINATES CENTERED IN ØPENING)
      NT2=NT-1
      DØ 900 I=1,NWIN
      PRINT 3
      PRINT 5,I
5     FØRMAT(13H ØPENING NØ. ,I1////16H INITIAL CØØRDS.,6X,
&     13HFINAL CØØRDS.,9X,11HFINAL SPEED/16H  X (FT)  Y (FT),5X,
&     16H  X (FT)  Y (FT),8X,5H(FPS)//)
7     FØRMAT(1H //////)
      B0=2.*SQRT(A(I,1)/3.14158)
      X1=4.5*B0
      X2=X1+2.2*B0
      X3=5.*X2
      DELX=X1/10.
      DELY=X1/2.
      NJ=1000
      NK=1000
      DØ 895 J=1,NK
      X0=(J-1)*DELY
      PRINT," "
      Y=0.
      M=0
      DØ 890 K=1,NJ
      Y=(K-1)*DELX
      X=X0
      V=0.
      DØ 880 L=1,NT2
      Q0=(Q3(L,I)+Q3(L+1,I))/2.
      IF(Q0)15,18,18
```

```
15  Q0=0.
18  IF(X.GE.X1)GØTØ 50
IF(Y.GT.(.1577*X+B0/2.))GØTØ 20
IF(Y.GT.B0/2.)GØTØ 30
GØTØ 40
20  Q=0.
M=1
GØTØ 100
30  B=.27*X
QA=Q0
10  E=(B-(Y-(X1-X)/9.))/B
Q=QA*(1.-(1.-E**1.5)**2.)**2.
GØTØ 100
40  R=Y/(X1-X)
IF(R-.1111)42,42,30
42  Q=Q0
GØTØ 100
50  IF(X-X2)60,60,70
60  B=.27*X1+(.22*X2-.27*X1)*(X-X1)/(X2-X1)
F=Y/B
IF(F.GT.1)GØTØ 20
E=B0/(1.08*X)+.584
QA=Q0*(1.-(1.-E**1.5)**2.)**2.
GØ TØ 10
62  E=Y/B
IF(E.GT.1)GØTØ 20
Q=Q0*((1.-E**1.5)**4.)*((6.2*B0/X)**2.)
GØTØ 100
70  B=.22*X
GØTØ 62
100  DT=T(L+1)-T(L)
V=V+AA*Q*DT
X=X+V*DT
IF(M-1)880,220,220
220  PRINT 25,X0,Y,X,Y,V
GØTØ 895
880  CØNTINUE
PRINT 25,X0,Y,X,Y,V
IF(V-10.)891,891,890
891  K=NJ
IF(Y.LT.DELX)J=NK
25  FØRMAT(1H ,F6.1,2X,F6.1,6X,F6.1,2X,F6.1,8X,F6.1/)
890  CØNTINUE
895  CØNTINUE
900  CØNTINUE
RETURN
END
```

Table E-3

SAMPLE PROBLEM LISTING TO SHOW TYPICAL INPUT AND OUTPUT

```
1. AMBIENT AIR PRESSURE (PSIA)?14.7
2. AMBIENT AIR DENSITY (SLUGS/CF)?.002378
3. RØØM VØLUME (CF)?1.311E6
4. NUMBER ØF ØPENINGS (NØT MØRE THAN 8)?8
5. AREAS ØF EACH ØPENING (SF)?25,25,12.6,77,139.8,125,125,229.4
6. LØCATIØN CØDE FØR EACH ØPENING?2,2,2,2,2,2,2,2
7. DELAY IN ENTRY AT EACH ØPENING (MS)?22,208,0,0,0,22,208,241
8. CØMMUNICATIØN DISTANCE (FT) FØR EACH ØPENING?3.5,3.5,2,7,6,3.5,3.5,6
9. CLEARING TIME (MS)?0
10. DRAG CØEFFS FØR LØCATIØN CØDES 1, 2 AND 3?1,0,-.4
11. PEAK FREE FIELD ØVERPRESSURE (PSIG)?10
12. DURATIØN ØF PØSITIVE PHASE (SEC)?4
13. WANT PEAK VALUES ØNLY (.TRUE. ØR .FALSE.)?F
14. INTERVAL BETWEEN VALUES ØF ØUTPUT (MS)?50
15. WANT  DECLINE ØF RØØM PRESSURE (.TRUE. ØR .FALSE.)?F
16. WANT ØUTSIDE PRESSURE (.TRUE. ØR .FALSE.)?T
17. WANT DYNAMIC PRESSURES (.TRUE. ØR .FALSE.)?T
18. WANT TRANSLATIØN EFFECTS (.TRUE. ØR .FALSE.)?T
19. ACCELERATIØN CØEFFICIENT (SF/SLUG)?.708
```

ØUTSIDE PRESSURES (PSIG) AT EACH ØPENING

ØPENING NØ. / TIME STEP NØ.	1	2	3	4	5	6	7	8
1	0.	0.	10.00	10.00	10.00	0.	0.	0.
2	9.75	0.	9.75	9.75	9.75	9.75	0.	0.
3	9.51	0.	9.51	9.51	9.51	9.51	0.	0.
4	9.27	0.	9.27	9.27	9.27	9.27	0.	0.
5	9.04	0.	9.04	9.04	9.04	9.04	0.	0.
6	8.81	8.81	8.81	8.81	8.81	8.81	8.81	8.81
7	8.58	8.58	8.58	8.58	8.58	8.58	8.58	8.58
8	8.36	8.36	8.36	8.36	8.36	8.36	8.36	8.36
9	8.14	8.14	8.14	8.14	8.14	8.14	8.14	8.14
10	7.93	7.93	7.93	7.93	7.93	7.93	7.93	7.93
11	7.72	7.72	7.72	7.72	7.72	7.72	7.72	7.72
12	7.52	7.52	7.52	7.52	7.52	7.52	7.52	7.52
13	7.32	7.32	7.32	7.32	7.32	7.32	7.32	7.32
14	7.12	7.12	7.12	7.12	7.12	7.12	7.12	7.12
15	6.93	6.93	6.93	6.93	6.93	6.93	6.93	6.93
16	6.74	6.74	6.74	6.74	6.74	6.74	6.74	6.74
17	6.55	6.55	6.55	6.55	6.55	6.55	6.55	6.55
18	6.43	6.43	6.43	6.43	6.43	6.43	6.43	6.43

TIME STEP NØ.	TIME(SEC)	INSIDE PRESSURE (PSIG)
1	0.	0.
2	0.5000E-01	0.2165E+00
3	0.1000E+00	0.4655E+00
4	0.1500E+00	0.7116E+00
5	0.2000E+00	0.9550E+00
6	0.2500E+00	0.1339E+01
7	0.3000E+00	0.1815E+01
8	0.3500E+00	0.2286E+01
9	0.4000E+00	0.2752E+01
10	0.4500E+00	0.3213E+01
11	0.5000E+00	0.3669E+01
12	0.5500E+00	0.4120E+01
13	0.6000E+00	0.4567E+01
14	0.6500E+00	0.5008E+01
15	0.7000E+00	0.5446E+01
16	0.7500E+00	0.5879E+01
17	0.8000E+00	0.6308E+01
18	0.8333E+00	0.6256E+01

CØRE DYNAMIC PRESSURES (PSI) AT EACH ØPENING

ØPENING NØ. / TIME(SEC)	1	2	3	4	5	6	7	8
0.	0.	0.	0.	0.	0.	0.	0.	0.
0.050	4.33	0.	4.33	4.33	4.33	4.33	0.	0.
0.100	4.21	0.	4.21	4.21	4.21	4.21	0.	0.
0.150	4.09	0.	4.09	4.09	4.09	4.09	0.	0.
0.200	3.98	0.	3.98	3.98	3.98	3.98	0.	0.
0.250	3.86	3.86	3.86	3.86	3.86	3.86	3.86	3.86
0.300	3.72	3.72	3.72	3.72	3.72	3.72	3.72	3.72
0.350	3.58	3.58	3.58	3.58	3.58	3.58	3.58	3.58

0.400	3.46	3.46	3.46	3.46	3.46	3.46	3.46	3.46
0.450	3.34	3.34	3.34	3.34	3.34	3.34	3.34	3.34
0.500	3.23	3.23	3.23	3.23	3.23	3.23	3.23	3.23
0.550	3.12	3.12	3.12	3.12	3.12	3.12	3.12	3.12
0.600	3.02	3.02	3.02	3.02	3.02	3.02	3.02	3.02
0.650	2.93	2.93	2.93	2.93	2.93	2.93	2.93	2.93
0.700	2.84	2.84	2.84	2.84	2.84	2.84	2.84	2.84
0.750	2.75	2.75	2.75	2.75	2.75	2.75	2.75	2.75
0.800	2.67	2.67	2.67	2.67	2.67	2.67	2.67	2.67
0.833	0.	0.	0.	0.	0.	0.	0.	0.

TRANSLATION OF OBJECT

ACCELERATION COEFFICIENT = 0.7080 (SF/SLUG)
COORDINATES CENTERED IN OPENING

OPENING NO. 1

INITIAL COORDS. X (FT)	Y (FT)	FINAL COORDS. X (FT)	Y (FT)	FINAL SPEED (FPS)
0.	0.	113.1	0.	197.1
0.	2.5	91.1	2.5	154.8
0.	5.1	0.	5.1	0.
12.7	0.	115.6	0.	173.7
12.7	2.5	80.7	2.5	123.1
12.7	5.1	12.7	5.1	0.
25.4	0.	110.0	0.	145.2
25.4	2.5	76.0	2.5	97.0
25.4	5.1	31.7	5.1	12.9
25.4	7.6	25.4	7.6	0.
38.1	0.	110.6	0.	121.2
38.1	2.5	83.6	2.5	85.5
38.1	5.1	47.7	5.1	21.8
38.1	7.6	38.1	7.6	0.1
50.8	0.	99.6	0.	88.4
50.8	2.5	85.5	2.5	67.1
50.8	5.1	65.5	5.1	31.3
50.8	7.6	53.1	7.6	5.2
63.5	0.	97.9	0.	65.8
63.5	2.5	89.9	2.5	52.3
63.5	5.1	78.1	5.1	30.6
63.5	7.6	68.7	7.6	11.2
63.5	10.2	64.3	10.2	1.8
76.2	0.	101.4	0.	49.9
76.2	2.5	96.6	2.5	41.2
76.2	5.1	89.2	5.1	27.2
76.2	7.6	82.6	7.6	13.8
76.2	10.2	78.4	10.2	4.7
88.9	0.	108.0	0.	38.7
88.9	2.5	104.9	2.5	32.9
88.9	5.1	100.2	5.1	23.6
88.9	7.6	95.5	7.6	14.1
88.9	10.2	92.0	10.2	6.7
101.6	0.	116.5	0.	30.6
101.6	2.5	114.5	2.5	26.6
101.6	5.1	111.2	5.1	20.2
101.6	7.6	107.9	7.6	13.5
101.6	10.2	105.2	10.2	7.7
114.2	0.	126.2	0.	24.7
114.2	2.5	124.8	2.5	21.9
114.2	5.1	122.5	5.1	17.4
114.2	7.6	120.2	7.6	12.4
114.2	10.2	118.0	10.2	8.0
126.9	0.	136.7	0.	20.3
126.9	2.5	135.7	2.5	18.3
126.9	5.1	134.1	5.1	15.0
126.9	7.6	132.3	7.6	11.3
126.9	10.2	130.6	10.2	7.8
139.6	0.	147.7	0.	16.9
139.6	2.5	147.0	2.5	15.5
139.6	5.1	145.8	5.1	13.0
139.6	7.6	144.5	7.6	10.2
139.6	10.2	143.2	10.2	7.5
152.3	0.	159.2	0.	14.3
152.3	2.5	158.6	2.5	13.2
152.3	5.1	157.7	5.1	11.3
152.3	7.6	156.7	7.6	9.2
165.0	0.	170.9	0.	12.3
165.0	2.5	170.5	2.5	11.4
165.0	5.1	169.8	5.1	10.0

Table E-3 (Concluded)

177.7	0.	182.8	0.	10.6
177.7	2.5	182.5	2.5	10.0
190.4	0.	194.8	0.	9.3

ØPENING NØ. 2

INITIAL CØØRDS. X (FT)	Y (FT)	FINAL CØØRDS. X (FT)	Y (FT)	FINAL SPEED (FPS)
0.	0.	66.2	0.	169.9
0.	2.5	54.2	2.5	128.7
0.	5.1	0.	5.1	0.
12.7	0.	75.1	0.	153.0
12.7	2.5	51.8	2.5	99.5
12.7	5.1	12.7	5.1	0.
25.4	0.	75.9	0.	124.9
25.4	2.5	53.8	2.5	75.6
25.4	5.1	28.8	5.1	9.3

between the blastward face and the opening; and an additional delay may be caused if a door or window resists blast entry for a certain time. Also, the user must type in the free-field duration of the positive overpressure, from which the program calculates the decay of the outside pressure by methods described in Refs. 1 and 3. Since both peak free-field overpressure and positive phase duration are specified, a specific value of weapon yield is tacitly implied.

Only three different pressure-time histories may be used in any one problem. The user must specify the history appropriate to each opening by the use of a "location code." The code number 1 means the history contains a reflected pressure pulse that clears during the "clearing time" (which also must be specified). The code numbers 2 and 3 are both for pressure-time histories that have no reflected pulse.

Corresponding to each location code number the user must specify a "drag coefficient," which is used by the program to calculate the drag pressure on the outside wall containing the opening (methodology is described in Section IIC3). The total pressure against an opening is the free-field pressure plus any pressure increments due to reflection and any increments or decrements due to drag. If the location code is 2 or 3 and the drag coefficient is zero, the total pressure is the free-field pressure (e.g., a fully buried structure's cover slab, in a Mach region). The program cannot compute pressure increments when the impact of the blast wave is not head-on. The user must estimate whether the conditions of impact at each wall of his problem are more nearly head-on or side-on.

Referring to Table E-3:

- The first two questions ask for the outside pressure and air density immediately before the arrival of the blast wave. In the sample these questions have been answered from information for the standard sea level atmosphere listed in Table 6.1 of Volume 1.

- In the third and fourth questions the program obtains pertinent physical parameters of the open shelter: room volume in cubic feet and number of openings through which it fills. If the user does not want translational (jet effect) information in the neighborhood of two or more openings, and if these openings are in the same wall, he should add their areas together and consider the several openings as a single opening. The computer output formats are arranged for a maximum of eight openings but the program will accept any integral number. The response to "Number of openings (not more than 8)?" must be an integer, typed with no decimal point.

- In answering the next four questions the user must enter data for each of the openings included in the response to the fourth question. The sequence of items in each list must be such that the openings to which the items pertain are in the same order after each question. Opening areas are entered in square feet, Location code for each opening must be an integer: 1, 2, or 3, typed without a decimal. Delay in entry at each opening is in milliseconds; in the absence of resistance to entry at the opening, the delay may be calculated by dividing the distance to the opening (measured along the line of blast travel from the blastward wall) by the shock speed. Such a delay for any opening in the blastward wall will be zero. Shock speed in standard air may be found in Table E-4 as a function of peak overpressure. Whenever the blast wave must break a structure, such as a door or window, to gain entry to the room, a breakage time delay must be included in the delay time. Breakage time for ordinary window glass is approximately 4 ms[4]. An independent estimate of time to failure must be made by the engineer for each door and wall subjected to blast. Communication distance (eighth question) is that distance over which sound waves must "communicate" to the entering wave the shape and size of the opening. Were there to be no effect on the blast wave arising from the edges of the aperture or entry channel, the entering air flow would remain what it is initially, that is, shock afterflow. At free-field overpressures above about 20 psig this afterflow is usually stronger than jet flow; below approximately 20 psig afterflow is usually weaker. The program interpolates between afterflow and jet flow, based on a "communication" time, or time to establish jet flow as described in Section IIC1, which in turn is based on the program user's input value of "communication distance." In the case of a simple opening, this distance is the shortest dimension of the opening. For baffled openings or entry channels through mazes the best estimate of communication distance is the distance along the shortest channel into the room. In the case of a composite opening, that is, an opening consisting of two or more actual windows or other apertures, the communication distance should be found by averaging the distances for all openings included in the composite opening. Each distance is entered in feet.

- The ninth question refers to clearing time of the reflected blast wave from the blastward face of the structure. It is used in calculating the outside pressure on all openings assigned location code number 1. If there is no such opening, any value whatever may be entered for "clearing time." There will be no such openings, for example, in an underground structure. Clearing time

Table E-4

SHOCK SPEEDS IN STANDARD ATMOSPHERE*

P Peak Overpressure (psig)	U Shock Speed (fps)
5.	1268.
10.	1404.
15.	1528.
20.	1714.
25	1750.
30.	1850.
50.	2208.
100.	2917.

---

* Computed from the formula given in Ref. 1:

$$U = c_o \left(1 + \frac{6p}{7P_o}\right)^{0.5}$$

in which P_o = 14.7 psi and c_o = 1116. fps

may be calculated by multiplying by three the shorter of the following two distances: the height of the blastward wall or half its width; and dividing the product by the free-field shock speed from Table E-4. Clearing time is expressed in milliseconds.

- The computer program will assign the three drag coefficients of the tenth question to the three location code numbers in ascending order. The three values shown in the tenth question in Table E-3 are those recommended by Ref. 1 for the reflecting blastward wall (location code 1), the slab at ground level over an underground structure (assigned location code 2 in this example), and the rear or side wall of an above ground structure located at a free-field pressure below 25 psig (assigned location code 3 in this example), respectively. The recommended values are: 1 for a front wall, 0 for a ground level slab in the Mach region, and -0.4 for a roof and walls other than the blastward wall.

- The eleventh and twelfth questions describe the free-field blast wave at the same range or position as the structure. Overpressure is in pounds per square inch and positive phase duration is in seconds. If weapon yield and overpressure are known, positive phase duration can be found in Ref. 1.

- The next seven questions provide the user some choice of output. By answering .TRUE. to the thirteenth question "Want peak values only?", the program will omit intermediate values of inside pressure and print out only the maximum pressure and the time it first occurs. In the answer to the fourteenth question the user specifies the time interval (milliseconds) for which he wants the inside pressure. If the positive phase duration divided by the specified time interval is greater than 500, the calculation will be stopped before the end of the positive phase duration and a warning message containing the value of the time at the end of the calculation printed out. Ordinarily the user will have no need for the inside pressure during the relatively long outflow phase and he may save computer time and shorten the output by answering the fifteenth question, "Want decline of room pressure?" by typing .FALSE. Should the user need the pressure difference across an exterior wall (outside face minus inside face), he will probably want to answer the sixteenth question, "Want outside pressure?" with .TRUE. The pressure difference is then found at any opening in that wall. Ordinarily dynamic pressures in the various openings will not be needed, and the user will answer the seventeenth question, "Want values of dynamic pressure?" by

typing .FALSE. However, the sample output in Table E-3 contains dynamic pressures at each of the eight specified openings. These are "core" values, viz., dynamic pressures in the heart of the jet just inside the opening, as illustrated in Figure E-10.

- The eighteenth question, "Want translation effects?" should be answered .TRUE. if the user wants to estimate the hazard to a shelteree, stores, equipment, or other object arising from the translation of the object by the winds entering through the openings (jet effect). In Table E-3 this question has been answered .TRUE. so that the next question asks for the value of Acceleration Coefficient of the object (in square feet per slug). Acceleration coefficient is defined briefly in Section IIC3 and in great detail in Ref. 14. Table E-5 is a list of some typical values, particularly those for a human body in various postures in relation to the wind. In estimating translation hazard to the human body in a shelter the value for the prone body athwart the wind stream is recommended: 0.708 sf/slug. Values for objects not listed in Table E-5 may in some cases be estimated by the calculations described in Section IIC3.

When computing translation, the program places the body initially at a number of different points on a grid or coordinate system centered at the center of each opening and compute a time-history of displacement and speed for each starting grid point. The x-coordinate lies in the direction of the wind; the y-coordinate lies in any direction normal to the wind. The final coordinates and final speed correspond to the position and speed the unimpeded object has reached at the time the pressure difference between inside and outside becomes zero and the air flow first ceases. Since no decelerating forces are taken into account, the reported speed will be an upper limit on the speed achieved by an actual object.

VI. Edge Diffraction of an Acoustic Wave

A weak planar shock striking a semi-infinite wall head-on can be treated approximately as a self-similar acoustic wave in the manner demonstrated by Ludloff.[16] By this means we can estimate the pressure distribution within an open room during the diffraction phase immediately following blast arrival. Hitherto in this Appendix we have tried to calculate only an average air pressure in the filling room. Such an average may be grossly inadequate in determining the interior pressure load on the blast-struck wall, which is strongly affected immediately after blast arrival and long before the room fills appreciably, by the shock front as it diffracts through openings in that wall.

Table E-6

TYPICAL ACCELERATION COEFFICIENTS[14]

	sf/slug
168-lb man:	
Standing facing wind	1.67
Standing sidewise to wind	0.708
Crouching facing wind	0.676
Crouching sidewise to wind	0.547
Prone aligned with wind	0.203
Prone perpendicular to wind	0.708
Average value for tumbling man in straight, rigid position	0.966
21-g mice, maximum presented area	12.2
180-g rats, maximum presented area	6.12
530-g guinea pigs, maximum presented area	4.83
2100-g rabbits, maximum presented area	2.54
Typical stones:	
0.1 g	21.6
1.0 g	10.3
10.0 g	4.83
Window-glass fragments, 1/8 in. thick:	
0.1 g, all orientations	25.1
1.0 g, edgewise and broadside to wind	15.4-18.4
10.0 g, edgewise and broadside to wind	10.9-23.2
Steel spheres:	
1/8 in. diameter	4.48
1/4 in. diameter	2.24
7/16 in. diameter	1.28
1/2 in. diameter	1.12
9/16 in. diameter	0.998

This acoustic treatment is deficient in several ways. Shock waves do not behave like sound waves but only approach acoustic behavior at low overpressure. However, up to 5 psi free-field overpressure the differences (for our purposes) are not serious, and even above that level acoustic behavior is suggestive of shock behavior. A more restrictive limitation on the usefulness of the acoustic treatment is its two-dimensionality. We find here solutions valid only in a plane normal to an infinite reflecting half-plane and normal to the edge of this half-plane. In other words, the influences of other edges of the opening and of other walls of the room cannot be properly taken into account. However, there may be situations when the two-dimensional acoustic solution presented here will give useful insight into the shock pressure distribution on the inside of a blast-struck wall during the critical period immediately after blast arrival when the exterior air pressure load on the wall is at its peak.

The derivation that follows requires an understanding of the theory of functions of a complex variable. Reference 29 can provide guidance to a reader unfamiliar with the subject. The reader not wishing to pursue the derivation appearing below may turn immediately to Figure E-27, where the results of the calculation will be found in graphic form. A numerical example illustrating the use of Figure E-27 follows the figure.

In the acoustic approximation, all disturbances of effects are assumed to be propagated with sound speed.* Thus, after the incoming wave front strikes the semi-infinite wall, the influence of the edge will be felt only within a cylinder whose axis is the edge and whose radius is

$$c\,t$$

where c is sound speed and t is elapsed time after initial impact. If a Cartesian coordinate system is placed so that the edge of the semi-infinite plane becomes the z-axis and the negative y-axis lies in the plane, the location of the circle of influence of the edge is

$$x^2 + y^2 = c^2 t^2$$

and the equation satisfied by the overpressure p is

$$\frac{\partial^2 p}{\partial x^2} + \frac{\partial^2 p}{\partial y^2} = \frac{1}{c^2}\frac{\partial^2 p}{\partial t^2} \qquad (84)$$

The orientation of the circle and the wall is shown in Figure E-24. If a change of variables is made:

* Which is assumed constant throughout the calculation. In an actual blast the temperature - and hence the sound speed - will change from time to time and place to place.

$$\eta = \frac{y}{ct}, \; \sigma = \frac{x}{ct}, \text{ and } \tan\theta = \frac{y}{x} = \frac{\eta}{\sigma} \tag{85}$$

then in the new coordinates (η, σ, θ) the disturbance is confined to a circle of unit radius. If, further, radii are changed in scale according to the formula:

$$\rho = \frac{r}{1 + (1 - r^2)^{1/2}} \tag{86}$$

where ρ is the new radius and $r^2 = \eta^2 + \sigma^2$, then the equation satisfied by p in the cylindrical polar coordinates (ρ, θ) can be written

$$\rho \frac{\partial}{\partial\rho}\left(\rho \frac{\partial p}{\partial\rho}\right) + \frac{\partial^2 p}{\partial\theta^2} = 0 \tag{87}$$

This is Laplace's equation and is satisfied by the imaginary component of any analytic function of the complex variable.

$$\zeta = \rho\, e^{i\theta}$$

In the case of edge diffraction of a weak shock this method yields a solution for $0 \le r \le 1$ (or $0 \le \rho \le 1$). The angle θ lies in the range $-\pi/2 \le \theta \le 3\pi/2$, as illustrated in Figure E-24. The origin of coordinates labeled 0.

The boundary conditions are determined by physical considerations. Because the acoustic Eq. (84) or (87) is linear, the incident overpressure may be taken as unity and the pressure reflected from the wall, as 2. The overpressure in the undisturbed air is of course zero. These conditions imply the following pressure values on the circumference of the circle of influence:

$$\left.\begin{array}{ll} -\frac{\pi}{2} \le \theta \le 0 & p = 0 \\ 0 \le \theta \le \pi & p = 1 \\ \pi \le \theta \le \frac{3\pi}{2} & p = 2 \end{array}\right\} \tag{88}$$

Outside the circle pressure takes on uniform values within certain areas, as marked in Figure E-24.

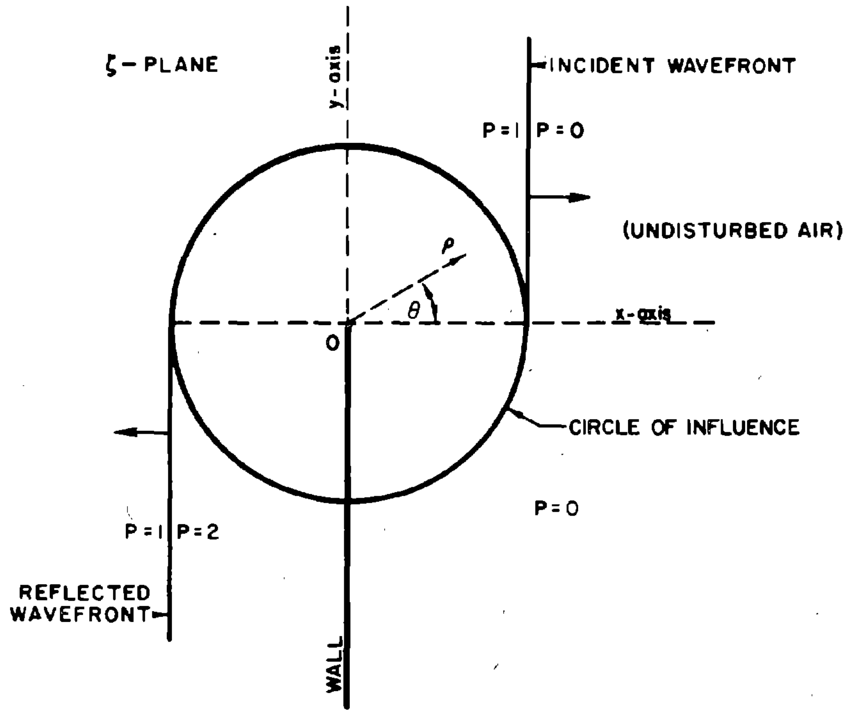

FIGURE E-24 BOUNDARY CONDITIONS ON CIRCLE OF INFLUENCE

Potential theory guarantees that there is only one pressure distribution within the unit circle that satisfies Eq. (87) and meets the foregoing boundary conditions. Equation (87) will be satisfied by any distribution function that is analytic.

A further transformation of variable will make the choice of the correct pressure distribution function clear. Let w be a complex variable defined by:

$$w = (i\zeta)^{1/2} = Re^{i\Phi} \tag{89}$$

where $R = \rho^{1/2}$ and $\Phi = \left(\frac{\pi}{2} + \theta\right)\frac{1}{2}$

In the w-plane, the unit circle of influence becomes a semicircle of radius 1; the back side of the wall lies along the line $\Phi = 0$ while the front side falls along $\Phi = \pi$. The line $\theta = 0$ in the ζ-plane rotates to $\Phi = \pi/4$ and the line $\theta = \pi$ is found along $\Phi = 3\pi/4$. Thus in the w-plane the boundary conditions on the semicircle $R = 1$ become

$$\left.\begin{array}{ll} p = 0 & 0 \le \Phi \le \frac{\pi}{4} \\ p = 1 & \frac{\pi}{4} \le \Phi \le \frac{3\pi}{4} \\ p = 2 & \frac{3\pi}{4} \le \Phi \le \pi \end{array}\right\} \tag{90}$$

Any analytic function of w will also be an analytic function of ζ.

The function $w - e^{\pi i/4}$ is represented by the line BA in Figure E-25 and its argument by the angle α. When A falls on the unit circle, α increased discontinuously from $-\pi/4$ to $3\pi/4$ as A moves counter-clockwise through the point B. The function $w - e^{5\pi i/4}$ is continuous within and on the upper semicircle DBE. Furthermore the included angle γ is

$$\gamma = \alpha + \beta$$

where $\text{Arg}\left[w - e^{i\frac{\pi}{4}}\right] = -\alpha$ and $\text{Arg}\left[w - e^{i\frac{5\pi}{4}}\right] = \beta$. But along the arc EB, $\gamma = \frac{\pi}{2}$. Hence the function

$$f_1 = \frac{1}{\pi}\left\{\text{Arg}\left[\frac{w - e^{i\frac{5\pi}{4}}}{w - e^{i\frac{\pi}{4}}}\right] - \frac{\pi}{2}\right\}$$

is zero along EB and one along BD.

By a similar argument based on Figure E-26 it is clear that the function

$$f_2 = \frac{1}{\pi}\left\{\text{Arg}\left[\frac{w - e^{i\frac{7\pi}{4}}}{w - e^{i\frac{3\pi}{4}}}\right] - \frac{\pi}{2}\right\}$$

is zero along the arc EB′ and one along B′D.

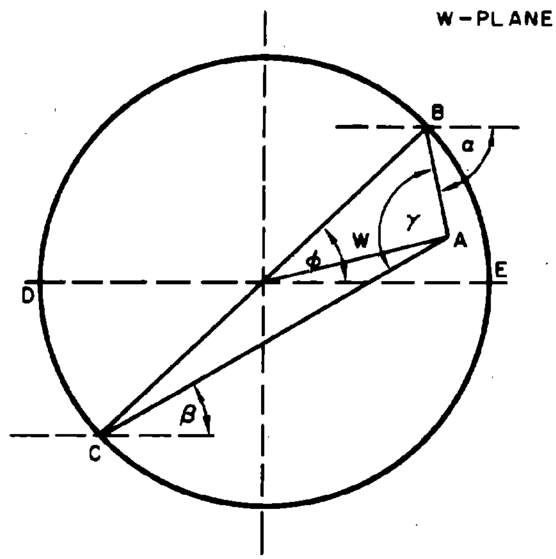

FIGURE E-25 COMPUTATION OF ARGUMENT $\left[\frac{w - e^{5\pi i/4}}{w - e^{\pi i/4}}\right]$

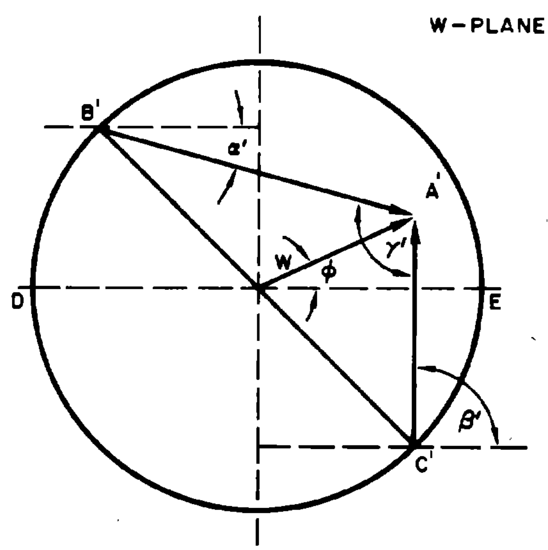

FIGURE E-26 COMPUTATION OF ARGUMENT $\left[\frac{w - e^{7\pi i/4}}{w - e^{3\pi i/4}}\right]$

Thus the sum

$$f_1 + f_2 = \frac{1}{\pi}\left\{ \text{Arg}\left[\frac{w - e^{i\frac{5\pi}{4}}}{w - e^{i\frac{\pi}{4}}} \cdot \frac{w - e^{i\frac{7\pi}{4}}}{w - e^{i\frac{3\pi}{4}}} \right] - \pi \right\} \tag{91}$$

meets the required boundary conditions along the semicircle EBD in the w-plane. But

$$F(w) = \frac{1}{\pi}\left\{ \ell n \left[\frac{w - e^{i\frac{5\pi}{4}}}{w - e^{i\frac{\pi}{4}}} \cdot \frac{w - e^{i\frac{7\pi}{4}}}{w - e^{i\frac{3\pi}{4}}} \right] - i\pi \right\}$$

is analytic in w and z and since $f_1 + f_2$ in Eq. (91) is evidently the imaginary part of F(w), Eq. (91) provides the sought-for expression giving the pressure distribution within and on the circle of disturbance $\rho = R = 1$.

Equation (91) can be written as

$$\pi p = \tan^{-1}\left(\frac{R \sin \Phi + \frac{1}{\sqrt{2}}}{R \cos \Phi - \frac{1}{\sqrt{2}}}\right) + \tan^{-1}\left(\frac{R \sin \Phi + \frac{1}{\sqrt{2}}}{R \cos \Phi - \frac{1}{\sqrt{2}}}\right)$$

$$- \tan^{-1}\left(\frac{R \sin \Phi - \frac{1}{\sqrt{2}}}{R \cos \Phi - \frac{1}{\sqrt{2}}}\right) - \tan^{-1}\left(\frac{R \sin \Phi - \frac{1}{\sqrt{2}}}{R \cos \Phi + \frac{1}{\sqrt{2}}}\right) - \pi \tag{92}$$

where

$$R = \rho^{1/2} = \left[\frac{r}{1 + (1 - r^2)^{1/2}} \right]^{1/2}$$

and

$$\Phi = \frac{\pi}{4} + \frac{\theta}{2}$$

The denominators of the four arctangents in Eq. (92) have real roots in the range $0 \le \Phi \le \pi$ when $\rho \ge 1/2$; and care must be taken to evaluate the inverse functions in such a way that p is continuous within the unit circle. There are no zeros in the denominators when $\rho < \frac{1}{2}$.

If $R \cos \Phi_1 + \frac{1}{\sqrt{2}} = 0$ and

$$R \cos \Phi_2 - \frac{1}{\sqrt{2}} = 0$$

then $\frac{3\pi}{4} \leq \Phi_1 \leq \pi$

and $0 \leq \Phi_2 \leq \frac{\pi}{4}$

If the FORTRAN algorithm is used to evaluate the arctangent terms in Eq. (92) then for

$$\Phi > \Phi_2 \text{ and } R > \frac{1}{\sqrt{2}}$$

the second term,

$$\tan^{-1}\left(\frac{R \sin \Phi + \frac{1}{\sqrt{2}}}{R \cos \Phi - \frac{1}{\sqrt{2}}}\right)$$

can be increased by π, and the third term

$$\tan^{-1}\left(\frac{R \sin \Phi - \frac{1}{\sqrt{2}}}{R \cos \Phi - \frac{1}{\sqrt{2}}}\right)$$

must be decreased by π, or the sum in Eq. (92) increased by 2π. When $\Phi > \Phi_1$ and $R > \frac{1}{\sqrt{2}}$ we must add another 2π to keep the expression for p continuous and insure the existence of its derivatives.

In order to assure continuity with respect to radius the foregoing choices limit the arctangents to certain quadrants where radius R is such that no zeros in the denominators exist, i.e., when $R < \frac{1}{2}$. Thus, since we have chosen to add π to

$$\tan^{-1}\left(\frac{R \sin \Phi + \frac{1}{\sqrt{2}}}{R \cos \Phi - \frac{1}{\sqrt{2}}}\right)$$

for $\Phi > \Phi_2$ and $R > \frac{1}{2}$, we must, when using the FORTRAN algorithm, add π to the same inverse tangent for all Φ when $R < \frac{1}{2}$ in order to place the angle computed in the second quadrant. Similarly, by subtracting π from

$$\tan^{-1}\left(\frac{R \sin \Phi - \frac{1}{\sqrt{2}}}{R \cos \Phi - \frac{1}{\sqrt{2}}}\right)$$

when $\Phi > \Phi_2$ and $R > \frac{1}{2}$ we are placing the arctangent in the range $-\frac{\pi}{2}$ to $-\pi$; hence the same function, when $R < \frac{1}{2}$, must be computed in the same range by subtracting π from the angle as computed by FORTAN. When $R < \frac{1}{2}$ the denominator

$$R \cos \Phi + \frac{1}{\sqrt{2}}$$

is always positive and when $R < \frac{1}{2}$ the FORTRAN choices of quadrant for the two arctangents containing it are consistent with those for $R > \frac{1}{2}$.

Pressure contours, located as outlined above, are shown in Figure E-27, in which the planar acoustic front is moving from left to right past the parallel wall shown as the heavy vertical line in the lower center of the Figure. The reflected wave is moving right to left off the wall (lower left); the incident wave (upper right) has passed the wall. The zone of influence of the edge is a circle centered at the edge.

Numerical Example No. 7 (Pressure Distribution over a Wall Near an Edge). Consider a large opening in a wall struck head-on by a 5-psig blast wave. Taking time t = o at the moment of impact, we estimate the pressure history over the inside and outside surfaces of the wall along a line normal to any edge of the opening. Standard atmospheric conditions are assumed to prevail inside and outside the wall before blast arrival.

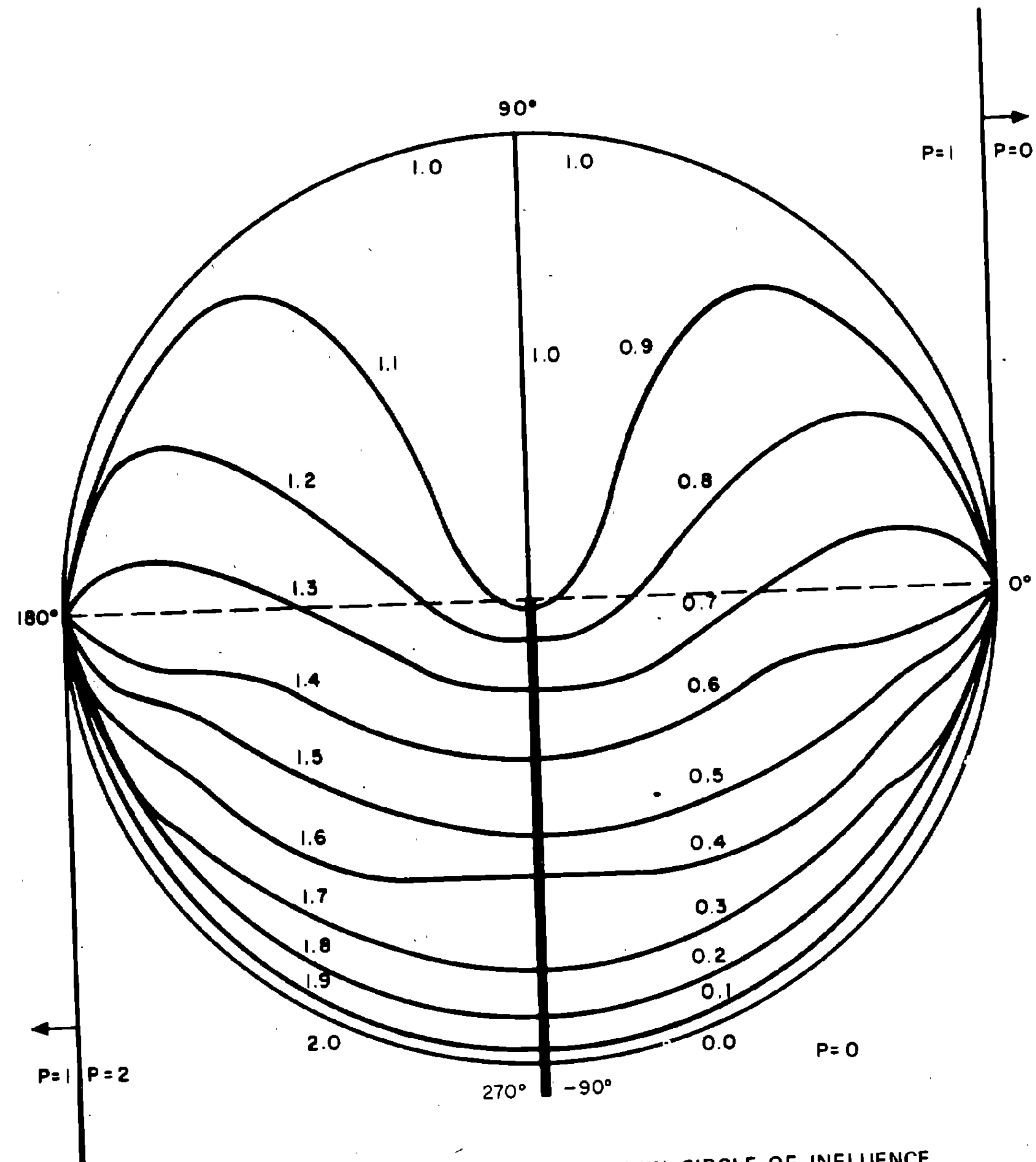

FIGURE E-27 PRESSURE CONTOURS WITHIN CIRCLE OF INFLUENCE

*The extent of the penetration y of the shock front is estimated from the speed of sound**

$$c = 1116 \text{ fps}$$

so that

$$y = ct = 1116\ t.$$

At t = 10 ms, for example, a distance of 11.2 ft along the wall inside the opening has been affected by the entering blast. The pressure distribution within that 11.2 ft can be found by reference to Figure E-27, in which the outermost (circular) contour now corresponds to 11.2 ft. The pressure along the lower right quadrant of that contour is zero. At a distance from the edge of the opening equal to 10.7 ft the pressure is 0.1 × 5 = 0.5 psig. This is where the 0.1 contour intersects the wall. At 5.68 ft from the edge the pressure at t = 10 ms is 0.5 × 5 = 2.5 psig, as given by the intersection of the 0.5 contour and the wall. Outside the wall these same contours are associated with pressures less than the pressure prevailing outside after reflection; that is, outside the wall the 0.1 contour becomes the 2- 0.1 = 1.9 contour, so that the pressure difference across the wall at t = 10 ms and y = 10.7 ft is (1.9 - 0.1) × 5 = 9.0 psig. Beyond the circle of influence, for example at y = 12, the pressure difference is (2.0 - 0.0) × 5 = 10.0 psig.

---

* *Calculated in Numerical Example No. 4.*

NOTATION*

A	Area
A_o	An additive term appearing in Eq. (5)
B	Constant equal to various functions of γ and/or of interior and exterior conditions, appearing in Eq. (5)
b	Half width of jet mixing zone
b_o	Maximum width of jet core
C	Constant
C_d	Drag coefficient
c	Speed of sound in air
c_o	Speed of sound in the standard atmosphere
c_v	Specific heat at constant volume for air
D	Diameter
F	Numerical factor for consistency of units
I	Integral
I	Impulse
K	Discharge coefficient
L	Linear dimension
ℓ	Distance along jet axis measured from opening
ℓ	Distance of travel along pipe

* Numerical subscripts may be used with variables to refer to a particular space or volume; see Preface.

M	Mass of object
M	Constant
m	Mass of air
Δm	Increment of air mass corresponding to time increment Δt
P	Air pressure
P'	Air pressure during immediately preceding time step
P_{1o}	Peak overpressure outside front or first wall
P_{1r}	Total overpressure outside rear wall
P_c	Sum of dynamic and side-on air pressure at time t_c
P_d	Free-field dynamic pressure
P_{dc}	Dynamic pressure in blast wave at time t_c
P_{do}	Peak dynamic pressure in blast wave
P_o	Ambient air pressure
P_R	Reflected pressure at a wall struck by blast wave
P_s	Free-field side-on overpressure
P_{sc}	Free-field side-on blast overpressure at time t_c
P_{so}	Free-field peak side-on overpressure
p	Overpressure
q	Dynamic pressure of air
q_{core}	Dynamic pressure of air in jet core
$\overline{q}$	(Spatial) average dynamic pressure in jet at one cross section
R	Gas constant for air (See Ref. 5)
R	Radius of jet of streming air

Re	Reynolds number
r	Radial coordinate, i.e., $r = (\eta^2 + \sigma^2)^{1/2}$
r	Radial coordinate measured from axis of jet
r	Ratio of pressures
S	Specific entropy of air
ΔS	Increment of entropy
s	Wall dimension used to compute clearing time
s	Distance
T	Absolute temperature
T	Time of passage of sound across object
ΔT	Filling time or interval between first arrival of blast and achievement of pressure equilibrium
t	Time measured from first arrival of blast at structure
t_c	Clearing time of structure in blast wave
t_o	Duration of positive side-on overpressure
t_1	Time required to establish jet flow through an opening
Δt	Increment of time
U	Blast front speed
u	Particle speed of air
u_m	Air particle speed along jet axis
u_o	Air particle (wind) speed in jet core
V	Volume of room or other space to be filled
ΔV	Increment of air volume

v	Speed of object in air stream
x	Cartesian coordinate
y	Cartesian coordinate
y	Unknown variable in Eq. (5)
y	Distance from outer jet boundary along normal to jet axis to point within mixing zone
y_o	A specific solution of Eq. (5), i.e., $y_o = 0.1912$
w	Complex variable $Re^{i\Phi}$
Δw	Energy increment
α	Angle in complex w-plane
α	A certain function of y
α	Angle between outer jet boundary and jet axis
β	Angle in complex w-plane
γ	Ratio of specific heat at constant pressure to specific heat at constant volume
γ	Angle in complex w-plane
Δ	Correction term applied to momentum balance associated with one control surface
ξ	Complex variable $\rho e^{i\theta}$
λ	Coefficient of resistance to flow in pipes
η	Viscosity of air
η	Coordinate of point in jet mixing zone; equal to y/b
η	Time independent coordinate, i.e., $\eta = y/ct$
θ	Angle between inward normal to surface and the positive direction of the x-axis

θ Angular coordinate, i.e., $\tan \theta = y/x$

θ Ratio between temperature in jet core and that in room

ρ Density of air

ρ Reduced radial coordinate

ρ' Air density during immediately preceding time step

ρ_{core} Air density in jet core

ρ_o Ambient air density

ρ_w Density of water

σ Time independent coordinate, i.e., $\sigma = x/ct$

τ Time required to transmit a sound signal over the longest room dimension

π Ratio of circumference to diameter of circle

E-134 BLANK

REFERENCES

1. Glasstone, S., editor, The Effects of Nuclear Weapons, U.S. Dept. of Defense and Atomic Energy Commission, Feb. 1964 reprint (with changes) of 1962 edition; Govt. Printing Office, Washington, D.C. 20402

2. Moulton, J., editor, Nuclear Weapons Blast Phenomena, Defense Atomic Support Agency (now Defense Nuclear Agency), Washington, D.C., DASA 1200 Vol. I, March 1960

3. Design of Structures to Resist the Effects of Atomic Weapons, EM 1110-345-413, Weapons Effects Data, Manuals - Corps of Engineers, U.S. Army, Washington, D.C., 1 July 1959

4. Iverson, J., Existing Structures Evaluation, Part II: Window Glass and Applications, Stanford Research Institute for the Office of Civil Defense, Menlo Park, Calif., December 1968 (AD-687 294)

5. Eshbach, O. W., editor, Handbook of Engineering Fundamentals, 2nd edition, John Wiley & Sons, 1952 (see chapter 8 for discussion of entropy and internal energy)

6. Oswatitsch, K., Gas Dynamics, Academic Press, 1956 (for a discussion of the concept and use of control surfaces in the study of flowing compressible fluids)

7. Eshbach, O. W., op. cit., pg 8-23

8. Eshbach, O. W., op. cit., pg 8-21

9. Coulter, G. A., Air Shock Filling of Model Rooms, Ballistic Research Laboratories Memorandum Report No. 1916, Aberdeen Proving Ground, Md., March 1968, Figure 28, pg 54 (AD-670 937)

10. Childers, H. M., C. A. Vansant and D. F. Mokrauer, Open Shelter Feasibility Study, The Vertex Corp. for the Office of Civil Defense, Kensington, Md., October 1968

11. Melichar, J. F., Air-Blast-Induced Aerodynamic Effects in Blast-Slanted Basement Shelters, URS Corporation for Office of Civil Defense, URS 692-3, OCD Work Unit 1126E, Burlingame, Calif., Jan. 1969 (AD-691 773)

12. Melichar, J. F., The Propagation of Blast Waves into Chambers: Aerodynamic Mechanisms, Terminal Ballistics Laboratory, Ballistic Research Laboratories, Aberdeen Proving Ground, Md., November 1967

13. Shapiro, A., The Dynamics and Thermodynamics of Compressible Fluid Flow, Volume I, The Ronald Press Co., 1953 (art. 4.7 for treating flow into a large reservoir which is steadily being evacuated)

14. Bowen, I. G., et al., A Model Designed to Predict the Motion of Objects Translated By Classical Blast Waves, Lovelace Foundation for Medical Education and Research, Albuquerque, N.M., U.S. Atomic Energy Commission CEX-58.9, June 29, 1961

15. Brode, H. L., Point Source Explosion in Air, RM-1824-AEC, the RAND Corporation, December 3, 1956

16. Ludloff, A. F., "On Aerodynamics of Blasts," Advances in Applied Mechanics, Vol. III, R. V. Mises, T. V. Kármán, editors, Academic Press, 1953

17. Air Blast Attentuation, IIT Research Institute for the Office of the Chief of Engineers, U.S. Army, Technical Manuscript S-1R, February 1971 (AD-729 425)

18. Coulter, G. A., op. cit., Figures 19 and 20, pp 43 and 44

19. Coulter, G. A., op. cit., Fig. 7, pg 27

20. Abramovich, G. N., The Theory of Turbulent Jets, M.I.T. Press, 1963

21. Coulter G. A., Flow in Model Rooms Caused by Air Shock Waves, Ballistic Research Laboratories Memorandum Report No. 2044, Aberdeen Proving Ground, Md., July 1970 (AD-711 885)

22. Melichar, J. F., Analysis of the Effect of Shelter Openings on Blast Protection, URS Research Company, San Mateo, Calif., for U.S. Office of Civil Defense, September 1970 (AD-724 710)

23. Taylor, W. J., Ballistic Research Laboratories, Aberdeen Proving Ground, Maryland, personal communication, March 1971

24. Kriebel, A. R., Airblast in Tunnels and Chambers, URS Research Company, San Mateo, Calif., for U.S. Defense Nuclear Agency, DRAFT Final Report, February 1972

25. Coulter, G. A., Blast Loading in Existing Structures - Basement Models, Ballistic Research Laboratories Memorandum Report No. 2208, Aberdeen Proving Ground, Md., August 1972 (AD-751 769)

26. Hoerner, S., Fluid Dynamic Drag, published by the author, Midland Park, N.J., Second Edition, 1958

27. Schlichting, H., Boundary Layer Theory, Fourth Edition, McGraw-Hill, 1960

28. Rouse, H., Elementary Mechanics of Fluids, John Wiley & Sons, 1953

29. Churchill, R. V., Complex Variables and Applications, Second Edition, McGraw-Hill, 1960

Appendix F

SLAB AND WALL DESIGN EXAMPLES

By C. K. Wiehle

Appendix F

SLAB AND WALL DESIGN EXAMPLES

By C. K. Wiehle

U.S. POST OFFICE AND COURTHOUSE
NEWNAN, GEORGIA

I. FIRST FLOOR SLAB

A. Loading *

$p_{so} = 15\,psi$; Assume zero rise-time

For $W = 1\,Mt$, $t_d = t_i = 1.0\,sec$ Ref. 1, p.3-45

B. Preliminary Slab Design #1

Slab over basement Reserve Room

Design as one-way simply supported slab, $\mu = 3.0$

1. Percent Reinforcing Steel, Assume $\phi_c = 2.0$ (max.) Ref. 1, p. 8-4

2. Dynamic Material Properties

$f_{dy} = 42{,}000\ psi$, structural grade Ref. 1, p.6-5

$f'_{dc} = 3{,}750\ psi$, for concrete with $f'_c = 3000\,psi$ " , p6-10

3. Slab Dead Load, Assume $t = 12''$

Equivalent dynamic load $= \frac{145}{1728}\, t\left(1-\frac{1}{2\mu}\right)$ Ref. 1, p. 9-4 & Ref. 2, p.145

$= \frac{145 \times 12}{1728}\left(\frac{5}{6}\right) = 0.84\,psi$

4. Required Resistance

$p_m = p_{so} + 0.84 = \left(1-\frac{1}{2\mu}\right) q$ Ref. 2, p.145

$q = \frac{6}{5}(15 + .84) = 19.0\ psi$

$\frac{d}{L} = \left(\frac{q_f}{0.072\,\phi_c \cdot f_{dy}}\right)^{1/2}$ Ref. 1, p. 8-5

where $q_f = q$

---

* Blast is assumed excluded from entering the shelter area.

$$\frac{d}{L} = \left(\frac{19.0}{(.072)(2.0)(42,000)}\right)^{1/2} = 0.05605$$

$L = 32'\text{-}2'' - (7'\text{-}7'' + 1'\text{-}0'' + 8'') = 22'\text{-}11''$ (clear span)

(Assume outer wall $t = 12''$; inner wall $t = 8''$)

Therefore, $d = (.05605)(22.92)(12) = 15.42''$

Use $d = 15\frac{1}{2}''$

5. Shear Check

For $\frac{d}{L} = 0.05605$, $f_c' = 3000$ psi — Ref. 1, Fig. 9-3

$p_m' \simeq 50$ psi > 15.84 psi — Ref. 1, Fig. 9-3

Therefore, section adequate for shear

6. Diagonal Tension Check

$$q_y = 100\left(\frac{1}{2 + \phi'/\phi_c}\right)\left(1 + \frac{2\phi_v f_{dy}}{10^5}\right)\left(\phi_c f_c'\right)^{1/2}\left(\frac{d}{L}\right)^2$$ Ref. 1, Fig. 8-2b

$$q_y = 100\left(\frac{1}{2+.25}\right)(1+0)(2\times 3000)^{1/2}(.05605)^2$$

where $\phi' = 0.25\,\phi_c$ (assumed)

$q_y = 10.8$ psi < 19.0 psi $\therefore$ Section inadequate

However, minimum $q_y = 3.5(f_c')^{1/2}\frac{d}{L}$ — Ref. 1, Fig. 8-2b

Therefore,

$q_y = (3.5)(3000)^{1/2}(.05605) = 10.7$ psi < 19.0 psi

and section is inadequate for diagonal tension.

Required ϕ_v for $q_y = 19.0$ psi is

$$19.0 = (100)\left(\frac{1}{2.25}\right)\left(1 + \frac{2\phi_v\, 42,000}{10^5}\right)(6000)^{1/2}(.05605)^2$$

or

$\phi_v = 0.90$

Since $\phi_c = 2.0$, provide required web reinforcement by bending up longitudinal rebar and stirrups if required.

7. Dynamic Analysis of Preliminary Slab Design #1

Determine slab thickness

$A_s = p b d = (.020)(12)(15.5) = 3.72\ \square''/ft$

Therefore use #11 @ 5", $A_s = 3.74\ \square''/ft$, $D = 1.410''$

For a 0.75" cover on the reinforcement Ref. 3

$t = 15.5 + 0.75 + \frac{1.410}{2} = 16.96''$ Use 17"

$W = \frac{(17)(1)(12)}{1728}(145)(22.92) = 392.3\ \#/\text{in. width}$

$m_t = \frac{W}{g} = \frac{392.3}{32.2} = 12.183\ \#\text{-sec}^2/ft/\text{in. width}$

$$I = \frac{b(k'd)^3}{3} + \frac{n b \phi d^3}{100}(1-k')^2$$ Ref. 1, Fig. 8-1

$$n = \frac{E_s}{E_c} = \frac{30}{3} = 10$$

For $f'_c = 3000$ psi, $\phi_c = 2.0$

$k' \simeq 0.46$ (By extrapolation) Ref. 1, Fig. 8-1

$$I = \frac{(1)(.46 \times 15.5)^3}{3} + \frac{(10)(1)(2.0)(15.5)^3(1-.46)^2}{100}$$

$I = 120.8 + 217.2 = 338\ \text{in.}^4/\text{in. width}$

$$k = \frac{384 E_c I}{5L^3} = \frac{(384)(3 \times 10^6)(338)}{(5)(22.92)^3(144)}$$ Ref. 1, Fig. 8-1

$k = 4.4915 \times 10^4\ \#/ft$

Equivalent Single-Degree-of-Freedom System Ref. 4 (-416)

Mass factor, $K_M = 0.5$ *
Load factor, $K_L = 0.64$ *
Resistance factor, $K_R = K_L = 0.64$ *

$m_e = m_t K_M = (12.183)(.5) = 6.0915\ \#\text{-sec}^2/ft/\text{in. width}$

$k_e = k K_L = (4.4915 \times 10^4)(.64) = 2.87456 \times 10^4\ \#/ft$

---

*See also Table 6.3 herein.

$$T_e = 2\pi\sqrt{\frac{m_e}{k_e}} = 2\pi\sqrt{\frac{6.0915}{2.87456 \times 10^4}}$$

$$T_e = 0.091 \text{ sec}$$

$$t_d = 1.0$$

$$\frac{t_d}{T_e} = \frac{1.0}{.091} = 10.99$$

For $\mu = 3.0$, $\quad \dfrac{p_{me}}{q_e} = 0.87$ Ref. 1, Fig. 9-1

$$p_{me} = (15.84)\,K_L$$

$$q_e = \frac{(15.84)\,K_L}{0.87}$$

$$q = \frac{q_e}{K_R} = \frac{15.84}{0.87} = 18.2 \text{ psi}$$

Therefore, preliminary design is adequate since the resistance required for dynamic load is less than the resistance required for design (see step 4). Section will not be redesigned for purposes of cost estimating.

8. Rebound

$$T = \frac{L^2}{(42,500)\sqrt{\phi_c}\;d}$$ Ref. 1, p. 8-11

$$T = \frac{(22.92 \times 12)^2}{(42,500)(2.0)^{1/2}(15.5)} = 0.081 \text{ sec}$$

$$\frac{t_d}{T} = \frac{1.0}{0.081} = 12.3$$

For $\mu = 3.0$ Ref. 1, Fig. B-10

$\phi' \simeq 0.25\phi_c$ *

$\phi' = (.25)(2.0) = 0.50$

$A_s' = p'bd = (.005)(12)(15.5)$

$A_s' = 0.93 \ \square''/ft$

Use #8 @ 10", $A_s' = 0.95 \ \square''/ft$

9. Slab Summary

$f_c' = 3000$ psi

$d = 15.5''$

$t = 17.0''$

$L = 22'\text{-}11''$ (Clear span)

A_s = #11 @ 5" with every other rebar bent up for diagonal tension.

A_s' = #8 @ 10", bent and anchored in both support walls.

Transverse $A_s = 0.0020\,tb$ Ref. 3

$= 0.41 \ \square''/ft$

Use #4 @ 11½" each face

$$\text{Wt. rebars} = (5.313)\left(\frac{12}{5}\right) + (2.670)\left(\frac{12}{10}\right) + (.668)\left(\frac{12}{11.5}\right)(2)$$

$= 17.35$ psf

* For simple supports, $\frac{r}{8y} = \frac{\phi'}{\phi_c}$

II. EXTERIOR WALL

A. Loading — Wall Design #1

Assume that the exterior dynamic soil pressure acts as a uniformly distributed load on the wall, without attenuation with depth. Since there is no interior pressure build-up in the basement, the horizontal dynamic pressure on the wall is taken as

$$p_h = K_o \, p_v$$ Ref. 1, p. 5-54

If it is assumed that $K_o = 0.5$, for an unsaturated cohesive soil of medium to stiff consistency, Ref. 1, p. 4-67 and that $p_v = p_{so}$, then the peak horizontal soil pressure due to the blast loading is

$$p_h = (.5)(15) = 7.5 \text{ psi}$$

The static soil pressure at the top of the wall, with the top of the first floor slab at grade, is

$$p_h = \frac{(30)(1)}{144} = 0.21 \text{ psi}$$ Ref. 5 Sec. 2310

The static soil pressure at the bottom of the wall, for a depth to the top of the footing of 14'-11", is

$$p_h = \frac{(30)(14.917)}{144} = 3.11 \text{ psi}$$

If it is assumed that the static soil pressure is equivalent to a uniformly distributed dynamic soil pressure of

$$p_h = \frac{(.21 + 3.11)}{2} \; \frac{5}{6} = 1.38 \text{ psi},$$ Ref. 1, p. 9-4

then the peak dynamic pressure for design of the wall is

$$p_m = 7.5 + 1.4 = 8.9 \text{ psi.}$$

B. Preliminary Wall Design # 1.

All exterior walls with soil backfill are of similar construction. Design as one-way, simply supported wall, with $\mu = 3.0$.

1. Percent Reinforcing Steel. Assume existing wall thickness is adequate and calculate required steel area. See step 3, below.

2. Dynamic Material Properties

See p. 1.

3. Required Resistance

$$p_m = \frac{5}{6} q = 8.9 \text{ psi}$$

$$q = \frac{6}{5}(8.9) = 10.7 \text{ psi}$$

$$t = 12''$$

For #5 rebar with 1" cover on interior surface

$$d = 12 - \left(1 + \frac{.625}{2}\right) = 10.69''$$

Use $d = 10.5''$

$$q_f = 0.072\, \phi_c\, f_{dy} \left(\frac{d}{L}\right)^2 \qquad \text{Ref. 1, p. 8-5}$$

The clear span of the wall, between the first floor slab and the top of the footing, varies from 13'-6" to 13'-11" (see p. F-10). Therefore assume a span

length of 13'-9" for design purposes. The required percent tensile steel is

$$p_c = \frac{(10.7)}{(.072)(42,000)}\left(\frac{13.75 \times 12}{10.5}\right)^2$$

$$p_c = 0.87$$

$$A_s = pbd = (.0087)(12)(10.5) = 1.10 \quad \square''/ft$$

Use #8 @ 8½", $A_s = 1.12$ □"/ft, $p_c = 0.89$

4. Shear Check

$$\frac{d}{L} = \frac{10.5}{(13.75)(12)} = 0.06364$$

For $f'_c = 3000$ psi

$p'_m \simeq 55$ psi $\gg$ 8.9 psi — Ref. 1, Fig. 9-3

Therefore, section adequate for shear.

5. Diagonal Tension Check

For the existing wall with #4 @ 18"

$A'_s = p'bd = 0.13$

where $d = 12 - \left(2 + \frac{0.5}{2}\right) = 9.75''$

Therefore,

$$p' = \frac{0.13}{(9.75)(12)} = 0.0011, \text{ or } p' = 0.11$$

For ductility $\phi_v = 0.25$ min., and Ref. 1, p.B-6

$$q_y = 100\left(\frac{1}{2+\frac{.11}{.89}}\right)\left(1+\frac{(2)(.25)(42{,}000)}{10^5}\right)(.89\times 3000)^{1/2}(.06364)^2 \quad p.F\text{-}4$$

$q_y = 11.9$ psi > 10.7 psi

Therefore, section adequate for diagonal tension.

6. Dynamic Analysis of Preliminary Wall Design #1

$$T = \frac{(13.75\times 12)^2}{(42{,}500)(.89)^{1/2}\ (10.5)} = 0.065 \text{ sec} \quad p.F\text{-}6$$

With $t_d = 1.0$ sec for dynamic portion of loading, a dynamic analysis is not warranted for cost estimating purposes. See p. F-4.

7. Rebound

$$\frac{t_d}{T} = \frac{1.0}{.065} = 15.4$$

For $\mu = 3.0$

$\phi' \simeq 0.25\,\phi_c$ Ref. 1, Fig. B-10

Existing reinforcement in wall provides

$$\phi' = \frac{.11}{.89}\ \phi_c = 0.12\,\phi_c$$

Therefore, since soil backfill would provide considerable rebound resistance, the existing reinforcing steel is assumed adequate.

8. Exterior Wall Summary

$f'_c = 3000$ psi

$d = 10.5''$

$t = 12''$

$A_s = \#8 @ 8\frac{1}{2}''$ Since $\phi_c = 0.89$ (p. F-8), provide minimum web reinforcement by bending up every third long. rebar.

$A'_s = \#4 @ 18''$ (existing)

Horizontal $A_s = \#4 @ 12''$ each face (existing)

$$Wt.\ rebars = (2.670)\left(\frac{12}{8.5}\right) + (.668)\left(\frac{12}{18}\right) + (.668)(2)$$

$$= 5.55 \text{ psf of wall.}$$

The height, or clear span, of the exterior wall varies due to differences in slab thickness as follows:

(a) Reserve Room

$L = (14'\text{-}11'') - (1'\text{-}5'') = 13'\text{-}6''$

(b) Shop Storage Room *

$L = (14'\text{-}11'') - (1'\text{-}0'') = 13'\text{-}11''$

(c) Shop Room *

$L = (14'\text{-}11'') - (1'\text{-}3\frac{1}{4}'') = 13'\text{-}7\frac{3}{4}''$

(d) Rooms Off Main Corridor *

$L = (14'\text{-}11'') - (1'\text{-}2\frac{1}{2})'' = 13'\text{-}8\frac{1}{2}''$

* Calculations for the slabs over these rooms not included in this example.

9. Check Wall Design #1 for Vertical Load

Maximum vertical load occurs in wall supporting Slab Design #1 in Reserve Room and is equal to

$V = 0.39\,Q + 0.11F$ Ref. 4

$L = (32'\text{-}2'') - (7'\text{-}7'') = 24'\text{-}7''$ p. F-4

$q = 19.0$ psi

$Q = qL = (19.0)(24.583 \times 12) = 5605$ #/in. width

$F = p_m L = (15.8)(24.583 \times 12) = 4661$ #/in. width

If it is assumed that the peak reaction occurs prior to any significant decay in the blast wave then,

$V = (.39)(5605) + (.11)(4661) = 2699$ #/in. width

From other wall analyses, it can be concluded that a vertical load of this magnitude would probably increase the wall resistance above that for lateral load only. Therefore, it is assumed for this example that the Wall Design #1 is adequate to resist the vertical load only, and the combined lateral and vertical load without modification.

10. Footing Design

(a) Allowable Soil Bearing Pressure

Assume a medium stiff clay or sandy clay

Static

$p_v = 2000 + 200H$ psf (max. = 6000 psf) Ref. 5 Sec. 2805

where H = depth below minimum depth

$\simeq 15-1 \simeq 14'$

$p_v = 2000 + (200)(14) = 4800$ psf

Dynamic

Allowable dynamic soil bearing is taken as twice the static value plus the peak free-field soil pressure. Ref. 1, p. 9-14

$$p_v = \frac{(2)(4800)}{144} + 15 = 82 \text{ psi}$$

(b) Total Force on Wall Footing

Slab

$t = 17''$, $L = 24'$-$7''$

$$D.L. = \frac{(17)(1)(12)}{1728}(145)\left(\frac{24.583}{2}\right) = 210 \text{ \#/in. wall width.}$$

$L.L. = 0$ (Assumed removed by blast)

Wall

$t = 12''$, $L = 13'$-$6''$

$$D.L. = \frac{(12)(1)(12)}{1728}(145)(13.5) = 163 \text{ \#/in. width}$$

Dynamic Equivalent for D.L. Ref. 1, p. 9-4

$P_1 = (210 + 163)\left(\frac{5}{6}\right) = 311$ #/in. width

Total Vertical Load on Wall Footing

$P_T = P_1 + V$ (neglecting footing weight)

$P_T = 311 + 2699 = 3010$ #/in. width.

(c) Wall Footing Width

Use continuous wall spread footing.

Required width

$$L = \frac{P_T}{p_v} = \frac{3010}{82} = 36.7''$$

Use $L = 38''$

Design pressure $p_m = \frac{3010}{38} = 79$ psi

(d) Wall Footing Thickness

Span from wall face

$$\ell = \frac{38-12}{2} = 13''$$

$$q_f = 0.018\,\phi_e\,f_{dy}\left(\frac{d}{\ell}\right)^2$$ Ref. 1, p. 8-47

For $q_f = p_m$, $d = 8.5''$, $t = 12''$

and

$$\phi_e = \frac{79}{(.018)(42{,}000)}\left(\frac{13}{8.5}\right)^2 = 0.244$$

$A_s = \rho b d = (.00244)(12)(8.5) = 0.25\ \square''/ft$

Use #4 @ 9½", $A_s = 0.25\ \square''/ft$

(e) Diagonal Tension Check

$$q_y \simeq 25\sqrt{f'_c\ \phi}\left(\frac{d}{L}\right)^2$$ Ref. 1, p. 8-48

For $f'_c = 2000$ psi

$$q_y \simeq (25)(.244 \times 2000)^{1/2}\left(\frac{8.5}{13}\right)^2$$

$$q_y \simeq 236\ psi > 79\ psi$$

Therefore, section is adequate for diagonal tension.

(f) Wall Footing Summary

$f'_c = 2000\ psi$

$d = 8.5''$

$t = 12''$

$L = 38''$

$A_s = \#4 @ 9½''$

Transverse $A_s = 0.0020\, t\, b$

$= 0.91\ \square''$

Use 3-#5, $A_s = 0.93\ \square''$

Dowels, 3'-0" long to match wall rebars

Use #8 @ 8½" and #4 @ 18"

$$Wt.\ rebars = (.668)\left(\frac{12}{9.5}\right)\left(\frac{38}{12}\right) + (1.043)(3) + (2.670)\left(\frac{12}{8.5}\right)(3) + (.668)\left(\frac{12}{18}\right)(3)$$

$\doteq 18.45\ plf$

$= 5.82\ psf$

III. INTERIOR SHELTER WALL

A. Loading - Wall Design #2

Assume that the blast loading on the interior shelter wall, due to the blast pressure build-up in the non-slanted area of the basement, is equal to the incident blast overpressure. The critical wall loading is for the lateral blast loading acting on the wall alone without considering vertical forces on the wall due to slab reactions.

B. Preliminary Interior Shelter Wall Design #2

Assume for design purposes that all interior walls enclosing the shelter area are similar. Design as one-way wall spanning between first and basement floor slabs, with $\mu = 3.0$.

1. Percent Reinforcing Steel, Assume $\phi_c = 2.0$ (max.) Ref. 1, p. B-4

2. Dynamic Material Properties

$f_{dy} = 42{,}000$ psi, structural grade

$f'_{dc} = 3{,}750$ psi, for concrete with $f'_c = 3000$ psi

3. Required Resistance

$$q = \frac{6}{5}(15) = 18.0 \text{ psi}$$ p. F-3

$$\frac{d}{L} = \left(\frac{q_f}{0.072\, \phi_c f_{dy}}\right)^{1/2}$$ Ref. 1, p. B-5

$L = (14'\text{-}0'') - (1'\text{-}2\tfrac{1}{2}'') = 12'\text{-}9\tfrac{1}{2}''$

(Maximum clear span for corridor wall).

$$d = (12.792 \times 12)\left(\frac{180}{(0.072)(2.0)(42{,}000)}\right)^{1/2}$$

$d = 8.4''$

Use $d = 8\frac{1}{2}''$, $\phi_c = 1.93$

$A_s = pbd = (.0193)(12)(8.50) = 1.97 \ \square''/ft$

Use #11 @ $9\frac{1}{2}''$, $A_s = 1.97 \ \square''/ft$

$t = 8.50 + 0.75 + \frac{1.410}{2} = 10.0''$

Use $10''$

4. Shear Check

$$\frac{d}{L} = \frac{8.50}{(12.792 \times 12)} = 0.0554$$

$p_m' \simeq 50 \text{ psi} > 15.8 \text{ psi}$ Ref. 1, Fig. 9-3

Therefore, section adequate for shear.

5. Diagonal Tension Check

For $\phi' = 0.25\,\phi_c$, $\phi_v = 0.25$ (min.) Ref. 1, p. 8-6

$$g_y = 100\left(\frac{1}{2+.25}\right)\left(1 + \frac{(2)(.25)(42{,}000)}{10^5}\right)(1.93 \times 3000)^{1/2}(.0554)^2$$ p. F-4

$g_y = 12.6 \text{ psi} < 18.0 \text{ psi}$

However, minimum p. F-4

$g_y = (3.5)(3000)^{1/2}(.0554) = 10.6 < 18.0 \text{ psi}$

Therefore, section insufficient for diagonal tension.

For $q_y = 18.0$ psi

$$18.0 = (100)\left(\frac{1}{2.25}\right)\left(1 + \frac{2\phi_v\, 42{,}000}{10^5}\right)(1.93 \times 3000)^{1/2}(.0554)^2$$

$\phi_v = 0.87$

Since $\phi_c = 1.93$, provide required web reinforcement by bending up every other longitudinal rebar.

6. Dynamic Analysis of Preliminary Wall Design #2

$$T = \frac{(12.792 \times 12)^2}{(42{,}500)(1.93)^{1/2}(8.50)} = 0.047 \text{ sec} \qquad \text{p. F-6}$$

With $t_d = 1.0$ sec for dynamic portion of loading, a dynamic analysis is not warranted for cost estimating purposes. See p. F-4.

7. Rebound

$$\frac{t_d}{T} = \frac{1.0}{.047} = 21.3$$

For $\mu = 3.0$

$\phi' \simeq 0.25\,\phi_c \simeq 0.48$ Ref. 1, Fig. B-10

$A_s' = p'bd = (.0048)(12)(8.50) = 0.49$ □"/ft

Use #6 @ 10½", $A_s' = 0.50$ □"/ft

B. Interior Wall Summary

$f'_c = 3000\ psi$

$d = 8\frac{1}{2}''$

$t = 10''$

A_s = #11 @ 9½" with every other rebar bent up for diagonal tension.

A'_s = #6 @ 10½"

Horizontal $A_s = 0.0020\ t\ b$

$= 0.24\ \square''/ft$

Use #4 @ 18", each face

$$Wt.\ rebars = (5.313)\left(\frac{12}{9}\right) + (1.502)\left(\frac{12}{10.5}\right) + (.668)\left(\frac{12}{18}\right)(2)$$

$$= 9.69\ psf$$

The height of the interior wall (for cost estimating) varies due to the difference in slab thickness as follows:

(a) Reserve Room

$L = 13'\text{-}6''$ p.F-12

(b) Elevator Corridor – South

$L = (14'\text{-}11'') - (1'\text{-}0'') = 13'\text{-}11''$

(c) Elevator Corridor – North

$L = (14'\text{-}11'') - (7\frac{3}{4}'') = 14'\text{-}3\frac{1}{4}''$

(d) Main Corridor

$L = 13'\text{-}8\frac{1}{2}''$ p.F-12

9. Check Wall Design #2 for Vertical Load.

Maximum vertical load occurs on interior wall supporting Slab Design #1 in Reserve Room, and is equal to

$V = 2699$ #/in. width p. F-13

This load is not critical, and the wall is assumed adequate to resist the vertical load without modification.

10. Footing Design

(a) Allowable Soil Bearing Pressure

$p_v = 82$ psi p. F-14

(b) Total Force on Wall Footing

Slab

D.L. = 210 #/in. p. F-14

Wall

$t = 10''$, $L = 13'-6''$

$$D.L. = \frac{(10)(1)(12)}{1728}(145)(13.5) = 136 \text{ \#/in.}$$

$P_T = 2699 + (210 + 136)\left(\frac{5}{6}\right) = 2987$ #/in. p. F-15

(c) Footing Width

Use continuous wall spread footing.

Required width

$$L = \frac{P_T}{p_v} = \frac{2987}{82} = 36.4''$$

Use $L = 38''$; design pressure $p_m = \frac{2987}{38} = 79$ psi.

(d) Footing Thickness

Span from wall face

$$\ell = \frac{38-10}{2} = 14''$$

For $q_f = p_m$, $d = 8.5$, $t = 12''$

$$\phi e = \frac{79}{(.018)(42{,}000)}\left(\frac{14}{8.5}\right)^2 = 0.283$$ p. F-15

$A_s = pbd = (.00283)(12)(8.5) = 0.29\ \square''/ft$

Use #5 @ 13'', $A_s = 0.29\ \square''/ft$

(e) Diagonal Tension Check

$$q_y \simeq (25)(.283 \times 2000)^{1/2}\left(\frac{8.5}{14}\right)^2$$ p. F-16

$q_y \simeq 219\ psi > 81\ psi$

Therefore, section is adequate for diagonal tension.

(f) Wall Footing Summary

$f'_c = 2000\ psi$

$d = 8.5''$

$t = 12''$

$L = 38''$

$A_s = \#5 @ 13''$

Transverse $A_s = (.002)(12)(38) = 0.91\ \square''$ p. F-16

Use 3-#5, $A_s = 0.93\ \square''$

Dowels, 3'-0" long to match vertical wall rebars

Use #11 @ 9" and #6 @ $10\frac{1}{2}$"

Wt. rebars $= (1.043)\left(\frac{12}{13}\right)\left(\frac{38}{12}\right) + (1.043)(3) + (5.313)\left(\frac{12}{9}\right)(3) + (1.502)\left(\frac{12}{10.5}\right)(3)$

$= 32.58$ plf

$= 10.29$ psf

F-24 BLANK

REFERENCES

1. Newmark, N. M., and J. D. Haltiwanger, Principles and Practices for Design of Hardened Structures, Air Force Design Manual, published by Air Force Special Weapons Center, Kirtland AFB, N.M., Rpt. No. SWC-TDR 62-138, December 1962. (AD-295 408)

2. Newmark, N. M., Design of Openings for Buried Shelters, Rpt. 2-67 U.S. Army Engineer Waterways Experiment Station, Vicksburg, Miss., July 1963.

3. Building Code Requirements for Reinforced Concrete (ACI 318-63), American Concrete Institute, Detroit, June 1963.

4. Manuals-Corps of Engineers, U.S. Army, Engineering and Design, Design of Structures to Resist the Effects of Atomic Weapons, EM 1110-345-413 (July 1959), -414 to -416 (March 1957), -417 (January 1958), and -418 to -421 (January 1960). Govt. Printing Office, Washington, D.C.

5. Uniform Building Code, 1967 edition, Vol. I, International Conference of Building Officials, Pasadena, California.

Appendix G

TYPICAL DESIGNS - PRELIMINARY DESIGN TECHNIQUES, COMPUTER PROGRAMS AND OTHER DATA

By H. L. Murphy and J. R. Rempel

Appendix G

TYPICAL DESIGNS - PRELIMINARY DESIGN TECHNIQUES, COMPUTER PROGRAMS AND OTHER DATA

By H. L. Murphy and J. R. Rempel

The purpose of this appendix is to present additional information relative to the Typical Designs section of Chapter 6 - information that includes backup and other data to allow the guide user to extrapolate/interpolate for additional values, delve into other situations, and gain further understanding of the approach and techniques used in the Typical Designs section, without further enlarging that section.

Preceding page blank

G-4 BLANK

Appendix G

TYPICAL DESIGNS - PRELIMINARY DESIGN TECHNIQUES, COMPUTER PROGRAMS AND OTHER DATA

I. One-Way Slabs - Simply Supported

Preliminary Design Procedure

This procedure is briefly described in the Slab Design section of Chapter 6 (and illustrated in Appendix F), and was used for preliminary design of several one-way slabs, based on the following common parameters:

$f'_c = 3$ ksi; $f'_{dc} = 1.25\ f'_c$; $f_{dy} = 42$ ksi; $p_{so} = 15$ psi;

$t_i = 1$ sec; $\mu = 3$.

The design steps were as follows: Using a step loading pulse, required unit resistance q (also termed an equivalent static load) equals $p_{so}/(1 - 1/2\mu)$. Flexural requirements were met by assuming d and using Equation 8-4* to obtain the slab clear span L. T was calculated from Equation 6-4, then Figure B-10* was entered with μ and t_d/T ($t_d = t_i = 1$ sec) to determine the required elastic rebound steel ratio p'. Diagonal tension requirements then dictated the required web steel ratio p_v by use of Equations 6-9a and 6-9b (first two equations of Figure 8-2b*; Equations 8-6 and 8-7* are also applicable but in a less convenient form). Pure shear capacity proved to be much larger than required, in all cases.

One-way slabs were similarly designed with p and p' adjusted so that the required web steel ratio p_v equaled zero.

Arithmetic plots of L versus d, L versus A_s, and L versus A'_s all yielded straight lines for each of the two families of slabs. One small and one large value of d for each slab family were, therefore, selected for further work (steel was detailed sufficiently to determine slab thickness); descriptive values for the four one-way slabs are:

---

* Reference 2 of Volume 1.

		Slab 1	Slab 2	Slab 3	Slab 4
Slab depth d*		7"	20.6"	10"	27.5"
Slab span L		130"	360"	135"	360"
Tens. steel p	At mid-	0.02	0.02	0.014	0.014
Compr. steel p'	span	.0052	.0052	.0029	.0029
Web steel p_v (required)		.0091	.0091	--	--
Slab thickness t*		8-5/8"	23-5/8"	11-9/6"	29-1/2"
Ratio t/d		1.233	1.148	1.156	1.072

Based on the steel detailing of these few slabs, approximate values of slab thickness versus depth were developed from slabs 1 and 2 into an upper limit equation for rough cost estimating and from slabs 3 and 4 into a lower limit equation that can be considered in estimating mass that is used later in equations of motion.† The resulting equations may be useful until a more complete study is made; they are as follows:

$t = 1.27d - 0.006d^2$, but t not less than 1.1d (for rough cost estimating) (6-7)

$t = 1.20d - 0.005d^2$, but t not less than 1.1d (for least mass estimate) (G-1)

Modified Preliminary Design Procedure

The preliminary design procedure described just above may well provide designs adequate for final design use - a few design comparisons are included below - but there were three changes in the procedure that were recognized and may be used to improve the resulting designs (that is, as a part of "Step 7" of Reference 2, art. 9.2), to make them give results closer to those from a final design technique that includes all refinements reasonably available at this time (Chapter 6).

The blast load pulse assumed to apply to one-way slabs over basements has a zero rise-time and an exponential decay from its peak value

---

* Such odd dimensions would certainly not be used in practice; however, it was the t/d ratios that were sought for rough cost and mass estimating purposes.

† Equation 6-7 was used for both purposes in the typical designs in Chapter 6.

(Eq. 3.51.1 of Ref. 1). The convenient chart solutions for single-degree-of-freedom dynamic systems, Figure 6-1 (p. 11-3), are exact only for triangular load pulses; however, techniques are available for using the chart solutions for decay pulses consisting of two or three straight lines (Figures 3-8 and -9*), thereby more closely approximating the exponential decay pulse. Some comparisons were made between the results from triangular and exponential decay pulses, using the positive phase duration times from Figures 3-7 and 3-5, respectively, of Reference 2. Solutions were obtained using dynamic load factors, Table 6.3, and the Newmark β Method[21] with a one msec time interval and $\beta = 1/6$. Using a single problem example about in the middle of a range of one-way slab designs and a peak blast overpressure p_{so} = 15 psi, the maximum resistance q and ductility μ values varied as follows:

q_{max}(psi)	23.6	17.0	16.0	15.8	14.5	13.8
$\mu_{triangular}$	1.24	2.69	3.43	3.71	6.27	8.83
$\mu_{exponential}$	1.25	2.75	3.57	3.88	6.86	10.03
μ_t/μ_e †	.995	.977	.961	.956	.914	.880

These tabulated values vary over a range of μ values, but are related to one midrange beam design situation. The following tabulated values compare μ_t with μ_e for a range of preliminary one-way slab designs, but with μ varied only over a narrow range (again, p_{so} = 15 psi):

d ;L	7" ;138"	20" ;398"	7" ;151"	20" ;440"
f'_c; f_{dy}(ksi)	3 ;44	3 ;44	5 ;52	5 ;52
q_{max}(psi)	16.2	16.0	16.1	15.5
$\mu_{triangular}$	4.31	3.42	4.41	3.71
$\mu_{exponential}$	4.40	3.57	4.53	3.92
μ_t/μ_e †	.979	.960	.974	.945

Using the 10 pairs of values tabulated, a curve-fitting equation for "adjusting" μ_t (calculated using a triangular decay pulse approximation, t_{00} of Figure 3-7*) to an estimated μ_e for an exponential decay pulse was developed; it is reiterated that the equation is for estimating only, and then only in the particular realm of applications from which it was derived:

---

* Reference 2 of Volume 1.

† Using more precise values of μ_t and μ_e than those tabulated.

$$\mu_e = \mu_t/(-.012747\ \mu_t + 1.00822)$$

where significant figures shown are simply those resulting from a library computer program run, not an implication of accuracy. The equation is most useful with computer programs; a simple figure is generally more useful (Figure G-1). This change in μ is the first of the three changes mentioned above.

The second change that may be readily applied as a part of "Step 7" is to use a "weighted" dynamic load factor, Table 6.3, tailored to the μ desired. In review, it should be recalled that only one (combined) dynamic load factor K_M/K_L need be used, applied to the mass as follows:

If the fundamental equation of motion

$$p(t) - kx = ma$$

includes dynamic load factors, it becomes

$$K_L\ p(t) - K_R\ kx = K_M\ ma$$

Recognizing that $K_R = K_L$* and dividing through by K_L leads to

$$p(t) - kx = (K_M/K_L)\ ma$$

The combined factor K_M/K_L is given directly in Table 6.3. The unanswered question is how K_M/K_L elastic and plastic values are to be "weighted" (a procedure suggested without explanation by at least two sources[22,33]). Two methods of weighting the factors were tested by use, first in a chart solution, discussed earlier in this section, then with the results compared to those from a full β-method solution (triangular decay load pulses used in both solutions). The two "weighting" methods were:

1. Apply elastic and plastic factors in accordance with relative areas under the elasto-plastic resistance plot (center figure, page 11-4) - for example, using K_e ($= K_M/K_L$ elastic) and K_p ($= K_M/K_L$ plastic) and $\mu = 7$, the weighted factor $K = (0.5/6.5)K_e + (6/6.5)\ K_p$.

2. Apply elastic and plastic factors in accordance with the relative displacements for elastic and plastic phases - for example, using K_e and K_p with $\mu = 7$, the weighted factor $K = (1/7)\ K_e + 6/7)\ K_p$.

The latter is recommended for use, because it is easier to apply and no discernible difference was found in the test applications of the two weighting methods.

---

* Reference 34 (Equation 7.17, p. 148) of Volume 1.

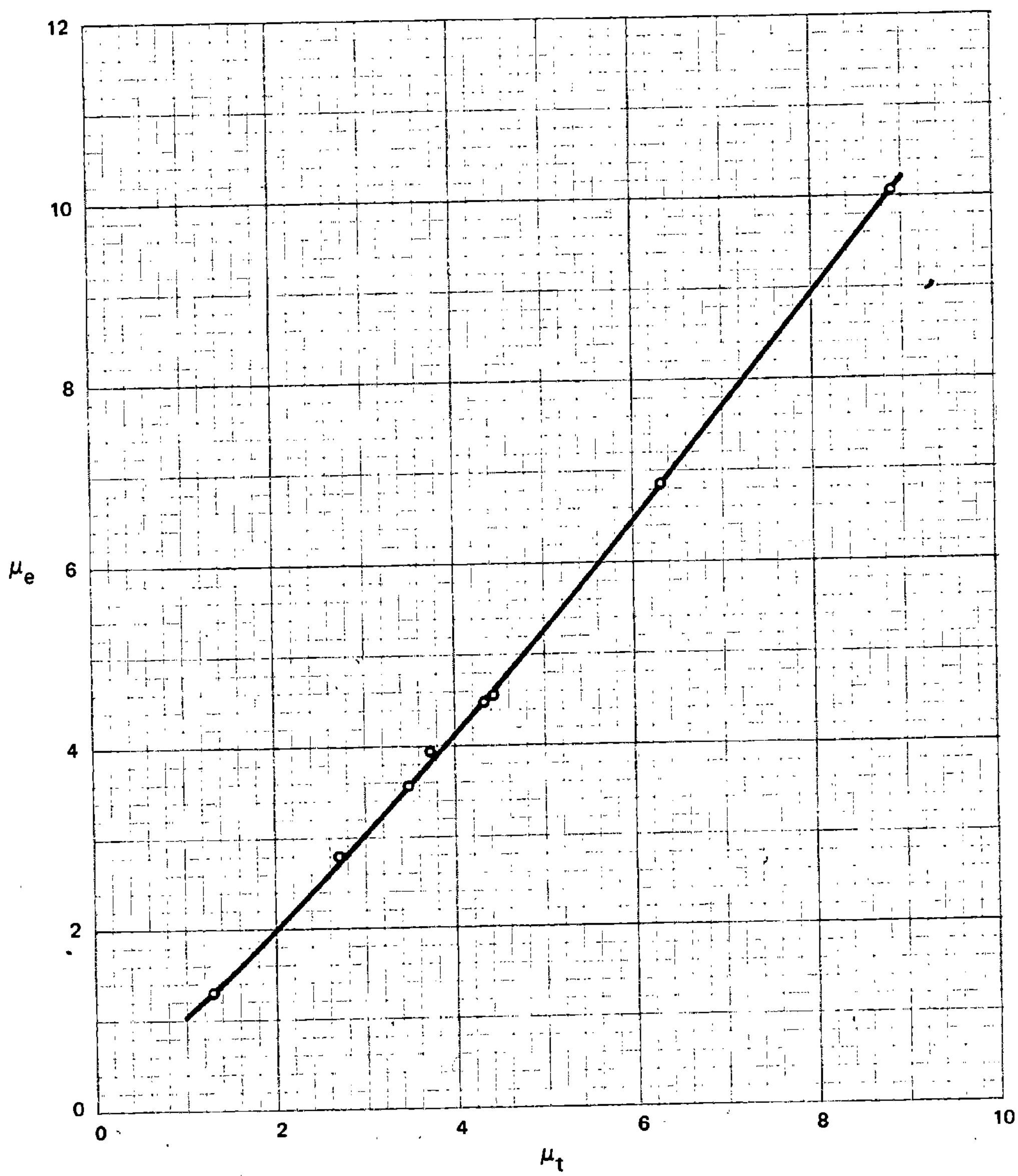

FIG. G-1 PEAK/YIELD DEFLECTION (μ): EXPONENTIAL VERSUS TRIANGULAR DECAY OF LOAD PULSE

The third change that may be readily applied as a part of "Step 7" is to use an ultimate moment capacity formula that takes into account rebound steel acting as compressive reinforcement. The change may be seen by comparing Equations 6-1 and 6-6; the effect is to allow a slighter smaller section depth d for a given clear span L.

The first two changes described for consideration involve changing a preliminary design procedure that already has certain elements incorporated in it that at least partially correct for the discrepancies discussed; for example, refer to the discussion of the calculation of the natural period of vibration T that follows Equation 6-5. On the other hand, incorporating a final "refinement" such as the third change discussed does not necessarily upset the assumptions made in the preliminary design procedure. For these reasons, the usefulness of the third change was tested first in developing the modified preliminary design procedure that follows.

A preliminary design (first cut) might then be improved ("Step 7") by using instead the following modified procedure:	Numerical Example:
1. Given values for the following parameters: f_c' (ksi); f_{dc}' (ksi); f_{dy} (ksi); p_{so} (psi); t_o (sec); L (in.); p; b (in.)	3; 3.75; 44; 15; 1.55; 255; .02; 1
2. Obtain t_{00} (sec) from Figure 3-7.*	0.71
3. Assume values for μ and T (sec); calculate t_{00}/T.	6; .08; 8.9
4. Using Figure 6-1, page 11-5, read p_m/q; calculate q, using $p_m = p_{so}$.	.985; 15.23
5. Calculate L/d, using the following modification of Equation 6.1: $(L/d)^2 = [8\ pbf_{dy}/aq]$ $[1 - 0.554\ pf_{dy}/(0.85\ f_{dc}')]$ (G-2) obtaining L/d, then calculating d (in.).	19.788; 12.89†
6. Using Equation 6-4, calculate T (sec), then t_{00}/T.	.0839; 8.46

* Reference 2 of Volume 1.

† Carrying more decimal places than justified, for demonstration purposes.

	Numerical Example:
7. Using Figure B-10* with μ and t_{00}/T, read r/q (equals p'/p); calculate p' ($=p(r/q)$, but not less than .0025), then μ ($= 0.1/(p-p')$); iterate this sequence until compatible values are found for p' and μ.	6; 8.46 .0046; 6.5
8. Using Equations 6-7 and -8, calculate "corrected" p_{so} to include effect of slab weight.	15+1.23 = 16.23†
9. Using corrected values for μ and t_{00}/T, repeat item 4 for new p_m/q and, with new p_m, calculate new q (psi); repeat item 5 for a new d(in.). Repeating items 6-8 should be unnecessary.	6.5; 8.46 1.00; 16.23; 16.23 13.31
10. Web steel to meet diagonal tension requirements should be calculated, and a check for pure shear strength should be made, using Equations 6-9 and -10, respectively.	

Another example with the same parameters except for changing f'_c (5 ksi), f'_{dc} (6.25 ksi), f_{dy} (78 ksi), and L (22'2") led to a design d = 10.21".†

A comparison with results from calculations using the final design procedure (Chapter 6) was then made at this point:

	d†	L	p'	μ	q
Trial 1, modified design	13.31"	21'3"	.0046	6.5	16.1
Final design	12.82"	21'3"	.0048	6.6	15.9
Trial 2, modified design	10.21"	22'2"	.0054	6.9	15.4
Final design	9.86"	22'2"	.0054	6.9	15.2

* Reference 2 of Volume 1.

† Carrying more decimal places than justified, for demonstration purposes.

Of the changes discussed earlier, the third one can be an inserted item in the modified procedure:

9.1 Adjust d slightly to take into account the rebound steel acting as compressive reinforcement, by using the following form of Equation 6-6 (with d appearing on both sides of the equation, a cut-and-try solution is indicated; however, for most designs it should be sufficiently accurate to simply use the d from item 9, in the right-end term below):

$$(L/d)^2 = [8\ (p-p')\ bf_{dy}/aq]\ [1 - 0.554\ (p-p')f_{dy}/(0.85\ f'_{dc})] + [8\ p'bf_{dy}/aq]\ [1 - d'/d]^* \quad (G-3)$$

A new comparison of results was made, adding those where step 9.1 had been applied:

	d†	L	p′	μ	q
Trial 1, modified design	13.31"	21'3"	.0046	6.5	16.1
Modified design with step 9.1	12.92"	21'3"	.0046	6.5	16.1
Final design procedure	12.82"	21'3"	.0048	6.6	15.9
Trial 2, modified design	10.21"	22'2"	.0054	6.9	15.4
Modified design with step 9.1	9.91"	22'2"	.0054	6.9	15.4
Final design procedure	9.86"	22'2"	.0054	6.9	15.2

The close agreement of results from the modified preliminary design procedure with step 9.1 inserted and the final design procedure results made it appear that further work on the modified form of the preliminary design procedure was unwarranted. If further design refinement is thought to be warranted, the final design procedure (Chapter 6) may be used.

* As in final design procedure (Chapter 6), d′ assumed as one in.

† Carrying more decimal places than justified, for demonstration purposes.

Tabular Data on Typical Designs

Table G.1 contains tabular data on the typical designs, made using the final design procedure of Chapter 6, for preparation of Figures 6-3 and 6-6. The significance of the two lines in italics in each figure is discussed in the next paragraph.

Computer Program Used for Typical Designs

Table G.2 shows a listing of the computer program used in calculating the typical designs for which data are shown in Table G.1. The programming language is Dartmouth BASIC as used by one of the largest commercial time-sharing organizations. For ease of handling data and plotting results, d was assumed and L calculated (rounded-off to a whole number, in inches). In retrospect, the beta method* time interval of one msec was smaller than necessary; one might calculate a time interval based on the estimated T in the program, using 0.05 T or 0.1 T (accuracy has been estimated to be within about 1% or 3.6%, respectively, of results obtained from a very small time interval, 0.001 T).† Also, the time interval could be increased considerably once the plastic phase is reached.

In reviewing the computer program, Table G.2, after publication of the Interim Report and in preparation for publication of the next report, the span factor (L-12)/L in lines 650 and 1140 was noticed with the realization that it was a carryover from an earlier time when L was tentatively used as a typical center-center span, rather than clear span as it is defined herein. The factor was applied to the design step that uses Equation 6-8, which makes a small increase in the value of the peak applied blast load p_{so} to allow for the member unit mass. As indicated by Table G.1, the computer program sought a "q" value to the nearest 0.1 psi that would come close to the allowed "μ" value $=0.1/(p-p')$ but ≤ 10 . Using the beta method[21] (which is a subroutine in Table G.2, lines 2440-3170) alone to solve the equations of motion and thereby test the effect of deleting the (L-12)/L factor, both original results and results from the new calculations were evaluated in terms of μ as follows. For each line of Table G.1, the coefficient or percentage of variation was calculated from results both with and without the span factor, i.e., $(\mu_{allowed} - \mu_{calculated})/\mu_{allowed}$; and eight cases, those with the largest positive and negative variation at each steel ratio p, were completely recalculated using the computer program (Table G.2) with the span factor removed from lines 650 and 1140. The results of these reruns

* Reference 21 of Volume 1.

† Reference 20 (p. 33) of Volume 1.

Table G.1

DATA FOR TYPICAL DESIGNS - ONE-WAY SLABS, SIMPLY SUPPORTED

$p = .02$

f'_c/f_{dy} (ksi)	d (in.)	L (in.)	p' (%)	p_v (%)	M_{max} (ft-kip)	q (psi)	x_e (in.)	x_m (in.)	μ	t_m (msec)	p_m (psi)
3/52	6	126	.38	.97	31.8	16.0	.896	5.6	6.25	89	15.59
	10	214	.45	1.04	90.4	15.8	1.58	10.3	6.54	148	15.96
	14	304	.52	1.10	179.9	15.6	2.31	15.6	6.76	204	16.32
	18	397	.61	1.18	301.8	15.3	3.125	22.5	7.20	265	16.66
	21	471	.71	1.25	416.4	15.0	3.82	29.2	7.65	315	16.91
4/52	6	128	.38	.77	32.9	16.0	.869	5.5	6.28	88	15.59
	10	217	.45	.83	93.2	15.8	1.52	10.1	6.60	147	15.96
	14	308	.53	.88	185.1	15.6	2.22	15.2	6.86	202	16.32
	18	402	.62	.94	309.4	15.3	2.97	21.8	7.35	262	16.66
	21	476	.73	1.01	425.6	15.0	3.615	28.4	7.85	313	16.91
5/52	6	130	.38	.62	33.6	16.0	.845	5.3	6.33	88	15.59
	10	218	.45	.67	94.9	15.9	1.465	9.3	6.36	140	15.96
	14	311	.53	.72	188.0	15.6	2.137	14.9	6.95	201	16.32
	18	405	.63	.77	313.9	15.3	2.858	21.3	7.47	261	16.66
	21	479	.74	.82	430.8	15.0	3.457	27.7	8.02	311	16.91
3/72	6	146	.41	1.15	41.9	15.7	1.58	10.3	6.48	118	15.59
	9	223	.48	1.23	96.7	15.5	2.53	16.3	6.45	173	15.87
	12	305	.56	1.30	175.6	15.1	3.62	25.2	6.95	237	16.14
	15	395	.71	1.43	282.6	14.5	4.995	39.3	7.86	319	16.41
	18	501	.99	1.65	424.0	13.5	6.99	68.0	9.74	440	16.66
4/72	6	150	.42	.99	44.0	15.7	1.58	10.2	6.48	118	15.59
	9	229	.49	1.05	101.0	15.4	2.52	17.0	6.77	178	15.87
	12	311	.58	1.12	182.7	15.1	3.55	24.8	7.00	237	16.14
	15	401	.73	1.21	291.6	14.5	4.82	38.5	8.00	317	16.41
	18	499	.95	1.35	430.1	13.8	6.37	58.4	9.16	410	16.66
5/72	6	152	.42	.85	45.2	15.7	1.56	10.1	6.50	118	15.59
	9	231	.49	.90	103.5	15.5	2.45	16.0	6.51	172	15.87
	12	314	.58	.96	186.7	15.1	3.455	24.4	7.07	235	16.14
	15	405	.74	1.05	296.7	14.5	4.655	37.8	8.13	315	16.41
	18	502	.97	1.17	435.4	13.8	6.095	57.2	9.39	408	16.66
3/52	*6*	*126*	*.38*	*.97*	*31.8*	*16.0*	*.896*	*5.5*	*6.13*	*92*	*15.59*
4/72	*18*	*506*	*1.02*	*1.39*	*432.3*	*13.5*	*6.58*	*65.4*	*9.94*	*438*	*16.66*

Table G.1 (continued)

p = .015

f'_c/f_{dy} (ksi)	d (in.)	L (in.)	p′ (%)	p_v (%)	M_{max} (ft-kip)	q (psi)	x_e (in.)	x_m (in.)	μ	t_m (msec)	p_m (psi)
3/52	6	112	.27	.76	24.7	15.7	.664	5.3	8.05	93	15.59
	11	210	.34	.83	84.8	15.4	1.296	11.4	8.79	170	16.05
	16	311	.42	.90	182.2	15.1	1.98	18.6	9.37	244	16.495
	20	395	.53	.99	288.8	14.8	2.60	25.9	9.95	306	16.83
	24	480	.63	1.07	420.9	14.6	3.245	32.6	10.05	358	17.15
4/52	6	114	.27	.57	25.3	15.7	.64	5.2	8.12	92	15.59
	11	212	.34	.63	86.7	15.4	1.24	11.1	8.93	169	16.05
	16	314	.43	.69	185.8	15.1	1.89	18.1	9.58	242	16.495
	20	397	.53	.76	293.2	14.9	2.44	24.0	9.82	296	16.83
	24	482	.63	.82	426.1	14.7	3.025	30.3	10.02	347	17.15
5/52	6	114	.27	.50	25.7	15.7	.62	5.1	8.19	92	15.59
	11	213	.34	.50	87.8	15.5	1.19	10.2	8.55	162	16.05
	16	314	.43	.53	187.8	15.2	1.81	16.8	9.29	234	16.495
	20	399	.54	.59	296.0	14.9	2.34	23.5	10.03	294	16.83
	24	482	.63	.64	429.1	14.8	2.87	28.3	9.88	337	17.15
3/72	6	131	.30	.98	32.9	15.4	1.20	10.0	8.33	124	15.59
	10	224	.38	1.06	94.0	15.0	2.176	19.2	8.82	205	15.96
	13	298	.47	1.15	162.0	14.6	3.023	28.7	9.51	272	16.23
	16	376	.59	1.25	250.6	14.2	3.99	40.1	10.04	340	16.495
	20	482	.74	1.38	400.5	13.8	5.37	54.5	10.14	418	16.83
4/72	6	133	.30	.80	34.1	15.4	1.18	9.9	8.37	124	15.59
	10	227	.38	.87	96.8	15.0	2.15	18.9	8.92	204	15.96
	13	302	.49	.95	166.3	14.6	2.92	28.2	9.67	271	16.23
	16	378	.59	1.02	255.4	14.3	3.77	37.3	9.90	329	16.495
	20	483	.74	1.12	405.7	13.9	5.013	50.9	10.15	406	16.83
5/72	6	134	.30	.67	34.8	15.4	1.159	9.8	8.42	123	15.59
	10	229	.39	.74	98.5	15.0	2.063	18.6	9.01	203	15.96
	13	304	.49	.80	168.8	14.6	2.825	27.7	9.82	270	16.23
	16	380	.60	.86	258.4	14.3	3.632	36.7	10.10	328	16.495
	20	483	.74	.95	408.9	14.0	4.756	47.8	10.05	395	16.83
4/52	*11*	*212*	*.34*	*.63*	*86.7*	*15.4*	*1.24*	*10.84*	*8.73*	*171*	*16.05*
4/72	*13*	*303*	*.48*	*.95*	*166.3*	*14.5*	*2.93*	*29.11*	*9.92*	*280*	*16.23*

Table G.1 (continued)

p = .01

f'_c/f_{dy} (ksi)	d (in.)	L (in.)	p′ (%)	p_v (%)	M_{max} (ft-kip)	q (psi)	x_e (in.)	x_m (in.)	μ	t_m (msec)	p_m (psi)
3/52	6	93	.25	.53	17.0	15.6	.421	4.10	9.79	87	15.59
	12	189	.25	.57	69.5	15.5	.887	8.70	9.77	160	16.14
	18	286	.27	.60	157.8	15.4	1.363	13.5	9.88	224	16.66
	24	385	.34	.66	283.5	15.3	1.87	18.5	9.92	282	17.15
	30	485	.42	.73	447.2	15.2	2.396	23.9	9.96	337	17.626
4/52	6	94	.25	.50	17.2	15.6	.402	4.0	9.91	86	15.59
	12	191	.25	.50	70.5	15.5	.847	8.4	9.94	158	16.14
	18	288	.28	.50	159.5	15.4	1.301	13.1	10.08	222	16.664
	24	387	.35	.50	286.6	15.3	1.774	18.0	10.17	280	17.15
	30	485	.42	.52	450.8	15.3	2.247	22.2	9.89	327	17.626
5/52	6	94	.25	.26	17.4	15.6	.389	3.9	10.00	85	15.59
	12	191	.25	.26	71.0	15.5	.818	8.2	10.06	157	16.144
	18	289	.28	.50	161.1	15.4	1.255	12.9	10.24	221	16.664
	24	387	.34	.50	288.2	15.4	1.694	16.8	9.94	271	17.15
	30	487	.42	.50	452.9	15.3	2.157	21.8	10.10	326	17.626
3/72	6	110	.25	.77	23.0	15.3	.788	8.0	10.21	117	15.59
	11	205	.25	.80	79.0	15.1	1.527	15.0	9.79	195	16.054
	15	283	.30	.85	148.8	14.9	2.165	21.2	9.81	254	16.408
	20	384	.40	.95	269.3	14.6	3.051	30.6	10.01	327	16.830
	25	488	.49	1.03	426.5	14.3	4.00	40.7	10.16	398	17.228
4/72	6	111	.25	.60	23.5	15.3	.762	7.9	10.34	117	15.59
	11	207	.25	.63	80.5	15.1	1.474	14.6	9.93	194	16.054
	15	285	.31	.68	151.4	14.9	2.083	20.8	9.99	252	16.408
	20	385	.40	.75	272.5	14.7	2.885	28.5	9.87	317	16.83
	25	489	.49	.82	430.2	14.4	3.758	38.1	10.13	387	17.228
5/72	6	111	.25	.50	23.7	15.4	.736	7.1	9.71	110	15.59
	11	208	.25	.50	81.5	15.1	1.434	14.4	10.04	193	16.054
	15	286	.31	.54	152.9	14.9	2.018	20.5	10.14	251	16.408
	20	386	.40	.60	274.5	14.7	2.782	28.0	10.06	316	16.83
	25	488	.49	.66	432.4	14.5	3.584	35.8	10.0	377	17.228
	26	508	.50	.67	468.2	14.5	3.736	36.8	9.85	385	17.305
5/52	12.2	195	.25	.26	73.4	15.5	.832	8.4	10.0	159	16.16
	12.4	198	.25	.26	75.9	15.5	.847	8.5	10.0	161	16.18
	12.6	201	.25	.26	78.4	15.5	.861	8.6	10.0	163	16.20
	12.8	204	.25	.50	80.9	15.5	.875	8.8	10.01	165	16.215
	12.9	206	.25	.50	82.2	15.5	.882	8.8	10.0	166	16.22
	13.0	208	.25	.50	83.5	15.5	.889	8.9	10.0	167	16.23
	14.0	224	.25	.50	97.0	15.5	.961	9.5	9.93	177	16.32
5/52	*18*	*289*	*.28*	*.50*	*161.1*	*15.4*	*1.255*	*12.6*	*10.04*	*221*	*16.664*
5/72	*6*	*111*	*.25*	*.50*	*23.7*	*15.3*	*.741*	*7.45*	*10.06*	*118*	*15.59*

Table G.1 (concluded)

p = .005

f'_c/f_{dy} (ksi)	d (in.)	L (in.)	p′ (%)	p_v (%)	M_{max} (ft-kip)	q (psi)	x_e (in.)	x_m (in.)	μ	t_m (msec)	p_m (psi)
3/52	6	66	.25	.26	8.5	15.8	.176	1.8	10.29	60	15.59
	16	179	.25	.28	63.7	16.0	.518	5.1	9.82	142	16.495
	25	280	.25	.29	157.4	16.1	.824	8.3	10.02	204	17.228
	36	402	.25	.30	328.5	16.3	1.187	12.0	10.08	270	18.15
	43	477	.25	.30	469.7	16.5	1.407	14.0	9.94	306	18.764
	47	520	.25	.31	561.7	16.6	1.532	15.2	9.93	326	19.114
4/52	6	66	.25	.26	8.5	15.8	.168	1.7	10.38	59	15.59
	16	179	.25	.26	63.9	16.0	.494	4.9	9.97	140	16.495
	26	291	.25	.26	170.9	16.2	.813	8.0	9.80	203	17.305
	36	401	.25	.26	329.4	16.4	1.125	11.1	9.89	261	18.151
	43	478	.25	.26	471.1	16.5	1.342	13.7	10.18	304	18.764
	47	519	.25	.26	563.4	16.7	1.452	14.3	9.83	317	19.114
5/52	6	66	.25	.26	8.5	15.8	.162	1.7	10.43	58	15.59
	16	179	.25	.26	64.0	16.0	.478	4.8	10.09	139	16.495
	26	291	.25	.26	171.2	16.2	.787	7.8	9.93	202	17.305
	36	401	.25	.26	330.0	16.4	1.088	10.9	10.05	260	18.151
	43	477	.25	.26	471.9	16.6	1.290	12.9	9.97	296	18.764
	47	520	.25	.26	564.3	16.7	1.404	14.0	10.00	316	19.114
3/72	6	77	.25	.50	11.7	15.7	.336	3.2	9.62	77	15.59
	14	185	.25	.54	66.9	15.6	.876	8.5	9.74	168	16.321
	22	294	.25	.55	167.6	15.5	1.423	14.2	9.97	245	16.992
	31	417	.25	.56	335.0	15.4	2.046	20.8	10.16	323	17.713
	36	485	.25	.56	452.8	15.4	2.387	24.2	10.15	362	18.15
	40	539	.26	.58	560.2	15.4	2.664	27.0	10.15	393	18.501
4/72	6	77	.25	.32	11.7	15.7	.322	3.1	9.73	76	15.59
	14	186	.25	.38	67.2	15.6	.837	8.3	9.92	166	16.321
	23	308	.25	.39	184.1	15.5	1.425	14.5	10.15	251	17.072
	32	430	.25	.40	358.6	15.5	2.008	20.1	10.01	321	17.801
	36	484	.25	.40	454.6	15.5	2.267	22.8	10.04	353	18.15
	40	539	.26	.41	562.3	15.5	2.528	25.5	10.07	383	18.501
5/72	6	77	.25	.26	11.8	15.7	.312	3.1	9.80	75	15.59
	14	186	.25	.27	67.4	15.6	.811	8.1	10.04	165	16.321
	22	294	.25	.28	168.6	15.6	1.309	12.9	9.85	235	16.992
	31	417	.25	.29	337.1	15.5	1.882	19.1	10.17	312	17.713
	36	483	.25	.29	455.7	15.6	2.181	21.5	9.86	344	18.151
	40	538	.26	.30	563.5	15.6	2.432	24.1	9.92	374	18.501
4/52	*43*	*478*	*.25*	*.26*	*471.1*	*16.5*	*1.342*	*13.48*	*10.05*	*304*	*18.764*
3/72	*6*	*77*	*.25*	*.50*	*11.7*	*15.6*	*.338*	*3.39*	*10.01*	*84*	*15.59*

Table G.2

COMPUTER PROGRAM

```
100 PRINT "LEVEL 1:"
110 PRINT "ENTER VALUES OF ELASTIC FACTOR,PLASTIC FACTOR"
120 PRINT "AND TIME INTERVAL (SEC)"
130 INPUT K0,K9,H
140 PRINT USING 150 ,K0,K9,H
150:DATA ARE  0.00  0.00  0.000
160 PRINT
170 PRINT "LEVEL 2:"
180 PRINT "ENTER VALUES OF PEAK OVERPRESSURE (PSI), RISE-TIME (SEC)"
190 PRINT "AND POSITIVE PHASE DURATION (SEC)"
200 INPUT P0,T1,T0
210:DATA ARE  00.0  0.000  0.000  0
220 PRINT "ENTER 1 IF BLAST DECAY LINEAR, 2 IF EXPONENTIAL"
230 INPUT Z
240 PRINT USING 210 ,P0,T1,T0,Z
250 PRINT
260 PRINT "LEVEL 3:"
270 PRINT "ENTER VALUES OF STEEL DYNAMIC YIELD STRESS (PSI),"
280 PRINT "CONCRETE COMPRESSIVE STRESS (STATIC) (PSI) AND TENSION"
290 PRINT "STEEL RATIO"
300 INPUT F2,F1,P9
310 PRINT USING 330 , F2,F1,P9
320 PRINT
330:DATA ARE 00000  0000  0.000
340 PRINT "LEVEL 4:"
350 PRINT "ENTER SLAB DEPTH (INCHES)"
360 INPUT D
370 PRINT USING 380 , D
380:DEPTH IS  00.0
390 PRINT
400 PRINT
410 PRINT
420 LET A=30000/F1
430 LET A1=P9*A
440 LET K0=SQR(2*A1+A1*A1)-A1
460 PRINT
470 PRINT
480 LET 80=15.9
490 LET 80 = INT(80*10+0.5)/10.+0.05
500 LET C=0
510 LET G2,G3,G4,H2,N1=0
520 LET G1=7
530 LET H2 = 0
540 REM                                FLEXURE (INCL. REBOUND)
550 LET H1 = P9*D*2*F2*(1 - .55*P9*F2/(1.0625*F1))
560 LET D1 = 1.2*D - .006*D*2
570 IF D1 >= 1.10D THEN 590
580 LET D1 = 1.10D
590 LET P1 = P0
600 LET P0 = P0 * (150/1728)*D1*(1 - 1/2/6)
610 LET T2 = .07*SQR(10/P1)*W*(1/3)
620 LET I1 = (K0*D)*3/3 + (30000/F1)*P9*D*3*(1-K0)*2
630 LET L = SQR(80*1/80)
640 PRINT "H1= ";H1;" L= ";L
650 LET M9 = D1*(L*12.)*150./1728./386./L
660 LET K1= 76800*F1*I1/L*4
680 LET T9 = T0*42S000*D*SQR(P9)/L*2
690 LET N1=N1+1
700 IF N1>100 THEN 720
710 GOTO 740
720 PRINT "LOOPING: 80= ";80
730 GOTO 3180
740 REM                                          REBOUND STEEL RATIO
750 LET X=T2*T9/T0
760 LET G3=X
770 IF X>50 THEN 990
780 LET Y=LOG(G1)*3.6916
790 LET G2=LOG(X)*3.6916
800 IF Y > 2.419*G2 THEN 820
810 GOTO 890
820 IF Y < 2.419*G2+11.3 THEN 850
830 PRINT "OUT OF RANGE OF CURVE-FITTING: MU=";G1;"  X=";X
840 GOTO 2280
850 LET Z6=Y/2.419-G2
860 LET Z7=Z6*Z6
870 LET P8=.4090+.0614*Z6+.3206*Z7-.12775*Z7*Z6
880 GOTO 1010
890 LET X=-4.67475475+.8550*G2+.520*Y
900 LET Y=-.806-.520*G2+.655*Y
910 IF Y>0 THEN 940
920 LET B=X-.151750*Y*Y-.1003
930 GOTO 950
940 LET B=X-.28110*Y*Y-.2380
950 LET B2=B*B
960 LET B4=B2*B2
970 LET P8=.40062-.046716*B+.001678*B2+.0003724*B*B2-.00003552*B4
980 GOTO 1010
990 PRINT "DURATION/NAT. PERIOD IS TOO LARGE",X
1000 GOTO 2250
1010 LET P8 = INT(10000*P8*P9+.5)/10000
1020 IF P8 < 0.0025 THEN 1040
1030 GOTO 1100
1040 LET P8 = 0.0025
1060 GOTO 1100
1070:REBOUND STEEL RATIO =  0.0000
1100 LET H2 = (P9-P8)*D*2*F2*(1-.55*(P9-P8)*F2/1.0625/F1)
1110 LET H2 = H2 + P8*D*F2*(D - 1)
1120 LET L = SQR(8*H2/80)
1130 LET K1=76800*F1*I1/L*4
1140 LET M9 = D1*(L*12.)*150./1728./386./L
1150 IF C < 3 THEN 1290
1160 PRINT USING 1090 , P8
```

```
1170 PRINT "M2= ";M2;"  L= ";L
1180 LET R=D/L
1190 IF R > .2 THEN 1210
1200 GØTØ 1240
1210 PRINT "PRØGRAM STØPPED BECAUSE DIAGØNAL TENSIØN PØRTIØN"
1220 PRINT "HANDLES THE CASE D/L < 0.2 ØNLY"
1230 GØTØ 3180
1240 LET Z9=.74*P0*(1.-R)/(R*F1)
1250 PRINT "BEAM THICKNESS, D1 ØR T= ";D1;" MASS, M9= ";M9
1260 PRINT "EQUIV. DURATIØN / NAT. PERIØD = ";G3
1270 PRINT "PURE SHEAR FACTØR= ";Z9
1280 PRINT
1290 GØSUB 2380
1300 GØ TØ 1310,1330,1650,ØN C
1310 LET S0 = 1.0
1320 LET J0 = 0
1330 LET J=.1/(P9-P8)
1340 IF J<=10 THEN 1360
1350 LET J=10
1360 LET J=X9/X8-J
1370 IF(J0*J)>=0 THEN 1580
1380 IF S0 > 0.1 THEN 1520
1390 IF X9/X8>10 THEN 1410
1400 GØTØ 1440
1410 IF Q3=0 THEN 1460
1420 IF (X9/X8-10)<Q3 THEN 1440
1430 LET Q0=Q4
1440 LET C=3
1450 GØTØ 1500
1460 LET Q4=Q0
1470 LET Q0=Q2
1480 LET Q3=(X9/X8-10)
1490 GØTØ 1600
1500 LET Q0=Q0+.05*J/ABS(J)
1510 GØTØ 1620
1520 LET S1=.5*S0
1530 IF S1 <= 0.1 THEN 1550
1540 GØTØ 1570
1550 LET S0 = 0.1
1560 GØ TØ 1580
1570 LET S0 = INT(10.*S1+0.5)/10.
1580 LET Q2=Q0
1590 LET Q0=Q0+S0*J/ABS(J)
1600 LET C = 2
1610 LET J0=J
1620 LET L=SQR(8*M2/Q0)
1630 GØTØ 680
1640 REM                                  DIAGØNAL TENSIØN
1650 GØ SUB 2980
1660 LET Q1=3.5*R*SQR(F1)
1670 LET P7=0
1680 IF Q1 >= Q0 THEN 1790
1690 LET P7=.0049
1700 FØR I = 1 TØ 200
1710      LET P7 = P7 + .0001
1720      LET Q1 = 1000*(1/(2+P8/P9))*(1+2*P7*F2/1000)*(R)↑2
1730      LET Q1 = Q1*SQR(P9*F1)
1740      IF Q1>=Q0 THEN 1840
1750 NEXT I
1760 PRINT
1770 PRINT "***NØT ENØUGH DIAGØNAL TENSIØN STEEL***"
1780 PRINT
1790 IF P7>=.0026 THEN 1840
1800 IF X9/X8<=1.5 THEN 1840
1810 LET P7=.0026
1830 GØTØ 1720
1840 PRINT USING 1850 ,P7,Q1,Q0
1850:FØR PV (P7)= 0.####   Q1=###.###   LAST Q0= ##.#
1860 PRINT
1870 PRINT USING 1880
1880:DEPTH  SPAN   T.STL   C.STL  WEB ST  Q-YLD   K1     X9     X9/X8=MU

1890 PRINT
1900 LET S1=INT(L+1/2)
1910 LET S2=INT(1E4*X9+1/2)/1E4
1920 LET S3=INT(1000*X9/X8+1/2)/1000
1930 PRINT USING 1940 ,D,S1,P9,P8,P7,Q0,INT(10*K1+.5)/10,S2,S3
1940: ###   ####  #.####  #.####  #.####  ###.#  ##.#  ###.####  ##.###

1950 PRINT
1960 PRINT
1970 LET N1,N2,N3,N4,N5,N6,N7,N8=0
1980 LET N1 = INT(100*12*P9*D + 1/2)/100
1990 LET N2 = INT(100*12*P8*D + 1/2)/100
2000 LET N3 = INT(100*12*.002*D1 + 1/2)/100
2010 LET N4 = INT(100*144*P7 + 1/2)/100
2020 LET L9 = (360 - L)/230
2030 IF L9 < 0 THEN 2050
2040 GØ TØ 2070
2050 LET L9 = 0
2060 GØ TØ 2100
2070 IF L9 > 1 THEN 2090
2080 GØ TØ 2100
2090 LET L9 = 1
2100 LET L9 = .23*L9 + 1.12
2110 LET N5 = INT(1000*L9 + 1/2)/1000
2120 LET N6=INT(12*D*(1.03*P9+1.15*P8)*(L+2*(D+11))*490/1728+.5)
2130 LET N7 = INT(12*.002*D1*(L-12)*490/1728 + 1/2)
2140 LET N8 = INT(144*P7*1.68*D*(L-12)/12*490/1728 + 1/2)
2150 PRINT USING 2170
2160 PRINT USING 2180
2170:    STEEL/FT WIDTH    STL/SF  LENGTH  TØTAL  STEEL/FT   WIDTH (LBS)
```

Table G.2 (concluded)

```
2180: AS-     AS+  A-TEMP   A-WEB  CORR.   AS-&+  TEMP  WEB    TOTAL
2190 PRINT
2200 PRINT USING 2210 ,N1,N2,N3,N4,N5,N6,N7,N8,N6+N7+N8
2210:##.##  ##.##  ##.##   ##.##  ##.##   #####  ###  ####    #####
2220 LET P0=P1
2230 LET N1,N2,N3,N4,N5,N6,N7,N8=0
2250 PRINT
2260 PRINT
2270 PRINT
2280 PRINT "IS THERE ANOTHER CASE (ENTER 0 FOR NO, 1 FOR YES)"
2290 INPUT N1
2300 IF N1 = 0 THEN 3180
2310 PRINT "ENTER INPUT LEVEL AT WHICH NEXT CASE BEGINS"
2320 INPUT N1
2330 PRINT
2340 PRINT
2350 PRINT
2360 GOTO 100,170,260,340, ON N1
2380 REM
2390 IF Q0 = 0 THEN 3170
2400 LET V0,X0,T=0
2410 LET X8 = Q0/K1
2420 GOSUB 2750
2430 LET A0 = P/K8/M9
2440 REM                         BETA EQUATIONS
2450 REM                 ASSIGN NEW BETA TO NEXT LINE IF DESIRED
2460 LET B = 1/6
2470 LET A2,A1=A0
2480 LET T = T + H
2490 GOSUB 2750
2500 FOR I = 1 TO 10
2510      LET A1 = A2
2520      LET V1 = V0 + (A0 + A1)*H/2
2530      LET X1 = X0 + H*V0 + (1/2 - B)*A0*H^2 + B*A1*H^2
2540      GOSUB 2900
2550      IF X1 <= X8 THEN 2580
2560      LET A2 = (P - Q)/K9/M9
2570      GO TO 2590
2580      LET A2 = (P - Q)/K8/M9
2590      IF ABS(A2-A1)/A1 <= .01 THEN 2630
2600 NEXT I
2610 IF ABS(A2-A1)/A1 <= .01 THEN 2630
2620 PRINT "AT T=";T;"ABS(A2-A1)/A2=";ABS(A2-A1)/A2
2630 LET V1 = V0 + (A0+A2)*H/2
2640 LET X1 = X0 + H*V0 + (1/2 - B)*A0*H^2 + B*A2*H^2
2650 LET X9 = (X0 + X1)/2
2660 LET G1=X9/X8
2670 IF G1 < 50 THEN 2690
2680 GO TO 3160
2690 IF V1 < 0 THEN 2970
2700  LET A0 = A2
2710  LET V0 = V1
2720  LET X0 = X1
2730 GO TO 2480
2740 REM                 FORCE FUNCTION SUBROUTINE
2750 IF T < T0 THEN 2790
2760 LET P = 0
2770 RETURN
2780 REM                           TRIANGULAR RISE PULSE
2790 IF T >= T1 THEN 2820
2800 LET P = P0 * T/T1
2810 RETURN
2820 IF Z = 2 THEN 2870
2830 REM                           TRIANGULAR DECAY PULSE
2840 LET P = P0 * (T0-T)/(T0-T1)
2850 RETURN
2860 REM                           EXPONENTIAL DECAY PULSE
2870 LET P=P0*(1-((T-T1)/(T0-T1)))*EXP(-((T-T1)/(T0-T1)))
2880 RETURN
2890 REM                 RESISTANCE FUNCTION SUBROUTINE
2900 IF Q0 - K1*X1 < 0 THEN 2950
2910 REM                           ELASTIC PHASE
2920 LET Q = K1*X1
2930 RETURN
2940 REM                           PLASTIC PHASE
2950 LET Q = Q0 + K2*(X1 - X8)
2970 RETURN
2980 REM                      BETA ROUTINE PRINTOUT
3000 PRINT "TIME    ACCELERATION    VELOCITY    DISPLACEMENT"
3010 PRINT
3020 LET S5=INT(1E4*A0+1/2)/1E4
3030 LET S6=INT(1E4*V0+1/2)/1E4
3040 LET S7=INT(1E4*X0+1/2)/1E4
3050 LET S8=INT(1E4*A2+1/2)/1E4
3060 LET S9=INT(1E4*V1+1/2)/1E4
3070 LET S0=INT(1E4*X1+1/2)/1E4
3080 PRINT USING 3100 ,T-H,S5,S6,S7
3090 PRINT USING 3100 ,T,S8,S9,S0
3100        :#.###     ######.##    ###.####       ###.####
3110 PRINT
3120 PRINT "P=";P;"   Q=";Q;"   YIELD DEFL.=";X8
3130 PRINT
3140 PRINT "MAX/YIELD DEFL = MU =";X9/X8
3150 PRINT
3170 RETURN
3180 END
```

are indicated in italics in Table G.1; because these are probably the cases most affected by the span factor's deletion, the design effect of originally using the factor in preparing Figures 6-3A and 6-6A/B/C is concluded to be inconsequential.

Suggested changes in the computer program, Table G.2, other than deleting the factor (L-12)/L in lines 650 and 1140, are as follows: In lines 480, change 15.5 to PO; in line 1210, change diagonal tension to pure shear; in line 1220, insert = following <; in line 1290, change 2380 to 2390; in line 2680, change 2680 to 2685 and change 3160 to 490; add a new line: 2680 LET Q0=1.5*Q0

NOTATION

See Notation section at end of Chapter 6.

Appendix G - Supplement

TYPICAL DESIGNS - PRELIMINARY DESIGN TECHNIQUES
COMPUTER PROGRAMS AND OTHER DATA

By H. L. Murphy and J. E. Beck

CONTENTS

TABLES

Appendix G - Supplement

TYPICAL DESIGNS - PRELIMINARY DESIGN TECHNIQUES, COMPUTER PROGRAMS AND OTHER DATA

By H. L. Murphy and J. E. Beck

The purpose of this appendix is to present additional information relative to the Typical Designs portion of Chapter 6 - information that includes backup and other data to allow the guide user to extrapolate/interpolate for additional values, delve into other situations, and gain further understanding of the approach and techniques used in the Typical Designs section, without further enlarging that section. Original Appendix G, Section I, is in Volume 2 of Reference 50.

G-28 BLANK

II. Typical Designs Section of Chapter 6

The Typical Designs portion of Chapter 6 herein consists of the following Sections:

A. One-Way Slabs - Simply Supported

B. One-Way Slabs - Continuous

C. One-Way Slabs - Design for Rebar Ratios Not in Design Graphs

D. One-Wal Walls - Simply Supported

E. Columns - Simply Supported

F. Footings (Wall and Square)

G. Wood Beams - Simply Supported

1. Computer Program for Beams and One-Way Slabs. To supplement Sections A-C of Chapter 6, Table G.3 provides a listing of the computer program used for design of rectangular R/C beams and one-way slabs (simply supported, propped cantilever, and fixed ends) and sample outputs therefrom. The program replaces that shown in Table G.2.[50*] The program is fully interactive (or conversational), and programming language used was Dartmouth BASIC, specifically as used by one of the largest commercial time-sharing firms.

The program has an option for using either of two subroutines for computing the dynamic response (i.e., solving the equation of motion) - one using the Newmark Beta Method (NBM)[21] and the other using a modified version (MNBM) developed by J. E. Beck. In the program, a note starting at line 1572 describes the procedure for changing from use of one subroutine to the other. The NBM is a general numerical method that can be applied with slight changes to any equation of motion. Its limiting characteristic, however, is an iterative inner loop (lines 3000 to 3100, Table G.3) that may make runs long in relation to other methods. The MNBM is limited to governing differential equations of motion that have linear equations of acceleration, velocity, and displacement. While the MNBM could be modified to handle other situations, the task would be monumental in comparison to the ease with which the NBM could be modified. The strength of the MNBM lies in the deletion of the iterative inner loop just mentioned. Experience in running the program has shown

---

* Superscript numerals are related to References listed on p. 11-35 and following.

Table G.3 INTERACTIVE COMPUTER PROGRAM FOR DESIGN OF R/C BEAMS AND ONE-WAY SLABS, WITH EXAMPLES

```
100 REM  PROGRAM FOR BLAST DESIGN OF BEAMS & ONE-WAY SLABS, VARIOUS
110 REM  SUPPORT CONDITIONS, WEAPON YIELD (0.5 MT OR MORE,
120 REM  OR ELSE EQUIVALENT TRIANGULAR PULSE LOAD (AFDM P.3-7&45)
130 REM  MUST BE CHANGED IN REBOUND SUBROUTINE)
140 REM ****************************************************
150 REM, VARIABLES (INPUTS PORTION): A,B,F1,F2,H,K8,K9,L,P0,P1,R1,R9,
160 REM                              T0,T1,U,U1,W,Z1,Z2,Z3,(Z9)
162 PRINT  USING "3D,4D,3D,2D";TIM(3),TIM(2),TIM(1),TIM(0)
164 PRINT
166 DIM A$[4],B$[2]
170 LET K8=.78
180 LET K9=.66
190 LET H=.001
195 LET Z7=4
200 PRINT "LEVEL 1:"
210 PRINT "ENTER PEAK OVERPRESSURE (PSI), RISE-TIME (SEC),"
220 PRINT "  POSITIVE PHASE DURATION (SEC) AND WEAPON YIELD (MT)"
230 INPUT P0,T1,T0,W
240 IF P0 <= 250 THEN 270
250 PRINT "PROGRAM NOT INTENDED FOR OVERPRESSURE > 250 PSI"
260 GOTO 200
270 IF W >= .499999 THEN 300
290 PRINT "PROGRAM NOT INTENDED FOR YIELD < .5 MT"
300 LET P0=INT(P0+1/2)
310 LET T1=INT(1000*T1+1/2)/1000
320 LET T0=INT(1000*T0+1/2)/1000
330 LET W=INT(10*W+1/2)/10
340 IF P0<1 THEN 200
350 IF T1<0 THEN 200
360 IF T0<.001 THEN 200
370 IF W<.49 THEN 200
380 LET P1=P0
390 PRINT "ENTER BLAST DECAY: 1=LINEAR, 2=EXPONENTIAL ";
400 INPUT Z1
410 LET Z1=INT(Z1)
420 IF Z1<1 THEN 390
430 IF Z1>2 THEN 390
440 PRINT
450 PRINT "LEVEL 2:"
460 PRINT "ENTER STEEL DYNAMIC YIELD STRESS (PSI) AND"
470 PRINT "  CONCRETE COMPRESSIVE STRESS (STATIC)(PSI)"
480 INPUT F2,F1
490 LET F2=INT(F2+1/2)
500 LET F1=INT(F1+1/2)
510 IF F2<1000 THEN 450
520 IF F1<1000 THEN 450
530 PRINT
540 PRINT "LEVEL 3:"
550 PRINT "SUPPORT CONDITIONS & BEAM/ONE-WAY SLAB. ENTER 2 SINGLE"
560 PRINT "  DIGITS, SEPARATED BY A COMMA: 1=SIMPLE SUPPORTS,"
570 PRINT "  2=PROPPED CANTILEVER, OR 3=FIXED ENDS; AND"
580 PRINT "  1=SLAB OR 2=BEAM ";
590 INPUT Z3,Z2
595 LET A$="SLAB"
600 LET Z3=INT(Z3)
610 LET Z2=INT(Z2)
615 LET W8=0
620 IF Z3<1 THEN 540
630 IF Z3>3 THEN 540
640 IF Z2<1 THEN 540
650 IF Z2>2 THEN 540
664 IF Z3=1 THEN 680
666 IF Z3=2 THEN 676
668 PRINT "ENTER AVERAGE WIDTH OF INTERIOR SUPPORTING WALLS";
674 GOTO 678
676 PRINT "ENTER WIDTH OF INTERIOR SUPPORTING WALL";
678 INPUT W8
680 IF Z2=1 THEN 770
690 PRINT "ENTER BEAM WIDTH (INCHES) & SUPPORTED AREA WIDTH (INCHES)"
700 INPUT B,A
705 LET A$="BEAM"
710 LET B=INT(B+1/2)
720 LET A=INT(A+1/2)
730 IF B >= A THEN 690
740 IF B<1 THEN 690
750 IF A<1 THEN 690
760 GOTO 789
770 LET A=B=1
789 PRINT
790 PRINT "LEVEL 4:"
800 PRINT "ENTER CLEAR SPAN (IN.) AND MU (>10 CAUSES USE OF"
810 PRINT "  MU=.1/(P-P')<=10; P & P'=TENS.& COMPR. STEEL)"
820 INPUT L,U
830 LET U=INT(10*U+1/2)/10
840 LET U0=U
850 IF L<10 THEN 790
860 LET L=INT(L+1/2)
870 IF U <= 0 THEN 790
880 PRINT
890 PRINT "LEVEL 5:"
900 PRINT "ENTER MAX. TENSILE STEEL RATIO (<=.02) ";
910 INPUT R1
920 LET R1=INT(10000*R1+1/2)/10000
922 IF R1>.02 THEN 890
924 IF R1 <= 0 THEN 890
926 LET Z5=0
928 PRINT "ENTER D' & D'' (ZEROES GIVE MIN.OF 1.3125; OR 1,1= USE"
930 PRINT "  STATISTICAL PGM HEREIN; OR ENTER ACTUAL VALUES>1.3125)"
932 INPUT D1,D2
934 IF Z3=1 THEN 945
936 LET Z9=D1
938 LET D1=D2
940 LET D2=Z9
945 IF D1=1 AND D2=1 THEN 953
946 IF D1<1 THEN 950
948 IF D2>.999999 THEN 956
950 LET D1=D2=1.3125
952 GOTO 958
953 LET Z5=1
954 LET D1=D2=1.45
955 GOTO 958
956 IF D1<1.3125 THEN 950
957 IF D2<1.3125 THEN 950
958 PRINT
960 LET R4=R1
970 LET R1=0
```

Table G.3 (continued)

```
0975 LET A3=A
0980 PRINT "LIST ALL VARIABLES TØ THIS PØINT (1=YES, 2=NØ)";
0990 INPUT Z9
1000 IF INT(Z9)=2 THEN 1131
1010 PRINT
1020 PRINT "P0","P1","T1","T0","W"
1030 PRINT P0,P1,T1,T0,W
1040 PRINT
1050 PRINT "Z1","F2","F1","Z3","Z2"
1060 PRINT Z1,F2,F1,Z3,Z2
1070 PRINT
1080 PRINT "W8","B","A","A3"
1090 PRINT W8,B,A,A3
1100 PRINT
1105 PRINT "L","U","U0","R1","R4"
1110 PRINT L,U,U0,R1,R4
1115 PRINT
1120 PRINT "D1","D2","Z9"
1125 PRINT D1,D2,Z9
1130 PRINT
1131 LET Z9=0
1132 LET Q2=0
1135 PRINT "ANY CHANGES? (6=NØ; 1 TØ 5=RETURN TØ LEVEL 1,2...5)"
1136 INPUT I
1137 LET I=INT(I)
1138 IF I<1 THEN 1135
1139 IF I>6 THEN 1135
1140 PRINT
1141 GØTØ I ØF 200,450,540,790,890,1150
1150 REM *** FLEXURE PØRTIØN  ****************************************
1160 REM
1170 REM, ADDITIØNAL VARIABLES: C3...C9,I,(J),Q0,(Q1),R2,R8
1180 REM                        X,X8,X9,Y,Z
1185 REM
1189 LET U=U0
1190 LET P0=P1
1210 GØTØ Z3 ØF 1220,1300,1390
1220 LET C3=C8=1/8
1225 LET B$="SS"
1230 LET C4=384/5
1240 LET C5=425000.
1250 LET C6=1
1260 LET C7=1
1270 LET R1=R4
1272 IF R1 >= .005 THEN 1276
1274 LET R1=.005
1276 LET R2=R1/4
1277 IF R2 >= .0025 THEN 1280
1278 LET R2=.0025
1280 LET C9=R9=R8=0
1290 GØTØ 1500
1300 LET C3=1/6
1305 LET B$="PC"
1310 LET C4=160
1320 LET C5=638000.
1330 LET C8=9/128
1340 LET C9=16/9
1350 LET R9=R4
1360 IF R9 >= .0089 THEN 1380
1370 LET R9=.0089
1380 GØTØ 1470
1390 LET C3=1/12
1395 LET B$="FF"
1400 LET C4=307
1410 LET C5=850000.
1430 LET C8=1/24
1440 LET C9=2
1450 LET R9=R4
1455 IF R9 >= .01 THEN 1470
1460 LET R9=.01
1470 LET R8=R9/4
1480 IF R8 >= .0025 THEN 1492
1490 LET R8=.0025
1492 LET R1=R9/C9
1494 LET R2=R1/4
1496 IF R2 >= .0025 THEN 1500
1498 LET R2=.0025
1500 LET J=0
1510 LET J1=2
1520  FØR I=1 TØ 3
1530  IF U0 <= 10 THEN 1550
1540  GØSUB 3850
1550  GØSUB 3900
1560  GØSUB 4030
1570  NEXT I
1571 REM
1572 REM *** IN LINES 1580, 1614, 1690, AND 1840 GØSUB 2820
1573 REM *** WILL CALL NEWMARK BETA-METHØD(NBM), AND GØSUB 7000
1574 REM *** WILL CALL MØDIFIED NEWMARK BETA-METHØD(MNBM).
1575 REM *** THE MNBM IS FASTER THAN THE NBM. THE MNBM CAN ØNLY BE
1576 REM *** USED WHEN THE DIFF. EQ. GØVERNING MØTIØN THAT INCLUDES
1577 REM *** ACCELERATIØN, VELØCITY ØR DISPLACEMENT HAS ØNLY ØNE ØF
1578 REM *** THESE VARIABLES AND ØNLY TØ THE FIRST PØWER. BØTH
1579 REM *** METHØDS CAN BE USED WITH VISCØUS DAMPING.
1580 GØSUB 7000
1585 LET Z9=0
1590 IF U-X9/X8 >= 0 THEN 1618
1592 LET Z9=Z9+1
1594 IF Z9 <= 3 THEN 1610
1600 PRINT "TRØUBLE: Q0 FRØM 1ST FLEXURE I-LØØP TØØ SMALL."
1605 STØP
1610 LET Q0=1.3*Q0
1612 GØSUB 4030
1614 GØSUB 7000
1616 GØTØ 1590
1618 LET Z9=0
1620 LET Q1=Q0
1630 LET U1=X9/X8
1640 LET Q3=0
1650 LET U3=100000.
1652 PRINT "HØW IS REBØUND RATIØ(RO) TØ BE GENERATED?"
1654 PRINT "  (O=BY INTERNAL EQN; 1=BY CHART, REF 2, PG B-32)";
1656 INPUT Q2
1658 PRINT
```

Table G.3 (continued)

```
1660  FØR I=1 TØ 20
1665  LET J1=0
1670  LET Q0=(Q1+Q3)/2
1680  GØSUB 4030
1690  GØSUB 7000
1695  REM
1700  IF X9/X8>U THEN 1740
1710  LET Q1=Q0
1720  LET U1=X9/X8
1730  GØTØ 1760
1740  LET Q3=Q0
1750  LET U3=X9/X8
1760  IF Q1-Q3 <= .1 THEN 1780
1770  NEXT I
1780  IF I<20 THEN 1800
1790  PRINT "RESULTS SUSPECT; 20 TRIALS IN 2ND FLEXURE I-LØØP."
1800  Q0=(Q1*(U3-U)+Q3*(U-U1))/(U3-U1)
1820  REM
1825  LET Q0=INT(10*Q0+1/2)/10
1828  LET J1=0
1830  GØSUB 4030
1840  GØSUB 7000
1980  LET Q1=X=Y=Z=0
1981  IF R9-R8 >= .4*1.25*F1/F2 THEN 1984
1983  IF R1-R2<.4*1.25*F1/F2 THEN 2020
1984  PRINT "SLANTING REPØRT TABLE 6.2 EQ.4 NØT MET; CHANGE PRØGRAM"
1985  STØP
1990  REM *** DIAGØNAL TENSIØN PØRTIØN ******************************
2000  REM
2010  REM, ADDITIØNAL VARIABLES: (Q2),R3,(Z9)
2020  REM
2022  IF Z3<1.5 THEN 2030
2023  IF Z3>2.5 THEN 2027
2024  LET C6=1+R9/R1/4
2025  LET C7=1+.75*R9/R1
2026  GØTØ 2030
2027  LET C6=1
2028  LET C7=1+1.5*R9/R1
2030  IF D/L <= .2 THEN 2060
2040  PRINT "PRØGRAM NØT APPLICABLE; D/L>.2 (DEEP BEAM PRØBLEM)"
2050  STØP
2060  LET Q1=3.5*SQR(F1)*D/L*B/A*C6
2070  LET Q2=SQR(R1*F1)/(2+R2/R1)*(D/L)^2*B/A*C7
2080  LET Z9=(Q0-1000*Q2)/2/F2/Q2
2090  IF Q1<Q0 THEN 2160
2100  LET R3=0
2110  IF U <= 1.5 THEN 2190
2120  LET R3=.0026
2130  GØTØ 2170
2140  LET R3=Z9
2150  GØTØ 2190
2160  LET R3=.005
2170  IF R3-Z9 >= 0 THEN 2190
2180  LET R3=Z9
2190  LET Q1=Q2=Z9=0
2200  LET R3=INT(10000*R3+1/2)/10000
2210  REM *** PURE SHEAR PØRTIØN ************************************
2220  REM
2260  LET Z9=.74*P0*(1-D/L)*C6/(D/L)/(B/A)/F1
2265  LET Z9=INT(1000*Z9+1/2)/1000
2267  PRINT ""
2270  PRINT "PURE SHEAR: F'C CØEFFICIENT APPROX ";Z9
2280  PRINT "ABSØLUTE MAX.=.2; DESIRABLE MAX.=.1; SEE TEXT & EQ.6-10"
2290  PRINT
2300  LET Z9=(L-D)/L*P0*L/2/.85/D/SQR(F1)
2310  IF Z3 <> 2 THEN 2330
2320  LET Z9=1.25*Z9
2330  PRINT "PURE SHEAR: SQR(F'C) CØEFFICIENT APPRØX ";Z9
2340  PRINT "ACI71(CH.11) ALLØWED=6 ØR MØRE"
2350  LET Z9=0
2352  REM *** BØND PØRTIØN ****************************************
2354  REM
2356  LET Z9=P0*L/2*B/.15/F1/.9/D
2360  REM *** ØUTPUT PØRTIØN **************************************
2370  REM
2380  GØSUB 3510
2390  PRINT
2400  PRINT "ØVERPR","F'C","FDY","D(+M)","D(-M)"
2410  PRINT P1,F1,F2,D3,D4
2420  PRINT
2430  PRINT "CL.SPAN","P(+M)","P'(+M)","PV","+M(IN.K/B)"
2440  PRINT L,R1,R2,R3,M1/1000
2450  PRINT
2460  PRINT "MU(DESIRED)","P(-M)","P'(-M)","Q","-M(IN.K/B)"
2470  PRINT U,R9,R8,Q0,M9/1000
2480  PRINT
2490  PRINT "XE","XM","MU(CALC'D)","TM(MSEC)","PRESS(MAX)"
2500  PRINT X8,X9,X9/X8,T3,P0
2510  PRINT
2520  PRINT "RISE-T.","PØS.DUR.","W(MT)","PERIØD(SEC)","DECAY"
2525  LET T2=T2/T8
2530  LET T8=(L*L/C5/D/SQR(R1)*100000.+1/2)/100000.
2540  PRINT T1,T0,W,T8,Z1
2550  PRINT
2560  PRINT "TD/T","K1","K2","K8","K9"
2570  PRINT T2,K1,K2,K8,K9
2580  PRINT
2590  PRINT "MASS","SLAB/BEAM","SUPP.CØND.","WIDTH(B,IN.)","LØADED WIDTH"
2600  LET M=INT(100000.*M+1/2)/100000.
2610  PRINT M,A$,B$,B,A
2620  PRINT
2630  PRINT "BETA H(SEC)","H(PLASTIC)","D'","D''","EST.THICK."
2632  IF Z3=1 THEN 2640
2634  PRINT H,H*Z7,D2,D1,D5
2636  GØTØ 2650
2640  PRINT H,H*Z7,D1,D2,D5
2650  PRINT
2660  PRINT "AS(+M)","A'S(+M)","AS(-M)","A'S(-M)"
2662  PRINT "  AND REBAR PERIMETER SUMS        (/FT. IF SLAB)"
2670  IF Z2>1.5 THEN 2700
2680  PRINT R1*12*B*D3,R2*12*B*D3,R9*12*B*D4,R8*12*B*D4
2681  LET Z9=Z9*12
2682  GØSUB 4900
```

```
2690  GØTØ 2710
2700  PRINT R1*B*D3,R2*B*D3,R9*B*D4,R8*B*D4
2704  GØSUB 4900
2710  LET Z9=0
2715  PRINT
2720  PRINT "RO","P'/P(+M)","P'/P(-M)","SUPP.THICK."
2724  IF Z3<1.5 THEN 2730
2726  PRINT RO,R2/R1,R8/R9,W8
2728  GØTØ 2736
2730  PRINT RO,R2/R1,"NA","NA"
2736  GOSUB 5000
2738  PRINT
2740  PRINT  USING "3D,4D,3D,2D";TIM(3),TIM(2),TIM(1),TIM(0)
2750  IF Z2>1.5 THEN 2778
2760  LET B=1
2778  PRINT ""
2780  PRINT "RETURN TØ WHAT LEVEL (1-5; USE 6=STØP) ";
2790  INPUT I
2792  PRINT
2794  PRINT
2796  PRINT
2800  GØTØ I ØF 200,450,540,790,890,2810
2810  STØP
2815  REM ****************************************************************
2820  REM *** BETA-METHØD SUBRØUTINE  **********************************
2830  REM
2840  REM  VARIABLES: AO,A1,A2,B9,D5,D9,H,(I),K1,K2,K8,K9,M,P,PO,Q0
2850  REM             T,TO,T1,T3,VO,V1,XO,X1,X8,X9,Z1
2860  REM
2870  IF Q0=0 THEN 3278
2890  LET VO=XO=T=0
2900  LET X8=Q0/K1
2910  GØSUB 3290
2920  LET M=D5*150/1728/386
2930  LET AO=P/K8/M
2940  REM                              BETA EQUATIØNS
2945  REM              BETA(B9) IS DESCRIBED IN LINES 7130 TØ 7160
2950  REM               ASSIGN NEW BETA TØ NEXT LINE IF DESIRED
2960  LET B9=1/6
2961  REM                      D9 = VISCØUS DAMPING RATIØ
2962  REM              ASSIGN NEW VISCØUS DAMPING RATIØ TØ
2963  REM              NEXT LINE IF DESIRED
2964  LET D9=0
2965  LET Z8=X9=0
2970  LET A2=A1=AO
2980  LET T=T+H
2990  GØSUB 3290
3000  FØR I9=1 TØ 10
3010  LET A1=A2
3020  LET V1=VO+(AO+A1)*H/2
3030  LET X1=XO+H*VO+(1/2-B9)*AO*H*H+B9*A1*H*H
3040  GØSUB 3440
3050  IF X1 <= X8 THEN 3080
3052  IF Z8>.5 THEN 3060
3054  LET Z8=1
3056  LET H=INT(1000*H*Z7+1/2)/1000
3060  LET A2=(P-Q)/K9/M-2*D9*SQR(K2/K9/M)*V1
3070  GØTØ 3090
3080  LET A2=(P-Q)/K8/M-2*D9*SQR(K1/K8/M)*V1
3090  IF ABS((A2-A1)/A2) <= .01 THEN 3140
3100  NEXT I9
3120  PRINT "AT T=";T;"ABS(A2-A1)/A2=";ABS(A2-A1)/A2
3130  STØP
3140  LET V1=VO+(AO+A2)*H/2
3150  LET X1=XO+H*VO+(1/2-B9)*AO*H*H+B9*A2*H*H
3160  IF X9 >= X1 THEN 3200
3170  LET X9=X1
3180  GØTØ 3200
3200  IF X9/X8<15 THEN 3220
3204  IF Z8<.5 THEN 3210
3206  LET H=INT(1000*H/Z7+1/2)/1000
3210  RETURN
3220  IF V1<0 THEN 3262
3230  LET AO=A2
3240  LET VO=V1
3250  LET XO=X1
3260  GØTØ 2980
3262  IF Z8>1.5 THEN 3278
3263  IF Z8<.5 THEN 3278
3264  LET Z8=2
3266  LET T=T-H
3268  LET A2=AO
3274  LET H=INT(1000*H/Z7+1/2)/1000
3276  GØTØ 2980
3278  RETURN
3280  REM *** FØRCE FUNCTIØN SUBRØUTINE  ****************************
3290  IF T<TO THEN 3330
3300  LET P=0
3310  RETURN
3320  REM                        TRIANGULAR RISE PULSE
3330  IF T >= T1 THEN 3360
3340  LET P=PO*T/T1
3350  RETURN
3360  IF Z1=2 THEN 3410
3370  REM                        TRIANGULAR DECAY PULSE
3380  LET P=PO*(TO-T)/(TO-T1)
3390  RETURN
3400  REM                        EXPØNENTIAL DECAY PULSE
3410  LET P=PO*(1-((T-T1)/(TO-T1)))*EXP(-((T-T1)/(TO-T1)))
3420  RETURN
3430  REM *** RESISTANCE FUNCTIØN SUBRØUTINE  **********************
3440  IF Q0-K1*X1<0 THEN 3490
3450  REM                        ELASTIC PHASE
3460  LET Q=K1*X1
3470  RETURN
3480  REM                        PLASTIC PHASE
3490  LET Q=Q0+K2*(X1-X8)
3500  RETURN
3510  PRINT
3530  PRINT
3540  PRINT "TIME","ACCELERATIØN","VELØCITY","DISPLACEMENT","DAMP.CØEF."
3560  LET T=INT(1000*T+1/2)/1000
3570  PRINT T-H,INT(10000*AO+1/2)/10000,INT(10000*VO+1/2)/10000,
3580  PRINT INT(10000*XO+1/2)/10000,D9
```

Table G.3 (continued)

```
3590 PRINT T,INT(10000*A2+1/2)/10000,INT(10000*V1+1/2)/10000,
3600 PRINT INT(10000*X1+1/2)/10000
3640 LET T3=INT(1000*(T-H)+V0/(V0-V1)+1/2)
3680 PRINT
3690 RETURN
3840 REM *** SUBRØUTINE FØR U FRØM FØRMULA **************************
3850 LET U=INT(1/(R1-R2)+1/2)/10
3860 IF U <= 10 THEN 3880
3870 LET U=10
3880 RETURN
3890 REM *** EARLY P0, Q0 ******************************************
3900 IF J>0 THEN 3940
3910 LET P0=1.3*P1
3920 LET J=1
3930 GØTØ 3950
3940 GØSUB 4000
3950 LET Q0=P0/(1-1/2/U)
3960 RETURN
3970 REM *** SUBRØUTINE FØR INCREASED P0 FØR DEAD LØAD *************
4000 LET P0=P1+150/1728*D5*(1-1/2/U)
4010 RETURN
4020 REM *** SUBRØUTINE FØR M1, D, K0, I1, K1, T8 ******************
4030 REM
4035 LET M1=R1*B*F2*(1-.554*R1*F2/.85/1.25/F1)
4040 IF Z3=1 THEN 4060
4050 LET M1=R9*B*F2*(1-.554*R9*F2/.85/1.25/F1)
4060 LET D=SQR(A*Q0*L↑2*C3/M1)
4130 LET T8=L↑2/C5/D/SQR(R1)
4135 LET D3=D4=D
4140 GØSUB 4470
4150 IF R9-R8 >= .4*1.25*F1/F2 THEN 4180
4170 IF R1-R2<.4*1.25*F1/F2 THEN 4200
4180 PRINT "SLANTING REPØRT TABLE 6.2 EQ.4 NØT MET; CHANGE PRØGRAM"
4190 STØP
4200 IF Z5=1 THEN 4204
4202 IF D2>1.3 THEN 4220
4204 GØSUB 6000
4220 IF Z3>1.5 THEN 4330
4240 LET X[1]=(R1-R2)*B*F2*(1-.554*(R1-R2)*F2/.85/1.25/F1)+R2*B*F2
4250 LET Y[1]=-R2*B*F2*D1
4260 LET Z[1]=M1=-A*Q0*L↑2*C8
4270 LET M1=-M1
4280 LET D=(-Y[1]+SQR(Y[1]↑2-4*X[1]*Z[1]))/2/X[1]
4290 LET D3=D4=D
4300 REM
4310 LET M9=0
4314 LET D5=D3+D2
4320 GØTØ 4410
4330 LET X[1]=(R9-R8)*B*F2*(1-.554*(R9-R8)*F2/.85/1.25/F1)+R8*B*F2
4340 LET Y[1]=-R8*B*F2*D2
4350 LET Z[1]=M9=-A*Q0*L↑2*C3
4360 LET M9=-M9
4365 LET M1=M9/C9
4370 LET D=(-Y[1]+SQR(Y[1]↑2-4*X[1]*Z[1]))/2/X[1]
4380 REM
4390 LET D4=D
4392 LET D5=D4+D1
4394 LET D3=D=D5-D2
4396 LET Y2=-B*D↑2*F2
4398 LET Y1=-Y2*.554*F2/.85/1.25/F1
4400 LET Y3=M1-B*D*F2*(D-D1)*R2
4402 LET Y0=2*Y3/(-Y2+SQR(Y2↑2-4*Y1*Y3))
4404 LET R1=INT(10000*(Y0+R2)+1/2)/10000
4410 LET X[1]=Y[1]=Z[1]=0
4412 IF D3>D4 THEN 4418
4414 LET D=D3
4416 GØTØ 4420
4418 LET D=D4
4420 IF U0 <= 10 THEN 4424
4422 GØSUB 3850
4424 GØSUB 4000
4426 LET K0=30000/F1*R1
4428 LET K0=SQR(2*K0+K0↑2)-K0
4430 LET I1=B*((K0*D)↑3/3+30000/F1*R1*D↑3*(1-K0)↑2)
4432 LET K1=C4*1000*F1*I1/L↑3/(B*L)
4434 LET K2=0
4440 LET J1=J1+1
4445 IF J1<2 THEN 4130
4450 RETURN
4460 REM *** SUBRØUTINE FØR REBØUND STEEL, R2 AND R3 ***************
4470 IF Z1=1 THEN 4500
4480 LET T2=.87*SQR(10/P0)*W↑(1/3)
4490 GØTØ 4510
4500 LET T2=T0
4510 IF T1=0 THEN 4532
4520 PRINT "REBØUND STEEL SUBRØUTINE BASED ØN ZERØ RISE-TIME BLAST;"
4530 PRINT "  RESULTS INVALID BECAUSE T1>0 ENTERED IN LEVEL 1."
4531 GØTØ 4660
4532 IF T2/T8 < 0.2 THEN 4660
4534 IF T2/T8>100 THEN 4660
4536 IF U<1 THEN 4660
4538 IF U>50 THEN 4660
4540 LET Y[2]=3.6916*LØG(U)
4550 LET X[2]=3.6916*LØG(T2/T8)
4551 IF Y[2] <= 2.419*X[2] THEN 4560
4552 IF Y[2] >= (2.419+2.419*X[2]) THEN 4554
4553 IF Y[2] < 6 THEN 4660
4554 IF Y[2] < (7.2905 + 2.419*X[2]) THEN 4557
4555 LET R0=1.0
4556 GØ TØ 4700
4557 LET R0=3.514+X[2]-Y[2]/2.419
4558 LET R0=0.9429+0.1839*R0-0.16*R0↑2+0.02022*R0↑3
4559 GØTØ 4700
4560 LET Y[3]=-.806-.52*X[2]+.855*Y[2]
4570 LET X[3]=-4.6748+.855*X[2]+.52*Y[2]
4580 IF Y[3]>0 THEN 4610
4590 LET R0=X[3]-.15175*Y[3]↑2-.1008
4600 GØTØ 4620
4610 LET R0=X[3]-.2811*Y[3]↑2-.238
4620 LET R0=.4008-.04672*R0+.001678*R0↑2+3.724E-04*R0↑3-3.552E-05*R0↑4
4630 IF R0>.5 THEN 4660
4640 IF R0<.1 THEN 4660
4650 IF Q2=0 THEN 4700
4660 PRINT "R0-EQUATION=";R0;", ENTER REBØUND STEEL RATIØ BY USING"
```

```
4670 PRINT "  CHART WITH TD/T=";T2/T6;"AND MU=";U
4680 PRINT "  (ENTER ABSOLUTE VALUE; 0 CAUSES USE OF RO-EQUATION)";
4684 INPUT O1
4685 PRINT
4686 IF O1 <= 0 THEN 4700
4690 LET RO=O1
4700 LET R2=INT(10000*RO*R1+1/2)/10000
4710 IF R2 >= .0025 THEN 4730
4720 LET R2=.0025
4730 IF Z3>1.5 THEN 4760
4740 LET R8=0
4750 RETURN
4760 LET R8=INT(10000*RO*R9+1/2)/10000
4764 IF R8 >= .0025 THEN 4770
4766 LET R8=.0025
4770 IF R8 >= INT(10000*R1/4+1/2)/10000 THEN 4790
4780 LET R8=INT(10000*R1/4+1/2)/10000
4785 LET R2=R8*R1/R9
4790 RETURN
4898 REM *** SUBROUTINE FOR OUTPUT PORTION *************************
4900 IF Z3>1.5 THEN 4930
4910 PRINT Z9,Z9*R2/R1,R9,R9
4920 RETURN
4930 PRINT Z9*R1/R9,Z9*R2/R9,Z9,Z9*R8/R9
4940 RETURN
5000 REM *** SUBROUTINE FOR ESTIMATED STEEL AND CONCRETE QUANITIES **
5010 REM  CHANGE SYMBOL MEANINGS OF R1,R2,R3,R9 TO BE AREAS PER
5020 REM  UNIT WIDTH INSTEAD OF DIMENSIONLESS RATIOS
5030 LET R1=R1*D3
5040 LET R1=4.41078E-03+1.00003*R1
5050 LET R2=R2*D3
5060 LET R2=7.1098E-03+.998029*R2
5070 LET R9=R9*D4
5080 LET R9=4.41078E-03+1.00003*R9
5090 LET R8=R8*D4
5100 LET R8=7.1098E-03+.998029*R8
5210 PRINT
5230 PRINT
5240 PRINT "ESTIMATE OF STEEL AND CONCRETE QUANTITIES (VER II)"
5245 REM ***WEIGHT OF PRIMARY REINFORCING STEEL***
5250 IF Z2=2 THEN 5290
5260 PRINT "FOR 12 INCH WIDTH OF SLAB."
5270 LET B=12
5275 LET W1=0
5280 GOTO 5300
5290 PRINT "FOR";B;"INCH WIDTH OF BEAM."
5300 PRINT
5310 IF R1>R8 THEN 5320
5312 PRINT "CHANGE PROGRAM TO ACCOUNT FOR R1<R8"
5314 GOTO 5500
5320 IF Z3=1 THEN 5410
5330 IF Z3=2 THEN 5370
5340 LET W2=(.4226*L+3*D)*(R8+R9)+(.5774*L-3*D)*(R1+R2)+.8284*(R1-R8)
5345 PRINT "WEIGHT OF LONG. STEEL IN FREE SPAN      =";W2*.28356*B
5350 LET W2=.28356*B*(W2+W8*(R8+R9))
5360 GOTO 5430
5370 LET W2=(.25*L+1.5*D)*(R8+R9)+(.75*L-1.5*D)*(R1+R2)+.4141*(R8+R9)
5375 PRINT "WEIGHT OF LONG. STEEL IN FREE SPAN      =";W2*.28356*B
5380 LET W2=.28356*B*(W2+W8/2*(R8+R9))
5390 LET W1=(21.735+2.93509E-02*L)*R1+(13.663+4.48492E-02*L)*R2
5395 LET W2=W2+.28356*B*W1
5400 GOTO 5430
5410 LET W2=.28356*B*L*(R1+R2)
5415 PRINT "WEIGHT OF LONG. STEEL IN FREE SPAN      =";W2
5420 LET W1=(21.735+2.93509E-02*L)*R1+(13.663+4.48492E-02*L)*R2
5425 LET W2=W2+.28356*B*2*W1
5430 PRINT "WEIGHT OF LONGITUDINAL REINFORCING STEEL=";W2
5440 W1=W2
5500 REM ***WEIGHT OF TEMP STEEL***
5501 LET D6=D1
5502 LET D7=D2
5503 LET D1=R9
5504 IF R9>R2 THEN 5506
5505 LET D1=R2
5506 LET D1=1.43502*EXP(.180369*D1*12)
5507 LET D2=R8
5508 IF R8>R1 THEN 5510
5509 LET D2=R1
5510 LET D2=1.43502*EXP(.180369*D2*12)
5512 LET D5=D2
5514 IF D5>D1 THEN 5518
5516 LET D5=D1
5518 D5=D5+D
5519 LET W2=.002*D5
5520 LET W2=2.60165E-03+1.03708*W2
5530 W2=.28356*B*L*W2
5540 PRINT "WEIGHT OF TEMPERATURE STEEL             =";W2
5560 LET W1=W1+W2
5600 REM ***WEIGHT OF STIRRUP STEEL***
5610 LET Z9=.7*EXP(-.08*D)
5620 IF .11/.75/D/D/(.3+Z9)>R3 THEN 5690
5630 LET W2=.11/.75/D/D/R3/(.3+Z9)
5640 LET W2=R3*(L+D+W2*W2*(L-D))
5660 LET W2=W2*.1417*(-.25+(1.3+Z9)*D+1.286*D1-.214*D2)*B
5680 GOTO 5710
5690 LET W2=.2834*(-.25+(1.3+Z9)*D+1.286*D1-.214*D2)
5700 LET W2=W2*.11/.75/D/D/(.3+Z9)*L*B
5710 LET W2=4.24137+.957262*W2
5720 PRINT "WEIGHT OF STIRRUP STEEL                 =";W2
5730 LET W1=W1+W2
5800 PRINT "TOTAL WEIGHT OF STEEL                   =";W1
5810 PRINT
5900 REM ***CUBIC YARDS OF CONCRETE IN FREESPAN***
5902 REM *** AND THICKNESS ***
5904 IF D2>D1 THEN 5910
5906 D2=D1
5910 PRINT  USING 5912;D,D2,D+D2
5912 IMAGE "D + D'' = T =",2X2D.5D2X,"+",2X2D.5D2X,"=",2X2D.5D
5914 LET W2=L*(D+D2)*B/46656.
5916 PRINT
5920 PRINT "CUBIC YARDS OF CONCRETE IN FREE SPAN    =";W2
5980 LET D1=D5
5990 LET D2=D6
```

Table G.3 (continued)

```
5999 RETURN
6000 REM *** SUBRØUTINE FØR D1 AND D2 ***************************
6010 LET D1=7.1098E-03+.998029*R2*D3
6020 LET Z9=4.41078E-03+1.00003*R9*D4
6030 IF D1>Z9 THEN 6050
6040 LET D1=Z9
6050 LET D1=1.43502*EXP(.180369*D1*12)
6060 LET D2=4.41078E-03+1.00003*R1*D3
6070 LET Z9=7.1098E-03+.998029*R8*D4
6080 IF D2>Z9 THEN 6100
6090 LET D2=Z9
6100 LET D2=1.43502*EXP(.180369*D2*12)
6110 LET Z9=0
6120 RETURN
7000 REM ************************************************************
7010 REM *** ALTERNATE BETA-METHØD SUBRØUTINE *********************
7020 REM
7030 REM  VARIABLES: A0,A1,A2,B9,D5,D9,H,K1,K2,K8,K9,M,Ø0,T
7040 REM             V0,V1,X0,X1,X8,X9,Z8
7050 REM
7060 IF Ø0=0 THEN 7640
7070 LET V0=X0=T=0
7080 LET X8=Ø0/K1
7090 GØSUB 3290
7100 LET M=D5*150/1728/386
7110 LET A0=P/K8/M
7120 REM ***          BETA EQUATIØNS
7130 REM ***          BETA(B9) = 1/6 CØRRESPØNDS EXACTLY TØ THE
7140 REM ***          LINEAR-ACCELERATIØN METHØD
7150 REM ***          BETA(B9) = 1/4 CØRRESPØNDS TØ THE MØDIFIED
7160 REM ***          ADAMS METHØD
7170 REM *** ASSIGN NEW BETA TØ NEXT LINE IF DESIRED (1/6<BETA<1/4)
7180 LET B9=1/6
7185 REM ***          D9 = VISCØUS DAMPING RATIØ
7187 REM *** ASSIGN NEW VISCØUS DAMPING RATIØ TØ NEXT LINE IF DESIRED
7189 LET D9=0
7190 LET X9=0
7200 REM
7210 REM *** ELASTIC PØRTIØN ***
7220 REM
7230 LET T=T+H
7240 GØSUB 3290
7250 LET Ø0=SQR(K1/K8/M)
7255 LET X1=B9*H*H*(P/K8/M-2*D9*Ø0/(1+D9*H*Ø0)*(V0+H/2*(A0+P/K8/M)))
7260 LET X1=X1+X0+V0*H+(1/2-B9)*A0*H*H
7265 LET X1=X1/(1+Ø0*Ø0*H*H*B9/(1+D9*H*Ø0))
7270 IF X1>X8 THEN 7380
7280 LET V1=(V0+H/2*(A0+P/K8/M-Ø0*Ø0*X1))/(1+D9*H*Ø0)
7290 LET A1=P/K8/M-2*D9*Ø0*V1-Ø0*Ø0*X1
7300 IF X9 >= X1 THEN 7320
7310 LET X9=X1
7320 IF V1<0 THEN 7630
7330 LET A0=A1
7340 LET V0=V1
7350 LET X0=X1
7360 GØTØ 7230
7370 REM
7380 REM *** PLASTIC PØRTIØN ***
7390 REM
7400 LET Z8=1
7410 LET T=T-H
7420 LET H=INT(1000*H*Z7+1/2)/1000
7430 LET T=T+H
7440 GØSUB 3290
7450 LET Ø0=SQR(K2/K9/M)
7452 LET P=(P-Ø0*K2*K8)
7455 LET X1=B9*H*H*(P/K9/M-2*D9*Ø0/(1+D9*H*Ø0)*(V0+H/2*(A0+P/K9/M)))
7460 LET X1=X1+X0+V0*H+(1/2-B9)*A0*H*H
7465 LET X1=X1/(1+Ø0*Ø0*H*H*B9/(1+D9*H*Ø0))
7470 LET V1=(V0+H/2*(A0+P/K9/M-Ø0*Ø0*X1))/(1+D9*H*Ø0)
7475 LET A1=P/K9/M-2*D9*Ø0*V1-Ø0*Ø0*X1
7480 IF X9 >= X1 THEN 7500
7490 LET X9=X1
7500 IF X9/X8<15 THEN 7530
7510 LET H=INT(1000*H/Z7+1/2)/1000
7520 GØTØ 7630
7530 IF V1<0 THEN 7580
7540 LET A0=A1
7550 LET V0=V1
7560 LET X0=X1
7570 GØTØ 7430
7580 IF Z8>1.5 THEN 7630
7590 LET Z8=2
7600 LET T=T-H
7610 LET H=INT(1000*H/Z7+1/2)/1000
7620 GØTØ 7430
7630 LET A2=A1
7640 RETURN
9999 END
```

Table G.3 (continued)

```
RUN
SLB

 74  70 1612

LEVEL 1:
ENTER PEAK OVERPRESSURE (PSI), RISE-TIME (SEC),
  POSITIVE PHASE DURATION (SEC) AND WEAPON YIELD (MT)
?15,0,1.55,1
ENTER BLAST DECAY: 1=LINEAR, 2=EXPONENTIAL ?2

LEVEL 2:
ENTER STEEL DYNAMIC YIELD STRESS (PSI) AND
  CONCRETE COMPRESSIVE STRESS (STATIC)(PSI)
?52000,30000.

LEVEL 3:
SUPPORT CONDITIONS & BEAM/ONE-WAY SLAB. ENTER 2 SINGLE
  DIGITS, SEPARATED BY A COMMA: 1=SIMPLE SUPPORTS,
  2=PROPPED CANTILEVER, OR 3=FIXED ENDS; AND
  1=SLAB OR 2=BEAM ?1,1-2
ENTER BEAM WIDTH (INCHES) & SUPPORTED AREA WIDTH (INCHES)
?30,100

LEVEL 4:
ENTER CLEAR SPAN (IN.) AND MU (>10 CAUSES USE OF
  MU=.1/(P-P')<=10; P & P'=TENS.& COMPR. STEEL)
?200,11

LEVEL 5:
ENTER MAX. TENSILE STEEL RATIO (<=.02) ?.01
ENTER D' & D'' (ZEROES GIVE MIN.OF 1.3125; OR 1,1= USE
  STATISTICAL PGM HEREIN; OR ENTER ACTUAL VALUES>1.3125)
?1,1

LIST ALL VARIABLES TO THIS POINT (1=YES, 2=NO)?1

PO                P1                T1                TO
 15                15                0                 1.55

Z1                F2                F1                Z3
 2                 52000.            3000              1

W8                B                 A                 A3
 0                 30                100               100

L                 U                 U0                R1
 200               11                11                0

D1                D2                Z9
 1.45              1.45              1

ANY CHANGES? (6=NO; 1 TO 5=RETURN TO LEVEL 1,2...5)
?6

 74  70 1615
```

```
HOW IS REBOUND RATIO(RO) TO BE GENERATED?
  (O=BY INTERNAL EQN: 1=BY CHART, REF 2, PG B-32)?0

PURE SHEAR: F'C COEFFICIENT APPROX  .102
ABSOLUTE MAX.=.2; DESIRABLE MAX.=.1; SEE TEXT & EQ.6-10

PURE SHEAR: SQR(F'C) COEFFICIENT APPROX  1.33499
ACI71(CH.11) ALLOWED=6 OR MORE

TIME            ACCELERATION    VELOCITY        DISPLACEMENT    DAMP.COEF.
 .094           -500.022         .3424           1.4253          0
 .095           -505.119        -.1602           1.4253

OVERPR          F'C             FDY             D(+M)           D(-M)
 15              3000            52000.          24.3198         24.3198

CL.SPAN         P(+M)           P'(+M)          PV              +M(IN.K/B)
 200             .01             .0025           .0057           8600

MU(DESIRED)     P(-M)           P'(-M)          Q               -M(IN.K/B)
 10              0               0               17.2            0

XE              XM              MU(CALC'D)      TM(MSEC)        PRESS(MAX)
 .146945         1.42535         9.69987         95              17.2078

RISE-T.         POS.DUR.        W(MT)           PERIOD(SEC)     DECAY
 0               1.55            1               .038705         2

TD/T            K1              K2              K8              K9
 17.137          117.051         0               .78             .66

MASS            SLAB/BEAM       SUPP.COND.      WIDTH(B,IN.)    LOADED WIDTH
 .00602         BEAM            SS               30              100

BETA H(SEC)     H(PLASTIC)      D'              D''             EST.THICK.
W .001           .004            1.66181         2.45256         26.7724
 1
  AS(+M)        A'S(+M)         AS(-M)          A'S(-M)
Z2  AND REBAR PERIMETER SUMS       (/FT. IF SLAB)
 2  7.29595      1.82399         0               0
    5.2412       1.3103          0               0

RO              P'/P(+M)        P'/P(-M)        SUPP.THICK.
 .175489         .25            NA              NA
R4
 .01
ESTIMATE OF STEEL AND CONCRETE QUANTITIES (VER II)
FOR 30  INCH WIDTH OF BEAM.

WEIGHT OF LONG. STEEL IN FREE SPAN        = 536.619
WEIGHT OF LONGITUDINAL REINFORCING STEEL= 679.019
WEIGHT OF TEMPERATURE STEEL               = 98.9032
WEIGHT OF STIRRUP STEEL                   = 190.195
TOTAL WEIGHT OF STEEL                     = 968.117
```

Table G.3 (continued)

```
D + D'' = T =  24.31982  +   2.45255  =  26.77237

CUBIC YARDS OF CONCRETE IN FREE SPAN     = 3.44295

 74  70 1623

RETURN TO WHAT LEVEL (1-5; USE 6=STOP) ?5


LEVEL 5:
ENTER MAX. TENSILE STEEL RATIO (<=.02) ?.005
ENTER D' & D'' (ZEROES GIVE MIN.OF 1.3125; OR 1,1= USE
  STATISTICAL PGM HEREIN; OR ENTER ACTUAL VALUES>1.3125)
?1,1

LIST ALL VARIABLES TO THIS POINT (1=YES, 2=NO)?2
ANY CHANGES? (6=NO; 1 TO 5=RETURN TO LEVEL 1,2...5)
?6

 74  70 1624
HOW IS REBOUND RATIO(RO) TO BE GENERATED?
  (0=BY INTERNAL EQN; 1=BY CHART, REF 2, PG B-32)?0

PURE SHEAR: F'C COEFFICIENT APPROX  .071
ABSOLUTE MAX.=.2; DESIRABLE MAX.=.1; SEE TEXT & EQ.6-10

PURE SHEAR: SQR(F'C) COEFFICIENT APPROX  .922593
ACI71(CH.11) ALLOWED=6 OR MORE
```

TIME	ACCELERATION	VELOCITY	DISPLACEMENT	DAMP.COEF.
.087	-367.081	.046	.895	0
.088	-370.993	-.323	.8949	

OVERPR	F'C	FDY	D(+M)	D(-M)
15	3000	52000.	34.7039	34.7039
CL.SPAN	**P(+M)**	**P'(+M)**	**PV**	**+M(IN.K/B)**
200	.005	.0025	.005	9050.
MU(DESIRED)	**P(-M)**	**P'(-M)**	**Q**	**-M(IN.K/B)**
10	0	0	18.1	0
XE	**XM**	**MU(CALC'D)**	**TM(MSEC)**	**PRESS(MAX)**
9.05658E-02	.895037	9.88273	87	18.0358
RISE-T.	**POS.DUR.**	**W(MT)**	**PERIOD(SEC)**	**DECAY**
0	1.55	1	3.83587E-02	2
TD/T	**K1**	**K2**	**K8**	**K9**
16.8906	199.855	0	.78	.66
MASS	**SLAB/BEAM**	**SUPP.COND.**	**WIDTH(B,IN.)**	**LOADED WIDTH**
.00828	BEAM	SS	30	100

BETA H(SEC)	H(PLASTIC)	D'	D''	EST.THICK.
.001	.004	1.75766	2.10921	36.8131

AS(+M)	A'S(+M)	AS(-M)	A'S(-M)
AND REBAR PERIMETER SUMS		(/FT. IF SLAB)	
5.20559	2.60279	0	0
3.84967	1.92483	0	0
RO	**P'/P(+M)**	**P'/P(-M)**	**SUPP.THICK.**
.176854	.5	NA	NA

```
ESTIMATE OF STEEL AND CONCRETE QUANTITIES (VER II)
FOR 30   INCH WIDTH OF BEAM.

WEIGHT OF LONG. STEEL IN FREE SPAN        = 462.147
WEIGHT OF LONGITUDINAL REINFORCING STEEL= 581.797
WEIGHT OF TEMPERATURE STEEL               = 134.336
WEIGHT OF STIRRUP STEEL                   = 235.168
TOTAL WEIGHT OF STEEL                     = 951.301

D + D'' = T =  34.70391  +   2.10920  =  36.81311

CUBIC YARDS OF CONCRETE IN FREE SPAN     = 4.7342

 74  70 1631

RETURN TO WHAT LEVEL (1-5; USE 6=STOP) ?3

LEVEL 3:
SUPPORT CONDITIONS & BEAM/ONE-WAY SLAB. ENTER 2 SINGLE
  DIGITS, SEPARATED BY A COMMA: 1=SIMPLE SUPPORTS,
  2=PROPPED CANTILEVER, OR 3=FIXED ENDS; AND
  1=SLAB OR 2=BEAM ?1,1
LEVEL 4:
ENTER CLEAR SPAN (IN.) AND MU (>10 CAUSES USE OF
  MU=.1/(P-P')<=10; P & P'=TENS.& COMPR. STEEL)
?500.,11
LEVEL 5:
ENTER MAX. TENSILE STEEL RATIO (<=.02) ?.01
ENTER D' & D'' (ZEROES GIVE MIN.OF 1.3125; OR 1,1= USE
  STATISTICAL PGM HEREIN; OR ENTER ACTUAL VALUES>1.3125)
?1,1
LIST ALL VARIABLES TO THIS POINT (1=YES, 2=NO)?2
ANY CHANGES? (6=NO; 1 TO 5=RETURN TO LEVEL 1,2...5)
?6

 74  70 1633
HOW IS REBOUND RATIO(RO) TO BE GENERATED?
  (0=BY INTERNAL EQN; 1=BY CHART, REF 2, PG B-32)?1
```

Table G.3 (continued)

```
RO-EQUATIØN= .543864        , ENTER REBØUND STEEL RATIØ BY USING
  CHART WITH TD/T= 2.7586     AND MU= 10
  (ENTER ABSØLUTE VALUE; 0 CAUSES USE ØF RO-EQUATIØN)?0

RO-EQUATIØN= .540563        , ENTER REBØUND STEEL RATIØ BY USING
  CHART WITH TD/T= 2.78511    AND MU= 10
  (ENTER ABSØLUTE VALUE; 0 CAUSES USE ØF RO-EQUATIØN)?0

RO-EQUATIØN= .460614        , ENTER REBØUND STEEL RATIØ BY USING
  CHART WITH TD/T= 3.46445    AND MU= 10
  (ENTER ABSØLUTE VALUE; 0 CAUSES USE ØF RO-EQUATIØN)?.44

RO-EQUATIØN= .47243         , ENTER REBØUND STEEL RATIØ BY USING
  CHART WITH TD/T= 3.35577    AND MU= 10
  (ENTER ABSØLUTE VALUE; 0 CAUSES USE ØF RO-EQUATIØN)?.44

RO-EQUATIØN= .437437        , ENTER REBØUND STEEL RATIØ BY USING
  CHART WITH TD/T= 3.69129    AND MU= 10
  (ENTER ABSØLUTE VALUE; 0 CAUSES USE ØF RO-EQUATIØN)?.42

RO-EQUATIØN= .446383        , ENTER REBØUND STEEL RATIØ BY USING
  CHART WITH TD/T= 3.60135    AND MU= 10
  (ENTER ABSØLUTE VALUE; 0 CAUSES USE ØF RO-EQUATIØN)?.43

RO-EQUATIØN= .453072        , ENTER REBØUND STEEL RATIØ BY USING
  CHART WITH TD/T= 3.53612    AND MU= 10
  (ENTER ABSØLUTE VALUE; 0 CAUSES USE ØF RO-EQUATIØN)?.43

RO-EQUATIØN= .458832        , ENTER REBØUND STEEL RATIØ BY USING
  CHART WITH TD/T= 3.48121    AND MU= 10
  (ENTER ABSØLUTE VALUE; 0 CAUSES USE ØF RO-EQUATIØN)?.43

RO-EQUATIØN= .459231        , ENTER REBØUND STEEL RATIØ BY USING
  CHART WITH TD/T= 3.47745    AND MU= 10
  (ENTER ABSØLUTE VALUE; 0 CAUSES USE ØF RO-EQUATIØN)?.44

RO-EQUATIØN= .465497        , ENTER REBØUND STEEL RATIØ BY USING
  CHART WITH TD/T= 3.41903    AND MU= 10
  (ENTER ABSØLUTE VALUE; 0 CAUSES USE ØF RO-EQUATIØN)?.44

RO-EQUATIØN= .455033        , ENTER REBØUND STEEL RATIØ BY USING
  CHART WITH TD/T= 3.5173     AND MU= 10
  (ENTER ABSØLUTE VALUE; 0 CAUSES USE ØF RO-EQUATIØN)?.43

RO-EQUATIØN= .462109        , ENTER REBØUND STEEL RATIØ BY USING
  CHART WITH TD/T= 3.45046    AND MU= 10
  (ENTER ABSØLUTE VALUE; 0 CAUSES USE ØF RO-EQUATIØN)?.44

RO-EQUATIØN= .453514        , ENTER REBØUND STEEL RATIØ BY USING
  CHART WITH TD/T= 3.53186    AND MU= 10
  (ENTER ABSØLUTE VALUE; 0 CAUSES USE ØF RO-EQUATIØN)?.43

RO-EQUATIØN= .460462        , ENTER REBØUND STEEL RATIØ BY USING
  CHART WITH TD/T= 3.46588    AND MU= 10
  (ENTER ABSØLUTE VALUE; 0 CAUSES USE ØF RO-EQUATIØN)?.44

RO-EQUATIØN= .454545        , ENTER REBØUND STEEL RATIØ BY USING
  CHART WITH TD/T= 3.52197    AND MU= 10
  (ENTER ABSØLUTE VALUE; 0 CAUSES USE ØF RO-EQUATIØN)?.43

RO-EQUATIØN= .461283        , ENTER REBØUND STEEL RATIØ BY USING
  CHART WITH TD/T= 3.45818    AND MU= 10
  (ENTER ABSØLUTE VALUE; 0 CAUSES USE ØF RO-EQUATIØN)?.44

RO-EQUATIØN= .45436         , ENTER REBØUND STEEL RATIØ BY USING
  CHART WITH TD/T= 3.52374    AND MU= 10
  (ENTER ABSØLUTE VALUE; 0 CAUSES USE ØF RO-EQUATIØN)?.43

RO-EQUATIØN= .461176        , ENTER REBØUND STEEL RATIØ BY USING
  CHART WITH TD/T= 3.45918    AND MU= 10
  (ENTER ABSØLUTE VALUE; 0 CAUSES USE ØF RO-EQUATIØN)?.44

PURE SHEAR: F'C CØEFFICIENT APPRØX  .066
ABSØLUTE MAX.=.2; DESIRABLE MAX.=.1; SEE TEXT & EQ.6-10

PURE SHEAR: SQR(F'C) CØEFFICIENT APPRØX  2.87287
ACI71(CH.11) ALLØWED=6 ØR MØRE

TIME          ACCELERATIØN   VELØCITY       DISPLACEMENT   DAMP.CØEF.
 .343         -827.996        .4247          23.9311        0
 .344         -831.234       -.4049          23.9311

ØVERPR        F'C            FDY            D(+M)          D(-M)
 15            3000           52000.         31.209         31.209

CL.SPAN       P(+M)          P'(+M)         PV             +M(IN.K/B)
 500           .01            .0044          .0072          478.125

MU(DESIRED)   P(-M)          P'(-M)         Q              -M(IN.K/B)
 10            0              0              15.3           0

XE            XM             MU(CALC'D)     TM(MSEC)       PRESS(MAX)
 2.41613       23.9311        9.9047         344            17.8085

RISE-T.       PØS.DUR.       W(MT)          PERIØD(SEC)    DECAY
 0             1.55           1              .188488        2

TD/T          K1             K2             K8             K9
 3.45918       6.33244        0              .78            .66

MASS          SLAB/BEAM      SUPP.CØND.     WIDTH(B,IN.)   LØADED WIDTH
 .00766       SLAB           SS              1              1

BETA H(SEC)   H(PLASTIC)     D'             D''            EST.THICK.
 .001          .004           1.96061        2.84729        34.0563

AS(+M)        A'S(+M)        AS(-M)         A'S(-M)
  AND REBAR PERIMETER SUMS       (/FT. IF SLAB)
 3.74508       1.64783        0              0
 4.22681       1.8598         0              0
```

Table G.3 (concluded)

```
RO              P'/P(+M)        P'/P(-M)        SUPP. THICK.
 .44             .44            NA              NA

ESTIMATE OF STEEL AND CONCRETE QUANTITIES (VER II)
FOR 12 INCH WIDTH OF SLAB.

WEIGHT OF LONG. STEEL IN FREE SPAN        = 783.763
WEIGHT OF LONGITUDINAL REINFORCING STEEL= 897.595
WEIGHT OF TEMPERATURE STEEL               = 124.606
WEIGHT OF STIRRUP STEEL                   = 279.198
TOTAL WEIGHT OF STEEL                     = 1301.4

D + D'' = T =  31.20897  +   2.84693  =   34.05590

CUBIC YARDS OF CONCRETE IN FREE SPAN      = 4.37962

 74  70 1652

RETURN TO WHAT LEVEL (1-5) USE 6=STOP) ?6


DONE
```

Table G.3 (addendum)

Experience in using the computer program for design of R/C beams and one-way slabs has indicated certain changes to make the program of broader use and easier to understand, the latter in terms of input and output. The following pages, therefore, include suggested program changes, an example run with the changes made, and an explanation of all program output values.

Three program changes were made. First, both input and confirming printout portions were modified to make data entry easier, and yet incorporate some added safeguards against unreasonable entries. Second, the equation for equivalent triangular decay in loading (used only in the rebound steel portion) was changed slightly. Third, program capability was expanded to include handling of a blast loading rise-time; for a rise-time that is longer than the beam/slab effective natural period of vibration, however, capability is limited to a blast loading decay phase that is linear. The entire program change is listed on the next page.

The third page of this addendum shows the example run, using the program change; the example used is the same as the first design example published with the unchanged program (page G-37). Program user inputs are on the left side of the page; the change is in the portion, optional to the user, wherein all entered data is listed for review, the change being that the data for review are identified by listing in the identical order first entered, rather than depending on brief headings as before. (Listing for review provides the bonus of assuring the user that no terminal-computer transmission errors have occurred.) Program outputs are on the right side of the same page; the outputs are explained on the last (fourth) page of this addendum.

The changed program requires slightly over 10,000 characters of storage on two low-cost local time-sharing vendors and pushes their computer limits. One means of reducing this required storage is to delete whichever of a pair of alternate subroutines that is not being used: the one for the Newmark β Method, Lines 2820-3278, or that for the Modified Newmark β Method, Lines 7000-7640; see Explanation, Lines 1571-9, and page G-29.

Table G.3 (addendum)

```
0162  REM
0240  IF P0 <= 200 THEN 270
0250  PRINT "** WARNING ØNLY:  PRØGRAM INTENDED FØR LØWER PEAK"
0260  PRINT "  ØVERPRESSURE, CHECKING WØRK SUGGESTED."
0270  REM
0290  REM
0360  IF T0<.01 THEN 200
0370  IF W <= 0 THEN 200
0372  IF W >= .5 THEN 360
0374  PRINT "** WARNING ØNLY:  PRØGRAM INTENDED FØR LARGER WEAPØNS."
0376  PRINT "  CHECKING WØRK SUGGESTED."
0390  PRINT "ENTER BLAST DECAY: 1=LINEAR, ";
0395  PRINT "2=EXPØNENTIAL(EQ. 3.51.1 REF. 1)";
0668  PRINT "ENTER AVERAGE WIDTH ØF INTERIØR SUPPØRTING WALLS (IN.)";
0676  PRINT "ENTER WIDTH ØF INTERIØR SUPPØRTING WALL (IN.)";
0931  INPUT D1,D2
0932  LET D0=D1
0933  LET D8=D2
0976  I0=I2=0
1020  PRINT "LEVEL 1:",P1,T1,T0,W
1030  PRINT "            ",Z1
1040  PRINT
1050  PRINT "LEVEL 2:",F2,F1
1060  PRINT
1070  PRINT "LEVEL 3:",Z3,Z2
1080  IF Z3=1 THEN 1095
1090  PRINT "            ",W8
1095  IF Z2=1 THEN 1105
1100  PRINT "            ",B,A
1105  PRINT
1110  PRINT "LEVEL 4:",L,U
1115  PRINT
1120  PRINT "LEVEL 5:",R4
1125  PRINT "            ",D0,D8
1131  LET Z9=Ø2=0
1132  IF T1 <= 0 THEN 1135
1133  IF U >= 1 THEN 1135
1134  GØTØ 1870
1571  REM *** IN LINES 1580, 1614, 1690 AND 1840, GØSUB 2820 WILL CALL
1572  REM *** NEWMARK BETA  METHØD (NBM), AND  GØSUB 7000  WILL  CALL
1573  REM *** MØDIFIED NEWMARK BETA METHØD (MNBM).  MNBM  FASTER  THAN
1574  REM *** NBM.  BØTH  LIMITED  TØ  EQ. ØF  MØTIØN  WITH  ANY  TERM
1575  REM *** CØNTAINING ACCELERATIØN, VELØCITY ØR DISPLACEMENT HAVING
1576  REM *** ØNLY ØNE ØF THESE  VARIABLES  AND  ØNLY  TØ FIRST PØWER.
1577  REM *** FØR ØTHER EQS. SEE  TEXT  P.G-29.  PGM HEREIN CAN HANDLE
1578  REM *** VISCØUS DAMPING (LINES 2961 & 7185)  &  FRICTIØN/CØULØMB
1579  REM *** DAMPING (ADD CØNSTANT, LINES 3460 & 3490).
1651  IF I0=1 THEN 1660
1850  IF T1 <= 0 THEN 1980
1860  IF U >= 1 THEN 1980
1870  PRINT "*** PRØGRAM NØT INTENDED FØR NØN-ZERØ ";
1875  PRINT "RISE-TIME & MU < 1 CØMBINATIØN."
1880  GØTØ 2750
1984  PRINT "*** DATA NØT CØMPATABLE WITH SLANTING ";
1985  PRINT "REPØRT TABLE 6.2 EQ. 4."
1986  GØTØ 2750
2740  REM
2862  GØSUB 8010
3210  GØTØ 3278
3278  GØSUB 8110
4472  LET T2=.87*SQR(10/P1)*W^(1/3)
4474  IF T2<.5 THEN 4480
4476  IF P1<2 THEN 4480
4478  IF P1 <= 30 THEN 4490
4480  IF I2=1 THEN 4510
4481  PRINT "** WARNING ØNLY:  REBØUND SUBRØUTINE MAY BE INVALID"
4482  PRINT "  E.G. LINE 4472, SEE PARAGRAPH 4 PAGE 6-33."
4483  I2=1
4511  IF I0=1 THEN 4660
4512  PRINT "*** RISE-TIME IS NØN-ZERØ ***"
4514  PRINT "  WITH FINITE RISE-TIME,REBØUND STEEL RATIØ (RO) MUST"
4520  PRINT "  CØME FRØM USE ØF CHARTS: FIRST ØN PAGE 11-5 SLANTING"
4525  PRINT "  VØLUME 1; SECØND ØN PAGE B-32, REFERENCE 2."
4530  I0=1
4660  IF T1=0 THEN 4668
4661  PRINT
4662  PRINT "  FIRST, USING MU=";U;" AND PMAX/Q=";P0/Q0;" ØBTAIN [D/T]"
4664  PRINT "  SECØND, ØBTAIN RO.  ENTER RO";
4665  INPUT RO
4666  GØTØ 4700
4668  PRINT "RO-EQUATIØN=";RO;", ENTER REBØUND STEEL RATIØ BY USING"
4683  INPUT Ø1
4684  PRINT
4685  LET Ø1=ABS(Ø1)
5910  PRINT "D + D'' = T =";D;"+";D2;"=";D+D2
5912  REM
7052  GØSUB 8010
7640  GØSUB 8110
7650  RETURN
8000  REM SUBRØUTINE TØ MØDIFY Q0 & T1 IF T1/T > 1.0
8010  Q4=Q0
8020  T4=T1
8030  IF T1/T8 <= 1 THEN 8090
8040  Q0=Q0*2*U/(2*U-1)
8050  T1=0
8090  RETURN
8100  REM  SUBRØUTINE TØ RESET Q0 & T1 IF T1/T > 1.0
8110  T1=T4
8120  Q0=Q4
8190  RETURN
```

Table G.3 (addendum)

```
RUN
SLB

LEVEL 1:
ENTER PEAK OVERPRESSURE (PSI), RISE-TIME (SEC),
  POSITIVE PHASE DURATION (SEC) AND WEAPON YIELD (MT)
?15,0,1.55,1
ENTER BLAST DECAY: 1=LINEAR, 2=EXPONENTIAL(EQ. 3.51.1 REF. 1)?2

LEVEL 2:
ENTER STEEL DYNAMIC YIELD STRESS (PSI) AND
  CONCRETE COMPRESSIVE STRESS (STATIC)(PSI)
?52000,3000

LEVEL 3:
SUPPORT CONDITIONS & BEAM/ONE-WAY SLAB. ENTER 2 SINGLE
  DIGITS, SEPARATED BY A COMMA: 1=SIMPLE SUPPORTS,
  2=PROPPED CANTILEVER, OR 3=FIXED ENDS; AND
  1=SLAB OR 2=BEAM ?1,2
ENTER BEAM WIDTH (INCHES) & SUPPORTED AREA WIDTH (INCHES)
?30,100

LEVEL 4:
ENTER CLEAR SPAN (IN.) AN) MU (>10 CAUSES USE OF
  MU=.1/(P-P')<=10; P & P'=TENS.& COMPR. STEEL)
?200,11

LEVEL 5:
ENTER MAX. TENSILE STEEL RATIO (<=.02) ?.01
ENTER D' & D'' (ZEROES GIVE MIN.OF 1.3125; OR 1,1= USE
  STATISTICAL PGM HEREIN; OR ENTER ACTUAL VALUES>1.3125)
?1,1

LIST ALL VARIABLES TO THIS POINT (1=YES, 2=NO)?1

LEVEL 1:      15          0           1.55        1
              2

LEVEL 2:      52000.      3000

LEVEL 3:      1           2
              30          100

LEVEL 4:      200         11

LEVEL 5:      .01
              1           1

ANY CHANGES? (6=NO; 1 TO 5=RETURN TO LEVEL 1,2...5)
?6

HOW IS REBOUND RATIO(RO) TO BE GENERATED?
  (0=BY INTERNAL EQN; 1=BY CHART, REF 2, PG B-32)?0
```

```
PURE SHEAR: F'C COEFFICIENT APPROX  .102
ABSOLUTE MAX.=.2; DESIRABLE MAX.=.1; SEE TEXT & EQ.6-10

PURE SHEAR: SQR(F'C) COEFFICIENT APPROX  1.33499
ACI71(CH.11) ALLOWED=6 OR MORE

TIME          ACCELERATION    VELOCITY      DISPLACEMENT    DAMP.COEF.
 .094         -500.022         .3424         1.4253          0
 .095         -505.119        -.1602         1.4253

OVERPR        F'C             FDY           D(+M)           D(-M)
 15            3000            52000.        24.3198         24.3198

CL.SPAN       P(+M)           P'(+M)        PV              +M(IN.K/B)
 200           .01             .0025         .0057           8600

MU(DESIRED)   P(-M)           P'(-M)        Q               -M(IN.K/B)
 10            0               0             17.2            0

XE            XM              MU(CALC'D)    TM(MSEC)        PRESS(MAX)
 .146945       1.42535         9.69987       95              17.2078

RISE-T.       POS.DUR.        W(MT)         PERIOD(SEC)     DECAY
 0             1.55            1             .038705         2

TD/T          K1              K2            K8              K9
 18.3556       117.051         0             .78             .66

MASS          SLAB/BEAM       SUPP.COND.    WIDTH(B,IN.)    LOADED WIDTH
 .00602       BEAM            SS             30              100

BETA H(SEC)   H(PLASTIC)      D'            D''             EST.THICK.
 .001          .004            1.66181       2.45256         26.7724

AS(+M)        A'S(+M)         AS(-M)        A'S(-M)
  AND REBAR PERIMETER SUMS        (/FT. IF SLAB)
 7.29595       1.82399         0             0
 5.2412        1.3103          0             0

RO            P'/P(+M)        P'/P(-M)      SUPP.THICK.
 .168779       .25            NA            NA

ESTIMATE OF STEEL AND CONCRETE QUANTITIES (VER II)
FOR 30   INCH WIDTH OF BEAM.

WEIGHT OF LONG. STEEL IN FREE SPAN           = 536.619
WEIGHT OF LONGITUDINAL REINFORCING STEEL     = 679.019
WEIGHT OF TEMPERATURE STEEL                  = 98.9032
WEIGHT OF STIRRUP STEEL                      = 190.195
TOTAL WEIGHT OF STEEL                        = 968.117

D + D'' = T = 24.3198     + 2.45255     = 26.7724

CUBIC YARDS OF CONCRETE IN FREE SPAN         = 3.44295
```

Table G.3 (addendum)

OUTPUT EXPLANATION

OUTPUT	Notation (p.6-119)	Comment
TIME		time from start of loading, sec
ACCELERATION		of lumped mass, ips/sec
VELOCITY		of lumped mass, ips
DISPLACEMENT		of lumped mass, in.
DAMP.COEF.		damping coefficient, applied to velocity in β equations; actually, the ratio (between 0 and 1) of assumed viscous damping to critical viscous damping (see Lines 2961 and 1577-9)
OVERPR	p_{so}	psi
D(+M),D(-M)	d	at point of maximum positive/negative moment, in.
P(+M),P'(+M)	p,p'	
PV	p_v	
P(-M),P'(-M)	p_e, p_e'	
Q	q	calculated to tenth (psi) for design nearest desired μ
XE,XM	x_e, x_m	in.
TM	t_m	msec (milliseconds; thousandths of a second)
PRESS(MAX)	p_m	psi
POS.DUR.	t_o	sec
TD/T	t_d/T	$= t_o/T$ (TD here is from Line 4480 equation; see Ref. 2, p.3-45)
K1,K2		stiffness, elastic phase/plastic phase
K8,K9		dynamic load-mass factor, elastic phase/plastic phase
MASS	m	mass per sq. in. of loaded surface, $lb\text{-}sec^2/in.$
BETA H(SEC)		elastic phase time interval in Newmark β Method, sec
H(PLASTIC)		plastic phase time interval in Newmark β Method, sec
D'	d'	in.
D''	d''	in.
AS(+M)	A_s	for maximum positive moment, sq in.
A'S(+M)	A_s'	for maximum positive moment, sq in.
RO		p'/p for +M, as calculated from internal curve-fit equations from, or as read and entered by computer program user from, Ref. 2, p. B-32 (Fig. B-10)
SUPP.THICK		width of interior support, in.
(weights of steel)		lbs.
D + D'' = T	d+d''=t	in.

that running times required for calculations by the MNBM are about one-third of those required by the NBM. Also, all of the illustrative problems used herein, and most of those occurring in structural engineering, are within the limitations of the MNBM, as stated above. Because of its efficiency, therefore, the MNBM is suggested for use whenever possible.

Estimation of slab thickness was needed in the program for rough cost estimating. In order to find an approximate function of slab thickness t versus depth d, many slabs were detailed from the design data given in Table G.1.[50] From this detailing experience, it was found that d'' (and thus t) correlates with A_s. A series of functions were then tested using a computer least squares fit numerical routine; the function with the best correlation was found to be

$$d = 1.44\ e^{(0.00467 + 0.180\ A_s)}$$

which value of d'' was then used to calculate the approximate slab thickness

$$t = d + d''$$

A least value of t recommended for rough estimating use would be

$$t = d + 1.3125$$

where the 1.3125 constant represents 0.75 in. for cover, plus a #3 bar for minimum stirrup size and a half-thickness of a #3 bar for minimum bottom steel.

A correction is needed in the computer program to update it from the former minimum stirrup spacing of 0.75 d to the current 0.5 d, but this is only of concern to those using the quantities estimating portion, not the design portion alone, of the program.[4,60] For this correction, change .75 to .5 in lines 5620, 5630, and 5700. To make a minor correction in the stirrup steel quantities estimating part of the beam portion of the program, the following change should be made in a program line:

```
5710 W2 = 4.24137*B/12 + 0.957262*W2
```

2. Computer Program for Wood Beams

To supplement Section G of Chapter 6, Table G.4 provides a listing of the computer program used for design of rectangular wood beams, simply supported. The program is fully interactive (or conversational).

Table G.4 COMPUTER PROGRAM - WOOD BEAMS, RECTANGULAR, SIMPLY SUPPORTED

```
0100  REM  PRØGRAM IS FØR DESIGN ØF WØØD BEAMS UNDER BLAST LØADING
0120  REM
0140  GØSUB 1740
0160  DIM N$(10)
0180  PRINT "STEP 1"
0200  PRINT "SUPPØRT CØNDITIØN: 1=SIMPLE SUPPØRTS: 2=PRØPPED CANTILEVER:"
0220  PRINT "  3=FIXED-FIXED ENDS";
0240  INPUT N9
0260  PRINT
0280  GØTØ N9 ØF 300,360,420
0300  LET C1=1/8
0320  LET C2=1/2
0340  GØTØ 460
0360  LET C1=1/8
0380  LET C2=5/8
0400  GØTØ 460
0420  LET C1=1/12
0440  LET C2=1/2
0460  PRINT "STEP 2"
0480  PRINT "ENTER CLEAR SPAN (IN.)";
0500  INPUT L
0520  PRINT
0540  PRINT "STEP 3"
0560  PRINT "ENTER DESIGN STRESSES: BENDING, HØRIZ.SHEAR, CØMPRESSIØN"
0580  PRINT "  PERPENDICULAR TØ GRAIN (PSI)";
0600  INPUT F1,F2,F3
0620  PRINT
0640  PRINT "STEP 4"
0660  PRINT "ENTER DEPTH (ACTUAL, NØT NØMINAL) ØF WØØD BEAM (IN.)";
0680  INPUT D
0700  PRINT
0720  LET Q1=2*F1*(D/L)↑2/3/C1
0740  LET Q2=8*F2*D/3/C2/(L-2*D)
0760  IF Q1>Q2 THEN 820
0780  LET Q=Q1
0800  GØTØ 840
0820  LET Q=Q2
0840  LET L1=Q*L*C2/F3
0860  REM    U IN NEXT LINE IS MU, DUCTILITY RATIØ
0880  LET U=3
0900  LET P1=Q*(1-1/(2*U))
0920  REM    P3 IN NEXT LINE IS ASSUMED AMBIENT AIR PRESSURE AT SITE
0940  LET P3=14.7
0960  LET A=8
0970  LET B=14*P3-P1
0980  LET C=-7*P1*P3
0990  LET D1=SQR(B*B-4*A*C)
1000  LET P2=(-B+D1)/2/A
1010  LET P5=(-B-D1)/2/A
1020  IF P5 <= 0 THEN 1220
1030  PRINT "MULTIPLE RØØTS AT LINE 1010"
1040  PRINT "P2=";P2,"P5=";P5
1050  LET P2=P2 MIN P5
1220  REM     ØUTPUT PØRTIØN
1240  GØSUB 1740
1260  PRINT "WØØD BEAM DESIGN (USING MU=3):"
1280  PRINT
1300  PRINT "SUPP.CØNDITIØN, CL.SPAN, DES.STRESSES, BEAM DEPTH ARE:"
1320  PRINT
1340  PRINT N9;L;F1;F2;F3;D
1360  PRINT
1380  PRINT "SIDE-ØN & HEAD-ØN(FULLY REFLECTED) ØVERPR.RESISTANCES ARE:"
1400  PRINT INT(P1*10+1/2)/10,INT(P2*10+1/2)/10;
1420  PRINT "USING AMBIENT AIR AT";P3;"PSI"
1440  PRINT
1460  PRINT "REQ'D BEARING LENGTH AT EACH END ØF BEAM (IN.) = ";
1480  PRINT INT(L1*10+1)/10
1500  GØSUB 1740
1520  PRINT "ANØTHER DESIGN PRØBLEM";
1540  INPUT N$
1560  IF N$="NØ" THEN 1820
1580  PRINT "RETURN TØ STEP 1, 2, 3 ØR 4";
1600  INPUT N8
1620  LET N8=INT(N8)
1640  IF N8<1 THEN 1580
1660  IF N8>4 THEN 1580
1680  GØSUB 1740
1700  GØTØ N8 ØF 180,460,540,640
1720  STØP
1740   FØR I=1 TØ 5
1760   PRINT
1780   NEXT I
1800  RETURN
1820  END
RUN
HLMWBM

STEP 1
SUPPØRT CØNDITIØN: 1=SIMPLE SUPPØRTS: 2=PRØPPED CANTILEVER:
  3=FIXED-FIXED ENDS?1

STEP 2
ENTER CLEAR SPAN (IN.)?40

STEP 3
ENTER DESIGN STRESSES: BENDING, HØRIZ.SHEAR, CØMPRESSIØN
  PERPENDICULAR TØ GRAIN (PSI)?1250,95,385

STEP 4
ENTER DEPTH (ACTUAL, NØT NØMINAL) ØF WØØD BEAM (IN.)?2.5

WØØD BEAM DESIGN (USING MU=3):

SUPP.CØNDITIØN, CL.SPAN, DES.STRESSES, BEAM DEPTH ARE:

 1      40     1250     95     385    2.5

SIDE-ØN & HEAD-ØN(FULLY REFLECTED) ØVERPR.RESISTANCES ARE:
 21.7           8.8          USING AMBIENT AIR AT 14.7        PSI

REQ'D BEARING LENGTH AT EACH END ØF BEAM (IN.) =  1.4
ANØTHER DESIGN PRØBLEM?NØ
```

3. <u>Design Examples Using Final Design Procedures of Chapter 6</u>

The following examples illustrate use of the final design procedures of Chapter 6 for simply supported one-way walls, both exterior and interior, Table G.5; and for simply supported spiral columns, Table G.6. These examples also parallel those used in the next section on preliminary design procedures for similar walls and columns.

TABLE G.5 EXAMPLE OF FINAL DESIGN PROCEDURE FOR SIMPLY SUPPORTED INTERIOR AND EXTERIOR WALLS

D. One-Way Walls - Simply Supported

This section includes - for simply supported one-way walls, both exterior (basement) and interior - typical designs and rough estimates of reinforcing steel and concrete quantities. A recommended final design procedure is described below. The procedure for estimating rebars is closely similar to that for one-way slabs;* thus, only deviations from that procedure, plus comments for text continuity, are noted herein. Further, the basic reasoning on use of stirrups in one-way slabs is also applicable to one-way walls, and rebar detailing (Fig. 6-5) should minimize potential moment transfer from basement shelter cover slab into walls or columns designed as simply supported.

Final Design Procedure. This procedure was developed for potential use in making design graphs and is therefore probably more elaborate than would be justified for normal design use. A preliminary design method is introduced later herein (Appendix G - Supplement).

1. Basic parameter values considered for use were: $f_c' = 3, 4, 5$ ksi; $f_{dc}' = 1.25\ f_c'$; $f_{dy} = 52, 72$ ksi; $p_{so} = 5, 10, 15, 20, 30$ psi, with $t_o \doteq 2.52, 1.85, 1.55, 1.38, 1.17$ sec, respectively (exponential decay). As recommended earlier herein: for wall and column design, either $\mu = 1.3$ and f_c' with no dynamic loading increase factor, or $\mu = 1$ and f_{dc}' may be used; the latter combination was used herein.

The in-plane loading P_u was assumed constant and taken as twice the design blast peak overpressure,† times the tributary area served.[2] (There is a blast wave transit time, and thus a finite rise-time, in the dynamic loading, which can be handled instead of using zero rise-time, but is generally considered as too design-time consuming and complex to be worthwhile.)

The lateral load p_m (psi) on exterior walls‡ was taken as 0.5 p_{so} (i.e., lateral soil coefficient $K_o = 0.5$§), plus the average static soil

Exterior Wall: without in-plane load, initial and final step	Exterior Wall: with in-plane load, initial step	Exterior Wall: with in-plane load, 2nd and final step	Interior Wall: without in-plane load, initial and final step	Interior Wall: with in-plane load, initial step	Interior Wall: with in-plane load, 3rd and final step
(1)	(2)	(3)	(4)	(5)	(6)
3			3		
3.75;52;15			3.75;52;15		
1.55			1.55		
1.0	1.0		1.0		
0	4320		0	8640	
7.5	7.5		—	—	

* Section A of this chapter.

† Which is equivalent to using a step pulse loading with $\mu = 1$; multiplier is thus $1/(1 - 1/(2\mu))$, or 2.

‡ See earlier section on loadings herein, including lateral loads on exterior (basement) walls; it is suggested there that the transit time of airslap down the wall may be used (thus a finite, or not zero, rise-time), but the simpler approach of a step pulse was adopted in the final design procedure above because of possible outrunning ground motion and other situations, as well as because of the simplicity. For further reading and details on this matter, the following sources are available: References 2 (Ch. 4,5), 16 (Ch. 2,5) and 18.

§ K_o varies with the soil, of course. For airslap, it may vary between about 0.15 and 0.75, but will be 1.0 for any saturated soil.[2(p.4-8), 16(p.10),18] For outrunning blast waves, it should probably be 1.0 applied to the free-field (in soil) loading (not necessarily p_{so}).

pressure acting on the wall multiplied by $(1 - 1/(2\mu))$. For purposes of preparing design graphs, the average soil pressure could be assumed to be 15L/1728 psi.* The lateral load on interior walls is, of course, zero within closed (to blast entry) shelters. The lateral load on interior walls exposed to blast requires some estimation of the interior air blast behavior - inflow rate, reflections, time-rates, etc. - for which reference is made to discussion in Chapter 8 and Appendix E of References 50 and 61. Interior walls in open shelter may be so located as to be potentially exposed to blast from either side (in which case $p = p'$); if only exposed on one side, rebound steel should be included per Section A, step 4.

Rules concerning selection of p and p′ in Table 6.2 also apply to one-way walls; however, for exterior walls where rebound is limited by earthfill, p′ may be taken as 0.25p or 0.0025, whichever is larger.

2. This step was to get a first trial value of d; the approach uses only the lateral loading p_m and ignores for now the axial loading P_u. An alternate approach is to assume d (from code, local practice, or judgment) and move directly to step 3.

2a. A value equal to $2p_m$ was assumed for q (psi), as the peak elastic value in an elasto-plastic resistance function for the wall section under design. Using q led to the first trial value for d as follows:

It was first necessary to compute k_3; (k_3d)† is the distance from extreme fiber to neutral axis in USD[4,60]:

$$k_3 = [pf_{dy} - p'(f_{dy} - 0.85f'_{dc})] / (0.85f'_{dc}\beta_1) \qquad (6\text{-}17)$$

where: $\beta_1 = 0.85$, for $f'_c \leq 4000$; or

$$\beta_1 = 0.85 - 0.00005(f'_c - 4000), \text{ for } f'_c > 4000$$

Next, the strain in the compression steel e'_s was calculated:[65,67]

$$e'_s = 0.00375\ (k_3 - d'/d)\ /\ k_3 \qquad (6\text{-}18)$$

where (d'/d) is assumed or estimated (0.1 suggested for first trial); for a trial d′ assume 3/4 in. concrete cover, 3/8 in. stirrup, and half-thickness of 3/8 in. rebar, total 1.3125 in.

Table G.5 (continued)

(1)	(2)	(3)	(4)	(5)	(6)
0.50	0.50				
L = 144; 1.25	144; 1.25		144, 0	144, 0	
p_m = 8.125	8.125		p_m = 15	15	
p = 0.01	0.01		p = 0.01	0.01	
p′ = 0.0025	0.0025		p′ = 0.01	0.01	
16.25	16.25		30	30	
0.147	0.147		0.012	0.012	
0.85	0.85		0.85	0.85	
0.0012	0.0012		-0.02370	-0.02370	

* L is clear wall height (in.).

† Termed "c" in latest ACI Code.[60]

The e_s' value was then to be compared to the yield strain:

$$e_y = f_{dy} / E_s \qquad (6\text{-}19)$$

where E_s (elastic modulus of rebars) was taken as 3×10^7 psi.

2b. If $e_s' \geq e_y$, then the first trial d was calculated:[65]

$$M_u = [(p - p') b f_{dy} (1 - \beta_1 k_3/2) + p'b (f_{dy} - 0.85 f_{dc}')(1 - d'/d)] d^2$$

$$= bq\, L^2 c \qquad (6\text{-}20)$$

where c = 1/8, and b is the width of wall section under design (usually 1 in., sometimes 1 ft).

2c. If $e_s' < e_y$, then k_3 had to be recomputed from the following quadratic equation solution:[65]

$$k_3 = \frac{-B + [B^2 - 4AC]^{0.5}}{2A} \qquad (6\text{-}21)$$

where: $A = 0.85 \beta_1 f_{dc}'$

$B = p' (0.00375\, E_s - 0.85\, f_{dc}') - p f_{dy}$

$C = -0.00375\, E_s p' (d'/d)$

and a first trial d was computed using[65]

$$M_u = \{0.85 \beta_1 b k_3 f_{dc}' (1 - \beta_1 k_3/2) + p'b\, [0.00375\, E_s (k_3 - d'/d)/k_3 - 0.85 f_{dc}'](1 - d'/d)\} d^2$$

$$= bq\, L^2 c \qquad (6\text{-}22)$$

where c = 1/8, and b was as defined in step 2b.

3a. The in-plane and flexural loadings interaction was then considered.* Using the applicable one of the six blocks of equations in Table 6.6, or a suitable interaction diagram,† a new M_u was calculated, including the in-plane loading P_u. Values of z_o and x_o were calculated from equations under the General Notes, Table 6.6; thickness of wall t may be estimated from t = d + 1.3125, using some trial assumptions of step 2a.

Table G.5 (continued)

(1)	(2)	(3)	(4)	(5)	(6)
0.001733	0.001733		0.001733	0.001733	
Go to 2c	Go to 2c		Go to 2c	Go to 2c	
0.1571	0.1571		0.124	0.124	
2709.4	2709.4		2709.4	273.13	
-246.72	-246.72		573.13	573.13	
-28.125	-28.125		-112.5	-112.5	
$M_u = 482.05 d^2$ $M_u = 42120$ d = 9.35	$482.05 d^2$ 42120 9.35		$M_u = 485.54 d^2$ $M_u = 77760$ d = 12.66	$485.54 d^2$ 77760 12.66	at end of 2nd trial d = 10.11
Eqn. #2 42142 $z_o = 1, \frac{x_o}{d} = NA$	Eqn. #1 58080 0.59,0.04	Eqn. #1 44938.50 0.59,0.04	Eqn. #2 77820 $z_o = 1, \frac{x_o}{d} = NA$	Eqn. #1 122860 0.55, 0	Eqn. #1 83605 0.55, 0

* The complexity of current procedures, both ACI and AISC, for handling the interaction of combined axial and flexural loads on beam-column structural members is the subject of much complaint among structural designers - as is the form of the interaction equations, which is such that no mental image of envisioned structural behavior comes from a study of the equations, as it could from older approaches. Nonetheless, use is made of the interaction equations herein because they are the current practice in design.

† That is, one based on the basic flexural design source,[32] not later sources that include a "safety" factor φ.[4,60]

Table G.5 (continued)

	(1)	(2)	(3)	(4)	(5)	(6)
3b. Then a new trial value for d was calculated:						
$d_{new} = [M_{u(old)} / M_{u(new)}]^{0.5}\, d_{old}$ (6-23)	9.35	7.96	skip	12.66	10.07	skip
This step was then repeated until the previously calculated M_u and the new M_u (and of course, the old and new d values) from this step 3 were acceptably close (say, within 2% to 5%); usually no more than 2 or 3 trials are necessary.	M_u=42142	after repeating d = 7.96 OK M_u=43668.59			after 2 more trials d = 9.67	
4. Cracked section moment of inertia I, and elastic and plastic phase stiffnesses, K and K_p, were then calculated:[67]						
$I = bd^3/12\ \{12\ np\ [(1 - k')^2 + r_o(k' - d'/d)^2] + 4(k')^3\}$ (6-24)	45.13	29.22	30.68	124.79	55.61	63.55
where: $n = 30{,}000/f_c'$; $r_o = (n-1)\ p'/(np)$; and k' is identical with k of balanced working stress design:	10, 0.225	10, 0.225	10, 0.225	10, 0.90	10, 0.90	10. 0.90
$k' = [(np(1 + r_o))^2 + 2np(1 + r_o d'/d)]^{0.5} - np(1 + r_o)$ (6-25)	0.346	0.346	0.346	0.314	0.314	0.314
$K = E_c I c'/L^3$ (6-26)	3482.25	2020.36	2132.71	9628.93	3824.09	4436.88
where: $c' = (384/5)/\delta$; $\delta = 12\ [2/\cos(u) - u^2 - 2] / [5\ u^4]$; $u = 0.5\pi\ (P/P_{cr})^{0.5}$; $P_{cr} = \pi^2 E_c I/L^2$; and $E_c = 1{,}000\ f_c'$ (Ref. 2,60,66,67).*	76.8, 1 0,64441, 3×10^6	68.82,1.116 .5054,41723, 3×10^6	69.19,1.110 .4933,43808, 3×10^6	76.8, 1 0,178187, 3×10^6	68.45,1.122 .5181,79406, 3×10^6	69,50,1.105 .4847,90746.80, 3×10^6
$K_p = 0$, if $P = 0$; if $P \neq 0$, then $\mu = 1$ and plastic range of resistance function is not used (thus $K_p = 0$ can be used generally, as in a computer program). With $\mu = 1$, the maximum displacement, or deflection at mid-height of the wall, is	$K_p = 0$	0	0	$K_p = 0$	0	0
$x_e = qL/K$ (6-27.1)	0.672	1.076	1.055	0.449	1.003	0.947
where q is redefined, using the value of δ calculated just above, as $q = 8\ M_u/(\delta L^2)$ (6-27.2)	16.26	15.10	15.62	30.02	26.83	29.18
5. As in Section A (step 8), load-mass-factors of 0.78 (elastic) and 0.66 (plastic), Table 6.3, were used to convert to an equivalent single-degree-of-freedom system, which was then solved for μ and maximum deflection, using the Newmark β Method or a modified version of it (with exponential decay and β = 1/6). Should chart solutions for the equation	μ = 0.981	1.051	1.016	μ = 0.987	1.111	1.010

* $\delta \approx 1/(1 - P/P_{cr})$, if $P \leq 0.6\ P_{cr}$ (Ref. 66).

of motion be needed, loading simplification to triangular pulse may be made[2(p.3-6)] and the elastic period of vibration T may be useful:*

$$T = L^2 \delta^{0.5} / [c'' d (p)^{0.5}] \qquad (6\text{-}28.1)$$

where $c'' = 425{,}000$ (Ref. 2,66).† Also needed is the unit mass (i.e., per square inch):

$$m \approx (150/1728)\ t\ /\ g \qquad (6\text{-}28.2)$$

where $g = 386.4$ and $t \approx d + 1.3125$ (step 2a trial assumptions). Care should be taken that the equation of motion is dimensionally consistent.)

6. If the calculated μ was not acceptably close (say, within 1% to 5%) to the desired $\mu = 1.0$, a new d was assumed from $d_{new} = [\mu_{calculated} / 1.0]^{1/3} d_{old}$ and step 3a, plus steps 4 through 6, was repeated (i.e., skipping step 3b).

7. The remaining checks - for diagonal tension, pure shear, and bond - were identical to Section A (steps 10, 11, and 12 of simply supported one-way slab design procedure).[2] Note: In step 10, use a = b; in step 11, $p_m = p_{so}$ because $\Delta p_{so} = 0$.

Table G.5 (concluded)

(1)	(2)	(3)	(4)	(5)	(6)
not needed	not needed	not needed	not needed	not needed	not needed
0.002395	0.002083	0.002112	0.003138	0.002467	0.002566
$t \approx 10.66$	9.27	9.40	$t \approx 13.97$	10.98	11.42
μ is OK		μ is OK	μ is OK		μ is OK
	8.09			10.02	
final d = 9.35	——	final d = 8.09	final d = 12.66	——	final d = 10.11
	use d = 9.35			use d = 12.66	

* T is related to behavior under lateral loading; under in-plane loading, the period is so short that a blast load can be handled as a step pulse because the loading lasts much longer than the period.

† $\delta \approx 1/(1 - P/P_{cr})$, if $P \le 0.6\ P_{cr}$ (Ref. 66).

‡ More precisely, a vertical load applied on top and bottom ends and located along the plastic centroid line (USD) or transformed section centroid line (WSD).
(Note: centroid lines are not neutral axis lines.)

TABLE G.6 EXAMPLE OF FINAL DESIGN PROCEDURE FOR SIMPLY SUPPORTED CIRCULAR COLUMNS

E. Columns - Simply Supported

This section covers design of simply supported columns, as well as rough estimates of related steel and concrete quantities. A final design procedure is described below. Comments on loading assumptions in Section D also apply herein. Only circular, spiral reinforcement columns are considered below; they are recommended for shelter use as preferable over square, tied columns.[2,16]

The basis for this recommendation is in the far greater energy absorption capacity of the spiral columns prior to complete collapse. Up to yield point, both types act almost identically, but after reaching this point, a tied column immediately fails with a shearing diagonal failure of the concrete and a buckling failure of the column steel between ties. While the tied and spiral columns act almost identically up to yield point, it is only after this point that the spiral steel becomes significantly effective because of gradual destruction of the shell concrete covering the spiral, which then provides radial compressive forces on the core concrete, thereby adding significantly to the load carrying capacity of the core.[65(p.28-)]

Selecting Column Steel Ratio. Many factors should be considered in selecting the (vertical) steel ratio used in a column (range of 0.01 to 0.06 is recommended*). In general, concrete is less expensive than steel in load-carrying capacity; therefore, as the steel ratio decreases, the total cost of column materials, excluding spiral steel, decreases. However, some of the savings will be offset by the increased spiral steel required as the column diameter increases, which in turn decreases usable space. Another factor in choosing the steel ratio would be the cost effectiveness of having fewer column form sizes by using various steel ratios; present practice is to try to keep column sizes constant throughout a building or at least its major areas. Since there are about as many reasons for selecting a large steel ratio as a small one, it is suggested that a first trial value of, say, 0.03 or 0.04 be used.

Final Design Procedure. This procedure was developed for potential use in making design graphs and is therefore probably more elaborate than would be justified for normal design use. A preliminary design method is introduced later herein (Appendix G - Supplement).

	initial trial (1)	2nd trial (2)	final trial (3)
1. Basic parameter values used were: $f'_c = 3, 4, 5$ ksi; $f'_{dc} = 1.25 f'_c$; $f_{dy} = 52, 72$ ksi. Select a trial steel ratio p of 0.01 to 0.06	3 3.75; 52; 0.04		

* Ref. 60, section A.6.1.

Table G.6 (continued)

	(1)	(2)	(3)
(see preceding section). Desired $\mu = 1$. For design, the axial load P_u to be resisted was taken as the product of the tributary area times twice the assumed blast overpressure p_{so}; by using this value as an independent variable, many combinations of p_{so} and tributary area may be covered by a given value of the load in a design graph or table. The load assumption amounts to use of a step pulse (i.e., resistance must equal peak blast load times $\frac{1}{1-1/(2\mu)}$, or 2 when $\mu = 1.0$); such an assumption is well justified when the structural member is extremely stiff (meaning that it has a very short natural period of vibration), as are columns. Any blast lateral load should be minor relative to P_u.	$\mu = 1$; $P_u = 311000$ $L = 144$		
2. The minimum eccentricity e under the current Code[60] was taken as one inch or 0.05 D (column diameter), whichever was larger. The approximate moment on the column was then calculated:	$e = 1.0$		
$M_u = P_u \delta e$ (6-29)	342,100		
where δ was assumed as 1.1 for this step, but is defined in step 4 for use after a trial column diameter D has been determined.			
3. Using M_u and P_u, a trial D was found through use of suitable interaction diagrams,* equations or tables,† as described below.			
Obtaining a trial column D appeared to be a simple matter using M_u and P_u in tables and diagrams.[69,70] It proved troublesome, however, in that the tables are for usual f_y and f_c' values, rather than f_{dy} and f_{dc}', and include a factor Φ that would not be used for blast design, necessitating multiplication of tabular values by $1/\Phi$ for use. Also, implicit in the procedure herein is that maximum concrete strain[2] is 1.25 times 0.003, whereas the tables[69] are based on 0.003. Finally, in developing a computer program for column design, use of equations was much more convenient than use of tables with a program stop for entry of a value read from a table(s).			
Using equations required the following iterative approach:			
3a. A trial value for D is provided by			
$D = [4P_u/(0.85\ \pi f_{dc}')]^{0.5}$ (6-30)	11.15 (first trial)		

* See similar footnote to step 4, Section D.
† Equations and tables used herein are in Ref. 69.

Table G.6 (continued)

	(1)	(2)	(3)
3b. Using Table 6.7, values of c were successively tried* until a calculated P_u matched the desired P_u (step 1). Other parameters needing values were D_s and β_1, obtainable as follows: β_1 is as defined in Section D (step 2a); and D_s may be estimated as 0.75 D, at least in early design trials. Figure 6-9 defines several parameters in column design.	cd = 8.35 β_1 = 0.85 D_s = 8.36		
3c. An M_u was calculated from Table 6.7. If this value was not satisfactorily close to the trial M_u (from step 2), a new trial D was chosen:	601,700		
$D_{(new\ trial)} = [\text{trial } M_u / \text{calculated } M_u]^{0.25} D_{(old\ trial\ value)}$ (6-31)	9.68		
and steps 3b and 3c were repeated. The latest D value was used for the design steps that follow.	final D = 10.17 (D_s = 7.63)		
4. Calculations could then be made toward a better check for lateral stability:[60,66]			
$EI = E_c I_g/5 + E_s I_s$ (6-32)	1,024,600,000		
where: $E_c = 1000\ f'_c$	3,000,000		
E_s = 30,000,000 psi	30,000,000		
$I_g = \pi D^4/64 = 0.049087\ D^4$	525.11		
$I_s = \pi D_s^3 A_{st}/(8\pi D_s) = 0.098175\ D_s^2 D^2 p$	23.65		
and $P_{cr} = \pi^2 EI/L^2$	487,670		
$\delta = 1/(1 - P_u/P_{cr})$ (6-33)	2.76		
Then, using the minimum eccentricity e = 0.05 D or one inch, whichever is larger, a revised trial value of M_u is calculated:	e = 1.0		
$M_u = P_u \delta e$ (6-29)	858,360		
5. This step is the same as step 3 except for the following modification of step "a.":			
5a. New trial D was estimated using			
$D = [(\delta e)_{current} / (\delta e)_{previous}]^{0.25} D_{previous}$ (6-34)	12.80 (D_s = 9.6)	10.30 (7.73)	11.00 (8.25)
where $(\delta e)_{current}$ is from step 4; $(\delta e)_{previous}$ is the next earlier one (from step 2 or 4); and $D_{previous}$ is the latest D preceding this step 5a. Steps 5b and 5c are the same as steps 3b and 3c, including the possible iterations.	final D = 12.02 (D_s = 9.02)	final D = 10.64 (D_s = 7.98)	final D = 11.05 (D_s = 8.29)

* First trial c might be D/2.

6. This step is the same as step 4.

7. If the new M_u value from step 6 was not satisfactorily close to the previous calue of M_u (from step 4 or 6), then steps 5 and 6 were repeated until the current and previous values of M_u from step 6 were satisfactorily close.

8. To complete the design, the required spiral steel ratio was calculated:

$$p_s = 0.45\ (A_g/A_c - 1)\ (f_c'/f_y) \text{ or } = 0.12\ f_c'/f_y \qquad (6\text{-}35)$$

whichever is larger, where: p_s (ρ_s in cited references) is the spiral steel ratio;* A_g is gross area of column; A_c is area of core (measured out-to-out of spiral steel).

Table G.6 (concluded)

(1)	(2)	(3)
EI = 1,999,600,000	1,226,800,000	1,427,600,000
P = 951,740	583,910	679,490
δ = 1.49	2.14	1.84
M_u = 463,390	665,540	572,240
Go to step 5	Go to step 5	
		~ 0.015

* For p_s definition: see ρ_s on page 30, Ref. 60. For help on design of spirals: see page 5-17, Ref. 69 or page 34, Ref. 65; and page C-9 is a useful table in Ref. 71 (included later herein as Table 6.8). Source of p_s equations is Ref. 60 (sections 10.9.2 and A.6.4.2).

† See also NOTE, Fig. 6-10.

4. Preliminary Design Procedures, with Examples

Limitations on the Preliminary Design Procedure for One-Way Walls. The preliminary design procedures for walls, described in the next two sections, are completely general except for Step 5.

In the preliminary design procedure for exterior walls, Step 5 is applicable only to cases where the stress pattern for $P_u = 0$ falls under Case 1, Table 6.6; this is usually the case when the rebound steel is less than about one-half the primary reinforcing steel. If the Case 1 equations are inapplicable, then the equations given in Step 5 (corresponding to Case 2, Table 6.6) of the preliminary design procedure for interior walls may be usable in computing d.

Similarly, in the preliminary design procedure for interior walls, Step 5 is applicable only to cases where the stress pattern for $P_u = 0$ falls under Case 2, Table 6.6; this is usually the case when the rebound steel is greater than about one-half the primary reinforcing steel. If the Case 2 equations are inapplicable, then the equations given in Step 5 (corresponding to Case 1, Table 6.6) of the preliminary design procedure for exterior walls may be usable in computing d.

One-Way Walls - Simply Supported (Interior). For interior one-way walls, simply supported, the following steps show a preliminary design procedure, with a numerical example in parallel to the right.

1. Given values for f_c' and f_{dc}'(ksi); f_{dy}(ksi); p_{so}(psi); t_o(sec); L(in.); p; b(in.).*	3; 3.75; 52; 15 1.55; 144; 0.01; 1
2. Obtain t_{oo}(sec) from Figure 3-7, Ref. 2.	0.71

* See Chapter 6, Typical Designs portion, Section D from opening through Step 1 of the final design procedure, for basic guidance on wall design, selection of p.

3. Calculate first trial using $\mu = 1$ and no vertical load.	
Assume value for T(sec); calculate t_{oo}/T.	0.04; 17.8
4. Using Figure 6-1, page 11-5,[50] read p_m/q; calculate	0.50
q, using $p_m = p_{so}$.	30
5. Calculate L/d, using following modifications of second	
set of equations in Table 6.6 (Chapter 6), assuming p = p'	
and $d'/d = 0.1$*: $C_1 = 0.85\, f'_{dc}\beta_1$;	2709.38
$C_2 = p\,(0.00375\, E_s - f_{dy} - 0.85\, f'_{dc})$; $C_3 = 0.00375\, E_s p d'/d$;	573.13; 112.50
$c = [-C_2 + (C_2^2 + 4\, C_1 C_3)^{0.5}] / (2C_1)$	0.1238
$(L/d)^2 = (8/q)\{0.85 f'_{dc}\beta_1 c(1 - \beta_1 c/2)$	129
$+ p(1 - d'/d)\,[0.00375 E_s (c - d'/d)/c - 0.85 f'_{dc}]\}$	
Then calculate d.	12.68
6. Using Equation 6-4 (Chapter 6), calculate T(sec),	0.03848
then t_{oo}/T.	18.45
7. Repeat Steps 4, 5, and 6 as necessary, until d	
predicted in Step 5 does not change appreciably.	12.68
	(last trial)
8. Estimate in-plane vertical load P; use $P = 2\,L(2\,p_{so})$.†	8640
9. Calculate T(sec) using Equation 6-4 (Chapter 6), with	
previous value of d (from Step 7 or 13).	0.03848
Then compute t_{oo}/T.	18.45
10. Using Figure 6-1, page 11-5,[50] read p_m/q; calculate	0.50
q by using $p_m = p_{so}$.	30

* Assume d'/d = 0.01 for first trial; if this varies significantly from the value found at the end of this procedure, assume a corrected value of d'/d and repeat the entire procedure.

† Here L is half the supported slab clear span on each side of wall (average if different).

11. Compute approximate moment of inertia I, also k'(using Equations 6-24 and 6-25, Chapter 6), critical buckling load P_{cr}, and amplification factor A: $P_{cr} = \pi^2 E_c I / L^2$	125.40; 0.3140 179,034
$A = 1 / (1 - P/P_{cr})$	1.051
12. Using the equations from Table 6.6 (Chapter 6), calculate M_u, then $AqL^2/8$.	123,189; 81,726
If $M_u > AqL^2/8$ and it is first time this step has been performed, go to Step 14.	
13. Calculate a new d: $d_{new} = d_{old} \left[AqL^2/(8M_u)\right]^{0.5}$	(skipped)
Repeat Steps 8 through 13 until $d_{new} \approx d_{old}$.	(skipped)
14. Using the latest value of d, calculate web steel needed for diagonal tension; check for pure shear and bond, using Step 7, Section D of Typical Designs portion of Chapter 6.	d = 12.68 (d = 12.66 by longer, final design method)

In general it was found, for small vertical loads, that the vertical load increases the moment capacity. Only when the vertical load is very large does it reduce moment carrying capacity.

<u>One-Way Walls - Simply Supported (Exterior)</u>. For exterior (basement) one-way walls, simply supported, the following steps show a preliminary design procedure, with a numerical example in parallel to the right. All steps are identical with the preceding preliminary design procedure for interior walls, except Steps 1, 4, 5, 8, and 10, thus all other steps are not described in the following.

1. Given values for: f'_c and f'_{dc}(ksi); f_{dy}(ksi); p_{so}(psi); t_o(sec); L(in.); p; b(in.).*	3; 3.75; 52; 15 1.55; 144; 0.01; 1
2.	0.71
3.	0.05; 14.2
4. Using Figure 6-1, page 11-5,(50) read p_m/q; calculate q, using $p_m \approx 0.5\ p_{so} + (15L/1728)\ [1 - 1/(2\mu)]$ (which assumes 0.5 is ratio of horizontal load to vertical load in soil; correct as appropriate).	0.50 16.25; $p_m = 8.125$
5. Calculate L/d, using following modification of Equation 6-6 (Chapter 6), assuming p' = 0.25 p and d'/d = 0.1 †:	
$(L/d)^2 \approx [8(p - p')bf_{dy}/(aq)][1 - 0.554(p - p')f_{dy}/(0.85f'_{dc})]$ $+ [8p'bf_{dy}/(aq)][1 - d'/d]$	232.87 $[= (15.26)^2]$
Then calculate d.	9.43
6.	0.5174; 13.72
7.	9.43 (last trial)
8. Estimate in-plane vertical load P; use $P = L\ (2\ p_{so})$.‡	4,320
9.	0.05174, 13.72

* See Chapter 6, Typical Designs portion, Section D from opening through Step 1 of the final design procedure, for basic guidance on wall design, including selection of p.

† Assume d'/d = 0.1 for first trial; if this varies significantly from the value found at the end of this procedure, assume a corrected value of d'/d and repeat the entire procedure.

‡ Here L is half the supported slab clear span.

10. Using Figure 6-1, page 11-5,(50) read p_m/q; calculate q, using $p_m = 0.5\ p_{so} + (15\ L/1728)[1 - 1/(2u)]$ (same assumption is made as in Step 4).	0.50 16.25, $p_m = 8.125$
11.	48.59; 0.346 69,381, 1.066
12.	58,970; 44,900
13.	(skipped)
14.	d = 9.43 (9.18 by final design method)

In general it was found, for small vertical loads, that the vertical load increases the moment capacity. Only when the vertical load is very large does it reduce moment carrying capacity.

Columns - Simply Supported. For circular, spirally reinforced, simply supported columns, the following steps show a preliminary design procedure, with a numerical example in parallel to the right; the design procedure uses Reference 67, a copy of which must, therefore, be at hand.

1. Given values for: f'_c and f'_{dc}(ksi); f_y and f_{dy}(ksi); P_u (kips); L(in.); p (ρ used in Ref. 67).*	3; 3.75; 40; 52 311; 144; 0.04
2. Assume code minimum eccentricity, e = 0.05 D, or 1 in., whichever is larger† (use first trial D = 12 in.‡); assume moment magnifier $\delta = 1.1$;‡ assume $D_s/D = 0.75$;‡ see Figure 6-9, Chapter 6 [note tables[67] use h for D herein and γ (p. 267) for D_s/D].	1 12 1.1; 0.75

* For guidance see Chapter 6, Typical Designs portion, Section E, subsection titled Selecting Column Steel Ratio.

† Or even larger, if indicated by experience

‡ Unless otherwise indicated by experience.

3. Calculate $\delta e/h$; find $(P_u/A_g)_{Table}$ (ksi), using table.[67] (p.xii-)	0.0917; 2.38 (Table 2.2).
4a. Calculate $f_d = [(f_{dy}/f_y + f'_{dc}/f'_c)/2]$ and note that φ is 0.75 (Ref. 67, p. 8). Eliminate safety factor φ and account for dynamic strengths of materials as indicated below:	1.275 (say 1.25)
Calculate $D = h = \{4\ P_u / [\pi (P_u/A_g)_{Table}\ (f_d/\varphi)]\}^{0.5}$	9.99
Skip to Step 5 if this is first time through Step 4a.	
4b. Average new D with D from previous iteration:	
$D = (D_{new} + D_{previous})/2$	
Then calculate $(P_u/A_g)_{Table} = 4\ P_u / (\pi D^2 f_d/\varphi)$	
5. Using same table as found for Step 3: k = 1 for simply supported column; ℓ_u is used for L herein; h_e is effective h (h = D herein).	
Find h_e/h from table; calculate h_e; then, using small table at top of right side page:	1.24; 12.39
Calculate $k\ell_u/h_e$ for rows scale; use $(P_u/A_g)_{Table}$ for columns scale ($\beta_d = 0$); interpolating, read δ/c_m; find	11.62
δ ($c_m = 1$).	2.26
If the new δ is close to δ of Step 3 (say, within about 1% or 2%), skip to Step 7.	
6. Correct e, if necessary under Step 2 guidance. Use latest values of all paramenters as initial values and repeat Steps 3-5.	
7. Calculate required spiral steel ratio p_s using Equation 6-35, Chapter 6.	0.026

From first trial design and from two iterations of Steps 3-5, resulting D (or h) values were 9.99, 10.94, and 10.82, respectively, when entering Step 5. (D = 11.05 by longer, final design method.)

NOTATION

See Notation section at end of Chapter 6.

Appendix H

BUILDING 4A VENTILATION

By F. C. Allen

Appendix H

BUILDING 4A VENTILATION

By F. C. Allen

Section 1 - Introduction

The parking garage in the Court House complex at Columbus, Muscogee County, Georgia, provides a good model to illustrate the fundamental rationale for adapting the electromechanical systems in a conventionally designed facility for use as a combined nuclear effects shelter. The spaces are geometrically simple, the original systems are elemental, and the potential for sheltering a large number of people is compatible with use of an auxiliary power supply at a relatively small increase in per capita costs. The basic principles can usually be applied to the ventilating system for each compartment in a more complex configuration, with the objective of supplying an adequate quantity of circulating and replacement air to every part of the shelter for maintaining therein an environment that remains within acceptable limits for air quality, temperature, and humidity during all seasons. For relatively small shelters, the per capita cost of a reliable auxiliary power system is likely to be dismayingly high, unless there is a technological innovation that leads to a substantial reduction in the cost of small power sources. In such cases, the use of manually powered apparatus for ventilating should be given serious consideration.

The purpose of this appendix is therefore to outline concepts for adapting electromechanical systems in a parking garage to shelter use, with the implication that the basic principles are generally applicable to other configurations.

Section 2 - Basic System for the Parking Garage

The prospective shelter spaces in Building 4, which is described in general terms in Chapter 7, are the two sub-levels of the parking garage. In the original plans, these spaces are ventilated by an independent system with 12 propeller fans, each of which has a rated capacity of 24,000 cfm at a static pressure of 0.125 in. of water. The fan wheels have a nominal

diameter of 48 in. and are belt-driven by 2-hp motors at a speed of 467 rpm. Six of the fans supply fresh air to the spaces, three to the upper sub-level and three to the lower sub-level. The other six fans exhaust air from the spaces, also three from each sub-level. Three vent shafts for supply air are provided at the east wall, and three for exhaust air are provided at the west wall of the structure. Each vent shaft extends down from its horizontal grating just above ground level to an elevation 2 ft above the 6 in. curb of the lower sub-level. The gratings and the tops of the vent shafts abut the street-side walls of the East and West office Buildings and are inside the rows of decorative columns that surround these buildings. Two fans are installed at framed openings in the building wall of each vent shaft, one fan at each sub-level. At designated fan capacity, each of the two sub-levels is normally ventilated at the rate of 72,000 cfm with unidirectional movement of air from the east side to the west side of each sub-level. Since the rated supply and exhaust capacities for each sub-level are equal, the system does not provide for air flow along the auto ramps. However, the fans are belt-driven, and pulleys could readily be changed to cause either an upward or downward air flow along the ramps.

Section 3 - Ventilation Requirements for Shelter Purposes

Summer Occupancy

Columbus, Georgia, the site of Building 4, is located between the isoventilation lines for 15 and 20 cfm of fresh air per person as shown in Figure 6-2.* For the reasons stated in the text accompanying Figure 6-2 and in accord with the cost/feasibility purposes of this case study, a unit ventilating rate of 17 scfm/person was used herein. With a floor area allowance of 10 sf/person, the indicated capacity of the shelter in Building 4A (slanted version of Building 4) is 12,700 persons and the required rate of ventilation is 216,000 cfm, or 108,000 cfm for each of the two sub-levels. This is 1.5 times the design ventilating rate (144,000 cfm) for normal operation of the parking garage.

Winter Occupancy

With an air flow rate of 108,000 cfm across each sub-level, the average air velocity in the space would be approximately 47 fpm. Local air velocities would be appreciably higher than this value because the

* In Volume 1 of this report.

gross area of the flow path is not uniform, the effective area is reduced by the presence of obstructions such as cars and people, and the ventilating air is supplied and exhausted at relatively high velocities through a few openings. Although air velocities of this magnitude may be advantageous for removing metabolic heat during warm seasons, the chilling effect associated with air motion would become increasingly objectionable as air temperatures in any occupied part of the shelter fall below 70 F. During cool weather, two-speed fan motors could be used to reduce the total rate of ventilation from the 216,000 cfm needed for shelter use during warm weather to the 144,000 cfm required for normal operation as a parking garage. The unit ventilating rate would then be reduced from 17 cfm/person to about 11 cfm/person, if the shelter were occupied during a cold season.

If air is not uniformly distributed but moves laterally through a large space, the environmental temperature and humidity tend to increase progressively as metabolic heat is added to the ventilating air.[1]* The environmental state at the entering-air end of the shelter will correspond closely to the state of the supply air. For climates in which temperatures below 50 F prevail during a significant proportion of the year, it is therefore necessary to provide means for limiting the supply air temperature to a minimum of 50 F, the recommended minimum temperature for a fallout shelter environment.[2] This can, of course, be accomplished by providing a heating system for tempering incoming fresh air. In connection with shelters, it is generally more realistic to use occupant-generated metabolic heat for this purpose by recirculating an appropriate part of the ventilating air and providing a means such as dampers for adjusting the percentage of recirculated air as ambient conditions change. This method also serves to maintain the rates of ventilation that are necessary for avoiding local stagnation and large temperature differences, even during cold weather.

Columbus, Georgia, the site of Building 4A, is not included among the 91 weather stations that provided climatic data for analyses of requirements for shelter ventilation during warm seasons and for the subsequent establishment of ventilating criteria, including the contour map shown in Figure 6-2. However, Montgomery, Alabama, is one of the 91 stations, is less than 100 miles west of Columbus, and occupies a similar position within the same ventilation zone of Figure 6-2. The climatic similarities between Columbus and Montgomery are apparent in Table H.1,

---

* Superscript numerals refer to publications listed at the end of this appendix.

Table H.1

COMPARISON OF CLIMATIC DATA

Quantity	Columbus, Georgia	Montgomery, Alabama
Dry-bulb temperatures, F		
Winter*		
Median of annual lows†	19	18
99% basis‡	23	22
97.5% basis	26	26
Summer§		
Daily range‖	21	21
1% basis‡	98	98
2.5% basis	96	95
5% basis	94	93
Wet-bulb temperatures, F		
Summer§		
1% basis‡	80	80
2.5% basis	79	79
5% basis	78	78
Elevation above sea level, ft	242	195

* Three-month period, December through February.
† Mean value of lowest temperature recorded each year.
‡ Average percentage of hours during period with temperature equal to or higher than listed values.
§ Four-month period, June through September.
‖ Difference between average maximum and average minimum temperature during hottest month.

Source: Reference 3.

for which data were abstracted from Reference 3.* For purposes of this study climatic data for Montgomery, Alabama, were considered to be sufficiently representative for Columbus, Georgia. The detailed computer-readout data for Montgomery[4] included frequency values for hourly dry-bulb and

* Reference 3, Chapter 22, Table 1.

wet-bulb temperature readings over a ten-year period from January 1949 through December 1958. These data were used herein to determine the percentages shown in Table H.2. It is significant that atmospheric temperatures would probably be less than 50 F about 18% of the time during an average year and that a system capability for controlled recirculation would be useful for shelter purposes in preventing the occurrence of environmental temperatures below 65 F about 44% of an average year. On the basis of the foregoing information, one can logically conclude that, in the absence of apparatus for tempering air, recirculation of air from occupied spaces is necessary as well as desirable. When controlled recirculation can be accomplished without extensive ductwork for return air, the added cost for providing this capability is small and may require only that adjustable dampers be provided for recirculated air.

Table H.2

ANNUAL DISTRIBUTION OF TEMPERATURE IN MONTGOMERY, ALABAMA

Hourly Readings of Dry-Bulb Temperature F	Percentages of Hourly Temperature Readings During an Average Year		
	Below Listed Value	At Listed Value	Above Listed Value
32	1.809%	0.363%	97.828%
35	3.087	0.616	96.297
40	6.903	0.956	92.141
45	11.992	1.249	86.759
50	18.444	1.529	80.027
55	26.066	1.690	72.244
60	34.536	1.993	63.471
65	43.791	2.128	54.081
70	54.407	2.425	43.168
75	68.182	3.007	28.811
80	80.851	2.113	17.036
85	89.215	1.346	9.439
90	95.204	1.013	3.783
95	98.995	0.358	0.647
100	99.910	0.034	0.056

Quantities for Partial Recirculation

The air quantities, temperatures, and humidities associated with recirculation of air from occupied spaces can be determined by a psychrometric analysis, using appropriate climatic data in conjunction with an equation that defines human metabolic responses to the thermal environment. The model system in this analysis consists of a rectangular, occupied space with a ventilating system that supplies a mixture of fresh and recirculated air through openings along one wall and removes an equivalent amount of air through openings along the opposite wall. During passage through the space, metabolic heat and moisture are gradually added to the air, thereby causing the environmental temperature and humidity to increase gradually in the direction of air movement. After passing through the space, an adjustable proportion of the air is returned for recirculation, and the remainder, which is equal in quantity to the amount of fresh air, is exhausted to the atmosphere. In accordance with the criterion for minimum environmental temperature, the minimum temperature of the fresh/recirculated air mixture is $t_2 = 50$ F. From an inspection of climatic data in Table H.1, a design ambient temperature of $t_1 = 20$ F was selected for winter conditions. The shelterees were assumed to be sedentary adults dressed in optimum clothing, that is, clothing appropriate for maintaining a sufficiently high skin temperature to avoid muscular tension or shivering in the environment to which each person is exposed.

During cool or cold seasons, the environment in all occupied parts of a shelter should be maintained at 50 F or higher for air entering the shelter and at 85 F or lower for air leaving the shelter. This can usually be accomplished by partial recirculation of ventilating air. The effects of heat transmission through walls and roof slabs, which were not considered in the analysis, would tend to increase the required proportion of recirculated air. In connection with a large, fully occupied, underground shelter, these effects appear to be relatively small on a long term basis, but the transient chilling effects of an initially cold structure may be important during the first day or two of occupancy. Heat emitted by lights would have a small but beneficial effect in cold seasons.

Computed quantities associated with cold season ventilating and mixing processes in Building 4A are shown in Table H.3 for several combinations of operating conditions, all with a design ambient or fresh air temperature of 20 F and a metabolic rate of 400 Btuh/person. The basis for these computations is outlined in the next subsection. To accommodate 12 values for each combination, the data are tabulated in pairs of rows in accordance with the upper and lower headings at the top of

Table H.3

RECIRCULATION OF AIR AT HIGH AND LOW FAN SPEEDS*

ELEVATION, FT= 242 , BAROMETER, ATM= .99127
AMBIENT TEMP, F= 20 , METABOLISM, BTUH= 400

MIXED TEMP	TOTAL SCFM	FRESH SCFM	RECRC SCFM	RATIO DH/DW	EVAP LB/DAY
RECRC TEMP	TOTAL CFM	FRESH CFM	RECRC CFM	DEW POINTS F MIXED	DEW POINTS F RECRC
	FRESH AIR: %RH= 0		, W1= 0		
40	17.00	7.55	9.45	4067.8	2.360
55.9	16.25	6.91	9.33	13.90	26.10
50	17.00	5.81	11.19	3797.2	2.528
65.5	16.60	5.31	11.29	24.30	33.40
60	17.00	4.60	12.40	3407.3	2.817
74.8	16.97	4.21	12.76	34.10	42.10
70	17.00	3.58	13.42	2813.4	3.412
83.3	17.37	3.27	14.10	47.40	53.70
	FRESH AIR: %RH= 100		, W1= 2.16137E-03		
40	17.00	7.54	9.46	4067.8	2.360
55.9	16.30	6.92	9.38	31.80	39.10
50	17.00	5.79	11.21	3797.2	2.528
65.5	16.66	5.32	11.34	37.90	44.30
60	17.00	4.58	12.42	3407.3	2.817
74.8	17.02	4.21	12.82	44.80	50.50
70	17.00	3.57	13.43	2813.4	3.412
83.3	17.43	3.27	14.16	54.70	59.70
	FRESH AIR: %RH= 0		, W1= 0		
40	11.33	6.14	5.19	3953.0	2.429
63.7	10.83	5.62	5.21	14.70	31.20
50	11.33	4.91	6.42	3634.0	2.642
72.9	11.07	4.49	6.58	25.60	38.70
60	11.33	3.95	7.38	3161.2	3.037
81.4	11.32	3.62	7.70	36.90	47.90
70	11.33	3.01	8.32	2446.2	3.925
88.1	11.61	2.75	8.86	53.80	62.20
	FRESH AIR: %RH= 100		, W1= 2.16137E-03		
40	11.33	6.13	5.20	3953.0	2.429
63.7	10.87	5.63	5.24	32.20	42.70
50	11.33	4.90	6.43	3634.0	2.642
72.9	11.10	4.50	6.61	38.80	48.10
60	11.33	3.94	7.39	3161.2	3.037
81.4	11.35	3.62	7.74	46.80	55.10
70	11.33	3.00	8.33	2446.2	3.925
88.1	11.65	2.76	8.90	59.80	66.90

* Total SCFM is 17.00 at high and 11.33 at low fan speed.

each column. The input data include the site elevation (242 ft), metabolic rate (400 Btuh), ambient temperature (20 F), ambient relative humidity (0% and 100%), temperature of mixed fresh and recirculated air supplied to the shelter (40, 50, 60 and 70 F), and the ventilating rates (17 scfm/person for high speed and 11.33 scfm/person for low speed operation of ventilating fans). The computed value for humidity ratio of ambient (fresh) air is identified by the symbol, W1. In column 1, the lower value in each pair of rows is the temperature of recirculated air and also the temperature of air leaving the shelter. In columns 2, 3, and 4, the upper values are the rate of total (mixed), fresh, and recirculated air in scfm/person, that is, in terms of standard air having a dry-air density of 0.075 pounds per cubic foot. The lower values are the corresponding ventilating rates corrected to actual conditions of temperature, humidity, and barometric pressure. In columns 5 and 6, the upper values are the slope of the mixing process line in the enthalpy-humidity coordinate system and the average mass of water evaporated in 24 hr by each person. The lower values are dew point temperatures of mixed and recirculated air, that is, the dew points at the supply and exhaust ends of the shelter. These are of interest because moisture would condense on any surface having a lower temperature. The mass of water evaporated per day is relevant to the problem of potable water storage in shelters; in addition to water losses by evaporation from skin surfaces and respiratory tract, water must be available to replace losses in urine and feces. It is significant that less severe environmental temperatures than the recommended minimum of 50 F can be maintained by partial recirculation without reducing the flow rate of fresh air below the recommended minimum of 3 cfm/person.

To demonstrate the effect of a change in site elevation or a change in ambient temperature, input parameters are modified in Tables H.4 and H.5. In both tables, the ambient relative humidity is 50%.

In the upper half of Table H.4, the parameters relate to conditions associated with Building 4A; in the lower half the elevation is increased by 1000 ft, with other input data unchanged. Although the values of corrected ventilating rates, humidity ratio, and dew point change appreciably, the effect of this modest change in elevation is not very significant. However, the effect of a change to an elevation of 5,000 ft, at which the barometric pressure is 0.83186 atmospheres, would be greatly increased.

The data in Table H.5 show the effect of changes in ambient fresh air temperature, with other input parameters appropriate to conditions at Building 4A. These values should be compared directly with corresponding values in the upper half of Table H.4. Among the data for ambient temperatures of 40, 20, and -20 F, it is most significant that, for

Table H.4

EFFECTS OF SITE ELEVATION ON VENTILATION

AMBIENT TEMP= 20 F, METABØLIC RATE= 400 BTUH
AMBIENT RELATIVE HUMIDITY= 50 %

MIXED TEMP	TØTAL SCFM	FRESH SCFM	RECRC SCFM	RATIØ DH/DW	EVAP LB/DAY
RECRC TEMP	TØTAL CFM	FRESH CFM	RECRC CFM	DEW PØINTS F MIXED	RECRC
ELEVATIØN, FT= 242 , BARØMETER, ATM= .99127					
AMBIENT HUMIDITY RATIØ, W1= 1.07881E-03					
50	17.00	5.80	11.20	3797.2	2.528
65.5	16.63	5.32	11.31	31.60	39.40
60	17.00	4.59	12.41	3407.3	2.817
74.8	16.99	4.21	12.79	40.00	46.60
50	11.33	4.90	6.43	3634.0	2.642
72.9	11.09	4.49	6.59	32.70	43.80
60	11.33	3.95	7.38	3161.2	3.037
81.4	11.34	3.62	7.72	42.30	51.70
ELEVATIØN, FT= 1242 , BARØMETER, ATM= .95587					
AMBIENT HUMIDITY RATIØ, W1= 1.11884E-03					
50	17.00	5.80	11.20	3797.2	2.528
65.5	17.24	5.51	11.73	31.10	38.70
60	17.00	4.59	12.41	3407.3	2.817
74.8	17.63	4.36	13.27	39.20	45.80
50	11.33	4.90	6.43	3634.0	2.642
72.9	11.50	4.66	6.84	32.00	43.00
60	11.33	3.95	7.38	3161.2	3.037
81.4	11.76	3.75	8.01	41.50	50.90

Table H.5

EFFECTS OF AMBIENT TEMPERATURE ON VENTILATION

ELEVATIØN, FT= 242 , BARØMETER, ATM= .99127
AMBIENT RELATIVE HUMIDITY= 50 %

MIXED TEMP	TØTAL SCFM	FRESH SCFM	RECRC SCFM	RATIØ DH/DW	EVAP LB/DAY
RECRC TEMP	TØTAL CFM	FRESH CFM	RECRC CFM	DEW PØINTS F MIXED	RECRC
AMBIENT TEMP, F= 40 , W1= 2.60775E-03					
50	17.00	10.34	6.66	3797.2	2.528
65.5	16.62	9.89	6.73	30.20	38.20
60	17.00	7.22	9.78	3407.3	2.817
74.8	16.98	6.91	10.08	37.20	44.40
50	11.33	7.88	3.45	3634.0	2.642
72.9	11.08	7.54	3.54	30.50	42.20
60	11.33	5.85	5.48	3161.2	3.037
81.4	11.32	5.60	5.73	38.50	49.00
AMBIENT TEMP, F=-20 , W1= 1.31986E-04					
50	17.00	3.09	13.91	3797.2	2.528
65.5	16.70	2.59	14.11	44.90	50.00
60	17.00	2.66	14.34	3407.3	2.817
74.8	17.08	2.23	14.86	52.40	56.90
50	11.33	2.79	8.54	3634.0	2.642
72.9	11.13	2.34	8.79	46.50	53.80
60	11.33	2.39	8.94	3161.2	3.037
81.4	11.40	2.01	9.40	55.40	61.80

similar values of mixed air temperature, the flow rate of fresh air decreases as either the ambient temperature or total ventilating rate decreases. When the ambient temperature is -20 F and the total ventilating rate is 11.33 scfm/person, the flow rates of fresh air at both 50 and 60 F mixture temperatures are less than the recommended minimum of 3 cfm/person. For climatic zones in which the recommended ventilating rate for limiting the hot season environment is 10 cfm/person or less, it may be necessary to increase the ventilating rate during the coldest season to meet criteria for both minimum temperature and minimum rate of air replacement without a heating system. There is a factor of safety in the recommended minimum 3 cfm of fresh air per person, but this factor is primarily intended to accommodate situations in which a ventilating system does not establish an adequate flow of air through each and every part of the shelter.

Analytical Basis for Computations

The computed data in Tables H.3, H.4, and H.5 are based on an analysis of the mixing process for fresh and recirculated air in conjunction with the heat-mass transfer process in occupied spaces. The analytical background is outlined in this subsection.

When air moves linearly through a space occupied by N people who are in thermal equilibrium with a metabolic rate of M Btuh/person, the change in specific enthalpy of the moving air is

$$N\dot{m}_a dh = NMdr \tag{1}$$

and the change in humidity ratio is

$$N\dot{m}_a dW = N\bar{m}dr \tag{2}$$

if all loads other than metabolic heat and moisture are negligible. In these equations:

$\dot{m}_a$ = mass flow rate of dry air (lb/hr/person)

h = specific enthalpy of dry air (Btu/lb of dry air)

N = number of people in the space

M = metabolic rate (Btuh/person)

W = humidity ratio = $\frac{\text{mass of moisture}}{\text{mass of dry air}}$

$\bar{m}$ = water evaporated from skin surfaces and respiratory track (lb/hr/person)

r = dimensionless ratio of coordinate distance to total length of space in direction of air movement.

If Equation 1 is divided by Equation 2, the result is

$$\frac{dh}{dW} = \frac{M}{\bar{m}} \tag{3}$$

which is an equation for the slope of the ventilating process line. The quantity $\bar{m}$ varies with the ratio of latent to total metabolic heat, which is a function of dry-bulb temperature. A rational expression for $\bar{m}$ is

$$\bar{m} = \frac{\rho M}{h_{fg} + \rho h_f} \tag{4}$$

in which

h_{fg} = latent heat of vaporization for saturated water at skin temperature

h_f = enthalpy of saturated water at skin temperature

ρ = ratio of latent to total metabolic heat.

In this analysis, the mean skin temperature is assumed to be 94 F, at which $h_{fg} \approx 1040$ and $h_f \approx 62$ Btu/lb. In the derivation of Equations 1 through 4, credit is given to the cooling effect of potable water consumed at a temperature less than skin temperature. If the quantity of water consumed were double the amount evaporated and if the remainder were excreted at a temperature of 98 F, a drinking water temperature of 65 F is consistent with the equations. These equations imply that metabolic heat removed by the air is $(M - \bar{m}h_f)$, but the heat added to the air is M Btu/hr. The difference is ascribed to the convention that the enthalpy of saturated water is zero at a temperature of 32 F. When Equation 4 is substituted for $\bar{m}$ in Equation 3, the result is

$$\frac{dh}{dW} = \frac{1040}{\rho} + 62 \tag{5}$$

A second and necessary equation for slope can be obtained by differentiating an equation for specific enthalpy of moist air. For the ventilating process in the shelter, it is convenient to use a constant value of $h_g = 1090$ Btu/lb for the enthalpy of saturated water vapor. The specific enthalpy of moist air is then

$$h = c_p t + 1090W \tag{6}$$

Btu/lb of dry air, and the appropriate derivative is

$$\frac{dh}{dW} = c_p \frac{dt}{dW} + 1090 \tag{7}$$

in which

t = dry-bulb temperature (F)

c_p = specific heat of dry air at constant pressure.

In this analysis, $c_p = 0.2402$ Btu/lb-F. The value $h_g = 1090$ Btu/lb is the true value for enthalpy of saturated water vapor at about 66 F, and is less than 1% in error at temperatures above 40 and below 90 F.* These limits cover the range of interest for temperatures in shelters during cold seasons.

When Equations 5 and 7 are combined, the result is

$$0.2402 \frac{dt}{dW} = \frac{1040}{\rho} - 1028 \tag{7}$$

Within the range of interest, the quantity ρ can be approximated by a single function of dry-bulb temperature

$$\rho = 0.19 + \frac{3.24}{95 - t} \tag{8}$$

* Reference 3, Chapter 21, Table 2.

This equation represents the ratio of latent to total metabolic heat losses from sedentary persons dressed in optimum clothing at dry-bulb temperatures of 89 F or less. With a constant metabolic rate of 400 Btu/hr, corresponding values of sensible heat loss are 300, 270 and 180 Btu/hr at dry-bulb temperatures of 41, 71 and 86 F, respectively, which are consistent with applicable data.[1,5] When Equation 8 is substituted in Equation 7, the numerical coefficients can be combined and the variables can be separated. Then, the differential equation for the ventilating process in the shelter is

$$dW = \frac{0.0060542 - 0.000054030t}{91.0568 - t}\,dt \tag{9}$$

In the combined processes for ventilating the shelter and for mixing fresh and recirculated air, there are three points of interest: (1) the state of fresh air, (2) the state of mixed air, and (3) the state of air that is either recirculated or exhausted to atmosphere. To identify air properties associated with each of these points, the corresponding numbers are used as subscripts. Then, integrating Equation 9 between points 2 and 3 yields the relationship between terminal temperatures and humidity ratios for air traversing the shelter,

$$W_3 - W_2 = 0.000054030(t_3 - t_2) + 0.0011344\,\ell n(R) \tag{10}$$

where $R = (91.0568 - t_2)/(91.0568 - t_3)$ and $\ell n(R)$ is the natural logarithm of R. In accordance with Equation 6, the corresponding increase in specific enthalpy is

$$h_3 - h_2 = 0.2402(t_3 - t_2) + 1090(W_3 - W_2) \tag{11}$$

Btu/lb of dry air. Combining Equations 10 and 11,

$$h_3 - h_2 = 0.299093(t_3 - t_2) + 1.23650\,\ell n(R) \tag{12}$$

Btu/lb of dry air, where $R = \dfrac{91.0568 - t_2}{91.0568 - t_3}$

For a metabolic rate, M = 400 Btu/hr/person, the quantity of mixed air is

$$V_2 = \frac{400}{4.5(h_3 - h_2)} \tag{13}$$

scfm/person (scfm refers to standard air having a dry-air density of 0.075 lb/cf of air). In general, the ventilating capacity V_2 will be determined by conditions during the hot season, the state of fresh air will be known or deduced from a study of climatic data, and the mixture temperature will be selected to meet a criterion for minimum temperature in the shelter, such as 50 F. The quantity $(h_3 - h_2)$ can then be determined from Equation 13, but the values of t_3 and $(W_3 - W_2)$ must be found by an iterative process, using Equations 10 and 12. When both $(h_3 - h_2)$ and $(W_3 - W_2)$ have been evaluated, their ratio is the slope of the mixing line and, consequently, the ratios of all similar pairs, that is

$$\frac{h_3 - h_2}{W_3 - W_2} = \frac{h_2 - h_1}{W_2 - W_1} = \frac{h_3 - h_1}{W_3 - W_1} = \frac{400}{\dot{m}} = S \tag{14}$$

For evaluating the specific enthalpy of fresh air at temperatures less than t_2, the specific enthalpy of saturated water vapor is assumed to vary linearly with temperature, because the fresh air temperature may vary over a wide range. Then the specific enthalpy of fresh air is

$$h_1 = 0.2402t_1 + EW_1 \tag{15}$$

where E = specific enthalpy of saturated water vapor

$$E = E_1 = (1061.09 + 0.4412t_1) \tag{16}$$

when $t_1 < 32$ F

$$\text{and } E = E_2 = (1061.25 + 0.4362t_1) \tag{17}$$

when $32 \le t_1 \le t_2$.

For evaluating vapor pressures or humidity ratios when the relative humidity is known, equations for the pressure of saturated water vapor are needed. Two equations derived from Clapeyron's relation and fitted to empirical data[1] are

$$p_s = 0.00602751R^{0.61775} \exp(z_1)^* \tag{18}$$

when $t \ge 32$ F

and

$$p_s = 0.00602792R^{8.0374} \exp(z_2) \tag{19}$$

when $t \ge 32$

in which

p_s = pressure of saturated water vapor (atmospheres)

$R = 491.67/(459.67 + t)$

t = saturation temperature (F)

$z_1 = 22.892(1-R) + 0.226568(1-R)/R$

$z_2 = 26.4051(1-R) + 1.48183(1-R)/R$

The vapor pressure of partially saturated air is

$$p_v = p_s(RH)/100 \tag{20}$$

in atmospheres, where (RH) = relative humidity expressed as a percentage. Equations 18 and 19 are also used in an iterative procedure to find the dew point temperature when the vapor pressure or humidity ratio is known. The relationship between vapor pressure and humidity ratio is

---

* Base e raised to the power z_1.

$$W_1 = 0.62197\, p_{v1}/(B - p_{v1}) \tag{21}$$

in which B = barometric pressure (atmospheres). The nominal or standard barometric pressure at elevations less than 35,333 feet above mean sea level can be determined with the equation[1]

$$B = (1 - 0.00000683432A)^{5.29478} \tag{22}$$

in atmospheres, where A is the elevation above mean sea level in feet.

From Equations 14 through 17, two equations for $(W_2 - W_1)$ can be derived,

$$W_2 - W_1 = \frac{0.2402(t_2 - t_1) + (E_2 - E_1)W_1}{S - E_2} \tag{23}$$

when $t_1 < 32F$, and

$$W_2 - W_1 = \frac{(0.2402 + 0.4362\, W_1)(t_2 - t_1)}{S - E_2} \tag{24}$$

when $32 \leq t_1 \leq t_2$

In Equations 23 and 24

S = slope of the mixing line (Equation 14)

$E_1 = 1061.09 + 0.4412\, t_1$ (Equation 16)

$E_2 = 1061.25 + 0.4362\, t_2$ (Equation 17)

From Equation 14,

$$h_2 - h_1 = S(W_2 - W_1) \tag{25}$$

Btu/lb of dry air, and

$$\bar{m} = 400/S \tag{26}$$

pounds of water evaporated/hr/person. The masses of dry air entering and leaving the structure are equal, and the difference in total enthalpies of leaving and entering air is equal to heat added in the shelter. That is,

$$\dot{m}_{a1}(h_3 - h_1) = \dot{m}_{a2}(h_3 - h_2) = 400 \text{ Btuh/person}$$

where

$\dot{m}_{a1}$ = $4.5\ V_1$ (lb/hr of dry fresh air per person)

$\dot{m}_{a2}$ = $4.5\ V_2$ (lb/hr of dry mixed air per person)

V_1 = scfm of fresh air per person

V_2 = scfm of mixed air per person .

It is obvious that

$$h_3 - h_1 = (h_3 - h_2) + (h_2 - h_1) \tag{28}$$

Then, the flow rate of fresh air is

$$V_1 = \frac{400}{4.5(h_3 - h_1)} = V_2 \frac{h_3 - h_2}{h_3 - h_1} \tag{29}$$

scfm/person, and the flow rate of recirculated air must be

$$V_3 = V_2 - V_1 \text{ scfm/person} \tag{30}$$

An equation[1] to convert ventilating rates in scfm units to actual volumetric rates at prevailing states is

$$U_n = \frac{0.001891\ V_n(459.67 + t_n)(1 + 1.6078\ W_n)}{B} \tag{31}$$

where

U_n = actual volumetric flow rate at point n (cfm)

V_n = standard flow rate at point n (scfm)

t_n = dry-bulb temperature at point n (F)

W_n = humidity ratio at point n

n = subscript 1, 2, or 3 for fresh, mixed, or recirculated air.

Finally, to determine dew point temperatures of mixed and recirculated air, the humidity ratios and vapor pressures at points 2 and 3 must be evaluated. Obviously, at point 2

$$W_2 = (W_2 - W_1) + W_1 \tag{32}$$

and at point 3

$$W_3 = W_2 + (W_3 - W_2) \quad (33)$$

Then, vapor pressures at points 2 and 3 are

$$p_{v2} = BW_2/(W_2 + 0.62196) \quad (34)$$

and

$$p_{v3} = BW_3/(W_3 + 0.62195) \quad (35)$$

atmospheres, where the barometric pressure is B atmospheres (Equation 22). In Equations 21, 34, and 35, the numerical constants are the ratios of the molecular weight of water to the apparent molecular weight of dry air. At low rates of air replacement, the concentration of carbon dioxide would increase appreciably with a consequent increase in the apparent molecular weight of dry air.[6] In token recognition of this effect, slightly different values for this ratio were used for the fresh, mixed, and recirculated air at points 1, 2, and 3. The dew point temperatures of mixed and recirculated air must then be found by an iterative procedure, using Equations 18 and 19, together with the vapor pressures determined by Equations 34 and 35. Superheated vapor in moist air becomes saturated vapor when cooled at constant pressure to the dew point.

The computer programs used for preparation of Tables H.3, H.4, and H.5 were based on the rationale described above.

Section 4 - Adaptation of Electromechanical Systems

Deficient or Marginal Elements of the Systems

In Section 2, the ventilating system provided for normal use in Building 4 is described, and in Section 3 a rationale for all-season ventilation of shelters in this type of structure is outlined. With this background for guidance, it is apparent that modifications for shelter purposes should be directed toward correction of the following deficiencies in the electromechanical systems and appurtenances:

1. The normal-use ventilating capacity of 144,000 cfm (72,000 cfm for each of the two sub-levels) is not sufficient for full occupancy shelter-use in the climatic zone containing Columbus, Georgia, for which a ventilating rate of 17 cfm/person is appropriate. This establishes a shelter-use requirement for 216,000 cfm of air (108,000 cfm for each sub-level), or 150% of the original design capacity.

2. The twelve 24,000 cfm propeller fans (3 supply and 3 exhaust on each of the two sub-levels) for normal-use ventilating of the garage do not adequately care for people in the south end for either normal use or shelter use.

3. At rated fan capacities, equal quantities of air are supplied to and exhausted from each sub-level. Thus, if these quantities are actually in balance, there is little or no movement of air along the ramps. Because some of the ramps constitute useful spaces for shelterees, a positive movement of air is needed for these spaces.

4. No provisions in normal use have been made for either tempering or recirculating air during cool or cold weather. The parking garage is an unheated structure.

5. The propeller fans that supply air to the spaces in normal use discharge directly at high velocity with no diffusion. This would be particularly objectionable for shelter use during cool or cold weather.

6. The vertical ventilation shafts for intake and exhaust air are adjacent to the outside walls of the office buildings, with openings just above ground level. The gratings and shafts would be vulnerable to blockage by debris if the office buildings were subjected to nuclear blast.

7. The propeller fans protrude from the wall openings at which they are installed. This interferes with the provision of panel closures for protecting these fans from blast effects within the shelter. Under the open shelter concept, it is intended that ramps and perhaps other access openings will remain open.

8. There is no auxiliary source of electric power in Building 4 for operating essential equipment and lights when commercial sources are disrupted by blast effects or system failure. (For this case study, the 500-kva, engine-generator set in the adjacent tower structure is assumed to be unavailable.)

9. The drainage sump and dual pumps provided on each side of the parking garage are located in two rooms; each contains the air-conditioning equipment and ductwork to serve one office building overhead. In combined effects slanting of the garage, these equipment rooms must be blast isolated from the garage by strengthening the planned interior partitions. Since the drainage function may be essential for shelter operation, the sumps and pumps should be relocated into a blast protected area.

10. Fluorescent lighting fixtures are hung from the ceilings of each sub-level. These fixtures would become dangerous missiles under air blast conditions in an open shelter.

Modifications Indicated for Shelter Purposes

The modified electromechanical system devised to correct the deficiencies enumerated above is shown by Figures 8-4A.1* and 8-4A.2; the slanting changes are described in the following paragraphs, which are keyed to corresponding numbers encircled in the figures and used in Table 8.4A:

9. Replace the twelve 24,000 cfm propeller fans with sixteen propeller fans each with a rated capacity of 27,000 cfm under a static pressure differential equal to 1/4-in. WG (water gage). These fans are to be mounted on either flanged rings or square panels and are to be

* In Volume 1 of this report.

V-belt-driven by 5-hp, two-speed (1800/1200 rpm) motors in place of single-speed 2-hp motors. These motor sizes are indicated for the specified operating conditions in catalog data for propeller fans. These data provide a factor of safety against motor overload caused by a substantial increase in flow resistance, e.g., from partial blockage of airways. The replacement fans, when operating on high speed, have a higher tip speed and sound level than the original fans. The V-belt drives provide a highly practical means for subsequent modification of fan speeds and volumetric capacities to match air flow characteristics of the system and to provide for air movement along the ramps. (Similar results could be obtained by providing volume dampers on the airways or by use of two-speed, direct-driven propeller fans with variable-pitch blades, if special impellers having this feature could be obtained.) Replacement of the original single-speed starters and pushbutton stations with two-speed starters and selector switches would also be required.

5. Change the design and location of the six vent shafts for intake and exhaust air, and provide two additional air shafts near the south end of the garage, one on the east and one on the west side. Typical configurations are shown by Figures 8-4A.3 and 8-4A.4. The shafts at the north end have been moved southward one bay to avoid the premature diversion of supply air toward the ramp entrance at the lower sub-level; in the original location, the stream of air discharged from a supply fan would be obstructed by the rear wall of the interior stairwell. To facilitate the partial recirculation of air without extensive ductwork, the ventilating system was changed to provide air flow in opposite directions on the two sub-levels. Thus, the supply side of the building for one sub-level will be the exhaust side for the other. Recirculation can be controlled by dampers at openings in the partitions that separate adjacent supply and exhaust chambers. With this objective, the grating at the top of each air shaft is replaced by a solid slab at grade, and each air shaft is divided into halves by either vertical partitions or horizontal slabs. On the east side of the building, these are vertical partitions, the north compartment is a plenum for supply air and the south compartment is a plenum for exhaust air. On the west side, these are horizontal slabs at the intermediate floor level, the upper compartment is a plenum for supply air and the lower compartment is a plenum for exhaust air. Each supply plenum, which is also a mixing plenum for fresh and recirculated air, is connected by a prefabricated conduit (such as corrugated-steel cattle-pass sections) to an air intake facility in the grass strip between the sidewalk and the street. Likewise, each exhaust plenum is connected to an exhaust facility along the center of the street. Each facility is an elongated concrete box covered by removable sections of steel grating. There is a ships ladder at each end. Thus, each of the

16 facilities can serve as an emergency exit for the shelter. A typical configuration is shown in Figure 8-0D.

The propeller fans for ventilating the structure are to be installed over openings in the building wall between each plenum and the shelter space. A manually operated multiblade damper for recirculating air is to be installed over an opening in the wall or slab that separates each pair of adjacent intake and exhaust plenums. Each propeller fan is to be supported in such a way that clearance is provided for installation of a recessed grille and a blast door on the shelter side of the wall openings. Flat diamond or wire mesh grilles are to be used over exhaust fans, and diffusion grilles with adjustable, vertical vanes are to be used over supply fans.

11. In the plan for design modifications or slanting, one room each is provided on the east and west sides of the structure for the installation of auxiliary power sources for the emergency operation of essential apparatus during shelter occupancy. These rooms are located at the lower sub-level and are an integral part of the exhaust plenums that are nearest the mechanical equipment rooms for the overhead office buildings, as shown in Figure 8-4A.5. Each of the two power systems is complete and independent. The apparatus includes an engine-generator set, starting batteries, battery rack, control cabinet with remote starting and manual transfer switches, protective devices and meters (including a running-time meter), all necessary circuit connections, disconnect switches for nonessential loads, an underground fuel storage tank, and all necessary piping for fuel supply to the engine, venting, and servicing. Each engine-generator set has a rated continuous capacity of 50 kw at 0.80 power factor. The generator is self-cooled, has a rotating field, and is compatible with building load requirements. The engine is liquid cooled with radiator and, for minimum first cost, uses gasoline fuel. (For maximum reliability and safety, a diesel engine would be preferred.) The engine-generator sets are mounted with vibration isolators on steel bases and installed on concrete pads in the designated rooms. An effective muffler-silencer is connected to the engine exhaust manifold with flexible connectors, and insulated exhaust piping extends through backfill materials alongside the exhaust airway to the air exhaust facility near the middle of the street. The fuel storage tank has a capacity of about 2,000 gallons, with diameter and length dimensions of 5 and 15 ft, respectively. The outside of the tank has a corrosion-resistant finish protected by an abrasion-resistant coating. Offset runs of pipe are used in the fuel lines to provide for differential movement of tank and structure. Switches are provided to isolate the circuits served by each of the two auxiliary power systems. Radiative heat losses from the engine-generator sets will be removed by air exhausted from the shelter; when

the auxiliary power systems are operating, at least 8,000 cfm of air must be exhausted through each generator room. To maintain a state of readiness and to minimize deterioration of stored fuel, the auxiliary power systems must be exercised periodically and a schedule for routine maintenance must be established. Commercial engine-generator sets of this size can be expected to have a predicted life of 10,000 hr or more between successive needs for major overhaul. However, reliable data on the predicted life of a specific manufacturer's apparatus may not be available without extensive tests of representative samples. The remaining time in any predicted period of maintenance should be sufficient to accommodate at least two weeks of shelter occupancy.

10. In this plan for modifications, a drainage sump with dual pumps is relocated from each of the two original mechanical equipment rooms to one lower sub-level supply air plenum on each side of the garage, as indicated in Figure 8-4A.2. Drainage, discharge, and vent piping are to be changed to accommodate the new location. (Although these pumps handle relatively clean water from floor drains and condensate from air-conditioning equipment, a more accessible location in the exhaust air streams might be preferred; plans for the auxiliary power rooms could readily be changed to provide the necessary space.)

12. Two floodlights are mounted in wall recesses adjacent to each ventilating fan, and two small lights are mounted in each emergency generator room. The floodlights in wall recesses are protected by the same blast doors that protect the fans.

X. Although planned modifications include the installation of grilles that provide horizontal diffusion for air discharged at high velocity from supply fans, a flat recessed grille can be only partially successful in reducing the velocities of such large quantities of air in a short distance. If the vanes of such a grille were set at oblique angles as large as 45-degrees with the axis of the fan, the effective area for air flow would be excessively reduced. An expedient solution can be employed to reduce velocities further before the air reaches the first ranks of people in the space. If a stream of air has an objectionable chilling effect, it is proposed to use boxes of shelter supplies or cans of stored water from the storeroom as building blocks to construct a deflecting barrier about seven ft high and eight ft from the wall at an angle to deflect the airstream in an appropriate direction. Spaces between boxes would permit passage of small streams of air, which would soon mix with air in the immediate environment. As the supplies are consumed, waste materials would be used as ballast to refill the boxes.

Section 5 - Alternative Electromechanical Systems

The ventilation modifications proposed for Building 4A and for other case studies are the result of many compromises among a variety of alternatives. Evaluation of these alternatives has necessarily been based not only on cost-effectiveness comparisons among alternative electromechanical systems, but also on the composite effects of system and structural changes on cost-effectiveness of a shelter. This has demonstrated that an optimum ventilating system may not be compatible with an optimum structure. In this context, an optimum facility of any kind can be defined as one that barely satisfies minimum performance requirements with minimum cost. Although the proposed system for Building 4A is capable of meeting criteria for performance at relatively low incremental costs, some additional comments regarding alternative systems or components may be appropriate because they may be applicable in other situations.

Parking garages are sometimes provided with ventilation galleries along two opposite ends or sides through which air is supplied or exhausted. With this arrangement, the air can be introduced and exhausted through many grilled openings without significant increase in cost, an essentially linear pattern of air flow can be established in the space, massive jets of high velocity air are avoided, and stagnant areas may be virtually eliminated. This arrangement inherently leads to a better environment for human habitation. With the addition of a capability for partial recirculation of air during cold seasons, such an arrangement should perform very well in a shelter, if the system has sufficient air handling capacity. In general, such a system would use a few large fans and intake or exhaust facilities in lieu of many small ones. Also, the fans would be remote from and would create less noise in occupied spaces. However, a system using this arrangement proved to be incompatible in terms of cost with structural requirements under the open shelter concept for Building 4A, largely because both inside and outside walls of the air galleries would require strengthening for blast resistance. Also, the arrangement would provide only 4 rather than 16 emergency exits.

In Building 4A, the recirculation of air without return ductwork was facilitated because the two-level structure provided a built-in return path. With such a configuration, ventilation and recirculation

could be accomplished with supply and exhaust facilities (fans and airways to atmosphere) on only one side of the shelter. All of the fresh air would then be introduced along one side of the upper sub-level, all air would be withdrawn through openings along the same side of the lower sub-level, and any proportion of the air could be recirculated through dampers in the floor between the plenums for fresh and return air. However, there are three objections to such an arrangement:

- In addition to the supply and exhaust fans at the near side, an intermediate set of fans would be required along the far side of the shelter for transferring air from the upper to the lower sub-level. Because the effective area of the ramp openings is so large, it would not be practicable to provide air shafts or grated floor openings that have the relatively larger free area needed to transfer most of the air at the far side of the shelter, as necessary for adequate ventilation.

- Velocities of air would be doubled, and the resultant average velocity of 94 fpm with high speed operation of the fans or 63 fpm with low speed operation would be undesirably high in the cool environment associated with winter conditions. There is a practical but undefined limit to the length of path for air flow in a large shelter.

- If an isolated fire should occur in a parking garage (or other facility), the ventilation of two or more levels in series would tend to spread fire and smoke through a more extensive area than with other ventilation schemes. To minimize this effect, it would be necessary to curtail ventilation at all levels.

In a shelter that occupies a large space on a single level, partial recirculation can be accomplished with dampers but little or no ductwork by using curtains or brattices to fold the path for air flow in a horizontal plane, thus bringing the supply and exhaust plenums into proximity. This method could, of course, be applied to each level for a multi-level shelter. To use this method in Building 4A, it would have been necessary to reverse the direction of rotation of half the supply and half the exhaust fans during occupancy of the shelter, because the brattices could not be left in place during normal operation of the parking garage. In general, higher efficiencies are obtainable with axial flow fans that have impellers designed for unidirectional operation. When possible, it is advantageous to use structural elements, whether they are floors or partitions, to define the folded path for air flow through a series of

spaces. In any such configuration, no excessively high air velocities should occur in any occupied space along either arm of the folded path.

During moderately cold weather, the minimum requirements for environmental temperature can usually be satisfied without excessive reduction in the flow rate of fresh air by recirculating an appropriate part of the ventilating air. However, this method may not be adequate in climatic locations where sub-zero temperatures occur frequently or in shelters that would have a relatively larger loss of heat by transmission through walls and roof. Table H.6 shows values of air properties when the quantity of fresh air is 3 scfm/person, the temperature of mixed air is either 50 or 65 F, and the total rate of ventilation is within a range of 6 to 30 scfm/person as shown in the second column. As in Tables H.3, H.4 and H.5, transmission heat losses were assumed to be small relative to metabolic loads. The BASIC computer program for preparing Table H.6 is listed in Table H.7; Tables H.3 to H.5 were prepared with earlier versions of the same program.

In the first column of Table H.6, the upper value in each pair is the minimum value of fresh air temperature at which the recommended minimum flow rate of 3 scfm/person can be maintained without reducing the mixed air temperature or increasing the total rate of ventilation. It is most significant that minimum environmental temperatures and rates of air replacement can be maintained at lower ambient temperatures when the total ventilating rate is increased. As shown in the first column lower value of each pair, the difference between mixed and recirculated air temperatures is reduced as the total rate of ventilation (second column) increases.

Thus, the ventilating capacity required in a northern climate may be higher during the cold than during the hot season. To obviate any need for increasing the ventilating capacity above that required during the hot season, waste heat from a liquid-cooled or ebullient-cooled engine-generator set can be used for tempering the air supplied to occupied spaces. This can be accomplished by passing the stream of fresh, recirculated, or mixed air through an extended-surface or pipe coil that has control valves and interconnecting water piping either in series or in parallel with the engine radiator. The heat conservation system should be controlled automatically (1) to maintain engine temperatures within an efficient operating range and (2) to temper air supplied to occupied spaces when and only when warmer air will improve the environment. Although heat transfer coils could readily be installed over the recirculation damper near each generator room in Building 4A, the additional costs associated with use of waste heat were not considered justifiable in the moderate winter climate of Columbus, Georgia.

Table H.6

QUANTITIES ASSOCIATED WITH MINIMUM RATE OF AIR REPLACEMENT

ELEVATIØN, FT= 242 , BARØMETER, ATM= .99127
AMBIENT REL HUMIDITY= 50 %, MR= 400 BTUH

FRESH TEMP	TØTAL SCFM	FRESH SCFM	RECRC SCFM	RATIØ DH/DW	EVAP LB/DAY
RECRC TEMP	TØTAL CFM	FRESH CFM	RECRC CFM	DEW PØINTS F MIXED	RECRC
		MIXED AIR TEMP= 50			
		AMBIENT HUMID RATIØ= 0.0007139			
11.6	6.00	3.00	3.00	2879.1	3.334
88.3	5.89	2.70	3.19	42.90	59.70
		AMBIENT HUMID RATIØ= 0.0002786			
-6.6	9.00	3.00	6.00	3473.9	2.763
78.2	8.83	2.59	6.24	43.30	53.60
		AMBIENT HUMID RATIØ= 0.0001890			
-13.6	11.33	3.00	8.33	3634.1	2.642
72.9	11.13	2.55	8.58	44.30	52.20
		AMBIENT HUMID RATIØ= 0.0001415			
-18.8	14.00	3.00	11.00	3732.1	2.572
68.7	13.75	2.52	11.23	45.10	51.30
		AMBIENT HUMID RATIØ= 0.0001137			
-22.6	17.00	3.00	14.00	3796.9	2.528
65.5	16.70	2.50	14.20	45.70	50.80
		AMBIENT HUMID RATIØ= 0.0000973			
-25.2	20.00	3.00	17.00	3838.6	2.501
63.2	19.65	2.49	17.17	46.20	50.40
		AMBIENT HUMID RATIØ= 0.0000723			
-30.2	30.00	3.00	27.00	3910.2	2.455
58.9	29.49	2.46	27.04	47.10	49.80
		MIXED AIR TEMP= 65			
		AMBIENT HUMID RATIØ= 0.0010870			
20.2	8.62	3.00	5.62	2470.1	3.886
89.0	8.75	2.75	6.00	53.90	64.50
		(RECRC TEMP > 89 F IF TØTAL SCFM= 6)			
		AMBIENT HUMID RATIØ= 0.0009853			
18.1	9.00	3.00	6.00	2539.7	3.780
88.5	9.13	2.74	6.40	53.50	63.50
		AMBIENT HUMID RATIØ= 0.0006333			
9.2	11.33	3.00	8.33	2838.0	3.383
85.1	11.49	2.69	8.81	52.10	59.90
		AMBIENT HUMID RATIØ= 0.0004632			
3.1	14.00	3.00	11.00	3023.4	3.175
81.9	14.20	2.65	11.55	51.60	57.80
		AMBIENT HUMID RATIØ= 0.0003683			
-1.3	17.00	3.00	14.00	3143.4	3.054
79.2	17.24	2.62	14.62	51.50	56.50
		AMBIENT HUMID RATIØ= 0.0003143			
-4.3	20.00	3.00	17.00	3219.0	2.982
77.2	20.28	2.61	17.68	51.50	55.70
		AMBIENT HUMID RATIØ= 0.0002331			
-9.8	30.00	3.00	27.00	3346.0	2.869
73.3	30.42	2.58	27.85	51.70	54.50

Table H.7

BASIC COMPUTER PROGRAM

```
200  REM: BASIC PRØGRAM > VFRMB4 <    7/71
210  REM: VENTILATIØN PRØCESS WITH RECIRCULATIØN
220  READ L9,MO,Y1,VO
230  LET P9=(1-6.83432E-06*L9)^5.29478
240  LET B9=INT(100000.*P9+.5)/100000.
250  PRINT
260  PRINT
270  LET Q1=Q2=Q3=Q4=0
280  PRINT  USING 380
290  PRINT "    ELEVATIØN, FT=";L9;", BARØMETER, ATM=";B9
300  PRINT "    AMBIENT REL HUMIDITY=";Y1;"%, MR=";MO;"BTUH"
310  PRINT  USING 380
320  PRINT  USING 390
330  PRINT  USING 400
340  PRINT  USING 410
350  PRINT  USING 420
360  PRINT  USING 430
370  PRINT  USING 380
380  IMAGE"-------------------------------------------------------------"
390  IMAGE" FRESH      TØTAL      FRESH      RECRC       RATIØ      EVAP"
400  IMAGE" TEMP       SCFM       SCFM       SCFM        DH/DW    LB/DAY"
410  IMAGE"- - - - - - - - - - - - - - - - - - - - - - - - - - - - - - -"
420  IMAGE"  RECRC       TØTAL      FRESH      RECRC        DEW PØINTS F"
430  IMAGE"  TEMP          CFM        CFM        CFM       MIXED      RECRC"
440  IMAGE 4D.D,3X4D.2D,2X4D.2D,2X4D.2D,3X5D.D,2X3D.3D
450  IMAGE X4D.D,3X4D.2D,2X4D.2D,2X4D.2D,3X4D.2D,2X4D.2D
460  GØTØ 600
470  REM: SUB > TRHSPW < IN T7(T1),Y1; OUT S1,P1,W1
480  LET R7=491.67/(459.67+T7)
490  IF T7<32 THEN 540
500  LET S0=6.02792E-03
510  LET X1=26.4051*(1-R7)+1.48183*(1-R7)/R7
520  LET S1=S0*R7^8.0374*EXP(X1)
530  GØTØ 570
540  LET S0=6.02751E-03
550  LET X1=22.892*(1-R7)+.226568*(1-R7)/R7
560  LET S1=S0*R7^.61775*EXP(X1)
570  LET P1=S1*Y1/100
580  LET W1=.62197*P1/(P9-P1)
590  RETURN
600  READ V4,T2
610  IF V4<.3 ØR T2<-.3 THEN 2070
620  LET G2=MO/(4.5*V4)
630  LET R0=(91.0568-T2)/2.0568
640  LET F0=.299093*(89-T2)+1.2365*LØG(R0)
650  IF G2>F0 THEN 680
660  IF V4<VO THEN 600
670  GØTØ 740
680  LET G2=F0
690  LET V2=MO/(4.5*F0)
700  IF V2<VO THEN 600
710  LET T3=T4=89
720  LET Q4=2
730  GØTØ 760
740  LET V2=V4
750  GØSUB 1360
760  LET R1=(91.0568-T2)/(91.0568-T3)
770  LET F1=5.403E-05*(T3-T2)+1.1344E-03*LØG(R1)
780  LET R4=G2/F1
790  LET M3=MO/R4
800  LET H6=MO/(4.5*VO)
810  LET H5=H6-G2
820  LET W5=H5/R4
830  LET Z1=T2
840  LET J=1
850  LET Z3=128/(-2)^J
860  FØR T7=Z1 TØ Z1+6*Z3 STEP Z3
870  GØSUB 480
880  LET K8=R4-1061.25-.4362*T2
890  IF T7<32 THEN 930
900  LET K1=.2402+.4362*W1
910  LET T8=T2-(K8*W5)/K1
920  GØTØ 950
930  LET K2=.2402+.4412*W1
940  LET T8=T2-(K8*W5+(.005*T2-.16)*W1)/K2
950  IF T7>T8-.01 AND T7<T8+.01 THEN 1050
960  IF Z3>0 THEN 990
970  IF T7<T8 THEN 1010
980  GØTØ 1000
990  IF T7>T8 THEN 1010
1000  NEXT T7
1010  IF ABS(Z3)<.02 THEN 1050
1020  LET Z1=T7
1030  LET J=J+1
1040  GØTØ 850
1050  LET T1=INT(10*T7+.5)/10
1060  LET W2=W5+W1
1070  LET P5=P9*W2/(W2+.62196)
1080  GØSUB 1600
1090  LET D2=D5
1100  IF D2>T2 THEN 2140
1110  LET V1=VO
1120  LET W3=W2+F1
1130  LET P5=P9*W3/(W3+.62195)
1140  GØSUB 1600
1150  LET D3=D5
1160  LET V3=V2-V1
1170  LET U1=V1*.001891*(459.67+T1)*(1+1.6078*W1)/P9
1180  LET U2=V2*.001891*(459.67+T2)*(1+1.6078*W2)/P9
1190  LET U3=V3*.001891*(459.67+T3)*(1+1.6078*W3)/P9
1200  IF T2<Q2+.1 AND T2>Q2-.1 THEN 1220
1210  PRINT "                    MIXED AIR TEMP=";T2
1220  LET Q2=T2
1230  PRINT  USING 1240;W1
1240  IMAGE 9X,"AMBIENT HUMID RATIØ=",2D.7D
1250  PRINT  USING 440;T1,V2,V1,V3,R4,24*M3
1260  PRINT  USING 450;T4,U2,U1,U3,D2,D3
1270  IF Q4>1 THEN 1290
1280  GØTØ 1300
1290  PRINT "     --- RECRC TEMP > 89 F IF TØTAL SCFM=";V4
1300  IF Q3>1 THEN 1320
1310  GØTØ 1330
1320  PRINT "     --- MØIST LØAD > MAX FØR FRESH SCFM=";VO
1330  LET Q3=Q4=0
1340  GØTØ 600
```

Table H.7 (continued)

```
1350  REM: SUB > RT3MSB < IN G2=H3-H2, OUT T3 AND T4 (F)
1360  LET N1=89.24
1370  LET J1=1
1380  LET C1=(89-T2)/2↑J1
1390  FOR T=N1 TO N1-2*C1 STEP -C1
1400  GOSUB 1540
1410  IF F2 <= G2 THEN 1430
1420  NEXT T
1430  IF C1<.04 THEN 1470
1440  LET N1=T+C1
1450  LET J1=J1+1
1460  GOTO 1380
1470  LET A1=T
1480  LET B1=G2-F2
1490  LET T=A1+C1
1500  GOSUB 1540
1510  LET B2=F2-G2+B1
1520  LET T3=A1+C1*B1/B2
1530  GOTO 1570
1540  LET R2=(91.0568-T2)/(91.0568-T)
1550  LET F2=.299093*(T-T2)+1.2365*LOG(R2)
1560  RETURN
1570  LET T4=INT(10*T3+.5)/10
1580  RETURN
1590  REM: SUB > DPTFSB < IN P5(ATM), OUT D5(F)
1600  IF P5<6.E-07 THEN 1940
1610  IF P5>1 THEN 1960
1620  IF P5<6.0277E-03 THEN 1660
1630  LET N2=31.9
1640  LET J2=6
1650  GOTO 1680
1660  LET N2=32.1
1670  LET J2=5
1680  LET C2=(-2)↑J2
1690  FOR T5=N2 TO N2+4*C2 STEP C2
1700  GOSUB 1840
1710  IF S5>.9995*P5 AND S5<1.0005*P5 THEN 1810
1720  IF C2<0 THEN 1750
1730  IF S5>P5 THEN 1770
1740  GOTO 1760
1750  IF S5<P5 THEN 1770
1760  NEXT T5
1770  IF ABS(C2)<.04 THEN 1810
1780  LET N2=T5
1790  LET J2=J2-1
1800  GOTO 1680
1810  LET T5=INT(10*T5)/10+.05
1820  GOSUB 1840
1830  GOTO 1980
1840  LET R=491.67/(459.67+T5)
1850  IF P5<6.0277E-03 THEN 1900
1860  LET S=6.02792E-03
1870  LET X=26.4051*(1-R)+1.48183*(1-R)/R
1880  LET S5=S*R↑8.0374*EXP(X)
1890  GOTO 1930
1900  LET S=6.02751E-03
1910  LET X=22.892*(1-R)+.226568*(1-R)/R
1920  LET S5=S*R↑.61775*EXP(X)
1930  RETURN
1940  LET D5=-111.11
1950  GOTO 2060
1960  LET D5=+212.12
1970  GOTO 2060
1980  IF S5<P5 THEN 2010
1990  IF S5>P5 THEN 2030
2000  GOTO 2050
2010  LET D5=T5+.05
2020  GOTO 2060
2030  LET D5=T5-.05
2040  GOTO 2060
2050  LET D5=T5
2060  RETURN
2070  PRINT  USING 380
2080  PRINT
2090  PRINT
2100  READ Q1
2110  IF Q1>9.5 THEN 220
2120  IF Q1>.5 AND Q1<9.5 THEN 250
2130  GOTO 2400
2140  LET T7=T2
2150  GOSUB 480
2160  LET W2=.62196*S1/(P9-S1)
2170  LET Z2=T2-254
2180  LET J=1
2190  LET Z4=256/2↑J
2200  FOR T7=Z2 TO Z2+2*Z4 STEP Z4
2210  GOSUB 480
2220  IF T7<32 THEN 2260
2230  LET K1=.2402+.4362*W1
2240  LET T8=T2-(K8*(W2-W1))/K1
2250  GOTO 2280
2260  LET K2=.2402+.4412*W1
2270  LET T8=T2-(K8*(W2-W1)+(.005*T8-.16)*W1)/K2
2280  IF T7>T8-.02 AND T7<T8+.02 THEN 2350
2290  IF T7>T8-Z4/2 AND T7<T8+Z4/2 THEN 2310
2300  NEXT T7
2310  IF Z4<.02 THEN 2350
2320  LET Z2=T7-Z4
2330  LET J=J+1
2340  GOTO 2190
2350  LET T1=INT(10*T7+.5)/10
2360  LET V1=V2*F1/(F1+W2-W1)
2370  LET D2=T2
2380  LET Q3=2
2390  GOTO 1120
2400  END

110   DATA 242,400,50,3
120   DATA 6,50,9,50,11.33,50,14,50,17,50,20,50,30,50
130   DATA 6,65,9,65,11.33,65,14,65,17,65,20,65,30,65
140   DATA -7,9,-23
```

Finally, an opportunity to use relatively cool water from a well or other reliable source for cooling purposes as well as potable uses in a shelter should not be overlooked. When this resource is available and utilized, the physical environment can readily be controlled regardless of atmospheric conditions, and an auxiliary power supply can be cooled directly without any requirement for air other than that needed for combustion of fuel.

Section 6 - Conclusions

The results of this study lead to the following conclusions:

1. The adequacy of a ventilating system is seriously eroded if the system cannot maintain a satisfactory environment during cold seasons.

2. In the absence of viable apparatus for tempering fresh air, a ventilating system that is capable of recirculating an adjustable proportion of the air is necessary for shelters located in climatic zones having a significant percentage of hourly temperature readings below 50 F.

3. The fragmentary data in Table H.6 indicate that the capacity of a ventilating system should be at least 10 cfm/persons, even though a lesser capacity is prescribed for preventing an excessively hot environment in a shelter.

4. With objective planning, means for recirculating air can be provided at low cost and the shelter system configuration can be arranged to eliminate virtually all stagnant spaces, in many if not most cases.

5. Further research is needed with regard to the ventilation of shelters during cool and cold seasons. The work should include the derivation of more complete data on recirculation of air under the probable range of operating conditions, the contribution made by lights, the use of waste heat, and the effects of heat conduction in surrounding materials.

6. More case studies in depth are needed to devise economical and effective techniques for adapting electromechanical systems to shelter uses in representative types of structures.

REFERENCES

1. Allen, F. C., Ventilating and Mixing Processes in Nonuniform Shelter Environments, Final Report under OCD Work Unit 1236A, Stanford Research Institute, January 1970 (AD-708 574).

2. Technical Standards for Fallout Shelters, Technical Memorandum 68-1, U.S. Office of Civil Defense, March 5, 1969.

3. ASHRAE Handbook of Fundamentals, American Society of Heating, Refrigerating and Air-Conditioning Engineers, Inc., New York, 1967.

4. Baschiere, R. J., and M. Lokmanhekim, Shelter Forced Ventilation Requirements Using Unconditioned Air, OCD Work Unit 1215A, General American Research Division, Niles, Illinois, February 1967. (Frequency tables of hourly temperature readings at 91 weather stations are in an unpublished supplement to this report.)

5. Humphreys, C. M., A. Henschel, and D.H.K. Lee, Sensible and Latent Heat Losses from Occupants of Survival Shelters, OCD Work Unit 1221C, U.S. Public Health Service, December 1966.

6. Allen, F. C., Shelter Configuration: Environmental Control Systems and Related Parameters, Final Report under OCD Work Unit 1236A, Stanford Research Institute, March 1969.

Appendix H.1

VENTILATION DESIGN CONSIDERATIONS

By F. C. Allen

CONTENTS

Preceding page blank

FIGURES

Appendix H.1

VENTILATION DESIGN CONSIDERATIONS

By F. C. Allen

Section I - Environmental Control Through Ventilation

It is assumed that for each phase in full slanting, the design of a building will be performed or supervised by professional engineers or architects who are familiar with specialized requirements associated with shelters. A qualifying background for slanting the design of ventilating or air-conditioning systems should include either completion of the DCPA-sponsored Environmental Engineering course or the equivalent in private study of relevant literature. Technical requirements and recommendations for environmental control and mechanical equipment in shelters are discussed in several documents.[1-5*]

In this section on ventilation and air conditioning, repetition of information contained in readily available publications is intentionally minimized. In Section I-A the environmental criteria are stated and supported by explanatory notes. Sufficient data are included to determine the required capacities of basic systems. The technical background for governing criteria is discussed in Section I-B, which relates to chemical vitiation of air, and Section I-C, which relates to thermal effects in shelters occupied during warm weather. The configuration of mechanical systems, including the arrangement of cost-effective ventilating systems, is discussed in Section I-D. Recommendations on the arrangement of ventilating systems are largely based on concepts relating to metabolic parameters, spatially nonuniform (varistate) environments, and partial recirculation of air during cold weather. These concepts were developed and used in evaluating the seasonal performance of ventilating systems for dual use of a parking garage (Appendix H, Volume 2, Reference 6). The concepts were subsequently developed further under a more rigorous analysis, and the results were used to obtain graphic data that are instructive and applicable to the design, evaluation, or operation of ventilating systems for shelters.[7] The scientific background and salient results of the advanced analysis are presented in Section II.

---

* Superscript numerals indicate references listed at the end of this Appendix.

A. Environmental Criteria for Shelters

The environment in a shelter must necessarily be isolated to some degree from the ambient atmosphere, and reliable means must therefore be available for maintaining habitable conditions during any anticipated period of occupancy. The ventilating, air-conditioning, or life support system provided for this purpose must be capable of maintaining throughout the shelter an air quality that is within acceptable limits with respect to both chemical composition and temperature.

Recommended criteria relating to systems for control of the environment in shelters are as follows:[4]

1. The rate of ventilation with outside (fresh) air should be not less than 3 scfm* per person. This specified minimum rate of air replacement will adequately dilute the carbon dioxide produced and replenish the oxygen consumed by metabolic processes in sedentary persons, but is not adequate for removal of metabolic heat during warm seasons.

2. Environmental temperatures in an occupied shelter should not fall below 50 F. Temperatures in vacant shelters should not fall below 33 F, if necessary to prevent frost damage to susceptible materials.

3. The daily average effective temperature (ET) in occupied spaces should be less than or equal to 82 F (82 FET) during 90 percent of the days in a year that is representative of the local climate. This criterion is based on the original effective temperature index, which relates to the thermal comfort of normally clothed sedentary persons in environments having equal air and mean radiant temperatures.[2,8] The index determines a value of ET, which is the temperature of saturated air that would produce the same sensory responses as an environment in which stated conditions prevail with respect to temperature, humidity, and air velocity. The effective temperature in a shelter environment is approximated by the equation:

$$ET \approx (62.3T+45.2D)/(62.3+D)$$

where

T = dry-bulb temperature, F

T_W = wet-bulb temperature, F

$D = T-T_W$ = wet-bulb depression

---

* Cubic feet per minute of "standard air," i.e., air having a specific volume of 13.33 cf per pound of dry air.

Values of the revised effective temperature (written with an asterisk, ET*) determined with the new ASHRAE Comfort chart are not applicable under this criterion.†

4. The required capacity of a ventilating system for a shelter (scfm units) is the product of the designated number of occupants and the per capita rate of air flow, as indicated on Figure H.1-1 in which the unit ventilation requirement is constant along each of the labeled lines. These "isoventilation lines" were determined by extensive analyses of the probable effects of local climates on system performance, under the following basic assumptions:[10]

a. The shelter walls are insulated or adiabatic, i.e., there is no heat transmitted across boundary surfaces.

b. Metabolic heat and moisture losses from sedentary occupants are the only thermal loads in the shelter; heat emitted by lights or other appliances is not considered.

c. The shelter environment is spatially uniform, i.e., air supplied at outside conditions of temperature and humidity is thoroughly and instantly mixed with air in the occupied space, and exhaust air is typical of the environment.

The title for Figure H.1-1 implies that a daily average, adjusted, effective temperature of 82 FET will not be exceeded during more than 10 percent of days in a typical year, if the shelter is ventilated at the indicated per capita rate. An adjusted value of 82 FET corresponds to an input value of 83 FET in computations that do not consider the transient effects of heat conduction in surrounding masses of building and fill materials. The one degree adjustment in ET is consistent with a comparison of computed and experimental data relating to concrete and masonry shelters.[10] Ventilation system capacities determined in accordance with Figure H.1-1 are presumed to meet the criterion for limiting the effective temperatures that would probably develop in shelter environments during warm weather.

† Reference 9, p. 137.

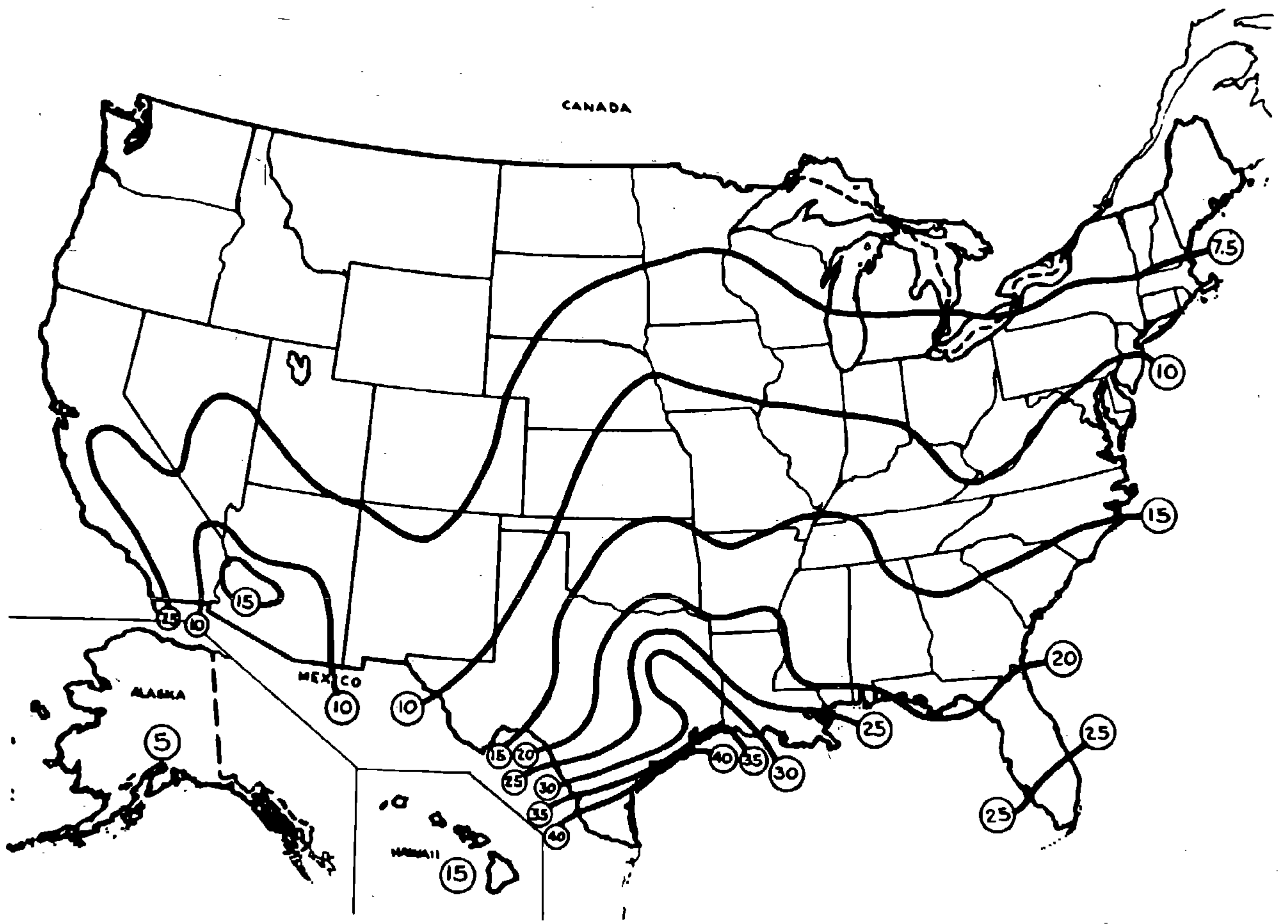

FIGURE H.1-1 AMENDED MAP OF FORCED VENTILATION REQUIREMENTS (SCFM/OCCUPANT) FOR 82 F ADJUSTED EFFECTIVE TEMPERATURE AND 90% ADEQUACY BASED UPON DAILY AVERAGE DATA (VENTILATION RATES FOR STANDARD AIR, DENSITY = 0.075 pcf)[10]

B. The Chemical Environment

During prolonged occupancy of a space by sedentary persons (metabolic rate = 400 Btuh*), volumetric concentrations of carbon dioxide and oxygen associated with several rates of ventilation tend to approach the following values:[1,2]

Ventilating Rate (scfm/Person)	Volumetric Concentration Carbon Dioxide	Oxygen
0.5	2.7%	17.2%
1.0	1.4	18.8
1.5	0.9	19.3
2.0	0.7	19.5
3.0	0.5	19.8
5.0	0.3	20.1

Oxygen concentrations of 17 to 21 percent by volume, which include all values listed above, are considered safe for prolonged exposures. A carbon dioxide concentration of 3 percent may be an appropriate design limit for acute exposures, i.e., 8 hours or less, but concentrations of 1 percent or less should be maintained when adverse effects must be minimized during prolonged exposures.[11] Values between 1 and 3 percent carbon dioxide could develop during an operational emergency in all or part of a shelter without serious consequences. Design criteria for shelters call for outside (fresh) air at 3 scfm per person, as a minimum.[4] The apparent concentration of carbon dioxide would then be only 0.5 percent, but higher values would occur in all or part of a shelter if: air is poorly distributed; the occupants are physically active; the space is overpopulated; or a ventilating fan is temporarily inoperative.[12] There is no compelling reason to reduce the criterion for minimum fresh air quantity, because required capacities and costs of ventilating systems are largely determined in all climatic zones by criteria for control of temperatures and humidities during warm seasons. However, minimum quantities of fresh air, spatial variations in temperature, and partial recirculation of air during cold weather should be considered when planning the system configuration.[7] Vitiated air from toilets, kitchens, engine-generator rooms, and spaces that may be contaminated by airborne pathogens should not be recirculated unless treated as necessary to remove noxious constituents.

---

* Btu per hour.

C. The Thermal Environment

With the sedentary levels of physical activity that would probably prevail in shelters, the unit metabolic rate would be about 50 kilogram calories per hour (kcal/hr) per square meter of skin surface area. For a typical man the total metabolic rate would be about 100 kcal/hr, 400 Btuh, or 117 watts.[7,9,10] To maintain a state of thermal equilibrium in which body temperatures are not changing with time, metabolic heat must be rejected to the environment at a rate that is substantially equal to the rate of production. Moreover, to avoid excessive discomfort or physiological stress, the transfer of metabolic heat must be accomplished with near-normal body temperatures and with rates of evaporation that are well below a maximum sustained sweat rate of about one liter per hour.[13] The total rate for transfer of metabolic heat is the almost constant sum of two variable components, "sensible heat" and "latent heat;" the first is associated with a change in temperature, and the second, with an increase in humidity of the ventilating air. During passage through an occupied space, the air temperature will increase if the air enters at less than 95 F, but will decrease if the air enters at more than 95 F, because evaporative regulation tends to limit mean skin temperatures at about 95 F.[14] The rationale for control of the thermal environment is treated in more detail in Section II, which includes graphic data relating to metabolic parameters, ventilation process lines, and partial recirculation of air during cold weather. Section II also includes a derivation of parametric relationships in the transfer of metabolic heat, and a psychrometric analysis of ventilating processes in varistate environment.

There is generally a requirement during all seasons for cooling rather than heating in fully occupied shelters of the types considered herein. Metabolic heat from shelterees tends to be much greater than the combined effects of other loads, including low-level lighting, heating appliances, and heat transmitted through structural elements. The effects of transient or periodic heat conduction in surrounding masses of materials contribute to control of a shelter environment by attenuating both the initial rise and the amplitude of diurnal variations in temperatures of occupied spaces.[1-3] These effects will be most apparent in small underground shelters that have relatively large, per capita areas of structural slabs or walls backed by cool earth. All heat generated in an underground shelter could be dissipated solely by conductive effects in contiguous materials - if the initial earth temperature is less than the upper limit for environmental temperature, and if the population density could be reduced as necessary to meet prevailing requirements for heat transfer at the interface.[2,12,15] In temperate regions, for example, an increase in per capita floor area to about 40 sf per person might be required for a stay time of two weeks. Per capita costs for shelter, however, may then be prohibitive.

D. Configuration of Mechanical Systems

With regard to slanting for combined effects of nuclear weapons (or full slanting), environmental control systems may be designed with either primary or secondary consideration given to shelter needs; for example, in most if not all buildings, a ventilating system will be provided, but air conditioning will be included only when required by non-shelter uses for the space.

The required capacity of a ventilating system for shelters is determined by prescribed criteria for control of the thermal environment during warm seasons. However, the fact that air-moving capacity is adequate does not assure satisfactory performance of a system that is improperly arranged. An extensive system of ducts and diffusion outlets can be provided to distribute air and create a virtually uniform environment in all spaces. Alternatively, the system can be arranged to move air in sequence through one or more contiguous spaces, with an objective of reducing costs for ductwork without sacrificing environmental quality. To move air linearly through a rectangular room, air should enter the occupied space at many points along one wall and leave the space at many points along the opposite wall. Thus, each person in the space will be in the moving air stream. This is the characteristic situation for creating a varistate environment.

In L-shaped rooms, rooms connected by doorways, and rooms with obstructions or reentrant corners, the ideal conditions present in a simple rectangular space can be simulated by using a combination of peripheral ducts, diffusion outlets, exhaust openings, portable screens and brattices, as necessary to direct the flow of air through every geometrical component of the occupied spaces. The objectives are to eliminate stagnant areas and to obtain a uniform difference between the temperatures of entering and leaving air. Such means are commonly used in ventilating mines.

Ventilating systems that tend to create a varistate environment should be capable of supplying a mixture of fresh and recirculated air to occupied spaces at a temperature of 50 F or higher during cold weather. Alternatively, heat recovery apparatus can be provided and used during cold weather to temper fresh air with heat extracted from relatively warm waste air. Metabolic heat losses in fully occupied underground shelters will usually be adequate for such tempering purposes, after steady state conditions have been established.

An auxiliary power source (engine-generator set) can contribute significantly to shelter operation and reliability. Heat losses from the engine can be used to heat water and to temper air during cold weather.

Heat recovered from the jackets, lubricating oil, and exhaust gases of a liquid or vapor cooled engine can be supplemented by resistance heaters when the generator is not otherwise loaded to capacity.

If ventilating air enters and leaves a shelter at widely separated points, a long run of return-air ductwork may be needed for partial recirculation of air. This can be avoided if the path of air flow through the shelter can be folded to bring the entering and leaving points into proximity.[16] However, when the intake and exhaust openings are close together, the possibility of short-circuiting (reentry of waste air) is increased. Such short-circuiting can usually be reduced or eliminated by discharging the waste air at high velocity in a nearly vertical direction. The use of ventilation intake and exhaust conduits as emergency entranceways for a large shelter in an underground parking garage (Building 4A) is illustrated in Chapter 8 of References 6 and 17 and discussed in Appendix H, Volume 2 of Reference 6.

In general, the operational integrity or reliability of the environmental control system should be consistent with the level of blast protection afforded by the shelter structure. System components that would be damaged or destroyed by anticipated blast effects must be either blast resistant or protected from blast effects. Shock-mounting of fragile apparatus may also be necessary. These requirements apply to all essential equipment and appurtenances, including ducts, piping, air-moving apparatus, heat transfer equipment, pumps, facilities associated with a heat sink (water, air, or earth), and any auxiliary power source needed to operate the system during an emergency.

For ever-ready protection of both equipment and personnel against relatively high overpressures, consideration should be given to the use of either blast-actuated or sensor-operated valves at air intake and exhaust openings. The penetration of blast resistant walls of a shelter structure by air ducts should be avoided, if possible, because such vulnerable openings must be provided with blast resistant closures.

In general, it is desirable to provide a separate system for environmental control in the protected shelter area. If the system includes air conditioning designed for nonshelter uses, the installation should be thoroughly examined to identify modifications needed for adapting the system to shelter use.[18] The examination should consider both operational and protective requirements. An air-conditioning system that uses chilled water and a package water chiller is well-adapted for use in blast resistant shelters, because refrigerant piping is contained within the package, and heat is transferred through less vulnerable water piping. When feasible, cooling can be accomplished reliably by means of a water well, a pump, and apparatus for air-to-water heat transfer.

Section II - Generalized Analyses of Ventilation Processes

A. Introduction

Two ventilation processes for controlling the thermal environment in shelters are considered in this Section. The first of these processes is associated with a spatially nonuniform or varistate environment; the second, which is a special case of the first, is associated with a uniform or isostate environment.

The first objective herein is to present data that are generally useful in the design, evaluation, or operation of shelter ventilating systems. The second objective is to document thoroughly the background and derivation of: (1) rationale for transfer of metabolic heat and moisture to the air; (2) psychrometric equations for ventilation process lines; and (3) relationships among parameters in the partial recirculation of air during cold weather. In approaching these objectives, a better understanding of the processes may be fostered, and points of departure for more advanced analyses may be established.

B. Metabolic Parameters

Published data on metabolic heat are largely based on experiments with subjects who were either nude or dressed in "normal" clothing. This "normal" clothing had a thermal resistance in the range of 0.5 to 1.0 clo units.[9,13,19] (A clothing ensemble that has a resistance of 1 "clo" unit will transmit heat at the rate of 1 watt/sf when the temperature difference from skin to exposed surface is about 3 F.) Because the temperature in a shelter may vary through a wide range, it is realistic to assume that clothing is many-layered, and at any time or place is adjusted to be "optimum" in the prevailing environment.

The metabolic parameters shown in Figure H.1-2 are based on numerical data obtained with a computer model in which are simulated seven simultaneous processes for exchange of heat and moisture between a sedentary person and his environment.[7] The seven metabolic processes are as follows:

1. Radiation at exposed surfaces of skin or clothing.

2. Convection at exposed surfaces.

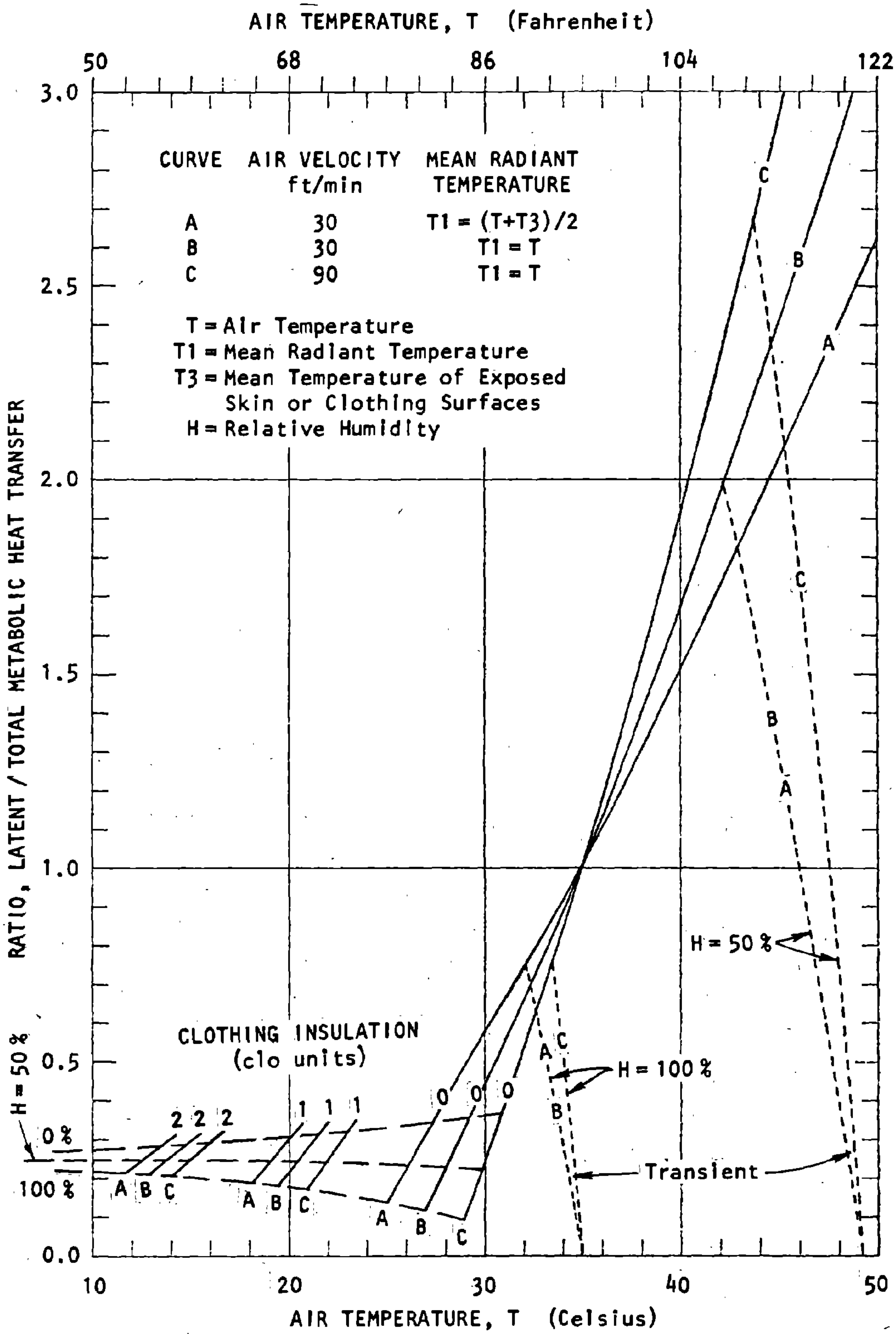

FIGURE H.1-2 METABOLIC DATA AT THERMAL EQUILIBRIUM FOR SEDENTARY PERSONS IN OPTIMUM CLOTHING

3. Heat associated with changes in temperature of respired air.

4. Conduction of heat through clothing, if any is worn (this process is in series with radiation and convection effects at exposed surfaces).

5. Passive diffusion of vaporized water through dry skin surfaces and any overlying clothing.

6. Evaporation of sweat at wet portions of skin surfaces (active sweating is initiated only when the body is virtually nude).

7. Evaporation of moisture in respiratory tract.

Correlated data for each of these processes and a rationale for their synthesis were derived from a literature study.[7] The first three processes contribute to the sensible heat component, the last three contribute to the latent heat component, and the algebraic sum of these six is the total rate for transfer of metabolic heat to the environment.

The model for thermal metabolism includes the following basic assumptions:

1. The subject is sedentary and in thermal equilibrium.

2. Mean skin temperature T_s is a function of air temperature T_a:

$$T_s = 34+1.5 \tan^{-1}\left[0.1967(T_a-31)\right] \qquad (1)$$

where the temperatures are Celsius. With this equation, maximum deviation from the median, $T_s = 34$ C, is plus or minus $0.75\,\pi$ C = 2.356 C. In general, optimum comfort is associated with a skin temperature of about 34 C (93.2 F), and the range from 32 C (89.6 F) to 36 C (96.8 F) is transitional between skin that is dry (no active sweating) and skin that is partially or completely wet with perspiration.

3. Clothing is permeable to water vapor and is "optimum" at any environmental temperature. This implies that model skin temperatures will be maintained in a cool environment by adding or removing clothing. When the optimum clo value is zero (i.e., nudity), a rise in air temperature must be accompanied by the secretion and evaporation of sweat, as necessary to maintain thermal equilibrium.

4. A maximum evaporative cooling effect is reached when the skin is completely wet and the vapor pressure gradient from skin to air will not support an increase in rate of evaporation. Submaximal evaporation requirements to reach thermal equilibrium come from involuntary changes in the proportionate area of wetted skin. The evaporative cooling effect may also be limited to about 600 kcal/hr (2400 Btuh) in very hot, dry environments by the maximum sustainable rate of sweat production.[13]

In evaluating the seasonal requirements for ventilation of shelters, the essential metabolic parameters are: (1) the metabolic rate, which is generally assumed to be 100 kcal/hr(400 Btuh) for sedentary persons; and (2) the ratio ρ ("rho") of latent to total metabolic heat, which is shown for several combinations of environmental conditions in Figure H.1-2. The graphic data demonstrate that humidity has virtually no effect on the value of ρ in the zone of evaporative regulation, unless the required rate of evaporative cooling exceeds the maximum rate attainable with wet skin. In a temperate or cool environment, where clothing variation is used as a control mechanism, humidity has a significant effect on the value of ρ and a small effect on the optimum value of clothing resistance. The effects of variations in mean radiant temperature or air velocity on the value of ρ are most apparent in a hot environment; in a cool environment these variations change the optimum value of clothing resistance.

If Q is the total rate for transfer of metabolic heat, the latent heat component is

$$q_L = \rho Q \tag{2}$$

Btuh per person, and the sensible heat component is

$$q_S = (1-\rho)\ Q \tag{3}$$

Btuh per person. Within the limits for thermal equilibrium, the metabolic data in Figure H.1-2 can be approximated by two equations for ρ, the dimensionless ratio of latent to total metabolic heat:

$$\rho = 0.25 \tag{4}$$

when $t \leq 82.5$ F (28.06 C), and

$$\rho = 0.06\ t - 4.7 \tag{5}$$

when $t \geq 82.5$ F, where t is the air temperature. Values along Curve B in Figure H.1-2 are simulated quite well by Equations 4 and 5, if the relative humidity is about 50 percent when $t < 82.5$ F.

C. Transfer of Metabolic Heat

Metabolic data obtained by short-term experiments do not reflect the effects of heat that may be exchanged when liquid or solid foods are ingested and either excreted or vaporized at different temperatures. It is therefore appropriate, in the analysis of ventilating processes, to establish a rationale for treating these effects.

Some of the energy generated by human metabolism may be dissipated by means other than the environmental control system. These means can be combined in an equation for "reduced metabolic rate,"

$$M = (MR) - S - X - q_e \tag{6}$$

Btuh per person, where

(MR) = metabolic rate

S = rate of heat storage in body

X = rate of external work (the heat resulting from this work may contribute to thermal loads on the control system)

$q_e = m_e c_e \, (t_b - t_e)$ = the heat absorbed by a quantity m_e (lb/hr per person) of materials, having a specific heat c_e (Btu/lb-F), when ingested at t_e (F) and excreted at body temperature, $t_b \approx 98$ F. The product $m_e c_e$ is the "water equivalent."

The total metabolic heat transfer to the environment Q is the sum of sensible and latent components,

$$Q = q_S + q_L \tag{7}$$

Btuh per person.

The latent heat associated with metabolism is

$$q_L = \rho Q = \bar{m} h_{fgs} \tag{8}$$

Btuh per person, where

$\emptyset$ = ratio of latent to total metabolic heat

$\bar{m}$ = moisture evaporated at skin surfaces and in respiratory tract (lb/hr per person). This moisture is ingested at a temperature t_i and vaporized at skin temperature t_s = 95 F.

h_{fgs} = latent heat of vaporization for water at skin temperature.

The increase in air enthalpy associated with metabolism is, alternatively,

$$\begin{aligned} E &= q_S + \bar{m}h_{gs} \\ &= q_S + \bar{m}h_{fgs} + \bar{m}h_{fs} \\ &= q_S + q_L + \bar{m}h_{fs} \\ &= Q + \bar{m}h_{fs} \end{aligned} \tag{9}$$

Btuh per person, where

h_{fs} = specific enthalpy of liquid water at skin temperature t_s = 95 F.

$h_{gs} = h_{fgs} + h_{fs}$ = specific enthalpy of saturated water vapor at skin temperature (Btu/lb).

For liquid water at a temperature $t > 32$ F, the specific heat $c_w \approx 1.0$, and the specific enthalpy is

$$h_f = c_w\ (t-32) \approx t-32 \tag{10}$$

Btu per pound of water.

A linear approximation for the specific enthalpy of saturated water vapor at a temperature t (F) is

$$h_g = A + Bt \tag{11}$$

Btu/lb, where regression coefficients derived from tabulated values are:[9]

A = 1061.25 and B = 0.4362 when $t \geq 32$ F

A = 1061.09 and B = 0.4412 when $t \leq 32$ F.

Then, for moisture evaporating at a skin temperature of $t_s \approx 95$ F, values of thermal properties are

$$\begin{aligned} J &= h_{fs} = 95-32 = 63 \\ h_{gs} &= 1102.69 \\ K &= h_{fgs} = h_{gs}-h_{fs} = 1039.69 \end{aligned} \tag{12}$$

Btu/lb of moisture evaporated.

If the water to be evaporated at skin temperature is ingested at t_i (F), the reduced metabolic rate is

$$\begin{aligned} M &= Q + \bar{m}\ (h_{fs}-h_{fi}) \\ &= Q + \bar{m}\ (95-t_i) \\ &= E - \bar{m}\ (t_i-32) \end{aligned} \tag{13}$$

Btuh per person, and from Equations 8, 9, and 13

$$E = \frac{(K+J\rho)M}{K+(95-t_i)\rho} \tag{14}$$

Btuh per person.

The rate of evaporation is, alternatively,

$$\begin{aligned} \bar{m} &= \frac{\rho Q}{K} = \frac{\rho E}{K+J\rho} \\ &= \frac{\rho M}{K+(95-t_i)\rho} \end{aligned} \tag{15}$$

lb/hr per person.

In general, there would be heat and moisture loads in addition to metabolic effects. If water or steam is added to the air in the form of a spray or jet at the rate of m_w (lb/hr per person), the total moisture added to the air would be

$$G = \bar{m} + m_w \tag{16}$$

lb/hr per person.

If there are also one or more sensible heat loads F (Btuh per person), the additional heat load would be

$$Z = F + m_w h_w \tag{17}$$

Btuh per person, where

h_w = specific enthalpy of added water or steam (Btu/lb).

The sensible loads F may be associated with lighting fixtures, heating appliances, or temperature-dependent effects of heat transmitted through structural elements. Then the increase in enthalpy of ventilating air is

$$H = E + Z \tag{18}$$

Btuh per person.

The addition of heat causes an increase in specific enthalpy h of the ventilating air

$$H = \dot{m}_a \Delta h = \dot{m}_a (h_3 - h_2) \tag{19}$$

Btuh per person, where

$\dot{m}_a = 4.5\ V_s$ = flow rate of dry ventilating air (lb/hr per person).

V_s = flow rate of standard air having a specific volume of 13.33 pounds per cubic foot of dry air (scfm/person).

$\Delta h = h_3 - h_2$ = change in specific enthalpy of air from initial state h_2 to final state h_3 (Btu/lb of dry air).

Similarly, the addition of moisture causes an increase in humidity ratio W of the ventilating air:

$$G = \dot{m}_a \Delta W = \dot{m}_a (W_3 - W_2) \tag{20}$$

lb/hr per person, where

$\Delta W = W_3 - W_2$ = change in humidity ratio of air from initial state W_2 to final state W_3 (pounds of moisture per pound of dry air).

For the general case, where the metabolized water $\bar{m}$ (lb/hr per person) is ingested at a temperature t_i (F), the increase in enthalpy of ventilating air is

$$H = E + Z$$

$$= \frac{(K+J\rho)M}{K+(95-t_i)\rho} + Z \tag{21}$$

Btuh per person, and the corresponding increase in moisture content is

$$G = \bar{m} + m_w$$

$$= \frac{\rho M}{K+(95-t_i)\rho} + m_w \tag{22}$$

lb/hr per person. The ratio of the change in specific enthalpy to the change in humidity ratio of the air is

$$\frac{dh}{dW} = \frac{H}{G}$$

$$= \frac{(K+J\rho)M + \left[K+(95-t_i)\rho\right]Z}{\rho M + \left[K+(95-t_i)\rho\right]m_w} \tag{23}$$

Btu per pound of moisture added. This is the slope of the ventilation process line on a psychrometric chart at a particular value of ρ, which is a temperature-dependent variable defined by Equation 4 or 5.

From an examination of Equations 13, 21, 22, and 23, it is convenient to assume that metabolized water is ingested at a temperature of 95 F or 32 F.

If t_i = 95 F:

$$M = Q$$

$$H = \frac{(K+J\rho)M}{K} + Z \tag{24}$$

Btuh per person,

$$G = \frac{\rho M}{K} + m_w \tag{25}$$

lb/hr per person, and the slope is

$$\frac{dh}{dW} = \frac{(K + J\rho)M + KZ}{\rho M + Km_w} \quad (26)$$

Btu per pound of moisture added.

If $t_i = 32$ F:

$$M = E$$

$$H = M + Z \quad (27)$$

Btuh per person,

$$G = \frac{\rho M}{K + J\rho} + m_w \quad (28)$$

lb/hr per person, and the slope is

$$\frac{dh}{dW} = \frac{(K + J\rho)\ (M + Z)}{\rho M + (K + J\rho)m_w} \quad (29)$$

Btu per pound of moisture added.

Moreover, if metabolic heat and moisture loads are the only thermal effects to be considered, $Z = m_w = 0$ and the transfer of metabolic heat reduces to two cases:

For Case I, $t_i = 95$ F.

The increase in enthalpy is

$$H = E = \frac{K + J\rho}{K} M \quad (30)$$

Btuh per person; the increase in moisture content is

$$G = \bar{m} = \frac{\rho M}{K} \quad (31)$$

lb/hr per person; and the slope of ventilating process lines is

$$\frac{dh}{dW} = \frac{E}{\bar{m}} = \frac{K}{\rho} + J \quad (32)$$

Btu per lb of moisture. The mass rate of ventilation associated with entering and leaving states of the air is[14]

$$\dot{m}_a = 4.5V_s = \bar{m}/(W_3-W_2)$$

$$= \frac{M}{(h_3-h_2) - J(W_3-W_2)} \qquad (33)$$

pounds of dry air per hour per person.

For Case II, $t_i = 32$ F.

The increase in enthalpy is

$$H = E = M \qquad (34)$$

Btuh per person; the increase in moisture content is

$$G = \bar{m} = \frac{\rho M}{K + J\rho} \qquad (35)$$

lb/hr per person; and the slope of ventilation process lines is

$$\frac{dh}{dW} = \frac{K}{\rho} + J \qquad (36)$$

Btu per lb of moisture. The mass rate of ventilation associated with entering and leaving states of the air is[7]

$$\dot{m}_a = 4.5V_s = \bar{m}/(W_3-W_2)$$

$$= \frac{M}{h_3-h_2} \qquad (37)$$

pounds of dry air per hour per person.

The derivation of equations for ventilation process lines in the next section is valid for either Case I or Case II; Equations 32 and 36 are identical. However, per capita ventilating rates determined by Equation 33 (Case I) are slightly higher than rates determined by Equation 37 (Case II).

The simplifying assumptions made in connection with Cases I and II may not be adequate in certain situations. For example, steady state heat loads associated with lighting fixtures or transmission effects may be relatively more significant for aboveground shelters in cold climates. The general equations, 21 to 29 inclusive, may then be used as a point of departure for a more definitive analysis.

D. Ventilation Processes

In this section, the rationale outlined in previous sections on Metabolic Parameters and Transfer of Metabolic Heat is used in the derivation of equations for families of ventilation process lines on a psychrometric chart. The derivations are based on assumptions that metabolic heat and moisture are the only significant internal loads and that water evaporated is ingested at a temperature of 32 F, the Case II assumption for transfer of metabolic heat.

When air moves linearly through an occupied space, heat and moisture associated with metabolism and other sources cause a gradual change in thermal properties of the air. In a differential length dx of a shelter, there are

$$dy = \frac{N}{\ell}\,dx = N dr \tag{38}$$

people, where

N = number of people in the space

ℓ = length of space in the direction of air movement (ft)

x = portion of length ℓ, measured from air entry end of space

y = number of people in length x

$r = \frac{x}{\ell}$ = dimensionless length ($0 \le r \le 1$).

The rates of increase in specific enthalpy and humidity ratio along the path of air flow are given by the differential equations

$$N\dot{m}_a dh = NH dr$$

or

$$\frac{dh}{dr} = \frac{H}{\dot{m}_a} \tag{39}$$

for the change in specific enthalpy, and

$$N\dot{m}_a dW = NG dr$$

or

$$\frac{dW}{dr} = \frac{G}{\dot{m}_a} \tag{40}$$

for the change in humidity ratio, where

$\dot{m}_a$ = mass flow rate of dry air (lb/hr per person)

h = specific enthalpy of moist air (Btu/lb of dry air)

W = humidity ratio (lb of moisture/lb or dry air)

H = M = unit change in enthalpy, as defined by Equations 6 and 34 (400 Btuh per person)

G = $\bar{m}$ = unit change in moisture, as defined by Equations 8 and 35 (lb/hr per person).

Then, from Equations 36, 39, and 40,

$$\frac{dh}{dW} = \frac{M}{\bar{m}} = \frac{K}{\rho} + J \tag{41}$$

Btu per pound of moisture.

The specific enthalpy of moist air h is[9]

$$\begin{aligned} h &= \varphi t + h_g W \\ &= \varphi t + (A+Bt)\ W \end{aligned} \tag{42}$$

Btu per pound of dry air, where

t = dry-bulb temperature F

φ = specific heat of dry air (Btu/lb-F)

$h_g \approx A+Bt$ = specific enthalpy of saturated water vapor (Equation 11).

From equation 42, the total derivative is

$$\frac{dh}{dW} = (\varphi + BW)\ \frac{dt}{dW} + Bt + A \tag{43}$$

Btu per pound of moisture.

Equating the two expressions for $\frac{dh}{dW}$, Equations 41 and 43, the general differential equation for families of ventilation process lines associated with metabolic heat is

$$(\varphi + BW)\,\frac{dt}{dW} = \frac{K}{\rho} + J - A - Bt \tag{44}$$

for which numerical values of physical constants are:

$A = 1061.25$,

$B = 0.4362$,

$\varphi = 0.24026$,

$K = 1039.69$, and

$J = 63$.

The differential equation then becomes

$$\frac{dW}{0.5508 + W} = \frac{\rho dt}{2383.51 - 2288.51\rho - \rho t} \tag{45}$$

for which the value of ρ (the ratio of latent to total metabolic heat) comes from Equation 4 or 5. In the low range of temperatures ($t \leq 82.5$ F), $\rho = 0.25$ and the differential equation is

$$\frac{dW}{0.5508 + W} = \frac{dt}{7245.6 - t}\,. \tag{46}$$

In the high range of temperatures ($t \geq 82.5$ F), $\rho = 0.06t-4.7$, and the differential equation is

$$\frac{dW}{0.5508 + W} = \frac{(t - 78.333)dt}{(95 - t)\,(2305.2 + t)} \tag{47}$$

In the low range of temperatures ($t \leq 82.5$ F), a direct solution to Equation 41 can be obtained in terms of specific enthalpy and humidity ratio because $\rho = 0.25$ = a constant. Equation 41 becomes

$$\frac{dh}{dW} = 4221.8 \tag{48}$$

and the solution is

$$h-h_o = 4221.8\,(W - W_o) \tag{49}$$

when $t \leq 82.5$ F.

In terms of humidity ratio and temperature, the solution to Equation 46 is

$$\frac{0.5508 + W}{0.5508 + W_o} = \frac{7245.6 - t_o}{7245.6 - t} \tag{50}$$

when $t \leq 82.5$ F.

The quantities h_o, W_o, and t_o are properties of moist air (specific enthalpy, humidity ratio, and temperature) at any state point on a particular ventilation process line, and h, W, and t are corresponding properties of moist air at any other point on the same process line.

In terms of humidity ratio and temperature, the solution of Equation 47 is

$$\frac{0.5508 + W}{0.5508 + W_o} = R_2 \left(\frac{R_3}{R_2}\right)^{0.0069439} \tag{51}$$

where $R_2 = \dfrac{2305.2 + t_o}{2305.2 + t}$

$R_3 = \dfrac{95 - t_o}{95 - t}$

and $t \geq 82.5$ F.

Several ventilation process lines determined analytically by Equations 49, 50, and 51 are shown on Figure H.1-3.* The lines are straight in the temperature range at or below 82.5 F. At higher temperatures, the environment tends to approach a temperature of 95 F asymptotically, because air and skin temperatures are then equal, and metabolic equilibrium is maintained entirely by evaporative cooling effects. The six lines that originate at a temperature of 50 F bracket the possible range of 0 to 100 percent relative humidity. Thus these lines represent process lines associated with the prescribed criterion for a minimum temperature of 50 F in a shelter environment. Across this group of six process lines are a number of heavier nearly vertical lines that terminate at dots. These are isoventilation lines, calculated in accordance with Equation 37, with the proviso that air is supplied to occupied spaces at a temperature of 50 F. The isoventilation lines show the condition

---

* Adapted from Reference 7.

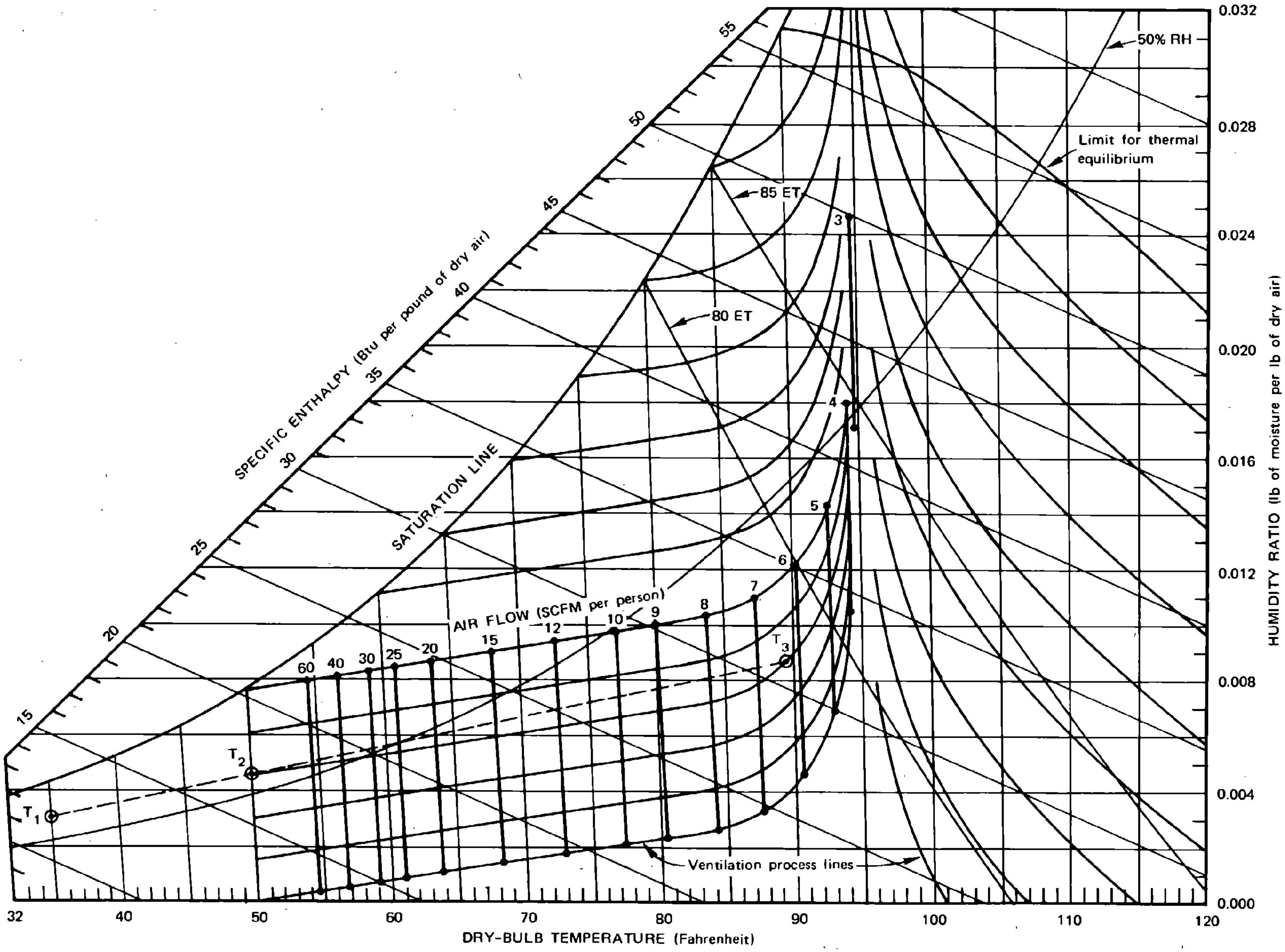

FIGURE H.1-3 PROCESS LINES FOR VENTILATING A SPACE WITH MIXED AIR AT 50 F

of exhaust or recirculated air when the space is ventilated at the indicated rate. A curve at the top of the figure shows the locus of points above which thermal equilibrium cannot be maintained. Effective temperature lines for 80 FET and 85 FET are also shown.

The metabolic data and rationale derived for environmental analyses are inherently applicable under both isostate and varistate conditions. The uniform state (isostate) is a special case of the variable (varistate) in which the ventilating process can be represented by two end points on a straight line on a psychrometric chart. The slope of this line is determined by the value of ρ at the resultant temperature of the environment, and the change in enthalpy of the air from intake to exhaust conditions is determined by the heat absorbed in occupied spaces.[14] When the environmental temperature is 95 F, metabolic heat is transferred only by evaporation; air temperatures are virtually uniform and constant; and ventilating rates associated with isostate and varistate processes are equal. The rate of ventilation required to maintain an effective temperature of 83 FET is somewhat higher for an isostate process than for a varistate process when the environmental temperature is more than 95 F, and correspondingly lower when the environmental temperature is less than 95 F.[14]

E. Recirculation of Air

During warm weather, the capabilities of a ventilating system will be used to best advantage if all air supplied to occupied spaces is fresh (outside) air. During cool weather, when atmospheric temperatures are within the range of 50 F to 70 F, partial recirculation of air would be beneficial in connection with systems that do not distribute air through ducts and diffusion outlets.

When outside temperatures are less than 50 F, which is the prescribed minimum temperature in shelters, the environment near openings through which air enters an occupied space may be too cold, unless the fresh air is either heated or mixed with relatively warm air from the space.[4] The mixing process is illustrated in Figure H.1-3 by a straight dash line through three points at which the temperatures, specific enthalpies, and humidity ratios are T_1, h_1 and W_1 for fresh air; T_3, h_3 and W_3 for recirculated air; and T_2, h_2 and W_2 for mixed air. The state points for mixed and recirculated air must be on the same ventilation process line. In accordance with the principles of conservation of mass and energy in a mixing process, the properties of moist air at the three state points are related by the equations,

$$\frac{h_3 - h_1}{W_3 - W_1} = \frac{h_2 - h_1}{W_2 - W_1} = \frac{h_3 - h_2}{W_3 - W_2} \quad (52)$$

and the ratio of flow rates for fresh and mixed air is

$$\frac{V_1}{V_2} = \frac{h_3 - h_2}{h_3 - h_1} = \frac{W_3 - W_2}{W_3 - W_1} \quad (53)$$

where the flow rates V_1 and V_2 are referred to standard conditions, that is, scfm per person. A true ventilating rate V can be determined for moist air under any stated condition by the equation

$$V = V_s \left[\frac{0.001891\ (459.67 + t)\ (1 + 1.6078W)}{P}\right] \quad (54)$$

where

$V_s = \dot{m}_a/4.5$ = scfm of standard air

$\dot{m}_a$ = mass flow rate, pounds of dry air per hour

t = air temperature F

W = humidity ratio (lb of moisture/lb of dry air)

P = barometric pressure (atmospheres)

The relationships among quantities associated with recirculation of ventilating air during cool or cold seasons are shown in Figure H.1-4 for a mixed-air temperature of 50 F.[7] The figure is based on a computer analysis of the combined mixing and varistate ventilating processes. Metabolic effects are assumed to be the only significant heat loads.*

The total flow rate of mixed air V_2 will usually correspond to the installed system capacity, as determined by probable requirements for ventilation in warm weather. For this or any selected rate of ventilation, Figure H.1-4 evaluates the temperature of leaving (exhaust) air T_3 when the mixed (supply) air temperature is 50 F. Then the Figure shows the flow rate of fresh air V_1 required at various values of outside temperature T_1 to maintain a mixture temperature of just 50 F.

---

* The use of Figure H.1-4 is illustrated by an example in Figure 6-2A, Chapter 6.

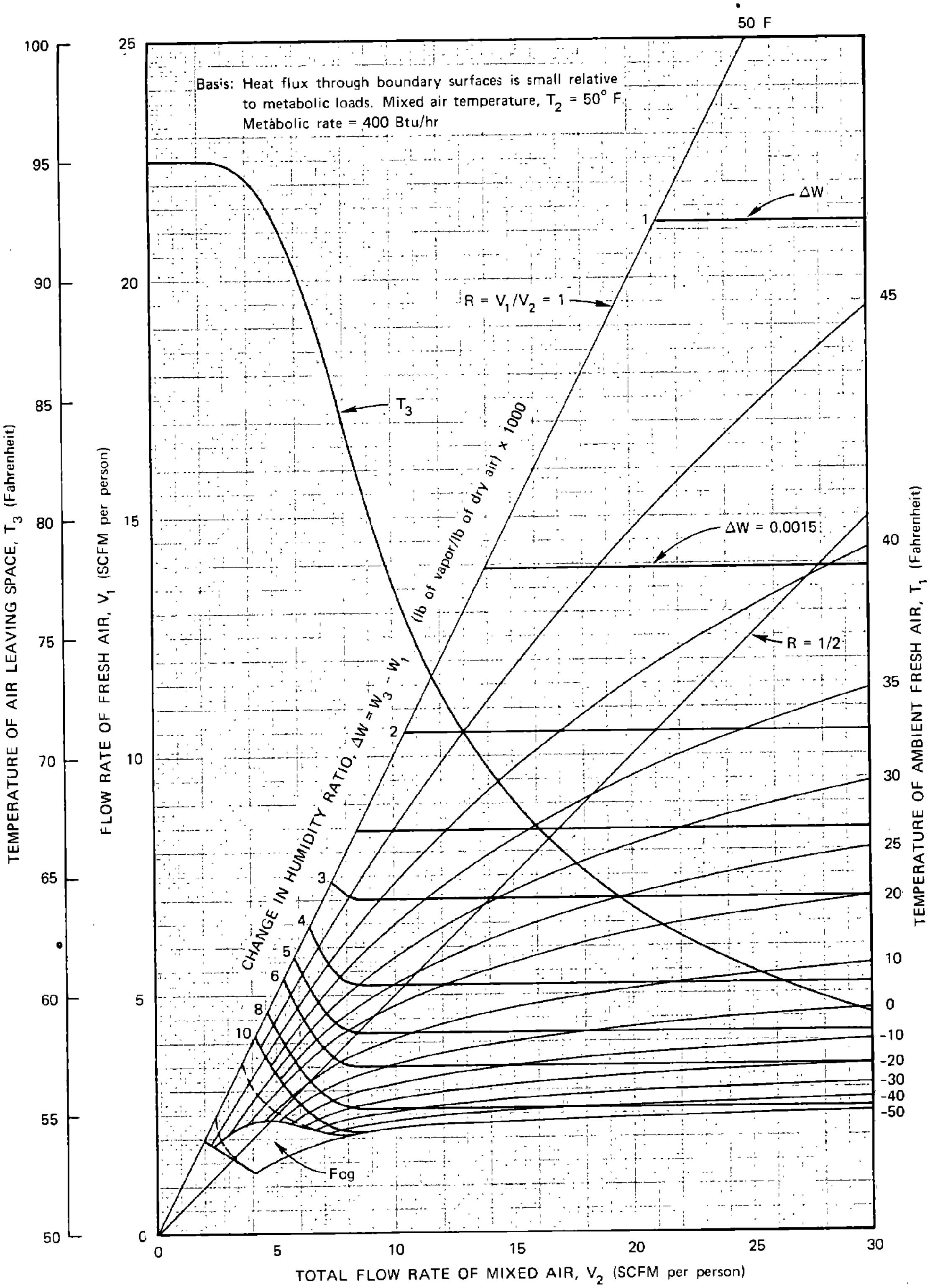

FIG. H.1-4 VENTILATION OF AN OCCUPIED SPACE WITH AIR SUPPLY AT 50 F[7]

The Figure also shows the increase in humidity ratio ($\Delta W = W_3 - W_1$) of fresh air during passage through the system. For example: If the unit capacity of a ventilating system is 12 scfm per person and the mixed air temperature is 50 F, the temperature of recirculated air will be 72.6 F. Then, if the outside air temperature is 20 F, the flow rate of fresh air should be 5.2 scfm per person. During passage through the shelter, about 0.004 pounds of moisture will be added to each pount of dry air in the fresh air stream.

If the state point for mixed air lies above the saturation line, droplets of condensed moisture will be present in air supplied to occupied spaces. This condition would prevail in the region labeled "Fog" in Figure H.1-4.

If the flow rate of fresh air V_1 is 3 scfm per person, in accordance with the criterion for control of chemical vitiation, a mixture temperature of 50 F can be maintained in an "insulated" shelter, unless the outside air temperature falls below values in the following tabulation:[4]

Flow Rate of Mixed Air, V_2 (scfm/person)	Minimum Temperature of Fresh Air, T_1 (F)
5	20
6	10
7	0
9	-10
13	-20
22	-30

These flow rates suggest minimum capacities for ventilating systems in northern regions where the indicated low temperatures frequently occur. The systems should be arranged to recirculate air.

NOTATION

c_e	specific heat of excreted materials (Btu/lb-F)
c_w	specific heat of water (Btu/lb-F)
D	wet-bulb depression F
E	enthalpy increase caused by metabolism (Btuh/person)
ET	effective temperature F (original version)
ET^*	effective temperature F (revised version)
F	sum of non-metabolic sensible heat loads (Btuh/person)
G	increase in moisture content of air (lb/hr/person)
H	increase in enthalpy of ventilating air (Btuh/person)
h	specific enthalpy of ventilating air (Btu/lb of dry air)*
h_f	specific enthalpy of water (Btu/lb)
h_{fgs}	latent heat of vaporization (water at t_s = 95 F)(Btu/lb)
h_{fi}	specific enthalpy of water at t_i (Btu/lb)
h_{fs}	specific enthalpy of water at t_S = 95 F (Btu/lb)
h_g	specific enthalpy of saturated water vapor (Btu/lb)
h_{gs}	specific enthalpy of saturated water vapor at t_s (Btu/lb)
h_w	specific enthalpy of added non-metabolic water or steam (Btu/lb)
h_1	specific enthalpy of fresh air (Btu/lb of dry air)
h_2	specific enthalpy of air entering space (Btu/lb of dry air)
h_3	specific enthalpy of air leaving space (Btu/lb of dry air)
J	$= h_{fs}$
K	$= h_{fgs}$
ℓ	length of space in direction of air movement (ft)
M	reduced metabolic rate (Btuh/person)
(MR)	metabolic rate (Btuh/person)
$\bar{m}$	body moisture evaporated (skin surfaces + respiratory tract)(lb/hr/person)
$\dot{m}_a$	flow rate of dry ventilating air (lb/hr/person)
m_e	quantity of excreted materials (lb/hr/person)
m_w	non-metabolic moisture added to air (lb/hr/person)
N	number of persons in ventilated space
P	barometric pressure (atmospheres)
Q	total metabolic heat transfer (Btuh/person)

H. 1-33

q_e	heat absorbed by excreted materials (Btuh/person)
q_L	latent heat transfer rate (Btuh/person)
q_S	sensible heat transfer rate (Btuh/person)
r	$= x/\ell$
S	rate of heat storage in body (Btuh/person)
T	dry-bulb temperature F
T_a	air temperature C
T_s	mean skin temperature C
T_w	wet-bulb temperature F
T_1	temperature of fresh air F
T_2	temperature of mixed (fresh and recirculated) air F
T_3	temperature of recirculated air F
t	temperature F*
t_b	body temperature F
t_e	ingestion temperature of materials later excreted F
t_i	ingestion temperature of water later evaporated F
t_s	skin temperature F
V	true flow rate or ventilating rate (cfm/person)
V_s	flow rate (scfm/person) of standard air (specific volume = 13.33 pcf dry air)
V_1	flow rate of fresh air (scfm/person)
V_2	flow rate of air entering space (scfm/person)
W	humidity ratio (lb moisture per lb dry air)*
W_1	W for fresh air supply
W_2	W for air entering space
W_3	W for air leaving space
W_3	W at final state
X	rate of external work (Btuh/person)
x	portion of length ℓ, measured from air entry end of space (ft)
y	number of persons in length x
Z	total added heat excluding metabolic (Btuh/person)
ρ	ratio of latent to total metabolic heat
c_p	specific heat of dry air (Btu/lb-F)

* With subscript o the variable is a property of moist air at the state point that determines the ventilation process line.

REFERENCES

1. Shelter Design and Analysis, Volume 3 - Environmental Engineering for Shelters, U. S. Office of Civil Defense, TR-20 (Vol. 3), May 1969.

2. "Survival Shelters," Chapter 16, ASHRAE Guide and Data Book - Applications, 1971, American Society of Heating, Refrigerating and Air-Conditioning Engineers, Inc., New York, New York.

3. Mechanical and Electrical System Design for Protective Shelters, prepared by Walter F. Spiegel, Consulting Engineer, for the U.S. Office of Civil Defense, Washington, D.C., June 1968.

4. Technical Standards for Fallout Shelters, Technical Memorandum 68-1, U.S. Office of Civil Defense (5 March 1969). Habitability requirements for fallout and blast shelters are quite similar.

5. Design Considerations for Fallout Shelter Ventilating Air Intake Systems, Technical Memorandum 71-1, U.S. Office of Civil Defense, January 1971. Intake facilities in shelters for combined weapons effects should be blast resistant as well as effective in reducing fallout ingress.

6. Murphy, H. L., Feasibility Study of Slanting for Combined Nuclear Weapons Effects (Revised), Volumes 1 and 2, SRI Technical Report for OCD (DCPA), July 1971 (AD-734 831 and 2).

7. Allen, F. C., Parametric Study of Thermal Problems in Densely Populated Shelters, Contract No. DAHC20-71-C-0290, prepared by Stanford Research Institute for Defense Civil Preparedness Agency, June 1972 (AD-749 796).

8. ASHRAE Handbook of Fundamentals, American Society of Heating, Refrigerating and Air-Conditioning Engineers, Inc., New York, New York; 1967, p. 117.

9. ASHRAE Handbook of Fundamentals, American Society of Heating, Refrigerating and Air-Conditioning Engineers, Inc., New York, New York, 1972.

10. Baschiere, R. J., and M. Lokmanhekim, Shelter Forced Ventilation Requirements Using Unconditioned Air, GARD final report 1266, General American Transportation Corp., Niles, Illinois, for U.S. Office of Civil Defense, February 1967.

11. Schaefer, K. E., "A Concept of Triple Tolerance Limits Based on Chronic CO_2 Toxicity Studies," Environmental Engineering in Protective Shelters, National Academy of Sciences - National Research Council, February 1960.

12. Allen, F. C., "Mechanical Equipment Requirements," Symposium on Survival Shelters, American Society of Heating, Refrigerating and Air-Conditioning Engineers, June 1962.

13. Humphreys, C. M., A. Henschel, and D.H.K. Lee, Sensible and Latent Heat Losses from Occupants of Survival Shelters, OCD Work Unit 1221C, final report by Occupational Health Research and Training Facility, Public Health Service, DHEW, December 1966.

14. Allen, F. C., Ventilating and Mixing Processes in Nonuniform Shelter Environments, Contract No. DAHC20-68-C-0155, prepared by Stanford Research Institute for Office of Civil Defense, January 1970 (AD-708 574).

15. Yaglou, C. P., "Tolerance Limits of People for Cold, Heat, and Humidity in Underground Shelters," Environmental Engineering in Protective Shelters, National Academy of Sciences - National Research Council, February 1960.

16. Allen, F. C., Shelter Configuration: Environmental Control Systems and Related Parameters (Contract No. DAHC20-68-C-0155) report prepared by Stanford Research Institute for Office of Civil Defense, March 1969.

17. Murphy, H. L., and J. E. Beck, Slanting for Combined Nuclear Weapons Effects: EXAMPLES WITH ESTIMATES, AND AIR BLAST ROOM FILLING, Stanford Research Institute Technical Report, for Defense Civil Preparedness Agency, June 1973. (AD-783 061)

18. Everetts, J., D. R. Witt, and E. R. McLaughlin, The Feasibility of Augmenting Below-Grade Shelter Habitability with Conditioned Air, OCD Contract No. DAHC-20-68-0175, The Pennsylvania State University, January 1970.

19. Houghten, F. C., W. W. Teague, W. E. Miller, and W. P. Yant, "Heat and Moisture Losses from the Human Body and Their Relation to Air Conditioning Problems," American Society of Heating and Ventilating Engineers, Transactions, Volume 35, 1929.